Monitoring immune responses in dendritic cell based vaccination

with a focus on *in vivo* imaging

Erik H.J.G. Aarntzen

Monitoring immune responses in dendritic cell based vaccination Erik H.J.G. Aarntzen

Monitoring immune responses in dendritic cell based vaccination

with a focus on in vivo *imaging*

Erik Hendrikus Johannes Gregorius Aarntzen

ISBN

Production

Design Erik Aarntzen

Layout Marjolein Hovestad

Print Ipskamp Drukkers B.V., Enschede

The work presented in this thesis was performed at the departments of Tumor Immunology, Nijmegen Centre for Molecular Life Sciences, and the department of Medical Oncology, Radboud University Nijmegen Medical Centre, Nijmegen, The Netherlands.

The studies described in this thesis were supported by the Radboud University Nijmegen Medical Centre (Agiko grant 2008-2-4), the European Network for Cell Imaging and Tracking Expertise (ENCITE, 7th Framework, WP5.1, task F) and Stichting Afweer Tegen Kanker.

Monitoring immune responses in dendritic cell based vaccination

with a focus on in vivo *imaging*

Proefschrift

ter verkrijging van de graad van doctor aan de Radboud Universiteit Nijmegen

op gezag van de rector magnificus prof. mr. S.C.J.J. Kortmann,

volgens besluit van het college van decanen

in het openbaar te verdedigen op vrijdag 18 januari 2013, om 10.30 uur precies

door

Erik Hendrikus Johannes Gregorius Aarntzen

geboren op 28 juni 1981

te Angeren

Promotoren:	prof. dr. C.J.A. Punt
	prof. dr. C.G. Figdor
	prof. dr. I.J.M. de Vries
Copromotor:	dr. J.F.M. Jacobs
Manuscriptcommissie:	prof. dr. O.C. Boerman
	prof. dr. J.B.A.G. Haanen (Antoni van Leeuwenhoek ziekenhuis - Nederlands Kanker Instituut)
	dr. H. Dolstra

Prelude

zo

zo doet

zo doe ik

doen wij

wat wij kunnen

zo

Bert Schierbeek

Contents

page

Scope of this thesis 1

Part 1. Strategies to optimize dendritic cell based vaccinations 3

1. Dendritic cell vaccines in melanoma: from promise to proof? 5

   Crit Rev Oncol Hematol. 2008; 66(2):118-34.

2. Targeting $CD4^+$ T-helper cells improves the induction of antitumor responses in dendritic cell based vaccination 27

   Cancer Res. 2012 Oct 18th (accepted)

3. Vaccination with mRNA-electroporated dendritic cells induces robust tumor antigen-specific CD4+ and CD8+ T cell responses in stage III and IV melanoma patients 45

   Clin Cancer Res. 2012; 18(19):5460-70.

4. Natural human plasmacytoid dendritic cells induce antigen specific T cell responses and enhance overall survival in melanoma patients 63

   (submitted)

Part 2. In vivo tracking of dendritic cell based vaccinations upon delivery 79

5. Maximizing dendritic cell migration in cancer immunotherapy 81

   Expert Opin Biol Ther. 2008; 8(7):865-74

6. Limited amounts of dendritic cells migrate into the T cell area of lymph nodes but have high immune activating potential in melanoma patients 97

   Clin Cancer Res. 2009; 15(7):2531-40

7. Targeting of ^{111}In-labeled dendritic cell human vaccines improved by reducing the number of cells 113

   (submitted)

Part 3. Monitoring immune responses in dendritic cell based vaccination studies *129*

8. Dendritic cell vaccination and immune monitoring *131*

Cancer Immunol Immunother. 2012; 57(10):1559-68

9. Imaging of cellular therapies *145*

Adv Drug Deliv Rev. 2010; 62(11):1080-93

10. Humoral anti-KLH responses in cancer patients treated with dendritic cell based immunotherapy are dictated by different vaccination parameters. *167*

Cancer Immunol Immunother. 2012; 61(11):2003-11

11. Skin-test infiltrating lymphocytes early predict clinical outcome of dendritic cell based vaccination in metastatic melanoma *179*

Cancer Res. 2012 Sept 24th (accepted)

12. Early identification of antigen-specific immune responses *in vivo* by ^{18}F-FLT PET imaging *197*

Proc Natl Acad Sci U S A. 2011; 108(45):13896-9

General discussion *209*

13. *In vivo* imaging of therapy-induced anti-cancer immune responses in humans

Cell Mol Life Sci. 2012 Oct 5th (accepted)

Concluding remarks *235*

Nederlandse samenvatting *237*

Dankwoord *245*

Curriculum Vitae *247*

List of publications *249*

Scope of this thesis

Immunotherapy aims to re-engage and revitalize the immune system in the fight against cancer. Our immune system is a highly organized multi-cellular system designed to protect us from invading pathogens and malignantly transformed cells. As such, the immune system acts with enormous specificity and great sensitivity, in concert with regulatory mechanisms, to avoid destructive self-reactivity. The notion of the immunogenic aspects of cancer, together with the attractive modes of action of the immune system, has initiated the development of treatments that rely on immune cells. Owing to their unique immune stimulatory properties, dendritic cells (DC) have become an essential target for anti-cancer immunotherapy. We, and others, have explored DC-based therapy to induce tumor-specific immune responses in metastatic melanoma patients. However, research in the past four decades has shown that the relationship between the immune system and human cancer is complex, highly dynamic and dependent on the individuals' characteristics.

Given this complexity, it is crucial to understand the processes that precede the failure or success of therapy-induced immune responses. This thesis focuses on the evaluation of DC-based therapy and the development of novel tools to monitor therapy-induced immune responses. Such monitoring tools would allow further optimizing therapy parameters and identifying probable responding patients early during treatment. Functional multimodal *in vivo* imaging is a powerful candidate to fulfil this task as it addresses critical steps in ensuing immune responses.

The first section is focused on clinical studies and describes three single-arm proof-of-principle studies investigating different vaccination parameters. **Chapter 1** provides a 'roadmap' for optimizing the efficacy of DC-based strategies. In **Chapter 2**, we studied the targeting of tumor-specific $CD4^+$ T cells by including MHC Class II binding epitopes for loading *ex vivo* generated DC. In **Chapter 3**, we investigate immune responses to mRNA transfected DC presenting a multitude of (un-)defined epitopes, in metastatic melanoma patients and patients with locoregional lymph node metastases. **Chapter 4** describes the immunological and clinical responses to vaccination with plasmacytoid DC, a naturally circulating subset with high capacity to produce type 1 interferons.

In the second section, we discuss the first step in the successful induction of anti-cancer immune responses; correct delivery of DC to the relevant sites. **Chapter 5** introduces this section by reviewing strategies to maximize the migration of vaccinated DC to lymph nodes. Next, we demonstrate in **Chapter 6** by scintigraphic imaging that even limited numbers of DC that reach the lymph nodes are capable of inducing tumor-specific immune responses. **Chapter 7** concludes this section by providing an *ex vivo* model using ^{19}F-MRI and *in vivo* experimental data, in order to speed up the optimization of intradermal delivery of DC.

The last section is devoted to the monitoring of the mainstay of immunotherapy; vaccine-specific effector immune cells. **Chapter 8** emphasizes that the concept of optimizing DC-based strategies by small proof-of-principle studies warrants intensive immune monitoring. **Chapter 9** highlights the contribution of functional *in vivo* imaging for real time assessment of parameters such as cell localization, numbers and viability. In **Chapter 10**, we investigate the patterns of humoral responses to keyhole limpet hemocyanin (KLH), as a surrogate marker, in response to varying vaccination parameters by developing a novel quantitative KLH-specific ELISA. The diversity and quality of tumor-

specific $CD8^+$ T cell responses after vaccination are evaluated in skin-test infiltrating lymphocyte cultures. We show in **Chapter 11** that this bioassay accurately identifies long-term survivors after completing of vaccination. **Chapter 12** demonstrates that already during the course of DC-based therapy, vaccine-specific immune responses in vaccinated lymph nodes can be assessed quantitatively using ^{18}F-FLT PET/CT; showing for the first time in human how functional *in vivo* imaging can aid physicians in individualized decision-making, by early discrimination of responding patients. The General Discussion, **Chapter 13**, provides an overview of the role of imaging modalities in the monitoring of therapy-induced anti-cancer immune responses and a visionary view on further development.

Part 1

Strategies to optimize dendritic cell based vaccinations

Dendritic cell vaccines in melanoma: from promise to proof?

Lesterhuis WJ

Aarntzen EH

De Vries IJ

Schuurhuis DH

Figdor CG

Adema GJ

Punt CJ

Crit Rev Oncol Hematol. 2008;66(2):118-34.

Abstract

Dendritic cells (DC) are the directors of the immune system, capable of inducing tumour antigen-specific T- and B cell responses. As such, they are currently applied in clinical studies in cancer patients. Early small clinical trials showed promising results, with frequent induction of anti-cancer immune reactivity and clinical responses. In recent years, additional trials have been carried out in melanoma patients, and although immunological responses are often reported, objective clinical responses remain anecdotal with objective response rates not exceeding 5-10%. Thus, DC vaccination research has now entered a stage in between 'proof of principle' and 'proof of efficacy' trials. Crucial questions to answer at this moment are why the clinical responses remain scarce and what can be done to improve the efficacy of vaccination. The answers to these questions probably lie in the preparation and administration of the DC vaccines. Predominantly, cytokine-matured DC are used in clinical studies, while from preclinical studies it is evident that DC that are activated by pathogen-associated molecules are much more potent T cell activators. For sake of easy accessibility monocyte-derived DC are often used, but are these cells also the most potent type of DC? Other yet unsettled issues include the optimal antigen-loading strategy and route of administration. In addition, trials are needed to investigate the value of manipulating tolerizing mechanisms, such as depletion of regulatory T cells or blockade of the inhibitory T cell molecule CTLA-4. These issues need to be addressed in well-designed comparative clinical studies with biological endpoints in order to determine the optimal vaccine characteristics. DC vaccination can then be put to the ultimate test of randomized clinical trials. Here, we review the immunobiology of DC with emphasis on the different aspects that are most relevant for the induction of anti-tumour responses *in vivo*. The different variables in preparing and administering DC vaccines are discussed in this context and the immunological and clinical results of studies with DC vaccines in melanoma patients are summarized.

1. Introduction

Melanoma is one of the more immunogenic cancer types and many strategies to enhance specific or non-specific immunity in melanoma patients have been explored in clinical studies (1). Dendritic cells (DC) are crucial as the sentinels of the immune system. It has been proposed that when the tumour reaches a certain size and causes damage to the surrounding tissues with release of products by the microenvironment, local DC are activated and subsequently the immune system is alerted (2). It then depends on the size of the tumour and its immunomodulatory characteristics, whether the immune system is able to eradicate the cancer. Often malignant growth is a slow and silent process that fails to provide a 'danger signal' necessary for the activation of the immune system. The goal of DC vaccination is to mend this inattention of the immune system by providing it with *ex vivo* 'educated' DC; appropriately activated and loaded with tumour antigen. The underlying principle is that DC are the most potent antigen presenting cells of the immune system that play a central role in the induction-phase of antigen-specific immunity. DC acquire and process antigen and migrate to the lymphoid organs where they present the antigen to the specific arm of the immune system, resulting in the induction of primary T- and B cell responses. Because of these unique qualities they represent an interesting tool in cancer immunotherapy. The possibility to generate DC in large amounts for clinical use has accelerated research in this field, and immunological and clinical responses have been reported in melanoma patients after vaccination with DC (Table 1-2) (3-5). Several years ago it was already estimated that more than thousand cancer patients had received some form of DC-based vaccination (6). In contrast to other systemic therapies in cancer treatment, it is not possible to pool these patients in a meta-analysis. This is due to the enormous diversity in terms of vaccine preparation and administration and immunomonitoring. Although much progress has been made in several of these areas over the past years, there seems still room for significant improvement before an optimal DC vaccine is to put to the ultimate test of large scale clinical studies.

2. DC subsets

Two distinct categories of DC exist: plasmacytoid DC and conventional or 'myeloid' DC (7). Plasmacytoid DC are circulating cells with a plasmacytoid morphology that are capable of producing large amounts of type I interferons upon activation by microbial stimuli (8). In addition, they can differentiate into DC that are capable of activating naïve T cells against allo-antigens (9) and exogenous antigens (10). In the context of cancer, plasmacytoid DC have been implicated in the induction of both immunity and tolerance, and their potential role in vaccination strategies in cancer patients still has to be determined (11). Conventional DC or 'myeloid' DC (12) can be further divided into migratory DC, which actively sample the peripheral tissues and migrate to draining lymph node to present antigens to T cells, and lymphoid-tissue-resident DC which captivate local (foreign and self-) antigens and present it to local T cells (13). Examples of lymphoid-tissue-resident DC are splenic and thymic DC. Migratory DC derived from both $CD34^+$ precursor cells and monocytes. Monocytes can differentiate into DC upon transendothelial migration (14). The presence of GM-CSF, in addition to other pro-inflammatory cytokines, can differentiate both $CD34^+$ precursor cells and monocytes into DC. Recently, it was proposed to recognize a third distinct group of conventional DC, 'inflammatory' DC: cells that are not present in the steady state, but that appear under the influence of inflammation or infection (13).

3. DC subsets in clinical trials

Monocyte-derived DC have been used in most vaccination studies because of the relative ease with which large quantities of cells can be obtained. Usually, one leukapheresis is enough to obtain approximately $100\text{-}150\times10^6$ cells. Yields are much lower with $CD34^+$ selection and repeated leukaphereses are often necessary to obtain enough cells (15). The same accounts for circulating blood DC, which can be obtained from peripheral blood after *in vivo* Flt-3L expansion and negative

selection *ex vivo* (16). Banchereau and collegues have reported impressive immunological and clinical results using Flt3-Ligand expanded $CD34^+$ DC (15). In other studies with $CD34^+$ DC, using different maturation and vaccination regimes, clinical responses were observed less frequently (17, 18). The same variable outcomes are seen in studies with monocyte-derived DC (Table 1 and 2, and section on clinical results). These differences may well be more related to the differences in culture and maturation protocols, than to the differences in DC subsets. Due to the fragmented nature of the available data and the absence of direct comparative studies, it is not possible at this moment to draw any firm conclusion on the most optimal DC subset to be used in clinical trials. In recent years, evidence is accumulating that considerable cross-talk takes place between the different DC subsets (7), and that perhaps it is beneficial even to combine different subsets of DCs, as has been done in the above mentioned studies (15).

4. Maturation

The term 'maturation' refers to the phenotypical and functional reaction of DC upon encountering danger signals. Maturation can be induced by pro-inflammatory cytokines such as IL-1β or IL-6, by interaction with T cells and by interaction with pathogens. DC can detect pathogens through pattern recognition receptors such as Toll-like receptors (TLR)(19). The TLR family consists of several receptors that recognize molecular patterns of pathogens, for example bacterial lipopolysaccharide (through TLR4) and single stranded viral RNA (through TLR7) (20). In the past 10 years, the term 'mature' DC has generally been used to describe T (helper 1) cell stimulatory DC. Immature DC were considered to be primarily involved in the recognition and uptake of antigen. Upon receiving maturation signals these immature DC would then change their chemokine receptor repertoire and upregulate their co-stimulatory molecules, thus acquiring the phenotype of mature DC that are capable of migration to the lymph nodes and activation of T cells. In the absence of maturation signals, DC would not upregulate their co-stimulatory molecules and would thus remain anergy- or tolerance-inducing antigen-presenting cells. Although this concept may not be entirely wrong, recent findings show that this is probably an oversimplification (for a comprehensive review on this topic see reference (21)). For instance, in the steady state, that is in the absence of 'danger', immature DC have been shown to be capable of circulating through the tissues and lymphoid organs, encountering and capturing both self-antigens and innocuous environmental antigens (22). It is suggested that through this mechanism immature DC play a critical role in the continuous induction of peripheral tolerance, thereby preventing both auto-immunity and hyperreactivity (23). In addition, although the expression of co-stimulatory molecules is one of the phenotypic markers of mature DC, the induction of a tolerogenic immune response depends on the presence of these molecules as well (24). In a chimeric murine model it was shown that although cytokine-matured DC demonstrated upregulation of co-stimulatory molecules and induction of T cell proliferation, the activated T cells did not fully develop into IFNγ-producing effector cells (25). Only when the DC were activated through Toll-like receptors (TLRs), also referred to as 'licensed' DC (26), the induced antigen-specific T cells were able to fully develop into effector cells. The 'licensing' of DC is not only restricted to pathogen-derived signals, since activation by bystanding T helper cells may also suffice (27, 28). Another level of complexity is added by the timing and duration of the maturation signal. For example, murine bone marrow-derived DC that are exposed to lipopolysaccharide for 48 hours have the same expression of costimulatory molecules CD80, CD86 and CD40 as compared to DC that are exposed to lipopolysaccharide for 8 hours and also have a comparable migratory capacity and allostimulatory potential. However, the former exhibit a decreased IL-12 production potential correlating with low antigen-specific T cell responses after vaccination in mice (29, 30). In addition, both the timing of the activation signal and the exposure to antigen are of crucial importance for optimal antigen presentation: only the simultaneous presence of apoptotic cells and TLR ligands to DC resulted in efficient antigen-presentation and subsequent T cell activation (31).

Table 1. Results of published DC-vaccination trials with non-matured DC in metastatic melanoma

DC culture method	Antigens	Ag-loading method	Route	No. pts	Clinical response	Immunological response [1]	Ref
IL-4/GM-CSF/FCS moDC	tyrosinase, gp100, MART-1, MAGE-1, MAGE-3 or lysate	peptides/ lysate	in	16	2 CR, 2 PR	not tested	49
IL-4/GM-CSF/FCS moDC	MAGE-3A.2, tyrosinase, gp100, MART-1 or lysate	peptides/ lysate	in	33	3 PR, 1MR, 6 SD	13	93
IL-4/GM-CSF moDC	MART-1, gp100	MHC-I peptides	iv	10	1 PR	1	85
IL-4/GM-CSF moDC	autologous peptides	autologous peptides	id	22	1 CR, 1 PR	not tested	96
IL-4/GM-CSF moDC	lysate	lysate	id	14	1 PR, 1 SD	4	91
IL-4/GM-CSF moDC	MART-1, gp100, tyrosinase	MHC-I peptides	iv	16	1 CR, 2 PR, 2 MR	5	76
IL-4/GM-CSF moDC	MART-1	MHC-I peptides	id	4	1 CR[2], 1 SD[2], 1 MR	4	86
IL-4/GM-CSF/FCS moDC	lysate	lysate	in/sc	4	1 PR, 1 CR	3	94
IL-4/GM-CSF moDC	gp100/tyrosinase	MHC-1 peptides	iv/id	9	-	-	52

Results of published DC-vaccination trials in which non-matured DC were used, only melanoma patients with distant metastases and evaluable disease are included. Abbreviations: IL, interleukin; GM-CSF, granulocyte macrophage-colony stimulating factor; FCS, fetal calf serum; moDC, monocyte-derived DC; sc, subcutaneous; in, intranodal; id, intradermal; iv, intraveneous; CR, complete response; PR, partial response; MR, mixed response; SD, stable disease (≥ 4 months).
[1]Immunological response is defined as any evidence of melanoma peptide or tumor-specific T cell response after vaccination by one or more test methods; the number of patients with an immune reponse are given.
[2]After DC-vaccination these patients received treatment with an anti-CTLA4 blocking antibody.

With respect to the type of TLR ligands, it has been shown that combinations of different TLR ligands can have a synergistic effect on the immunogenic potential of DC *in vitro* (32) and *in vivo* (33). For example, a combination of triggering via TLR3 and TLR 7 leads to a ten- to hundred-fold higher IL-12 production, when compared to DC that have been activated by one of the respective TLRs alone (32). In concordance with these data, Querec *et al.* recently showed that broad immunity that was induced by a Yellow fever vaccine was dependent on triggering multiple TLRs simultaneously (notably TLR 2,7,8,9) (34). In terms of IL-12 production, it appears that monocyte-derived DC activation via TLR3 and 7 leads to the most potent Th1 T cell responses (32, 35, 36). However, migratory capacity is somewhat hampered in these cells as compared to cytokine-matured DC, which can be restored by co-culturing the DC in PGE_2 (36). If DC with similar expression of co-stimulatory molecules can exert entirely different functions, what then determines the nature of the induced T cell response? The ability of DC to produce IL-12, TNF-α and IL-6 is thought to be important for the induction of robust T cell responses and to bypass suppressor T cell-induced tolerance (37-39). In addition, several factors such as IL-10, vitamin-D3 and cortico-steroids can skew the DC into a more suppressive T cell type of inducer (40). However, it still remains poorly understood which mechanisms truly determine the nature of the T cell response as instructed by the DC. Taken together, these findings show that the process of maturation is highly complex and that different maturation stimuli do not lead to one common 'mature DC', but that there are in fact a lot of different types of mature DC that exert different functions ranging from the induction of strong Th1-type responses to the induction of tolerance. These data also show that the maturation stage of DC cannot be fully characterized by the expression of costimulatory molecules and surface-MHC. When reporting clinical DC vaccination trials it is therefore of crucial importance that the phenotypic and functional characteristics of the DC

are carefully described. Thus far, T cells have been the primary target of DC vaccination protocols. In the last few years more evidence is accumulating that also DC-induced activation of natural killer (NK) cells (41) and natural killer T (NKT) cells (42) can eradicate cancer. NKT cells and DC activate each other communally. DC activate NKT cells by presentation of exogenous (microbial) and endogenous glycolipid antigens, thereby inducing IFNγ release and CD40-ligand upregulation by the NKT cells (43, 44) Reciprocally, NKT cells activate DC via CD40-CD40L interaction. This in turn causes the DC to produce IL-12, which further activates the NKT cells (reviewed in (42)). Because glycolipid antigens induce both NKT and DC activation in this manner, they offer an interesting target in cancer immunotherapy. The synthetically produced, marin sponge-derived glycolipid α-galactosylceramide (αGalCer) has been studied in murine and human studies. A single injection of αGalCer combined with a model antigen induced strong $CD4^+$ and $CD8^+$ T cell responses, through activation of DC in a TLR-independent but NKT cell-dependent manner (45). The results were confirmed using tumour vaccines instead of a model antigen (46, 47). Thus far, one phase I dose-escalation study with clinical-grade αGalCer (KRN7000) has been carried out in 24 patients with solid tumours, in which no clinical responses were observed (48).

5. Maturation of DC in clinical trials

In early clinical trials only immature DC were used (49, 50). Some of these DC might have been 'semi-mature' due to the addition of fetal calf serum in the culture medium (49, 51). Although objective clinical remissions were observed in these studies, there is now strong evidence that immature DC should no longer be used in clinical practice. In a comparative study in metastatic melanoma patients cytokine-matured, peptide-pulsed DC were superior to immature DC, with no immune induction against the control protein keyhole limpet hemocyanine (KLH) in the latter arm of the study, while all patients that were vaccinated with cytokine-matured DC showed a strong T cell and B cell response against KLH (52). In addition, only in patients vaccinated with mature DC, delayed type hypersensitivity (DTH) responses against the vaccine were observed. Using immature DC in vaccination protocols in cancer patients might in fact be hazardous due to the induction of tolerance instead of immunity (23, 53, 54). Several maturation methods have been applied with maturation being defined by a high expression of mature DC-specific surface markers (which is a rather limited description a discussed in the previous paragraph). Most widely used is a cytokine cocktail that includes TNFα, with any of the following cytokines in any combination: IL-1β, IL-6, PGE_2, or the supernatant of activated autologous monocytes, (Monocytes Conditioned Medium) (55-59). There is some evidence that culturing DC with IL-15 may lead to a type of mature DC that induces stronger Th1 effector type of immune responses (60), however no comparative studies have been reported yet. Lastly, CD40-ligation has been used as a method of activation of DC in a clinical setting (61, 62). None of these different maturation methods has shown to be clearly superior, which is mainly due to the fact that there are no direct comparative studies, neither in animal models nor in cancer patients. It is important to realize that to date no trial has been published in which TLR-matured, truly Th1-polarized DC were used in cancer patients. *In vitro* data are promising (63), but clinical results with TLR-matured DC are eagerly awaited.

6. Antigen-processing and presentation

Intracellular endogenous antigens usually are presented in MHC class I, whereas exogenous antigens are usually presented in class II by antigen-presenting cells (Figure 1a) (64). Of crucial importance for DC-based vaccines in cancer immunotherapy is the finding that internalized antigens from exogenous sources, such as apoptotic or necrotic tumour cells (65, 66) are also presented in MHC class I to cytotoxic T cells, a process referred to as cross presentation (Figure 1a) (67, 68). Thus, tumour antigens derived from necrotic or apoptotic tumour cells can be presented by the DC to both $CD4^+$

Table 2. Results of published DC-vaccination trials with matured DC.

DC culture method	Antigens	Ag-loading method	Route	No. pts	Clinical response	Immune response	Ref
IL-4/GM-CSF/MCM/ TNF-α/ moDC	MAGE-3	MHC I peptides	sc, id, iv	13	6 MR	9	56
IL-4/GM-CSF/IL-1b/ IL-6/TNF-α/PGE_2 moDC	MAGE-3, MAGE-1, tyrosinase, MAGE-4, MAGE-10, gp100, MART-1	MHC I+II peptides	sc	19	1 CR, 4 SD	12	57
IL-4/GM-CSF/MCM/ TNF-α moDC	MAGE-3	MHCI peptides	sc, iv	8	1 SD	8	59
GM-CSF/Calcium-ionophore/IL-2/IL-12 moDC	MART-1, gp100, tyrosinase,	MHC I peptides	in, id, iv	27	3 PR	13	78
IL-4/GM-CSF/MCM/ TNF-α+PGE2 moDC	gp100, tyrosinase	MHC I peptides	id, iv	10	1 PR, 1 MR, 3 SD	2	52
Flt3L/GM-CSF/TNFα CD34+ DC	MART-1, MAGE-3, gp100, tyrosinase	MHC I peptides	sc	18	4 CR[1], 4 PR, 3 SD	17	15, 82, 83
IL-4/GM-CSF/TNFα/IL-3/ IL-6/SCF CD34+ DC	MART-1, gp100, tyrosinase, MAGE-1, MAGE-3	MHC I peptides	iv	14	1 PR, 6 SD	1	18
Flt3L/GM-CSF/TNFα/ IFNα CD34+ DC	MART-1, MAGE-3, gp100, tyrosinase	MHC I peptides	sc	20	1 SD	7	17
IL-4/GM-CSF/TNF-α/ CD40L moDC	Allogeneic lysate	Allogeneic lysate	sc	20	1 CR, 1 PR	2	61
IL-4/GM-CSF/IL-1β/ IL-6/TNF-α/PGE_2 moDC	Autologous tumor RNA	RNA-electroporation	id or in	21	1 MR	9	110, 111
IL-4/GM-CSF/TNFα moDC ± sc IL-2	Allogeneic lysate	lysate	id	15	6 SD	9	99
IFNβ/IL-3/polyI:C moDC	NA17, MAGE-3	MHCI +II peptides	sc, id	4	1 SD	1	84
IL-4/GM-CSF/IL-1β/IL-6/ TNF-α/PGE_2 moDC	MAGE-1, MAGE-3, tyrosinase, gp100, MART-1	MHCI +II peptides	sc	53	2 PR, 8 SD[2]	Not given	87
GM-CSF/IL-13 moDC	Allogeneic lysate	Allogeneic lysate	in, sc, id	10	1 SD	3	98
GM-CSF/IL-13/ Ribomunyl/IFNg	MART-1, ± NA17	MHCI+II peptides	il then in	14	2 SD	5	133

Results of published DC-vaccination trials in which DC were used that had received some form of maturation signals, only melanoma patients with distant metastases and evaluable disease are included. Abbreviations: IL, interleukin; GM-CSF, granulocyte macrophage-colony stimulating factor; MCM, monocyte-conditioned medium; TNFα, tumor necrosis factor alpha; PGE2, PGE_2; moDC, monocyte-derived DC; Flt3L, Flt3-Ligand; SCF, stem cell factor; IFN, interferon; sc, subcutaneous; in, intranodal; id, intradermal; iv, intraveneous; il, intralymfatic; CR, complete response; PR, partial response; MR, mixed response; SD, stable disease (≥ 4 months).

[1] In a follow-up report, all complete responders were still free of disease with a median of 5 years.

[2] This is a multi-instutional, randomized phase III trial. In the other treatment-arm 55 patients were treated with DTIC, in which 3 PR and 10 SD were seen. No differences in overall or progression-free survival were observed.

(in MHC class II) and $CD8^+$ T cells (in MHC class I), which implies that a broad effector and memory immune response can be induced against tumour antigens.Apoptosis is a physiological 'silent' immunologic event, pertaining millions of cells per second. However, with regard to the immunogenicity of apoptotic cancer cells the data are less clear (69-73). Recently it was shown in a murine model that chemotherapy-induced apoptosis results in cross-presentation and T cell activation, thereby preventing tumour outgrowth in a prophylactic setting (74). The same authors show in another study that apoptotic tumour cells induce immune responses in a TLR-4 dependent

manner via secretion of HMBG1 (75). The importance of these findings is that apoptosis of cancer cells may be an immunologic event without the need of an extra 'danger signal', and that this can be accomplished by the administration of cytotoxic drugs or radiotherapy.

7. DC Antigen-loading in clinical trials

In most clinical DC vaccination studies synthetic MHC class I-binding peptides have been used (15, 17, 18, 49, 52, 56, 76-86), with class II-binding peptides being added in some (Figure 1b) (57, 87). There is convincing preclinical evidence that targeting both cytotoxic T cells and T helper cells is of crucial importance for the induction of a strong and sustained anti-tumour T cell response (88, 89). However, no clinical trial has yet been performed in which MHC class I antigen-loaded DC are compared to the combination of both MHC class I and II antigen-loaded DC. Instead of HLA-binding peptides, whole antigenic proteins can be used. The DC processes the protein into peptides, which has the advantage that multiple epitopes are presented in both MHC class I and II and that there is no HLA-restriction. Unfortunately, little recombinant proteins are clinically grade available (90). Autologous (49, 91-96) or allogeneic (61, 97-99) tumour cell lysates have also been applied as a source of antigens. This has several advantages: the antigen expression by the tumour does not need to be defined and a wide array of both MHC class I and II epitopes are presented including tumour-unique antigens. Possible drawbacks include the presentation of auto-antigens, the requirement of a sufficient volume of tumour tissue and difficulties in monitoring tumour-specific T cell responses since the antigens relevant to T cell responses are not known. Palucka *et al.* partly circumvented the latter problem by using large peptide libraries to pinpoint the dominant T cell responses in advanced melanoma patients after vaccination with allogeneic tumour lysate-loaded DC (61). Transfection of DC with RNA concerns a novel antigen-loading technique (100), with either tumour-derived RNA (101, 102) or synthetic RNA encoding specific melanoma-associated antigens being used (103). A benefit of this technique lies in the presentation of several MHC class I epitopes and sometimes also MHC class II epitopes, depending on the presence of an endosomal targeting sequence (104). Also, it may lead to a more prolonged presentation of the antigen as compared to peptide-loading which appears to be short-lived (105). Potential drawbacks of RNA transfection include a variable expression and a low yield of viable cells after transfection, especially with respect to the most widely used technique of RNA electroporation. However, several studies have shown that this technique is feasible and results in highly efficient DC-transfection (103, 106-109). Furthermore, anti-tumour T cell responses and clinical responses have been reported in patients vaccinated with DC electroporated with tumour-derived RNA (110, 111). In a study with 33 metastatic melanoma patients vaccination with autologous tumour lysate-loaded DC resulted in a slightly higher response rate compared to peptide-pulsed DC, (3 versus no partial remissions, respectively) (93). Equal immunogenicity was demonstrated for peptide- and RNA-pulsed DC in colorectal cancer patients (112). However, immature DC were used in both studies. Mature DC have not been used in clinical studies comparing different antigen-loading techniques. Therefore at this moment the optimal method for antigen loading is unknown. Antigens that target DC *in vivo* would obviate the need for laborious *ex vivo* culturing protocols (113). Although this appears to be feasible through DC specific molecules such as the C-type lectins DC-SIGN (114) and DEC-205 (115) using model antigens, it will probably take some years before this can be applied in clinical experiments in cancer patients. In addition, a DC maturation stimulus should be applied *in vivo*. Another approach concerns the targeting of intratumoural DC by delivering danger signals *in situ*, which can be combined with chemokine treatment in order to increase the number of intratumoural DC (116). In addition, local tumour-destructing therapies can induce antigen-release *in situ*, for example by using radiotherapy (117), chemotherapy (118) or radiofrequency ablation (119). The immunogenicity of these methods may then be further enhanced by the local delivery of DC activating signals (120, 121).

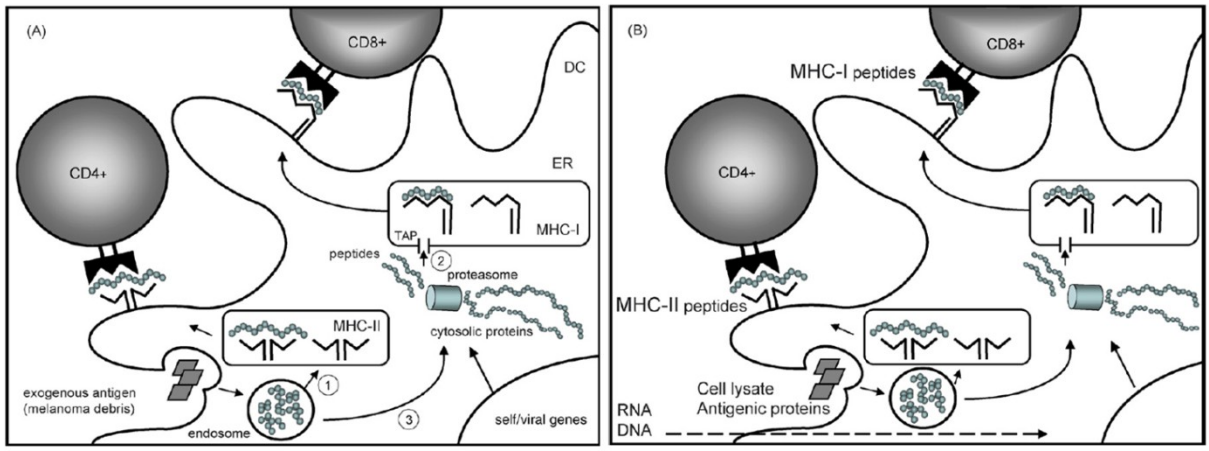

Figure 1. Antigens can be processed by the DC through three major pathways. (A) Exogenous antigens will be internalized by the DC and enter the endocytic pathway in which they are targeted to lysosome-related MHCclass II-rich compartments. In these compartments the antigens are degraded and loaded onto MHC class II molecules. During maturation of the DC the MHC-peptide complexes are released to the surface, thus making the cell ready for antigen presentation to $CD4^+$ T helper cells (route 1 in the Figure). Intracellular endogenous antigens, such as unstable self-proteins or viral proteins, are cleaved into peptides in the proteasome and subsequently translocated into the lumen of the endoplasmatic reticulum (ER) by transporters associated with antigen processing (TAP), where stable MHC class I-peptide complexes are assembled. Upon binding of the peptide, the complex is released from the endoplasmatic reticulum and transferred to the cell surface (route 2 in the Figure), where it is presented to $CD8^+$ cytotoxic T cells. Lastly, DC have the unique capacity to present exogenous antigens, such as necrotic or apoptotic tumour cells, in MHC class I to cytotoxic T cells, a process referred to as cross presentation (route 3 in the Figure). (B) Melanoma antigens can be loaded onto the DC for antigen presentation either by transfection with DNA or RNA encoding melanoma antigens, or pulsing with tumour lysate, antigenic proteins or peptides.

8. Migration

DC are the sentinels of the immune system and therefore need efficient migratory capacity. In peripheral tissues they continuously sample the environment for antigens. After antigen uptake DC must migrate to the secondary lymphoid organs, in particular the lymph nodes for presentation of the antigens to the adaptive arm of the immune system. The lymph node homing chemokine receptor CCR7 is essential for DC migration to the lymph nodes (122, 123). CCR7 guides the DC towards and through the lymphatic vessels to the lymph nodes in response to chemotactic gradients of its ligands CCL19 and CCL21 that are expressed by lymphatic vessels and lymph node-residing cells (Figure 2a) (124). Expression of CCR7 is upregulated upon DC maturation, resulting in an enhanced migratory capacity of matured DC as compared to immature DC (73). In addition, inflammatory signals such as PGE_2 are needed to further sensitize CCR7 to its ligands (125, 126). These findings are of importance for DC-based vaccination, since they show that it may be beneficial to culture DC in the presence of PGE_2 in order to get a good migratory capacity after vaccination, even though PGE_2 has been described to skew DC under some circumstances towards a Th2 type of immune response (40). Interestingly, in a murine model DC migration could be increased up to ten-fold after pretreatment of the injection site with TNFα or unloaded DC, due to the upregulation of CCR7-ligand CCL21 in lymphatic endothelial cells, resulting in a superior magnitude and quality of the T cell response (123).

9. Route of DC administration in clinical trials

For the effective induction of immunity it is obligatory for the DC to interact with T cells, which takes place in the peripheral lymphoid organs: mainly in the lymph nodes but to some extent also in the spleen. Recent evidence suggests that also the bone marrow may be a site for primary immune responses (127). As different routes lead to different sites of accumulation of the vaccinated DC, these issues are of importance when considering the route of delivery of the DC (Figure 2b). Murine models have shown that after intravenous injection the majority of DC accumulate in the spleen and

to a lesser extent in the lungs, kidneys and liver, while hardly any DC end up in peripheral lymph nodes (128). *In vivo* studies in cancer patients have shown that after intradermal injection approximately 2-4% of the DC migrate to draining lymph nodes (129). There is now convincing evidence from several independent human studies that migration after subcutaneous injection is much lower compared with intradermal injection (84, 129-131). Intranodal injection results in a much higher amount of DC accumulating in lymph nodes, not only in the injected node, but also in subsequent draining nodes (129). Migration to these subsequent nodes via the physiological pathway through lymph vessels can be as much as 80%. However, the magnitude of DC migration that is observed after intranodal injection is more variable than after intradermal vaccination (129). Intranodal injections are usually administered under ultrasound guidance. Supposedly, this would result in an assured accurate delivery, which was the reason for some studies to prefer this route of administration (54). However, using paramagnetic beads-labeled DC that can be tracked in patients after injection by MR imaging, we recently found that intranodal injection is complicated by inaccurate delivery: in a considerable proportion of patients the DC were misinjected, in the perinodal fat (132). Inaccurate injection correlated with absent migration to remote lymph nodes. These results explain the variability in migratory outcome after intranodal administration and underscore the importance of accurate delivery (133). Recently, Lesimple and colleagues showed that intralymphatic delivery into a lymph vessel in the dorsum of the foot is also feasible (134). Migration of administered cells however, is only a surrogate endpoint. The true value of the different routes of delivery can only be determined with immune response or even clinical response as an endpoint. One study in melanoma patients found a small benefit in peptide-specific T cell responses after intranodal injection as compared to intradermal or intravenous injection (78). Another study in advanced melanoma patients showed no benefit for intranodal vaccination as compared to intradermal vaccination: of 22 evaluable patients a positive DTH reaction against the vaccine was detected in 7/10 intradermal vaccinated patients and in 3/12 intranodal vaccinated patients (135). Fong et al compared vaccination with DC enriched from peripheral blood mononuclear cells injected via three different routes in advanced prostate cancer patients: intradermal, intravenous and intralymphatic injection via a canule in a lymphatic channel in the dorsum of the foot (136). Antigen-specific T cell responses were observed regardless of the route of delivery, although IFNγ production after antigen stimulation *in vitro* was only demonstrated in the intradermally and intralymphaticly vaccinated patients. However, the intravenous route gave rise to a more pronounced antibody response. In an important study performed by the same group intravenous injection of DC was shown to be essential for immune responses against visceral melanoma metastases, whereas for subcutaneous vaccination this was true for non-visceral metastases (137). These findings indicate that the combination of different routes of administration may be beneficial to target different tumour locations in the entire body (138). In conclusion, to date no specific route of administration has unequivocally been shown to be superior in terms of induction of immune or clinical responses.

10. Tolerance

The immune system has several pathways to tune down immune responses In order to prevent autoimmunity or excessively long or vigorous inflammatory reactions. These many pathways include antigen-presentation by tolerizing DC (as discussed above), the suppressive activity of so-called regulatory T cells (Treg) and tolerance induction via inhibitory molecules on T cells. According to current insights there are two major distinct populations of Treg: naturally occurring $CD4^+/CD25^+$ Treg which at the time they leave the thymus already have a suppressive potential, and induced Treg that are 'conventional' $CD4^+$ or $CD8^+$ T cells but transformed into cells with an immunosuppressive function under the influence of tolerizing conditions (139, 140). Treg can affect immune responses at the level of antigen-presentation and during the effector phase of T cells at the site of inflammation or tumour growth (139).

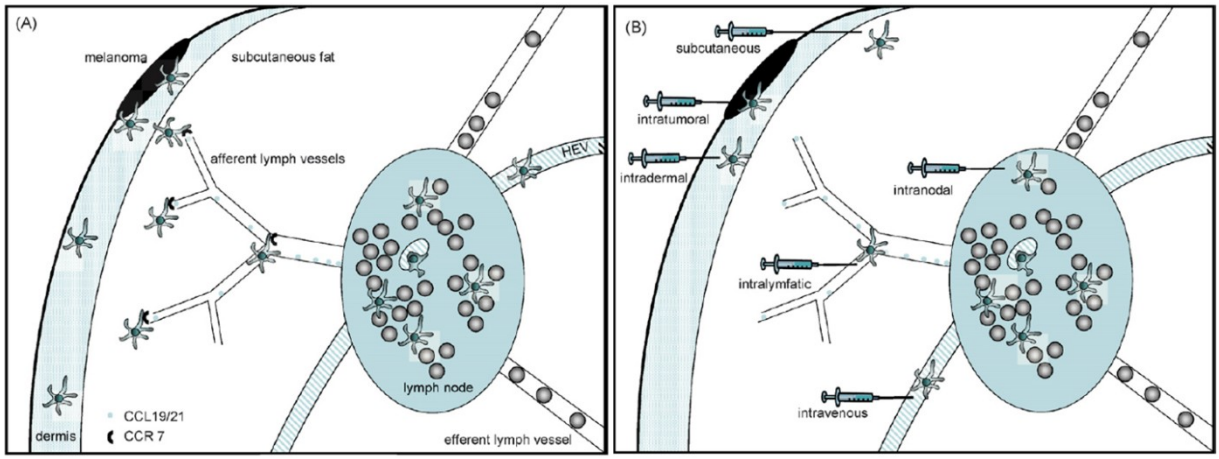

Figure 2. Routes of DC administration in clinical trials. (A) DC that reside in the periphery migrate to draining lymph nodes through afferent lymphatic vessels following chemotactic gradients of CCL19and CCL21. These chemokines are expressed by lymphatic endothelial cells and lymph node-residing cells. Blood DC enter the lymph nodes through high endothelial venules (HEV). After interaction with DC, the T cells leave the lymph node through efferent lymphatic vessels and disseminate throughout the body via the circulation. (B) Several routes of administration are used in clinical DC vaccination trials: intradermal, subcutaneous, intratumoural, intralymphatic, intranodal and intraveneous.

Treg function is controlled by cytokines, cross-talk with antigen-presenting cells, but also by direct interaction with pathogens via TLRs (141). The mechanisms by which Treg exert their suppressive function are not completely elucidated, but it may happen in a cell-cell contact dependent manner via camp as second messenger (142) as well as through cytokines such as IL-10 or TGFβ (140). The clinical importance of Treg in cancer has been demonstrated by Curiel *et al.* (143). A high number of Treg in tumours of ovarian cancer patients correlated with poor survival. In other tumor types, these data have been confirmed (144-146). Furthermore, depletion of naturally occurring Treg by anti-CD25 or anti-GITR monoclonal antibodies in murine models resulted in enhanced therapeutic efficacy of a cancer vaccine (147, 148). Since T effector cells also upregulate CD25 upon activation (the β-chain of the IL-2 receptor), a potential drawback of targeting Tregs via CD25 may be the depletion of newly activated T effector cells along with the Tregs (148). It may therefore be a meticulous task to find the optimal dosing and timing of anti-CD25 treatment to deplete Tregs via anti-CD25 antibodies without affecting the activate T cell population. Another important pathway through which tolerance or anergy may be induced involves inhibitory molecules on the T cells, such as cytotoxic T lymphocyte-associated antigen-4 (CTLA-4) or programmed death-1 receptor (PD-1) (149). The ligands of CTLA-4 are the DC co-stimulatory molecules CD80 and CD86. Binding of these costimulatory molecules to the inhibitory molecule CTLA-4 instead of the activating T cell molecule CD28, results in suppression of T cell activation and proliferation. Activated T cells express CTLA-4. Since the affinity of CTLA-4 for CD80 and CD86 is higher than that of CD28, eventually the tolerogenic pathway prevails, thereby terminating immune reactions (149, 150). PD-1 is another inhibitory T cell surface molecule that upon binding to its ligands PD-L1 and PD-L2 induces anergy or tolerance (149). Interestingly, PD-L1 and 2 are expressed by several types of cancer, which may allow the tumour to escape from immune surveillance (151, 152). This phenomenon can be reversed in mice by treatment with an anti-PD-L1 antibody (152, 153). Although this has been confirmed *in vitro* for the human situation, studies using PD-L1 blockade in cancer patients have not been reported yet (154).

11. Breaking tolerance in melanoma patients

Several new drugs have entered the clinic that target immunosuppressive mechanisms and may therefore be relevant in combination with anti-cancer vaccines. Treg can be efficiently depleted in prostate cancer patients with denileukin diftitox, a compund that consists of a diphteria toxin coupled to IL-2, resulting in enhanced antigen-specific T cell responses after DC vaccination (155).

Denileukin diftitox as a single agent has shown promising immunological and clinical results in phase I and II studies in ovarian cancer (Barnet ASCO 2006). In melanoma however, thus far the data are conflicting, with one study failing to show any efficient Treg (156), while another preliminary study showed tumour regression in two patients (Chesney ASCO 2006). Mahnke *et al.* found enhanced antigenic immune responses after peptide vaccination and a significant reduction in Treg frequencies in melanoma patients after denileukin diftitox (157). The combination of DC vaccination with denileukin diftitox has not yet been reported in melanoma patients. This also holds true for the combination with anti-CD25 antibodies, despite the fact that these are commonly used in transplant patients. The recent unexpected results with the anti-CD28 monoclonal antibody TGN1412-trial again demonstrated the enormous potency of drugs that manipulate the co-stimulatory pathways (158, 159). Blockade of CTLA-4 has been shown to induce durable objective responses in metastatic melanoma patients, at the cost of autoimmune side effects (160-163). Anti-CTLA-4 treatment in melanoma patients did not result in depletion or decreased suppressive activity of Treg (which highly express CTLA-4), suggesting that the anti-tumour efficacy of the treatment is caused by an increased T cell activation and not by inhibition or depletion of Treg (164). Since treatment with anti-CTLA-4 is antigen is non-specific, the combination with a vaccine could potentially direct the T cell response in a more specific manner, thereby diminishing autoimmune side effects. There is anecdotal information that anti-CTLA4 treatment after DC vaccination may indeed enhance DC vaccine-induced T cell responses (163), however clinical trials that are specifically designed to answer this question are lacking.

12. Clinical results of DC vaccination studies in melanoma

Proof of principle studies were performed in the late nineties, showing the feasibility and the potential efficacy of DC vaccination in cancer patients (49, 50, 56). Since then numerous small studies have been performed, especially in melanoma patients (Table 1 and 2). Given the enormous variations in culturing protocols and frequency, dose and route of administration, it is not possible to pool all these data in a meta-analysis. Nevertheless, some general observations can be made. Objective response rates in these selected patients do not exceed 5-10%, with disease stabilization and mixed responses being observed more often. As discussed above, there is convincing evidence from preclinical and clinical studies that immature DC are not proper T cell activators, and could even induce tolerance. Strikingly however, this does not translate into a dramatic difference in clinical outcome when studies with immature DC are compared with studies in which matured DC have been used (Table 1 and 2). Perhaps this hints at the relatively low immunogenicity of the mature DC vaccines that are currently applied: using cytokines to mature the DC without activation by Toll-like receptor triggers. In a recent phase III multi-institutional, randomized controlled trial the standard chemotherapy regimen for patients with metastatic melanoma, DTIC, was compared with cytokine-matured DC vaccination and no difference in survival was observed after inclusion of all patients, upon which the study was discontinued (87). How can this disappointing result be explained? As reported by the authors themselves, the DC displayed a variable maturation status and the subcutaneous route of administration that was used is inferior. In addition, not all patients received the anticipated numbers of DC. Others have pointed at the enormous complexity of performing a multi-center study with patient-specific vaccines and the difficulties in establishing a standardized vaccine product as a possible explanation of the negative outcome of this study (90). Together these factors may explain why no clinical benefit was found for the DC vaccine. In a subgroup-analysis a correlation was found between response to DC vaccination and HLA-type, with a favorable outcome for the HLA-2+/HLA-B44- haplotype. Although this trial could be interpreted as a negative trial for DC vaccination, in our view equality with the standard therapy for the last 30 years is perhaps not a bad starting point, given the the fact that there are many parameters regarding DC vaccination that can still be optimized, as we have discussed above.

13. Immunological results of DC vaccination studies in melanoma

Successful development of DC vaccines in cancer patients much depends on obtaining biological information that correlates with clinical efficacy. A clear correlation between immunological response and clinical outcome has been observed in some studies (15, 165), but not in all (93). Monitoring immune responses in DC vaccination trials is difficult and laborious, since very low frequencies of high-affinity melanoma antigen-specific T cells in peripheral blood may be sufficient for tumour rejection. These frequencies can be as low as 1 in 40.000 T cells (166). These low responses are often not detected by the most frequently used techniques such as Elispot-analysis and direct tetramer-staining of peripheral blood lymphocytes. In order to detect these low frequencies Coulie *et al.* stimulated blood lymphocyte cultures from peptide-vaccinated melanoma patients *in vitro* with melanoma antigens, followed by cloning of the antigen-specific cells and T-cell receptor sequence analysis of the clones (166). We took another approach by analyzing T cell responses in vaccinated patients from biopsies of delayed type hypersensitivity reactions (DTH) that were performed with the peptide-loaded DC vaccine (165, 167). In these DTH biopsies we found evidence for functional antigen-specific T cell responses after vaccination. Moreover, the presence of these specific T cells was significantly correlated with a prolonged progression-free survival in metastatic melanoma patients (165). These data suggest that the success or failure of tumour-specific T cels to migrate towards the DTH site reflects the potency of the T cells at the site of disease. In a provocative study Lonchay *et al.* showed that although frequencies of vaccine-specific T cell may be higher after vaccinations, this does not necessarily mean that these cells are the true effector cells that actually cause the tumour regression (168). They found that other tumour-specific T cells that were already present prior to vaccination were much more expanded after vaccination than the vaccine-specific T cells. The current hypothesis is that vaccine-specific T cells ignite a certain 'spark' in the tumour, causing the non-active tumour-residing specific T cells to become active and proliferative. Thus, the expanded specific T cell frequencies that are observed upon DC vaccination and correlate with an improved clinical outcome may cause tumour regression either in a direct or in an indirect manner.

14. Study design and clinical endpoints in DC vaccination

The study design and clinical endpoints that should be used in therapeutic cancer vaccine studies, were recently defined in a consensus process by the Cancer Vaccine Clinical Trial Working Group, representing academia and pharmaceutical and biotechnology industries with participation from the US Food and Drug Administration (169), There are several differences between cytostatic drugs and therapeutic vaccines that should be taken into account when designing and evaluating clinical cancer vaccine trials. Firstly, conventional RECIST criteria may not always be the most appropriate endpoint to decide which DC vaccine will be the most optimal vaccine to be tested in large clinical trials. Because vaccine-induced immune responses will take some time before they become clinically apparent, initial minor progression could be accepTable. (169). In fact, adequate immune induction could theoretically first induce enlargement of tumour lesions through T cell infiltration and local inflammation. For these reasons, it may be proper to deviate from standard RECIST criteria, provided that the new criteria are pre-defined and clearly described, as proposed before (4). Whether functional *in vivo* imaging has a role in the monitoring of clinical responses in cancer vaccine trials remains to be determined. It has been shown that upon DC vaccination regional non-tumourous lymph nodes become FDG-positive on positron emission tomography-scanning, reflecting immune activation rather than tumour progression (170). A second major difference between conventional cytostatic therapy and DC vaccination is that the highest dose is not necessarily the most effective one. And because DC vaccines have an almost negligible toxicity, conventional dose-escalating phase I trials with toxicity as the primary endpoint would not result in the selection of the optimal dose to be used in further clinical testing. This problem has been circumvented by performing dose-

escalation studies with immune response as the primary endpoint rather than toxicity (see for example (15)). Another difference is that in patients with advanced disease, the patient group in which normally phase I trials are performed, immunotherapy will probably have little chances of being successful because of immunosuppressive mechanisms at the tumour site. For these reasons, the conventional phase I-II-III trial paradigm that is applied in the field of cytostatic therapy, may not be the most optimal trial design for DC vaccination. The Cancer Vaccine Clinical Trial Working Group concensus recently proposed a two-step development in clinical trial design in cancer vaccination: proof of principle trials and efficacy trials (169). The following criteria were proposed for proof-of-principle trials. They should include a minimum of 20 or more patients in a homogenous, well-defined population. The disease should not be rapidly progressive in order to allow the vaccines adequate time to induce immunological activity. Study objectives should include determination of dose and schedule and demonstration of immunological activity as proof-of-principle. Immunological activity is demonstrated if determined in 2 separate, established and reproducible assays at 2 consecutive follow-up time points after the baseline assessment. Efficacy trials then formally establish clinical benefit, either directly or through a surrogate endpoint. In contrast with the field of conventional cytostatic therapies, it is promoted that these trials are randomized. We believe that these guidelines are of great practical use and could help the field forward. And although in some instances it may be sufficient to include smaller numbers of patients (for example in trials investigating DC migration *in vivo*), we believe that adherence to these guidelines should be encouraged.

15. DC Companies

The preparation of a standard high-quality DC vaccine that meets Good Manufacturing Practice/Good Laboratory Practice (GMP/GLP), and clinical grade criteria is a laborious and costly process. Dedicated GMP/GLP cleanrooms are needed. Culturing a DC vaccine for one patient takes at least two persons two to three full working days. Even more costly are the culture media and cytokines that need to be toxin-free, clinical grade materials. Together with the fact that the vaccines are patient-specific, 'tailor-made', these issues gave rise to the long-held believe that companies would not be interested in DC vaccination. However, at the moment several companies are trying to get approval from official regulatory authorities (171). One company-made DC vaccine is Sipuleucel-T, which is made of antigen-presenting cells that are collected by two density centrifugation steps, pulsed with recombinant prostatic acid phosphatase fused to GM-CSF (172). A placebo-controlled phase III trial in hormone-refractory metastatic cancer patients was not able to show improvement in time to progression, the primary endpoint, although overall survival was prolonged from 21.4 to 25.9 months (173). Initially an FDA Advisory Committee recommended to approve Sipuleucel-T, but the FDA decided to await further proof of efficacy. This should come from an ongoing phase III trial with overall survival as primary endpoint of which the first interim analysis is planned in 2008 (171, 174). Other firms are seeking approval by the European and US regulatory authorities for vaccines targeted at lymphoma, sarcoma, glioblastoma and acute myelogenous leukaemia (171).

16. Combination therapies

There is a need to test combinations with more cytotoxic therapies, given the low frequency of clinical responses in patients with advanced disease upon DC vaccination alone. Although initially chemotherapy was believed to be detrimental to T cell-directed immunotherapy because most chemotherapy regimens have a myelosuppressive effect, now more evidence is accumulating that some forms of chemotherapy may not harm T cell responses (175) and may in fact have a synergistic effect together with immunotherapeutic approaches (reviewed in (176)) (75, 118). It is tempting to speculate on the possibility of tumour debulking by chemotherapy, combined with immune surveillance and immune memory induction by vaccination therapy to prevent relapses. The same

applies to radiotherapy (177) and targeted therapy (178). Another interesting approach involves *in situ* tumor destruction by cryo- or radiofrequency ablation in combination with immune activation, including injection of DC (119-121, 179). However, clinical data are lacking, trials combining chemotherapy and DC vaccination are in progress. As discussed above, also combination therapy with anti-CTLA4 and DC vaccination may have a synergistic effect. It is currently under study whether DC vaccination can enhance the graft-versus-tumour effect of stem cell transplantation and donor lymphocyte infusions in haematological malignancies (180). Adoptive T cell transfer following non-myeloablative but lymphodepleting chemotherapy showed impressive clinical results in advanced melanoma patients (181, 182). Adoptive T cell transfer generates a high, but short peek of antigen-specific T cells, whereas DC vaccination induces T cell responses more gradually that endure longer (183), providing a rationale to combine the two treatment modalities. In preclinical models DC vaccination indeed boosted and sustained anti-tumour T cell responses after adoptive T cell transfer (183, 184). Trials in the near future will have to answer the question whether DC vaccination can add to the efficacy of these other anti-cancer treatment modalities.

17. Conclusion and future prospects

DC vaccination has shown to be feasible and safe. Immunological responses are frequently observed. Clinical responses have been reported, but the incidence is low. Exciting new insights arise from preclinical studies, some of which are currently being applied in clinical studies. For example, depletion of suppressor T cells combined with DC vaccination may enhance the immunogenicity of the vaccine, as has been shown in prostate cancer patients (155). Also blockade of the inhibitory T cell molecule CTLA-4 by monoclonal antibodies could enhance the immunogenicity of DC vaccines (162). Combination treatment with chemotherapy, radiotherapy or other tumour ablative treatments needs to be further investigated. Trials with TLR-ligand activated DC are eagerly awaited. Although these novel treatment strategies are now entering clinical studies, the pace of *in vitro* and animal research is inevitably faster than that of clinical research. For this reason a lot of crucial questions regarding the optimal DC vaccine for clinical use remain unanswered to date. These questions concern the optimal methods for culture, maturation and antigen-loading, route of administration, subsets of DC and effects of suppressor T cell-depletion or blockade of other inhibitory pathways. Significant progress is only to be expected from well-designed, properly conducted and comparative studies with biological endpoints.

References

1. Rosenberg SA. Progress in human tumour immunology and immunotherapy. Nature 2001; 411: 380-384.
2. Finn OJ. Cancer vaccines: between the idea and the reality. Nat Rev Immunol 2003; 3: 630-641.
3. Lesterhuis WJ, de Vries IJ, Adema GJ, Punt CJ. Dendritic cell-based vaccines in cancer immunotherapy: an update on clinical and immunological results. Ann Oncol 2004; 15 Suppl 4: iv145-151.
4. Figdor CG, de Vries IJ, Lesterhuis WJ, Melief CJ. Dendritic cell immunotherapy: mapping the way. Nat Med 2004; 10: 475-480.
5. Banchereau J, Palucka AK. Dendritic cells as therapeutic vaccines against cancer. Nat Rev Immunol 2005; 5: 296-306.
6. Ridgway D. The first 1000 dendritic cell vaccinees. Cancer Invest 2003; 21: 873-886.
7. Villadangos JA, Schnorrer P. Intrinsic and cooperative antigen-presenting functions of dendritic-cell subsets *in vivo*. Nat Rev Immunol 2007; 7: 543-555.
8. Soumelis V, Liu YJ. From plasmacytoid to dendritic cell: morphological and functional switches during plasmacytoid pre-dendritic cell differentiation. Eur J Immunol 2006; 36: 2286-2292.
9. Grouard G, Rissoan MC, Filgueira L *et al.* The enigmatic plasmacytoid T cells develop into dendritic cells with interleukin (IL)-3 and CD40-ligand. J Exp Med 1997; 185: 1101-1111.
10. Benitez-Ribas D, Adema GJ, Winkels G *et al.* Plasmacytoid dendritic cells of melanoma patients present exogenous proteins to CD4+ T cells after Fc gamma RII-mediated uptake. J Exp Med 2006; 203: 1629-1635.
11. Kim R, Emi M, Tanabe K, Arihiro K. Potential functional role of plasmacytoid dendritic cells in cancer immunity. Immunology 2007; 121: 149-157.
12. Steinman RM, Banchereau J. Taking dendritic cells into medicine. Nature 2007; 449: 419-426.
13. Shortman K, Naik SH. Steady-state and inflammatory dendritic-cell development. Nat Rev Immunol 2007; 7: 19-30.
14. Randolph GJ, Beaulieu S, Lebecque S *et al.* Differentiation of monocytes into dendritic cells in a model of transendothelial trafficking. Science 1998; 282: 480-483.
15. Banchereau J, Palucka AK, Dhodapkar M *et al.* Immune and clinical responses in patients with metastatic melanoma to CD34(+) progenitor-derived dendritic cell vaccine. Cancer Res 2001; 61: 6451-6458.
16. Fong L, Hou Y, Rivas A *et al.* Altered peptide ligand vaccination with Flt3 ligand expanded dendritic cells for tumor immunotherapy. Proc Natl Acad Sci U S A 2001; 98: 8809-8814.
17. Banchereau J, Ueno H, Dhodapkar M *et al.* Immune and clinical outcomes in patients with stage IV melanoma vaccinated with peptide-pulsed dendritic cells derived from CD34+ progenitors and activated with type I interferon. J Immunother 2005; 28: 505-516.
18. Mackensen A, Herbst B, Chen JL *et al.* Phase I study in melanoma patients of a vaccine with peptide-pulsed dendritic cells generated *in vitro* from CD34(+) hematopoietic progenitor cells. Int J Cancer 2000; 86: 385-392.
19. Akira S, Takeda K. Toll-like receptor signalling. Nat Rev Immunol 2004; 4: 499-511.
20. Iwasaki A, Medzhitov R. Toll-like receptor control of the adaptive immune responses. Nat Immunol 2004; 5: 987-995.
21. Reis e Sousa C. Dendritic cells in a mature age. Nat Rev Immunol 2006; 6: 476-483.
22. Steinman RM, Turley S, Mellman I, Inaba K. The induction of tolerance by dendritic cells that have captured apoptotic cells. J Exp Med 2000; 191: 411-416.
23. Steinman RM, Nussenzweig MC. Avoiding horror autotoxicus: the importance of dendritic cells in peripheral T cell tolerance. Proc Natl Acad Sci U S A 2002; 99: 351-358.
24. Sharpe AH, Freeman GJ. The B7-CD28 superfamily. Nat Rev Immunol 2002; 2: 116-126.
25. Sporri R, Reis e Sousa C. Inflammatory mediators are insufficient for full dendritic cell activation and promote expansion of CD4+ T cell populations lacking helper function. Nat Immunol 2005; 6: 163-170.
26. Heath WR, Villadangos JA. No driving without a license. Nat Immunol 2005; 6: 125-126.
27. Albert ML, Jegathesan M, Darnell RB. Dendritic cell maturation is required for the cross-tolerization of CD8+ T cells. Nat Immunol 2001; 2: 1010-1017.
28. Alpan O, Bachelder E, Isil E *et al.* 'Educated' dendritic cells act as messengers from memory to naive T helper cells. Nat Immunol 2004; 5: 615-622.
29. Camporeale A, Boni A, Iezzi G *et al.* Critical impact of the kinetics of dendritic cells activation on the *in vivo* induction of tumor-specific T lymphocytes. Cancer Res 2003; 63: 3688-3694.
30. Langenkamp A, Messi M, Lanzavecchia A, Sallusto F. Kinetics of dendritic cell activation: impact on priming of TH1, TH2 and nonpolarized T cells. Nat Immunol 2000; 1: 311-316.
31. Blander JM, Medzhitov R. Toll-dependent selection of microbial antigens for presentation by dendritic cells. Nature 2006; 440: 808-812.
32. Napolitani G, Rinaldi A, Bertoni F *et al.* Selected Toll-like receptor agonist combinations synergistically trigger a T helper type 1-polarizing program in dendritic cells. Nat Immunol 2005; 6: 769-776.
33. Warger T, Osterloh P, Rechtsteiner G *et al.* Synergistic activation of dendritic cells by combined Toll-like receptor ligation induces superior CTL responses *in vivo*. Blood 2006; 108: 544-550.
34. Querec T, Bennouna S, Alkan S *et al.* Yellow fever vaccine YF-17D activates multiple dendritic cell subsets via TLR2, 7, 8, and 9 to stimulate polyvalent immunity. J Exp Med 2006; 203: 413-424.
35. Lehner M, Morhart P, Stilper A *et al.* Efficient chemokine-dependent migration and primary and secondary IL-12 secretion by human dendritic cells stimulated through Toll-like receptors. J Immunother (1997) 2007; 30: 312-322.
36. Boullart ACI, Aarntzen EHJG, Verdijk P *et al.* Maturation of monocyte-derived dendritic cells with Toll-like receptor 3 and 7/8 ligands combined with prostaglandin E2 results in high interleukin-12 production and cell migration. Cancer Immunol Immunother. 2008 Nov;57(11):1589-97.
37. Trinchieri G. Interleukin-12 and the regulation of innate resistance and adaptive immunity. Nat Rev Immunol 2003; 3: 133-146.

38. Pasare C, Medzhitov R. Toll pathway-dependent blockade of CD4+CD25+ T cell-mediated suppression by dendritic cells. Science 2003; 299: 1033-1036.
39. Pulendran B, Ahmed R. Translating innate immunity into immunological memory: implications for vaccine development. Cell 2006; 124: 849-863.
40. Kapsenberg ML. Dendritic-cell control of pathogen-driven T-cell polarization. Nat Rev Immunol 2003; 3: 984-993.
41. Wallace ME, Smyth MJ. The role of natural killer cells in tumor control--effectors and regulators of adaptive immunity. Springer Semin Immunopathol 2005; 27: 49-64.
42. Bendelac A, Savage PB, Teyton L. The biology of NKT cells. Annu Rev Immunol 2007; 25: 297-336.
43. Mattner J, Debord KL, Ismail N *et al.* Exogenous and endogenous glycolipid antigens activate NKT cells during microbial infections. Nature 2005; 434: 525-529.
44. Zhou D, Mattner J, Cantu C, 3rd *et al.* Lysosomal glycosphingolipid recognition by NKT cells. Science 2004; 306: 1786-1789.
45. Fujii S, Shimizu K, Smith C *et al.* Activation of natural killer T cells by alpha-galactosylceramide rapidly induces the full maturation of dendritic cells *in vivo* and thereby acts as an adjuvant for combined CD4 and CD8 T cell immunity to a coadministered protein. J Exp Med 2003; 198: 267-279.
46. Liu K, Idoyaga J, Charalambous A *et al.* Innate NKT lymphocytes confer superior adaptive immunity via tumor-capturing dendritic cells. J Exp Med 2005; 202: 1507-1516.
47. Shimizu K, Kurosawa Y, Taniguchi M *et al.* Cross-presentation of glycolipid from tumor cells loaded with {alpha}-galactosylceramide leads to potent and long-lived T cell mediated immunity via dendritic cells. J Exp Med 2007; 204: 2641-2653.
48. Giaccone G, Punt CJ, Ando Y *et al.* A phase I study of the natural killer T-cell ligand alpha-galactosylceramide (KRN7000) in patients with solid tumors. Clin Cancer Res 2002; 8: 3702-3709.
49. Nestle FO, Alijagic S, Gilliet M *et al.* Vaccination of melanoma patients with peptide- or tumor lysate-pulsed dendritic cells. Nat Med 1998; 4: 328-332.
50. Hsu FJ, Benike C, Fagnoni F *et al.* Vaccination of patients with B-cell lymphoma using autologous antigen-pulsed dendritic cells. Nat Med 1996; 2: 52-58.
51. Gilliet M, Kleinhans M, Lantelme E *et al.* Intranodal injection of semimature monocyte-derived dendritic cells induces T helper type 1 responses to protein neoantigen. Blood 2003; 102: 36-42.
52. de Vries IJ, Lesterhuis WJ, Scharenborg NM *et al.* Maturation of dendritic cells is a prerequisite for inducing immune responses in advanced melanoma patients. Clin Cancer Res 2003; 9: 5091-5100.
53. Dhodapkar MV, Steinman RM, Krasovsky J *et al.* Antigen-specific inhibition of effector T cell function in humans after injection of immature dendritic cells. J Exp Med 2001; 193: 233-238.
54. Jonuleit H, Giesecke-Tuettenberg A, Tuting T *et al.* A comparison of two types of dendritic cell as adjuvants for the induction of melanoma-specific T-cell responses in humans following intranodal injection. Int J Cancer 2001; 93: 243-251.
55. Jonuleit H, Kuhn U, Muller G *et al.* Pro-inflammatory cytokines and prostaglandins induce maturation of potent immunostimulatory dendritic cells under fetal calf serum-free conditions. Eur J Immunol 1997; 27: 3135-3142.
56. Thurner B, Haendle I, Roder C *et al.* Vaccination with mage-3A1 peptide-pulsed mature, monocyte-derived dendritic cells expands specific cytotoxic T cells and induces regression of some metastases in advanced stage IV melanoma. J Exp Med 1999; 190: 1669-1678.
57. Schuler-Thurner B, Schultz ES, Berger TG *et al.* Rapid induction of tumor-specific type 1 T helper cells in metastatic melanoma patients by vaccination with mature, cryopreserved, peptide-loaded monocyte-derived dendritic cells. J Exp Med 2002; 195: 1279-1288.
58. de Vries IJ, Eggert AA, Scharenborg NM *et al.* Phenotypical and functional characterization of clinical grade dendritic cells. J Immunother 2002; 25: 429-438.
59. Schuler-Thurner B, Dieckmann D, Keikavoussi P *et al.* Mage-3 and influenza-matrix peptide-specific cytotoxic T cells are inducible in terminal stage HLA-A2.1+ melanoma patients by mature monocyte-derived dendritic cells. J Immunol 2000; 165: 3492-3496.
60. Pulendran B, Dillon S, Joseph C *et al.* Dendritic cells generated in the presence of GM-CSF plus IL-15 prime potent CD8+ Tc1 responses *in vivo*. Eur J Immunol 2004; 34: 66-73.
61. Palucka AK, Ueno H, Connolly J *et al.* Dendritic cells loaded with killed allogeneic melanoma cells can induce objective clinical responses and MART-1 specific CD8+ T-cell immunity. J Immunother 2006; 29: 545-557.
62. Davis ID, Chen Q, Morris L *et al.* Blood dendritic cells generated with Flt3 ligand and CD40 ligand prime CD8+ T cells efficiently in cancer patients. J Immunother 2006; 29: 499-511.
63. Mailliard RB, Wankowicz-Kalinska A, Cai Q *et al.* alpha-type-1 polarized dendritic cells: a novel immunization tool with optimized CTL-inducing activity. Cancer Res 2004; 64: 5934-5937.
64. Trombetta ES, Mellman I. Cell biology of antigen processing *in vitro* and *in vivo*. Annu Rev Immunol 2005; 23: 975-1028.
65. Russo V, Tanzarella S, Dalerba P *et al.* Dendritic cells acquire the MAGE-3 human tumor antigen from apoptotic cells and induce a class I-restricted T cell response. Proc Natl Acad Sci U S A 2000; 97: 2185-2190.
66. Fields RC, Shimizu K, Mule JJ. Murine dendritic cells pulsed with whole tumor lysates mediate potent antitumor immune responses *in vitro* and *in vivo*. Proc Natl Acad Sci U S A 1998; 95: 9482-9487.
67. Bevan MJ. Cross-priming for a secondary cytotoxic response to minor H antigens with H-2 congenic cells which do not cross-react in the cytotoxic assay. J Exp Med 1976; 143: 1283-1288.
68. Heath WR, Carbone FR. Cross-presentation in viral immunity and self-tolerance. Nat Rev Immunol 2001; 1: 126-134.
69. Strome SE, Voss S, Wilcox R *et al.* Strategies for antigen loading of dendritic cells to enhance the antitumor immune response. Cancer Res 2002; 62: 1884-1889.

70. Bartholomae WC, Rininsland FH, Eisenberg JC *et al.* T cell immunity induced by live, necrotic, and apoptotic tumor cells. J Immunol 2004; 173: 1012-1022.
71. Chen Z, Moyana T, Saxena A *et al.* Efficient antitumor immunity derived from maturation of dendritic cells that had phagocytosed apoptotic/necrotic tumor cells. Int J Cancer 2001; 93: 539-548.
72. Scheffer SR, Nave H, Korangy F *et al.* Apoptotic, but not necrotic, tumor cell vaccines induce a potent immune response *in vivo*. Int J Cancer 2003; 103: 205-211.
73. Goldszmid RS, Idoyaga J, Bravo AI *et al.* Dendritic cells charged with apoptotic tumor cells induce long-lived protective CD4+ and CD8+ T cell immunity against B16 melanoma. J Immunol 2003; 171: 5940-5947.
74. Casares N, Pequignot MO, Tesniere A *et al.* Caspase-dependent immunogenicity of doxorubicin-induced tumor cell death. J Exp Med 2005; 202: 1691-1701.
75. Apetoh L, Ghiringhelli F, Tesniere A *et al.* Toll-like receptor 4-dependent contribution of the immune system to anticancer chemotherapy and radiotherapy. Nat Med 2007; 13: 1050-1059.
76. Lau R, Wang F, Jeffery G *et al.* Phase I trial of intravenous peptide-pulsed dendritic cells in patients with metastatic melanoma. J Immunother 2001; 24: 66-78.
77. Slingluff CL, Jr., Petroni GR, Yamshchikov GV *et al.* Clinical and immunologic results of a randomized phase II trial of vaccination using four melanoma peptides either administered in granulocyte-macrophage colony-stimulating factor in adjuvant or pulsed on dendritic cells. J Clin Oncol 2003; 21: 4016-4026.
78. Bedrosian I, Mick R, Xu S *et al.* Intranodal administration of peptide-pulsed mature dendritic cell vaccines results in superior CD8+ T-cell function in melanoma patients. J Clin Oncol 2003; 21: 3826-3835.
79. Butterfield LH, Ribas A, Dissette VB *et al.* Determinant spreading associated with clinical response in dendritic cell-based immunotherapy for malignant melanoma. Clin Cancer Res 2003; 9: 998-1008.
80. Linette GP, Zhang D, Hodi FS *et al.* Immunization using autologous dendritic cells pulsed with the melanoma-associated antigen gp100-derived G280-9V peptide elicits CD8+ immunity. Clin Cancer Res 2005; 11: 7692-7699.
81. Tuettenberg A, Becker C, Huter E *et al.* Induction of strong and persistent MelanA/MART-1-specific immune responses by adjuvant dendritic cell-based vaccination of stage II melanoma patients. Int J Cancer 2006; 118: 2617-2627.
82. Fay JW, Palucka AK, Paczesny S *et al.* Long-term outcomes in patients with metastatic melanoma vaccinated with melanoma peptide-pulsed CD34(+) progenitor-derived dendritic cells. Cancer Immunol Immunother 2006; 55: 1209-1218.
83. Paczesny S, Banchereau J, Wittkowski KM *et al.* Expansion of melanoma-specific cytolytic CD8+ T cell precursors in patients with metastatic melanoma vaccinated with CD34+ progenitor-derived dendritic cells. J Exp Med 2004; 199: 1503-1511.
84. Trakatelli M, Toungouz M, Blocklet D *et al.* A new dendritic cell vaccine generated with interleukin-3 and interferon-beta induces CD8+ T cell responses against NA17-A2 tumor peptide in melanoma patients. Cancer Immunol Immunother 2006; 55: 469-474.
85. Panelli MC, Wunderlich J, Jeffries J *et al.* Phase 1 study in patients with metastatic melanoma of immunization with dendritic cells presenting epitopes derived from the melanoma-associated antigens MART-1 and gp100. J Immunother 2000; 23: 487-498.
86. Ribas A, Glaspy JA, Lee Y *et al.* Role of dendritic cell phenotype, determinant spreading, and negative costimulatory blockade in dendritic cell-based melanoma immunotherapy. J Immunother 2004; 27: 354-367.
87. Schadendorf D, Ugurel S, Schuler-Thurner B *et al.* Dacarbazine (DTIC) versus vaccination with autologous peptide-pulsed dendritic cells (DC) in first-line treatment of patients with metastatic melanoma: a randomized phase III trial of the DC study group of the DeCOG. Ann Oncol 2006; 17: 563-570.
88. Toes RE, Ossendorp F, Offringa R, Melief CJ. CD4 T cells and their role in antitumor immune responses. J Exp Med 1999; 189: 753-756.
89. Bevan MJ. Helping the CD8(+) T-cell response. Nat Rev Immunol 2004; 4: 595-602.
90. Gilboa E. DC-based cancer vaccines. J Clin Invest 2007; 117: 1195-1203.
91. Chang AE, Redman BG, Whitfield JR *et al.* A phase I trial of tumor lysate-pulsed dendritic cells in the treatment of advanced cancer. Clin Cancer Res 2002; 8: 1021-1032.
92. O'Rourke MG, Johnson M, Lanagan C *et al.* Durable complete clinical responses in a phase I/II trial using an autologous melanoma cell/dendritic cell vaccine. Cancer Immunol Immunother 2003; 52: 387-395.
93. Hersey P, Menzies SW, Halliday GM *et al.* Phase I/II study of treatment with dendritic cell vaccines in patients with disseminated melanoma. Cancer Immunol Immunother 2004; 53: 125-134.
94. Griffioen M, Borghi M, Schrier PI *et al.* Analysis of T-cell responses in metastatic melanoma patients vaccinated with dendritic cells pulsed with tumor lysates. Cancer Immunol Immunother 2004; 53: 715-722.
95. Ridolfi R, Petrini M, Fiammenghi L *et al.* Improved overall survival in dendritic cell vaccination-induced immunoreactive subgroup of advanced melanoma patients. J Transl Med 2006; 4: 36.
96. Smithers M, O'Connell K, MacFadyen S *et al.* Clinical response after intradermal immature dendritic cell vaccination in metastatic melanoma is associated with immune response to particulate antigen. Cancer Immunol Immunother 2003; 52: 41-52.
97. Berard F, Blanco P, Davoust J *et al.* Cross-priming of naive CD8 T cells against melanoma antigens using dendritic cells loaded with killed allogeneic melanoma cells. J Exp Med 2000; 192: 1535-1544.
98. Salcedo M, Bercovici N, Taylor R *et al.* Vaccination of melanoma patients using dendritic cells loaded with an allogeneic tumor cell lysate. Cancer Immunol Immunother 2006; 55: 819-829.
99. Escobar A, Lopez M, Serrano A *et al.* Dendritic cell immunizations alone or combined with low doses of interleukin-2 induce specific immune responses in melanoma patients. Clin Exp Immunol 2005; 142: 555-568.
100. Sullenger BA, Gilboa E. Emerging clinical applications of RNA. Nature 2002; 418: 252-258.

101. Nair SK, Morse M, Boczkowski D *et al.* Induction of tumor-specific cytotoxic T lymphocytes in cancer patients by autologous tumor RNA-transfected dendritic cells. Ann Surg 2002; 235: 540-549.
102. Kyte JA KG, Aamdal S, Saeboe-Larssen S, Gaudernack G. Preclinical full-scale evaluation of dendritic cells transfected with autologous tumor-mRNA for melanoma vaccination. Cancer Gene Ther 2005; 12: 579-591.
103. Schaft N, Dorrie J, Thumann P *et al.* Generation of an optimized polyvalent monocyte-derived dendritic cell vaccine by transfecting defined RNAs after rather than before maturation. J Immunol 2005; 174: 3087-3097.
104. Bonehill A, Heirman C, Tuyaerts S *et al.* Messenger RNA-electroporated dendritic cells presenting MAGE-A3 simultaneously in HLA class I and class II molecules. J Immunol 2004; 172: 6649-6657.
105. Laverman P, de Vries IJ, Scharenborg NM *et al.* Development of 111In-labeled tumor-associated antigen peptides for monitoring dendritic-cell-based vaccination. Nucl Med Biol 2006; 33: 453-458.
106. Van Tendeloo VF, Ponsaerts P, Lardon F *et al.* Highly efficient gene delivery by mRNA electroporation in human hematopoietic cells: superiority to lipofection and passive pulsing of mRNA and to electroporation of plasmid cDNA for tumor antigen loading of dendritic cells. Blood 2001; 98: 49-56.
107. Ponsaerts P, Van Tendeloo VF, Cools N *et al.* mRNA-electroporated mature dendritic cells retain transgene expression, phenotypical properties and stimulatory capacity after cryopreservation. Leukemia 2002; 16: 1324-1330.
108. Ueno H, Tcherepanova I, Reygrobellet O *et al.* Dendritic cell subsets generated from CD34+ hematopoietic progenitors can be transfected with mRNA and induce antigen-specific cytotoxic T cell responses. J Immunol Methods 2004; 285: 171-180.
109. Mu LJ, Gaudernack G, Saeboe-Larssen S *et al.* A protocol for generation of clinical grade mRNA-transfected monocyte-derived dendritic cells for cancer vaccines. Scand J Immunol 2003; 58: 578-586.
110. Kyte JA, Mu L, Aamdal S *et al.* Phase I/II trial of melanoma therapy with dendritic cells transfected with autologous tumor-mRNA. Cancer Gene Ther 2006; 13: 905-918.
111. Kyte JA, Kvalheim G, Lislerud K *et al.* T cell responses in melanoma patients after vaccination with tumor-mRNA transfected dendritic cells. Cancer Immunol Immunother 2006.
112. Nair SK, Hull S, Coleman D *et al.* Induction of carcinoembryonic antigen (CEA)-specific cytotoxic T-lymphocyte responses *in vitro* using autologous dendritic cells loaded with CEA peptide or CEA RNA in patients with metastatic malignancies expressing CEA. Int J Cancer 1999; 82: 121-124.
113. Tacken PJ, de Vries IJ, Gijzen K *et al.* Effective induction of naive and recall T-cell responses by targeting antigen to human dendritic cells via a humanized anti-DC-SIGN antibody. Blood 2005; 106: 1278-1285.
114. Bonifaz LC, Bonnyay DP, Charalambous A *et al. In vivo* targeting of antigens to maturing dendritic cells via the DEC-205 receptor improves T cell vaccination. J Exp Med 2004; 199: 815-824.
115. Furumoto K, Soares L, Engleman EG, Merad M. Induction of potent antitumor immunity by *in situ* targeting of intratumoral DCs. J Clin Invest 2004; 113: 774-783.
116. Milas L, Mason KA, Ariga H *et al.* CpG oligodeoxynucleotide enhances tumor response to radiation. Cancer Res 2004; 64: 5074-5077.
117. Nowak AK, Robinson BW, Lake RA. Synergy between chemotherapy and immunotherapy in the treatment of established murine solid tumors. Cancer Res 2003; 63: 4490-4496.
118. den Brok MH, Sutmuller RP, van der Voort R *et al. In situ* tumor ablation creates an antigen source for the generation of antitumor immunity. Cancer Res 2004; 64: 4024-4029.
119. den Brok MH, Sutmuller RP, Nierkens S *et al.* Synergy between *in situ* cryoablation and TLR9 stimulation results in a highly effective *in vivo* dendritic cell vaccine. Cancer Res 2006; 66: 7285-7292.
120. den Brok MH, Sutmuller RP, Nierkens S *et al.* Efficient loading of dendritic cells following cryo and radiofrequency ablation in combination with immune modulation induces anti-tumour immunity. Br J Cancer 2006; 95: 896-905.
121. Forster R, Schubel A, Breitfeld D *et al.* CCR7 coordinates the primary immune response by establishing functional microenvironments in secondary lymphoid organs. Cell 1999; 99: 23-33.
122. MartIn-Fontecha A, Sebastiani S, Hopken UE *et al.* Regulation of dendritic cell migration to the draining lymph node: impact on T lymphocyte traffic and priming. J Exp Med 2003; 198: 615-621.
123. Randolph GJ, Angeli V, Swartz MA. Dendritic-cell trafficking to lymph nodes through lymphatic vessels. Nat Rev Immunol 2005; 5: 617-628.
124. Scandella E, Men Y, Legler DF *et al.* CCL19/CCL21-triggered signal transduction and migration of dendritic cells requires prostaglandin E2. Blood 2004; 103: 1595-1601.
125. Morelli AE, Thomson AW. Dendritic cells under the spell of prostaglandins. Trends Immunol 2003; 24: 108-111.
126. Feuerer M, Beckhove P, Garbi N *et al.* Bone marrow as a priming site for T-cell responses to blood-borne antigen. Nat Med 2003; 9: 1151-1157.
127. Eggert AA, Schreurs MW, Boerman OC *et al.* Biodistribution and vaccine efficiency of murine dendritic cells are dependent on the route of administration. Cancer Res 1999; 59: 3340-3345.
128. De Vries IJ, Krooshoop DJ, Scharenborg NM *et al.* Effective migration of antigen-pulsed dendritic cells to lymph nodes in melanoma patients is determined by their maturation state. Cancer Res 2003; 63: 12-17.
129. Ridolfi R, Riccobon A, Galassi R *et al.* Evaluation of *in vivo* labelled dendritic cell migration in cancer patients. J Transl Med 2004; 2: 27.
130. Morse MA, Coleman RE, Akabani G *et al.* Migration of human dendritic cells after injection in patients with metastatic malignancies. Cancer Res 1999; 59: 56-58.
131. de Vries IJ, Lesterhuis WJ, Barentsz JO *et al.* Magnetic resonance tracking of dendritic cells in melanoma patients for monitoring of cellular therapy. Nat Biotechnol 2005; 23: 1407-1413.
132. Zitvogel L, Tursz T. *In vivo* veritas. Nat Biotechnol 2005; 23: 1372-1374.

133. Lesimple T, Neidhard EM, Vignard V *et al.* Immunologic and clinical effects of injecting mature peptide-loaded dendritic cells by intralymphatic and intranodal routes in metastatic melanoma patients. Clin Cancer Res 2006; 12: 7380-7388.
134. Kyte JA AS, Kvalheim G, Dueland S, Hauser M, Gullestad HP, Ryder T, Lislerud K, Hammerstad H, Gaudernack G. Phase I/II trial of melanoma therapy with dendritic cells transfected with autologous tumor-mRNA. Cancer Gene Ther 2006; Epub ahead of print.
135. Fong L, Brockstedt D, Benike C *et al.* Dendritic cells injected via different routes induce immunity in cancer patients. J Immunol 2001; 166: 4254-4259.
136. Mullins DW, Sheasley SL, Ream RM *et al.* Route of immunization with peptide-pulsed dendritic cells controls the distribution of memory and effector T cells in lymphoid tissues and determines the pattern of regional tumor control. J Exp Med 2003; 198: 1023-1034.
137. Adema GJ, de Vries IJ, Punt CJ, Figdor CG. Migration of dendritic cell based cancer vaccines: *in vivo* veritas? Curr Opin Immunol 2005; 17: 170-174.
138. Fehervari Z, Sakaguchi S. CD4+ Tregs and immune control. J Clin Invest 2004; 114: 1209-1217.
139. Bluestone JA. Regulatory T-cell therapy: is it ready for the clinic? Nat Rev Immunol 2005; 5: 343-349.
140. Sutmuller RP, Morgan ME, Netea MG *et al.* Toll-like receptors on regulatory T cells: expanding immune regulation. Trends Immunol 2006; 27: 387-393.
141. Bopp T, Becker C, Klein M *et al.* Cyclic adenosine monophosphate is a key component of regulatory T cell-mediated suppression. J Exp Med 2007; 204: 1303-1310.
142. Curiel TJ, Coukos G, Zou L *et al.* Specific recruitment of regulatory T cells in ovarian carcinoma fosters immune privilege and predicts reduced survival. Nat Med 2004; 10: 942-949.
143. Grauer OM, Nierkens S, Bennink E *et al.* CD4+FoxP3+ regulatory T cells gradually accumulate in gliomas during tumor growth and efficiently suppress antiglioma immune responses *in vivo*. Int J Cancer 2007; 121: 95-105.
144. Gao Q, Qiu SJ, Fan J *et al.* Intratumoral balance of regulatory and cytotoxic T cells is associated with prognosis of hepatocellular carcinoma after resection. J Clin Oncol 2007; 25: 2586-2593.
145. Petersen RP, Campa MJ, Sperlazza J *et al.* Tumor infiltrating Foxp3+ regulatory T-cells are associated with recurrence in pathologic stage I NSCLC patients. Cancer 2006; 107: 2866-2872.
146. Sutmuller RP, van Duivenvoorde LM, van Elsas A *et al.* Synergism of cytotoxic T lymphocyte-associated antigen 4 blockade and depletion of CD25(+) regulatory T cells in antitumor therapy reveals alternative pathways for suppression of autoreactive cytotoxic T lymphocyte responses. J Exp Med 2001; 194: 823-832.
147. Ko K, Yamazaki S, Nakamura K *et al.* Treatment of advanced tumors with agonistic anti-GITR mAb and its effects on tumor-infiltrating Foxp3+CD25+CD4+ regulatory T cells. J Exp Med 2005; 202: 885-891.
148. Khoury SJ, Sayegh MH. The roles of the new negative T cell costimulatory pathways in regulating autoimmunity. Immunity 2004; 20: 529-538.
149. Walunas TL, Bakker CY, Bluestone JA. CTLA-4 ligation blocks CD28-dependent T cell activation. J Exp Med 1996; 183: 2541-2550.
150. Ohigashi Y, Sho M, Yamada Y *et al.* Clinical significance of programmed death-1 ligand-1 and programmed death-1 ligand-2 expression in human esophageal cancer. Clin Cancer Res 2005; 11: 2947-2953.
151. Iwai Y, Ishida M, Tanaka Y *et al.* Involvement of PD-L1 on tumor cells in the escape from host immune system and tumor immunotherapy by PD-L1 blockade. Proc Natl Acad Sci U S A 2002; 99: 12293-12297.
152. Blank C, Brown I, Peterson AC *et al.* PD-L1/B7H-1 inhibits the effector phase of tumor rejection by T cell receptor (TCR) transgenic CD8+ T cells. Cancer Res 2004; 64: 1140-1145.
153. Blank C, Kuball J, Voelkl S *et al.* Blockade of PD-L1 (B7-H1) augments human tumor-specific T cell responses *in vitro*. Int J Cancer 2006; 119: 317-327.
154. Dannull J, Su Z, Rizzieri D *et al.* Enhancement of vaccine-mediated antitumor immunity in cancer patients after depletion of regulatory T cells. J Clin Invest 2005; 115: 3623-3633.
155. Attia P, Maker AV, Haworth LR *et al.* Inability of a fusion protein of IL-2 and diphtheria toxin (Denileukin Diftitox, DAB389IL-2, ONTAK) to eliminate regulatory T lymphocytes in patients with melanoma. J Immunother 2005; 28: 582-592.
156. Mahnke K, Schonfeld K, Fondel S *et al.* Depletion of CD4+CD25+ human regulatory T cells *in vivo*: kinetics of Treg depletion and alterations in immune functions *in vivo* and *in vitro*. Int J Cancer 2007; 120: 2723-2733.
157. Suntharalingam G, Perry MR, Ward S *et al.* Cytokine storm in a phase 1 trial of the anti-CD28 monoclonal antibody TGN1412. N Engl J Med 2006; 355: 1018-1028.
158. Sharpe AH, Abbas AK. T-cell costimulation--biology, therapeutic potential, and challenges. N Engl J Med 2006; 355: 973-975.
159. Phan GQ, Yang JC, Sherry RM *et al.* Cancer regression and autoimmunity induced by cytotoxic T lymphocyte-associated antigen 4 blockade in patients with metastatic melanoma. Proc Natl Acad Sci U S A 2003; 100: 8372-8377.
160. Attia P, Phan GQ, Maker AV *et al.* Autoimmunity correlates with tumor regression in patients with metastatic melanoma treated with anti-cytotoxic T-lymphocyte antigen-4. J Clin Oncol 2005; 23: 6043-6053.
161. Maker AV, Yang JC, Sherry RM *et al.* Intrapatient dose escalation of anti-CTLA-4 antibody in patients with metastatic melanoma. J Immunother 2006; 29: 455-463.
162. Ribas A, Camacho LH, Lopez-Berestein G *et al.* Antitumor activity in melanoma and anti-self responses in a phase I trial with the anti-cytotoxic T lymphocyte-associated antigen 4 monoclonal antibody CP-675,206. J Clin Oncol 2005; 23: 8968-8977.
163. Maker AV, Attia P, Rosenberg SA. Analysis of the cellular mechanism of antitumor responses and autoimmunity in patients treated with CTLA-4 blockade. J Immunol 2005; 175: 7746-7754.

164. de Vries IJ, Bernsen MR, Lesterhuis WJ *et al.* Immunomonitoring tumor-specific T cells in delayed-type hypersensitivity skin biopsies after dendritic cell vaccination correlates with clinical outcome. J Clin Oncol 2005; 23: 5779-5787.
165. Coulie PG, Karanikas V, Colau D *et al.* A monoclonal cytolytic T-lymphocyte response observed in a melanoma patient vaccinated with a tumor-specific antigenic peptide encoded by gene MAGE-3. Proc Natl Acad Sci U S A 2001; 98: 10290-10295.
166. Lesterhuis WJ, de Vries IJ, Schuurhuis DH *et al.* Vaccination of colorectal cancer patients with CEA-loaded dendritic cells: antigen-specific T cell responses in DTH skin tests. Ann Oncol 2006; 17: 974-980.
167. Lonchay C, van der Bruggen P, Connerotte T *et al.* Correlation between tumor regression and T cell responses in melanoma patients vaccinated with a MAGE antigen. Proc Natl Acad Sci U S A 2004; 101 Suppl 2: 14631-14638.
168. Hoos A, Parmiani G, Hege K *et al.* A clinical development paradigm for cancer vaccines and related biologics. J Immunother (1997) 2007; 30: 1-15.
169. Shu CJ, Guo S, Kim YJ *et al.* Visualization of a primary anti-tumor immune response by positron emission tomography. Proc Natl Acad Sci U S A 2005; 102: 17412-17417.
170. Fox JL. Uncertainty surrounds cancer vaccine review at FDA. Nat Biotechnol 2007; 25: 827-828.
171. Small EJ, Fratesi P, Reese DM *et al.* Immunotherapy of hormone-refractory prostate cancer with antigen-loaded dendritic cells. J Clin Oncol 2000; 18: 3894-3903.
172. Small EJ, Schellhammer PF, Higano CS *et al.* Placebo-controlled phase III trial of immunologic therapy with sipuleucel-T (APC8015) in patients with metastatic, asymptomatic hormone refractory prostate cancer. J Clin Oncol 2006; 24: 3089-3094.
173. Provenge delayed. Nat Biotechnol 2007; 25: 703.
174. Correale P, Del Vecchio MT, Di Genova G *et al.* 5-fluorouracil-based chemotherapy enhances the antitumor activity of a thymidylate synthase-directed polyepitopic peptide vaccine. J Natl Cancer Inst 2005; 97: 1437-1445.
175. van der Most RG, Currie A, Robinson BW, Lake RA. Cranking the immunologic engine with chemotherapy: using context to drive tumor antigen cross-presentation towards useful antitumor immunity. Cancer Res 2006; 66: 601-604.
176. Kim KW, Kim SH, Shin JG *et al.* Direct injection of immature dendritic cells into irradiated tumor induces efficient antitumor immunity. Int J Cancer 2004; 109: 685-690.
177. Pedersen AE, Buus S, Claesson MH. Treatment of transplanted CT26 tumour with dendritic cell vaccine in combination with blockade of vascular endothelial growth factor receptor 2 and CTLA-4. Cancer Lett 2006; 235: 229-238.
178. Udagawa M, Kudo-Saito C, Hasegawa G *et al.* Enhancement of immunologic tumor regression by intratumoral administration of dendritic cells in combination with cryoablative tumor pretreatment and Bacillus Calmette-Guerin cell wall skeleton stimulation. Clin Cancer Res 2006; 12: 7465-7475.
179. Schattenberg AV, Dolstra H. Cellular adoptive immunotherapy after allogeneic stem cell transplantation. Curr Opin Oncol 2005; 17: 617-621.
180. Dudley ME, Wunderlich JR, Yang JC *et al.* Adoptive cell transfer therapy following non-myeloablative but lymphodepleting chemotherapy for the treatment of patients with refractory metastatic melanoma. J Clin Oncol 2005; 23: 2346-2357.
181. Dudley ME, Wunderlich JR, Robbins PF *et al.* Cancer regression and autoimmunity in patients after clonal repopulation with antitumor lymphocytes. Science 2002; 298: 850-854.
182. Park MY, Kim CH, Sohn HJ *et al.* The optimal interval for dendritic cell vaccination following adoptive T cell transfer is important for boosting potent anti-tumor immunity. Vaccine 2007.
183. Lou Y, Wang G, Lizee G *et al.* Dendritic cells strongly boost the antitumor activity of adoptively transferred T cells *in vivo*. Cancer Res 2004; 64: 6783-6790.

Targeting $CD4^+$ T helper cells improves the induction of anti-tumor responses in dendritic cell based vaccination

Aarntzen EH

De Vries IJ

Lesterhuis WJ

Schuurhuis DH

Jacobs JF

Bol K

Schreibelt G

Mus R

De Wilt JH

Haanen JB

Schadendorf D

Croockewit A

Blokx WA

Van Rossum MM

Kwok WW

Adema GJ

Punt CJ

Figdor CG

Cancer Res. 2012 Oct 18th (accepted)

Abstract

To determine the relevance of targeting antigen-specific $CD4^+$ T helper cells in anti-cancer immunotherapy, we investigated the immunological and clinical responses to vaccination with dendritic cells (DC) pulsed with either MHC Class I (MHC-I) restricted epitopes alone or both MHC Class I and II (MHC-I/II) restricted epitopes.

We enrolled thirty-three stage III and IV HLA-A*02:01 positive melanoma patients in this study, 29 patients were evaluable for immunological response. Patients received intranodal vaccinations with cytokine-matured DC loaded with keyhole limpet hemocyanin and MHC-I *alone* or MHC-I/II restricted tumor associated antigens (TAA) of tyrosinase and gp100, depending on their HLA-DR4 status.

In 4/15 patients vaccinated with MHC-I/II loaded DC and 1/14 patients vaccinated with MHC-I loaded DC, we detected TAA-specific $CD8^+$ T cells with maintained IFNγ production in skin-test infiltrating lymphocyte (SKIL) cultures and circulating TAA-specific $CD8^+$ T cells. If TAA-specific $CD4^+$ T cell responses were detected in SKIL cultures, it coincided with TAA-specific $CD8^+$ T cell responses. In 3/13 patients tested, we detected TAA-specific $CD4^+CD25^+FoxP3^-$ T cells with high proliferative capacity and IFNγproduction, indicating that these were not regulatory T cells. Vaccination with MHC-I/II loaded DC resulted in improved clinical outcome compared to matched control patients treated with DTIC, median OS 15.0 versus 8.3 months (p=0.089) and median PFS 5.0 versus 2.8 months (p=0.0089) . In conclusion, co-activating TAA-specific $CD4^+$ T helper cells with DC pulsed with both MHC Class I and II restricted epitopes augments TAA-specific $CD8^+$ T cell responses, contributing to improved clinical responses.

Introduction

Dendritic cells (DC) are considered the most effective antigen-presenting cells to activate naïve T cells (1). Immunotherapy exploiting *ex vivo* generated autologous DC pulsed with tumor peptides has shown proof of principle (2). We and others have shown that tumor-specific immune responses can be induced in both stage III and IV melanoma patients (2). Nevertheless, further optimization is warranted before this approach is accepted for clinical practice (3).

The role of $CD8^+$ cytotoxic T cells (CTL) in the eradication of tumor cells that express tumor associated antigens (TAA) in the context of MHC class I (MHC-I), has clearly been established (4). For melanoma, many HLA-A*01, A*02 and A*03 restricted epitopes derived from gp100, tyrosinase, MAGE-3 or MART-1 have been identified (5). The majority of clinical studies have been performed with MHC-I peptide-pulsed DC (6-11). A potential disadvantage of this method is that exclusively $CD8^+$ cytotoxic T cells are targeted, without involving $CD4^+$ T helper cells in the induction of anti-tumor responses.

The role of T helper cells has recently been better characterized. It has been shown that the presentation of tumor peptides in both MHC class I and II (MHC-I/II) induces high-affinity T cells reactive to multiple MHC-I/II epitopes (12). Subsequent direct activation of APC by T helper cells leads to stimulation of precursor CTL to become effector CTL (13). Several studies have shown a critical role for T helper cells in the maintenance of long-term protective immunity (14, 15). Furthermore, T helper cells themselves can also have a direct anti-tumor effect (13). This effect may be particularly relevant to melanoma, since melanoma cells often constitutively express MHC-II molecules (16), which are not down-regulated during progression (17). Recently, MHC-II epitopes derived from gp100 and tyrosinase have been made available for use in clinical trials (18-20). To determine the additional value of co-activating $CD4^+$ T helper cells we investigated the immunological and clinical responses after vaccination with DC either pulsed with MHC-I or MHC-I/II restricted epitopes of g100 and tyrosinase.

Materials and methods

Patient population

Melanoma patients with regional lymph node metastases (American Joint Committee on Cancer criteria stage III) scheduled for radical lymph node dissection (RLND) or with distant metastases (AJCC stage IV) were included. Additional eligibility criteria included HLA-A*02:01 genotype, known HLA-DR4 status, expression of melanoma-associated antigens gp100 and tyrosinase, WHO performance status 0 or 1, lactate dehydrogenase within 2x upper limit of normal (reference value 450 U/L). Patients with symptomatic brain metastases, serious concomitant disease or a history of second malignancy were excluded. The trial was registered at ClinicalTrials.gov, identifier NCT00243529 and approved by the local Institutional Review Board. Written informed consent was obtained from all patients.

Study protocol

Patients received the vaccine intranodally (i.n.) injected in a clinically tumor-free lymph node under ultrasound guidance. All administered vaccines consisted of autologous mature monocyte-derived DC pulsed with gp100 and tyrosinase peptides and keyhole limpet hemocyanin (KLH) protein. Patients were assigned to two different groups, depending on their HLA-DR4 genotype. Patients with HLA-DR4 genotype were vaccinated with DC loaded with MHC-I/II peptides (group A), patients without HLA-DR4 genotype were vaccinated DC loaded with MHC-I peptides only (group B). Patients were evaluable for immunological response, as they completed at least one cycle of three vaccinations with a biweekly interval, followed by delayed type hypersensitivity skin test (21). All seven patients with regional lymph node metastases received one extra vaccination 2 days prior to scheduled RLND for additional imaging studies (Aarntzen et al, *Clin Cancer Res. 2012)* and started thereafter with the standard schedule of 3 biweekly vaccinations. Patients without progression after

the first vaccination cycle were eligible for a maximum of two maintenance cycles at 6-month intervals. All vaccinations were administered between February 2002 and February 2009. The primary study endpoint was vaccine-specific immune response; secondary endpoints included the clinical response (progression-free survival and overall survival on intention to treat bases, calculated from the time of apheresis to event) and toxicity.

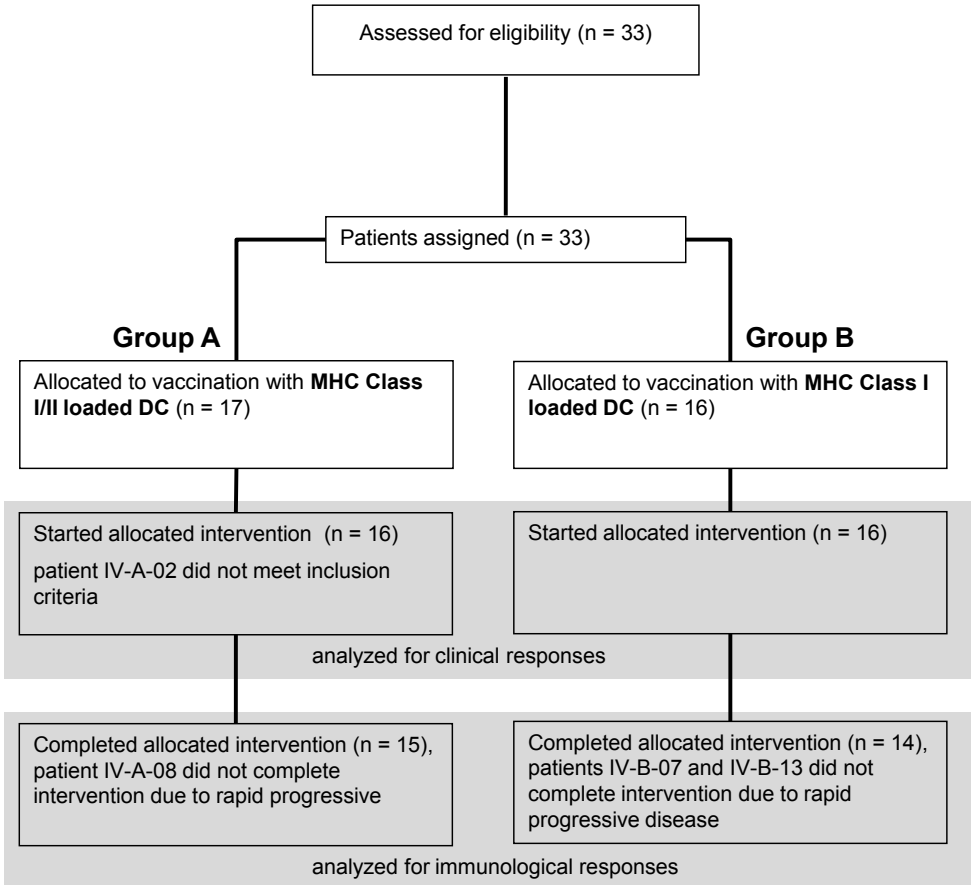

Supplementary Figure 1. CONSORT flow chart.

DC preparation and characterization

DC were generated from peripheral blood mononuclear cells (PBMC) prepared from leukapheresis products as described previously (8). Part of the PBMC was used to generate monocyte-conditioned medium (MCM). Plastic-adherent monocytes were cultured in X-VIVO-15™ medium (BioWhittaker, Walkersville, Maryland) supplemented with 2% pooled human serum (HS) (Bloodbank Rivierenland, Nijmegen, The Netherlands), IL-4 (500 U/ml) and GM-CSF (800 U/ml) (both CellGenix, Freiburg, Germany). Immature DC were pulsed at day 3 with Keyhole limpet hemocyanin (KLH, 10 μg/ml; Calbiochem, San Diego, CA). Two days prior the harvesting, cells were matured with autologous MCM with prostaglandin E_2 (10 □g/ml; Pharmacia & Upjohn, Puurs, Belgium) and 10 ng/ml of recombinant tumor necrosis factor alpha (provided by dr. G. Adolf, Bender Wien, Vienna, Austria). This protocol gave rise to mature DC (22). Patients received at maximum 15×10^6 DCs per injection.

Peptide-pulsing of DC

DC were pulsed with the MHC-I-restricted peptides gp100:154-162 (KTWGQYWQV) (23) and gp100:280-288 (YLEPGPVTA) (24) and tyrosinase:369-377 (YMDGTMSQV); MHC-II-restricted peptides gp100:44-59 (WNRQLYPEWTEAQRLD) (25) and tyrosinase:448-462 (DYSYLQDSDPDSFQD) (26). Peptide pulsing was performed as described previously (8), and cells were suspended in 0.1 ml for injection.

Flow cytometry

The following FITC-conjugated mAbs were used: anti-HLA-Class-I (W6/32), and anti-HLA-DR/DP (Q5/13); and PE-conjugated mAbs: anti-CD14, anti-CD83, anti-CD28 (Beckman Coulter, Mijdrecht, The Netherlands), and anti-CD80, anti-CD8, anti-CD86, anti-CD45RA, anti-CD62L (BD Biosciences, San Diego, CA). Directly labelled mAbs against CD4, CD8, CD25, CD127, CTLA-4 (BD Pharmingen) and FoxP3 (eBiosciece, San Diego, CA, USA), all according to the manufacturer's protocol, were used to characterize T cells. Regulatory T cells were defined as $CD4^{+}FoxP3^{+}CD25^{high}CD127^{low}$ cells. The FACSCalibur™ flow cytometer equipped with CellQuest software (BD Biosciences) was used.

Evaluation of immunological responses

Peripheral blood sampling was performed prior to and after each vaccination and at every follow-up visit thereafter, for the evaluation of KLH-specific responses and tetramer staining. Delayed type hypersensitivity skin-test procedures were performed at the completion of each cycle of 3 biweekly vaccinations, up to a total 3 cycles at a 6 month interval in case of no progression. For evaluation of the immunological responses we compared the maximum vaccine-induced responses per individual, as this most accurately reflects the competence of an individual to mount an immune response (Aarntzen et al, *Cancer Res. 2012*).

KLH-specific proliferation

PBMC were isolated from heparinized blood by Ficoll-Paque density centrifugation, stimulated with KLH (4 μg/2×10^5 PBMC) in X-VIVO with 2% HS. After 3 days, cells were incubated with ^{3}H-thymidine for 8 hours, incorporation was measured with a β-counter. Experiments were performed in triplicate.

KLH-specific antibodies

Antibodies against KLH were measured in the serum of vaccinated patients using enzyme-linked immunosorbent assays (ELISA) (21). Microtiter plates were coated with KLH and different concentrations of patient serum were allowed to bind. After washing, patient antibodies were detected with mouse-anti-human IgG, IgA or IgM antibodies labeled with horseradish peroxidase; 3,3'-5,5-tetramethyl-benzidine was used as a substrate. An isotype-specific calibration curve for the KLH response was included in each plate, the detection limit was determined at >20mg/l (27).

Skin-test infiltrating lymphocyte (SKIL) analyses

Skin tests were performed as described before (21) and at Labtube.tv [internet], available from www.labtube.tv/playvideo.aspx?vid+131825. Briefly, $2–10\times10^6$ DC pulsed with the indicated peptides were injected intradermally at different sites. After 48 hours, punch biopsies (6 mm) were taken, half of the biopsy was manually cut and cultured in RPMI-1640 containing 7% HS and IL-2 (100 U/ml).
No SKIL cultures were obtained prior to therapy since we previously demonstrated that, although induration might be present, no vaccine-specific T cells were detected prior to DC-based vaccination (28).

Tetramer staining

SKIL cultures and PBMC were stained with tetrameric-MHC complexes containing the MHC-I epitopes gp100:154-168, gp100:280-288 or tyrosinase:369-377 (Sanquin, Amsterdam, The Netherlands) or MHC-II epitopes gp100:44-59 and tyrosinase:448-462 (provided by William Kwok, Benaroya Research Institute, Seattle, WA) as described previously (21). In addition, PBMCs were restimulated for 8 days with DR4-binding gp100 or tyrosinase peptides and stained with tetrameric-MHC complexes containing MHC-II epitopes gp100:44-59 and tyrosinase:448-462. Tetrameric-MHC complexes recognizing HIV were used as correction for background binding. Tetramer positivity was defined as at least two-fold increase in the double positive population.

Antigen and tumor recognition

SKIL cultures were challenged with T2 cells pulsed with the indicated peptides or control antigen G250; or an allogenic HLA-A*02:01-positive, HLA-DR4 negative, gp100-positive and tyrosinase-positive tumor cell line (MEL624), which was stimulated with IFNγ (400 U/L) for 48 hours prior to stimulation. Cytokines were measured in supernatants after 16 hours by the cytometric bead array (Th1/Th2 Cytokine CBA 1; BD Pharmingen). Positive and specific cytokine production was defined as a two-fold increase compared to stimulation with the cell lines pulsed with an irrelevant peptide.

Cytotoxic activity

Cytotoxic activity of SKILs was measured using the chromium release assay as described previously (29). Briefly, T2 or MEL624 cells were incubated with 100 μCi $Na_2[^{51}Cr]O_4$ (Amersham, Bucks, UK) and, after washing, added to lymphocytes (1×10^5 cells) and unlabeled K562 cells (1×10^4 cells) in triplicate wells of a round bottom microtiter plate (E/T ratio 10/1). After 4 hours, supernatants were harvested and radioactivity was measured. The specific percentage of cytotoxicity was defined by the following formula:

$$specific\ cytotoxicity\ = \frac{(experimental\ release\ (cpm) - spontaneous\ release\ (cpm)}{maximum\ release\ (cpm) -\ spontaneous\ release\ (cpm)}\ x\ 100\%$$

Matched controls

Matched controls were identified from records of metastatic melanoma patients from the Radboud University Nijmegen Medical Centre (Nijmegen, The Netherlands), The Netherlands Cancer Institute – Antoni van Leeuwenhoek Hospital (Amsterdam, The Netherlands) and University Hospital Essen (Essen, Germany) who had received first-line dacarbazine (DTIC) chemotherapy at 850–1000 mg/m^2 i.v. at 3 weekly intervals, between March 2000 and March 2010. All matched controls were HLA-A*02:01 positive and were required to have received at least 3 infusions, a therapy time-frame that is consistent with one cycle of vaccinations.

Control patients were matched to study subjects, in ratio 1:3, primarily for M substage at baseline according to AJCC criteria, number of distant metastases, number of metastatic sites, localization of distant metastases and baseline serum LDH. These criteria currently represent the most important prognostic factors for survival (30). In case of more than three matches for one study subject, demographic criteria (age, gender) and systemic salvage treatment after progression on DTIC were used to select the closest match.

Statistical analysis

Differences between the groups were evaluated using an unpaired non-parametric t-test (Mann-Whitney U). Differences between pre- and post-vaccination were evaluated by a Wilcoxon's signed-ranks test, p-values are two-tailed. Kaplan-Meier probability estimates of PFS and OS were calculated, statistical differences between groups were determined by a log-rank test. Statistical significance was defined as $p<0.05$. SPSS19.0 was used for all analyses.

Results

Patient and vaccine characteristics

A total of 33 patients were enrolled (Supplementary Figure 1, available online). Three patients were considered as non-evaluable for immunological response, since they did not complete 3 vaccinations and DTH skin test because of rapid progressive disease. One patient did not meet eligibility criteria. Thus, a total of 29 stage III (n=7) and IV (n=22) melanoma patients completed at least one cycle of vaccinations. Group A (vaccination with MHC-I/II loaded DC) consisted of 15 patients (4 stage III and

11 stage IV), and group B (vaccination with MHC-I loaded DC) of 14 patients (3 stage III and 11 stage IV. Patient and treatment characteristics are summarized in Table 1.
The genotype of the *ex vivo* generated DC was determined by flow cytometry and in both groups the vaccine met the standard release criteria , with respect to expression of MHC-Class I and II, co-stimulatory molecules, CD83 and CCR7 (Supplementary Figure 2).

Table 1. Patient and treatment characteristics

	sex	age (yrs)	AJCC stage	N stage	M stage	LDH[a] (U/L)	number of mets	localization of mets	prior systemic treatment
IV-A-01	m	69	IV	N1b	M1a	384	>10	LN, skin	Cx
IV-A-03	m	57	IV	Nx	M1b	n.a.	n.a.	LN, lung	no
IV-A-04	m	51	IV	Nx	M1c	417	6	liver	no
IV-A-05	m	37	IV	Nx	M1a	253	3	skin	Ix[b]
IV-A-06	m	66	IV	Nx	M1c	345	6	adrenal gland, intestine	no
IV-A-07	m	38	IV	N1b	M1b	315	6	LN, skin, lung	no
IV-A-08	m	55	IV	N3	M1c	652	3	LN	no
IV-A-09	f	44	IIIa	N1a	M0	319	2	LN	no
IV-A-10	f	54	IV	Nx	M1c	432	2	liver, lung	no
IV-A-11	m	64	IV	Nx	M1b	361	3	lung	Ix [b]
IV-A-12	m	41	IV	N3	M1c	334	4	liver, LN, skin	Cx, Ix[c]
IV-A-13	f	55	IV	Nx	M1c	532	6	liver, LN, lung	no
IV-A-14	m	22	IIIb/c	N1b	M0	267	1	LN	no
IV-A-15	f	70	IIIb/c	N1b	M0	318	1	LN	no
IV-A-16	m	56	IIIc	N3	M0	346	9	LN	no
IV-A-17	m	59	IV	N2c	M1c	459	6	LN, lung, intestine	no
IV-B-01	m	48	IIIb/c	N2b	M0	298	3	LN	no
IV-B-02	f	57	IIIb/c	N1b	M0	403	1	LN	no
IV-B-03	m	54	IV	N2b	M1a	456	6	skin	no
IV-B-04	f	65	IV	Nx	M1b	469	2	lung	no
IV-B-05	m	50	IV	N3	M1c	1834	>10	liver, LN, lung, bone, skin	no
IV-B-06	m	50	IV	N3	M1c	735	6	liver, LN	no
IV-B-07	f	42	IV	Nx	M1c	487	>10	LN, lung, bone, skin	Cx
IV-B-08	m	43	IV	N2b	M1c	324	5	LN, lung, skin, bladder	no
IV-B-09	m	65	IV	N1b	M1c	449	6	liver, bone, skin	no
IV-B-10	f	37	IV	N1b	M1b	334	6	LN, lung, skin	no
IV-B-11	m	65	IV	Nx	M1c	640	>10	liver, LN, lung	Cx
IV-B-12	f	38	IV	Nx	M1b	387	>10	lung, skin	no
IV-B-13	m	30	IV	N3	M1c	464	3	LN, bone	Cx
IV-B-14	f	20	IV	N2a	M1b	293	5	LN, lung, skin	no
IV-B-15	m	69	IV	N2b	M1c	788	6	LN, lung, skin, adrenal gland	no
IV-B-16	f	46	IIIb	N2b	M0	292	3	LN	no

Abbreviations: LN, lymph nodes; Cx, chemotherapy; Ix, immunotherapy; n.a., not available; mets, metastases; [a]ULN = 450 U/L; [b] IFNγ adjuvant; [c] MAGE-A3 peptide vaccination

No grade 3 or 4 toxicities were observed (Table 2). In group A, 4 patients experienced grade 1 and 4 patients experienced grade 2 flu-like symptoms; 3 patients had grade 2 injection site reaction consisting of induration and redness. One patient developed vitiligo during the course of vaccination. In group B, 7 patients developed grade 1 flu-like symptoms and 6 patients had grade 1 injection site reactions. No grade 2 toxicities were observed in group B.

Immunological response to the control antigen KLH

To test the capacity of the patients in this study to generate an immune response we loaded the DC with the control antigen KLH. Most patients showed increased T cell proliferation upon stimulation with KLH, to comparable extent in both groups (Supplementary Figure 3, available online). Anti-KLH IgG antibodies were detected in 10 out of 15 patients tested in group A and 7 out of 14 patients in group B, to comparable levels. Anti-KLH IgA and IgM antibodies were detected in a minority of patients (Supplementary Figure 3, available online).

Table 2. Toxicity and clinical outcome.

	number of vaccinations	flu-like symptoms (CTC grade)	injection site reaction (CTC grade)	other immune related side effects (CTC grade)	Best response	PFS (months)	Salvage systemic treatment	OS (months)
IV-A-01	9	2	2	vitiligo	MR	39	no	119+
IV-A-03	6	0	0	no	SD	12	CIx	16
IV-A-04	3	1	0	no	SD	5	Cx	19
IV-A-05	6	0	0	no	SD	12	Cx	20
IV-A-06	3	1	0	no	PD	2	Cx	14
IV-A-07	3	1	0	no	SD	4	Cx	9
IV-A-08	1	0	0	no	PD	1	Cx	5
IV-A-09	9	2	0	no	NED	36	no	86+
IV-A-10	6	1	0	no	SD	14	unknown	51
IV-A-11	3	0	0	no	SD	7	no	14
IV-A-12	3	0	0	no	PD	1	no	14
IV-A-13	3	0	0	no	SD	5	Cx	20
IV-A-14	9	2	2	no	NED	83+	n.a.	83+
IV-A-15	3	0	0	no	NED	5	no	6
IV-A-16	9	2	2	no	NED	40	no	41
IV-A-17	3	0	0	no	PD	2	no	7
IV-B-01	9	0	1	no	NED	19	Cx	22
IV-B-02	9	1	1	no	NED	18	no	23
IV-B-03	3	0	0	no	PD	2	CIx	7
IV-B-04	3	1	0	no	PD	2	CIx	16
IV-B-05	3	1	0	no	PD	2	Cx	3
IV-B-06	3	0	0	no	PD	2	Cx	7
IV-B-07	3	0	0	no	PD	1	no	3
IV-B-08	3	1	0	no	PD	4	Cx	7
IV-B-09	3	0	1	no	PD	2	Cx	6
IV-B-10	3	0	0	no	SD	6	Cx	12
IV-B-11	3	0	1	no	SD	5	no	9
IV-B-12	3	0	0	no	PD	2	no	4
IV-B-13	3	1	0	no	PD	3	no	3
IV-B-14	3	0	1	no	SD	8	no	46
IV-B-15	3	1	0	no	PD	2	no	3
IV-B-16	9	1	1	no	NED	69+	n.a.	69+

Abbreviations: MR, mixed response; SD, stable disease; PD, progressive disease; NED, no evidence of disease; Cx, chemotherapy; CIx, chemoimmunotherapy; n.a., not available

Tumor-specific CD8$^+$ T cell responses in skin test infiltrating lymphocyte (SKIL) cultures

In group A, 7 out of 14 patients tested showed tetramer-positive CD8$^+$ T cells against at least 1 epitope and 3 patients had tetramer-positive CD8$^+$ T cells against multiple epitopes present in SKIL cultures. In group B this was 6 and 5 out of 14 patients, respectively (Figure 1).

In order to test the functionality of TAA-specific CD8$^+$ T cells, we measured cytokine production upon *in vitro* challenge with either peptide pulsed T2 cells or a gp100 and tyrosinase expressing HLA-A*02:01positive melanoma cell line (Figure 1). In 4 out of 11 patients tested in group A, we observed increased levels of IFNγ production upon challenge with the melanoma cell line, indicative of development of high affinity CTL which maintain tumor reactivity in a suppressive microenvironment. In contrast, in group B, antigen-specific IFNγ production was measured in 6 out of 6 patients tested, but only one patient maintained IFNγ production upon encounter of the melanoma cell line, suggesting that most T cells developed peptide specificity but cannot recognize naturally processed tumor antigen. In two patients, IV-A-05 and IV-A-07, the cytokine production was dominated by IL-5 (Figure 1).

Tumor-specific CD4$^+$ T cell responses in SKIL cultures

Similarly, we analyzed SKIL cultures for the presence of TAA-specific CD4$^+$ T cells in group A. In 4 out of 10 patients tested with cytokine bead assays, we observed specific IFNγ production to stimulation; in 3 patients (A-01, A-06 and A-16) to both gp100 and tyrosinase and 2 patients (A-09 and A-10) to

one TAA. Interestingly, in 4 out of 6 patients with a CD4$^+$ T cell response in either peripheral blood or in SKIL cultures, concurrent TAA-specific CD8$^+$ T cells were detected.

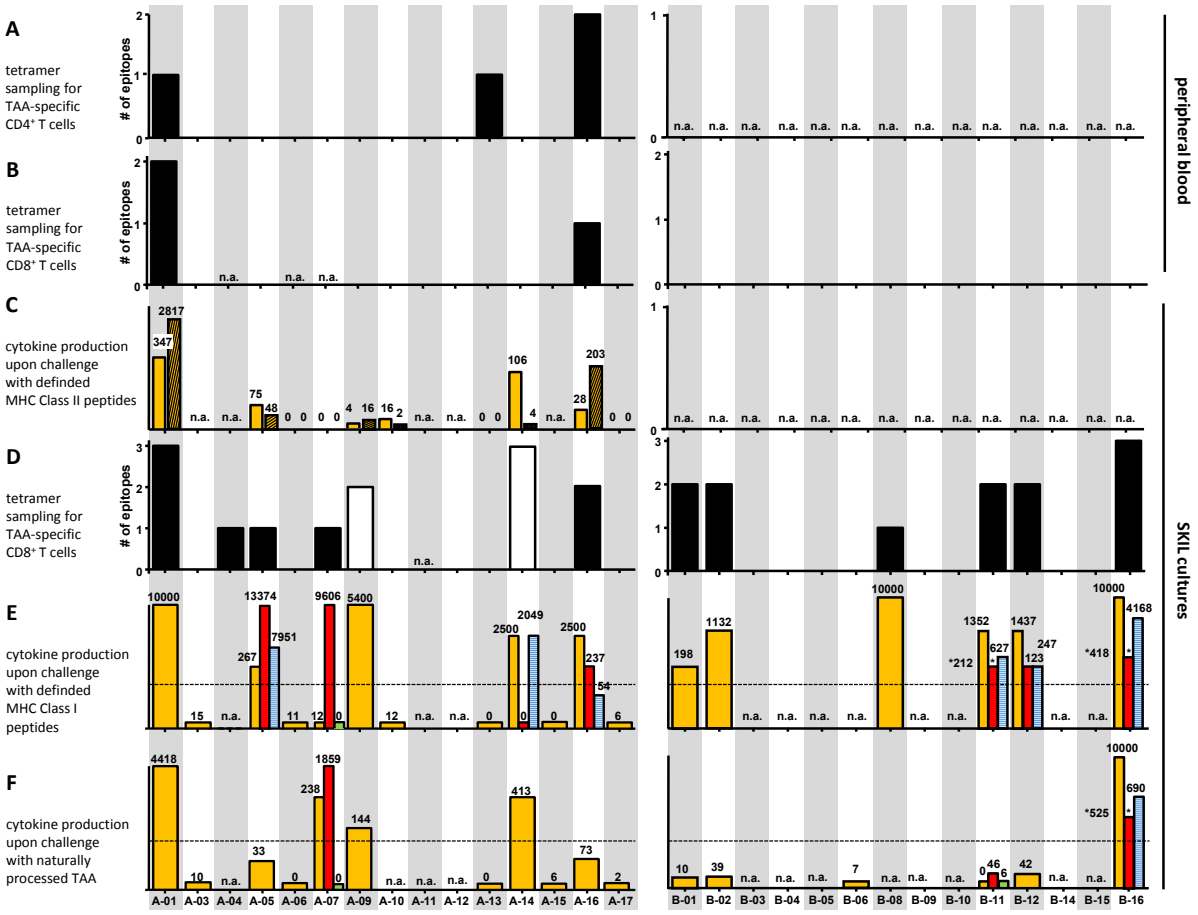

Figure 1. Tumor specific immune responses upon vaccination with MHC-I or MHC-I/II loaded dendritic cell vaccination. (A) Tetramer screening for vaccine induced CD4$^+$ T cell responses in peripheral blood. (B) Tetramer screening for vaccine induced CD8$^+$ T cell responses in peripheral blood. (C) The production of IFNγ in SKIL cultures upon stimulation with gp100 (open light grey bars) or tyrosinase (hatched light grey bars). (D) Tetramer screening for vaccine induced CD8$^+$ T cell responses in SKIL cultures (open bars represent percentages of tetramerspecific T cell populations that did not meet the predefined criteria for positivity, but positive IFNγ production was measured upon stimulation with their cognate antigen). To test their functionality, TAA-specific CD8$^+$ T cells were challenged with specific epitopes presented by T2 cell line (E) or with naturally processed gp100 and tyrosinase presented by an allogeneic tumor cell line Mel 624 (F), cytokine production was measured (pg/ml). Figure explanation: n.a., not available; dashed line is cut-off value for positivity as defined in Materials and Methods, light grey bars represent IFNγ production upon challenge, dark grey bars represent IL-5 production upon challenge and dotted grey bars represent IL-2 production upon challenge, the Y-axis is not scaled; bar heights are for visualization only, actual cytokine-concentrations (pg/ml) are denoted on top of the bars.

Tumor-specific responses in peripheral blood

We detected TAA-specific CD8$^+$ T cells in 2 out of 12 patients tested in group A and none in group B (Figure 1). In 3 out of 13 patients tested in group A, we detected tetramer-positive CD4$^+$ T cells. In all three patients, TAA-specific CD4$^+$ T cells were characterized as CD25$^+$FoxP3$^-$ with maintained capacity to proliferate and produce IFNγ (Figure 2).

Clinical responses

Clinical responses are summarized in Table 2. The median PFS of stage III patients was 37 months (range 5 – 76), however their number is too limited to draw meaningful conclusions on the clinical response. For patients with distant metastatic disease we retrospectively compared survival data to carefully matched controls (Supplementary Table 1, available online). The median PFS in group A was

Table 3. Immunological responses in SKIL cultures and peripheral blood

	tetramer specific CD8⁺Tcellsin SKIL cultures						tetramer specific CD8⁺Tcells in blood						tetramer specific CD4⁺Tcells in blood				after re-stimulation			
	gp100-154		gp100-280		tyrosinase		gp100-154		gp100-280		tyrosinase		gp100		tyrosinase		gp100		tyrosinase	
	% gated	% control	% gated	% control	% gated	% control	% gated	% control	% gated	% control	% gated	% control	% gated	% control	% gated	% control	% gated	% control	% gated	% control
group A																				
IV-A-01	4,18	0,05	0,70	0,02	10,9	0,20	0,09	0,00	-	-	0,08	0,00	- [a]	-	0,12	0,02	-	-	0,37	0,12
IV-A-03	-	-	-	-	-	-	-	-	-	-	-	-	-	-	-	-	-	-	-	-
IV-A-04	0,99	0,17	-	-	-	-	n.a.	n.a.	n.a.	n.a.	n.a.	n.a.	-	-	-	-	-	-	-	-
IV-A-05	0,20	0,00	-	-	-	-	-	-	-	-	-	-	-	-	-	-	-	-	-	-
IV-A-06	-	-	-	-	-	-	n.a.	n.a.	n.a.	n.a.	n.a.	n.a.	-	-	-	-	-	-	-	-
IV-A-07	0,04	0,02	-	-	-	-	n.a.	n.a.	n.a.	n.a.	n.a.	n.a.	-	-	-	-	-	-	-	-
IV-A-09	- [a]	-	-	-	- [a]	-	-	-	-	-	-	-	-	-	- [a]	-	-	-	-	-
IV-A-10	-	-	-	-	-	-	-	-	-	-	-	-	- [a]	-	-	-	-	-	-	-
IV-A-11	n.a.	n.a.	n.a.	n.a.	n.a.	n.a.	-	-	-	-	-	-	-	-	-	-	-	-	-	-
IV-A-12	-	-	-	-	-	-	-	-	-	-	-	-	-	-	-	-	-	-	-	-
IV-A-13	-	-	-	-	-	-	-	-	-	-	-	-	-	-	0,02	0,00	-	-	2,74	0,07
IV-A-14	0,44	0,00	- [a]	-	- [a]	-	-	-	-	-	-	-	-	-	-	-	-	-	-	-
IV-A-15	-	-	-	-	-	-	-	-	-	-	-	-	-	-	-	-	-	-	-	-
IV-A-16	1,80	0,04			0,41	0,06	10,37	1,18	-	-	-	-	0.1	0,02	0,08	0,02	3,03	0,3	0,45	0,01
IV-A-17	-	-	-	-	-	-	-	-	-	-	-	-	-	-	-	-	-	-	-	-
group B																				
IV-B-01	1,60	0,17	0,40	0,17	-	-	-	-	-	-	-	-	n.a.	n.a.	n.a.	n.a.	n.a.	n.a.	n.a.	n.a.
IV-B-02	0,25	0,09	0,43	0,09	-	-	-	-	-	-	-	-	n.a.	n.a.	n.a.	n.a.	n.a.	n.a.	n.a.	n.a.
IV-B-03	-	-	-	-	-	-	-	-	-	-	-	-	n.a.	n.a.	n.a.	n.a.	n.a.	n.a.	n.a.	n.a.
IV-B-04	-	-	-	-	-	-	-	-	-	-	-	-	n.a.	n.a.	n.a.	n.a.	n.a.	n.a.	n.a.	n.a.
IV-B-05	-	-	-	-	-	-	-	-	-	-	-	-	n.a.	n.a.	n.a.	n.a.	n.a.	n.a.	n.a.	n.a.
IV-B-06	-	-	-	-	-	-	-	-	-	-	-	-	n.a.	n.a.	n.a.	n.a.	n.a.	n.a.	n.a.	n.a.
IV-B-08	-	-	0,09	0,01	-	-	-	-	-	-	-	-	n.a.	n.a.	n.a.	n.a.	n.a.	n.a.	n.a.	n.a.
IV-B-09	-	-	-	-	-	-	-	-	-	-	-	-	n.a.	n.a.	n.a.	n.a.	n.a.	n.a.	n.a.	n.a.
IV-B-10	-	-	-	-	-	-	-	-	-	-	-	-	n.a.	n.a.	n.a.	n.a.	n.a.	n.a.	n.a.	n.a.
IV-B-11	0,35	0,07	0,36	0,07	-	-	-	-	-	-	-	-	n.a.	n.a.	n.a.	n.a.	n.a.	n.a.	n.a.	n.a.
IV-B-12	0,45	0,01	-	-	0,12	0,02	-	-	-	-	-	-	n.a.	n.a.	n.a.	n.a.	n.a.	n.a.	n.a.	n.a.
IV-B-13	-	-	-	-	-	-	-	-	-	-	-	-	n.a.	n.a.	n.a.	n.a.	n.a.	n.a.	n.a.	n.a.
IV-B-14	-	-	-	-	-	-	-	-	-	-	-	-	n.a.	n.a.	n.a.	n.a.	n.a.	n.a.	n.a.	n.a.
IV-B-15	-	-	-	-	-	-	-	-	-	-	-	-	n.a.	n.a.	n.a.	n.a.	n.a.	n.a.	n.a.	n.a.
IV-B-16	0,34	0,01	2,52	0,01	0,05	0,01	-	-	-	-	-	-	n.a.	n.a.	n.a.	n.a.	n.a.	n.a.	n.a.	n.a.

[a] The percentages of tetramer-positive cells did not meet the predefined criteria for positivity, nevertheless positive levels of cytokines were measured upon stimulation with their cognate antigen.

significantly improved compared to controls, with 5.0 months versus 2.8 months (p=0.0089), Hazard Ratio (HR) 0.39 (95%CI 0.19 – 0.79) (Figure 3A). There was no significant difference in median PFS between patients vaccinated in group B versus matched controls; 2.0 months versus 2.5 months (p = 0.891), HR 1.05 (95%CI 0.52 – 2.14).

With regard to overall survival, patients in group A showed increased 1-year survival rates as compared to matched controls, 80% versus 36%. Median OS was improved, 15.0 months compared to 8.3 months for matched historic controls (p=0.089), HR 0.57 (95%CI 0.30 – 1.09). In comparison, patients in group B did not show improved 1-year survival rates nor median OS over DTIC; 27% versus 36% and 7.0 months versus 7.9 months (p=0.202), HR 1.32 (95%CI 0.64 – 2.71).

In group A, the presence of vaccine-specific CD4+ T cell responses in peripheral blood or SKIL cultures was not significantly associated with OS: HR 0.21 (95%CI 0.03 – 1.70, p=0.144). In group A and B, the presence of vaccine-specific CD8+ T cell responses in peripheral blood or SKIL cultures was not associated with OS: HR 0.65 (95%CI 0.19 – 2.29, p=0.507) and HR 1.16 (95%CI 0.30 – 4.50, p=0.834).

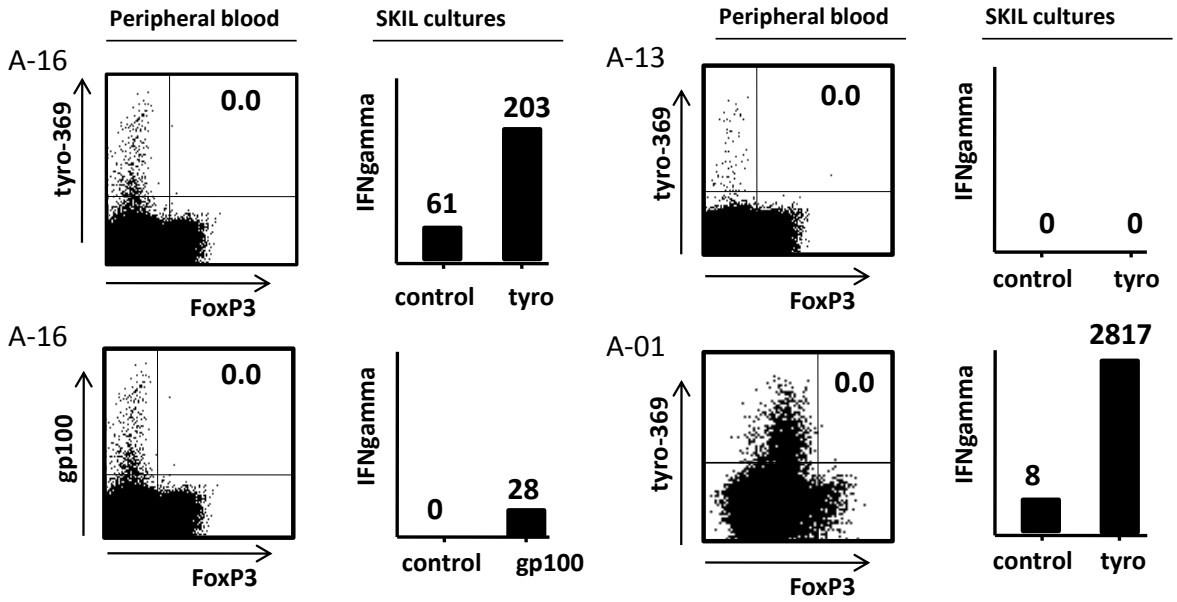

Figure 2. Vaccine-induced CD4$^+$ T cells are not regulatory T cells. In 3 patients, TAA-specific CD4$^+$ T cells were detected in peripheral blood, recognizing 1 or more MHC Class II epitopes (Table 3). A flowcytometric analysis was performed to further characterize these cells. In all patients, the tetramer-positive cells were CD25$^+$FoxP3$^-$, maintained their proliferative capacity (Table 3) and produced marked levels of IFNγ upon restimulation.

Discussion

The efficacy of DC-based vaccination in cancer patients has significantly improved over the past decade, as several vaccine parameters have been optimized. We initiated the current study to compare immunological responses to DC pulsed with MHC-I restricted melanoma epitopes alone or MHC-I/II restricted epitopes. Upon vaccination with MHC-I/II loaded DC we detected highly functional vaccine-specific CD8$^+$ T cells. These cells maintained their IFNγ production even in a suppressive milieu of an IL-10 producing melanoma cell-line. Interestingly, only in patients vaccinated with MHC-I/II loaded DC we found circulating TAA-specific CD8$^+$ T cells. The induction of regulatory CD4$^+$ T cells is of particular concern in immunotherapies targeting MHC-II restricted antigens (31, 32). We demonstrated in all patients that TAA-specific CD4$^+$ T cells were FoxP3 negative which is in line with the high proliferative capacity and production of significant levels of IFNγ. Furthermore, in most patients we detected concomitant TAA-specific CD8$^+$ T cell responses. These findings strongly support the hypothesis that co-activating TAA-specific CD4$^+$ T helper cells augments the induction and proliferation of TAA-specific CD8$^+$ T cells.

Our findings are in line with previous reports on vaccination with MHC-I/II loaded DC (33-36), but direct comparison is hampered by the large variation in study protocols. This is the first paper that evaluates the immunological responses upon vaccination with MHC-I/II loaded DC in direct comparison to MHC-I loaded DC.

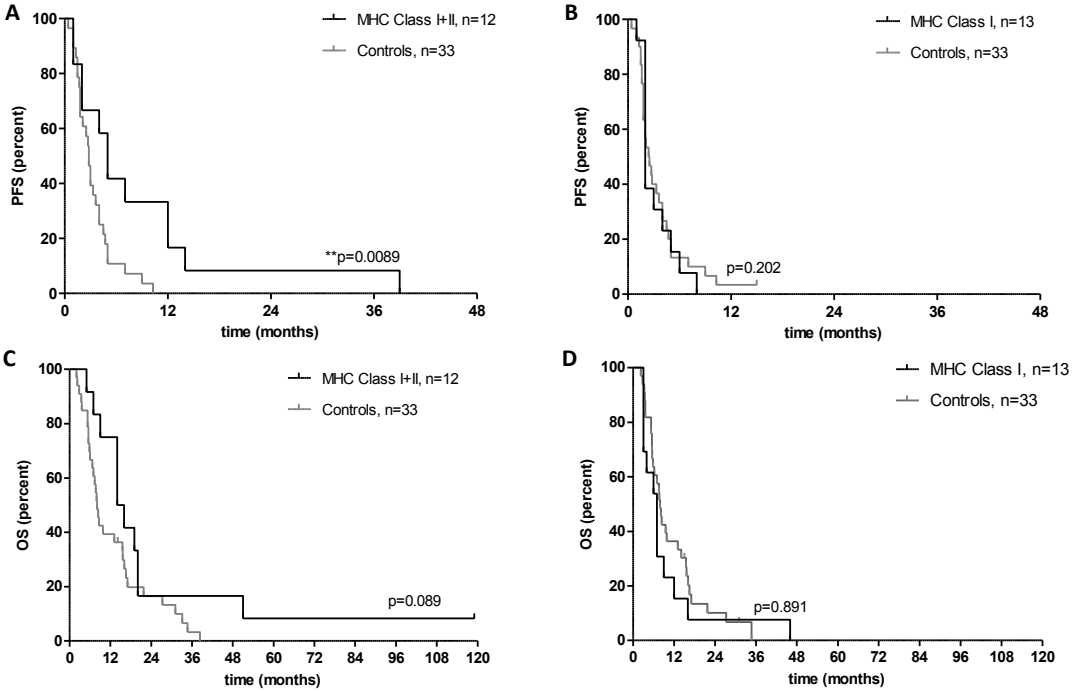

Figure 3. Improved clinical responses upon vaccination with MHC Class I and II loaded DC. In patients with distant metastatic or irresectable melanoma (stage IV), vaccination with MHC/I-II loaded DC resulted in significantly improved PFS compared to controls (A). Vaccination with MHC-I loaded DC only did not improve PFS (B). Median OS was improved for vaccination with MHC-I/II loaded DC compared to DTIC chemotherapy (C). Accordingly, one year survival rates improved upon vaccination with MHC-I/II loaded DC. Vaccination with MHC- loaded DC did not result in improved OS (D).

However, our findings are in contrast to previously published trials on peptide vaccination in melanoma patients (37-39). In a recent randomized multicentre trial Slingluff et al. report on 167 stage IIB to IV melanoma patients vaccinated with either MHC-I or MHC-I/II restricted peptides, with or without cyclophosphamide pretreatment (37). In this trial, the inclusion of melanoma-associated helper peptides paradoxically decreased $CD8^+$ T cell responses. The discrepancy with our findings might be explained by the intradermal/subcutaneous delivery of peptides, since it might target different DC subsets, compared to direct delivery of antigen-loaded DC into lymph nodes. To our opinion, controlling antigen presentation is crucial since the induction of $CD4^+$ T cells with improved functionality depends on density and potency of peptide-MHC complexes (40, 41).

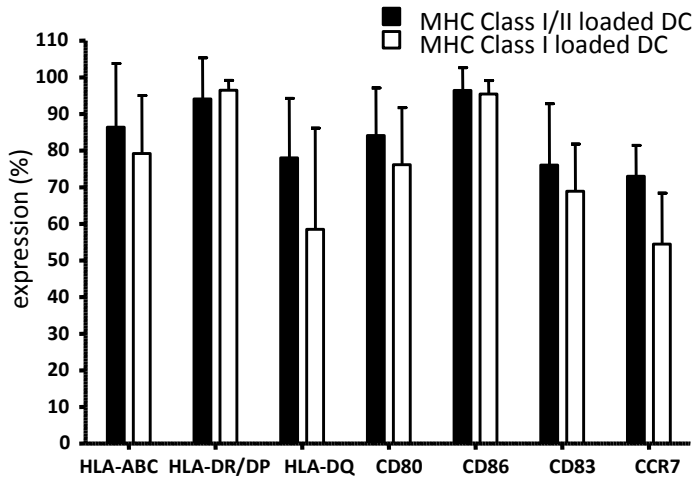

Supplementary Figure 2. Vaccine characteristics. The expression of surface markers, measured by flow cytometry on mature DCs for the first vaccination, is shown. Data are represented as percentage of cells (mean with SD) expressing the surface marker. Analyses was performed with one-way ANOVA with post-hoc (Dunn's Multiple Comparison Test) comparison of 2 groups per surface marker. Abbreviations: n.s. denotes not significant.

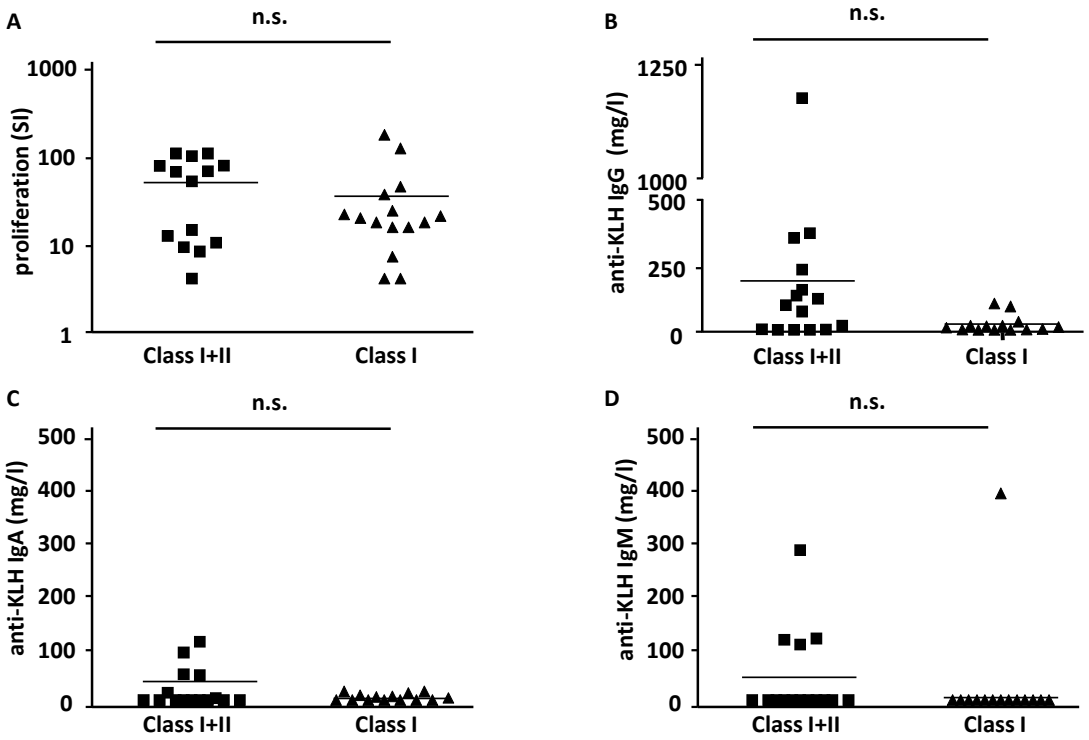

Supplementary Figure 3. KLH specific responses. KLH-specific T-cell proliferation was analyzed before vaccination and after each DC vaccination (A), maximum responses are depicted. KLH-specific IgG (B), IgA (C) and IgM (D) antibodies were quantitatively measured in sera after each DC vaccination during the treatment course, maximum responses are depicted. Per isotype, each dot represents 1 patient. Horizontal lines represent averages per group. Abbreviations: n.s. denotes not significant.

Although in a previous vaccination study in 108 melanoma patients no benefit was found for HLA-DR4 expression (42), we cannot exclude that this haplotype forms a possible confounding bias in our study when interpreting the clinical data. In order to obtain more insight in the clinical efficacy of our DC vaccination, we compared the clinical outcome to carefully selected control patients treated with standard DTIC chemotherapy. Comparison with control patients is based on the assumption that the observed historical control response rate is equal to the true control response rate (43). In this respect, survival rates of our matched controls treated with DTIC chemotherapy is comparable to the survival rates reported in recent large randomized trials using DTIC as comparative arm (44, 45). The observed clinical responses are in line with the trend in the differences in the immunological responses. Only patients who received MHC-I/II loaded DC showed increased PFS and 1-year overall survival as compared to matched control patients. Strikingly, the presence of circulating TAA-specific $CD4^+$ or $CD8^+$ T cells or IFNγ production upon challenge with naturally processed antigens was clearly linked to a more beneficial clinical course of disease (Figure 1 and Table 1). It is tempting to speculate that part of the clinical response is related to action of the $CD4^+$ T helper cell at the tumor site itself. $CD4^+$ T helper cells have been demonstrated to play an important role in assisting infiltration of the tumor by CTLs and can exert a direct cytotoxic effect themselves as well ((46, 47). In 2006, a randomized trial comparing MHC-I/II loaded DC vaccination to DTIC chemotherapy was reported (42). This study failed to demonstrate improved clinical outcome to DC-based vaccination. As discussed previously (48), the exploited DC-based vaccine in this study was far from optimized. Due to the subcutaneous delivery and low number of injected DC, it is questionable how many antigen-loaded DC were available for immune induction. Furthermore, injected DC mostly had a low mature genotype and lacked a non-specific T helper antigen, so their immune stimulatory capacity is suboptimal (48). Our study suggests that optimized DC-based vaccination harbors more potential than has been concluded from this study. The importance of antigen-specific $CD4^+$ T cell stimulus by the same antigen-presenting cell that present tumor-antigen in MHC Class I to $CD8^+$ T cells, has been

demonstrated in previous studies (49, 50). Optimal $CD4^+$ T cell help might mediated by CD40-CD40L interaction and cytokines like IL-2. These studies support our findings of superior immune responses in patients vaccinated with DC loaded with tumor-antigen in both MHC Class I and II. Finally, the current vaccination protocol might be further improved by overcoming the disadvantages of peptide-pulsing of DC; e.g. the dissociation of peptides from MHC complexes and the lack of post-translational modification by the use of mRNA-electroporation (51, 52). This method has shown to result in mature and migratory DCs expressing the encoded antigens *in situ* (52).
In conclusion, our results show that targeting $CD4^+$ T helper cells with DC pulsed with both MHC Class I and II restricted epitopes enhances vaccine-specific immunological responses.

Supplementary Table 1. Matched controls.

		control group A		**control group B**	
		n=33	%	n=33	%
sex	male	20	61	21	64
	female	13	39	12	36
age	median (range)	57 (31 - 77)		57 (31 - 74)	
M stage	M1a	5	15	3	9
	M1b	9	27	12	36
	M1c	19	58	18	55
nr of mets	<5	3	9	3	9
	>5	19	58	20	61
	n.a.	11	33	10	30
nr of organs	1	10	30	12	36
	>1	23	70	21	64
LDH at baseline	<ULN	18	55	14	42
	>ULN	9	27	11	33
	n.a.	6	18	8	24
prior systemic treatment[b]	immunotherapy[a]	9	27	9	27
	chemotherapy	0	0	0	0
	none	16	48	16	48
	n.a.	8	24	8	24
salvage systemic treatment[b]	immunotherapy	7	21	9	27
	chemotherapy	3	9	2	6
	chemoimmunotherapy	1	3	1	3
	none	17	52	16	48
	n.a.	5	15	5	15

[a] in adjuvant setting; [b] multiple entries possible

References

1. Steinman RM, Pope M. Exploiting dendritic cells to improve vaccine efficacy. J Clin Invest. 2002;109:1519-26.
2. Lesterhuis WJ, Aarntzen EH, De Vries IJ, Schuurhuis DH, Figdor CG, Adema GJ, et al. Dendritic cell vaccines in melanoma: from promise to proof? Crit Rev Oncol Hematol. 2008;66:118-34.
3. Schadendorf D, Ugurel S, Schuler-Thurner B, Nestle FO, Enk A, Brocker EB, et al. Dacarbazine (DTIC) versus vaccination with autologous peptide-pulsed dendritic cells (DC) in first-line treatment of patients with metastatic melanoma: a randomized phase III trial of the DC study group of the DeCOG. Ann Oncol. 2006;17:563-70.
4. Rosenberg SA, Yang JC, Restifo NP. Cancer immunotherapy: moving beyond current vaccines. Nat Med. 2004;10:909-15.
5. Wang RF, Rosenberg SA. Human tumor antigens for cancer vaccine development. Immunol Rev. 1999;170:85-100.
6. Schuler-Thurner B, Dieckmann D, Keikavoussi P, Bender A, Maczek C, Jonuleit H, et al. Mage-3 and influenza-matrix peptide-specific cytotoxic T cells are inducible in terminal stage HLA-A2.1+ melanoma patients by mature monocyte-derived dendritic cells. J Immunol. 2000;165:3492-6.
7. Bedrosian I, Mick R, Xu S, Nisenbaum H, Faries M, Zhang P, et al. Intranodal administration of peptide-pulsed mature dendritic cell vaccines results in superior CD8+ T-cell function in melanoma patients. J Clin Oncol. 2003;21:3826-35.
8. de Vries IJ, Lesterhuis WJ, Scharenborg NM, Engelen LP, Ruiter DJ, Gerritsen MJ, et al. Maturation of dendritic cells is a prerequisite for inducing immune responses in advanced melanoma patients. Clin Cancer Res. 2003;9:5091-100.
9. Paczesny S, Banchereau J, Wittkowski KM, Saracino G, Fay J, Palucka AK. Expansion of melanoma-specific cytolytic CD8+ T cell precursors in patients with metastatic melanoma vaccinated with CD34+ progenitor-derived dendritic cells. J Exp Med. 2004;199:1503-11.
10. Mackensen A, Herbst B, Chen JL, Kohler G, Noppen C, Herr W, et al. Phase I study in melanoma patients of a vaccine with peptide-pulsed dendritic cells generated in vitro from CD34(+) hematopoietic progenitor cells. Int J Cancer. 2000;86:385-92.
11. Thurner B, Haendle I, Roder C, Dieckmann D, Keikavoussi P, Jonuleit H, et al. Vaccination with mage-3A1 peptide-pulsed mature, monocyte-derived dendritic cells expands specific cytotoxic T cells and induces regression of some metastases in advanced stage IV melanoma. J Exp Med. 1999;190:1669-78.
12. Berard F, Blanco P, Davoust J, Neidhart-Berard EM, Nouri-Shirazi M, Taquet N, et al. Cross-priming of naive CD8 T cells against melanoma antigens using dendritic cells loaded with killed allogeneic melanoma cells. J Exp Med. 2000;192:1535-44.
13. Baxevanis CN, Voutsas IF, Tsitsilonis OE, Gritzapis AD, Sotiriadou R, Papamichail M. Tumor-specific CD4+ T lymphocytes from cancer patients are required for optimal induction of cytotoxic T cells against the autologous tumor. J Immunol. 2000;164:3902-12.
14. Janssen EM, Lemmens EE, Wolfe T, Christen U, von Herrath MG, Schoenberger SP. CD4+ T cells are required for secondary expansion and memory in CD8+ T lymphocytes. Nature. 2003;421:852-6.
15. Faiola B, Doyle C, Gilboa E, Nair S. Influence of CD4 T cells and the source of major histocompatibility complex class II-restricted peptides on cytotoxic T-cell priming by dendritic cells. Immunology. 2002;105:47-55.
16. Rodriguez T, Mendez R, Del Campo A, Aptsiauri N, Martin J, Orozco G, et al. Patterns of constitutive and IFN-gamma inducible expression of HLA class II molecules in human melanoma cell lines. Immunogenetics. 2007;59:123-33.
17. Ruiter DJ, Mattijssen V, Broecker EB, Ferrone S. MHC antigens in human melanomas. Semin Cancer Biol. 1991;2:35-45.
18. Kierstead LS, Ranieri E, Olson W, Brusic V, Sidney J, Sette A, et al. gp100/pmel17 and tyrosinase encode multiple epitopes recognized by Th1-type CD4+T cells. Br J Cancer. 2001;85:1738-45.
19. Schultz ES, Chapiro J, Lurquin C, Claverol S, Burlet-Schiltz O, Warnier G, et al. The production of a new MAGE-3 peptide presented to cytolytic T lymphocytes by HLA-B40 requires the immunoproteasome. J Exp Med. 2002;195:391-9.
20. Cochlovius B, Stassar M, Christ O, Raddrizzani L, Hammer J, Mytilineos I, et al. In vitro and in vivo induction of a Th cell response toward peptides of the melanoma-associated glycoprotein 100 protein selected by the TEPITOPE program. J Immunol. 2000;165:4731-41.
21. de Vries IJ, Bernsen MR, Lesterhuis WJ, Scharenborg NM, Strijk SP, Gerritsen MJ, et al. Immunomonitoring tumor-specific T cells in delayed-type hypersensitivity skin biopsies after dendritic cell vaccination correlates with clinical outcome. J Clin Oncol. 2005;23:5779-87.
22. Figdor CG, de Vries IJ, Lesterhuis WJ, Melief CJ. Dendritic cell immunotherapy: mapping the way. Nat Med. 2004;10:475-80.
23. Bakker AB, Schreurs MW, Tafazzul G, de Boer AJ, Kawakami Y, Adema GJ, et al. Identification of a novel peptide derived from the melanocyte-specific gp100 antigen as the dominant epitope recognized by an HLA-A2.1-restricted anti-melanoma CTL line. Int J Cancer. 1995;62:97-102.
24. Cox AL, Skipper J, Chen Y, Henderson RA, Darrow TL, Shabanowitz J, et al. Identification of a peptide recognized by five melanoma-specific human cytotoxic T cell lines. Science. 1994;264:716-9.
25. Li K, Adibzadeh M, Halder T, Kalbacher H, Heinzel S, Muller C, et al. Tumour-specific MHC-class-II-restricted responses after in vitro sensitization to synthetic peptides corresponding to gp100 and Annexin II eluted from melanoma cells. Cancer Immunol Immunother. 1998;47:32-8.
26. Topalian SL, Gonzales MI, Parkhurst M, Li YF, Southwood S, Sette A, et al. Melanoma-specific CD4+ T cells recognize nonmutated HLA-DR-restricted tyrosinase epitopes. J Exp Med. 1996;183:1965-71.

27. Aarntzen EH, de Vries IJ, Goertz JH, Beldhuis-Valkis M, Brouwers HM, van de Rakt MW, et al. Humoral anti-KLH responses in cancer patients treated with dendritic cell-based immunotherapy are dictated by different vaccination parameters. Cancer Immunol Immunother. 2012.
28. Lesterhuis WJ, de Vries IJ, Schuurhuis DH, Boullart AC, Jacobs JF, de Boer AJ, et al. Vaccination of colorectal cancer patients with CEA-loaded dendritic cells: antigen-specific T cell responses in DTH skin tests. Ann Oncol. 2006;17:974-80.
29. de Vries IJ, Bernsen MR, Lesterhuis WJ, Scharenborg NM, Strijk SP, Gerritsen MJ, et al. Immunomonitoring tumor-specific T cells in delayed-type hypersensitivity skin biopsies after dendritic cell vaccination correlates with clinical outcome. J Clin Oncol. 2005;23:5779-87.
30. Balch CM, Gershenwald JE, Soong SJ, Thompson JF, Atkins MB, Byrd DR, et al. Final version of 2009 AJCC melanoma staging and classification. J Clin Oncol. 2009;27:6199-206.
31. Correll A, Tuettenberg A, Becker C, Jonuleit H. Increased regulatory T-cell frequencies in patients with advanced melanoma correlate with a generally impaired T-cell responsiveness and are restored after dendritic cell-based vaccination. Exp Dermatol.19:e213-21.
32. de Vries IJ, Castelli C, Huygens C, Jacobs JF, Stockis J, Schuler-Thurner B, et al. Frequency of circulating Tregs with demethylated FOXP3 intron 1 in melanoma patients receiving tumor vaccines and potentially Treg-depleting agents. Clin Cancer Res.17:841-8.
33. Schuler-Thurner B, Schultz ES, Berger TG, Weinlich G, Ebner S, Woerl P, et al. Rapid induction of tumor-specific type 1 T helper cells in metastatic melanoma patients by vaccination with mature, cryopreserved, peptide-loaded monocyte-derived dendritic cells. J Exp Med. 2002;195:1279-88.
34. Trakatelli M, Toungouz M, Blocklet D, Dodoo Y, Gordower L, Laporte M, et al. A new dendritic cell vaccine generated with interleukin-3 and interferon-beta induces CD8+ T cell responses against NA17-A2 tumor peptide in melanoma patients. Cancer Immunol Immunother. 2006;55:469-74.
35. Lesimple T, Neidhard EM, Vignard V, Lefeuvre C, Adamski H, Labarriere N, et al. Immunologic and clinical effects of injecting mature peptide-loaded dendritic cells by intralymphatic and intranodal routes in metastatic melanoma patients. Clin Cancer Res. 2006;12:7380-8.
36. Schultz ES, Schuler-Thurner B, Stroobant V, Jenne L, Berger TG, Thielemanns K, et al. Functional analysis of tumor-specific Th cell responses detected in melanoma patients after dendritic cell-based immunotherapy. J Immunol. 2004;172:1304-10.
37. Slingluff Jr. CL, Petroni GR, Chianese-Bullock KA, Smolkin ME, Ross MI, Haas NB, et al. Randomized multicenter trial of the effects of melanoma-associated helper peptides and cyclophosphamide on the immunogenicity of a multipeptide melanoma vaccine. J Clin Oncol.29:2924-32.
38. Phan GQ, Touloukian CE, Yang JC, Restifo NP, Sherry RM, Hwu P, et al. Immunization of patients with metastatic melanoma using both class I- and class II-restricted peptides from melanoma-associated antigens. J Immunother. 2003;26:349-56.
39. Rosenberg SA, Sherry RM, Morton KE, Yang JC, Topalian SL, Royal RE, et al. Altered CD8(+) T-cell responses when immunizing with multiepitope peptide vaccines. J Immunother. 2006;29:224-31.
40. Erskine CL, Krco CJ, Hedin KE, Borson ND, Kalli KR, Behrens MD, et al. MHC Class II Epitope Nesting Modulates Dendritic Cell Function and Improves Generation of Antigen-Specific CD4 Helper T Cells. J Immunol.187:316-24.
41. Skokos D, Shakhar G, Varma R, Waite JC, Cameron TO, Lindquist RL, et al. Peptide-MHC potency governs dynamic interactions between T cells and dendritic cells in lymph nodes. Nat Immunol. 2007;8:835-44.
42. Schadendorf D, Ugurel S, Schuler-Thurner B, Nestle FO, Enk A, Brocker EB, et al. Dacarbazine (DTIC) versus vaccination with autologous peptide-pulsed dendritic cells (DC) in first-line treatment of patients with metastatic melanoma: a randomized phase III trial of the DC study group of the DeCOG. Ann Oncol. 2006;17:563-70.
43. Lee JJ, Tseng C. Uniform power method for sample size calculation in historical control studies with binary response. Control Clin Trials. 2001;22:390-400.
44. Robert C, Thomas L, Bondarenko I, O'Day S, M DJ, Garbe C, et al. Ipilimumab plus dacarbazine for previously untreated metastatic melanoma. N Engl J Med.364:2517-26.
45. Chapman PB, Hauschild A, Robert C, Haanen JB, Ascierto P, Larkin J, et al. Improved survival with vemurafenib in melanoma with BRAF V600E mutation. N Engl J Med. 2011;364:2507-16.
46. Wong SB, Bos R, Sherman LA. Tumor-specific CD4+ T cells render the tumor environment permissive for infiltration by low-avidity CD8+ T cells. J Immunol. 2008;180:3122-31.
47. Wang LX, Shu S, Disis ML, Plautz GE. Adoptive transfer of tumor-primed, in vitro-activated, CD4+ T effector cells (TEs) combined with CD8+ TEs provides intratumoral TE proliferation and synergistic antitumor response. Blood. 2007;109:4865-76.
48. Lesterhuis WJ, Haanen JB, Punt CJ. Cancer immunotherapy - revisited. Nat Rev Drug Discov. 2011;10:591-600.
49. Bennett SR, Carbone FR, Karamalis F, Miller JF, Heath WR. Induction of a CD8+ cytotoxic T lymphocyte response by cross-priming requires cognate CD4+ T cell help. J Exp Med. 1997;186:65-70.
50. Ossendorp F, Mengede E, Camps M, Filius R, Melief CJ. Specific T helper cell requirement for optimal induction of cytotoxic T lymphocytes against major histocompatibility complex class II negative tumors. J Exp Med. 1998;187:693-702.
51. Van Tendeloo VF, Ponsaerts P, Lardon F, Nijs G, Lenjou M, Van Broeckhoven C, et al. Highly efficient gene delivery by mRNA electroporation in human hematopoietic cells: superiority to lipofection and passive pulsing of mRNA and to electroporation of plasmid cDNA for tumor antigen loading of dendritic cells. Blood. 2001;98:49-56.
52. Schuurhuis DH, Verdijk P, Schreibelt G, Aarntzen EH, Scharenborg N, de Boer A, et al. In situ expression of tumor antigens by messenger RNA-electroporated dendritic cells in lymph nodes of melanoma patients. Cancer Res. 2009;69:2927-34.

Vaccination with mRNA-electroporated dendritic cells induces robust tumor antigen-specific $CD4^+$ and $CD8^+$ T cell responses in stage III and IV melanoma patients

Aarntzen EH*

Schreibelt G*

Bol K

Lesterhuis WJ

Croockewit AJ

De Wilt JH

Van Rossum MM

Blokx WA

Jacobs JF

Duiveman-de Boer T

Schuurhuis DH

Mus R

Thielemans K

De Vries IJ

Figdor CG

Punt CJ

Adema GJ

* contributed equally

Clin Cancer Res. 2012;18(19):5460-70

Abstract

Electroporation of dendritic cells (DC) with mRNA encoding tumor associated antigens (TAA) has multiple advantages over peptide loading. We investigated the immunological and clinical responses to vaccination with mRNA-electroporated DC in stage III and IV melanoma patients. Twenty-six stage III HLA*02:01 melanoma patients scheduled for radical lymph node dissection (stage III) and 19 melanoma patients with irresectable locoregional or distant metastatic disease (referred to as stage IV) were included. Monocyte-derived DC, electroporated with mRNA encoding gp100 and tyrosinase, were pulsed with keyhole limpet hemocyanin (KLH) and administered intranodally. TAA-specific T cell responses were monitored in blood and skin-test infiltrating lymphocyte (SKIL) cultures. Comparable numbers of vaccine-induced $CD8^+$ and/or $CD4^+$ TAA-specific T cell responses were detected in SKIL cultures; 17/26 stage III patients and 11/19 stage IV patients. Strikingly, in this population, TAA-specific $CD8^+$ T cells that recognize multiple epitopes and produce elevated levels of IFNγ upon antigenic challenge in vitro, were significantly more often observed in stage III patients; 15/17 versus 3/11 stage IV patients, p=0.0033. In stage IV patients, one mixed and one partial response were documented. The presence or absence of IFNγ-producing TAA-specific $CD8^+$ T cells in stage IV patients was associated with marked difference in median OS of 24.1 months versus 11.0 months, respectively. Vaccination with mRNA-electroporated DC induces a broad repertoire of IFNγ producing TAA-specific $CD8^+$ and $CD4^+$ T cell responses, particularly in stage III melanoma patients.

Introduction

Dendritic cells (DC) are the most effective antigen-presenting cells (APC) of the immune system, highly capable of stimulating naïve T cells. Immunotherapy with *ex vivo*-generated autologous DC pulsed with tumor peptides has provided proof of concept in clinical trials (1). We, and others, have demonstrated that tumor-specific immune responses can be induced in both stage III and IV melanoma patients (1-5). Since objective clinical responses are observed in a minority of patients, further optimization of DC based immunotherapy is warranted. To date, the majority of clinical studies on DC based vaccinations have been performed with MHC class I restricted peptide-pulsed monocyte derived DC in patients with measurable distant metastatic disease. However, there are at least several theoretical disadvantages against these protocols, which might be improved to induce more effective and sustained immunological responses. First, the exploitation of MHC class I restricted peptide epitopes target $CD8^+$ cytotoxic T cells (CTL) only, without involving $CD4^+$ T helper cells to enhance and sustain anti-tumor CTL responses. Secondly, pulsing DC with peptide epitopes implicates the use of a given HLA type, with defined tumor associated antigens (TAA). Moreover, peptide-loaded DC expose the antigen only for a short period of time (6), since the peptides may readily dissociate from the MHC molecules (7). Importantly, peptide loading does not account for post-transcriptional modifications of peptide epitopes (8;9). One strategy to circumvent most of these disadvantages of peptide pulsing is electroporation with synthetic mRNA encoding TAA, resulting in endogenous synthesis of the complete TAA. It has been shown previously that electroporation of DC with mRNA is effective and safe (7;10;11). DCs retain their phenotype and maturation potential upon electroporation, as well as their migratory capacities (10;12). Electroporated DC express TAA antigens, encoded by the electroporated mRNA and induce specific $CD8^+$ T cell responses in melanoma patients (10). Importantly, since mRNA lacks the potential to integrate into the host genome, it obviates safety concerns associated with gene therapy trials. It is now widely recognized that high tumorload in end-stage cancer patients often induces local, or even systemic, immune suppression by the secretion of suppressive cytokines and attraction of regulatory T cells (13-15). This suppressive tumor microenvironment will hamper the effective anti-tumor responses. Melanoma patients with locoregional lymph node metastases are at high risk of relapse and currently no standard adjuvant treatment is available which results in overall survival benefit (16). Given the minimal burden of tumor; we hypothesized that vaccination of patients adjuvant to therapeutic radical lymph node dissection might enhance vaccine efficacy. In this study we investigated in detail the immunological responses to intranodal vaccination with monocyte-derived DC electroporated with mRNA encoding gp100 and tyrosinase in 2 cohorts of melanoma patients; with distant metastatic or irresectable locoregional disease following radical regional lymph node dissection.

Translational relevance

Electroporation of dendritic cells (DC) with mRNA encoding tumor associated antigens (TAA) has multiple advantages over the conventional peptide loading. The presentation of multiple naturally processed epitopes in both MHC Class I and II should broaden the repertoire of responding lymphocytes. We studied in detail the immunological response to vaccination with mRNA-electroporated DC in 2 cohorts of melanoma patients: as palliative treatment for distant or irresectable locoregional metastatic disease and as adjuvant treatment following radical dissection of regional lymph nodes. A wide spectrum of tumor-specific IFNγ producing $CD8^+$ T cells was detected, in particular in patients vaccinated in the adjuvant setting. Furthermore, vaccine-induced $CD4^+$ T cells were shown to be FoxP3 negative. In conclusion, vaccination with mRNA-electroporated DC successfully enhances anti-tumor cytotoxic T cell responses and appears to be a promising adjuvant treatment for stage III melanoma patients.

Patients and methods

Patient population

Melanoma patients with locoregional resectable disease (further referred to as stage III), before or within 2 months after radical dissection of regional lymph node metastases, and patients with irresectable locoregional or distant metastatic disease (further referred to as stage IV) were included. Additional inclusion criteria were HLA*02:01 phenotype, melanoma expressing the melanoma-associated antigens gp100 and tyrosinase, and WHO performance status 0 or 1. Patients with brain metastases, serious concomitant disease or a history of a second malignancy were excluded. The study was approved by our Institutional Review Board, and written informed consent was obtained from all patients. Clinical trial registration number is NCT00243529.

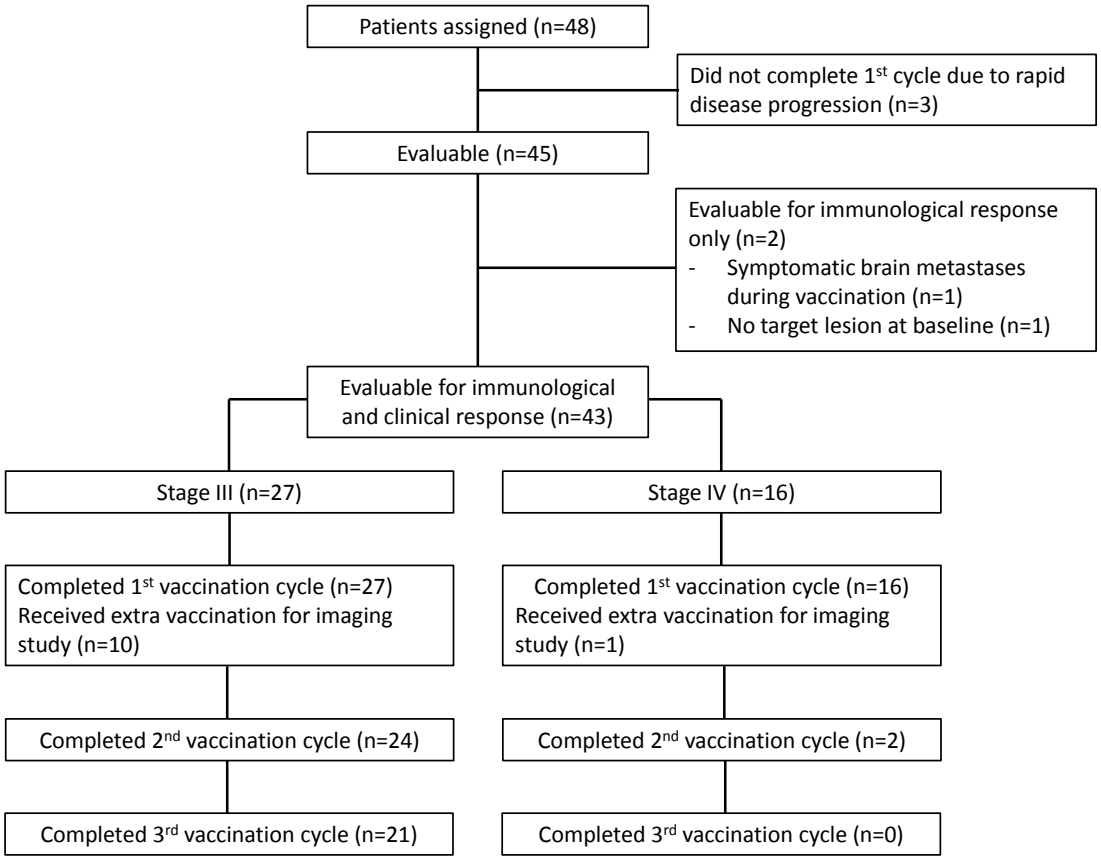

Supplementary Figure 1. CONSORT flowchart.

Study protocol

Patients received a DC vaccine intranodally, injected into a clinically tumor-free lymph node under ultrasound guidance. The DC vaccine consisted of autologous mature monocyte-derived DC electroporated with mRNA encoding for gp100 and tyrosinase protein, and pulsed with keyhole limped hemocyan (KLH) protein. Patients received three vaccinations with a biweekly interval. Ten patients received an extra vaccination 1 or 2 days before the radical lymph node dissection for additional imaging studies (*see Chapter 7*). One to two weeks after the last vaccination a skin test was performed. In absence of disease progression or recurrence, patients received a maximum of two maintenance series at 6-month intervals, each consisting of three biweekly intranodal vaccinations (Supplementary Figure 1). All vaccinations were administered between May 2006 and May 2010. Patients were considered evaluable when they had completed the first vaccination cycle. Vaccine-specific immune response was the primary endpoint, clinical response was a secondary endpoint in stage IV patients. Progression-free and overall survival were calculated from the time from apheresis to recurrence (for stage III patients) or progression (for stage IV patients), or death.

DC preparation and characterization

DC were generated from peripheral blood mononuclear cells (PBMC) prepared from leukapheresis products as described previously (17). After leukapheresis, part of the PBMC was used for the generation of monocyte-conditioned medium (MCM) (18). Plastic-adherent monocytes or monocytes isolated by centrifugal elutriation were cultured for 5-7 days in X-VIVO 15^{TM} medium (BioWhittaker, Walkersville, Maryland) supplemented with 2% pooled human serum (HS) (Bloodbank Rivierenland, Nijmegen, The Nethterlands), IL-4 (500 U/ml) and GM-CSF (800 U/ml) (both from Cellgenix, Freiburg, Germany). Immature DCs were pulsed at day 3 with Keyhole limpet hemocyanin (KLH, 10 μg/ml; Calbiochem, San Diego, CA). Two days prior the harvesting, cells were matured with autologous MCM, prostaglandin E_2 (10 μg/ml; Pharmacia & Upjohn, Puurs, Belgium) and recombinant tumor necrosis factor alpha (10 ng/ml; provided by dr. G. Adolf, Bender Wien, Vienna, Austria) (19). This protocol gave rise to a mature phenotype meeting the release criteria described previously (20): low expression of CD14, high expression of MHC class I, MHC class II, CD83, CD80, CD86, and CCR7, and expression of gp100 and tyrosinase after electroporation with mRNA (Supplementary Figure 2). Harvested DCs were tested by FACS analysis as described below.

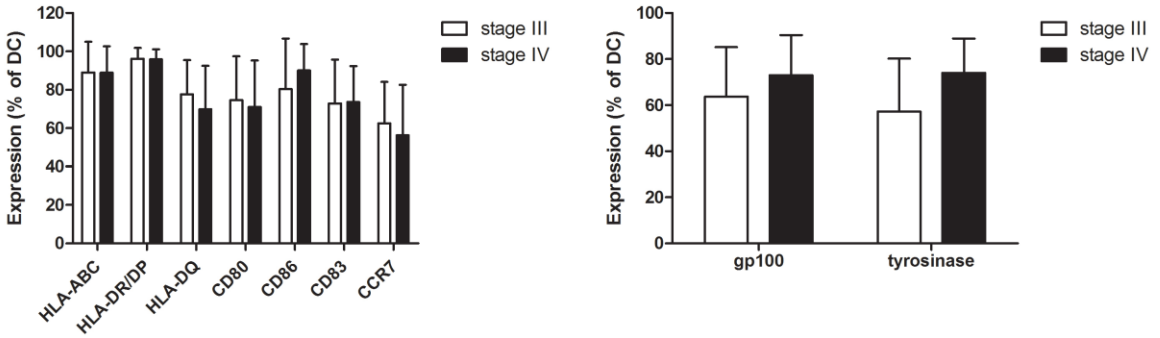

Supplementary Figure 2. Vaccine characteristics of first cycle of all patients. (A) Expression of HLA-ABC, HLA-DR/DP, HLA-DQ, CD80, CD86, CD83, and CCR7 was analyzed by flow cytometry. (B) Tumor antigen expression by DCs 2-4 hrs after electroporation with mRNA encoding gp100 and tyrosinase. Data are shown as percentage of positive DCs used for the first vaccination. The graphs represent mean ± SD of all patients.

Plasmids and in vitro mRNA transcription

Plasmids have been sent to CureVac GmbH (Tübingen, Germany) for the production of documented GMP grade gp100 and tyrosinase RNA for *ex vivo* use in clinical DC vaccination. The documented gp100 and tyrosinase mRNA was produced from the plasmids pGEM4Z/hgp100/A64 and pGEM4Z/tyrosinase/A64 (provided by Kris Thielemans, Free University Brussels, Belgium) according to GMP guidelines. CureVac mRNA contains a 5' cap and 3' poly A-tail that leads to high RNA stability and increased protein expression in transfected cells. The mRNA is purified by PUREmessenger^{TM} technology. This chromatography method efficiently eradicates traces of DNA and proteins. The mRNA production process is performed in clean room facilities and is documented by in-process controls. RNA quality was verified by agarose gel electrophoresis, RNA concentration was measured spectrophotometrically, and RNA was stored at -80ºC in small aliquots.

Electroporation of DC

Mature DCs were electroporated as described previously (10). Briefly, DC were washed twice in PBS and once in OptiMEM without phenol red (Invitrogen, Breda, The Netherlands). Twenty micrograms of RNA encoding either gp100 or tyrosinase were transferred to a 4 mm cuvette (Bio-Rad, Hercules, CA) and 8×10^6 cells were added in 200 μl OptiMEM and incubated for 3' before being pulsed in a Genepulser Xcell (Bio-Rad) by an exponential decay pulse of 300 V, 150 μF, as described before(10). Immediately after electroporation, cells were washed and were transferred to warm (37ºC) X-VIVO 15^{TM} without phenol red (Cambrex Bio Science, Verviers, Belgium) supplemented with 5% HS and left

for at least 2 hours at 37ºC, before further manipulation. The first vaccination was given with fresh DC 4 hours after electroporation. DC for subsequent vaccinations were frozen 2 hours after electroporation, thawed at the day of vaccination and incubated for 2 more hours at 37°C before injection. Electroporation efficiency was analyzed by intracellular staining and flow cytometric analysis for each separate TAA, electroporated DC were mixed before vaccination.

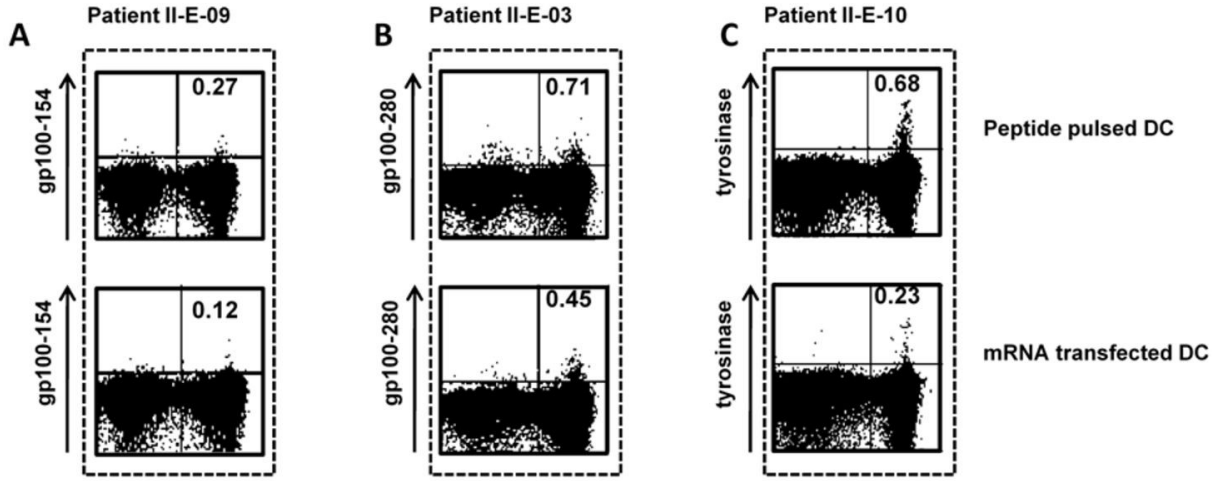

Supplementary Figure 3. Detection of tumor-specific T cells in SKIL cultures does not require challenge with defined epitopes. Tetramer analysis of SKILs cultured from biopsies of DTH reactions to DCs pulsed with tumor peptides (upper plots) or DCs electroporated with mRNA encoding tumor proteins (lower plots) of patients II-E-09 (A), II-E-03 (B), and II-E-10 (C). This figure shows that sampling DTH biopsy cultures with tetramers yields similar results when the patient is challenged with intradermal injections with DC pulsed with defined epitopes or DC electroporated with mRNA encoding the full tumor antigen.

Flow cytometric analysis

The following FITC-conjugated mAbs were used: anti-HLA class I (W6/32), and anti-HLA DR/DP (Q5/13); and PE-conjugated mAbs: anti-CD80 (BD Biosciences, Mountain View, CA), anti-CD14, anti-CD83 (Beckman Coulter, Mijdrecht, The Netherlands), and anti-CD83 (BD Pharmingen, San Diego, CA). For intracellular staining of the TAA the following mAb were used: NKI/beteb (IgG2b) (purified antibody) against gp100, T311 (IgG2a) (Cell Marque Corp., Rocklin, CA) against tyrosinase. For intracellular staining cells were fixed for 4' on ice in 4% (w/v) paraformaldehyde (Merck, Darmstadt, Germany) in PBS, permeabilized in PBS/2%BSA/0.02% azide/0.5% saponin (Sigma-Aldrich) (PBA/saponin), and stained with mAb diluted in PBA/saponin/2%HS, followed by staining with allophycocyanin-labeled goat-anti-mouse (BD PharMingen). Flow cytometry was performed with FACSCalibur^{TM} flow cytometer equipped with CellQuest software (BD Biosciences).

Flow cytometric analysis of T cells was performed using directly labelled mAbs against CD4, CD8, CD25, CD127, CTLA-4 (BD Pharmingen) and FoxP3 (eBioscience, San Diego, CA, USA), all according to the manufacturer's protocol. Tregs were defined as $CD4^+FoxP3^+CD25^{high}CD127^{low}$ cells; percentage of Tregs was defined as the number of $CD4^+FoxP3^+CD25^{high}CD127^{low}$ cells divided by the total number of $CD4^+$ cells x100.

KLH-specific proliferation

KLH-specific cellular responses were measured before and after vaccination by proliferation assay. Peripheral blood mononuclear cells (PBMC) were isolated from heparinised blood by Ficoll-Paque density centrifugation. PBMC were stimulated with KLH (4 µg/2×10^5 PBMC) in medium with 10% human AB serum. After 3 days, cells were pulsed with ^{3}H-thymidine for 8 hours, and incorporation was measured with a betacounter. Experiments were performed in triplicate.

KLH-specific antibody production

KLH-specific antibodies were measured in the sera of patients before and after vaccination. Microtiter plates (96 wells) were coated overnight at 4ºC with KLH (25 µg/ml in PBS). Different concentrations of patient serum (range 1:100 to 1:50,000) were added for 60' at room temperature. After extensive washing, patient antibodies were detected with mouse anti-human IgG, IgA, or IgM antibodies labelled with horseradish peroxidase (Invitrogen, San Diego, CA). 3,3' 5,5-tetramethyl-benzidine was used as a substrate and plates were measured with a microtiter plate reader at 450 nm. For quantification, an isotype-specific calibration curve for the KLH response was included in each microtiter plate.

Skin-test infiltrating lymphocyte (SKIL) cultures

0.2 - 1 x 10^6 DC pulsed with the gp100 and/or tyrosinase peptides and DC electroporated with gp100 and/or tyrosinase mRNA each were injected i.d. in the skin of the back of the patient at four or six different sites(21). The maximum diameter of induration was measured after 48 hours. From each site induration was measured and punch biopsies (6 mm) were obtained. Half of the biopsy was cryopreserved and the other part was manually cut and cultured in RPMI 1640 containing 7% HS and IL-2 (100 U/ml). Every 7 days, half of the medium was replaced by fresh medium containing HS and IL-2. After 2 to 4 weeks of culturing, SKILs were tested. In general, similar results were obtained per patient, regardless of the method of antigen-presentation (Supplementary Figure 3).

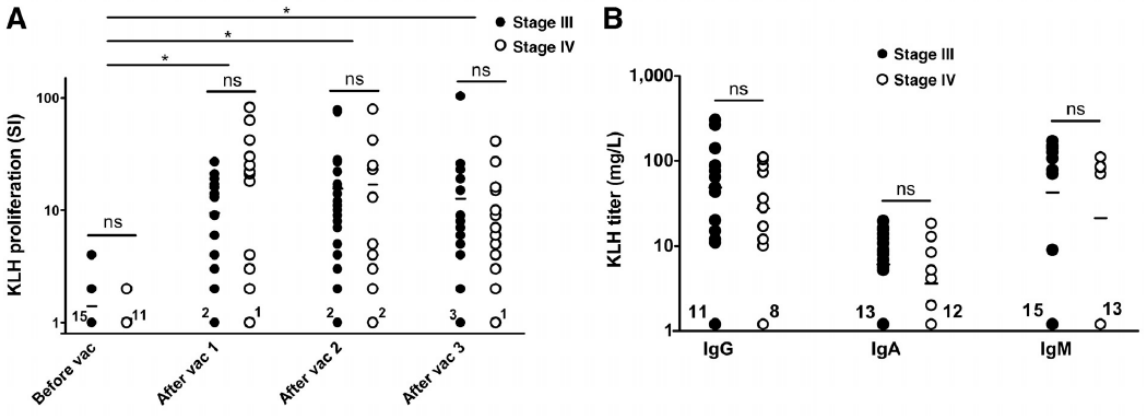

Figure 1. KLH-specific immune responses before and after DC vaccination. (A) KLH-specific T cell proliferation was analysed before the first vaccination and after each DC vaccination during the first vaccination cycle in PBMC of stage III (filled circles) and stage IV (open circles) melanoma patients. Per time point each dot represents one patient. Proliferative response to KLH is given as proliferation index (proliferation with KLH/proliferation w/o KLH). * p <0.05; NS, not significant. (B) KLH-specific IgG, IgA, and IgM antibodies were quantitatively measured after the first vaccination cycle in sera of vaccinated patients. Numbers indicate the number of patients without proliferative (A) or humoral (B) KLH-response.

Tetramer staining

SKILs and freshly isolated PBMC were stained with tetrameric-MHC complexes containing the HLA-A2-binding epitopes gp100:154-168, gp100:280-288 or tyrosinase:369-377 (Sanquin, Amsterdam, The Netherlands) or HLA-DR4-binding epitopes gp100:44-59 and tyrosinase:448-462 (provided by William Kwok, Benaroya Research Institute, Seattle, WA) as described previously(19). In addition, PBMCs of patients with tetramer positive CD4+ T cells were restimulated for 8 days with DR4-binding gp100 or tyrosinase peptides and stained with tetrameric-MHC complexes containing class II epitopes gp100:44-59 and tyrosinase:448-462. Tetrameric-MHC complexes recognizing HIV were used as controls; at least a two-fold increase of the double-positive population compared to control was regarded to be positive.

Antigen and tumor recognition

Antigen recognition was determined by the production of cytokines and cytotoxic activity of SKILs in response to T2 pulsed with the indicated peptides or BLM (a melanoma cell line expressing HLA*02:01 but no endogenous expression of gp100 and tyrosinase), transfected with control antigen G250, with gp100 or tyrosinase, or an allogenic HLA*02:01-positive, gp100-positive, and tyrosinase-positive tumor cell line (MEL624) were measured. Cytokine production was measured in supernatants after 16 hours of co-culture by a cytrometric bead array (Th1/Th2 Cytokine CBA 1; BD PharMingen). Positive and specific cytokine production was defined as a two-fold increase compared to stimulation with the cell lines pulsed with an irrelevant peptide.

Statistical analysis

Differences between the groups were evaluated using the Fisher's exact test or one-way ANOVA. Statistical significance was defined as $p<0.05$. GraphPad Prism 5.0 was used for all analyses.

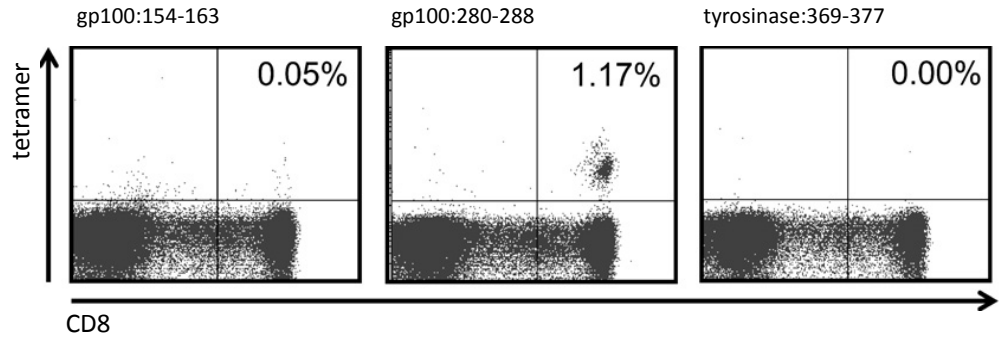

Figure 2. Tumor antigen-specific CD8$^+$ T cell responses in peripheral blood. An example of tetramer analysis of PBMCs from patient II-E-08 is shown. Cells were stained with tetramers encompassing the HLA*02-specific gp100:154-168, gp100:280-288, tyrosinase:369-377 peptide or an irrelevant peptide and with anti-CD8 mAb. The irrelevant control peptide stained 0.01% of the PBMCs.

Results

Patient characteristics

A total of 48 HLA*02:01 positive melanoma patients were enrolled (Supplementary Figure 1), of which 3 patients (IV-D-13, IV-D-12, IV-D-07) were regarded as non-evaluable, since they did not complete the first cycle due to rapid progressive disease. Two stage IV patients were only evaluable for immunologic response; patient IV-C-05 had no measurable disease at baseline and patient IV-D-15 had proven brain metastasis after the second vaccination but completed the first cycle. Twenty-six stage III and 19 stage IV patients were included. Twenty-three stage III patients received 1 cycle of maintenance vaccinations and 20 patients completed the full three cycles. Three stage IV patients received 1 cycle of maintenance vaccinations; one patient completed the full three vaccination cycles. No unexpected or severe adverse events were observed. Patient characteristics are summarized in Table 1.

Vaccine characteristics

Phenotypic and functional release criteria were defined for DC vaccines to ensure minimal quality criteria and the usage of mature DC in clinical vaccination protocols (22). The phenotype of the *ex vivo*-generated DC was determined by flow cytometry and all produced vaccines met the standard release criteria, with respect to expression of MHC class I and II, and co-stimulatory molecules, CD83 and CCR7 (Supplementary Figure 2). Furthermore, we confirmed the intracellular expression of tumor associated antigens gp100 and tyrosinase after electroporation by flow cytometry (Supplementary Figure 2). Patients received on average 12×10^6 DC per vaccination with a maximum of 15×10^6 DC per vaccination.

Table 1. Patient characteristics.

Patient	Sex	Age (yrs)	Origin of primary tumor	Stage on entry	Site of metastatic disease	LDH (U/l)	gp100[c]	tyro[c]	HLA-DR4 status	# of DC per vaccination (x 10^6)			# of vacc	previous systemic treatment	salvage systemic treatment
Stage IV										**mean**	**min**	**max**			
II-E-01	m	54	skin	M1c	LN	542	++	+	-	8,8	6	13	3	no	DTIC
IV-C-01	f	60	skin	M1b	lung, LN	343	+++	+++	+	10,7	9	12	3	no	DTIC
IV-C-02	f	48	skin	M1c	liver, lung, skin	318	+++	++	+	11,0	8	14	3	no	TMZ
IV-C-05	f	31	skin	M1c	lung, skin, breast	301	+++	+	+	14,0	9	15	12	no	no
IV-C-06	m	57	skin	M1c	lung, bladder, skin	412	++	-	+	12,3	11	15	3	no	no
IV-C-09	f	48	skin	M1b	lung, skin, LN	402	+++	-	+	12,0	10	15	3	DTIC	no
IV-C-13	f	47	skin	M1c	skin, LN	531	+	+	+	12,3	9	15	3	DTIC	no
IV-D-01	m	75	skin	M1c	liver, lung, bladder	334	+++	+++	-	11,5	11	12	3	DTIC	no
IV-D-02	m	69	skin	M1c	liver, lung, bone, adrenal	502	+	++	-	10,0	7	12	3	no	no
IV-D-03	f	42	eye	M1c	liver, lung	344	+++	+	-	7,3	6	9	3	DTIC	TMZ
IV-D-04	m	59	skin	M1c	lung, bladder, LN	381	+++	++	-	9,7	8	12	3	no	DTIC, TMZ, AZD6244
IV-D-06	f	61	skin	M1a	LN	459[a]	+	+	-	11,5	5	15	6	no	no
IV-D-09	m	50	skin	M1a	LN	431	+++	+++	-	15,0	15	15	3	no	DTIC
IV-D-11	m	44	mucosa	N3	LN, maxillary sinus	351	+++	++	-	14,2	12	15	12	no	no
IV-D-15	m	58	skin	M1c	lung, bone, LN	523	+++	+++	-	14,7	14	15	3	no	DTIC
IV-D-17	m	66	skin	M1c	lung, adrenal, intracardial	387	+++	+++	-	15,0	15	15	3	no	no
IV-D-18	m	57	skin	M1a	skin, LN	369	+++	+++	-	13,0	11	15	6	no	DTIC, AZD6244
IV-D-20	m	62	skin	M1c	liver, LN, adrenal	390	+++	+	-	15,0	15	15	3	no	DTIC
IV-D-21	f	30	skin	M1c	liver, lung, LN, skin	421	+++	+++	-	9,3	5	15	3	no	DTIC
Stage III															
II-E-02	m	38	skin	N3	LN	368	+++	++	-	11,3	6	15	12	n.a.	no
II-E-03	m	45	skin	N1a	LN	351	+++	++	+	13,9	10	15	12	n.a.	
II-E-04	m	41	skin	N2a	LN	392	+++	+	-	6,8	3	11	12	n.a.	
II-E-05	f	49	skin	N2a	LN	279	-	++	-	11,2	6	15	12	n.a.	DTIC
II-E-06	m	48	skin	N2a	LN	356	+++	++	-	12,6	10	15	12	n.a.	no
II-E-07	f	59	skin	N3	LN	422	+	n.a.	-	14,1	12	15	12	n.a.	
II-E-08	m	56	skin	N3	LN	598[a]	++	++	-	12,0	9	15	3	n.a.	DTIC
II-E-09	m	26	skin	N3	LN	352	+++	+++	-	13,5	10	15	12	n.a.	unknown
II-E-10	f	34	skin	N1a	LN	348	+++	+++	-	14,5	13	15	12	n.a.	
II-E-11	m	47	skin	N1a	LN	299	+++	++	-	13,8	10	15	12	n.a.	
IV-C-03	m	37	skin	N1a	LN	393	+++	+++	+	12,2	8	15	12	n.a.	DTIC
IV-C-04	m	45	skin	N3	LN	408	+	+	+	9,0	8	10	7	n.a.	no
IV-C-07	m	35	skin	N1a	LN	335	+++	+++	+	13,0	9	15	12	n.a.	
IV-C-08	m	35	skin	N1a	LN	390	++	++	+	14,2	8	15	12	n.a.	
IV-C-10	f	36	skin	N1a	LN	361	+++	++	+	13,1	9	15	12	n.a.	
IV-C-11	m	50	no primary	N1b	LN	379	+	+	+	14,0	11	15	12	n.a.	
IV-C-12	f	38	no primary	N1b	LN	360	+++	+++	+	13,7	11	15	3	n.a.	DTIC
IV-C-14	f	54	skin	N1b	LN	458	+++	+	+	12,2	7	15	12	n.a.	
IV-D-05	m	48	skin	N3	LN	388	++	++	-	7,0	6	8	6	n.a.	DTIC
IV-D-08	f	54	skin	N2b	LN	416	+++	+	-	15,0	15	15	6	n.a.	no
IV-D-10	f	37	skin	N1a	LN	342	++	++	-	11,6	10	15	12	n.a.	no
IV-D-14	m	63	skin	Nxb	LN	348	+++	+	-	13,3	10	15	12	n.a.	
IV-D-16	m	31	skin	N2b	LN	517[a]	+++	+++	-	12,1	8	15	12	n.a.	
IV-D-19	m	62	skin	N1b	LN	280	+++	+	-	10,8	7	15	12	n.a.	ITx
IV-D-22	m	23	skin	N1b	LN	394	++	-	-	13,3	12	15	3	n.a.	DTIC, anti-CTLA4
IV-D-24	m	65	skin	N2a	LN	350	++	++	-	14,2	12	15	12	n.a.	no

[a] LDH normalized after RLND

[b] Patients stopped because of burden of skin test

[c] gp100 and tyrosinase expression on the primary tumor was analyzed by immunohistochemistry. Intensity of positive cells were scored centrally and semi-quantitatively by a pathologist. Intensity was scored as low (+), intermediate (++), or high (+++).

Abbreviations: f=female, m=male, nr= number, LN=lymph node, n.a.=not applicable.

Immunological response to KLH

For immunomonitoring purposes all DC have been loaded with the control antigen KLH. PBMC, isolated after each vaccination, showed increased proliferation upon stimulation with KLH after vaccination in almost all patients in the first cycle (Figure 1a). One patient first developed a proliferative response to KLH in the second cycle. Anti-KLH antibodies were detected in 9 out of 17 stage IV patients tested, and 15 out of 26 stage III patients tested (Figure 1b). These data demonstrate that the vaccine effectively induced de novo immune responses.

Tumor-associated antigen specific responses in blood

To investigate TAA-specific immune responses, PBMC were screened with tetrameric-MHC complexes before and after each cycle of 3 vaccinations at the time point of SKIL test. TAA-specific $CD8^+$ T cells were only found in freshly isolated PBMC from 3 stage III and 3 stage IV patients after vaccination (Figure 2 and Table 2). Since it has been described that melanoma patients can already have a substantial number of TAA-specific T cells circulating in their blood, we analysed the presence of TAA-specific T cells in PBMC isolated prior to vaccination. Three out of these 6 patients had no detectable TAA-specific $CD8^+$ T cells circulating before vaccination, suggesting that TAA-specific $CD8^+$ T cells were newly induced, or at least enhanced, by the DC vaccinations in these patients, in concordance with previous reports (23).

Evidence is emerging that $CD4^+$ T cells needs to be antigen-specific in order to potentiate the $CD8^+$ immune response. Therefore we analysed the presence of TAA-specific $CD4^+$ T cells in PBMCs of all 15 $DR4^+$ patients. Four patients were positive after vaccination (patients IV-C-01, IV-C-02, IV-C-03, IV-C-08; Figure 3 and Table 2). Tetramer analysis of PBMCs restimulated *in vitro* with DR4-binding peptides confirmed the presence of TAA-specific $CD4^+$ T cells (Figure 3). TAA-specific $CD4^+$ T cells were detectable before vaccination in only one patient (IV-C-03), but only after *in vitro* restimulation of PBMCs with DR4-binding peptides, suggesting that tumor-specific $CD4^+$ T cells were induced, or at least enhanced, by DC vaccinations in these patients. We identified concurrent TAA-specific $CD8^+$ T cells in SKIL cultures in 3 of the 4 patients with tumor-specific $CD4^+$ T cells in their blood (patients IV-C-01, IV-C-02, IV-C-03; Table 2). To exclude that the TAA-specific $CD4^+$ T cells have a suppressor phenotype, we tested their FoxP3 expression, all were negative (Figure 3).

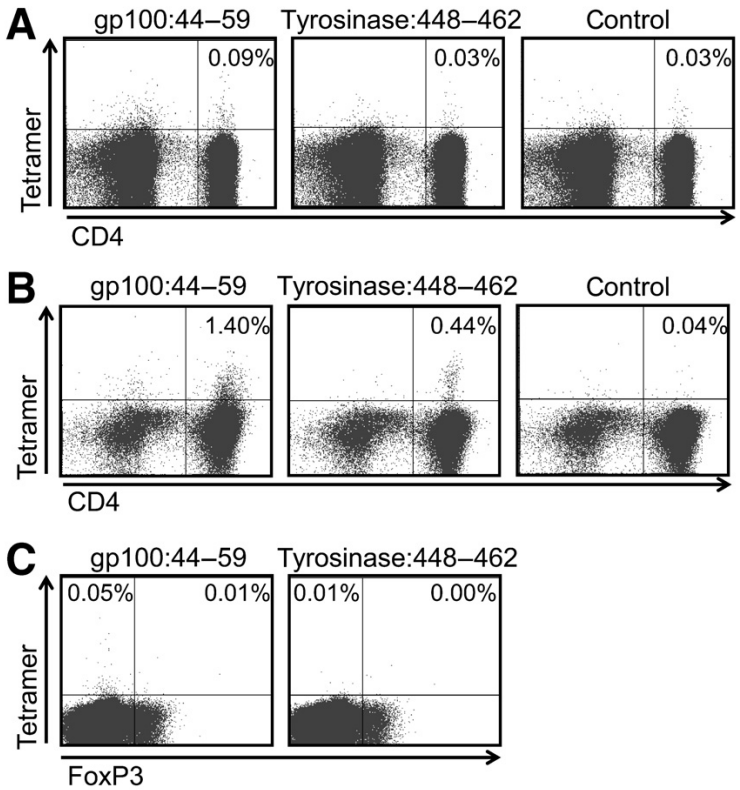

Figure 3. Tumor antigen-specific $CD4^+$ T cell responses in peripheral blood. An example of tetramer analysis of PBMCs of patient IV-C-02 after the first cycle of DC vaccination is shown. (A) Freshy isolated PBMCs were stained directly after isolation with tetramers encompassing the HLA-DR4-specific gp100:44-59 peptide, tyrosinase:448-462 peptide, or an irrelevant peptide and with anti-CD4 mAb. (B) Tetramer analysis of PBMC after 8 days of in vitro restimulation with DR4-binding gp100 or tyrosinase peptides. Note that before restimulation (A), only gp100-specific $CD4^+$ T cells are found, whereas after restimulation (B) both gp100- and tyrosinase-specific $CD4^+$ T cells are detectable. (C) The in vitro stimulated population of gp100- or tyrosinase-specific $CD4^+$ PBMC of patient IV-C-02 was further characterized for FoxP3 expression. TAA-specific $CD4^+$ T cells did not express FoxP3.

TAA-specific responses in skin-test infiltrating lymphocyte (SKIL) cultures

Previously we showed that the presence of TAA-specific T cells in SKIL cultures positively correlates with clinical outcome in stage IV melanoma patients (22). Skin tests were performed after each cycle of vaccinations. Since performing skin tests and taking biopsies puts a great burden to the patient, and previously we observed in a series of patients who underwent pre-vaccination skin test analysis that none of the patients had detectable levels of TAA-specific T cells prior to vaccination, we choose

not to perform pre-vaccination skin-tests, but rather perform in-depth analysis on the post-vaccination samples. Tetramer positive $CD8^+$ SKILs were detected in 17 stage III patients and in 11 stage IV patients (p=0.7574 Fischer's exact test). In 8 stage III patients and in 2 stage IV patients, $CD8^+$ SKILs were specific for all 3 tested epitopes (Table 2, Figure 4). Six stage III and 3 stage IV patients had TAA-specific $CD8^+$ T cells against 2 of the 3 epitopes tested, while $CD8^+$ T cells of the other patients recognized one epitope.

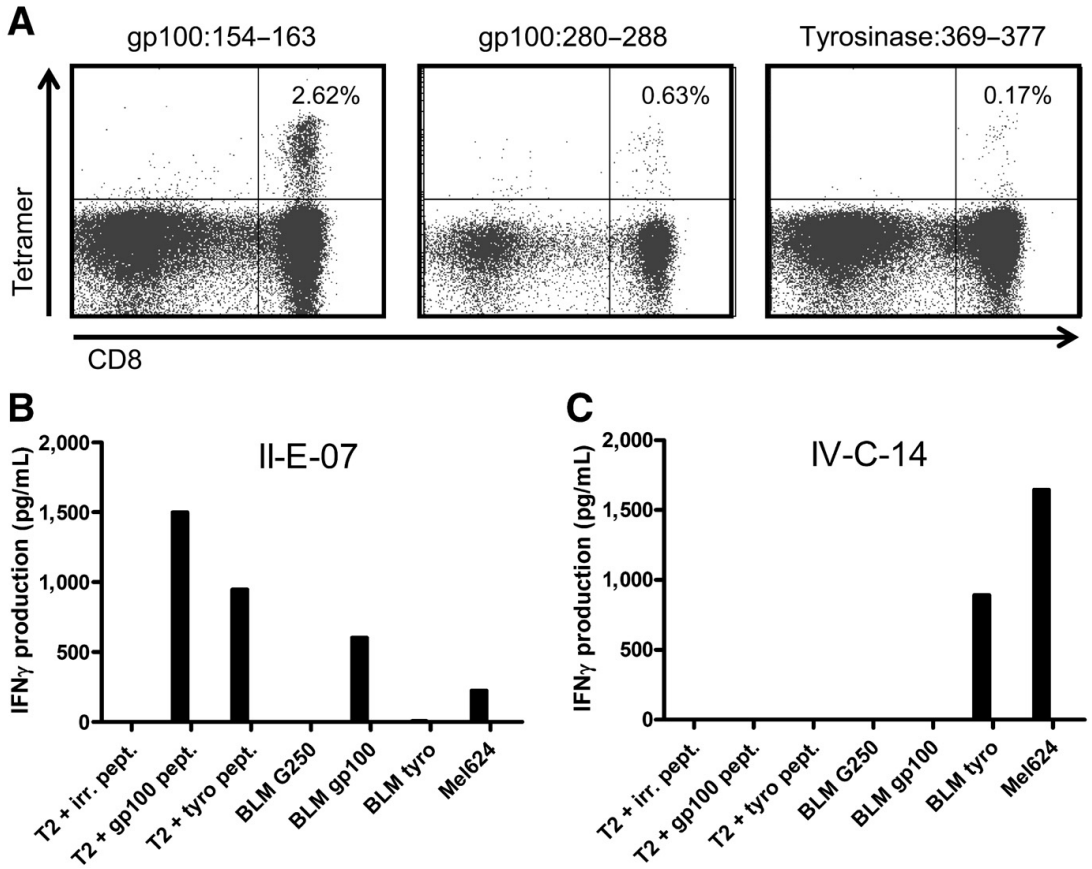

Figure 4. Tumor antigen-specific $CD8^+$ T cell responses in post-treatment SKIL cultures. The presence and functionality of TAA-specific T cells were tested in lymphocytes cultured form skin-test biopsies (SKILs). (A) An example is shown of tetramer analysis of SKILs from patient II-E-07, cultured from a DTH reaction to DC pulsed with tumor peptides. Cells were stained with tetramers encompassing the gp100:154 peptide, gp100:280, tyrosinase or an irrelevant peptide (control) and with anti-CD8 mAb. The irrelevant control peptide stained 0.07% of the T cells. The biopsy contains gp100- and tyrosinase-specific $CD8^+$ T cells. (B) IFNγ production by the same T cells after stimulation with T2 cells loaded with gp100:154-168 peptide and gp100:280-288 or tyrosinase:369-377 peptide (peptide stimulation), BLM cells expressing gp100- or tyrosinase protein (protein stimulation), or Mel624 cells expressing both gp100 and tyrosinase (tumor stimulation). (C) Example of functional responses of SKILs of patient IV-C-14, cultured from a biopsy of a DTH reaction to DC electroporated with tyrosinase mRNA, showing recognition of tyrosinase epitopes when presented by HLA-A2.1 positive tyrosinase-transfected BLM cells or endogenously tyrosinase expressing Mel624 cells, by the specific and elevated production of IFNγ, although it does not recognize the specific epitopes used in previous vaccination studies. This indicates that a broad repertoire of TAA-specific T cells can be stimulated by vaccination with mRNA-transfected DC.

Merely the presence of TAA-specific $CD8^+$ T cells is not necessary sufficient for effective anti-tumor responses. Therefore we tested whether the vaccine-induced TAA-specific $CD8^+$ T cells were 'functional' in terms of selective IFNγ production upon coculture with peptide-, or protein-loaded target cells or tumor cells (Table 2, Figure 4). Strikingly, although we detected tetramer-specific $CD8^+$ T cells in both stage III and IV melanoma patients to similar extend, we found increased IFNγ production only in 3 out of 11 stage IV melanoma patients. In contrast, in stage III patients with no measurable disease, we found IFNγ production in 15 out of 17 patients with tetramer-positive $CD8^+$ SKIL cultures, (p=0.0033 Fisher's exact test).

Interestingly, SKILs of three patients (IV-C-02, IV-C-10, IV-C-14) that did not produce cytokines upon co-culture with the HLA*02:01 binding peptides, produced IFNγ upon co-culture with the respective tumor protein, indicating that T cells recognized different epitopes. SKILs derived from three additional patients (II-E-04, II-E-05, IV-C-12) that produced IFNγ upon stimulation with only one of the HLA*02:01 binding peptides, produced IFNγ upon co-culture with gp100-expressing cell lines or tyrosinase-expressing cell lines (Table 2, Figure 4), suggesting that TAA-specific T cells with another specificity than the epitopes used for peptide stimulation and tetramer staining were induced by the DC vaccine.

Clinical outcome in stage III patients

One patient had progressive disease within 4 months after start of vaccinations. As of June 2011, 15 out of 26 patients progressed at 3 to 37 months after the start of vaccination. Twelve of 26 patients are in ongoing remission for up to 45 months. The median progression free survival (PFS) is 34.3 months, and the median overall survival has not yet been reached. Extended follow-up is necessary to draw conclusions on the potency of vaccination with mRNA electroporated dendritic cells as an adjuvant therapy in melanoma patients.

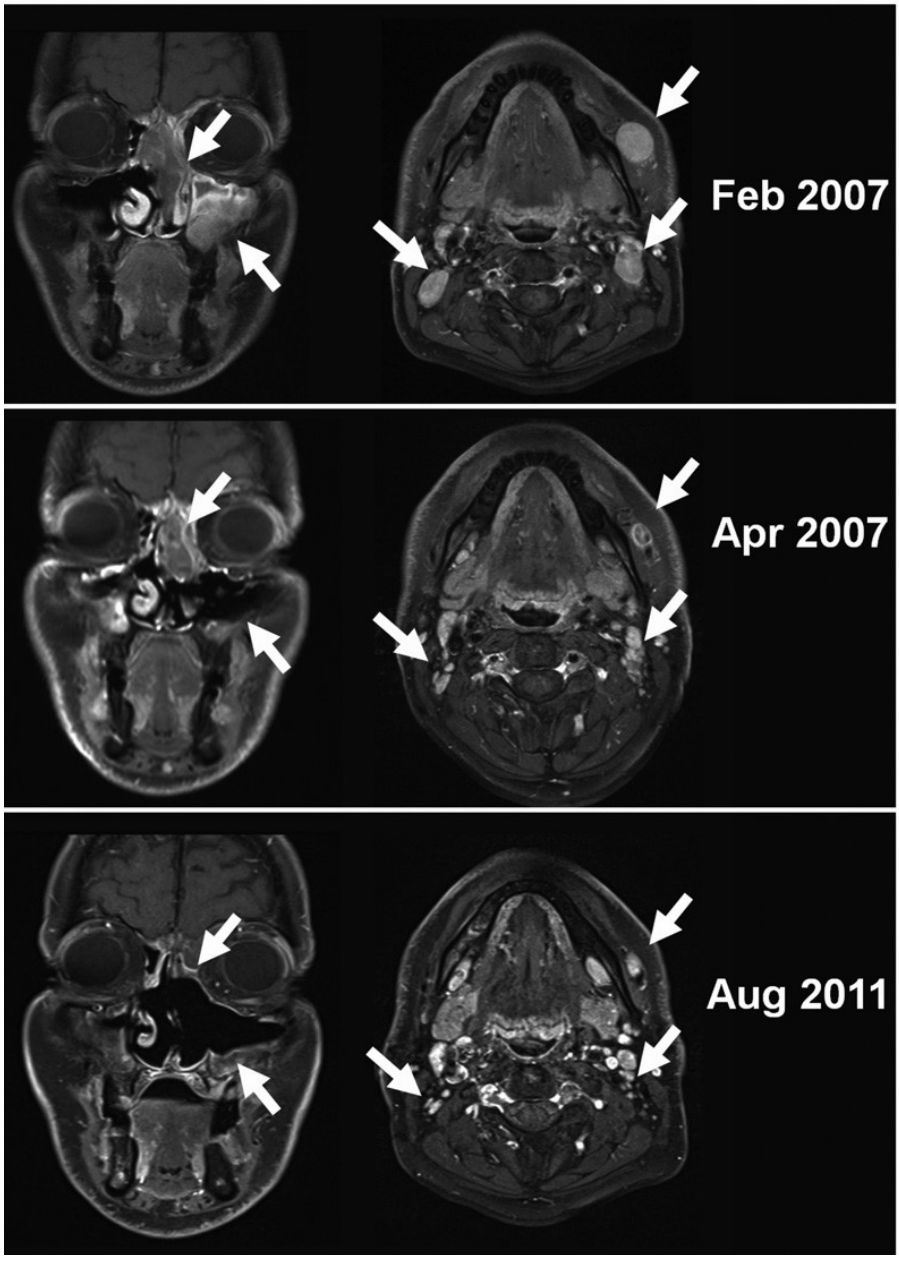

Figure 5. Partial reponse after three i.n. vaccinations with mRNA-transfected DC. (A) Patient IV-D-11 presented with a irresectable primary melanoma from nasal mucosa with extension into the nasal septum, maxillary and ethmoid sinus, and bilateral lymphadenopathy of level 1, 2 and 5. (B) Three intranodal vaccinations with mRNA-transfected DC induce a partial response, allowing resection of the primary tumor. (C) Patient is in ongoing remission.

Table 2. Immunological and clinical responses

Patient	Flu like symptoms	Injection site reaction	TAA specific T cells in blood, pre-vaccination [a]		TAA specific T cells in blood, post- vaccination [a]		TAA specific T cells in SKIL cultures				Clinical response[g]	PFS	OS
	CTC grade	CTC grade	CD4+ tetramer+	CD8+ tetramer+	CD4+ tetramer+	CD8+ tetramer+	CD8+ tetramer+ [a]	peptide [b]	protein [b]	tumor [b]		(months)	(months)
Stage IV													
II-E-01	1	0	n.a.	-	n.a.	-	-	-	-	-	PD	3	11
IV-C-01	0	0	-	-	++	-	+++	-	-	-	SD	6	14
IV-C-02	1	0	-	-	++	-	+	-	++	+	MR	5	10
IV-C-05	1	1	-	-	-	+	++	-	-	-	SD	16[d]	49[d]
IV-C-06	0	0	-	-	-	-	-	-	-	-	PD	1	3
IV-C-09	1	2	-	-	-	-	-	-	-	-	PD	3	15
IV-C-13	0	0	-	-	-	-	-	-	-	-	PD	1	5
IV-D-01	0	0	n.a.	-	n.a.	-	++	-	-	-	PD	3	5
IV-D-02	1	0	n.a.	-	n.a.	-	+	-	-	-	PD	2	5
IV-D-03	0	0	n.a.	-	n.a.	+	-	-	-	-	SD	6	26
IV-D-04	1	1	n.a.	-	n.a.	-	-	-	-	-	PD	3	22
IV-D-06	2	1	n.a.	+	n.a.	+	+	+	+	-	SD	16	24
IV-D-09	1	0	n.a.	-	n.a.	-	-	-	-	-	SD	7	14
IV-D-11	1	1	n.a.	-	n.a.	-	+++	+	+	+	PR	8	52+
IV-D-15	0	0	n.a.	-	n.a.	-	+	-	-	-	PD	1[e]	8[e]
IV-D-17	0	0	n.a.	-	n.a.	-	-	-	-	-	PD	2	2
IV-D-18	2	1	n.a.	-	n.a.	-	+	-	-	-	SD	10	22
IV-D-20	0	0	n.a.	-	n.a.	-	++	-	-	-	PD	4	21
IV-D-21	1	0	n.a.	-	n.a.	-	+	-	-	-	PD	1	7
Stage III													
II-E-02	0	0	n.a.	-	n.a.	-	-	-	-	-	NED	34	54+
II-E-03	2	1	-	-	-	-	+++	+++	++	+	NED	53+	53+
II-E-04	1	1	n.a.	-	n.a.	-	++	+	++	-	NED	52+	52+
II-E-05	1	1	n.a.	-	n.a.	-	+	+	++	-	NED	37	52+
II-E-06	2	0	n.a.	-	n.a.	-	+++	+++	++	+	NED	14	17
II-E-07	2	1	n.a.	-	n.a.	-	+++	++	++	+	NED	51+	51+
II-E-08	1	0	n.a.	+	n.a.	+	+++	+++	++	+	NED	9	50+
II-E-09	0	1	n.a.	-	n.a.	+	+++	++	++	+	NED	24	25
II-E-10	1	1	n.a.	-	n.a.	-	+++	+	+	-	NED	48+	48+
II-E-11	2	1	n.a.	-	n.a.	-	++	-	-	-	NED	47+	47+
IV-C-03	2	1	-[f]	-	+	-	++	+	+	+	NED	21	30
IV-C-04	1	0	-	-	-	-	-	-	-	-	NED	8	22
IV-C-07	1	1	-	-	-	-	+++	++	+	+	NED	46+	46+
IV-C-08	2	1	-	-	+	-	-	-	-	-	NED	40+	40+
IV-C-10	2	1	-	-	-	-	+++	-	++	-	NED	37+	37+
IV-C-11	1	1	-	-	-	-	-	-	-	-	NED	36+	36+
IV-C-12	1	1	-	+	-	+	+	+	++	+	NED	8	16
IV-C-14	1	0	-	-	-	-	-[c]	-	+	+	NED	15	28+
IV-D-05	1	1	n.a.	-	n.a.	-	++	++	+	+	NED	8	16
IV-D-08	2	1	n.a.	-	n.a.	-	-	-	-	-	NED	10	12
IV-D-10	0	1	n.a.	-	n.a.	-	++	+++	-	-	NED	23	28
IV-D-14	0	0	n.a.	-	n.a.	-	+	+	-	-	NED	51+	51+
IV-D-16	0	1	n.a.	-	n.a.	-	-	-	-	-	NED	50+	50+
IV-D-19	1	1	n.a.	-	n.a.	-	++	+	+	-	NED	26	48+
IV-D-22	0	0	n.a.	-	n.a.	-	-	-	-	-	PD	3	47+
IV-D-24	0	0	n.a.	-	n.a.	-	-	-	-	-	NED	36+	36+

Abbreviations: n.a. = not applicable; n.t.= not tested; SKIL= Skin-test Infiltrating Lymphocytes; PFS= Progression free survival; OS= Overall survival

[a] Tetramer staining of freshly isolated PBMC or SKILs. - no recognition, + one epitope recognized, ++ two epitopes recognized, +++ three epitopes recognized.

[b] Antigen recognition of SKILs after stimulation with T2 cells loaded with HLA-A2.1-binding gp100 or tyrosinase peptides (peptide recognition), BLM transfected with gp100 or tyrosinase protein (protein recognition) or the gp100 and tyrosinase-expressing tumor cell line Mel624 (tumor recognition) as analyzed by IFNγ production. Responses were scored as the best immunological response after 1-3 cycles of DC vaccinations.

[c] Patient IV-C-14 had functional T cells without recognizing the tested epitopes (see Figure 4).

[d] not evaluable for clinical response because no target lesion at start of vaccination.

[e] not evaluable for clinical response because of symptomatic brain metastases during 1st cycle

[f] gp100-specific CD4+ T cells were found after in vitro restimulation with DR4-binding peptides

[g] SD = stable disease, PD= progressive disease, NED=no evidence of disease, PR= partial response, MR= mixed response

Clinical responses in stage IV patients

All stage IV patients were evaluated for clinical response at 3-month intervals with CT scan. Five patients had stable disease up to 15 months and one patient (IV-C-02) showed a mixed response. One patient (IV-D-11) with irresectable primary melanoma of the nasal mucosa with bilateral lymph node metastases in the neck region and metastases in the maxillary sinus, showed a partial response of the primary tumor after three vaccinations, allowing resection of the primary tumor. The lymph node metastases and sinus metastases completely regressed upon further vaccination and this patient is in ongoing complete remission for 52+ months (Figure 5). DR4 expression was not correlated with survival (data not shown) in the vaccinated patients.

We observed a trend towards improved PFS in patients with TAA-specific T cells in their blood or SKIL cultures compared to patients without TAA-specific responses, with 8.1 month versus 2.8 months, respectively (p= 0.062). Similarly, patients with TAA-specific T cells showed improved OS compared to patients without TAA-specific T cells, 24.1 months versus 11.0 respectively (p = 0.101).

Discussion

Early clinical trials have shown that vaccination with DC loaded with tumor peptides is feasible, safe and can induce tumor-specific immune responses in advanced cancer patients (1;5;24). Although these results are promising, further improvement is warranted before its use can be accepted in clinical practice. In the present study we show that DC presenting multiple naturally processed epitopes following mRNA electroporation, enhance tumor-specific $CD8^+$ and $CD4^+$ T cell responses in melanoma patients. Importantly, both the presence of TAA-specific $CD8^+$ T cells and their capacity to produce IFNγ upon encounter of their cognate antigen was significantly increased in stage III patients treated in the adjuvant setting.

Long-lasting T cell receptor stimulation of several hours by fully matured DCs is necessary to activate naïve T cells to proliferate and differentiate into effector cells (25;26). The generated DCs highly and sustainably expressed gp100 and tyrosinase after electroporation with mRNA. *In vitro*, DCs were able to activate gp100-specific CTL up to 48 hours after electroporation. Previously, we demonstrated that gp100 and tyrosinase protein can be detected inside lymph nodes up to 24 hours after intranodal injection of mRNA electroporated DC (10). In this study, TAA-specific T cells were induced in the majority of patients which clearly demonstrates that electroporated DC are indeed potent inducers of tumor-specific T cells.

We detected TAA-specific $CD8^+$ T cells in peripheral blood of only 6 of the 45 patients. This is an underestimation, likely due to the low frequencies of these cells in the circulation and the observation that substantially more TAA-specific $CD8^+$ T cells were detected in SKIL cultures. Still, the number of TAA-specific T cells measured in this study might be underestimated because we screened with HLA*02:01 binding tetramers only. Indeed, in six patients SKILs produced IFNγ upon co-culture with the protein gp100 and/or tyrosinase, while no IFNγ production was detected upon co-culture with the corresponding HLA*02-binding peptide(s), supporting the notion that T cells with a broader specificity than the HLA*02:01 epitopes were induced. Recently, Bonehill *et al.* reported on the use of monocyte-derived DC electroporated with mRNA encoding multiple tumor antigens, CD40 ligand, active TLR4 and CD70 (TriMix-DC) (27). Although they monitored tumor-specific T cells by using autologous EBV-transformed B cells transfected with tumor antigens as target cells, comparable frequencies of gp100 and tyrosinase-specific $CD8^+$ T cells were found.

In 4 out of 10 patients tested, mRNA-electroporated DC induced concomitant TAA-specific $CD4^+$ T cells. The observation that these cells did not express FoxP3, suggest that these cells were T helper cells and not regulatory T cells. Initially, the main function of $CD4^+$ T helper 1 cells was thought to be the production of cytokines providing growth and differentiation signals to precursor CTL to become effector CTL (28). However, $CD4^+$ T cells have also been demonstrate to participate in the elimination of tumor and the maintenance of long-term protective immunity (29-31). In addition, activated T

helper cells can stimulate precursor CTLs by reciprocal activation of APCs, for instance via CD40-CD40L interactions (32). Recently it was shown that $CD4^+$ T cells enhance the recruitment of $CD8^+$ T cells to the lymph nodes(33) and tumor(34-36). Moreover, a direct antitumor effect of T helper cells has been demonstrated (37-39). This may be of particular relevance for the antitumor response against melanoma since this tumor type frequently expresses class II molecules constitutively (40;41). Indeed, $CD4^+$ T cell responses have been identified in peripheral blood from melanoma patients who remained disease-free after treatment for multiple relapses (39).

Our data suggests a trend towards improved overall survival, when compared to recently reported survival data in comparative arms from large randomized prospective studies on immunotherapy with anti-CTLA4 antibodies in irresectable metastatic melanoma patients (42;43). It is tempting to speculate that the observed clinical responses result from vaccine-induced immune responses. Indeed, stage IV melanoma patients with TAA-specific T cell responses showed increased clinical outcome after vaccination with mRNA-loaded DC when compared to patients with no vaccine-enhanced TAA-specific T cell responses. These data confirm and extend our previous findings that the presence of tumor-specific T cells in SKIL cultures identifies a subgroup of patients that might benefit from immunotherapy (21). Moreover, these studies demonstrate that sustained disease control can be achieved in increasing numbers of patients, but objective anti-tumor responses might take several months to years to develop (44;45). The, generally, delayed response patterns in immunotherapy and the high response rates to novel targeted therapies in melanoma, obviously warrants future studies that combine both modalities to achieve durable tumor control. Such studies should implement SKIL culture analyses pre- and post-intervention in both active and comparative arms in order to elucidate the dynamics and nature of the induced immune responses.

The higher tumor burden in stage IV as compared to stage III melanoma patients may hamper the induction of effective immune responses but instead favour local immune suppression. The present study demonstrates that robust immunological responses are more frequently induced in patients with no evidence of disease compared to patients with macroscopic tumor burden. Based on the association of tumor-specific T cells and improved clinical outcome, this suggests that DC based vaccination is a promising adjuvant treatment for stage III melanoma patients. However, extended follow-up is warranted to draw conclusions on the clinical efficacy of DC based vaccination in this stage of disease.

In summary, the advantages of vaccination with DC electroporated with mRNA encoding TAA include lack of HLA-restriction, presentation of multiple TAA epitopes to both $CD8^+$ and $CD4^+$ T cells, and the subsequent induction of a large repertoire of TAA-specific T cells. We demonstrate that vaccination of melanoma patients with mRNA-electroporated DC induces robust tumor-specific $CD4^+$ and $CD8^+$ T cell responses, in particular in stage III melanoma patients treated adjuvant to radical lymph node dissection.

References

1 Lesterhuis WJ, Aarntzen EHJG, Vries IJM, Schuurhuis DH, Figdor CG, Adema GJ, et al. Dendritic cell vaccines in melanoma: From promise to proof? Critical Reviews in Oncology Hematology 2008;66(2):118-34.

2 Lesterhuis WJ, de V, I, Schreibelt G, Lambeck AJ, Aarntzen EH, Jacobs JF, et al. Route of administration modulates the induction of dendritic cell vaccine-induced antigen-specific T cells in advanced melanoma patients. Clin Cancer Res 2011;17(17):5725-35.

3 Schultz ES, Schuler-Thurner B, Stroobant V, Jenne L, Berger TG, Thielemanns K, et al. Functional analysis of tumor-specific Th cell responses detected in melanoma patients after dendritic cell-based immunotherapy. J Immunol 2004;172(2):1304-10.

4 Verdijk P, Aarntzen EHJG, Lesterhuis WJ, Boullart ACI, Kok E, van Rossum MM, et al. Limited Amounts of Dendritic Cells Migrate into the T-Cell Area of Lymph Nodes but Have High Immune Activating Potential in Melanoma Patients. Clinical Cancer Research 2009;15(7):2531-40.

5 Wilgenhof S, Van Nuffel AM, Corthals J, Heirman C, Tuyaerts S, Benteyn D, et al. Therapeutic vaccination with an autologous mRNA electroporated dendritic cell vaccine in patients with advanced melanoma. J Immunother 2011;34(5):448-56.

6 Laverman P, de Vries IJM, Scharenborg NM, de Boer A, Broekema M, Oyen WJG, et al. Development of In-111-labeled tumor-associated antigen peptides for monitoring dendritic-cell-based vaccination. Nuclear Medicine and Biology 2006;33(4):453-8.

7 Mitchell DA, Nair SK. RNA-transfected dendritic cells in cancer immunotherapy. Journal of Clinical Investigation 2000;106(9):1065-9.

8 Skipper JCA, Hendrickson RC, Gulden PH, Brichard V, Vanpel A, Chen Y, et al. An HLA-A2-restricted tyrosinase antigen on melanoma cells results from posttranslational modification and suggests a novel pathway for processing of membrane proteins. Journal of Experimental Medicine 1996;183(2):527-34.

9 Zarling AL, Ficarro SB, White FM, Shabanowitz J, Hunt DF, Engelhard VH. Phosphorylated peptides are naturally processed and presented by major histocompatibility complex class I molecules in vivo. Journal of Experimental Medicine 2000;192(12):1755-62.

10 Schuurhuis DH, Verdijk P, Schreibelt G, Aarntzen EHJG, Scharenborg NM, de Boer A, et al. In situ expression of tumor antigens by messenger RNA-electroporated dendritic cells in lymph nodes of melanoma patients. Cancer Research 2009;69(7):2927-34.

11 Van Tendeloo V, Ponsaerts P, Lardon F, Nijs G, Lenjou M, Van Broeckhoven C., et al. Highly efficient gene delivery by mRNA electroporation in human hematopoietic cells: superiority to lipofection and passive pulsing of mRNA and to electroporation of plasmid cDNA for tumor antigen loading of dendritic cells. Blood 2001;98(1):49-56.

12 Schuurhuis DH, Lesterhuis WJ, Kramer M, Looman MGM, Hout-Kuijer M, Schreibelt G, et al. Polyinosinic polycytidylic acid prevents efficient antigen expression after mRNA electroporation of clinical grade dendritic cells. Cancer Immunology Immunotherapy 2009;58(7):1109-15.

13 Gajewski TF, Meng Y, Harlin H. Immune suppression in the tumor microenvironment. J Immunother 2006;29(3):233-40.

14 Gajewski TF. Failure at the effector phase: immune barriers at the level of the melanoma tumor microenvironment. Clin Cancer Res 2007;13(18 Pt 1):5256-61.

15 Gajewski TF, Meng Y, Blank C, Brown I, Kacha A, Kline J, et al. Immune resistance orchestrated by the tumor microenvironment. Immunol Rev 2006;213:131-45.

16 Eggermont AM, Testori A, Marsden J, Hersey P, Quirt I, Petrella T, et al. Utility of adjuvant systemic therapy in melanoma. Ann Oncol 2009;20 Suppl 6:vi30-vi34.

17 de Vries IJM, Lesterhuis WJ, Scharenborg NM, Engelen LPH, Ruiter DJ, Gerritsen MJP, et al. Maturation of dendritic cells is a prerequisite for inducing immune responses in advanced melanoma patients. Clinical Cancer Research 2003;9(14):5091-100.

18 Jonuleit H, Kuhn U, Muller G, Steinbrink K, Paragnik L, Schmitt E, et al. Proinflammatory cytokines and prostaglandins induce maturation of potent immunostimulatory dendritic cells under FCS-free conditions. Effect of culture conditions on the type of T cell response. Journal of Investigative Dermatology 1997;109(2):26.

19 de Vries IJM, Eggert AAO, Scharenborg NM, Vissers JLM, Lesterhuis WJ, Boerman OC, et al. Phenotypical and functional characterization of clinical grade dendritic cells. Journal of Immunotherapy 2002;25(5):429-38.

20 Figdor CG, de Vries IJM, Lesterhuis WJ, Melief CJM. Dendritic cell immunotherapy: mapping the way. Nature Medicine 2004;10(5):475-80.

21 de Vries IJM, Bernsen MR, Lesterhuis WJ, Scharenborg NM, Strijk SP, Gerritsen MJP, et al. Immunomonitoring tumor-specific T cells in delayed-type hypersensitivity skin biopsies after dendritic cell vaccination correlates with clinical outcome. Journal of Clinical Oncology 2005;23(24):5779-87.

22 Morse MA, Lyerly HK. Clinical applications of dendritic cell vaccines. Curr Opin Mol Ther 2000;2(1):20-8.

23 Germeau C, Ma WB, Schiavetti F, Lurquin C, Henry E, Vigneron N, et al. High frequency of antitumor T cells in the blood of melanoma patients before and after vaccination with tumor antigens. Journal of Experimental Medicine 2005;201(2):241-8.

24 Kyte JA, Mu L, Aamdal S, Kvalheim G, Dueland S, Hauser M, et al. Phase I/II trial of melanoma therapy with dendritic cells transfected with autologous tumor-mRNA. Cancer Gene Therapy 2006;13(10):905-18.

25 Hugues S, Fetler L, Bonifaz L, Helft J, Amblard F, Amigorena S. Distinct T cell dynamics in lymph nodes during the induction of tolerance and immunity. Nat Immunol 2004;5(12):1235-42.

26 Iezzi G, Karjalainen K, Lanzavecchia A. The duration of antigenic stimulation determines the fate of naive and effector T cells. Immunity 1998;8(1):89-95.

27 Bonehill A, Tuyaerts S, Van Nuffel AM, Heirman C, Bos TJ, Fostier K, et al. Enhancing the T-cell stimulatory capacity of human dendritic cells by co-electroporation with CD40L, CD70 and constitutively active TLR4 encoding mRNA. Molecular Therapy 2008;16(6):1170-80.

28 Keene JA, Forman J. Helper activity is required for the in vivo generation of cytotoxic T lymphocytes. J Exp Med 1982;155(3):768-82.

29 Hu HM, Winter H, Urba WJ, Fox BA. Divergent roles for CD4+ T cells in the priming and effector/memory phases of adoptive immunotherapy. J Immunol 2000;165(8):4246-53.

30 Ossendorp F, Mengede E, Camps M, Filius R, Melief CJM. Specific T helper cell requirement for optimal induction of cytotoxic T lymphocytes against major histocompatibility complex class II negative tumors. Journal of Experimental Medicine 1998;187(5):693-702.

31 Toes REM, Ossendorp F, Offringa R, Melief CJM. CD4 T cells and their role in antitumor immune responses. Journal of Experimental Medicine 1999;189(5):753-6.

32 Schoenberger SP, Toes RE, van d, V, Offringa R, Melief CJ. T-cell help for cytotoxic T lymphocytes is mediated by CD40-CD40L interactions. Nature 1998;393(6684):480-3.

33 Kumamoto Y, Mattei LM, Sellers S, Payne GW, Iwasaki A. CD4+ T cells support cytotoxic T lymphocyte priming by controlling lymph node input. Proc Natl Acad Sci U S A 2011;108(21):8749-54.

34 Bos R, Sherman LA. CD4+ T-cell help in the tumor milieu is required for recruitment and cytolytic function of CD8+ T lymphocytes. Cancer Res 2010;70(21):8368-77.

35 Marzo AL, Kinnear BF, Lake RA, Frelinger JJ, Collins EJ, Robinson BWS, et al. Tumor-specific CD4(+) T cells have a major "post-licensing" role in CTL mediated anti-tumor immunity. Journal of Immunology 2000;165(11):6047-55.

36 Wong SB, Bos R, Sherman LA. Tumor-specific CD4+ T cells render the tumor environment permissive for infiltration by low-avidity CD8+ T cells. J Immunol 2008;180(5):3122-31.

37 Baxevanis CN, Voutsas IF, Tsitsilonis OE, Gritzapis AD, Sotiriadou R, Papamichail M. Tumor-specific CD4+ T lymphocytes from cancer patients are required for optimal induction of cytotoxic T cells against the autologous tumor. J Immunol 2000;164(7):3902-12.

38 Mellman I, Steinman RM. Dendritic cells: specialized and regulated antigen processing machines. Cell 2001;106(3):255-8.

39 Takahashi T, Chapman PB, Yang SY, Hara I, Vijayasaradhi S, Houghton AN. Reactivity of autologous CD4+ T lymphocytes against human melanoma. Evidence for a shared melanoma antigen presented by HLA-DR15. J Immunol 1995;154(2):772-9.

40 Campillo JA, Martinez-Escribano JA, Muro M, Moya-Quiles R, Marin LA, Montes-Ares O, et al. HLA class I and class II frequencies in patients with cutaneous malignant melanoma from southeastern Spain: the role of HLA-C in disease prognosis. Immunogenetics 2006;57(12):926-33.

41 Rodriguez T, Mendez R, Del CA, Aptsiauri N, Martin J, Orozco G, et al. Patterns of constitutive and IFN-gamma inducible expression of HLA class II molecules in human melanoma cell lines. Immunogenetics 2007;59(2):123-33.

42 Hodi FS, O'Day SJ, McDermott DF, Weber RW, Sosman JA, Haanen JB, et al. Improved survival with ipilimumab in patients with metastatic melanoma. N Engl J Med 2010;363(8):711-23.

43 Robert C, Thomas L, Bondarenko I, O'Day S, JW MD, Garbe C, et al. Ipilimumab plus dacarbazine for previously untreated metastatic melanoma. N Engl J Med 2011;364(26):2517-26.

44 Hoos A, Eggermont AM, Janetzki S, Hodi FS, Ibrahim R, Anderson A, et al. Improved endpoints for cancer immunotherapy trials. J Natl Cancer Inst 2010;102(18):1388-97.

45 Lesterhuis WJ, Haanen JB, Punt CJ. Cancer immunotherapy--revisited. Nat Rev Drug Discov 2011;10(8):591-600.

Chapter 4

Natural human plasmacytoid dendritic cells induce antigen specific T cell responses and enhance overall survival in melanoma patients

Tel J

Aarntzen EH

Baba T

Schreibelt G

Schulte BM

Benitez-Ribas D

Boerman OC

Croockewit A

Oyen WJ

Van Rossum MM

Winkels G

Coulie PG

Punt CJ

Figdor CG

De Vries IJ

Submitted

Abstract

Vaccination against cancer exploiting dendritic cells (DCs) has for more than a decade been based on DCs generated *ex vivo* from monocytes or $CD34^+$ progenitors. Here, we report on the first clinical study of therapeutic vaccination against cancer exploiting activated naturally occurring plasmacytoid DCs (pDCs). Fifteen metastatic melanoma patients received intranodal injections of pDCs activated *ex vivo* and loaded with tumor-associated peptides. *In vivo* imaging demonstrated that administered pDCs migrated and distributed over multiple lymph nodes. Several patients mounted anti-vaccine $CD4^+$ and $CD8^+$ T cell responses. Despite the limited number of administered pDCs, an IFN signature was observed after each vaccination. Finally, patients that received the pDC-vaccine not only had a significant difference in the median survival (22 months) compared to patients that received standard DTIC chemotherapy (7.6 months), but also had a significant increase in the overall survival. These results indicate that vaccination with activated natural pDCs is feasible with minimal toxicity and that in patients with metastatic melanoma it induces immune responses and improve survival rate.

Introduction

Dendritic cells (DCs) constitute a family of antigen-presenting cells defined by their morphology, phenotype and unique capacity to process exogenously encountered antigens and to present them to naive T cells. Following infection or inflammation, DCs undergo a complex process of maturation and migrate to lymph nodes to present antigens and activate T cells. This decisive role in inducing immunity was the rationale for DC based immunotherapy, in which DCs loaded with tumor antigens were injected into cancer patients to stimulate T cells to eradicate tumors (1-3). So far, most DC-based vaccination studies were conducted in patients with metastatic melanoma because of the immunogenicity of this tumor and the characterization of antigens such as gp100 and tyrosinase (4, 5). Although numerous vaccination studies demonstrated the immunogenicity of tumor antigen-loaded DCs, the number of objective clinical responses has been limited, hampering its implementation as a novel form of standard treatment (6). Because of the limited number of naturally circulating DCs, virtually all vaccination studies have used DCs differentiated *ex vivo* from monocytes or $CD34^+$ progenitors. Recently we proposed that these 'artificial' DCs may be less effective than their natural counterparts that circulate in the blood (7). Two major subsets of natural circulating DCs can be found; plasmacytoid DCs (pDCs) and myeloid DCs.

Plasmacytoid DCs are the major producers of type I interferon (IFN), which is of major importance in combatting viral infections. Freshly isolated pDCs have been associated with tolerance or Th2 responses (8, 9), but several groups have now demonstrated that human pDCs produced large amounts of type I IFNs and induced Th1 responses (8, 10). Human pDCs induced strong allogeneic T cell responses (11), and primed $CD4^+$ and $CD8^+$ T cells against viruses or tumor antigens (12, 13). Preclinical studies showed that antigen-loaded pDCs protected against *Leishmania major* (14), and induced anti-tumor responses that inhibited tumor growth (15, 16). Recently, Takagi *et al* demonstrated that pDCs were crucial for the initiation of inflammation and T cell immunity (17). Together, these findings prompted us to test the capacity of activated human pDCs to elicit anti-tumor immune responses in patients.

In this first-in-human study, we report on vaccinating metastatic melanoma patients, with autologous activated pDCs loaded with tumor-associated peptides. Despite their low abundance in peripheral blood, we succeeded in isolating sufficient numbers (0.3-3 million per vaccination) of highly purified cells to carry out this study. We used the inactivated thick-borne encephalitis virus vaccine as a natural TLR agonist to activate pDCs and used these antigens as an immunomonitoring tool. We demonstrate that these activated pDCs induced antigen-specific $CD4^+$ and $CD8^+$ T cell responses associated with a significantly enhanced overall survival.

Material and Methods

Patient characteristics

Sixteen distant metastatic melanoma patients (according to the 2001 American Joint Committee on Cancer staging system) (18) were enrolled in this feasibility study. One patient did not complete the scheduled vaccinations and monitoring due to rapid progression of disease. Fifteen of the patients were considered evaluable. Eligibility criteria included measurable target lesions, HLA-A2.1 phenotype, histologically documented metastatic melanoma expressing gp100 (compulsory) and tyrosinase (non compulsory), no active infection or immune suppressive conditions, serum LDH concentration within normal limits (< 450 U/l) and WHO performance status 0 or 1. Primary endpoint was toxicity related to vaccination and immunological response. Informed consent was obtained from all patients and the study was approved by the local medical ethics committee.

CliniMACS pDC isolation and immunization schedule

Patients were vaccinated with autologous pDCs loaded with HLA-A2.1-binding tumor peptides derived from the melanoma-associated antigens gp100 and tyrosinase. The following HLA-A2.1-

restricted peptides were used: gp100-derived peptides gp100:154-162 (KTWGQYWQV) and gp100:280-288 (YLEPGPVTA) and tyrosinase-derived peptide tyrosinase:369-377 (YMNGTMSQV). The clinical study was designed as a feasibility study. The first patient received $0.3x10^6$ pDCs per vaccination, patients 2 and 3 received $1.0x10^6$ pDCs per vaccination, and patients 4 and 5 received $3x10^6$ pDCs per injection. Considering the yield from pDC isolation, this is the maximum feasible dose, and was also given to patients 6 to 15. Three intranodal injections were given once every two weeks followed by a DTH challenge. In the absence of disease progression, patients were eligible for a maximum of two maintenance cycles consisting of three biweekly vaccinations and a DTH challenge, each with a 6 month interval.

Plasmacytoid DCs were directly isolated from aphaeresis products using the fully closed immunomagnetic CliniMACS isolation system (Miltenyi Biotec, Bergisch-Gladbach, Germany). GMP-grade magnetic bead-coupled BDCA4 antibodies were used, following the manufacturer's guidelines. This procedure resulted in clinically applicable purified pDCs, which had an average purity of 75% and a yield between $13x10^6$ and $33x10^6$ (Supplementary Figure S1). Following aphaeresis and CliniMACS isolation, pDCs were cultured overnight at a concentration of 10^6 cells/ml in X-VIVO-15 (Cambrex, Belgium) containing 2% pooled human serum (HS) (Sanquin, Nijmegen, The Netherlands), supplemented with 10 ng/ml recombinant human interleukin-3 (rhIL-3) (Cellgenix, Freiburg, Germany). For the first vaccination, these pDCs were subsequently activated for 6 hours by addition of FSME-IMMUN® (1:10 v/v) (Baxter AG). During the last 3 hours of activation, pDCs were loaded with the melanoma-associated peptides gp100:154, gp100:280 and tyrosinase (19). For subsequent vaccinations and DTH skin tests, overnight IL-3 cultured pDCs were activated for 3 hours by addition of FSME-IMMUN® (1:10 v/v). Thereafter, these 3-hour activated pDCs were frozen in X-vivo 15 medium containing 10% DMSO. The peptide-loaded pDCs were administered intranodally in a clinically tumor-free lymphnode region under ultrasound guidance (20).

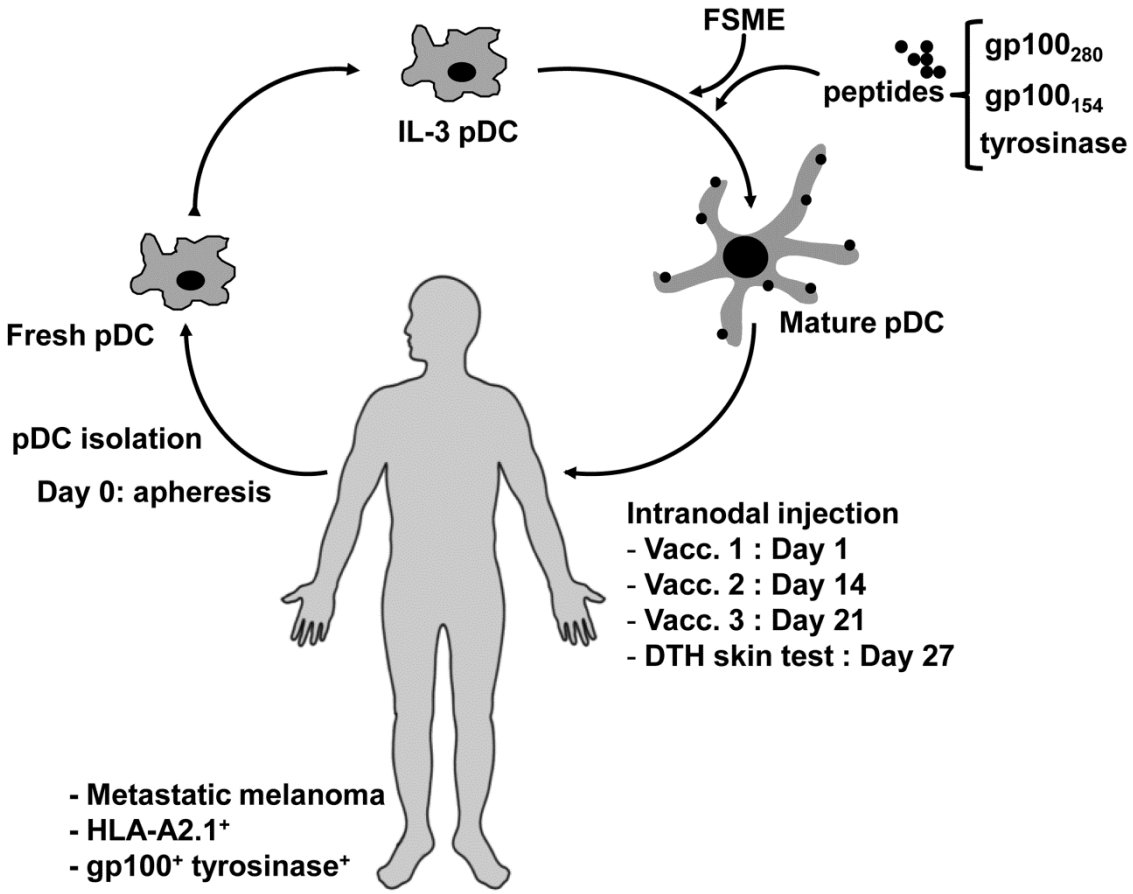

Figure 1 Schematic overview of the pDC culture protocol and vaccination strategy.

Phenotype

The purity of pDCs after CliniMACS isolation and the phenotype of the pDCs were determined by flow cytometry. The following primary monoclonal antibodies (mAbs) and the appropriate isotype controls were used: anti-CD45-FITC, anti-BDCA2-PE and anti-CD123-APC (all Miltenyi Biotec); anti-HLA-ABC-PE (W6/32), anti-HLA-DR/DP-FITC (Q5/13), anti-CD80-PE and CD86-PE (all BD Bioscience Pharmingen, San Diego, CA, USA); anti-CD83 (Beckman Coulter, Mijdrecht, the Netherlands) and anti-CCR7 (R&D Systems); followed by goat-anti-mouse PE.

Cytokine detection

Supernatants were collected from pDC cultures either directly after 6 h of stimulation or after 6 h of stimulation followed by a washing step and subsequent reconstitution of cells in fresh medium for an additional 12 hours, and IFNα production was analyzed with murine monoclonal capture and HRP-conjugated anti-IFNα antibodies (BenderMed Systems, Vienna, Austria) using standard ELISA procedures. To analyze the T helper cell profile, supernatants were collected after 2 days of pDC-PBL coculture. Cytokine production (IL-1β, IL-2, IL-4, IL-5, IL-6, IL-8, IL-10, IL-12 (p70), TNFα, TNFβ, IFNγ) in the supernatant was analyzed with a human Th1/Th2 Multiplex kit (BenderMed System) according to the manufacturer's instructions.

^{111}In-oxinate labeling and scintigraphic imaging

Six-hour FSME-activated pDCs were labeled with 5 MBq ^{111}In-oxinate (GE Healthcare, Eindhoven, The Netherlands) in 0.1 M Tris-HCl (pH 7.0) for 15 minutes at room temperature as described previously (21, 22). Cells were washed three times with PBS/1%HSA, and the labelling efficiency was calculated as the percentage of the activity that remained associated with the cell pellet. ^{111}In-labeled pDCs (3×10^6; 4 MBq) in 200 µl saline were injected under ultrasound guidance directly into a clinically tumor-free lymph node. *In vivo* planar scintigraphic images (256 × 256 matrix, 174 and 247 keV ^{111}In photopeaks with 15% energy window) of the injection depot and corresponding lymph node basin were acquired with a gamma camera (Siemens ECAM, Hoffman Estates, IL) equipped with medium energy collimators, 15 minutes, 24 hours and 48 hours after injection. Migration was quantified by region-of-interest analysis of the individual nodes visualized on the images and expressed as the fraction of ^{111}In-labeled DC that had migrated from the injection depot to following lymph nodes after 15 minutes, 24 hours and 48 hours.

Immunomonitoring of patients

Blood samples were obtained before the start of the vaccination regimen and after each individual vaccination. Each sample was tested for the presence of FSME-specific T cells by proliferation and ^{3}H-thymidine incorporation, and for the presence of FSME-specific antibodies in the serum using an ELISA specific for Tick-Borne Encephalitis IgG (Serion/Virio, Würzburg, Germany). Four days after the third vaccination, a DTH skin test was performed as described previously (23). moDCs pulsed with gp100 or tyrosinase peptides ($1x10^6$) and pDCs pulsed with gp100 or tyrosinase peptides ($0.2x10^6$) were injected intradermally in the skin of the back of the patient at 4 different sites. The maximum diameter of induration was measured after 48 hours. Punch biopsies (6 mm) were obtained from all DTH sites. Half of the biopsy was cryopreserved and the other half was manually cut and cultured in RPMI 1640 (Gibco-BRL Life Technologies) containing 7% HS and IL-2 (100 U/ml, Proleukin®, Chiron, the Netherlands). Every 7 days, half of the medium was replaced by fresh medium containing HS and IL-2. After 2 to 5 weeks of culturing, T cells were tested for specificity against gp100 and tyrosinase (19). DTH-derived cells were stained with tetrameric-MHC complexes containing the gp100:154-167, gp100:280-288 or tyrosinase:369-376 peptide (Sanquin, Amsterdam, The Netherlands) combined with CD8 staining as described previously (23). All samples were tested with HIV:77–85 HLA-A2.1-tetramers recognizing the irrelevant HIV-peptide (SLYNTVATL) for background staining.

Mixed lymphocyte-peptide cultures

Blood frequencies of anti-vaccine $CD8^+$ T cells were estimated using mixed lymphocyte-peptide cultures (MLPCs) as described previously (24). Briefly, PBMCs isolated before and after one cycle of three pDC injections, were thawed and divided in three groups incubated for 1 h at room temperature in Iscove's medium (Life Technologies, Carlsbad, CA, USA) with 1% HS and 2 μM of the peptides tyrosinase:369 (YMDGTMSQV), wild-type gp100:154 (KTWGQYWQV), or wild-type gp100:280 (YLEPGPVVTA). These pulsed cells were then washed, pooled, and distributed at 2 x 10^5 cells/0.2 ml in round-bottom microwells in Iscove's with 10% HS, L-arginine (116 mg/l), L-asparagine (36 mg/l), L-glutamine (216 mg/l), 1-methyl-L-tryptophan (100 μM), IL-2 (20 U/ml), and IL-7 (10 ng/ml). On day 7, 50% of the medium was replaced by fresh medium containing IL-2 and peptides at 4 μM. Tetramer labeling was performed on day 14 as described previously (24). Anti-gp100:154 T cell clones were derived that represented either the spontaneous anti-gp100 T cells present prior to vaccination in patients 2, 5, 6, 10 and 11, or the pDC-induced anti-gp100 T cells present after vaccination in patients 1, 4, 8 and 12. Tetramer-positive $CD8^+$ T cells were sorted at 1 cell/well and restimulated weekly with irradiated HLA-$A2^+$ EBV-transformed B cells pulsed with the gp100:154 peptide at 2 μM and irradiated allogeneic PBMC as feeder cells, in medium supplemented with IL-2 and IL-7. Established T cell clones were stained with the relevant tetramer and their functional avidity was evaluated by testing their production of IFNγ after stimulation with HLA-$A2^+$ EBV-B cells pulsed with various concentrations (from 10 pM up to 10 μM) of the gp100:154 peptide.

RNA isolation and qPCR

To determine mRNA expression of IFN and IFN-stimulated genes (ISGs) blood was drawn from one patient during one cycle of 3 vaccinations before each vaccination and at 4 and 24 hours after each vaccination using PAXgene tubes. RNA isolation was performed using PAXgene blood RNA kit according to the manufacturer's instructions (Qiagen). RNA isolations from PBMCs from healthy volunteers were done using the ZR RNA isolation kit (Zymo Research) according to manufacturer's instructions. RNA was treated with DNase I (amplification grade; Invitrogen) and reverse-transcribed into cDNA by using random hexamers and Moloney murine leukemia virus reverse transcriptase (Invitrogen). To exclude genomic DNA contamination we included a "-RT" control in which the reverse transcriptase was replaced with RNase-free water. The "-RT" control was taken along in the qPCR analysis, and was used as a cut-off value. cDNA was stored at -20°C until further use. mRNA levels for the genes of interest were determined by quantitative PCR (qPCR) with a Biorad CFX apparatus (Biorad) with SYBR Green (Applied Biosystems). Analysis was done using Biorad CFX-1.6 software, and expression levels were determined relative to PBGD expression. Primer sequences are available on request and were from the Primer Bank database (25).

Matched controls

Matched controls were identified from records of metastatic melanoma patients from the Radboud University Nijmegen Medical Centre (Nijmegen, The Netherlands), The Netherlands Cancer Institute – Antoni van Leeuwenhoek Hospital (Amsterdam, The Netherlands) and University Hospital Essen (Essen, Germany) who had received first-line dacarbazine (DTIC) chemotherapy at 850–1000 mg/m^2 i.v. at 3 weekly intervals, between March 2000 and March 2010. All matched controls were HLA-A*02:01 positive and were required to have received at least 3 infusions, a therapy time-frame that is consistent with one cycle of vaccinations.

Controls were matched to study subjects, in ratio 1:3, primarily for M substage at baseline according to AJCC criteria, number of distant metastases, number of metastatic sites, localization of distant metastases and baseline serum LDH. These criteria currently represent the most important prognostic factors for survival (26). In case of more than three matches for one study subject,

demographic criteria (age, gender) and systemic salvage treatment after progression on DTIC were used to select the closest match.

Statistical analysis

Significant differences from controls were determined according to paired student t-test or by one-way ANOVA analysis followed by the Tukey's post-hoc test. Differences between the groups were evaluated using an unpaired t-test. Differences between pre- and post-vaccination were evaluated with a Wilcoxon signed-rank test. Kaplan-Meier probability estimates of PFS and OS were calculated, statistical differences between the survival of the groups were determined with a log-rank test. Statistical significance was defined as $p<0.05$. SPSS19.0 was used for survival analyses.

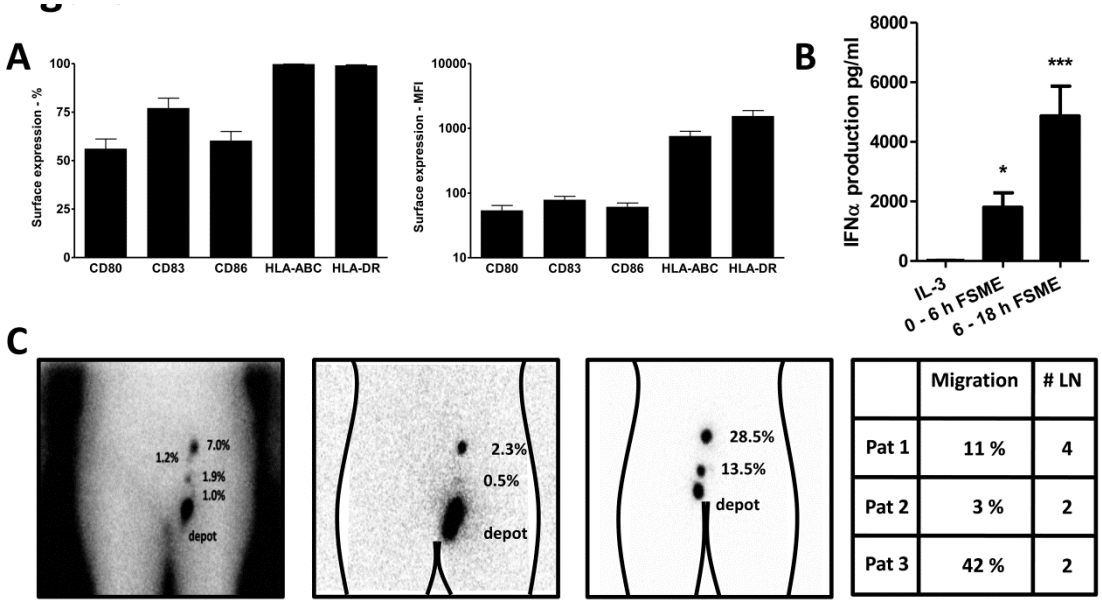

	Migration	# LN
Pat 1	11 %	4
Pat 2	3 %	2
Pat 3	42 %	2

Figure 2. Activated pDCs are mature and migrate to distinct lymph nodes in vivo. (A) Expression levels of the surface molecules CD80, CD83, CD86, MHC class I and MHC class II on pDCs after 6 hours of activation with the FSME-vaccine. Surface receptor expression levels of all molecules of the pDC vaccines depicted in the percentage of positive cells (left graph) and mean fluorescence intensity (right graph) after 6 hours of activation with the FSME-vaccine (n=15). (B) IFNα production by pDCs after 6 hours of cultivation/activation with rhIL-3 or FSME-vaccine or after 6 hours of activation followed by a washing step and reconstitution of pDCs in fresh medium for an additional 12 hours (n=9; *: P<0.05, ***: P<0.001). (C) Tracking of pDC migration i*n vivo*. Migration and biodistribution of ^{111}In-labeled pDCs visualized by scintigraphical imaging. Forty-eight hours after administration, 11% (Pt 01), 3% (Pt 02) and 42% (Pt 03) of injected pDCs were distributed over up to 4 distant lymph nodes away from the injection depot.

Results

Vaccination of metastatic melanoma patients with activated pDCs is safe with minimal side effects

It is of utmost importance that pDCs administered to cancer patients have an immunostimulatory phenotype (19). Previously we demonstrated that the commonly used preventive FSME-vaccine induced both IFNα secretion and a mature pDC phenotype (27). Thus FSME could be used as a clinically applicable natural TLR agonist. In this first-in human study we vaccinated 15 patients with increasing pDC numbers, ranging from 0.3 to 3 million per vaccination, with three vaccinations at bi-weekly intervals. Patient characteristics are shown in Table 1. The expression of CD80, CD83, CD86, MHC class I and II upon FSME-induced activation indicated that the generated pDCs were highly mature and capable of providing costimulatory signals needed for optimal T cell activation (Figure 2A). Furthermore, pDC activation for 6 hours led to the secretion of high levels of type I IFN (Figure 2B). Additionally, we also washed 6 hour activated pDCs and reconstituted the cells in fresh medium. Thereafter, pDCs were maintained for an additional 12 hours to demonstrate that pDCs have a sustained ability to secrete IFNα (Figure 2B). Thus, all patients received purified and activated peptide-loaded pDCs that met the predefined release criteria with the ability to secrete type I IFN *in*

vivo (6). Furthermore, the vaccines were well tolerated and no signs of severe toxicity (common toxicity criteria grade 3-4) were observed. Six vaccinated patients developed grade 1 flu-like symptoms and one patient reported grade 2 non-treatment related pain resulting from progressive subcutaneous metastasis. In none of the vaccinated patients did we detect antibodies to the murine antibody used during the isolation procedure (data not shown). We conclude that it is feasible and safe to administer activated and tumor-peptide loaded pDCs to patients.

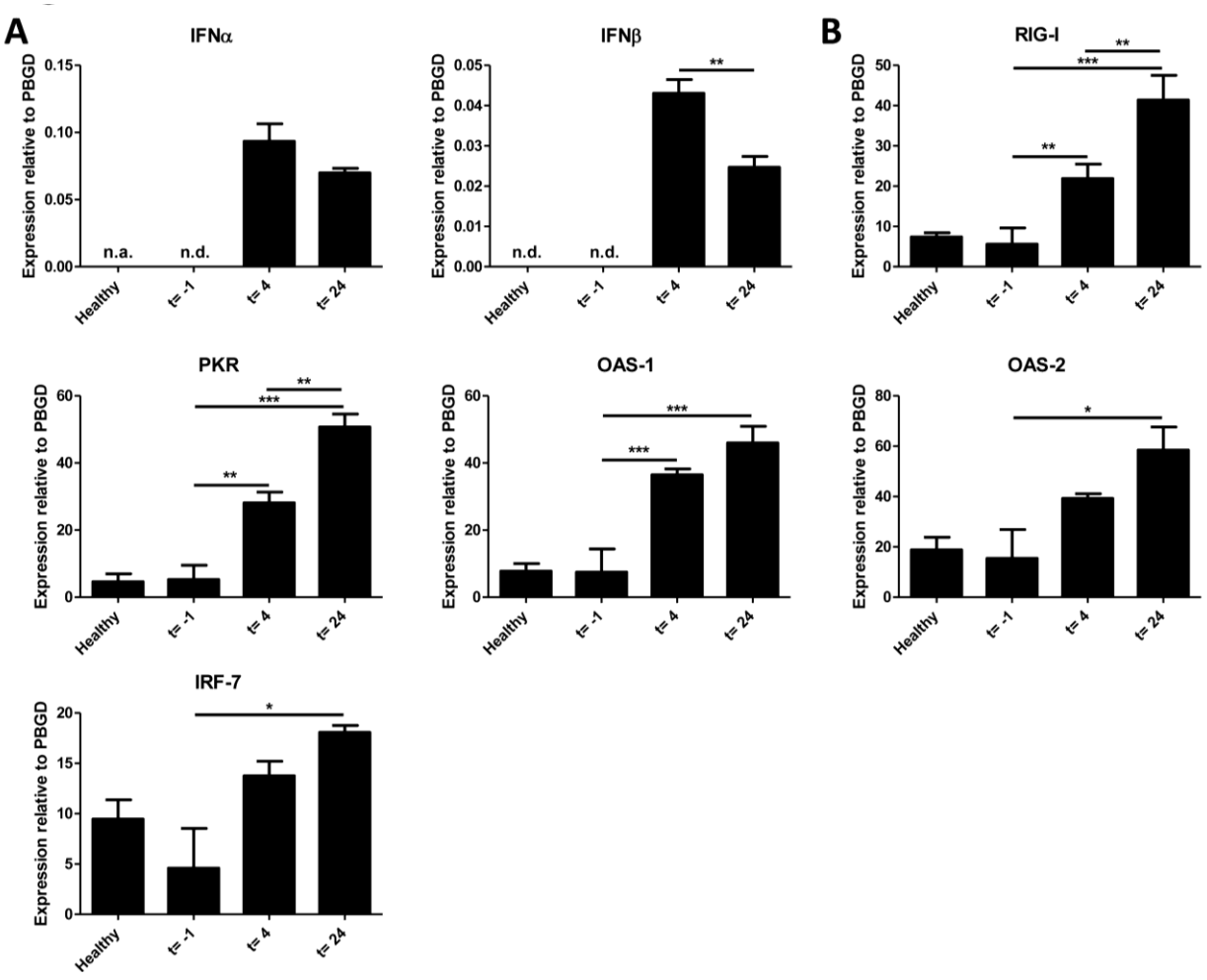

Figure 3. Vaccination with activated pDCs induces an IFN signature. (A) The graphs show the IFNα and IFNβ gene expression levels in the blood relative to PBGD expression at indicated times after each vaccination. (B) The graphs show the mRNA expression of indicated ISGs determined as in (A). Healthy indicates steady state expression levels of indicated genes in 8 healthy individuals. n.a.: not analyzed, n.d.: not detected (* $p<0.05$; ** $p<0.01$; *** $p<0.001$).

Migration of activated pDCs in vivo

For effective immunization, injected DCs have to migrate into the T cell areas of draining lymph nodes to present antigens to naive T cells. Because of the limited amount of pDCs available, we opted for intranodal injection to maximize the number of pDCs in the lymph node. In three patients we examined the migration *in vivo* of activated pDCs labelled with ^{111}In (21, 28). Forty-eight hours after intranodal injection a significant proportion of ^{111}In-labeled pDCs remained at the injection site and distinct amounts were detected in distant lymph nodes (Figure 2C). These results demonstrated that the pDCs injected in a single lymph node distributed into downstream nodes.

Vaccination with activated pDC induce an IFN signature in vivo

To verify whether activated pDCs secreted significant quantities of type I IFNs *in vivo*, we investigated in one patient the IFN signatures in great detail (multiple time points / three vaccinations). We measured in blood mononuclear cells the expression of type I IFNs genes and of five IFN-induced

genes in blood mononuclear cells one hour before and four and 24 hours after vaccination, and compared these expression levels to those of healthy individuals. Transcription of both IFNα and IFNβ genes was clearly induced four hours after vaccination and decreased 20 hours later (Figure 3A), indicating a temporal systemic induction of type I IFNs. As expected, we observed increases in the expression of the IFN-induced genes RIG-I, PKR, OAS-1, OAS-2 and IRF-7 after four hours and further increases after 24 hours (Figure 3B). These results demonstrate that after each vaccination even small numbers of injected pDCs induced a systemic type I IFN signature.

Plasmacytoid DC vaccination leads to CD4$^+$ T cell proliferation and antibody production

We next analyzed the ability of activated pDCs to prime T cell responses to the FSME antigens, which served as an internal control for the tumor-associated antigenic peptides. After 3 pDC vaccinations, FSME-stimulated T cell proliferation increased in 9 out of 14 tested patients (Figure 4A, Table 1). Cytokine production experiments carried out in 6 patients showed higher levels of IFNγ, IL-10 and IL-5 after vaccinations than before (Figure 4B, and data not shown).

Furthermore, we followed the levels of serum anti-FSME antibodies after each vaccination. Twelve out of the 15 tested patients significantly increased their anti-FSME IgG titers sstarting after the second vaccination (Figure 4C, Table 1). One patient (pt 14) already had anti-FSME antibodies prior to vaccination.

In only one of the 15 patients neither T cells nor antibodies to FSME were detected. Thus the majority of patients developed *de novo* proliferative and humoral FSME-specific immune responses upon vaccination, indicative of a functional immune system that can be primed by activated and antigen-loaded pDCs.

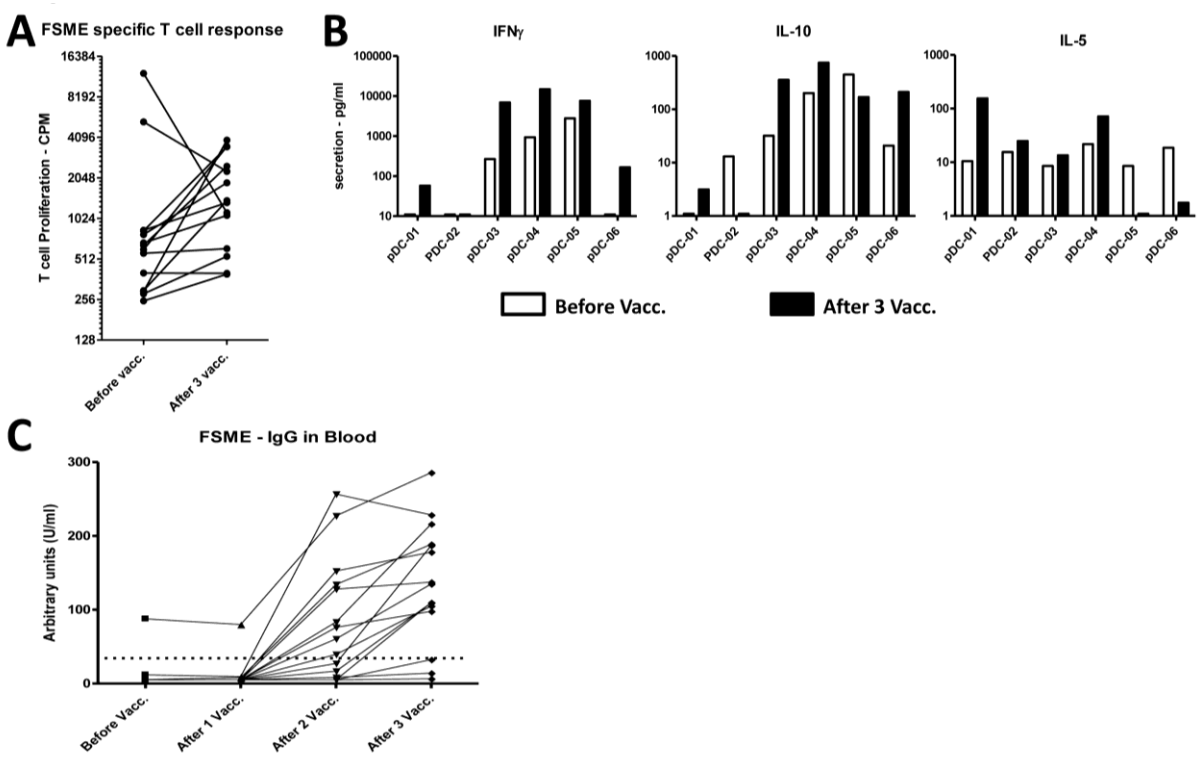

Figure 4. Activated pDCs induce de novo FSME-specific cellular and humoral immune response in vivo. (A) Proliferation of anti-FSME blood T cells collected before and after three vaccinations with tumor-peptide loaded pDCs. Proliferation of T cells was measured by ^{3}H-Thymidine incorporation and depicted as proliferation in counts per minute (log scale). (B) Cytokine production pre- (white bars) and post-vaccination (black bars); IFNγ, IL-10 and IL-5 production by T cells stimulated overnight by FSME-activated pDCs (log scale). The graphs show the cytokine production of T cells from 6 patients. (**C**) FSME-specific IgG detected in the serum of patients before and after the first, second and third vaccination. The dotted line represents the threshold (28 Units) for positivity. (ns, not significant; *** p<0.001).

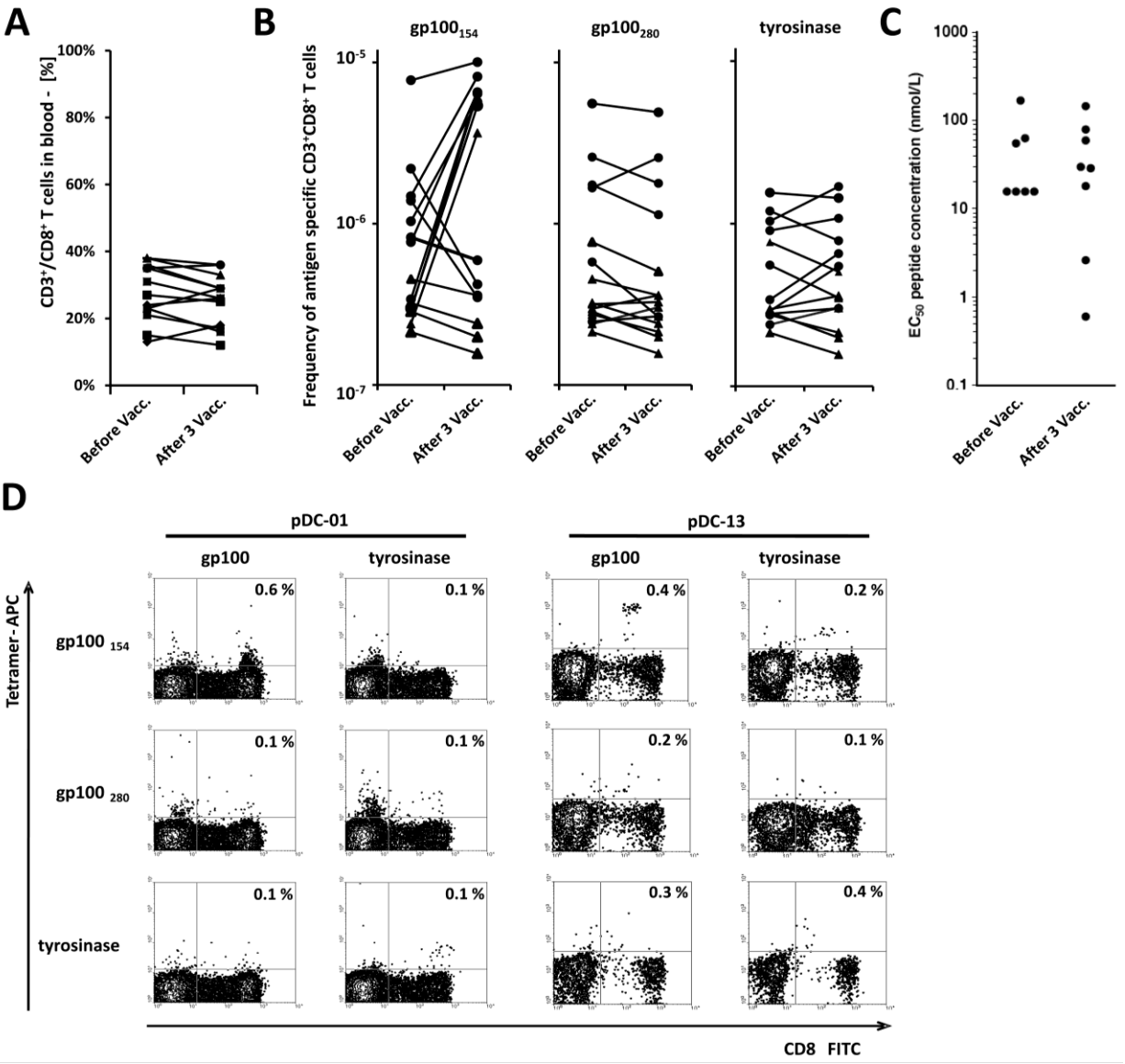

Figure 5. Activated pDCs induce tumor-antigen specific CD8$^+$ T cell responses in patients. (A) Proportions of blood CD3$^+$ CD8$^+$ T cells before and after 1 cycle of vaccination. (B) pDC vaccine-related CD8$^+$ T cell responses are detected in the blood after MLPCs. The graphs show the blood frequencies of gp100$_{154}$, gp100$_{280}$ and tyrosinase tetramer$^+$ CD8$^+$ T cells before and after 1 cycle of vaccination on a log scale. (C) Functional avidities of anti-gp100$_{154}$ CD8$^+$ T cell clones derived from selected patients before (7 clones) or after (8 clones) one cycle of vaccination. The graph shows the concentrations of antigenic peptide, pulsed on HLA-A2$^+$ cells, required to obtain 50% of maximal IFN-g production by each of the T cell clones on a log scale. (D) pDC vaccine-related CD8$^+$ T cell responses are detected in biopsies taken from DTH skin tests. Two weeks after the third pDC injection, a DTH skin test was performed by injecting intradermally pDCs and moDCs loaded with either the gp100 or the tyrosinase peptides. Biopsies taken 2 days later were cultured for 3-4 weeks in low dose IL-2, and proliferating T cells were stained with specific tetramers. FACS plots from patients 01 (after one vaccination cycle) and 13 (after two vaccination cycles)show DTH-infiltrating lymphocytes stained by gp100$_{154}$ tetramers. (ns, not significant; ** p<0.01).

Activated pDCs induce tumor antigen-specific CD8$^+$ T cell responses in vivo

We used tetramers to detect the presence of tumor antigen-specific CD8$^+$ T cells in blood, and in biopsies taken from skin delayed-type hypersensitivity (DTH) reactions as described previously (23). In blood, the proportions of total CD8$^+$ T cells did not change following vaccination (Figure 5A), and *ex vivo* tetramer staining was negative both before and after vaccination (data not shown). We resorted to an *in vitro* restimulation of blood mononuclear cells in limiting dilution conditions over two weeks with the 3 antigenic peptides, before screening all microcultures for the presence of CD8$^+$ tetramer$^+$ cells. This procedure allows estimating the frequencies of blood CD8$^+$ T cells that recognize a given antigen and proliferate *in vitro* in response to this antigen. As shown in Figure 5B, 7 out of 15

patients showed a significant increase (≥5-fold) of the frequency of $gp100_{154}$-specific $CD8^+$ T cells in (Figure 5B). To evaluate the affinity of these anti-vaccine T cells, we derived anti-$gp100_{154}$ T cell clones from pre- and -postvaccination PBMC and measured IFNg production after stimulation with various concentrations of peptide. The concentration of peptide that stimulates a half-maximal cytokine production reflects the functional avidity of the T cells. As shown in Figure 5C, 2 out of the 8 post-vaccination clones had a higher (>10-fold) functional avidity than that of all the other pre- or post-vaccination clones, suggesting the efficacy of pDCs at priming high affinity T cells.
In the skin, we observed in 10 out of the 15 patients positive DTH responses with indurations of up to 22 mm at the sites of intradermal injection of 0.2 x 10^6 peptide-loaded activated pDCs (Supplementary Table S1). Furthermore we detected anti-gp100:154 $CD8^+$ T cells in one DTH biopsy obtained after one cycle of vaccination (pt 1) and in one obtained after two cycles (pt 13) (Figure 5D). T cells obtained from biopsies of DTH reactions to unloaded pDCs did not proliferate demonstrating the specificity of this response. We conclude that vaccination with small numbers of peptide-loaded and activated pDCs can induce tumor-specific $CD8^+$ T cell responses in metastatic melanoma patients.

Plasmacytoid DC vaccination enhances the overall survival of late stage melanoma patients
Two patients (pt 13 and 14) showed durable stable disease and were eligible for two additional cycles consisting of three pDC vaccinations. Patient 14 developed a mixed response with regression of lung metastases and progression of a nodal metastasis. Patient 10 had a documented progression but achieved complete remission after surgery and subsequently received maintenance treatment. We compared the clinical outcome of these 15 patients to that of carefully matched historical control patients (n=72) who received standard DTIC (Dacarbazine) chemotherapy as a first line treatment (Supplementary Table S2). The median progression-free survival in the pDC group was 4.0 months versus 2.1 months in the control group (not significant; Figure 6A). Although the initial endpoint of this study was safety and feasibility, the median overall survival showed a remarkable improvement compared to matched control patients: 22.0 months (95%CI 1.8 – 42.2) versus 7.6 months (95%CI 5.8 – 9.4), p=0.001. Furthermore, based on a log-rank test, patients vaccinated with pDCs also showed a significant overall survival, p=0.001. Seven out of the 15 patients were alive, even 2 years after the start of treatment, compared to 6 out of 72 patients treated with standard chemotherapy (Figure 6B).

Table 1 Patient characteristics & clinical and immunological responses after pDC vaccination

						Anti FSME response		Anti tumor response				
Pt	**Sex/ age**	**Prior therapy**	**Stage**	**Site of metastases**	**Injected pDCs**	**T cell[a]**	**Ab[b]**	**$CD8^+$ T cell**	**Clinical response[c]**	**PFS[d]**	**OS[e]**	**Salvage treatment[g]**
01	M / 43	S	M1b	Lung, skin	0,3*106	++	++	+	PD	< 4	10	RT
02	F / 45	-	M1b	Lymph nodes, lung	1*106	+	++	-	PD	< 4	3	CT
03	M / 62	-	M1c	Liver, lung	1*106	++	++	+	SD	6	36+	CT, IT[1,2]
04	M / 35	-	M1c	Liver, lymph nodes, esophagus, omentum	3*106	-	++	+	SD	5	27	CT, IT[1,3]
05	F / 53	S	M1c	Liver, lung, skin, spleen	3*106	-	++	+	PD	< 4	5	RT
06	M / 59	S	M1b	Lung, skin	3*106	n.a.	-	-	PD	< 4	6	RT
07	M / 43	-	M1c	Lymph nodes, skin, testis	3*106	+	++	-	PD	4	5	None
08	F / 51	-	M1b	Lung	3*106	+	++	+	PD	< 4	13	None
09	M / 36	-	M1b	Lung, skin	3*106	+	+	+	SD	5	23	CT, IT[3,4]
10	M / 52	S	M1a	Lymph nodes	3*106	-	-	-	SD	7	28+	S
11	M / 66	-	M1c	Liver, lymph nodes, lung	3*106	-	++	-	PD	< 4	12	CT
12	F / 39	S	M1b	Lung	3*106	++	++	+	SD	5	27+	RT, CT, IT[1]
13	F / 56	S	M1b	Lung	3*106	++	++	+	SD	15	26+	CT, IT[1]
14	M / 69	S	M1c	Lung, skin, adrenal gland	3*106	+	++	-	MR	14+	24+	None
15	M / 67	S, RT, CT	M1b	Lymph nodes, lung, skin	3*106	++	-	-	PD	< 4	24+	IT[1]

[a] – No T cell response; + Stimulation index >1<2; ++ SI ≥2<10.
[b] – No Ab or < 15 U/ml; +/- Ab titer < 28 U/ml; + Ab titer > 28 <100 U/ml; ++ Ab titer >100 U/ml
[c] PD, progressive disease; SD, stable disease; MR, mixed response.
[d] Progression free survival (PFS) in months.
[e] Overall survival (OS) in months
[g] RT, radiotherapy; CT, chemotherapy; S, surgery; IT, immunotherapy
[1] anti-CTLA4 antibody,[2] Akt inhibitor,[3] Ifosfamide-pazopanib,[4] MEK inhibitor (AZD6244)

Discussion

After almost 15 years of DC based immunotherapy, the clinical efficacy of the *ex vivo* generated monocyte- or $CD34^+$ progenitor derived-DCs is disappointing. Therefore, properly activated naturally occurring dendritic cells might represent the next generation of anti-cancer cellular therapy to induce tumor-specific immunological responses and improved clinical efficacy. In this first clinical study with plasmacytoid DCs in metastatic melanoma patients, with activated pDCs injected into lymph nodes, we noted a significant increase in overall survival. In these patients we observed: 1) distribution of injected pDCs over multiple lymph nodes, 2) enhanced systemic secretion of type I IFNs, 3) *de novo* T and B cell responses to control antigen, and 4) induction of tumor antigen specific $CD8^+$ T cells, including some with high functional avidity.

Plasmacytoid DCs are known to sense viral or self nucleic acids and to become activated to produce type I IFN at sites of inflammation. These IFNs initiate protective immunity through maturation of resident myeloid DCs and subsequent activation of infiltrating T cells and NK cells. By contrast, non-activated pDCs promote T regulatory cell-mediated immunosuppression (29), and the presence of pDCs in tumors has been correlated with poor clinical outcome (30, 31). We hypothesized that properly activated pDCs, because of their IFN production, might stimulate myeloid DCs and enhance their ability to cross-prime $CD8^+$ T cells, thereby inducing more efficient anti-tumor T cell responses when compared to *in vitro* generated DCs. This notion is supported by two independent studies demonstrating in mice that type I IFNs were critical for the induction of anti-tumor immune responses (32, 33). Therefore, to warrant clinical efficacy, pDCs should secrete type I IFN at the time of administration. Since previous studies showed that pDCs produced IFNα within 12 hours after activation and then became refractory to further stimulation (34-36), isolated pDCs were maintained overnight in IL-3 and subsequently activated for 6 hours with FSME. Our approach resulted in clinically applicable pDCs with a stimulatory phenotype and secretion of type I IFNs *in vivo*. Accordingly, we now demonstrate that vaccination with such pDCs indeed induced an IFN signature based on the upregulated IFN-induced genes in the blood after vaccination, validating our approach.

For an optimal immune response the injected pDCs should migrate to neighboring lymph nodes and then to T cell areas. The observed migratory behavior and distribution over multiple lymph nodes of the injected pDCs might be linked to the expression of CCR7 (Supplementary Figure S2), the homing receptor for the chemokines CCL19 and CCL21 that are expressed by high endothelial venules and stromal cells in the T cell areas (29, 37, 38). The pDC migratory behavior is in agreement with previous studies, where although the majority of injected DCs reside at the injection depot (22, 28, 39, 40), a substantial fraction of the pDCs migrated to subsequent lymph nodes. It is important to consider that the microenvironment influences cell migration (41). Therefore, a high number of pDCs at the injection site might affect the microenvironment. For example, pDC-derived IFNs could drive expression of chemokines resulting in the recruitment of immune cells, thereby circumventing the need for active migration of the pDCs themselves. Unfortunately, the clinical protocol did not allow lymph node resections, to further substantiate this important aspect.

We used FSME as natural TLR agonist to activate pDCs. As FSME comprises a total inactivated virus we reasoned that during activation pDCs will process FSME-derived antigens and present antigenic peptides on HLA molecules. Indeed, we observed cellular as well as humoral responses against FSME in almost all patients. Therefore, commonly used vaccines are potentially interesting, to serve both as a TLR agonist and as a control antigen. In addition, it cannot be excluded that anti-FSME Th1 responses contribute to the expansion of $CD8^+$ tumor specific T cells.

We previously demonstrated that the presence of anti-vaccine $CD8^+$ T cells at sites of vaccine-induced skin DTH reactions was correlated with favorable clinical outcome (23, 42). Several clinical studies in cancer patients have reported anti-vaccine T cell responses in the blood, but only in a minority of patients or after prolonged *in vitro* restimulation with antigen (43-46). Here, we observed the specific induction of tumor specific $CD8^+$ T cells, which indicates that even small numbers of pDCs

can evoke antigen-specific immune responses. To verify if this tumor specific T cell response contributed to long-term tumor control, we compared the clinical outcome of our patients to that of carefully selected historical controls treated with standard DTIC chemotherapy. Although it must be emphasized that this study was not designed to evaluate clinical outcome, several interesting observations were made. First, progression-free survival in vaccinated patients was similar to that of the matched control patients, matching progression-free survival reported in literature (47-49). Remarkably, the 1-year and 2-year survival rates were 60% and 45% after pDC vaccination compared to 30% and less than 10% of the matched control patients respectively. To exclude that this discrepancy in survival might partially be influenced by subsequent salvage treatments, we carefully matched the total number of different treatments and the types of salvage treatments for both control group and the vaccinated patients (Supplementary Table S1). Secondly, we detected tumor-specific $CD8^+$ T cells almost in all patients with a long overall survival. Therefore, we hypothesize that the improved overall survival is related to the priming or restimulation of anti-tumor $CD8^+$ T cells, which would be in line with our previous findings (23). Thirdly, given the low numbers of cytotoxic T cells that we detected, as compared to number reported in trials with monocyte- or $CD34^+$ progenitor-derived DCs, it is tempting to speculate that other immune cells from the innate arm play an important role in assisting cytotoxic T cells. Therefore it would be extremely interesting to study the immune cell repertoire within resected lymph nodes in more detail. Comparable patterns, no effect on progression free survival but significantly extended overall survival, were recently described for other immunotherapies, especially anti-CTLA4 blockade (48). These findings support the notion that immunotherapy may act indirectly, rather than having a direct cytotoxic anti-tumor effect.
The remarkable extended 2-year overall survival by a significant number (7 out of 15) of patients, urge for a randomized phase II clinical trial to confirm the potential of natural pDCs as an anti-cancer vaccine.

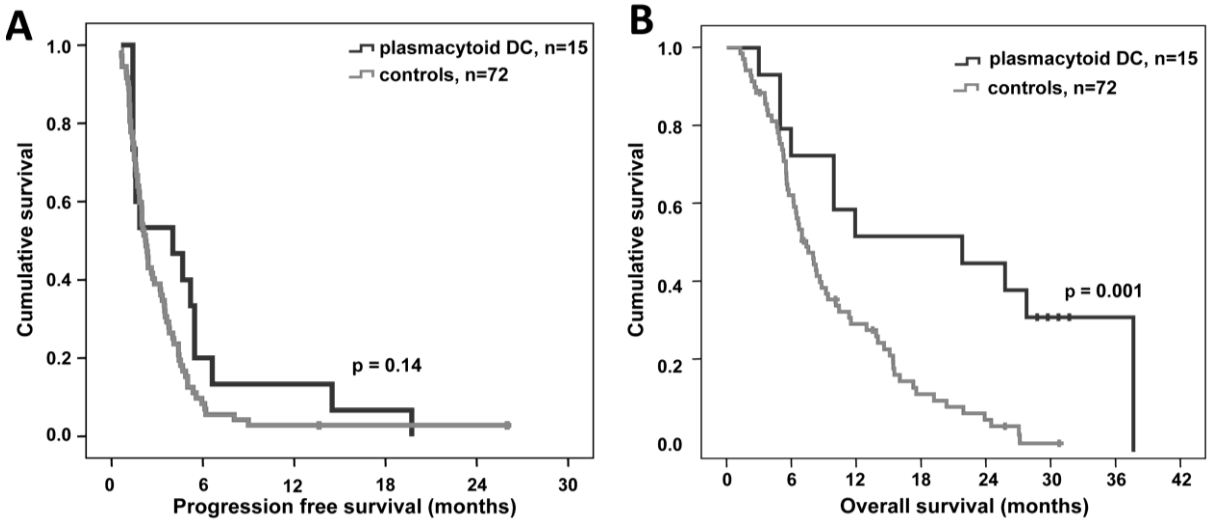

Figure 6. pDC vaccination improves overall survival. Clinical outcome to pDC vaccination was compared to a group of carefully matched historical control patients who received Dacarbazine as first line treatment. (A) Progression-free survival for pDC vaccination was 4.0 months versus 2.1 months in the control group. Median overall survival data showed a remarkable improvement compared to matched control patients; 22.0 months versus 7.6 months. (B) Overall survival of pDC vaccinated patients was significantly improved compared to matched controls. Statistical significance between the survival of the groups was determined by a log-rank test, p=0,001.

References

1. Banchereau, J. and A.K. Palucka, *Dendritic cells as therapeutic vaccines against cancer.* Nat Rev Immunol, 2005. 5(4): p. 296-306.
2. den Brok, M.H., et al., *Dendritic cells: tools and targets for antitumor vaccination.* Expert Rev Vaccines, 2005. 4(5): p. 699-710.
3. Nestle, F.O., A. Farkas, and C. Conrad, *Dendritic-cell-based therapeutic vaccination against cancer.* Current Opinion in Immunology, 2005. 17(2): p. 163-169.
4. Alexander B. H. Bakker, et al., *Identification of a novel peptide derived from the melanocyte-specific gp100 antigen as the dominant epitope recognized by an HLA-A2.1-restricted anti-melanoma CTL line.* International Journal of Cancer, 1995. 62(1): p. 97-102.
5. Brichard, V., et al., *The tyrosinase gene codes for an antigen recognized by autologous cytolytic T lymphocytes on HLA-A2 melanomas.* J. Exp. Med., 1993. 178(2): p. 489-495.
6. Figdor, C.G., et al., *Dendritic cell immunotherapy: mapping the way.* Nat Med, 2004. 10(5): p. 475-80.
7. Schreibelt, G., et al., *Commonly used prophylactic vaccines as an alternative for synthetically produced TLR ligands to mature monocyte-derived dendritic cells.* Blood, 2010. 116(4): p. 564-74.
8. Kadowaki, N., et al., *Natural interferon alpha/beta-producing cells link innate and adaptive immunity.* J Exp Med, 2000. 192(2): p. 219-26.
9. Farkas, L., et al., *Plasmacytoid dendritic cells activate allergen-specific TH2 memory cells: modulation by CpG oligodeoxynucleotides.* J Allergy Clin Immunol, 2004. 114(2): p. 436-43.
10. Ito, T., Y.J. Liu, and N. Kadowaki, *Functional diversity and plasticity of human dendritic cell subsets.* Int J Hematol, 2005. 81(3): p. 188-96.
11. Cella, M., et al., *Plasmacytoid dendritic cells activated by influenza virus and CD40L drive a potent TH1 polarization.* Nat Immunol, 2000. 1(4): p. 305-10.
12. Fonteneau, J.F., et al., *Activation of influenza virus-specific CD4+ and CD8+ T cells: a new role for plasmacytoid dendritic cells in adaptive immunity.* Blood, 2003. 101(9): p. 3520-6.
13. Salio, M., et al., *Plasmacytoid dendritic cells prime IFN-gamma-secreting melanoma-specific CD8 lymphocytes and are found in primary melanoma lesions.* Eur J Immunol, 2003. 33(4): p. 1052-62.
14. Remer, K.A., et al., *Vaccination with plasmacytoid dendritic cells induces protection against infection with Leishmania major in mice.* Eur J Immunol, 2007. 37(9): p. 2463-73.
15. Schlecht, G., et al., *Murine plasmacytoid dendritic cells induce effector/memory CD8+ T-cell responses in vivo after viral stimulation.* Blood, 2004. 104(6): p. 1808-15.
16. Salio, M., et al., *CpG-matured murine plasmacytoid dendritic cells are capable of in vivo priming of functional CD8 T cell responses to endogenous but not exogenous antigens.* J Exp Med, 2004. 199(4): p. 567-79.
17. Takagi, H., et al., *Plasmacytoid dendritic cells are crucial for the initiation of inflammation and T cell immunity in vivo.* Immunity, 2011. 35(6): p. 958-71.
18. Balch, C.M., et al., *Final version of the American Joint Committee on Cancer staging system for cutaneous melanoma.* J Clin Oncol, 2001. 19(16): p. 3635-48.
19. de Vries, I.J., et al., *Maturation of dendritic cells is a prerequisite for inducing immune responses in advanced melanoma patients.* Clin Cancer Res, 2003. 9(14): p. 5091-100.
20. de Vries, I.J.M., et al., *Magnetic resonance tracking of dendritic cells in melanoma patients for monitoring of cellular therapy.* Nat Biotech, 2005. 23(11): p. 1407-1413.
21. de Vries, I.J., et al., *Phenotypical and functional characterization of clinical grade dendritic cells.* J Immunother, 2002. 25(5): p. 429-38.
22. Eggert, A.A.O., et al., *Biodistribution and Vaccine Efficiency of Murine Dendritic Cells Are Dependent on the Route of Administration.* Cancer Res, 1999. 59(14): p. 3340-3345.
23. de Vries, I.J.M., et al., *Immunomonitoring Tumor-Specific T Cells in Delayed-Type Hypersensitivity Skin Biopsies After Dendritic Cell Vaccination Correlates With Clinical Outcome.* J Clin Oncol, 2005. 23(24): p. 5779-5787.
24. Karanikas, V., et al., *Monoclonal anti-MAGE-3 CTL responses in melanoma patients displaying tumor regression after vaccination with a recombinant canarypox virus.* J Immunol, 2003. 171(9): p. 4898-904.
25. Wang, X. and B. Seed, *A PCR primer bank for quantitative gene expression analysis.* Nucleic Acids Res, 2003. 31(24): p. e154.
26. Balch, C.M., et al., *Final version of 2009 AJCC melanoma staging and classification.* J Clin Oncol, 2009. 27(36): p. 6199-206.
27. de Vries, I.J., et al., *Prophylactic vaccines mimic synthetic CpG oligonucleotides in their ability to modulate immune responses.* Mol Immunol, 2011. 48(6-7): p. 810-7.
28. Cambi, A., et al., *The C-type lectin DC-SIGN (CD209) is an antigen-uptake receptor for Candida albicans on dendritic cells.* Eur J Immunol, 2003. 33(2): p. 532-8.
29. Conrad, C., S. Meller, and M. Gilliet, *Plasmacytoid dendritic cells in the skin: To sense or not to sense nucleic acids.* Seminars in Immunology, 2009. 21(3): p. 101-109.
30. Treilleux, I., et al., *Dendritic cell infiltration and prognosis of early stage breast cancer.* Clin Cancer Res, 2004. 10(22): p. 7466-7474.
31. Labidi-Galy, S.I., et al., *Quantitative and functional alterations of plasmacytoid dendritic cells contribute to immune tolerance in ovarian cancer.* Cancer Res, 2011. 71(16): p. 5423-34.
32. Diamond, M.S., et al., *Type I interferon is selectively required by dendritic cells for immune rejection of tumors.* J Exp Med, 2011. 208(10): p. 1989-2003.
33. Fuertes, M.B., et al., *Host type I IFN signals are required for antitumor CD8+ T cell responses through CD8{alpha}+ dendritic cells.* J Exp Med, 2011. 208(10): p. 2005-16.

34. Kadowaki, N., et al., *Subsets of human dendritic cell precursors express different toll-like receptors and respond to different microbial antigens.* J Exp Med, 2001. 194(6): p. 863-869.
35. Siegal, F.P., et al., *The nature of the principal type 1 interferon-producing cells in human blood.* Science, 1999. 284(5421): p. 1835-7.
36. Cella, M., et al., *Plasmacytoid monocytes migrate to inflamed lymph nodes and produce large amounts of type I interferon.* Nat Med, 1999. 5(8): p. 919-923.
37. Penna, G., et al., *Differential migration behavior and chemokine production by myeloid and plasmacytoid dendritic cells.* Hum Immunol, 2002. 63(12): p. 1164-1171.
38. Yoneyama, H., et al., *Evidence for recruitment of plasmacytoid dendritic cell precursors to inflamed lymph nodes through high endothelial venules.* Int Immunol, 2004. 16(7): p. 915-28.
39. Morse, M.A., et al., *Migration of Human Dendritic Cells after Injection in Patients with Metastatic Malignancies.* Cancer Research, 1999. 59(1): p. 56-58.
40. Mackensen, A., et al., *Homing of intravenously and intralymphatically injected human dendritic cells generated in vitro from CD34+ hematopoietic progenitor cells.* Cancer Immunol Immunother, 1999. 48(2-3): p. 118-22.
41. Gunzer, M., et al., *Migration of dendritic cells within 3-D collagen lattices is dependent on tissue origin, state of maturation, and matrix structure and is maintained by proinflammatory cytokines.* J Leukoc Biol, 2000. 67(5): p. 622-629.
42. Lopez, M.N., et al., *Prolonged Survival of Dendritic Cell-Vaccinated Melanoma Patients Correlates With Tumor-Specific Delayed Type IV Hypersensitivity Response and Reduction of Tumor Growth Factor {beta}-Expressing T Cells.* J Clin Oncol, 2009. 27(6): p. 945-952.
43. Brossart, P., et al., *Induction of cytotoxic T-lymphocyte responses in vivo after vaccinations with peptide-pulsed dendritic cells.* Blood, 2000. 96(9): p. 3102-3108.
44. Lau, R., et al., *Phase I Trial Of Intravenous Peptide-Pulsed Dendritic Cells in Patients With Metastatic Melanoma.* J Immunotherapy 2001. 24((1)): p. 66-78.
45. Speiser, D.E., et al., *In vivo activation of melanoma-specific $CD8^+$ T cells by endogenous tumor antigen and peptide vaccines. A comparison to virus-specific T cells.* Eur J Immunol, 2002. 32(3): p. 731-741.
46. Valmori, D., et al., *Vaccination with a Melan-A Peptide Selects an Oligoclonal T Cell Population with Increased Functional Avidity and Tumor Reactivity.* J Immunol, 2002. 168(8): p. 4231-4240.
47. Robert, C., et al., *Ipilimumab plus dacarbazine for previously untreated metastatic melanoma.* N Engl J Med, 2011. 364(26): p. 2517-26.
48. Hodi, F.S., et al., *Improved survival with ipilimumab in patients with metastatic melanoma.* N Engl J Med, 2010. 363(8): p. 711-23.
49. Chapman, P.B., et al., *Improved survival with vemurafenib in melanoma with BRAF V600E mutation.* N Engl J Med, 2011. 364(26): p. 2507-16.

Part 2

In vivo tracking of DC-based vaccinations upon delivery

Chapter 5

Maximizing dendritic cell migration in cancer immunotherapy

Verdijk P

Aarntzen EH

Punt CJ

De Vries IJ

Figdor CG

Expert Opin Biol Ther. 2008;8(7):865-74.

Abstract

The success of dendritic cell (DC) based immunotherapy to induce cellular immunity against tumors is highly dependent on accurate delivery and trafficking of the DC to T cell-rich areas of secondary lymphoid tissues. This article aims to provide an overview on DC migration *in vivo* and how migration to peripheral lymph nodes might be improved to optimize DC therapy. We focused on DC migration in preclinical models and human skin explants and on clinical vaccination trials studying migration of *in vitro* generated DC.DC migration requires an intricate interplay between the cell and its environment. To maximize migration for cellular therapy, it is important to optimize the generation of migratory DC as well as treatment strategies.

1. DC cancer immunotherapy

Immunotherapy in patients with cancer aims to activate the immune system to eradicate the tumor and to induce specific and long lasting immunity to protect against recurrent disease. Since the discovery of dendritic cells as antigen presenting cells with the unique capacity to induce naive antigen-specific T cells, many experimental immune therapies are now based on the vaccination of cancer patients with *ex vivo* generated autologous DC loaded with tumor antigens. Although immunological responses are observed in most studies, clinical responses are limited to a minority of patients. Opportunities for improvement of clinical outcome lie in a number of variables, such as DC subsets and culture methods used for the generation of DC, antigen loading, route of administration, dose and frequency and others (1). One important aspect of cell based immune therapy is accurate delivery of the vaccine. DC must closely encounter and interact with T cells to exert their action. Therefore DC must reach the secondary lymphoid tissues, and enter the T cell-rich areas. It has now been generally accepted that the site at which T cell priming occurs significantly influences the homing characteristics of the effector cells. For example, subcutaneous (s.c.), but not intravenous (i.v.), injection of DC in a mouse melanoma model induced protective immunity against subcutaneously growing tumors (2-4). In contrast, metastatic-like lung lesions were controlled by i.v. immunization and only partially by s.c. immunization (4). Similarly, only DC from mesenteric lymph nodes (5) and Peyer's patches (6) induced the expression of the gut-homing integrin $\alpha_4\beta_7$ on T cells. It is therefore not only essential to generate DC with high immunostimulatory capacity but research should also focus on maximizing migratory capacities and vaccine delivery. In this review we will discuss how endogenous DCs migrate and how this can be exploited to improve DC immunotherapy.

2. *In vivo m*igration of DC for therapy

For the delivery of DC three different options for administration can be distinguished: in peripheral tissue, such as skin (intradermal (i.d.) or s.c.) and mucosa, into the lymphatic system (intralymphatic (i.l.) or intranodal (i.n.)), and intravenous administration (i.v.). Vaccine delivery and distribution after injection has been studied in several clinical trials. In these trials DC generated from blood-derived monocytes or $CD34^+$ progenitor cells were radio-labeled with ^{111}Indium or ^{99m}Technetium and the distribution after injection was imaged and quantified by scintigraphic imaging of the patients. This approach showed that after i.v. injection DC are found in liver, lung, spleen and bone marrow (7; 8). In mice, DC reach the liver and spleen after a short accumulation in the lungs, and in some studies very low amounts of DC were detected in mesenteric and mediastinal nodes (2; 9). This is consistent with the finding that myeloid DC in the peripheral blood do not enter lymph nodes via the high endothelial venules, but first migrate to peripheral tissues and subsequently to draining lymph nodes via the afferent lymphatics (10). To target peripheral lymph nodes DC can be injected into the skin or directly into the skin-draining lymphatics or lymph node. In mice, subcutaneous (s.c.) injection is effective in both targeting DC to draining lymph nodes and inducing immune responses (2-4; 9; 11; 12). However, significantly more DC reached the draining lymph nodes after intradermal (i.d.) injection compared with s.c. injection (13). In human, no (7; 14; 15) or little (16; 17) migration of DC to skin-draining lymph nodes was found after s.c. injection of DC. Intradermal injection is more effective although the number of DC that reach the regional lymph nodes did not exceed 4% (7; 14-20). Best results have been accomplished with DC administered directly into the nasal submucosa. In this clinical study, DC showed rapid migration to the regional lymph nodes (21), however, whether this also leads to (systemic) immunity is not known. Alternatively, *ex vivo* generated DC can also be injected directly into lymph nodes or lymphatic vessels draining the skin, as a result of which all cells will be targeted to the draining lymph nodes (8; 18; 19; 22). Initial analyses showed that intranodal (i.n.) injection is not always successful, even when it is performed under ultrasound guidance by a highly experienced radiologist (22). Intralymphatic (i.l.) injection is an even more challenging technique that requires a highly skilled surgeon and hospital admission. Importantly, despite the fact

that most of the injected cells reach one or in most cases multiple lymph nodes, DC still need to migrate into the T cell-rich areas. Thus to conclude, for large-scale clinical trials i.d. and i.v. administration of DC are preferred, while they are simple and robust, although one important drawback is the low efficiency in targeting DC to peripheral lymph nodes. Inefficient delivery of *ex vivo* generated DC to T cell rich areas in secondary lymphoid organs may contribute to the limited clinical responses to DC based immunotherapy. Maximizing the migration of DC for cellular therapy might enhance these responses.

3. What can be learned from endogenous DC migration?

In the human body DC continuously migrate from the periphery into lymphatic tissues to orchestrate the immune system both in the presence and the absence of 'danger' signals. In an effort to maximize the migration of DC for cellular therapy it is indispensable to know how DC migration is initiated and what factors are essential for the cell to move towards the draining lymph node and enter the T cell-rich areas.

3.1 Emigration of DC from peripheral tissues towards lymph nodes

In a steady state, immature myeloid DC mainly reside in peripheral tissues where they continuously sample the environment for 'danger' signals. When they sense such signals the DC rapidly become activated, mature and emigrate from the tissue. Langerhans cells (LC) migrate from the epidermis to the draining lymph node upon application of proinflammatory mediators on the skin, such as contact allergens (23; 24) or toll-like receptor (TLR) ligands like CpG (25) and lipopolysaccharide (LPS) (26; 27). Critical factors are the local production of tumor necrosis factor α (TNFα) and interleukin (IL)-1β and of prostaglandin E_2 (PGE_2). Indeed, direct injection of TNFα (28-30) or IL-1β (31; 32) into the dermis of mice or human skin explants induces the emigration of LC (reviewed in (33)). Similarly, neutralizing antibodies to TNFα and IL-1β inhibit the spontaneous migration of DC from skin explants in mice and human (34). Interestingly, TNFα effects were neutralized by anti-IL-1β and vice versa (32; 34; 35), demonstrating that both cytokines are required for the initiation of DC migration. That the emigration upon proinflammatory stimuli is very rapid is illustrated by the fact that lung DC and LC migrate within 2 hours to draining lymph nodes after viral inoculation (36) or upon the application of the proinflammatory cytokines, respectively (30; 32). Importantly, TNFα effects were dose dependent: low concentrations (50 U/ml) of TNFα augmented LC migration, whereas high doses (5000 U/ml) of the same cytokine inhibited LC migration in human skin explant (34).

Proinflammatory mediators exert their effects on different levels: while they act directly on the DC by inducing DC maturation and initiation of DC migration to the draining lymph nodes, they also stimulate the local environment to produce factors, such as chemokines that promote emigration of DC and recruitment of circulating immune cells. Furthermore, LPS, IL-1β, and TNFα also induce the production of PGE_2 (37), which has proven to be required for DC migration and increases the responsiveness of monocyte-derived DC of the lymph node homing receptor, CCR7 (38-41). When applying DC therapy, we may benefit from these effects by stimulating the migration of injected DC *in situ*. By applying proinflammatory stimuli to the site where *ex vivo* generated DC will be injected, the local environment will be conditioned such that the emigration of the injected cells is favored. Indeed, Martín-Fontecha *et al.* (42) described that in mice conditioning of the injection site increased the migration of subcutaneously injected BM-DC up to 10-fold. The footpath of mice was pretreated by injection of TNFα or IL-1 or with DC, respectively 8 or 24 hours before vaccination. As a result 5- to 10 fold more fluorescently-labeled DCs were recovered from the draining lymph nodes. Accordingly, the T cell responses were up to 10 fold enhanced. The authors hypothesized that local inflammation induced by the injection of DC or pro-inflammatory cytokines conditioned the environment to promote rapid migration of DC towards the lymph nodes. To support this, they showed that the

lymph node chemokine CCL21 is up-regulated in the local lymphatics. These data show that conditioning of the skin has potential in increasing DC migration to lymph nodes after i.d. or s.c. injection. Skin conditioning prior to vaccination with mature DC has not yet been described in humans, but is a promising opportunity to improve DC migration. When proinflammatory mediators act directly on the DC, DC migration to the draining lymph nodes is likely initiated by the induction of DC maturation. With the use of radio-labels it was shown that immature, monocyte-derived DC are not able to migrate to subsequent lymph nodes upon injection in patients. Stimulating the maturation of immature DC after i.d. injections may improve migration and circumvents the need for *in vitro* maturation. Prins *et al.* showed that the combination of Imiquimod (containing TLR7 ligand) and s.c. injection of immature DC dramatically increased both the persistence and the trafficking of DC into the draining lymph nodes of mice (43). In mice, migration of immature DC was enhanced from 1.8 to 6.5% when cells were injected into skin that was pretreated with Imiquimod. Importantly, although migration of mature DC injected in untreated skin was higher (10%), the CTL responses induced after injection of immature DC in pretreated skin were superior to those induced by mature DC alone (20). In follow-up studies, Nair et al. injected immature DC intradermally in human skin pretreated with Imiquimod. Application of Imiquimod onto the injection site every other day for three times before injection of immature DC increased migration of DC compared to immature DC alone. Again the percentage of migrating cells did not exceed that of injections with mature DC (20). Application of Imiquimod before injection of immature DC for cellular therapy seems therefore a valid alternative to circumvent *ex vivo* maturation of DC, but not for amplifying the percentage of migrating DC. Its effect may increase after optimization of the timing and dose of Imiquimod, for example to apply the agent not before but after the injection of the immature cells, so that Imiquimod can directly stimulate the injected DC. Interestingly, it has been described that DC that migrate into the lymph nodes are not uniquely responsible for the activation of specific T cells. They can transfer antigen to resident DC and thereby spread antigens to a larger pool of DC to increase priming efficiency (44; 45). This would mean that, when antigen loading is sufficient, only a small number of cells need to reach the draining lymph node. How antigens are being transferred to lymphoid DC and what the requirements are for the maturation state of the immigrating DC to induce effective T cell responses is yet unknown. Addressing these questions may renew the insights on the type of DC and method of antigen-loading that are most appropriate for DC immunotherapy.

3.2 DC phenotype

Homing to specific tissues is controlled by the combined expression of different chemokine receptor and specific adhesion molecule receptors. After stimulation with proinflammatory stimuli, DC maturation is initiated and many molecules that are important for their change in function are either up- or down-regulated. Not only must DC change from an endocytic sentinel into a professional antigen presenting cell, but it also needs to detach from its local environment, migrate through surrounding tissues, enter the lymphatics and subsequent the draining lymph node and in particular penetrate the T cell area. To emigrate from the periphery towards the draining lymph nodes, DC rapidly change their repertoire of chemokine receptor and adhesion molecules and the expression of many other migration related proteins, such as matrix metalloproteases and cytoskeletal proteins. In this section an overview will be presented of chemokine receptors, adhesion molecules and MMP that were found essential in lymph node homing of endogenous DC.

3.2.1 Chemokine receptors

The dominant mediator in the mobilization of DC to lymph nodes via lymphatics is CCR7 (46-48). Constitutive expression of ligands CCL19 and CCL21 is found at the luminal site of high endothelial venules and in the T cell rich areas of secondary lymphoid tissues, such as tonsil, spleen and lymph nodes (49). CCL21 is also expressed on lymphatic vessels in the peripheral tissues and its expression

is increased during inflammation (42). The expression of CCR7 is essential for both the entry of DC into lymphatic vessels at peripheral sites and the entry into T cell rich areas of lymphoid tissues in both steady state and under inflammatory conditions (48). Besides CCR7 several other chemokine receptors play a role in DC homing from the periphery to draining lymph nodes but appear less important. Lung myeloid DCs are dependent on CCR5 and its ligand CCL5 for migration and maturation, since these events are significantly impaired in $CCL5^{-/-}$ and $CCR5^{-/-}$ mice. However, this effect seems to be mediated via CCR7 as in these mice the failure of DC to migrate to draining lymph nodes is associated with impaired up-regulation of CCR7 (36). Similarly, emigration of skin-DC (50) and lung-DC (51) to the draining LN was only partially blocked in CCR8-deficient mice. Migration of plasmacytoid DC matured with CpG for 24 hour from peripheral blood into the lymph nodes was described to depend on the CXCR3 ligand CXCL9 (10). But also pDC express high levels of CCR7 and gain responsiveness to CCR7 upon maturation (10; 52), suggesting that CCR7 is also important in lymph node homing of pDC. Overall, it appears that CCR7 is the main receptor for lymph node homing and that targeting from the periphery to the lymph node is promoted by additional chemokine receptors. For cellular therapy, chemokine-mediated migration of DC may be enhanced in two ways, by manipulating the local chemokine expression or by manipulating the expression of chemokine receptors by the DC itself. As described in the previous section, conditioning of the skin injection site, increased the expression of CCL21 on the local lymphatics (42). Inducing the expression of chemokines, such as CCL21, on (local) lymphatics before or together with the DC injection may improve the recruitment of CCR7-expressing cells to afferent lymphatics and eventually the draining lymph nodes. The chemokine receptor expression profile of DC is dependent on DC culture and maturation methods. The addition of PGE_2 as maturation stimulus enhances CCR7 expression and its activation, and drives effective migration of monocyte-derived DC towards CCR7 ligands CCL19 and 21 (38-40; 53). Another approach could be to introduce the expression of chemokine receptors in the *ex vivo* generated DC, which will be discussed below.

3.2.2 Adhesion molecules

Adhesion molecules play a pivotal role in successive steps in the process of migration. Therefore, their expression profile is tightly controlled. A switch in adhesion molecule expression profile is required to allow detachment of resident DC from existing interactions and to enable migration through the lymphatic system and into the lymph node. Thus far, no extensive analysis of the molecules implicated in transendothelial migration of DC into the lymphatic system has been carried out (54), but a variety of adhesion molecules is involved in the emigration of DC through the extracellular matrix (ECM) and in emigration of LC from skin. In mice LC, α_6 and α_4 integrins are oppositely regulated during migration to lymph nodes. α6 integrin is up-regulated and contributes to migration of LC (55). When the interaction between α6 and laminin was blocked, the emigration of LC from the epidermis was completely abrogated, although the cells had lost their cellular processes and seemed to have detached from neighboring keratinocytes. By contrast, blocking of α_4 integrin had no effect on LC migration (55). In addition, ICAM-1 and LFA-1 ($\alpha_L\beta_2$) were found to play a significant role in contact hypersensitivity-induced migration of LC to regional lymph nodes (56). Also non-integrins are regulated during DC migration and maturation. In mice CD44 is described as an adhesion molecule that binds to ECM-compound hyaluronic acid, which is expressed on the leading edge of migrating cells. Migrating and lymph node LC and DC express different CD44 splicing variants (57). CD44 can also bind the matrix metalloprotease MMP9 to the cells surface and mediate degredation of extracellular matrix (58). Blocking of CD44 inhibited the migration of LC from the epidermis. Furthermore, it prevented binding of both activated LC and DC to the T cell rich areas of lymph nodes (57). Another example of adhesion molecules regulated during DC migration are the syndecans (SDC), a family of transmembrane proteoglycans. In human skin explants, SDC1 and 4 (59)

have been implicated in the migration of LC. SDC1 was down-regulated and SDC4 was strongly up-regulated during LC emigration and within the first hours of LPS-induced DC maturation (59). Blocking SDC4 decreased DC motility. Thus, SDC1 may be involved in stable adhesive interactions with the ECM, whereas SDC4 seems involved in trafficking through the ECM. Lymph node homing from the peripheral blood is dependent on L-selectin, and is required for efficient rolling and attachment on HEV. L-selectin is expressed on a subset of circulating leukocytes, such as naive T cells (60) and pDC (61), but not on DC of the myeloid lineage. Next to L-selectin, pDC depend on the inducible endothelial adhesion molecule E-selectin to enter lymph nodes (10). CD44, which is a ligand for E-selectin, may therefore also play a role in pDC migration. In addition to chemokine responsiveness, manipulation of the expression of adhesion molecules on *ex vivo* generated DC may improve the migratory capacities of the cellular vaccine.

3.2.3 Matrix metalloproteases

To move through the physical obstacles, such as basement membranes and ECM, they express and secrete matrix metalloproteases (MMP). Upon triggering with IL-1β and TNFα, murine LC increase the expression of MMP9, (57; 62). Human immature monocyte derived-DC secrete MMP1, 2, 3 and 9 (63; 64), and their inhibitors (TIMP1 and 2) (63; 64), which are down-regulated upon stimulation with TNFα (64). The importance of MMP in DC migration through tissues is demonstrated in MMP9-deficient mouse, where DC migration through tracheal epithelial tight junctions was impaired (65). Furthermore, in human skin explants antibodies against MMP2 and 9 and inhibitors of MMP markedly reduced the migration of human LC and dermal DC (66; 67). Also, up-regulation of genes encoding matrix metalloproteinases (MMP), such as MMP1, 10 and 12 correlated with enhanced migratory capacity of DC measured in Matrigel (68). Thus, MMP are essential for effective migration through extracellular matrix. In brief, DC need to express appropriate chemokine receptors, adhesion molecules, and other migration-related proteins in addition to high T cell stimulatory capacities. To achieve maximal DC migration after injection, we need to exploit this information for the development of better DC or DC vaccination protocols.

4. Generating DC with migratory capacities

The characteristics of DC that are cultured *in vitro* are determined by the source and subset of the DC but even more by the culture and maturation procedures. Thus the migratory capacities can be manipulated by choosing the right subsets and culture conditions or by introducing migration-related proteins.

4.1 Dendritic cell subsets

The isolation of DC and DC precursors for cellular therapy DC or DC precursors is dependent on the availability of these cells and is therefore constrained to the peripheral blood leukocytes. From the circulation, monocytes and $CD34^+$ progenitor cells can be isolated that can be differentiated into DC, but also myeloid and plasmacytoid DC (precursors) that already have DC phenotype. The method of isolation and the subsequent culture methods can influence the final characteristics of the DC. For example, isolation of cells by immunoselection via subset-specific membrane markers may preactivate the cells. Monocytes that are immunoselected via the novel monocyte specific molecule CD300e, differentiate into DC that show greater migration towards CCL21 compared with CD14-immunoselected DC (69). Currently, most clinical trials use DC generated from monocytes or $CD34^+$ progenitor cells, as high numbers can be obtained from the peripheral blood after leukopheresis. A drawback is the relatively long necessity of *in vitro* culturing to generate fully differentiated DC of more than one week. Recently, also peripheral blood plasmacytoid DC are considered for immunotherapy, since pDC not only can directly induce antigen-specific $CD8^+$ T cell immune responses (70; 71), but are also thought to enhance the priming ability of myeloid DC (71). Another

interesting aspect is that they can enter the lymph nodes directly from the blood (10). pDC isolated from blood already have DC phenotype and only require additional activation to induce DC maturation, which makes them potential candidates for cellular therapy, despite their low frequency in the blood.

4.2 Ex vivo culture of monocyte derived DC

The phenotype of *ex vivo* differentiated DC depends greatly on the culture conditions. Generally, monocytes are differentiated into DC in the presence of IL-4 and GM-CSF. Different cytokine cocktails, using cytokines such as IL-15, IL-13, IFNα, IFNγ and TNFα, have been used for DC differentiation and function. Monocytes cultured with IFNα instead of IL-4 differentiate into immature DC with high expression of MMP9 and enhanced migration through ECM in response to CCL3 and CCL5. However, IFNα-DC migrated similarly towards the lymph node chemokine CCL21 compared to LPS-matured DC (72). Perhaps even more important than the differentiation conditions is the maturation procedure of the DC. In current clinical trials exploiting DC for cellular therapy, monocyte-derived DC are generally matured with cytokine cocktail containing PGE_2, which was first described by Jonuleit et al., based on inflammation induced monocyte-derived cytokines TNFα, IL-1β, IL-6 and PGE_2. PGE_2 greatly enhanced the migratory capacities by increasing the CCR7 responsiveness (38-40; 53) and inducing high-speed migration (41). The effect of different maturation stimuli on the migratory capacities of DC is broadly studied. According to the hypothesis of Luft et al. mature DC can be either migratory or cytokine-secreting (73). Maturation with TLR-ligands or with strong and sustained CD40 signaling induce DC with high IL-12p70 secretion and low migratory capacities (68; 73-76), whereas DC matured with PGE_2 containing cocktails show a migratory-type functional profile but produce little or no IL-12p70 (38; 77). Recently, galectin-1 was described as a new DC maturation factor resulting in up-regulation of genes related to cell migration through ECM (tenascin, MMP1, -10 and -12) and better chemotactic migration through Matrigel compared to LPS-matured DC, but also these cells did not produce IL-12p70 (68). The addition of IFNγ enhances the IL-12p70 production by DC, but at the same time negatively influences DC migratory capacities both *in vitro* (76; 78; 79), and *in vivo* (80). So indeed, upon maturation DCs seem to differentiate toward either a migratory or a cytokine producing phenotype, while in fact both are important. For DC therapy, the lack of production of Th1 inducing cytokines, such as IL-12p70, by DC matured with PGE_2 containing cocktails, is regarded as a major drawback. However, primary IL-12p70 production occurs during the first 24 hours of DC maturation and may not be relevant for DC therapy, since *ex vivo* generated DC are generally exposed to maturation stimuli for 24 to 48 hours. Recently, we observed that although PGE_2 inhibits the primary production of IL-12p70 upon DC maturation with TLR-ligands, it does not prevent IL-12p70 production upon DC-T cell contact (76). Thus, by stimulating DC with a combination of maturation stimuli that both promote cytokine-secretion and PGE_2, DC can be generated that have the ability to migrate to draining lymph nodes and to secrete IL-12p70 locally.

4.3 Manipulation of DC expression profiles

When specific DC characteristics cannot be attained via culture of maturation methods, phenotypic features of DC necessary for migration or T cell stimulation can also be achieved by manipulation of the cell by transducing the desired gene of gene transcript into the *ex vivo* generated cells. For example the homing of DC can be manipulated by transfection with specific homing receptors. Transduction of the CCR7 gene by RGD fiber-mutant adenovirus vector generated DC with strong chemotactic activity for CCL19 and a mature phenotype. Importantly, CCR7-DC injected i.d. into mice did accumulate in draining lymph nodes about 5.5 fold as efficient as the control vector-applied DC (81). DC that normally only enter lymph nodes via the lymphatics can be manipulated to enter lymph nodes via the peripheral blood by transfecting the appropriate receptors. Robert et al. retrovirally-

transduced murine DC with a chimeric E/L-selectin, providing them with the ability to extravasate directly from blood by binding to peripheral node addressin (PNAd), an adhesion molecule present on the lymph node vascular endothelium (60). As ethical and regulatory restrictions hamper the use of retrovirally-transduced DC in human, alternatives are being developed. To avoid the introduction of foreign DNA into patients, cells can now be transduced with mRNA encoding the molecules of interest. Already, transfection with mRNA encoding for tumor antigens is now being employed in clinical trials for the antigen-loading of DC, circumventing the use of HLA-restricted peptides. Recently, Dörrie et al. elegantly showed that human monocyte derived DC electroporated with E/L selectin-encoding mRNA indeed gained the capacity to role by binding to sialyl-Lewisx, creating the potential to extravasate through the HEV into the lymph node. Thus mRNA transfection opens many opportunities to manipulate DC to express proteins essential for either migration of immune activation, which may lead to the creation of DC with both migratory and immune stimulatory capacities.

5. Expert Opinion

DC migration requires an intricate interplay between the cell and its environment. To maximize migration for cellular therapy, it is important to take into account all the different variables and realize that the route of administration may have great influence on the homing of the activated T cells and therefore the clinical outcome, and that for example, DC for intravenous injection will need different characteristics than when injected into the skin. In mice it was demonstrated that in DC immunotherapy the spleen is essential for the clearance of lung metastasis, but not subcutaneously growing tumors. In contrast, peripheral lymph nodes were essential for the rejection of subcutaneously growing tumors and not lung metastasis (4). Similarly, only DC from mesenteric lymph nodes could induce gut-homing T cells (5). Thus, to induce systemic immunity, both the spleen and lymph nodes should be targeted during immunotherapy. This can be achieved by combining intravenous injections with intradermal or intranodal injection in the case of cutaneous tumors or with intraperitoneal injections in the case of intestinal tumors. Alternatively, DC can be injected that enter the peripheral lymph nodes directly from the blood, like pDC or *ex vivo* generated DC in which the required receptors for blood-lymph node homing are introduced. Identification of the factors that determine the homing of T cells might make it possible to create DC that can instruct T cells to home to specific tissues regardless of the route of administration.

When the choice is for i.d. injection, DC migration can be stimulated by manipulating either the injection site or the DC itself. Conditioning of the skin injection site can act in two ways: Induce the local production of factors that promote the emigration of DC, such as chemokines, or directly stimulate the DC to migrate. An important factor in this is the timing. If pretreatment of the skin is to early, the stimulatory effect may have faded away, or induce inflammatory conditions that retain DC rather than stimulate emigration. Focusing only on conditioning of the site of injection might not be sufficient. It is important to consider that emigration of resident DC is interrelated with DC maturation. In the first hours after the initiation of migration to the draining lymph nodes DC rapidly change the expression levels of chemokine receptors, adhesion molecules and other migration-related MMP and TIMP that are important for trafficking through the ECM and via lymphatics. For immunotherapy, DC are generally cultured with maturation stimuli for 24 to 48 hours prior to injection. These cells have excellent migratory capacities in *in vitro* assays, but their capability to migrate through barriers such as ECM, and lymphatic or blood endothelium, has been poorly studied. Intradermal injection of immature instead of mature DC in combination with conditioning of the skin with TLR-ligands, such as Imiquimod, is an interesting approach and should be further developed. Important is to realize that also here timing is crucial. Delivery of the maturation stimuli simultaneously with the immature DC or perhaps just prior to injection may ensure a direct effect of the stimuli on the DC. Alternatively, preactivated but not yet fully mature DC could be injected in the

skin, possibly combined with local conditioning of the injection site. Whatever route of administration of DC subsets is selected, to improve the proficiency of the cells, they can be endowed with molecules that improve lymph node homing, and DC can be provided with T cell stimulatory molecules, like IL-12 or costimulatory molecules.

Now RNA transfection of DC has proven safe and effective this should be exploited to manipulate and control DC function including migratory and costimulatory properties. Similary, proteins that compromise the immunostimulatory and migratory capacities of DC may be silenced using small interfering RNA (siRNA). That this may indeed be effective was recently demonstrated by.Kang *et al.* (83) who demonstrated that by silencing pro-apoptotic proteins the survival of DC was significantly increased and lead to an enhanced T cell response upon vaccination in mice. At the same time, Dannull *et al.* (84) showed that the ability of DC to stimulate anti-tumor immunity could be enhanced by down-modulating the immunoproteasome with siRNA.

In conclusion, optimal DC migration for cellular therapy against tumors, may be attained by creating both a stimulatory environment and generating of DC with a high migratory capacity and immune activation potential. Maximizing DC trafficking, homing to lymph nodes and T cell activation to a level that is adequate to induce a competent immune response against the tumor and long-lasting protection against recurrence disease is essential for the development of DC immune therapy into a valid treatment. Exploiting RNA and or siRNA to enhance DC function will certainly contribute to the next generation of DC vaccines.

References

1. FIGDOR CG, DE VRIES IJ, LESTERHUIS WJ, and MELIEF CJ: Dendritic cell immunotherapy: mapping the way. (2004) Nat. Med. 10(5), 475-480.
   • In this review, the status of DC immunotherapy in cancer patients is evaluated, and its application in a variety of immune-mediated diseases, such as transplantation and autoimmunity is discussed.
2. EGGERT AA, SCHREURS MW, BOERMAN OC et al.: Biodistribution and vaccine efficiency of murine dendritic cells are dependent on the route of administration. (7-15-1999) Cancer Res. 59(14), 3340-3345.
3. OKADA N, TSUJINO M, HAGIWARA Y et al.: Administration route-dependent vaccine efficiency of murine dendritic cells pulsed with antigens. (6-1-2001) Br. J Cancer 84(11), 1564-1570.
4. MULLINS DW, SHEASLEY SL, REAM RM, BULLOCK TN, FU YX, and ENGELHARD VH: Route of immunization with peptide-pulsed dendritic cells controls the distribution of memory and effector T cells in lymphoid tissues and determines the pattern of regional tumor control. (10-6-2003) J Exp. Med. 198(7), 1023-1034.
   •• In this paper, preclinical findings are described which indicate that it might be beneficial to combine different routes of administration; depending on the localization of the tumor, intravenous or intradermal vaccination might be preferential for visceral and nonvisceral metastases, respectively.
5. DUDDA JC, SIMON JC, and MARTIN S: Dendritic cell immunization route determines CD8+ T cell trafficking to inflamed skin: role for tissue microenvironment and dendritic cells in establishment of T cell-homing subsets. (1-15-2004) J Immunol 172(2), 857-863.
6. MORA JR, BONO MR, MANJUNATH N et al.: Selective imprinting of gut-homing T cells by Peyer's patch dendritic cells. (7-3-2003) Nature 424(6944), 88-93.
7. MORSE MA, COLEMAN RE, AKABANI G, NIEHAUS N, COLEMAN D, and LYERLY HK: Migration of human dendritic cells after injection in patients with metastatic malignancies. (1-1-1999) Cancer Res. 59(1), 56-58.
8. MACKENSEN A, KRAUSE T, BLUM U, UHRMEISTER P, MERTELSMANN R, and LINDEMANN A: Homing of intravenously and intralymphatically injected human dendritic cells generated *in vitro* from CD34+ hematopoietic progenitor cells. (1999) Cancer Immunol. Immunother. 48(2-3), 118-122.
9. HUCK SP, TANG SC, ANDREW KA, YANG J, HARPER JL, and RONCHESE F: Activation and route of administration both determine the ability of bone marrow-derived dendritic cells to accumulate in secondary lymphoid organs and prime CD8(+) T cells against tumors. (7-3-2007) Cancer Immunol Immunother.
10. YONEYAMA H, MATSUNO K, ZHANG Y et al.: Evidence for recruitment of plasmacytoid dendritic cell precursors to inflamed lymph nodes through high endothelial venules. (2004) Int. Immunol 16(7), 915-928.
11. BEDROSIAN I, MICK R, XU S et al.: Intranodal administration of peptide-pulsed mature dendritic cell vaccines results in superior CD8+ T-cell function in melanoma patients. (10-15-2003) J Clin. Oncol. 21(20), 3826-3835.
12. LAPPIN MB, WEISS JM, DELATTRE V et al.: Analysis of mouse dendritic cell migration *in vivo* upon subcutaneous and intravenous injection. (1999) Immunology 98(2), 181-188.
13. EGGERT AA, VAN D, V, TORENSMA R et al.: Analysis of dendritic cell trafficking using EGFP-transgenic mice. (10-9-2003) Immunol. Lett. 89(1), 17-24.
14. TRAKATELLI M, TOUNGOUZ M, BLOCKLET D et al.: A new dendritic cell vaccine generated with interleukin-3 and interferon-beta induces CD8+ T cell responses against NA17-A2 tumor peptide in melanoma patients. (2006) Cancer Immunol Immunother. 55(4), 469-474.
15. BLOCKLET D, TOUNGOUZ M, KISS R et al.: 111In-oxine and 99mTc-HMPAO labelling of antigen-loaded dendritic cells: *in vivo* imaging and influence on motility and actin content. (2003) Eur. J. Nucl. Med. Mol. Imaging 30(3), 440-447.
16. RIDOLFI R, RICCOBON A, GALASSI R et al.: Evaluation of *in vivo* labelled dendritic cell migration in cancer patients. (7-30-2004) J. Transl. Med. 2(1), 27.
17. THOMPSON M, WALL DM, HICKS RJ, and PRINCE HM: *In vivo* tracking for cell therapies. (2005) Q. J Nucl. Med. Mol. Imaging 49(4), 339-348.
18. DE VRIES IJ, KROOSHOOP DJ, SCHARENBORG NM et al.: Effective migration of antigen-pulsed dendritic cells to lymph nodes in melanoma patients is determined by their maturation state. (1-1-2003) Cancer Res. 63(1), 12-17.
   • In this article it is shown that *in vitro* generated mature, but not immature, DC efficiently migrate into the T cell areas of lymph nodes of melanoma patients. In general, less than 5% of intradermally administered mature DC reached the lymph nodes.
19. QUILLIEN V, MOISAN A, CARSIN A et al.: Biodistribution of radiolabelled human dendritic cells injected by various routes. (2005) Eur J Nucl. Med. Mol. Imaging 32(7), 731-741.
20. NAIR S, MCLAUGHLIN C, WEIZER A et al.: Injection of immature dendritic cells into adjuvant-treated skin obviates the need for *ex vivo* maturation. (12-1-2003) J. Immunol. 171(11), 6275-6282.
21. HORIGUCHI S, MATSUOKA T, OKAMOTO Y et al.: Migration of Tumor Antigen-Pulsed Dendritic Cells After Mucosal Administration in the Human Upper Respiratory Tract. (6-28-2007) J Clin. Immunol .
22. DE VRIES IJ, LESTERHUIS WJ, BARENTSZ JO et al.: Magnetic resonance tracking of dendritic cells in melanoma patients for monitoring of cellular therapy. (2005) Nat. Biotechnol. 23(11), 1407-1413.
23. RAMBUKKANA A, PISTOOR FH, BOS JD, KAPSENBERG ML, and DAS PK: Effects of contact allergens on human Langerhans cells in skin organ culture: migration, modulation of cell surface molecules, and early expression of interleukin-1 beta protein. (1996) Lab Invest 74(2), 422-436.
24. ENK AH and KATZ SI: Early molecular events in the induction phase of contact sensitivity. (2-15-1992) Proc. Natl. Acad. Sci. U. S. A 89(4), 1398-1402.
25. BAN E, DUPRE L, HERMANN E et al.: CpG motifs induce Langerhans cell migration *in vivo*. (2000) Int. Immunol 12(6), 737-745.

26. ROAKE JA, RAO AS, MORRIS PJ, LARSEN CP, HANKINS DF, and AUSTYN JM: Dendritic cell loss from nonlymphoid tissues after systemic administration of lipopolysaccharide, tumor necrosis factor, and interleukin 1. (6-1-1995) J. Exp. Med. 181(6), 2237-2247.
27. MACPHERSON GG, JENKINS CD, STEIN MJ, and EDWARDS C: Endotoxin-mediated dendritic cell release from the intestine. Characterization of released dendritic cells and TNF dependence. (2-1-1995) J Immunol 154(3), 1317-1322.
28. CUMBERBATCH M, FIELDING I, and KIMBER I: Modulation of epidermal Langerhans' cell frequency by tumour necrosis factor-alpha. (1994) Immunology 81(3), 395-401.
29. CUMBERBATCH M and KIMBER I: Dermal tumour necrosis factor-alpha induces dendritic cell migration to draining lymph nodes, and possibly provides one stimulus for Langerhans' cell migration. (1992) Immunology 75(2), 257-263.
30. CUMBERBATCH M, GRIFFITHS CE, TUCKER SC, DEARMAN RJ, and KIMBER I: Tumour necrosis factor-alpha induces Langerhans cell migration in humans. (1999) Br. J. Dermatol. 141(2), 192-200.
31. BHUSHAN M, CUMBERBATCH M, DEARMAN RJ, KIMBER I, and GRIFFITHS CE: Exogenous interleukin-1beta restores impaired Langerhans cell migration in aged skin. (2004) Br. J. Dermatol. 150(6), 1217-1218.
32. CUMBERBATCH M, BHUSHAN M, DEARMAN RJ, KIMBER I, and GRIFFITHS CE: IL-1beta-induced Langerhans' cell migration and TNF-alpha production in human skin: regulation by lactoferrin. (2003) Clin. Exp. Immunol. 132(2), 352-359.
33. GRIFFITHS CE, DEARMAN RJ, CUMBERBATCH M, and KIMBER I: Cytokines and Langerhans cell mobilisation in mouse and man. (10-21-2005) Cytokine 32(2), 67-70.
34. STOITZNER P, ZANELLA M, ORTNER U et al.: Migration of langerhans cells and dermal dendritic cells in skin organ cultures: augmentation by TNF-alpha and IL-1beta. (1999) J Leukoc. Biol. 66(3), 462-470.
35. CUMBERBATCH M, DEARMAN RJ, and KIMBER I: Langerhans cells require signals from both tumour necrosis factor-alpha and interleukin-1 beta for migration. (1997) Immunology 92(3), 388-395.
36. GRAYSON MH, RAMOS MS, ROHLFING MM et al.: Controls for lung dendritic cell maturation and migration during respiratory viral infection. (8-1-2007) J Immunol 179(3), 1438-1448.
37. HARIZI H and GUALDE N: The impact of eicosanoids on the crosstalk between innate and adaptive immunity: the key roles of dendritic cells. (2005) Tissue Antigens 65(6), 507-514.
38. LUFT T, JEFFORD M, LUETJENS P et al.: Functionally distinct dendritic cell (DC) populations induced by physiologic stimuli: prostaglandin E(2) regulates the migratory capacity of specific DC subsets. (8-15-2002) Blood 100(4), 1362-1372.
39. SCANDELLA E, MEN Y, GILLESSEN S, FORSTER R, and GROETTRUP M: Prostaglandin E2 is a key factor for CCR7 surface expression and migration of monocyte-derived dendritic cells. (8-15-2002) Blood 100(4), 1354-1361.
40. SCANDELLA E, MEN Y, LEGLER DF et al.: CCL19/CCL21-triggered signal transduction and migration of dendritic cells requires prostaglandin E2. (3-1-2004) Blood 103(5), 1595-1601.
    • In this paper, the authors show that DC migration could be increased up to 10-fold by preinjection of inflammatory cytokines such as TNF-a. In these mouse studies, the number of DCs reaching the lymph node was a critical parameter for the outcome of DC-based vaccination.
41. VAN HELDEN SF, KROOSHOOP DJ, BROERS KC, RAYMAKERS RA, FIGDOR CG, and VAN LEEUWEN FN: A critical role for prostaglandin E2 in podosome dissolution and induction of high-speed migration during dendritic cell maturation. (8-1-2006) J Immunol 177(3), 1567-1574.
42. MARTIN-FONTECHA A, SEBASTIANI S, HOPKEN UE et al.: Regulation of dendritic cell migration to the draining lymph node: impact on T lymphocyte traffic and priming. (8-18-2003) J. Exp. Med. 198(4), 615-621.
43. PRINS RM, CRAFT N, BRUHN KW et al.: The TLR-7 agonist, imiquimod, enhances dendritic cell survival and promotes tumor antigen-specific T cell priming: relation to central nervous system antitumor immunity. (1-1-2006) J Immunol 176(1), 157-164.
44. ALLAN RS, WAITHMAN J, BEDOUI S et al.: Migratory dendritic cells transfer antigen to a lymph node-resident dendritic cell population for efficient CTL priming. (2006) Immunity. 25(1), 153-162.
    •• This paper demonstrates that tissue-derived migratory DC are not uniquely involved in antigen presentation to CD8 T cells, and that lymph node resident DC also have a potentially critical role in this process.
45. CARBONE FR, BELZ GT, and HEATH WR: Transfer of antigen between migrating and lymph node-resident DCs in peripheral T-cell tolerance and immunity. (2004) Trends Immunol 25(12), 655-658.
46. SAEKI H, MOORE AM, BROWN MJ, and HWANG ST: Cutting edge: secondary lymphoid-tissue chemokine (SLC) and CC chemokine receptor 7 (CCR7) participate in the emigration pathway of mature dendritic cells from the skin to regional lymph nodes. (3-1-1999) J Immunol 162(5), 2472-2475.
47. DIEU MC, VANBERVLIET B, VICARI A et al.: Selective recruitment of immature and mature dendritic cells by distinct chemokines expressed in different anatomic sites. (7-20-1998) J Exp Med 188(2), 373-386.
48. OHL L, MOHAUPT M, CZELOTH N et al.: CCR7 governs skin dendritic cell migration under inflammatory and steady-state conditions. (2004) Immunity. 21(2), 279-288.
49. WILLIMANN K, LEGLER DF, LOETSCHER M et al.: The chemokine SLC is expressed in T cell areas of lymph nodes and mucosal lymphoid tissues and attracts activated T cells via CCR7. (1998) Eur J Immunol 28(6), 2025-2034.
50. QU C, EDWARDS EW, TACKE F et al.: Role of CCR8 and other chemokine pathways in the migration of monocyte-derived dendritic cells to lymph nodes. (11-15-2004) J. Exp. Med. 200(10), 1231-1241.
51. JAKUBZICK C, TACKE F, LLODRA J, VAN ROOIJEN N, and RANDOLPH GJ: Modulation of dendritic cell trafficking to and from the airways. (3-15-2006) J Immunol 176(6), 3578-3584.
52. DE LA RG, LONGO N, RODRIGUEZ-FERNANDEZ JL et al.: Migration of human blood dendritic cells across endothelial cell monolayers: adhesion molecules and chemokines involved in subset-specific transmigration. (2003) J Leukoc. Biol. 73(5), 639-649.

53. LEE JJ, TAKEI M, HORI S et al.: The role of PGE(2) in the differentiation of dendritic cells: how do dendritic cells influence T-cell polarization and chemokine receptor expression? (2002) Stem Cells 20(5), 448-459.
54. RODRIGUEZ-FERNANDEZ JL and CORBI AL: Adhesion molecules in human dendritic cells. (2005) Curr. Opin. Investig. Drugs 6(11), 1103-1111.
55. PRICE AA, CUMBERBATCH M, KIMBER I, and AGER A: Alpha 6 integrins are required for Langerhans cell migration from the epidermis. (11-17-1997) J Exp. Med. 186(10), 1725-1735.
56. MA J, WANG JH, GUO YJ, SY MS, and BIGBY M: *In vivo* treatment with anti-ICAM-1 and anti-LFA-1 antibodies inhibits contact sensitization-induced migration of epidermal Langerhans cells to regional lymph nodes. (10-15-1994) Cell Immunol 158(2), 389-399.
57. WEISS JM, SLEEMAN J, RENKL AC et al.: An essential role for CD44 variant isoforms in epidermal Langerhans cell and blood dendritic cell function. (6-2-1997) J Cell Biol. 137(5), 1137-1147.
58. YU Q and STAMENKOVIC I: Localization of matrix metalloproteinase 9 to the cell surface provides a mechanism for CD44-mediated tumor invasion. (1-1-1999) Genes Dev. 13(1), 35-48.
59. AVERBECK M, GEBHARDT C, ANDEREGG U, TERMEER C, SLEEMAN JP, and SIMON JC: Switch in syndecan-1 and syndecan-4 expression controls maturation associated dendritic cell motility. (2007) Exp. Dermatol. 16(7), 580-589.
60. ROBERT C, KLEIN C, CHENG G et al.: Gene therapy to target dendritic cells from blood to lymph nodes. (2003) Gene Ther. 10(17), 1479-1486.
61. DIACOVO TG, BLASIUS AL, MAK TW, CELLA M, and COLONNA M: Adhesive mechanisms governing interferon-producing cell recruitment into lymph nodes. (9-5-2005) J Exp. Med. 202(5), 687-696.
62. KOBAYASHI Y: Langerhans' cells produce type IV collagenase (MMP-9) following epicutaneous stimulation with haptens. (1997) Immunology 90(4), 496-501.
63. KOUWENHOVEN M, OZENCI V, TJERNLUND A et al.: Monocyte-derived dendritic cells express and secrete matrix-degrading metalloproteinases and their inhibitors and are imbalanced in multiple sclerosis. (2002) J Neuroimmunol. 126(1-2), 161-171.
64. OSMAN M, TORTORELLA M, LONDEI M, and QUARATINO S: Expression of matrix metalloproteinases and tissue inhibitors of metalloproteinases define the migratory characteristics of human monocyte-derived dendritic cells. (2002) Immunology 105(1), 73-82.
65. ICHIYASU H, MCCORMACK JM, MCCARTHY KM, DOMBKOWSKI D, PREFFER FI, and SCHNEEBERGER EE: Matrix metalloproteinase-9-deficient dendritic cells have impaired migration through tracheal epithelial tight junctions. (2004) Am. J Respir. Cell Mol. Biol. 30(6), 761-770.
66. RATZINGER G, STOITZNER P, EBNER S et al.: Matrix metalloproteinases 9 and 2 are necessary for the migration of Langerhans cells and dermal dendritic cells from human and murine skin. (5-1-2002) J Immunol 168(9), 4361-4371.
67. LEBRE MC, KALINSKI P, DAS PK, and EVERTS V: Inhibition of contact sensitizer-induced migration of human Langerhans cells by matrix metalloproteinase inhibitors. (1999) Arch. Dermatol. Res. 291(7-8), 447-452.
68. FULCHER JA, HASHIMI ST, LEVRONEY EL et al.: Galectin-1-matured human monocyte-derived dendritic cells have enhanced migration through extracellular matrix. (7-1-2006) J Immunol 177(1), 216-226.
69. CLARK GJ, JAMRISKA L, RAO M, and HART DN: Monocytes immunoselected via the novel monocyte specific molecule, CD300e, differentiate into active migratory dendritic cells. (2007) J Immunother. (1997.) 30(3), 303-311.
70. SALIO M, CELLA M, VERMI W et al.: Plasmacytoid dendritic cells prime IFN-gamma-secreting melanoma-specific CD8 lymphocytes and are found in primary melanoma lesions. (2003) Eur J Immunol 33(4), 1052-1062.
71. LOU Y, LIU C, KIM GJ, LIU YJ, HWU P, and WANG G: Plasmacytoid dendritic cells synergize with myeloid dendritic cells in the induction of antigen-specific antitumor immune responses. (2-1-2007) J Immunol 178(3), 1534-1541.
72. HU Y and IVASHKIV LB: Costimulation of chemokine receptor signaling by matrix metalloproteinase-9 mediates enhanced migration of IFN-alpha dendritic cells. (5-15-2006) J Immunol 176(10), 6022-6033.
73. LUFT T, MARASKOVSKY E, SCHNURR M et al.: Tuning the volume of the immune response: strength and persistence of stimulation determine migration and cytokine secretion of dendritic cells. (8-15-2004) Blood 104(4), 1066-1074.
74. NAPOLITANI G, RINALDI A, BERTONI F, SALLUSTO F, and LANZAVECCHIA A: Selected Toll-like receptor agonist combinations synergistically trigger a T helper type 1-polarizing program in dendritic cells. (2005) Nat. Immunol 6(8), 769-776.
75. LEHNER M, MORHART P, STILPER A et al.: Efficient chemokine-dependent migration and primary and secondary IL-12 secretion by human dendritic cells stimulated through Toll-like receptors. (2007) J Immunother. 30(3), 312-322.
76. BOULLART ACI, AARNTZEN EHJG, VERDIJK P et al.: Maturation of monocyte-derived dendritic cells with Toll-like receptor 3 and 7/8 ligands combined with prostaglandin E2 results in high interleukin-12 production and cell migration. (2008) Cancer Immunol. Immunother. (In press).
77. KALINSKI P, VIEIRA PL, SCHUITEMAKER JH, DE JONG EC, and KAPSENBERG ML: Prostaglandin E(2) is a selective inducer of interleukin-12 p40 (IL-12p40) production and an inhibitor of bioactive IL-12p70 heterodimer. (6-1-2001) Blood 97(11), 3466-3469.
78. ALDER J, HAHN-ZORIC M, ANDERSSON BA, and KARLSSON-PARRA A: Interferon-gamma dose-dependently inhibits prostaglandin E2-mediated dendritic-cell-migration towards secondary lymphoid organ chemokines. (11-30-2006) Vaccine 24(49-50), 7087-7094.
79. LEHNER M, STILPER A, MORHART P, and HOLTER W: Plasticity of dendritic cell function in response to prostaglandin E2 (PGE2) and interferon-{gamma} (IFN-{gamma}). (1-8-2008) J Leukoc. Biol.

80. WU X, HOU W, SUN S et al.: Novel function of IFN-gamma: negative regulation of dendritic cell migration and T cell priming. (7-15-2006) J Immunol 177(2), 934-943.
81. OKADA N, MORI N, KORETOMO R et al.: Augmentation of the migratory ability of DC-based vaccine into regional lymph nodes by efficient CCR7 gene transduction. (2005) Gene Ther. 12(2), 129-139.
82. DORRIE J, SCHAFT N, MULLER I et al.: Introduction of functional chimeric E/L-selectin by RNA electroporation to target dendritic cells from blood to lymph nodes. (9-2-2007) Cancer Immunol Immunother.
•• In this paper, the authors describe how DC properties can be manipulated by the introduction of RNA encoding for a lymph node homing receptor. This technique offers many opportunities to improve migratory and immunostimulatory capacities of DC for immunotherapy.
83. KANG TH, LEE JH, NOH KH et al.: Enhancing dendritic cell vaccine potency by combining a BAK/BAX siRNA-mediated antiapoptotic strategy to prolong dendritic cell life with an intracellular strategy to target antigen to lysosomal compartments. (4-15-2007) Int. J. Cancer 120(8), 1696-1703.
84. DANNULL J, LESHER DT, HOLZKNECHT R et al.: Immunoproteasome down-modulation enhances the ability of dendritic cells to stimulate antitumor immunity. (12-15-2007) Blood 110(13), 4341-4350.

Limited amounts of dendritic cells migrate into the T cell area of lymph nodes but have high immune activating potential in melanoma patients

Verdijk P

Aarntzen EH

Lesterhuis WJ

Boullart AC

Kok E

Van Rossum MM

Strijk S

Eijckeler F

Bonenkamp JJ

Blokx WA

Van Krieken JH

Joosten I

Boerman OC

Oyen WJ

Adema GJ

Punt CJ

Figdor CG

De Vries IJ

Clin Cancer Res. 2009;15(7):2531-40

Abstract

Success of immunotherapy with dendritic cells (DC) to treat cancer is dependent on effective migration to lymph nodes and subsequent activation of antigen-specific T cells. In this study, we investigated the fate of DC after intradermal or intranodal administration and the consequences for the immune activating potential of DC vaccines in melanoma patients. DC were intradermally or intranodally administered to 25 patients with metastatic melanoma scheduled for regional lymph node resection. To track DC *in vivo* with scintigraphic imaging and in lymph nodes by immunohistochemistry, cells were labeled with both ^{111}In and superparamagnetic iron oxide. After intradermal injection maximally 4% of the DC reached the draining lymph nodes. When correctly delivered, all DC were delivered to one or more lymph nodes after intranodal injection. Independent of the route of administration, large numbers of DC remained at the injection site, lost viability and were cleared by infiltrating $CD163^+$ macrophages within 48 hours. Interestingly, $87\pm10\%$ of surviving DC preferentially migrated into the T cell areas, where they induced antigen-specific T cell responses. Even though more DC reached the T cell areas, intranodal injection of DC induced similar antigen-specific immune responses as intradermal injection. Efficient immune responses were already induced with less than 5×10^5 DC migrating into the T cell areas.

Monocyte-derived DCs have high immune activating potential, irrespective of the route of vaccination. Limited numbers of DC in the draining lymph nodes are required to induce antigen-specific immunological responses.

Introduction

In cancer patients the immune system has not been able to establish an effective immune response against the tumor. Immunotherapy aims at educating the immune system to generate effective tumor-specific immune responses. Dendritic cells (DC) are specialized antigen presenting cells that can induce de novo anti-tumor responses and are excellent candidates for cell-based immunotherapy. While many DC-based clinical studies for the treatment of cancer have shown the feasibility and safety of DC vaccinations (reviewed in 1,2), clinical efficacy of the therapy still needs to be improved (3). One important factor that determines the outcome of DC therapy is the delivery of the vaccine to immune-reactive sites, such as lymph nodes, and more specifically to the T cell-rich area, the paracortex. To exert their action DC must closely encounter and interact with T cells. In addition, it has now been generally accepted that the site at which T cell priming occurs significantly influences the homing characteristics of the effector cells (4-8). Therefore, the route of administration may be of crucial importance. Currently, for treatment of solid tumors intradermal or subcutaneous administration of DC is most frequently used (91 clinical trials), followed by intravenous (47 trials) and intranodal (9 trials) injection (reported on www.mmri.mater.org.au). Scintigraphic imaging of cancer patients injected with DC labeled with ^{111}In or ^{99m}Tc demonstrated that only after intradermal (i.d.) or subcutaneous (9-16) intranodal (i.n.) (9,11,17) and intralymphatic (11,18) injection DC migrated to the draining lymph node regions. More substantial evidence was obtained in our previous study where DC were labeled with both ^{111}In and paramagnetic iron oxide particles (SPIO), which is a suitable contrast agent for magnetic resonance imaging (17). We demonstrated that after i.n. injection DC were indeed present in the injected node and had migrated to nearby lymph nodes. However, these images do not show how many cells actually reach the T cell area and provide no information on the phenotype and quality of the injected cells and whether the label is still present in the administered cells. SPIO-labeled DC can be easily visualized in resected lymph nodes and allow detailed analysis of the fate and local immune effects of the injected DC in the targeted lymph nodes. We demonstrate that, although the majority of non-migrating DC at the injection site are phagocytosed by macrophages, part of the SPIO-labeled cells migrate into the T cell areas, exhibit a DC phenotype, and activate specific T cells. Since immune responses in both groups of patients were comparable, there was no advantage of i.n. injection over i.d. administration.

Materials and methods

Patients

Eligibility criteria included stage III and IV melanoma according to AJCC criteria (19), HLA-A2.1 phenotype, and melanoma expressing the melanocyte-associated antigens gp100 and tyrosinase. The study was approved by our Institutional Review Board, and written informed consent was obtained from all patients.

Treatment schedule

At day -7 peripheral blood mononuclear cells were obtained by leukapheresis for DC-culturing. DC loaded with both KLH and tumor associated antigen peptides were injected either i.n. into a lymph node of the region that was to be resected or i.d. in close vicinity of this lymph node region. On day 0, patients received either an i.n. injection of ^{111}In-labeled DC (7.5×10^6) mixed with SPIO-labeled DC (7.5×10^6, total volume 100 µl) directly into a lymph node, or an i.d. injection of DC labeled with both ^{111}In and SPIO (15×10^6, total volume 100 µl). I.n. injections were performed under ultrasound guidance by an experienced radiologist. Scintigraphic imaging of the lymph node region was performed 30 minutes after i.n. injection and 24, 48, and/or 48 hours after i.n. or i.d. injection, before dissection of the regional lymph nodes. Two patients received an i.n. injection in both the left and right lymph node region. Radiolabeled lymph nodes were dissected from the surgical specimen

under guidance of a gamma probe (Europrobe®, Eurorad, Strasbourg, France) and then fixed in Unifix® (Klinipath; Duiven, The Netherlands). The lymph nodes were embedded in paraffin and processed for histology and immunohistochemistry. Patients received three more vaccinations at days 14, 28 and 42.

DC culture and labeling

DC were generated from adherent peripheral blood mononuclear cells by culturing in the presence of interleukin-4 (500 U/ml) and granulocyte-monocyte colony stimulating factor (800 U/ml) (both Cellgenix, Freiburg, Germany). On day 4 the immature DC were loaded with the control antigen keyhole limpet hemocyanin (KLH, 10 μg/ml, Calbiochem, Darmstadt, Germany) and labeled with SPIO by adding 100 μg Ferumoxide/ml (Endorem®, Laboratoire Guerbet, Aulnay-sous-Bois, France) three days after the onset of DC culturing (17). On day 5, DC were matured with autologous monocyte-conditioned medium supplemented with prostaglandin E_2 (10 μg/ml, Pharmacia & Upjohn, Puurs, Belgium) and 10 ng/ml recombinant tumor necrosis factor-α (Cellgenix, Freiburg, Germany) for 48 hours, as described previously (20,21). DC were pulsed with the melanoma peptides gp100:154-167, gp100:280-288, tyrosinase:369-376 as described previously (9). Mature DC were labeled with ^{111}In-oxine (Covidien, Petten, The Netherlands) in 0.1 M Tris-HCl (pH 7.0) for 15 minutes at room temperature as described previously (9,20) resulting in 4 MBq activity per 7.5×106 cells.

Scintigraphic imaging

In vivo and ex vivo planar scintigraphic images (256×256 matrix, 174 and 247 keV 111In photopeaks with 15% energy window) of the injection depot and corresponding lymph node basin were acquired with a gamma camera (Siemens ECAM, Hoffman Estates, IL) equipped with medium energy collimators, at day 0 and day 2). Migration was quantified by region of interest analysis of the individual nodes visualized on the images and expressed as the relative fraction of ^{111}In-labeled DC that had migrated from the injection depot to successive lymph nodes after 2 days.

Iron-staining and immunohistochemistry of histopathological sections

Sections (5 μm) of the resected radiolabeled lymph nodes were stained stained with hematoxilin and eosin (HE) or with Prussian blue to detect SPIO-labeled cells. Slides were stained with 2% potassium hexacyanoferrate (II)-trihydrate in 0.2 M HCl for 15 minutes and counterstained with 0.05% nuclear fast red in 5% aluminum sulphate. Immunohistochemical stainings were performed on paraffin-embedded tissue sections using monoclonal antibodies. Paraffin sections were de-waxed and rehydrated. All reactions were performed at room temperature, unless stated otherwise. Endogenous peroxidase activity was blocked by incubation in phosphate-buffered saline (PBS) containing 3% H_2O_2 for 30 min. After rinsing with PBS, antigen retrieval consisted of microwave boiling in either 10 mM sodium citrate buffer (pH 6.0) or 10 mM EDTA/1 mM Tris buffer (pH 8.0 or 9.0) for 10 min, depending on the primary antibody. After boiling, the slides were allowed to cool down for at least 2 h. After rinsing with PBS, slides were pretreated with 20% normal horse serum for 10 minutes to reduce nonspecific staining. All sera and antibodies were dissolved in PBS with 1% BSA. Subsequently, slides were incubated in a humidity chamber with the primary antibody at 4° C for 16–20h. The following primary monoclonal antibodies were used: CD4, CD8 (both from Beckman Coulter, Mijdrecht, The Netherlands) CD25, CD69, CD83 and CD163 (Novocastra, Newcastle upon Tyne, UK). The ABC (avidin–biotin complex, Vector, Burlingame, USA) method was used for visualization with 3, 3'-diaminobenzide hydrochloride solution (DAB). Staining of the DAB substrate was intensified with a 0.5% copper sulfate solution. Slides were counterstained with hematoxylin solution or nuclear fast red. Sections were analyzed by microscopy (Zeiss Axioskop 2 plus, Zeiss,

Sliedrecht, The Nehterlands or Leica DMLB microscope, Lieca, , Wetzlar, Germany) using ProgRes Capture Pro (Jenoptik, Jena, Germany) or Leica IM500 (Leica) software.

Humoral responses to KLH

Antibodies against KLH were measured in the serum of vaccinated patients by enzyme-linked immunosorbent assays (ELISA) (22). Microtiter plates (96 wells) were coated overnight at 4°C with KLH (25 μg/ml in PBS per well). After washing the plates, different concentrations of patient serum (range 1 in 100 to 1 in 500,000) were added for 1 hour at room temperature. After extensive washing, specific Ab (total IgG, IgG1, IgG2, and IgG4) labeled with horseradish peroxidase were allowed to bind for 1 hour at room temperature. Peroxidase activity was revealed using 3,3' 5,5-tetramethyl-benzidine as substrate and measured in a microtiter plate reader at 450nm.

Proliferation assay

Cellular responses against KLH were measured in a proliferation assay. Briefly, peripheral blood mononuclear cells (PBMC) isolated from blood samples taken before each DC vaccination were plated in a 96-well tissue culture microplate with or without KLH. After 4 days of culture, 1 μCi/well of tritiated thymidine was added for 8 hours, and incorporation of tritiated thymidine was measured in a β-counter.

Isolation of lymph node DC and T cells

Cell suspensions were made from resected radiolabeled lymph nodes from 3 patients. Lymph node tissue was cut into small fragments in Hanks Balanced salts solution medium (HBBS, GIBCO), with 50 μg/ml collagenase type 1A , 10 μg/ml DNAse and 1 μg/ml trypsin inhibitor (Sigma Chemical Co., St. Louis, MO). The fragments were incubated for 30 minutes at 37°C. For the isolation of DC-T cell rosettes, the large fragments were left to settle down and the supernatant was transferred to a fresh tube. SPIO-containing DCs were isolated with the use of a Dynal MPC® magnet. Cells were washed with RPMI supplemented with 7% human serum. The isolated SPIO-DC were spun onto microscope slides and stained with HE. From 2 patients lymph node cells were cultured 4 to 6 weeks in RPMI/7% human serum and 200 IU/ml of IL-2. KLH-specific T cell proliferation was measured in a proliferation assay. Fresh autologous PBMC were loaded with KLH overnight, irradiated and used as stimulator cells for lymph node T cells (ratio 1:1). After 4 days of culture, 1 μCi/well of tritiated thymidine was added for 8 hours, and incorporation of tritiated thymidine was measured in a β-counter.

Delayed Type Hypersensitivity

One to two weeks after the four DC vaccinations a delayed type hypersensitivity (DTH) skin test was performed. Briefly, DC pulsed with peptides and DC pulsed with peptides plus KLH ($2x10^5$ DC each) were injected i.d. in the skin of the back of the patients at four different sites. The diameter (in millimeters) of induration was measured after 48 hours, and punch biopsies (6 mm) were obtained under local anesthesia. Biopsies were cut in half, one part was frozen directly in liquid nitrogen for immunohistochemistry and the other part was cut in small pieces and cultured in RPMI/7% HS supplemented with IL-2 (100 U/ml). Every 7 days, half of the medium was replaced by fresh IL-2-containg RPMI/7%HS. After 2 to 4 weeks of culturing, T cells were tested for antigen recognition or tested for tetramer binding. For tetramer binding PBMC of T cells were incubated with allophycocyanin-labeled tetrameric-MHC complexes containing the gp100:154-167, gp100:280-288 or tyrosinase:369-376 peptide (Sanquin, Amsterdam, The Netherlands) for 1 h, washed and analyzed by flowcytometry.

Antigen recognition assay

Antigen recognition was determined by the production of cytokines by DTH-derived cells in response to T2 cells pulsed with the indicated peptides or BLM (a melanoma cell line expressing HLA-A2.1 and no endogenous expression of gp100 and tyrosinase), transfected with control antigen G250, or with gp100 or an allogenic HLA-A2.1-positive, gp100-positive, and tyrosinase-positive tumor cell line (MEL624) were measured. Cytokine production was measured in supernatants after 16 hours of coculture by the cytometric bead array (Th1/Th2 Cytokine CBA 1; BD Pharmingen).

Statistics

Data were analyzed using unpaired student t-test, p-values <0.05 were considered to be statistically significant.

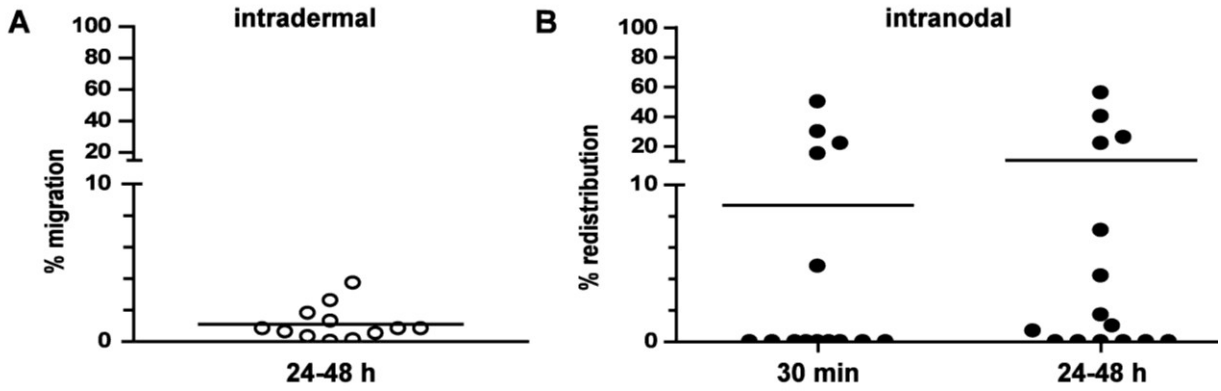

Figure 1. DC migration to nearby lymph nodes after vaccination in melanoma patients. Percentage of cells redistributed to nearby lymph nodes after i.d. (A) and i.n. (B) injection of ^{111}In- and SPIO-labeled DC, imaged by scintigraphy of the lymph node region. Each symbol represents one injection of 15×10^6 cells (open symbols: i.d., closed symbols: i.n.). The line indicates the mean redistribution. Migration of radiolabeled DC was measured 30 minutes and/or 24-48 hours after injection.

Results

Biodistribution of ^{111}In/SPIO-DC after i.d. and i.n. vaccination

To study the distribution of the dendritic cell vaccine after i.d. and i.n injection in patients with metastatic melanoma, DC were labeled with ^{111}In and SPIO for the first vaccination and injected in (the vicinity of) a lymph node region 24-72 hours before scheduled lymph node resection. Delivery of the DC to skin-draining lymph nodes after i.d. (n=12) and i.n. injection (13 patients) was monitored by scintigraphic imaging of the lymph node region (Supplementary table 1). After i.d. administration never more than 4% migration was observed (Figure 1A, mean 1.1±1.1%). In contrast, the percentage of cells reaching nearby lymph nodes after i.n. administration was highly variable and ranged from 0 to 56% (Figure 1B, mean 10.6±17.5%). In 5 patients distribution to more than one lymph node had already taken place within the first 30 minutes after injection, indicating that DC had spread via the lymphatics system during injection. Migration to subsequent lymph nodes increased in the next 24-72 h. In 6 patients DC remained localized at the injection site, suggesting that either DC had not (detectably) migrated, or that DC were not correctly injected into a lymph node. For 5 patients the latter was indeed confirmed with magnetic resonance imaging as previously described 17. In the resected lymph node basin from the sixth patient an ^{111}In-positive lymph node was isolated, demonstrating that injection was correct but that the cells had not migrated to nearby lymph nodes. Taken together, while maximally 4% of the DC reached the draining lymph nodes after i.d. injection, all DC were delivered to one or more lymph nodes after i.n. injection, when correctly delivered.

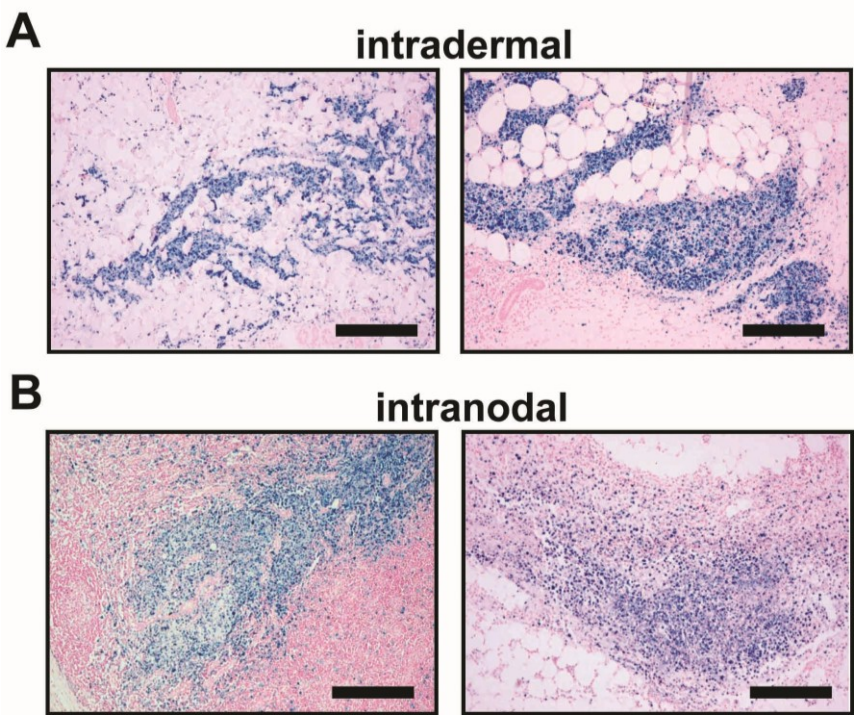

Figure 2. Most ^{111}In/SPIO-DC remain at site of injection. Melanoma patients received i.d. or i.n. injections of ^{111}In- and SPIO labeled DC 48 hours before surgery. Resected lymph nodes and skin biopsies were analyzed for the presence of SPIO-labeled cells by Prussian blue staining. (A) Injection site in the dermis after i.d. vaccination (two patients) (50×). (B) Injection site in the lymph node after i.n. vaccination (two patients) (50×). Bar, 500 μm.

Numerous ^{111}In/SPIO-DC die at the injection site and are phagocytosed by macrophages

Because the presence of ^{111}In/SPIO-DC inside lymph nodes does not necessarily imply that DC actually reach the T cell area, we analyzed the dissected radiolabeled lymph nodes by immunohistochemistry to visualize ^{111}In/SPIO-DC. Lymph nodes were obtained from 8 and 9 patients that received i.d. or i.n injections, respectively. In addition, biopsies from the i.d. injection site were obtained and analyzed in the same way. Although single ^{111}In/SPIO-DC were present in the sinuses and paracortex of draining lymph nodes, a large depot of SPIO+ cells was found at the site of injection, as was expected from the scintigraphs. This was not only observed after i.d. vaccination (Figure 2A), but also after i.n. injection (Figure 2B). In lymph nodes from patients where immediate redistribution of the DC after injection was observed, ^{111}In/SPIO-DC also accumulated in the sinuses of subsequent nodes (not shown). To verify whether the SPIO$^+$ cells at the i.d. or i.n. injection site were indeed DC and not phagocytes that have taken up label, lymph node sections were stained for the DC marker CD83, and for the macrophage marker CD163 23. This revealed that in the dermis only part of the SPIO$^+$ cells in the injection site expressed CD83 (Figure 3A). In the CD83 negative areas, all SPIO$^+$ cells were positive for the macrophage marker CD163 (Figure 3A-C). Staining with hematoxylin-eosin revealed that in areas with the most CD83$^+$ ^{111}In/SPIO-DC cells were enlarged and exhibited pale pink nuclei, typical for necrotic cells (Figure 3D right panel). At the same time the SPIO$^+$ cells in the CD163$^+$ area appeared viable, exhibiting regular hematoxilin staining of the nuclei (Figure 3D left panel), suggesting that macrophages had infiltrated the injection site and had phagocytosed dead ^{111}In/SPIO-DC. Comparable results were found after i.n. injection (Figure 3E-I). Most of the SPIO$^+$ cells at the site of injection still expressed CD83 at 24 h (1 patient), but numerous small macrophages containing no or little SPIO were present in-between enlarged SPIO$^+$ cells (Figure 3E). In lymph nodes resected after 48 hours, CD83 expression was rare and mainly found in the centre of the depot, while macrophages were present throughout the injection site (Figure 3F-H). Like in i.d. injection sites, necrotic cells were found at sites where CD83 expression was most abundant, whereas in areas with only CD83$^-$ SPIO$^+$ macrophages cells seemed viable (Figure 3I). Thus, the majority of the ^{111}In/SPIO-DC remained at the injection site and had lost viability, while macrophages infiltrated the depot and phagocytosed dead ^{111}In/SPIO-DC.

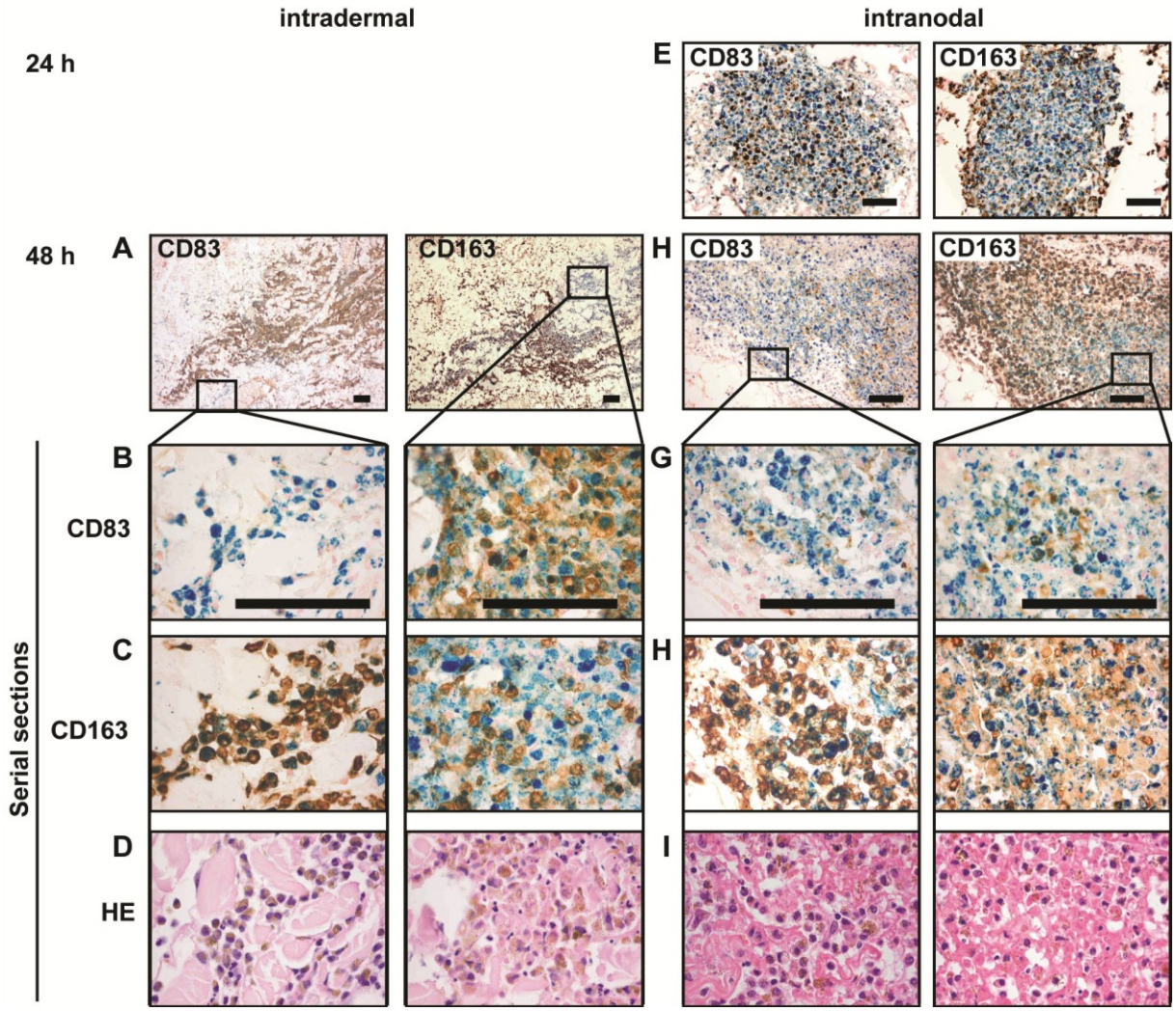

Figure 3. Expression of DC and macrophage markers on SPIO$^+$ cells in the injection depot. (A-I). Paraffin-embedded sections of i.d. (A-D) and i.n. (E-I) injection sites were stained with HE or with antibodies for CD83 and CD163. (A) Overview of CD83 (left panel)and CD163 (right panel) expression in injection site 48 hours after i.d. injection of 111In/SPIO-DC (50×). (E,F) Overview of CD83 (left panel) and CD163 (right panel) expression in injection site in lymph nodes resected 24 h (E) or 48 h (F) after injection of ^{111}In/SPIO-DC (100×). (B-D, G-I) Higher magnifications (400×) of indicated areas in C and H, stained for CD83 (B and G), CD163 (C and H), or with HE (D and I) (400×). Bar, 100 μm. In HE stainings SPIO is visible as brown granula. In immunostainings SPIO was visualized by Prussian blue staining and nuclei were stained with nuclear fast red.

^{111}In/SPIO-DC migrate into the T cell areas and activate antigen-specific T cells.

Although most ^{111}In/SPIO-DC were trapped at the site of injection, single SPIO$^+$ cells were found scattered in draining lymph nodes both after i.d. injection and in the injected and subsequent nodes after i.n. injection. We evaluated the CD83 expression and location within the lymph node of these SPIO$^+$ cells. After i.d. injection SPIO$^+$ cells can only reach the draining lymph nodes by active migration via the afferent lymphatics. Indeed, SPIO$^+$ cells were predominantly found in the T cell areas (93±9%) and sometimes in the subcapsular sinuses (Figure 4A, left panels). Of all SPIO$^+$ cells in the paracortex 85±13% were CD83$^+$ DC (Figure 4B), indicating that mainly viable ^{111}In/SPIO-DC and only few SPIO$^+$ macrophages had migrated to the draining lymph nodes and into the T cell areas. After i.n. injection more SPIO$^+$ cells were dispersed over lymph nodes than after injection in the dermis. SPIO$^+$ cells were present in high numbers both in the sinuses and the paracortex. We estimated the total number of SPIO$^+$ cells in the paracortex in single lymph node sections after i.n. injection to be 10-30 fold higher than after i.d. administration. However, also many SPIO$^+$ macrophages were present both in the injected node and in nearby lymph nodes. Analysis of the paracortex of all lymph nodes revealed that 54±21% of all SPIO$^+$ cells in the paracortex were DC. Within each section the ratio between ^{111}In/SPIO-DC and SPIO$^+$ macrophages was variable and correlated with the distance from the depot.

In close vicinity of the injection depot 5% SPIO$^+$ cells were CD83$^+$ ^{111}In/SPIO-DC, whereas at more distant sites virtually all of the SPIO+ cells expressed CD83 (not shown). Quantitative analysis of the total number of SPIO$^+$ cells was only possible in sections of lymph nodes where DC had migrated to. Quantification of CD83$^+$ and CD163$^+$ expression revealed that only 35±26% of all SPIO$^+$ cells were CD83$^+$ DC (Figure 4A, right panels, and 4C). Interestingly, 87±10% of these CD83$^+$ ^{111}In/SPIO-DC were found in the T cell area, indicating that ^{111}in/SPIO-DC that do survive preferentially migrate into the paracortex.

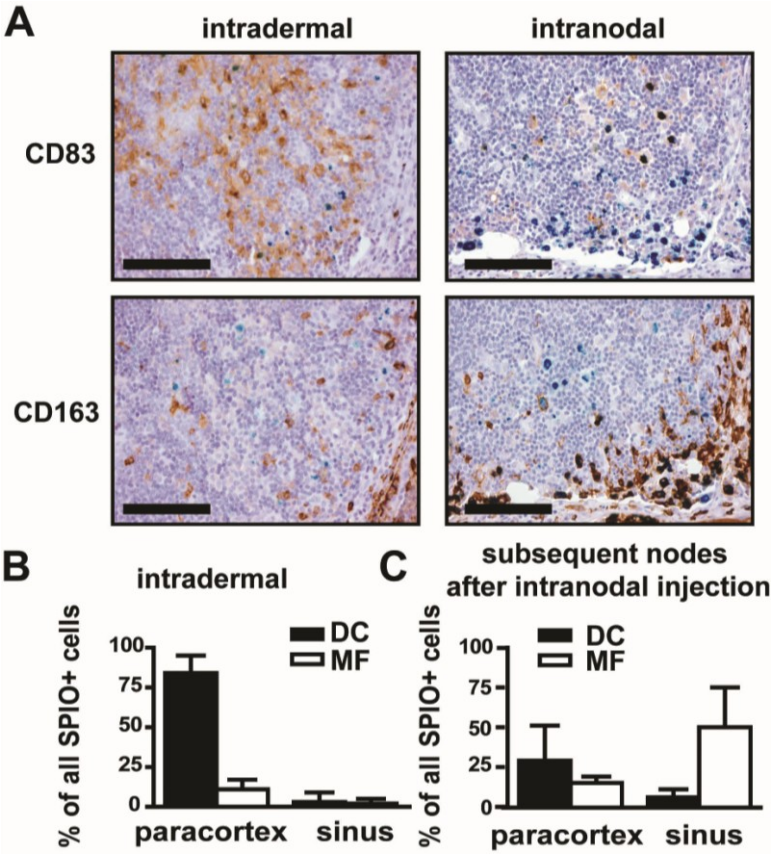

Figure 4. ^{111}In/SPIO-DC preferentially migrate into the T cell area. Immuno-histochemistry of paraffin-embedded sections of lymph nodes to which DC had migrated after i.d. and i.n. injection. A. T cell area of lymph nodes after i.d. (left panels) and i.n. (right panels) stained for CD83 and CD163 (200×). B-C. Graphs representing the percentage of SPIO$^+$ cells expressing CD83 or CD163 in the paracortex and sinuses of draining lymph nodes after i.d. injection (B) and of lymph nodes after i.n. injection that do not contain injection depots (C). Bar, 100 μm.

DCs in T cell area are fully functional and activate T cells

We next analyzed whether ^{111}in/SPIO-DC that had migrated into the paracortex of the (draining) lymph nodes were still functional and able to interact with resident T cells. SPIO$^+$ DC in the T cell area colocalized with both CD4$^+$ and CD8$^+$ T cells (Figure 5A). Interestingly, the staining for CD8 was most prominent at the interface between the T cell and the SPIO-positive cells (Figure 5B, second panel). This explicit localized expression of CD8 molecules suggests that the T cells are actively engaged with the DC in a way that stimulated redistribution of the CD8 molecules and likely the formation of an immunological synapse. Activation of T cells surrounding the injected DC was further supported by the expression of the early T cell activation marker CD69 and the activation marker CD25 (Figure 5B). Of the SPIO$^+$ cells in the T cell area 65±22% were in the immediate proximity of CD69$^+$ cells (8 lymph nodes from 6 patients). Similarly, 64±13% of the SPIO$^+$ cells in the paracortex were surrounded by CD25$^+$ T cells (10 lymph nodes from 6 patients). To further investigate the immune-activating potential of the migrated ^{111}In/SPIO-DC, they were isolated from a lymph node cell suspension by a magnet. We found that some of these DC were still forming rosettes with T cells (Figure 5C). In addition, we could demonstrate that T cells cultured from lymph node suspensions of two i.n. vaccinated patients showed KLH-specific proliferation (Figure 5D). Thus, ^{111}In/SPIO-DC interacted with T cells and induced antigen-specific T cell responses within 48 hours after vaccination.

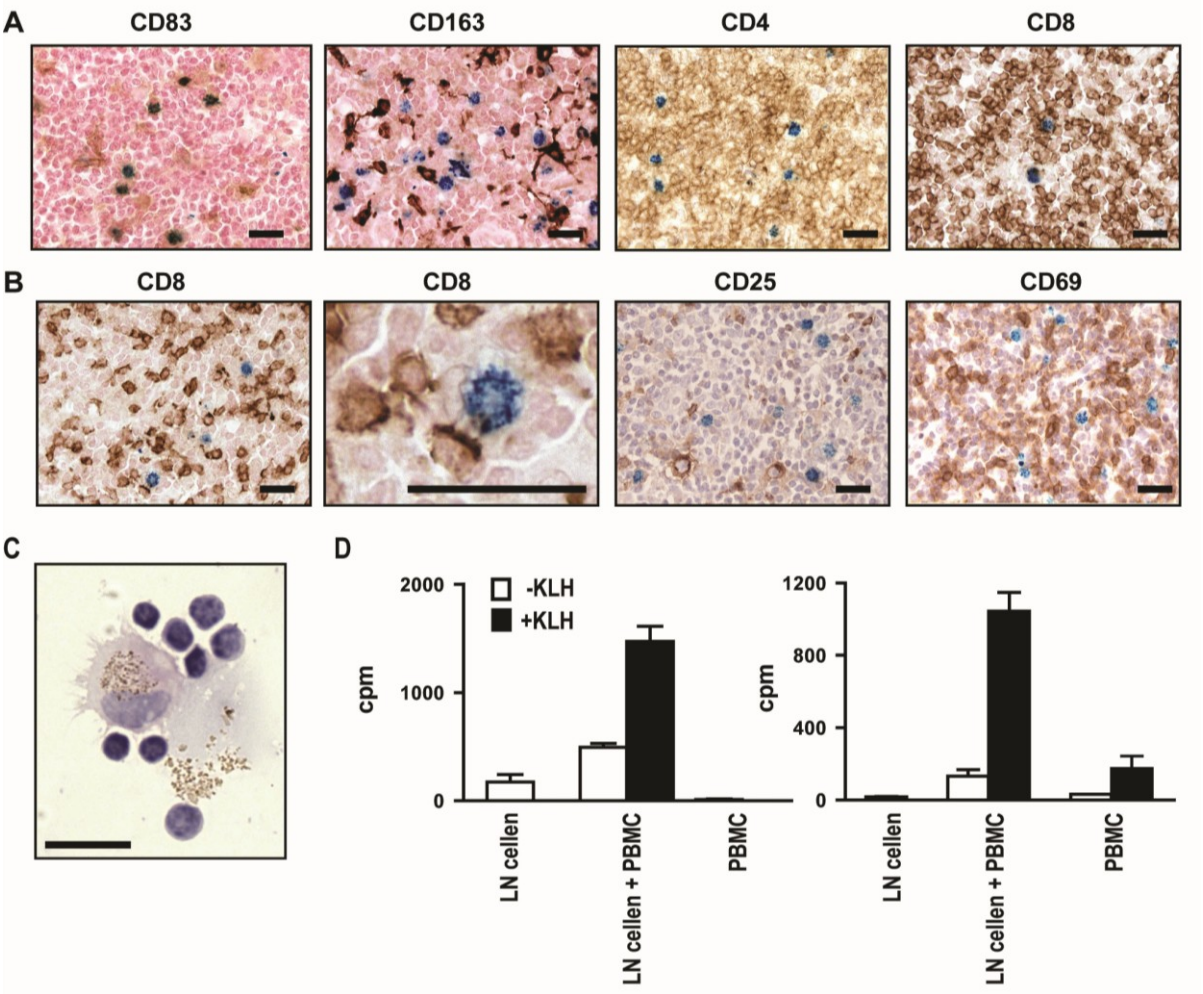

Figure 5. ^{111}*In/SPIO-DC interact with lymph node T cells and activate KLH-specific T cells. (*A) T cell area after i.n. injection stained for CD83, CD163, CD4 and CD8 (630x). Bar, 20 μm. (B) T cell area of lymph node after i.n. injection stained for CD8 (2nd panel shows a detail of the first panel), CD69 (3rd panel) and CD25 (last panel) (original magnification: 630x). Bar, 20 μm. Iron oxide was visualized by Prussian blue staining. Nuclei were stained with hematoxilin (A, E right panels) or nuclear fast red (D, E left panels). (C) Rosette of a SPIO-labeled DC with T cells magnetically isolated from a lymph node of a patient after i.n. injection. Bar, 20 μm. (D) KLH-specific proliferation of lymph node-derived T cells from two patients after one i.n. DC injection. T cells were cocultured with irradiated, autologous PBMC loaded with (black bars) or without KLH (white bars). Proliferation was measured in a tritiated-thymidin incorporation assay.

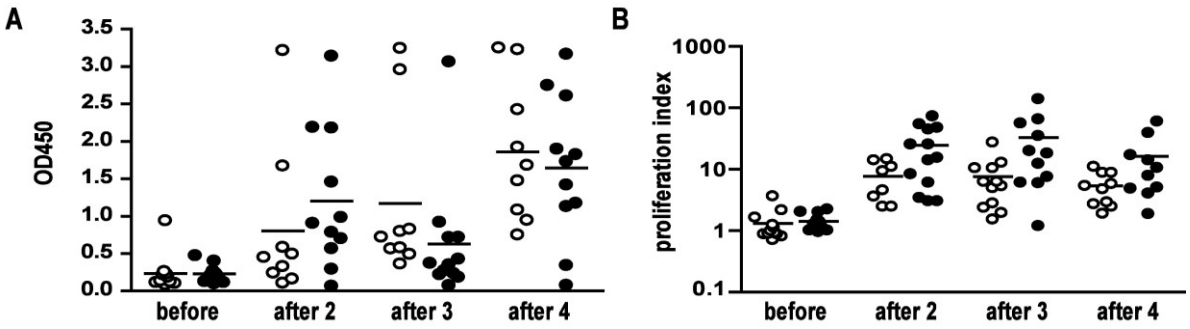

Figure 6. Immune activation by DC vaccination. Immunological response against KLH in the peripheral blood of patients before and after DC vaccination. PBMC and serum were isolated from blood from vaccinated patients at day 30, 44 and 56, respectively after 2, 3 and 4 vaccinations. Symbols represent individual patients (open circles: i.d. vaccination, closed circles: i.n. vaccination). The line indicates the mean. (A) Antibody response against KLH. Graphs shows the OD450 values of total IgG directed to KLH in serum of individual patients diluted 1 in 200. (B) KLH-induced proliferation of PBMC of melanoma patients before and after DC vaccination. Each symbol represents one patient (open symbols: i.d. injections, closed symbols: i.n. injections). The line indicates the mean.

Systemic immune responses after i.d. and i.n. vaccination with DC are comparable despite difference in number of DC in T cell area

To test whether the differences in ^{111}In/SPIO-DC distribution after vaccination by different routes of administration had any effect on the strength of immune activation, we compared the immune responses elicited in patients that received multiple injections. To monitor the capacity of vaccinated DC to initiate an immune response, DC were not only pulsed with TAA peptides, but also loaded with the foreign protein KLH. We observed that most patients (i.n. 11/13, i.d. 10/11) developed an IgG antibody response against KLH after DC vaccination, with serum levels increasing after each vaccination (Figure 6A). Levels of KLH specific IgG antibody were comparable after i.n. and i.d. vaccination. In addition, KLH-specific proliferation of $CD4^+$ T cells was induced in all i.n. and i.d. injected patients (Figure 6B). Thus, despite the difference in the number of DC that reach the skin draining lymph nodes, there was no effect on the strength of the immune response against KLH after i.n. or i.d. injection. Next we compared the capacity of i.d. and i.n. injected DC to induce specific $CD8^+$ T cell responses against the tumor associated peptides used for loading. Tumor associated antigen responses were tested by staining T cells with HLA-A2.1 tetramers encompassing gp100:154, gp100:280 or tyrosinase:369 peptides. In one patient in each group we could already detect tetramer-specific T cells in PBMC freshly isolated after four vaccinations. Because the frequency of peptide-specific T cell in the blood is very low and often undetectable, DTH responses were induced by injecting peptide-loaded DC intradermally. We have shown previously that sampling of DTH sites is a very powerful approach to detect vaccine-related T cells (24). No significant differences were found in the number of patients with tetramer+ and IFN-γ-producing T cells isolated from DTH reactions. TAA-tetramer-positive T cells were found in 4 out of 11 patients after i.d. vaccination and in 6 out of 11 patients after i.n. vaccination (Supplementary Table 1). The functionality of these T cells was tested by coculturing with T2 cells loaded with TAA-peptides and measuring the IFN-γ-production. Both after i.d. (4/10 patients) and after i.n. (4/8 patients) T cells from DTH biopsies produced IFN-γ in cocultures with peptide loaded target cells (Supplementary Table 1). Thus, despite the limited number of DC migrating to subsequent lymph nodes, immulological responses were found in most patients and no significant differences were found in the immunological responses after i.n. and i.d. DC vaccination.

Discussion

Previously, we have demonstrated that DC can be tracked *in vivo* both by scintigraphic imaging and MRI (9,17). In this study we monitored the migration of DC into the T cell area, paracortex, of the lymph node at microscopical level. Although *in vivo* imaging provided us with much information on the distribution of the DC vaccine after injection, the limitation is that lymph nodes can only be generally qualified as positive for the cell tracking label. Here we exploit immunohistochemistry to show that many DC remained at the site of injection where they died and were cleared by macrophages. Nevertheless, small numbers of labeled DC did reach the lymph node and migrated into the T cell area, where they interacted with T cells and induced immune responses against KLH and TAA. Importantly, despite the fact that more DC reached the T cell areas after i.n. injection, DCs were equally well capable of inducing immune responses. *In vivo* tracking of *ex vivo* generated cells is an important read-out for evaluation of cellular therapy. Our results explicate that *in vivo* tracking of therapeutic cells primarily tracks the cell label and may need to be confirmed with immunohistochemical studies. For example, whereas quantification of migrated DC after i.d. injection proved to be quite accurate (approximately 85% of the migrated cells were indeed DC), quantification of the number of viable therapeutic cells that had actually migrated after i.n. injection was not possible, because the migrated cells as well as the depot were present within the same lymph nodes. Therefore, not only viable DC, but also non-viable DC and phagocytes that have taken up the tracking agent were imaged. Moreover, migration may be overestimated because therapeutic

cells and phagocytes containing the tracking label cannot be distinguished by *in vivo* imaging. Thus, depending on the method of administration and the nature of the vaccine, immunohistochemical analysis of target organs will still be decisive for quantitative and qualitative evaluation of the efficacy of cellular therapy. Intradermal administration of DC vaccines is not only attractive for imaging purposes, it is also easier to perform and less time consuming and less expensive than i.n. injection, which needs to be performed under ultrasound guidance by an experienced radiologist. We found that after i.d. injection never more than 4% of DC migrated to the draining lymph node, while up to 56% of the DC redistributed to distinct lymph nodes after i.n. injection. Despite these major differences in migrating DC, immunological responses were comparable after both i.n. and i.d. DC injection. Up till now, the minimal amount of DC that is needed to induce an efficient immune response in humans is unknown. From our data we can calculate that after i.d. injection less than 5×10^5 DC reach the T cell area (in the case of maximal migration of 4%, of which 84% accounts for viable DC after injection of 15×10^6 DC). Apparently this low number of DC is sufficient to induce de novo immune responses. It is interesting that after 4 vaccinations immune responses after i.n. injection of DC were not significantly higher than after i.d. injection, even though at least 10-30 fold more $SPIO^+$ cells reach the paracortex with each vaccination. Important difference is that after intradermal injection only few macrophages migrate from the injection site into the lymph nodes, whereas after intranodal injection all macrophages are already inside. The presence of macrophages that have phagocytosed ^{111}In/SPIO-DC in the paracortex (ca. 50% of $SPIO^+$ cells after i.n. injection versus 13% after i.d. injection) may have a negative effect on the immune response, for instance by the secretion of anti-inflammatory cytokines. CD163 was found to be exclusively expressed by anti-inflammatory (mφ2) and not by pro-inflammatory macrophage (mφ1) subsets cultured from monocytes (25). These mφ2 macrophages can induce regulatory T cells via the expression of membrane bound tumor growth factor (TGF)-β (26). Thus, the presence of large numbers of $CD163^+SPIO^+$ macrophages may dampen the immune response induced by the ^{111}In/SPIO-DC. Although we detected anti-KLH immune responses in most patients, TAA-specific immune response were observed less frequently. One of the reasons may be the absence of MHC class II-restricted peptides. Also, the threshold for the activation of T cells specific for TAA tyrosinase and gp100 is likely higher than for the immunogenic foreign antigen KLH. Most importantly, the binding of exogenous-loaded TAA-peptides to DC is not stable and peptides may therefore be presented by less cells at lower densities and for a shorter period of time (27). An alternative way of antigen delivery would be loading of DC with antigens that need to be intracellularly processed. The use of antigens requiring processing results in prolonged antigen presentation (27), thereby increasing the time span during which the DC can activate specific T cells. Furthermore, DC may amplify the response by the transfer of antigen to resident DC, in addition to presenting processed antigen to T cells themselves (28,29). Increasing antigen presentation, immune-stimulatory potential and migratory capacities of DC for immunotherapy may greatly enhance the efficacy of DC therapy (reviewed in 30). At present, we are comparing peptide-loaded DC with DC loaded with mRNA encoding for TAA. Initial findings demonstrate that when DC electroporated with TAA-mRNA are injected into a lymph node, TAA-protein expression was detectable up till 24 hours after injection (Schuurhuis *et al.* submitted). Simultaneously, our research focuses on the generation of DC with high immune-stimulatory capacity (31) and on maximizing migratory capacities and vaccine delivery. In addition, it will be worthwhile to investigate whether the injection of no more than 5×10^6 DC directly into a lymph node will already be sufficient to induce immunological responses, as this will greatly reduce the need for large-scale production of DC and may make the use of DC that circulate in small numbers in the peripheral blood feasible. Optimizing both the generation of high migratory and immune-stimulatory DC and improving application and treatment strategies will be necessary to enhance the number of responding patients and advance experimental DC immune therapy into a standard treatment.

References

1. Figdor, C. G., de Vries, I. J., Lesterhuis, W. J., and Melief, C. J. Dendritic cell immunotherapy: mapping the way. Nat.Med., 10: 475-480, 2004.
2. Nencioni, A., Grunebach, F., Schmidt, S. M., Muller, M. R., Boy, D., Patrone, F., Ballestrero, A., and Brossart, P. The use of dendritic cells in cancer immunotherapy. Crit Rev.Oncol.Hematol., 65: 191-199, 2008.
3. Lesterhuis, W. J., Aarntzen, E. H., de Vries, I. J., Schuurhuis, D. H., Figdor, C. G., Adema, G. J., and Punt, C. J. Dendritic cell vaccines in melanoma: from promise to proof? Crit Rev.Oncol.Hematol., 66: 118-134, 2008.
4. Eggert, A. A., Schreurs, M. W., Boerman, O. C., Oyen, W. J., de Boer, A. J., Punt, C. J., Figdor, C. G., and Adema, G. J. Biodistribution and vaccine efficiency of murine dendritic cells are dependent on the route of administration. Cancer Res., 59: 3340-3345, 1999.
5. Okada, N., Tsujino, M., Hagiwara, Y., Tada, A., Tamura, Y., Mori, K., Saito, T., Nakagawa, S., Mayumi, T., Fujita, T., and Yamamoto, A. Administration route-dependent vaccine efficiency of murine dendritic cells pulsed with antigens. Br.J Cancer, 84: 1564-1570, 2001.
6. Mullins, D. W., Sheasley, S. L., Ream, R. M., Bullock, T. N., Fu, Y. X., and Engelhard, V. H. Route of immunization with peptide-pulsed dendritic cells controls the distribution of memory and effector T cells in lymphoid tissues and determines the pattern of regional tumor control. J Exp.Med., 198: 1023-1034, 2003.
7. Dudda, J. C., Simon, J. C., and Martin, S. Dendritic cell immunization route determines CD8+ T cell trafficking to inflamed skin: role for tissue microenvironment and dendritic cells in establishment of T cell-homing subsets. J Immunol, 172: 857-863, 2004.
8. Mora, J. R., Bono, M. R., Manjunath, N., Weninger, W., Cavanagh, L. L., Rosemblatt, M., and von Andrian, U. H. Selective imprinting of gut-homing T cells by Peyer's patch dendritic cells. Nature, 424: 88-93, 2003.
9. de Vries, I. J., Krooshoop, D. J., Scharenborg, N. M., Lesterhuis, W. J., Diepstra, J. H., van Muijen, G. N., Strijk, S. P., Ruers, T. J., Boerman, O. C., Oyen, W. J., Adema, G. J., Punt, C. J., and Figdor, C. G. Effective migration of antigen-pulsed dendritic cells to lymph nodes in melanoma patients is determined by their maturation state. Cancer Res., 63: 12-17, 2003.
10. Morse, M. A., Coleman, R. E., Akabani, G., Niehaus, N., Coleman, D., and Lyerly, H. K. Migration of human dendritic cells after injection in patients with metastatic malignancies. Cancer Res., 59: 56-58, 1999.
11. Quillien, V., Moisan, A., Carsin, A., Lesimple, T., Lefeuvre, C., Adamski, H., Bertho, N., Devillers, A., Leberre, C., and Toujas, L. Biodistribution of radiolabelled human dendritic cells injected by various routes. Eur J Nucl.Med.Mol.Imaging, 32: 731-741, 2005.
12. Ridolfi, R., Riccobon, A., Galassi, R., Giorgetti, G., Petrini, M., Fiammenghi, L., Stefanelli, M., Ridolfi, L., Moretti, A., Migliori, G., and Fiorentini, G. Evaluation of *in vivo* labelled dendritic cell migration in cancer patients. J.Transl.Med., 2: 27, 2004.
13. Blocklet, D., Toungouz, M., Kiss, R., Lambermont, M., Velu, T., Duriau, D., Goldman, M., and Goldman, S. 111In-oxine and 99mTc-HMPAO labelling of antigen-loaded dendritic cells: *in vivo* imaging and influence on motility and actin content. Eur.J.Nucl.Med.Mol.Imaging, 30: 440-447, 2003.
14. Nair, S., McLaughlin, C., Weizer, A., Su, Z., Boczkowski, D., Dannull, J., Vieweg, J., and Gilboa, E. Injection of immature dendritic cells into adjuvant-treated skin obviates the need for ex vivo maturation. J.Immunol., 171: 6275-6282, 2003.
15. Thompson, M., Wall, D. M., Hicks, R. J., and Prince, H. M. *In vivo* tracking for cell therapies. Q.J Nucl.Med.Mol.Imaging, 49: 339-348, 2005.
16. Trakatelli, M., Toungouz, M., Blocklet, D., Dodoo, Y., Gordower, L., Laporte, M., Vereecken, P., Sales, F., Mortier, L., Mazouz, N., Lambermont, M., Goldman, S., Coulie, P., Goldman, M., and Velu, T. A new dendritic cell vaccine generated with interleukin-3 and interferon-beta induces CD8+ T cell responses against NA17-A2 tumor peptide in melanoma patients. Cancer Immunol Immunother., 55: 469-474, 2006.
17. de Vries, I. J., Lesterhuis, W. J., Barentsz, J. O., Verdijk, P., van Krieken, J. H., Boerman, O. C., Oyen, W. J., Bonenkamp, J. J., Boezeman, J. B., Adema, G. J., Bulte, J. W., Scheenen, T. W., Punt, C. J., Heerschap, A., and Figdor, C. G. Magnetic resonance tracking of dendritic cells in melanoma patients for monitoring of cellular therapy. Nat.Biotechnol., 23: 1407-1413, 2005.
18. Mackensen, A., Krause, T., Blum, U., Uhrmeister, P., Mertelsmann, R., and Lindemann, A. Homing of intravenously and intralymphatically injected human dendritic cells generated *in vitro* from CD34+ hematopoietic progenitor cells. Cancer Immunol.Immunother., 48: 118-122, 1999.
19. Balch, C. M., Buzaid, A. C., Soong, S. J., Atkins, M. B., Cascinelli, N., Coit, D. G., Fleming, I. D., Gershenwald, J. E., Houghton, A., Jr., Kirkwood, J. M., McMasters, K. M., Mihm, M. F., Morton, D. L., Reintgen, D. S., Ross, M. I., Sober, A., Thompson, J. A., and Thompson, J. F. Final version of the American Joint Committee on Cancer staging system for cutaneous melanoma. J.Clin.Oncol., 19: 3635-3648, 2001.
20. de Vries, I. J., Eggert, A. A., Scharenborg, N. M., Vissers, J. L., Lesterhuis, W. J., Boerman, O. C., Punt, C. J., Adema, G. J., and Figdor, C. G. Phenotypical and functional characterization of clinical grade dendritic cells. J.Immunother., 25: 429-438, 2002.
21. Thurner, B., Haendle, I., Roder, C., Dieckmann, D., Keikavoussi, P., Jonuleit, H., Bender, A., Maczek, C., Schreiner, D., von den, D. P., Brocker, E. B., Steinman, R. M., Enk, A., Kampgen, E., and Schuler, G. Vaccination with mage-3A1 peptide-pulsed mature, monocyte-derived dendritic cells expands specific cytotoxic T cells and induces regression of some metastases in advanced stage IV melanoma. J.Exp.Med., 190: 1669-1678, 1999.
22. Holtl, L., Rieser, C., Papesh, C., Ramoner, R., Herold, M., Klocker, H., Radmayr, C., Stenzl, A., Bartsch, G., and Thurnher, M. Cellular and humoral immune responses in patients with metastatic renal cell carcinoma after vaccination with antigen pulsed dendritic cells. J Urol., 161: 777-782, 1999.
23. Vakkila, J., Lotze, M. T., Riga, C., and Jaffe, R. A basis for distinguishing cultured dendritic cells and macrophages in cytospins and fixed sections. Pediatr.Dev.Pathol., 8: 43-51, 2005.

24. de Vries, I. J., Bernsen, M. R., Lesterhuis, W. J., Scharenborg, N. M., Strijk, S. P., Gerritsen, M. J., Ruiter, D. J., Figdor, C. G., Punt, C. J., and Adema, G. J. Immunomonitoring tumor-specific T cells in delayed-type hypersensitivity skin biopsies after dendritic cell vaccination correlates with clinical outcome. J.Clin.Oncol., 23: 5779-5787, 2005.
25. Verreck, F. A., de Boer, T., Langenberg, D. M., van der, Z. L., and Ottenhoff, T. H. Phenotypic and functional profiling of human proinflammatory type-1 and anti-inflammatory type-2 macrophages in response to microbial antigens and IFN-gamma- and CD40L-mediated costimulation. J Leukoc.Biol., 79: 285-293, 2006.
26. Savage, N. D., de Boer, T., Walburg, K. V., Joosten, S. A., van Meijgaarden, K., Geluk, A., and Ottenhoff, T. H. Human anti-inflammatory macrophages induce Foxp3+ GITR+ CD25+ regulatory T cells, which suppress via membrane-bound TGFbeta-1. J Immunol, 181: 2220-2226, 2008.
27. Schnurr, M., Chen, Q., Shin, A., Chen, W., Toy, T., Jenderek, C., Green, S., Miloradovic, L., Drane, D., Davis, I. D., Villadangos, J., Shortman, K., Maraskovsky, E., and Cebon, J. Tumor antigen processing and presentation depend critically on dendritic cell type and the mode of antigen delivery. Blood, 105: 2465-2472, 2005.
28. Allan, R. S., Waithman, J., Bedoui, S., Jones, C. M., Villadangos, J. A., Zhan, Y., Lew, A. M., Shortman, K., Heath, W. R., and Carbone, F. R. Migratory dendritic cells transfer antigen to a lymph node-resident dendritic cell population for efficient CTL priming. Immunity., 25: 153-162, 2006.
29. Kleindienst, P. and Brocker, T. Endogenous dendritic cells are required for amplification of T cell responses induced by dendritic cell vaccines *in vivo*. J Immunol, 170: 2817-2823, 2003.
30. Verdijk, P., Aarntzen, E. H. J. G., Punt, C. J., Vries IJ, M. d., and Figdor, C. G. Maximizing dendritic cell migration for cancer immunotherapy. Expert Opin.Biol.Ther., 8: 865-874, 2008.
31. Boullart, A. C. I., Aarntzen, E. H. J. G., Verdijk, P., Jacobs, J. F. M., Schuurhuis, D., Benitez-Ribas, D., Schreibelt, G., van de Rakt, M. W. M. M., Scharenborg, N. M., de Boer, A., Kramer, M., Figdor, C. G., Punt, C. J., Adema, G. J., and de Vries, I. J. Maturation of monocyte-derived dendritic cells with Toll-like receptor 3 and 7/8 ligands combined with prostaglandin E2 results in high interleukin-12 production and cell migration. Cancer Immunol.Immunother., -In press, 2008.

Targeting of ^{111}In-labeled dendritic cell human vaccines improved by reducing number of cells

Aarntzen EH*

Srinivas M*

Bonetto F

RicondoCruz LJ

Verdijk P

Schreibelt G

Van de Rakt MM

Lesterhuis WJ

Van Riel M

Punt CJ

Adema GJ

Heerschap A

Figdor CG

Oyen WJ

De Vries IJ

* contributed equally

Submitted

Abstract

Anti-cancer dendritic cell (DC) vaccines require the DC to relocate to lymph nodes (LN) to trigger immune responses. However, these migration rates are typically very poor. Improving the targeting of *ex vivo* generated DC to LN might increase vaccine efficacy and reduce costs. We investigated DC migration *in vivo* in humans in different conditions. HLA-A*02:01 melanoma patients were vaccinated with mature DC loaded with tyrosinase and gp100 peptides together with keyhole limpet hemocyanin (KLH) (NCT00243594). For this study, patients received an additional intradermal (i.d.) vaccination with ^{111}In-labeled mature DC. The injection site was pretreated with nonloaded, activated DC, TNFα or Imiquimod; GM-CSF was co-injected or smaller numbers of DC were injected. Migration was measured by scintigraphy and compared to an intra-patient control vaccination. In an *ex vivo* tissue model, we measured CCL21-directed migration of ^{19}F-labeled DC over a period of up to 12 hours using ^{19}F MRI to supplement our patient data. Pretreatment of the injection site induced local inflammatory reactions but did not improve migration rates. Both *in vitro* and *in vivo*, reduction of cell numbers to 5×10^6 or less cells per injection improved migration. Furthermore, scintigraphy is insufficient to study migration of such small numbers of ^{111}In-labeled DC *in vivo*.

Reduction of cell density, not pretreatment of the injection site, is crucial for improved migration of DC to lymph nodes *in vivo*.

Introduction

Cellular therapy in cancer patients aims to activate the immune system in a highly specific response against the tumor. In most studies, autologous antigen-presenting cells, principally dendritic cells (DC), are activated and loaded with tumor antigen *ex vivo* (1). To trigger an effective immune response, the DC need to relocate to immune reactive sites, such as lymph nodes (LN) upon injection back into the patient. Different routes are used to administer the DC to the patients, of which intradermal (i.d.) injection is the most frequently used (2). The biodistribution of DC after vaccination has been studied in humans, primarily using ^{111}In or ^{99m}Tc-labeled DC and scintigraphy (2). However, even though about 20 clinical trials have been carried out with DC delivered intradermally, the number of cells that reach a LN has never reproducibly exceeded 4% of the total cells injected (2). Why migration of mature DC from the vaccination site is so poor is still unknown. Several reasons have been suggested, for example the lack of an inflammatory microenvironment which would promote emigration of immune cells to afferent lymphatic vessels. In a mouse model, the migration of bone marrow derived DC into the draining lymph node could be dramatically increased by pretreating the injection site (3, 4). Prior to the vaccination the skin was injected with either an extra dose of DC, pro-inflammatory cytokines (TNFα or IL-1α) or Toll-like receptor ligands before injection of the vaccine-DC. This pretreatment of the skin resulted in a five to ten-fold increase in the number of DC in the draining lymph node that correlated with a similar increase in T cell activation. Other parameters of DC delivery might also contribute to more efficient emigration of DC from the skin to the draining LN, e.g. the frequency of delivery, the infrastructure in terms of vascular and lymphatic networks at site of transplant and the local availability of oxygen and nutrients (5-7).Thus conditioning the injection site, and perhaps indirectly the draining lymph nodes, may stimulate the emigration of DC from the skin and directly improve the clinical efficacy of DC-based therapy. Given this multitude of parameters, *in vitro* cell migration assays are warranted, as they allow high-throughput screening of influences of single parameters or combinations of parameters. The common *in vitro* cell migration assays that do exist, such as those based on microscopy or plate-based migration assays, have some major drawbacks: these techniques typically only work with small numbers of cells or non-opaque samples and thus do not replicate clinical conditions. Furthermore, most techniques assess migration in two-dimensional setting, whereas *in vivo* migration requires motility in 3D. Thus, studying cell migration in a sensitive and quantitative manner for clinical application is extremely challenging, and not readily feasible with current technology (2).

In this study, we investigated DC migration *in vivo* in humans after pretreatment of the injection site, using nonloaded but activated DC, TNFα or Imiquimod (a synthetic TLR7/8 ligand), to induce a local inflammatory microenvironment; or co-injection with GM-CSF to enhance DC survival. We tracked ^{111}In-labeled vaccine-DC over a period of 48 hours by planar scintigraphy and compared migration to the LN to a standardized control vaccination in the same patient. Furthermore, we modified an *in vitro* assay that closely reflects *in vivo* vaccination conditions to measure human DC migration in a standardized manner in tissue samples (8). By using this model, we measured CCL21 directed migration of ^{19}F-labeled vaccine-DC over a period of up to 12 hours using ^{19}F MRI. We show that reduction of cell density, not pretreatment, at the injection site is crucial for improved DC migration *in vivo*. In particular, we found that cell numbers greater than 1 million reduced migration both *in vitro* and *in* vivo. However, current clinical imaging modalities for clinical *in vivo* tracking of DC are insufficient to study migration of reduced numbers of DC in human studies.

Materials and Methods

DC vaccination in melanoma patients

In this study, stage III and IV melanoma patients (according to American Joint Committee on Cancer criteria) who were scheduled for regional lymph node dissection with either curative or palliative intention were included. Additional inclusion criteria included HLA*A02:01 phenotype, melanoma expressing the melanoma-associated antigens gp100 and tyrosinase, and WHO performance status 0 or 1. Patients with brain metastases, serious concomitant disease, or a history of a second malignancy were excluded (see Supplementary Table 1 for details). The study was approved by the Regional Review Board, and written informed consent was obtained from all patients. Clinical trial registration number is NCT00243594.

Patients received a DC vaccine via intradermal or intranodal injection, either with or without systemically administered IL-2. Intranodal vaccination was conducted in a clinically tumor-free lymph node under ultrasound guidance. Intradermal vaccination was conducted at 5 to 10 cm distal from a (preferably inguinal) clinically tumor-free lymph node, by clinicians with extensive experience with the procedure (W.J. Lesterhuis, E.H.J.G. Aarntzen, C.J.A. Punt). Because the first vaccination was administered 1-2 day before regional lymph node dissection, presumably a significant benefit to the patient could not be expected. For this reason, the first vaccination always consisted of an injection of ^{111}In-labeled, but not peptide-pulsed and not keyhole limpet hemocyanin (KLH)-loaded DCs on the side of the lymph node dissection, and an injection of peptide-pulsed DCs on the contralateral side. The latter vaccine could be ^{111}In-labeled or not. The DC vaccine consisted of autologous mature DCs pulsed with gp100 and tyrosinase peptides and KLH. Patients received 1 cycle consisting of 4 DC vaccinations administered at a biweekly interval. IL-2 was administered by subcutaneous injections (at 9 MIU) once daily for 1 week starting 3 days after each DC vaccination. Twenty-four to 48 hours after the first vaccination, a radical lymph node dissection was conducted. One to 2 weeks after the fourth vaccination, a DTH test was conducted (9). All patients who remained free of disease progression after the first vaccination cycle were eligible for 2 maintenance cycles, each at 6-month intervals and each consisting of 3 biweekly intranodal vaccinations without IL-2. Patients were considered evaluable when they had completed the first vaccination cycle. Vaccine-specific immune response was the primary endpoint, as reported in previous publication (10).

DC preparation and characterization

KLH-loaded DCs were generated from peripheral blood mononuclear cells (PBMC) and matured with autologous monocyte-conditioned medium containing prostaglandin E2 (10 mg/mL; Pharmacia & Upjohn) and recombinant TNFα (10 ng/mL; provided by Dr. G. Adolf, Bender Wien GmbH), as described (29, 30). This procedure gave rise to mature DCs meeting the release criteria (29) and detailed vaccine phenotype is reported in previous publication (10).

Peptide pulsing

DCs were pulsed with the HLA class I gp100-derived peptides gp100:154–162 and gp100:280–288 and the tyrosinase-derived peptide tyrosinase: 369–377 (31–33). Peptide pulsing was conducted as described (13), and cells were resuspended in 0.1 mL for injection.

^{111}In-labeling and scintigraphy

For ^{111}In labeling, ^{111}In-oxine (Covidien, Petten, The Netherlands) in 0.1 M Tris-HCl (pH 7.0) was added to mature DC for 15 min at room temperature as described previously (11). This results in 5 μCi per 15×10^6 cells. Cells were washed three times with PBS. Radiolabeling efficiency was determined by measuring activity in both the cell pellet and the washing buffer.

For this study, patients received an extra injection prior to scheduled RLND as mentioned above, or during the course of vaccination with increasing numbers of DC resuspended in 100 μl of injection

liquid and distributed over one or multiple injection sites, as indicated. At 24 hours and 48 hours post-injection, migration of DC was imaged by planar scintigraphy (256 × 256 matrix, 174 and 247 keV ^{111}In photopeaks with 15% energy window) of the injection depot and corresponding LN basin with a gamma camera (Siemens ECAM, Hoffman Estates, Ill) equipped with medium energy collimators). Migration was quantified by region of interest (ROI) analysis of the individual nodes visualized on the images and expressed as the relative fraction of ^{111}In-labeled DC that had migrated from the injection depot to draining LN.

^{19}F-labeling and MR imaging in vitro

For ^{19}F labeling, the label particles were prepared using perfluoro-[15]-crown-5 ether ($C_{10}F_{20}O_5$) (Exfluor Research Corp., Round Rock, TX, USA) and PLGA (Resomer RG 502 H, lactide: glycolide molar ratio 48:52 to 52:48; Boehringer Ingelheim, Ingelheim am Rhein, Germany) as described (12). 10 mg per 10^6 cells of particles was added to the DC culture at day 3. Upon harvesting (day 8), cells were washed three times in PBS to remove excess particles.

For the migration assay, the technique was adapted from (8) to replace the gel scaffold with a tissue sample, in this case bovine muscle. DC were injected as a bolus in the center of a 2 ml Eppendorf tube filled with a single piece of tissue, leaving about 1cm above the tissue as space for medium (see Figure 3a). The region below the cells formed the control layer to account for nonspecific motion, and the region above was the migration region through the use of a chemokine gradient consiting of 0.2μg recombinant human CCL21 (R&D Systems, Minneapolis, MN, USA).

^{1}H and ^{19}F images were acquired on a 7T horizontal bore MR-system with a ^{1}H/^{19}F volume coil. ^{1}H 2D spin echo images were taken for localization and nine ^{19}F chemical shift spectroscopic imaging (CSI) was done every hour for up to 9 hours, to measure cell migration. Proton images were acquired with TR/TE=1000/22 ms and 0.125×0.125×1 mm^3 resolution. A 0.94×0.94×10 mm^3 matrix size with TR/TE=400/2.94ms was used for CSI. The sample was sealed and not moved for the duration of the imaging experiment. Temperature was maintained at 37 ^{o}C using regulated warm air flows.

Histology

Sections (5 μm) of the resected skin from the injection sites were stained with hematoxilin. The staining protocol was done as in (13). Similar sections were cut from the tissue used for the *ex vivo* migration assay. These were stained with hematoxilin and an antibody against carbonic anhydrase 9(CAIX; Novus Biologicals)..

Statistical analyses

All comparisons were performed using a two-tailed unpaired t-test with the intradermal migration after 48 hours without pretreatment as comparator.

Results

DC migration to LN is poor after intradermal vaccination

In current and previous studies (10, 14), migration of DC to skin-draining lymph nodes after i.d. injection (n=18) was monitored by labeling the DC vaccine with ^{111}In and subsequent scintigraphy of injected region (14, 15). Figure 1A shows the percentage of migrating DC after i.d. injection of 15×10^6 DC at 24 or 48 hrs post-injection. The average migration achieved was 1.2% after 24 hours and 1.4% after 48 hrs, indicating that most of the migration occurred within 24 hrs after injection. Migration rates never exceeded 4% of the total cells injected. Figure 1B shows representative scintigraphs, with the arrow indicating a pretreated site.

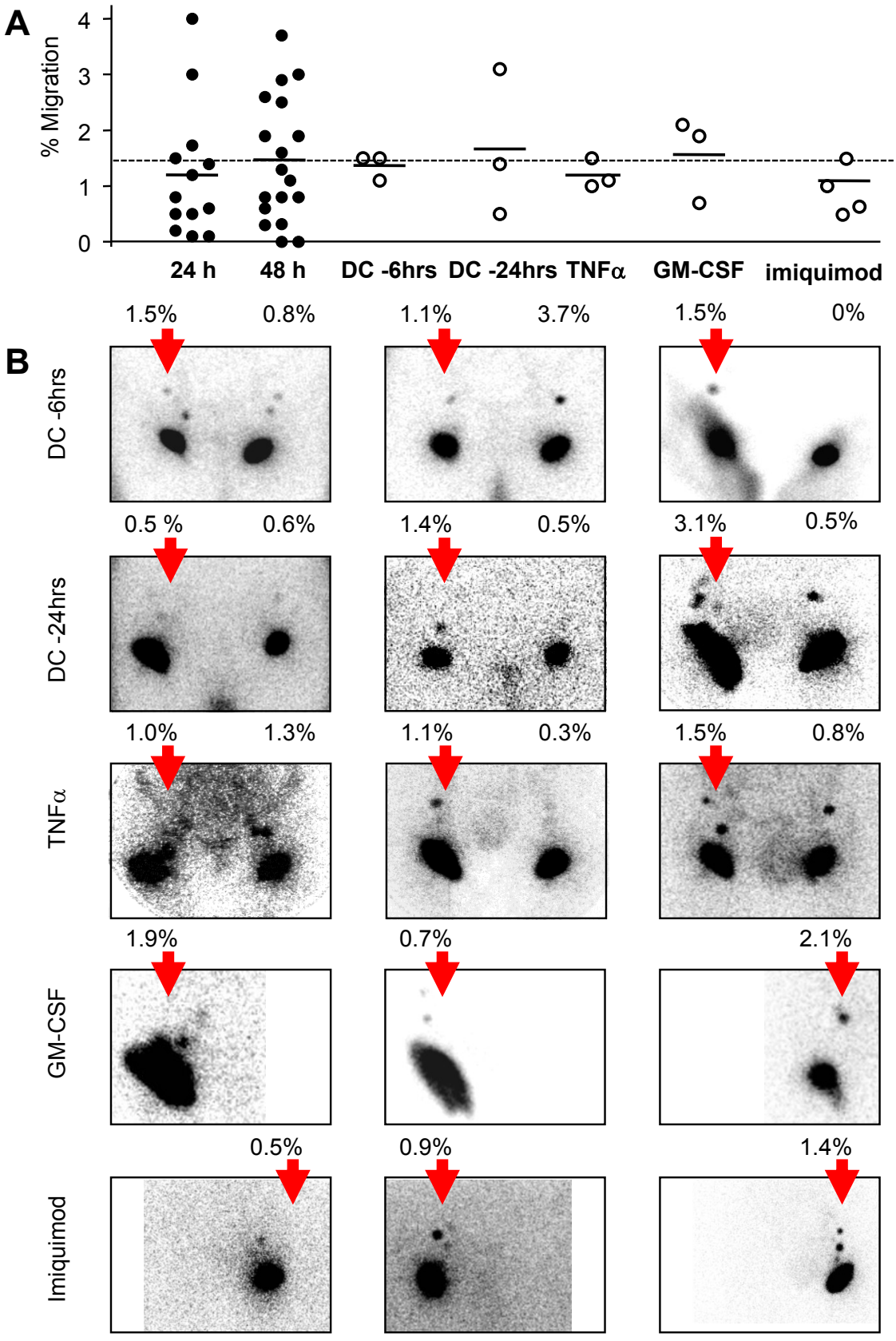

Figure 1. Pretreatment of the skin does not improve DC migration. Migration of DC to skin-draining lymph nodes (n=18) was monitored after intradermal injection with 15×10^6 ^{111}In-labeled DC vaccine and planar scintigraphy of injected region. (A) The percentage of migrating DC at 24 or 48 hrs post-injection, or after different pretreatments, never exceeded 4% of the total cells injected. Statistical analyses using a two-tailed unpaired t-test showed no significant differences between the experimental conditions or migration at 48 hours after intradermal migration without pretreatment. (B) For each pretreatment condition, TNFα(n=3), GM-CSF (n=3), Imiquimod (n=4) or unloaded but activated DC 6 hours (n=3) or 24 hours (n=3) prior to vaccination, the individual images are shown. Upon GM-CSF addition, the induration and migration at the site of injection was markedly larger than after injection of DC alone, suggesting random migration into surrounding dermis. Red arrows indicate the pretreated site.

The induction of local inflammation of does not improve DC migration

Based on data from mice studies (3, 4), we investigated whether pretreatment of the injection site to create a local inflammatory microenvironment, optimized DC migration. To this end, we pretreated the injection sites with TNFα(n=3), imiquimod (n=4) or unloaded but activated DC 6 hours (n=3) or 24 hours (n=3) prior to vaccination (Figure 1A,B). In patients pretreated with TNFα or activated DC, the contralateral administration of 15×10^6 ^{111}In-labelled vaccine-DC served as intra-patient control. Although the migration from the pretreated site was higher than in the control site in the majority of those patients, it still did not exceeded 4% and did not significantly increase migration compared to unconditioned sites. Our previous studies have shown that vaccine-DC rapidly lose viability at the injection site after intranodal or intradermal delivery, which might contribute to defective migration to LN (15). Addition of GM-CSF as an adjuvant during DC vaccination might increase the survival of DC and thereby increase migration rates. Three patients were injected with 15×10^6 DC in normal saline containing 14×10^4 IU GM-SCF. Although the percentage of migrating cells after 48hours was higher than average in 2 of 3 patients, migration was still within the established range. Of note, the induration at the site of injection was markedly larger than after injection of DC alone, suggesting random migration into surrounding dermis. Lastly, we pretreated the injection site of 4 patients by imiquimod application every 12 hours for 2 days prior to vaccination. Again, no significant changes in migration rates were documented. Overall, the effects of pretreatment were limited and did not significantly improve subsequent migration of vaccine-DC to the draining LN.

Local cell density is limiting factor

We performed histological analysis of the pretreatment injection sites 48 hours post-injection in order to validate our imaging findings. Injection of DC consistently induced local inflammation, demonstrated by infiltrates of leukocytes around vessels in the dermis, mainly neutrophils and eosinophils. The number of lymphocytes in the dermis increased, compared to normal skin. Pretreatment of the injection site with either TNFα (Figure 2A,B) or unloaded DC (Figure 2C); or co-injection with GM-CSF (Figure 2D) induced some inflammation, as evidenced by the infiltration of leukocytes. However, this did not affect DC emigration.

Histology showed that macrophages had infiltrated the dermis and subcutis around the injection site. In areas with SPIO+ cells were enlarged and exhibited pale pink nuclei, typical for necrotic cells. Thus, the histological evidence shows that DCs die at the site of injection and invariably induce an inflammatory response consisting of macrophages and neutrophils. As no apparent differences were noted after different pretreatment regimens, together with the notion that dying vaccine-DC were found at higher rates with larger numbers of injected cells; these data suggests that it must be the local cell density itself that hampers efficient emigration of the injection site.

An in vitro assay to study migration of small numbers of DC

To test this hypothesis, we adapted a novel assay we developed to mimic clinical vaccine conditions and which allows reliable quantification of reduced numbers of cells (8). The assay was modified to use a tissue sample instead of a gel scaffold, as done previously. DCs were cultured as used in patient vaccinations, with the addition of a labeling step for ^{19}F detection. This labeling has previously been shown to have no effect on the DCs, including their migration (8), (Figure 3A). The grid overlay shows the voxels used in the ^{19}F CSI scans. Imaging was carried out at hourly intervals without moving the sample, and the temperature was regulated. A control area under the cell injection was used to measure passive cell movement due to gravity. CCL21 was used to create a chemokine gradient for active CCR7-mediated migration. The percentage of total cells that migrated was calculated to represent the migratory cells. Figure 3B shows representative cell numbers at 1, 5 and 9 hours after injection of 5×10^6 DCs. The migratory and control regions are highlighted.

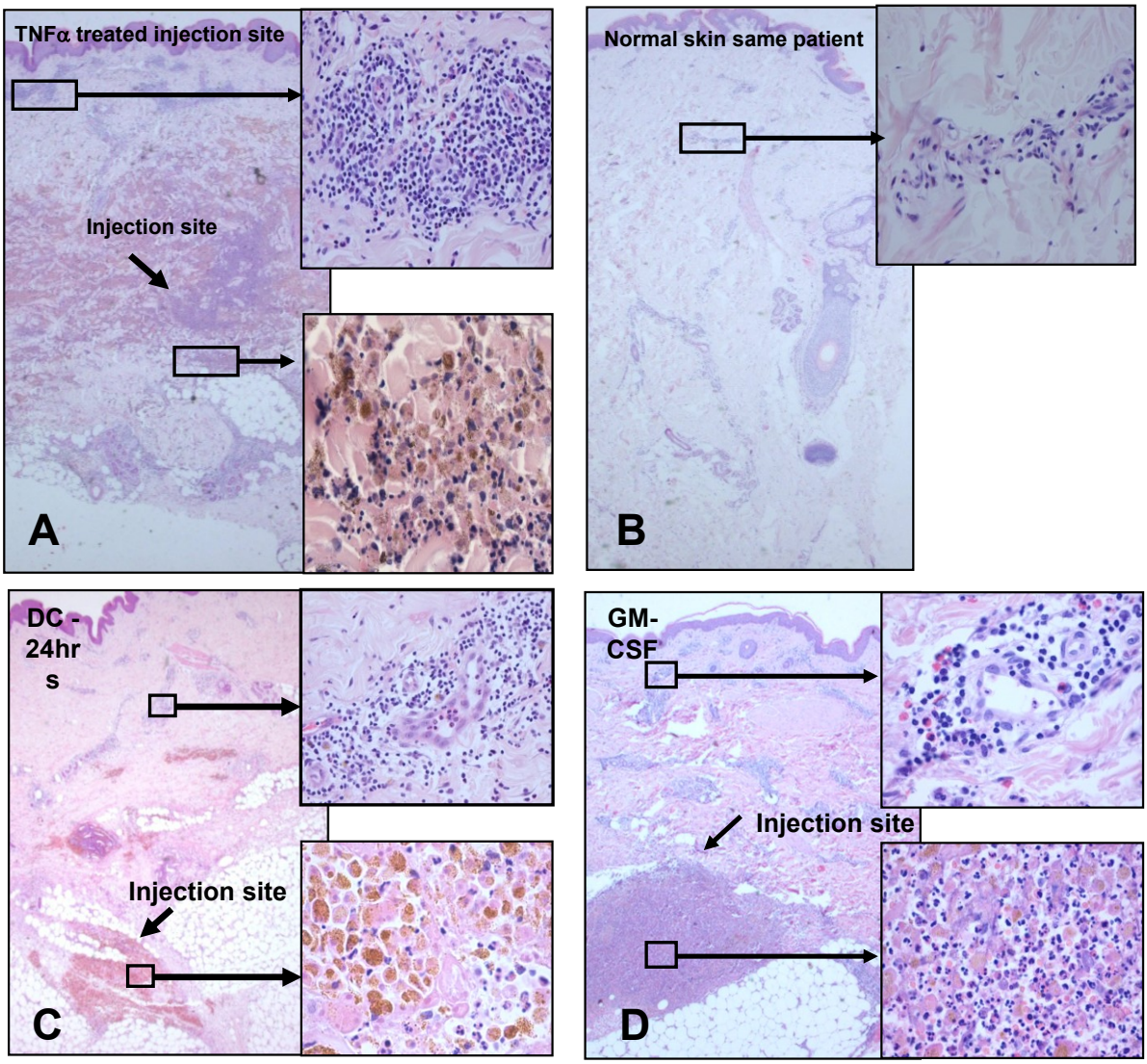

Figure 2. Immunohistochemical analyses of the injection site. We performed histological analysis of the pretreatment injection sites 48 hours post-injection in order to validate our imaging findings. (A-C) Pretreatment of the injection site with TNFα, GM-CSF or unloaded DC, consistently induced local inflammation, demonstrated by infiltrates of leukocytes around vessels in the dermis, mainly neutrophils and eosinophils. Within areas with high cell density, especially at the injection sites, there is a high proportion of dying cells, including vaccine-DC. (D) Normal skin from patient in Figure 2C, for comparison.

Reducing the cell density improves migration rates

The following figure (Figure 4A) shows the migration over time for 5×10^6 DCs, for the migratory region (red) and the control region under the cell layer (blue). These data show that clear migration which is absent in the control region. The overall numbers of cells that migrated were 3×10^4 and 4.5×10^5 with 5×10^5 and 5×10^6 cells, respectively, demonstrating the sensitivity of this assay. Figure 4B summarizes the results of three individual experiments with varying cell numbers in the gel scaffold. The data indicate that indeed increasing cell number suppresses migration. Thus, the percent of migratory cells is nearly 3% with 0.5 $x10^6$ and 0% with 15 $x10^6$ DC. Finally, histological analyses on the tissue samples, taken over and around the injection site, were analysed (Figure 4C). Extensive hypoxia was observed at the injection site (CAIX stain (brown); top panel). Furthermore, at the lower cells numbers, we observed trains of migratory cells (lower panels). These trains appear to be migrating along the muscle tissue, and were completely absent with samples with 15 and 10 x 10^6 million DCs.

Planar scintigraphy not sufficient for imaging of low numbers of injected cells in vivo

Finally, we compared the migration data obtained *in vitro* using our ^{19}F MRI assay with the clinical data obtained using scintigraphy on ^{111}In-labeled DCs (Figure 5a). Due to the difficulties of testing different conditions in patients, our clinical data only reflects migration with 10^5 and 10^6cells per injection. Five injections of 1×10^6 or 5 injections of 1×10^5 cells were injected intradermally, at different sites 1 centimeter apart. The average percentage of migratory cells was significantly increased to 5×10^6 cells compared to 1 injection with 15×10^6 cells; 1.9% ($p<0.05$), but not with 5×10^5 cells; 0.5% (not significant) respectively. Thus, lowering the number of cells to 10^6 cells per injection improved migration by about 1.5-fold, in terms of percentage, relative to a single bolus injection of 15×10^6 DC. So, trend in percentage of migratory cells is comparable with our *in vitro* data for 5 and 10×10^6 cells, respectively. The percentage of migratory DC in patients would be expected to be highest with 0.5×10^6 cells, as predicted by the *in vitro* results. However, this apparent discordance is due to the sensitivity limits of scintigraphy (16), where the smaller numbers of migratory cells were probably simply not detected due to sensitivity issues.

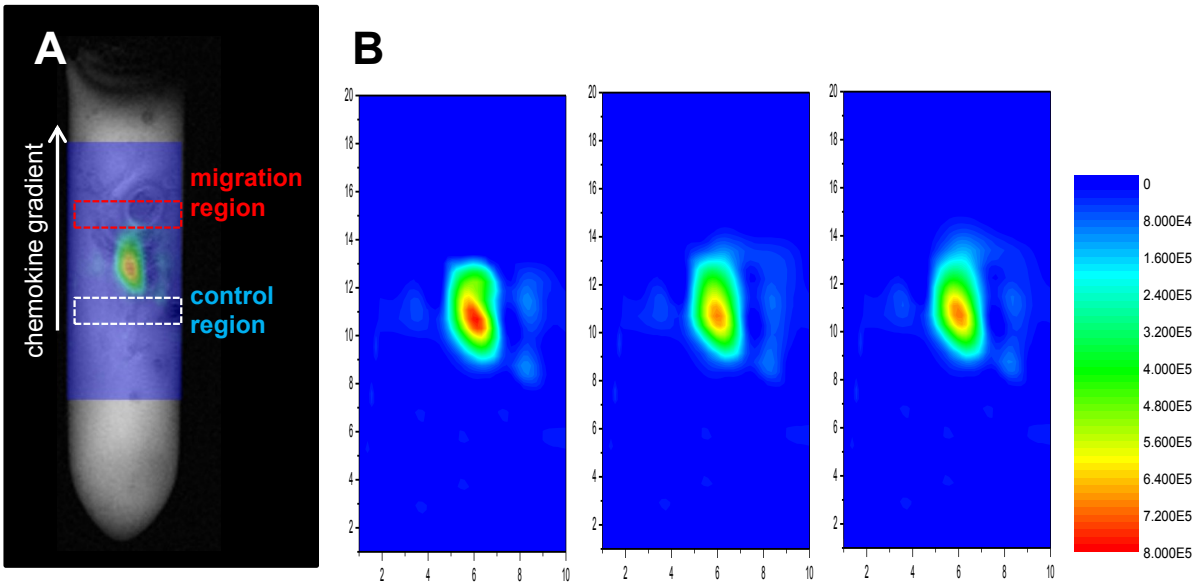

Figure 3. In vitro model to study migration of small numbers of cells. (A) Cell bolus position within the sample. Overlay of a ^{1}H MRI image and ^{19}F CSI cell map showing the position and the density of the cell bolus injection in the tissue sample. The *migration region* is vertically above the cell pellet and the *control region* below. (B) The panels show representative data obtained at 1, 5 and 9 hrs after injection of 5×10^6 DCs. The scale bar represents the number of cells.

Discussion

The interest in cellular therapy is increasing at fast pace, in particular research towards harnessing immune cells for anti-cancer therapy, which has been revived by recent key developments (17, 18). Owing to their unique immune stimulating properties, DCs have been the "hot" target for anti-cancer immunotherapy in the past decades. Endowed with knowledge of the crucial steps which underlie successful induction of tumor specific immune responses, various vaccination parameters have been optimized in previous studies (19). At this point, the paradigm shifts from small proof-of-principle studies to large randomized controlled trials. Accordingly, attention should be paid to the feasibility of cellular therapy at large scale. Intradermal injection of DC for immunotherapy is generally the easiest approach and therefore preferred in most clinical trials involving DC-based therapy (2). Unfortunately only limited numbers of DC will reach the draining lymph nodes. Improving the efficiency of DC migration might therefore increase the immunological response (20) and reduce costs while potentially improving patient response. In mice, immune responses were dose dependent (3, 21) and could be increased by conditioning of the injection site. We show here that migration rates of human monocyte-derived DC after intradermal injection in melanoma patients

could not be increased by pretreatment to induce a pro-inflammatory microenvironment at the injection site. Instead, by using a novel model, we demonstrate *in vitro* and *in vivo* that a reduction of cell numbers at the injection site is key to improved migration.

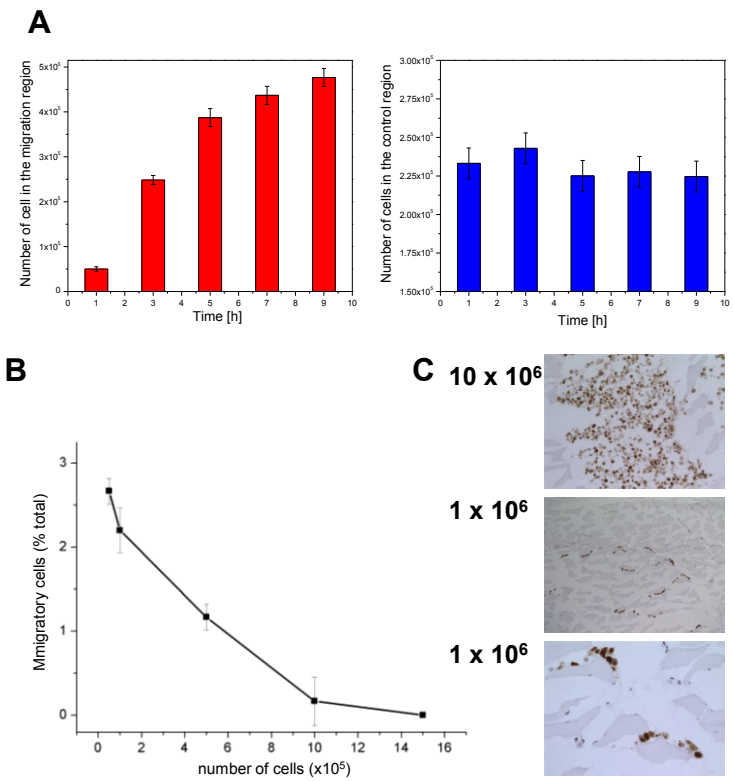

*Figure 4. Reducing the cell density improves migration rates in vitro.*The change in time in the cell numbers within the migration and the control regions are plotted for 5×10^6 DCs (n=3). (A) A clear trend is observed for the cell number time dependence in the migration region (left, in red); improved migration is observed for 5×10^6 and 1×10^6 cells. No pattern is observed for the control region (right, in blue). (B) Summary of three individual experiments with varying cell numbers in the tissue assay. The data indicate that increasing cell number suppresses migration. Thus, the percent of migratory cells is nearly 3% 0.5×10^6 and 0% with 15×10^6 DCs. (C) Sections from the tissue used for the migration assay were cut and stained for hypoxia (brown); cell nuclei are purple. Note that nuclei are sparse in the surrounding muscle tissue. Representative images are shown for 10×10^6 DC (top; low magnification), and 1×10^6 DC (low and high magnification respectively). Migratory cells are evident in the lower panels.

A number of factors might explain the discrepancy between our negative results and the positive effects of pretreatment of the injection site on migration in mice skin. First, closer analysis of the results in mouse models by Martin-Fontecha *et al*. revealed that migration rates were indeed dramatically increased by conditioning but even in their experiments never exceeded approximately 2% (3). Conditioning of the skin was only effective in increasing the migration of suboptimal doses of DC from 0.01-0.1% to 1%. No increases in migration rates were observed when the migration rate of the untreated control was around 1-2%. Moreover, high doses of TNFα have been demonstrated, to the contrary, to inhibit migration from the skin (22). Thirdly, the timing of pretreatment is critical. Clinical studies show that intradermal administration of TNFα or IL1-β induced the emigration of resident Langerhans cells to draining lymph nodes. In this setting, application of those pro-inflammatory cytokines may act both directly on the DC and indirectly via the surrounding accessory cells. In our study, TNFα is injected to the skin 8 hours prior to DC vaccination and will therefore exert its effect on the microenvironment and not directly on the DC. Given the burden for patients in terms of injections and logistics, we chose not to titrate the dose and timing of TNFα to find the optimal. Moreover, Nair et al demonstrated that by conditioning the skin with the TLR-ligand Imiquimod, the migration of *immature* DC could be stimulated (21). However, even in this trial no improvement in migration rate was achieved as the injected DC had a mature, and thus highly migratory, phenotype. Finally, note that while several factors contribute to the migration of DC, these can be very difficult to study individually and even more so when considering the costs and logistics of a clinical study. Hence, such factors may best be studied *in vitro* before final optimization *in vivo*.

The use of ^{19}F MRI for quantitative cell tracking is a relatively new technique (12). Here we applied this technology to track migratory DC over 10 hours, in order to optimize the cell numbers used in DC vaccinations in the clinic. This technique allows us to use a wide range of cell numbers, up to the

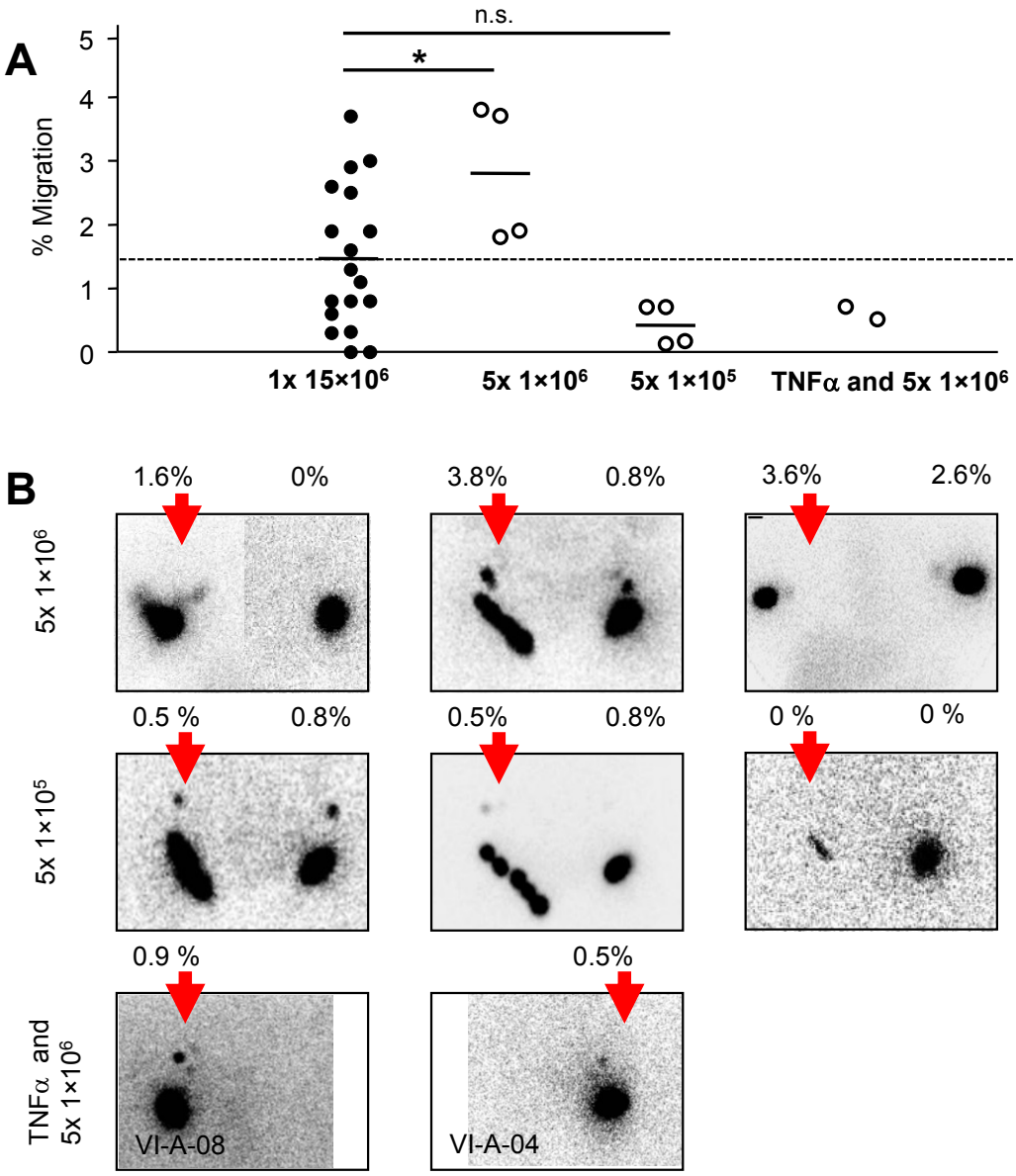

*Figure 5. Reducing the cell density improves migration rates in vivo.*Migration of DC to skin-draining lymph nodes was monitored after intradermal injection with reduced numbers of ^{111}In-labeled DC vaccine and planar scintigraphy of injected region. (A) The percentage of migration with 15×10^6 DC at 48 hrs post-injection (as a reference), 5×10^6 (n=4), 5×10^5 DC (n=4) or TNFα pretreatment together with 5×10^6 cells (n=2). The mean percentage of migration with 5×10^6 DC was 2.6%, significantly higher than 15×10^6 DC (p=0.0496, unpaired two-tailed t-test), whereas further reduction of cell number or pretreatment with TNFα combined with reduced cell number, did not significantly improve migration rates (n.s. denotes not significant). (B) For each condition with reduced number of cells, the individual images are shown. Red arrows indicate the experimental site.

millions of cells that are typical for current DC vaccination and to use opaque samples, such as tissue. Other migration assays require either small cell numbers or transparent samples (23). The ^{19}F particles used to label the DC are not toxic to the cells and do not affect their migration, when compared to unlabeled cells (24). The expression of typical cell surface markers, used in chemotaxis and migration, is also unaffected. Although ^{19}F MRI has not currently been applied to clinical cell tracking, the technique will be available for the clinic in the near future. The label we used here can also be adapted for clinical use. Furthermore, the assay conditions can easily be modified to include different cytokines or combinations of cytokines to study their effect on migration. Different cell types can also be used, as long as the cells can be labeled with a ^{19}F agent. Some ^{19}F labels may also be sensitive to oxygen partial pressures, and thus these can be measured during the experiments to indicate hypoxic regions. In this paper, we used bovine tissue instead of human tissue to avoid differences due to mismatched immune cells and the inflammatory condition of the tissue. However,

Supplementary Table 1. Patient characteristics

study code	sex	age	Primary tumor Breslow thickness (mm)	ulceration	Clark level	histological type	origin	N stage	AJCC stage	Site	M stage	prior therapy
II-A-11	m	64	1,25	no	4	SSM	skin	N1a	3	inguinal	M0	
II-C-03	m	60	9	yes	3	NM	skin	N1b	3	axilla	M0	
II-C-14	f	65	n.a.	n.a.	n.a.	n.a.	skin	N1b	3	inguinal	M0	
II-D-01	m	51	1,2	n.a.	n.a.	n.a.	skin	N1a	3	inguinal	M0	
II-D-02	f	58	2,5	no	3	NM	skin	N1a	3	inguinal	M0	
II-D-03	m	65	2,5	yes	4	SSM	skin	N1a	3	inguinal	M0	
II-D-04	f	53	0,73	no	4	SSM	skin	Nx	3	inguinal	M0	
II-D-05	m	58	4,5	yes	4	NM	skin	N1b	3	inguinal	M0	
II-D-06	m	58	2,55	no	4	SSM	skin	Nx	3	inguinal	M0	
II-D-08	f	50	4,5	yes	5	SSM	skin	Nx	3	head/neck	M0	
II-D-09	f	39	1,1	no	3	SSM	skin	N2a	3	axilla	M0	
II-D-10	m	51	10	yes	5	SSM	skin	N3	3	axilla	M0	
II-D-11	f	37	6	yes	4	NM	skin	N3	3	inguinal	M0	
II-D-12	m	48	8	yes	4	NM	skin	Nx	3	axilla	M0	
II-E-03	m	45	5,8	no	4	SSM	skin	N1a	3	axilla	M0	
II-E-04	m	42	3,6	no	4	NM	skin	N2a	3	axilla	M0	
II-E-06	m	49	3,2	n.a.	n.a.	SSM	skin	N2a	3	axilla + inguinal	M0	
II-E-07	f	60	1,11	no	3	SSM	skin	Nx	3	axilla	M0	
IV-B-11	m	66	n.a.	n.a.	n.a.	n.a.	uveal	Nx	4	liver, lung, distant lymph nodes	M1c	DTIC, RTx
IV-C-04	m	45	2,8	n.a.	4	n.a.	skin	Nx	3	head/neck	M0	
IV-C-10	f	36	1,6	no	4	SSM	skin	N1a	3	axilla	M0	
IV-D-09	m	51	1,4	no	4	SSM	skin	Nx	4	axilla or distant lymph nodes	M1a	no
IV-D-11	m	45	n.a.	n.a.	n.a.	n.a.	mucosal	N3	4	head/neck	M0	
VI-A-04	f	67	1,6	n.a.	4	SSM	skin	Nx	4	distant lymph nodes	M1a	no
VI-A-08	m	66	2,4	yes	n.a.	NM	skin	N0	4	liver, lung, distant lymph nodes	M1c	no

n.a., not available; SSM, superficial spreading melanoma; NM, nodular melanoma; DTIC, Dacarbazine; RTx, irradiation

the assay can readily be adapted to use other tissue types. Here we used CCL21 to provide a chemotactic gradient for DC migration. CCL21 is known to induce the active migration of DCs towards lymphatic vessels *in vivo* (25).

One of the main issues with ^{19}F MRI is its sensitivity in terms of detectable cells/voxel/unit imaging time. Under our conditions, we found the sensitivity to be higher than that of clinical scintigraphy (Figure 5A); the sensitivity in our set-up allows the detection of as little as 5000 cells/voxel, compared to 2×10^4 with scintigraphy (16). This is 4-fold higher than the sensitivity of scintigraphy *in vivo.* Note that the MRI was carried out on a clinical scanner using sequences that can be applied to humans; using a higher field research magnet and faster imaging sequences would improve sensitivity further. In our experiments, we chose to measure only migration in the vertical plane (i.e. along the chemokine gradient), as we felt this was the most relevant direction. However, it would certainly be feasible to measure migration in both planes or even in 3D in this setup. Furthermore, the relatively poor sensitivity of scintigraphy might be one reason why smaller numbers of migratory cells are not detected, and thus the percentage of migratory cells calculated is artificially low, especially when smaller cell numbers were injected initially. Although the spatial resolution has improved with more recent nuclear imaging modalities (SPECT, SPECT/CT) it is still far behind on MRI especially in soft tissues like lymph nodes. We previously demonstrated examination of intra-lymph node distribution of labeled DC at 7 Tesla MRI (16).

The high density of cells at the injection site may prevent the access to sufficient oxygen and nutrients, and may therefore hamper cell movement and active migration. Indeed, hypoxia is evident at the injection site (Figure 4C). Hypoxia suppresses the production of matrix metallo-proteinasesand the migration of human monocyte derived-DC (3). After injection of a cell suspension in the dermis, the fluid will be readily drained into the afferent lymphatic vessels, due to elasticity of the skin. The cells however, will be caught in the extracellular matrix and will be packed together, devoid of nutrients and oxygen. The cells on the border of the injection depot may have the opportunity to move away from the depot.

The optimal numbers of DC per LN for adequate immune induction in clinical studies has not been established. Some studies report a dose-dependent relation with immune responses in human (26, 27). Given the high immune stimulating potential of DC *in vitro*, it may not be surprising that even small numbers of DC, as in clinical studies, are sufficient. Indeed, we have shown previously that even small numbers of DC are capable of effective interacting with T cells (10, 15). Hypothetically, the unfavorable conditions at the site of delivery may select the most fit DC with high stimulatory potency, or simply those at the periphery of the bolus, which are then able to migrate to the LN and adequately induce immune responses. Combining this information with the current data, we suggest that multiple intradermal injections with small numbers of cells to target multiple lymph node basins would increase DC migration to LN, for example using a 'tattoo' delivery device (28). In particular, cells that appear to be actively migratory were only evident with the lower cell numbers (Figure 4C). It is possible that DC aggregation or chemotaxis could also be involved in reducing emigration with larger cell numbers, although these factors were not studied here.

In conclusion, we have shown that pretreatment of the skin to create an inflammatory microenvironment at the injection site does not improve DC migration to LN after i.d. delivery. To the contrary, we demonstrate that reduction of cell density at the injection site is key to improved DC migration, both *in vitro* and *in vivo*. Since current imaging modalities for clinical *in vivo* tracking of DC are not sensitive enough to study migration of small numbers of DC, the *in vitro* model developed here facilitates further studies for improving migration rates.

References

1. Palucka K, Banchereau J. Cancer immunotherapy via dendritic cells. Nat Rev Cancer 2012; 12:265-77.
2. Srinivas M, Aarntzen EH, Bulte JW, et al. Imaging of cellular therapies. Adv Drug Deliv Rev 2010; 62:1080-93.
3. MartIn-Fontecha A, Sebastiani S, Hopken UE, et al. Regulation of dendritic cell migration to the draining lymph node: impact on T lymphocyte traffic and priming. J Exp Med 2003; 198:615-21.
4. Tripp CH, Ebner S, Ratzinger G, Romani N, Stoitzner P. Conditioning of the injection site with CpG enhances the migration of adoptively transferred dendritic cells and endogenous CD8+ T-cell responses. J Immunother 2010; 33:115-25.
5. Verdijk P, Aarntzen EH, Punt CJ, de Vries IJ, Figdor CG. Maximizing dendritic cell migration in cancer immunotherapy. Expert Opin Biol Ther 2008; 8:865-74.
6. Randolph GJ, Angeli V, Swartz MA. Dendritic-cell trafficking to lymph nodes through lymphatic vessels. Nat Rev Immunol 2005; 5:617-28.
7. Angeli V, Randolph GJ. Inflammation, lymphatic function, and dendritic cell migration. Lymphat Res Biol 2006; 4:217-28.
8. Bonetto F, Srinivas M, Weigelin B, et al. A large-scale (19) F MRI-based cell migration assay to optimize cell therapy. NMR Biomed 2012.
9. Aarntzen EH, Bol K, Schreibelt G, et al. Skin-test infiltrating lymphocytes early predict clinical outcome of dendritic cell based vaccination in metastatic melanoma. Cancer Res 2012.
10. Lesterhuis WJ, de Vries IJ, Schreibelt G, et al. Route of administration modulates the induction of dendritic cell vaccine-induced antigen-specific T cells in advanced melanoma patients. Clin Cancer Res 2011; 17:5725-35.
11. de Vries IJ, Lesterhuis WJ, Scharenborg NM, et al. Maturation of dendritic cells is a prerequisite for inducing immune responses in advanced melanoma patients. Clin Cancer Res 2003; 9:5091-100.
12. Srinivas M, Heerschap A, Ahrens ET, Figdor CG, de Vries IJ. (19)F MRI for quantitative in vivo cell tracking. Trends Biotechnol 2010; 28:363-70.
13. Aarntzen EH, Srinivas M, De Wilt JH, et al. Early identification of antigen-specific immune responses in vivo by [18F]-labeled 3'-fluoro-3'-deoxy-thymidine ([18F]FLT) PET imaging. Proc Natl Acad Sci U S A 2011; 108:18396-9.
14. De Vries IJ, Krooshoop DJ, Scharenborg NM, et al. Effective migration of antigen-pulsed dendritic cells to lymph nodes in melanoma patients is determined by their maturation state. Cancer Res 2003; 63:12-7.
15. Verdijk P, Aarntzen EH, Lesterhuis WJ, et al. Limited amounts of dendritic cells migrate into the T-cell area of lymph nodes but have high immune activating potential in melanoma patients. Clin Cancer Res 2009; 15:2531-40.
16. Verdijk P, Scheenen TW, Lesterhuis WJ, et al. Sensitivity of magnetic resonance imaging of dendritic cells for in vivo tracking of cellular cancer vaccines. Int J Cancer 2007; 120:978-84.
17. Mellman I, Nussenzweig M. Retrospective. Ralph M. Steinman (1943-2011). Science 2011; 334:466.
18. Kantoff PW, Higano CS, Shore ND, et al. Sipuleucel-T immunotherapy for castration-resistant prostate cancer. N Engl J Med; 363:411-22.
19. Figdor CG, de Vries IJ, Lesterhuis WJ, Melief CJ. Dendritic cell immunotherapy: mapping the way. Nat Med 2004; 10:475-80.
20. Celli S, Day M, Muller AJ, Molina-Paris C, Lythe G, Bousso P. How many dendritic cells are required to initiate a T cell response? Blood 2012.
21. Nair S, McLaughlin C, Weizer A, et al. Injection of immature dendritic cells into adjuvant-treated skin obviates the need for ex vivo maturation. J Immunol 2003; 171:6275-82.
22. Geissmann F, Dieu-Nosjean MC, Dezutter C, et al. Accumulation of immature Langerhans cells in human lymph nodes draining chronically inflamed skin. J Exp Med 2002; 196:417-30.
23. Toetsch S, Olwell P, Prina-Mello A, Volkov Y. The evolution of chemotaxis assays from static models to physiologically relevant platforms. Integr Biol (Camb) 2009; 1:170-81.
24. Srinivas M, Cruz LJ, Bonetto F, Heerschap A, Figdor CG, de Vries IJ. Customizable, multi-functional fluorocarbon nanoparticles for quantitative in vivo imaging using 19F MRI and optical imaging. Biomaterials 2010; 31:7070-7.
25. Tal O, Lim HY, Gurevich I, et al. DC mobilization from the skin requires docking to immobilized CCL21 on lymphatic endothelium and intralymphatic crawling. J Exp Med 2011; 208:2141-53.
26. Dillman RO, Fogel GB, Cornforth AN, Selvan SR, Schiltz PM, DePriest C. Features associated with survival in metastatic melanoma patients treated with patient-specific dendritic cell vaccines. Cancer Biother Radiopharm 2011; 26:407-15.
27. Engell-Noerregaard L, Hansen TH, Andersen MH, thor SP, Svane IM. Review of clinical studies on dendritic cell-based vaccination of patients with malignant melanoma: assessment of correlation between clinical response and vaccine parameters. Cancer Immunol Immunother 2008.
28. van den Berg JH, Nujien B, Beijnen JH, et al. Optimization of intradermal vaccination by DNA tattooing in human skin. Hum Gene Ther 2009; 20:181-9.

Part 3

Monitoring immune responses in DC-based vaccination studies

Chapter 8

Dendritic cell vaccination and immune monitoring

Aarntzen EH

Figdor CG

Adema GJ

Punt CJ

De Vries IJ

Cancer Immunol Immunother. 2008;57(10):1559-68.

Abstract

We exploited dendritic cells (DC) to vaccinate melanoma patients. We recently demonstrated a statistical significant correlation between favorable clinical outcome and the presence of vaccine-related tumor antigen specific T cells in delayed type hypersensitivity (DTH) skin biopsies. However, favorable clinical outcome is only observed in a minority of the treated patients. Therefore, it is obvious that current DC-based protocols need to be improved. For this reason, we study in small proof of principle trials the fate, interactions and effectiveness of the injected DC.

Antigen presenting dendritic cells

DC are the professional antigen presenting cells (APC) of the immune system that instruct and control the activation of B and T lymphocytes, the mediators of specific immunity (1). DC are highly mobile cells and by their sequential migration from peripheral tissues to lymphoid organs they serve as sentinels of the immune system. Immature DC are very efficient in antigen uptake, mediated by high endocytotic activity and expression of an array of cell surface receptors capable of capturing antigens (2, 3). Inflammatory mediators and 'danger signals' promote maturation and re-routing of DC to the secondary lymphoid organs (1, 4). In the secondary lymphoid tissues, DC are mature and well equipped to attract, interact and activate naive T cells to initiate a primary immune response (1, 5). DC are also able to directly activate NK cells (6) and can produce large amounts of interferon upon encounter with viral pathogens (7), thus providing a link between the adaptive and innate immune system. In murine tumor models protective immunity as well as regression of established tumors have been observed after vaccination with DC loaded with tumor antigens (8-10). Their unique capacity to initiate and modulate immune responses is currently exploited by many groups, including ours, to fight infectious diseases and cancer. One aspect of DC biology that is rapidly evolving is the apparent diversity of DC subsets (11). At least two distinct ontogenic pathways for DC development have been reported, the myeloid progenitor- and the lymphoid progenitor derived DC (12). Part of these different DC subsets may also be explained by differences in the maturation stage of DC and the local cytokine environment. The geographical localization of the DC-subsets in secondary lymphoid tissues is distinct, myeloid derived DC mainly migrate to or reside in the marginal zone (a primary entry point for blood-born antigens) whereas the lymphoid DC mainly reside in the T cell areas. This supports distinct functions for the DC-subsets, as been shown in murine studies (1, 12). It is now well appreciated that the DC subset, its maturation state and the microenvironment or type of pathogen a DC encounters in the periphery, determine the type of immune response that is induced, ranging from a TH1 or TH2 response to immune tolerance (12-14). Data are now accumulating that immature DC can induce tolerance and are able to induce regulatory T cells *in vitro* (15, 16) and *in vivo* (17). Regulatory T cells are involved in the control of peripheral tolerance (18) and the prevention of vigorous inflammatory reactions. These regulatory T cells affect immune responses at the level of antigen-presentation and during the effector phase of T cells at the site of the tumor. Although the exact mechanisms by which regulatory T cells exert their suppressive functions are not yet elucidated, direct cell-cell contact and cytokines like IL-10 and TGF have demonstrated to play a role. Our data on vaccination of melanoma patients also demonstrate that mature DC, but not immature DC, induce strong immune responses *in vivo* (19). Another aspect in the evolving field of immunotherapy is the re-acknowledgement of the role of the innate immune system. The eradication of a malignancy is the result of a concerted action of adaptive and innate immunity, in which natural killer (NK) cells and natural killer T (NKT) cells are important effector cells (20). Next to the direct cytotoxic effect on tumor cells, NK cells produce type I interferons that contribute to a great extent to a proinflammatory microenvironment. Clinical studies on adoptive NK-cell immunotherapy have shown that NK cells can target human tumors (21, 22).

DC-based cancer vaccines: current status

Over 60 different clinical studies have been carried out between 1996 and 2004, applying tumor antigen-loaded DC-based vaccines (23). The vast majority of these studies have been performed in melanoma patients (24, 25). In our studies, as well as in other groups, immunological and, notably long-lasting, clinical responses have consistently been observed following cellular therapy (24, 26, 27). In several patients these clinical responses coincide with the induction of specific cytotoxic T cell responses. We have explored vaccination of cancer patients with monocyte-derived DC loaded with peptides derived from tumor-associated antigens. In our current culture protocol (28), we routinely generate large amounts of clinical grade mature and immature DC. DC maturation is induced using

MCM, TNFα and PGE2. The first DC-trial at our institution has been initiated in 1998. Herein, the safety of DC based vaccines and the efficacy of immature DC versus mature DC was studied. HLA-A2.1$^+$, gp100$^+$, tyrosinase$^+$ metastatic melanoma patients were treated with peptide-pulsed immature or mature DC. As peptides we used two HLA-A2.1 restricted gp100 peptides (either native or modified peptides to improve their HLA-A2.1 binding affinity) (29, 30) and a tyrosinase peptide (31). All DC vaccines were co-loaded with the foreign protein KLH (Calbiochem, Darmstadt, Germany) that serves as a control for immune competence and stimulation of a T-helper response. Vaccinations were given 3 times with 2-week intervals, followed by injections with the peptides alone. Immune monitoring consisted of 1) DTH responses with pulsed- and unpulsed DC, 2) ELIspot-assays (32, 33) and 3) tetramer assays (34-36). In addition to peripheral blood, immune monitoring was also performed using biopsies taken from DTH sites (see below). The results of the first clinical trial have been published (19), and unequivocally demonstrated that mature but not immature DC are capable of inducing potent anti-KLH specific T-cell, and B-cell responses (19). Clinical results demonstrated that 3/20 objective remissions were observed in stage IV melanoma patients vaccinated with mature DC. In this group 10 patients were vaccinated with mature DC, of these patients 1 was not evaluable because of detoriating condition and of the remaining 9 patients, 3 showed stable disease >4 months (respectively 4.5, 7.5 and 22) 1 patient showed a mixed response and 1 patient achieved a partial response with complete remission after surgical intervention, that now lasts >7 years. All patients in this study were melanoma patients with metastatic disease (M1c, 1 patient M1a) in WHO performance status 0. Moreover, clinical results correlated with the presence of vaccine-induced immune responses against the tumor-peptides (see below) (37). To date, >200 melanoma patients have been vaccinated in our ongoing DC-trials, we observed no clinical benefit from vaccinations in patients with high tumor load (as judged by the clinician), elevated serum LDH, brain metastases or rapid progressive disease. Therefore, we excluded these patients, with a life expectancy less than 3 months, in ongoing studies. While on the down side the vaccine is not yet very effective, with an objective clinical response rate (i.e. > 1 year SD or better, stage IV melanoma patients) of approximately 10-15%, the positive message is that we clearly find T cell mediated immunological responses: 60% in patients with regional lymph node metastasis and 30% in patients with metastatic disease. Patients exhibiting these responses show an significantly improved progression free survival. Nevertheless, a number of variables need to be evaluated and controlled to further improve clinical outcome in cellular therapies, amongst these are generation of DC, use of different DC subsets, route of administration, optimal activation stimuli for DC (38), antigen-loading of dendritic cells, selection of tumor-derived antigens and so on (24). These variables are in ongoing debate, but one can conclude that the full potential of DC-based cellular therapy has not yet fully been exploited. However, the current consensus is to continue cellular therapy in well-designed small trials that meet a standardized list of quality criteria. This consensus list should at least describe quality-control criteria for *ex vivo* generated DC, patient characteristics, trial design including the different variables that are investigated, and tests for clinical and immunological responses (24, 39). Significant progress in cellular therapy against cancer, including DC vaccination, is only to be expected by careful immune monitoring studies in order to obtain detailed insight of the underlying (patho-) physiological processes that determine the success or failure of treatment. Different compartments and modalities are considered to monitor induced immune responses; e.g. accuracy of delivery, immune responses in peripheral blood, tumor and delayed type hypersensitivity (DTH) test biopsies, and clinical evaluation. Recently, it was shown that the modality of vaccination with a tumor-specific antigen influences the differentiation pathway of the anti-vaccine CD8 T cells, which may have an effect on their capacity to trigger a tumor rejection response (40). Palucka *et al.* observed that patients with a high baseline level of melanoma antigen-specific immunity more often show an immune response to the vaccine (41). Furthermore they show that patients who survived longer are those who showed immune response against two melanoma antigens presented on the

DC vaccine (42). Although sometimes correlations between tumor regression and T cell responses are observed (42, 43), the immunological studies performed so far are too diverse in their set-up to pool them in a meta-analysis (44). However, some lessons can be drawn from these studies. For example, an intact and proper functioning immune system seems to have a higher potential to react on immune therapy. From our immune monitoring data, mentioned below, we might not only conclude that the presence of tetramer specific T cells is correlated with an improved progression free survival. Another conclusion should be that in end-stage melanoma patients these tetramer specific T cells are less frequently induced (8 out of 26 patients) than in melanoma patients with regional lymph node metastasis (24 out of 31 patients). Secondly, upon induction of tumor antigen specific T cells, the next hurdle to take is the local immune suppressive environment created by the tumor. In end-stage melanoma patients, the misbalance is already in favor of the metastasizing tumor. In our ongoing studies we have seen that in some patients tetramer specific T cells are present after DC vaccination, but still experience progression. It became clear that these tetramer specific T cells did not produce interferon-□ nor showed cytotoxic activity upon tumor challenge. Apparently, these effector cells were not capable of breaking the local suppressive tumor-environment. We might take better advantage of the unique capacity of DC to direct the immune response by exploiting DC-based cellular therapy earlier in the disease course. It has been demonstrated that already in sentinel nodes melanoma-specific T cells are present, together with antigen-presenting cells. In this window between primary tumor and metastasis, immunological processes can be crucial. It might be at this turning point in the development of melanoma, that *ex vivo* generated DC can assist the immune system.

DC migration *in vivo*

For DC to induce potent immune responses their migration towards lymph nodes is essential. In mice, we have demonstrated that major differences can be found in numbers of migrating DC depending on the route of administration (subcutaneous gave the best results) and the maturation state (mature gave the best results) (45). With respect to the latter we were able to confirm these data in stage III melanoma patients with lymph node metastases who were scheduled for radical lymph node resection (46). During the first vaccination these patients received an injection of ^{111}In-labeled mature or immature DC to allow scintigraphic imaging to study *in vivo* migration (46). Regardless of the route of administration (intradermal or intranodal) mature DC were more efficient than immature DC in reaching the draining lymph node *in vivo* (46). The results described above were obtained by our developed method of radioactive labeling of DC (Figure 1) (45, 46). DC have therefore been labeled with radionuclides for scintigraphic imaging of cell trafficking, which is until to date the only FDA-approved clinical cellular imaging modality (46, 47). A major drawback of scintigraphy, however, is the lack of anatomical detail allowing only gross anatomical determination of migration between LNs without the ability to assess the intranodal distribution pattern of DC within each LN. Furthermore, due to its low spatial distribution, accurate delivery of cells which may be essential for subsequent migration into nearby lymph nodes cannot be properly evaluated using scintigrapy. In contrast, MR imaging is well suited to obtain three-dimensional whole body high-resolution images and is widely used in clinical practice. The currently most sensitive markers to label cells for MR detection are (ultrasmall) superparamagnetic iron oxide ((U)SPIO) particles (48). We took advantage of the fact that DC naturally endocytose clinically applied, FDA-approved SPIO-labels in significant amounts, obviating these concerns. This provided us with the opportunity to label cells with high efficiency without affecting their function and use these cells in humans (49). We investigated the biodistribution of these SPIO-prelabeled DC applied as cancer vaccines in melanoma patients using MR imaging. In our DC vaccination protocols, *in vitro* generated DC loaded with tumor-derived antigenic peptides were administered to stage III melanoma patients as outlined in Figure 1 (46),(19). DC were labeled with ^{111}In-oxine and SPIO (Endorem®) separately and co-injected in a LN

in the lymph node basin to be resected. This provided the unique opportunity to not only obtain MR scans at 3 Tesla (T) before surgery, but also to generate high resolution MR images at 7T of individual

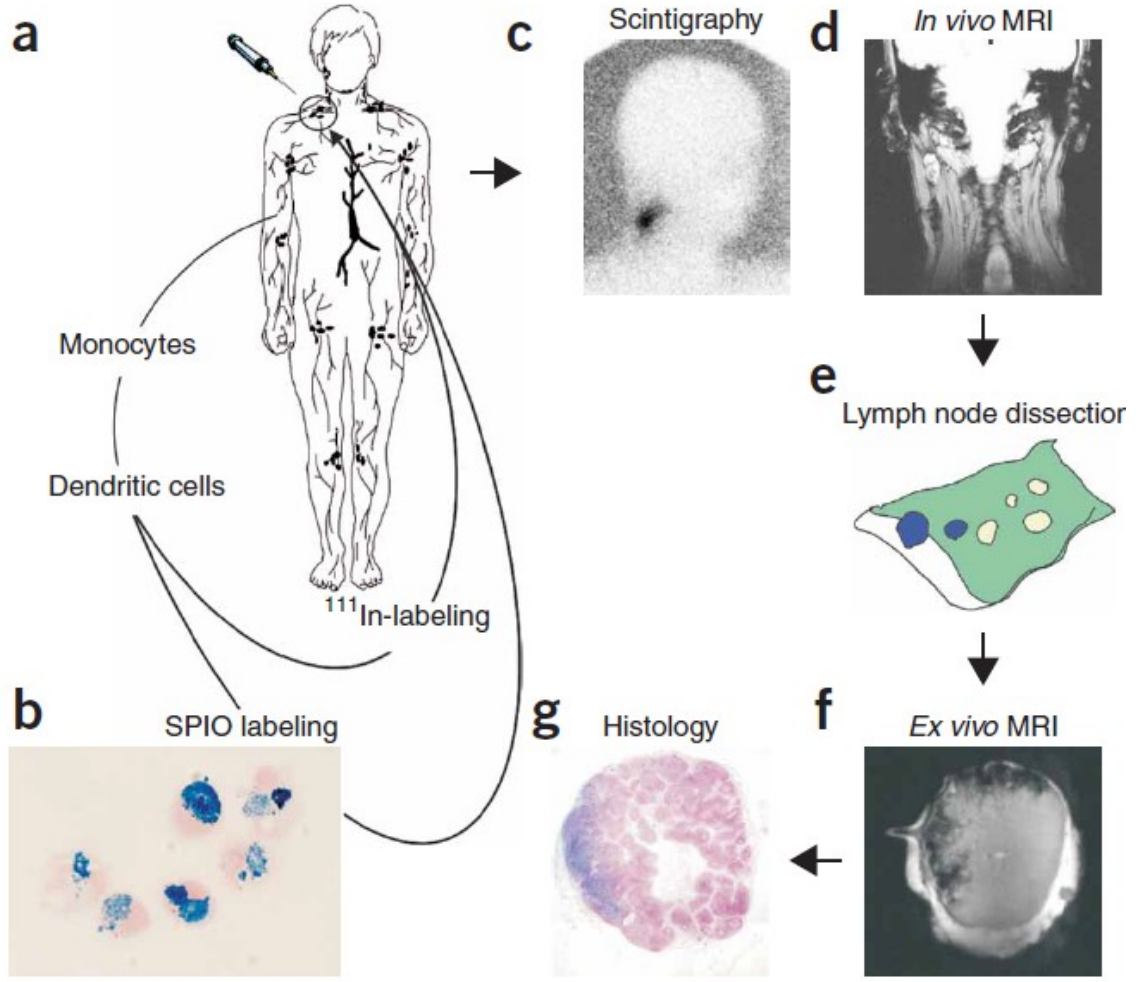

Figure 1. Monitoring the accuracy of delivery of SPIO-labelled cells using MR imaging and scintigraphy. Monocytes are obtained by cytopheresis from stage III melanoma patients (A), they are cultured and labeled with SPIO particles and ^{111}In (B). The cells are then injected intranodally into the lymph node basin that is to be resected and their biodistribution is monitored *in vivo* by scintigraphy (C) and MRI (D). The lymph node basin is resected (E) and separate lymph nodes are visualized with high resolution MRI at 7 Tesla (F) and histology (G) (Adapted from De Vries et al. *Nat Biotechnol.* 2005)

resected LNs, and to correlate the results with scintigraphy and (immuno-) histopathology. Interestingly, we found that in only approximately 50% of the cases DC were correctly injected into the LN, despite ultrasound guidance of the injection needle by a highly experienced radiologist. Subsequent migration could be observed only when DCs were correctly injected into the lymph node, demonstrating not only the importance of accurate delivery, but also of careful monitoring of cell tracking in cellular therapy. Inadequate delivery may be an important reason why only a limited proportion of patients respond in ongoing clinical trials using DC vaccines. We found that the accuracy of MR imaging to visualize truly DC-positive LNs was significantly better than scintigraphy. These findings illustrate the power of additional anatomical information, which can also be of value for other fields of biomedical research. With Prussian blue staining we can visualize SPIO-labeled cells. We observed immunohistologically that the SPIO-labeled DC that do migrate enter the lymph nodes via the sinuses and reach the T cell areas where the actual DC-T cell interaction takes place. At this stage we were able to demonstrate that intranodally injected SPIO-labeled DC, electroporated with RNA encoding the tumor antigen gp100, express the gp100 protein. From resected lymph nodes rosettes, containing SPIO-labeled DC surrounded by enlarged and activated T cells, were isolated. So we disclosed the desired “functional unit” within a lymph node.

Immune monitoring in tissues

Another aspect is monitoring the immune response that is thought to induce tumor regression. Immune monitoring is most straightforward after vaccination with defined antigens, however, responses have also been detected after lysate or total RNA loaded DC vaccines. Fortunately, many novel tools are now available to detect immune responses against known and unknown tumor antigens, including MHC-tetramers, Eli-spot- and cytokine release/catch assays (32-34, 36). No correlation was observed between the reactivity against KLH and the clinical outcome. We developed a novel approach to efficiently monitor DC vaccine related T cell responses in vaccinated patients using biopsies derived from delayed type hypersensitivity (DTH) sites (37). The results of this monitoring method correlated with the clinical outcome in stage III and IV melanoma patients. DTH challenges consisting of peptide-loaded DC plus or minus KLH, DC loaded with KLH, and unloaded DC revealed that essentially all patients mounted a positive DTH response with indurations up to 33 mm.

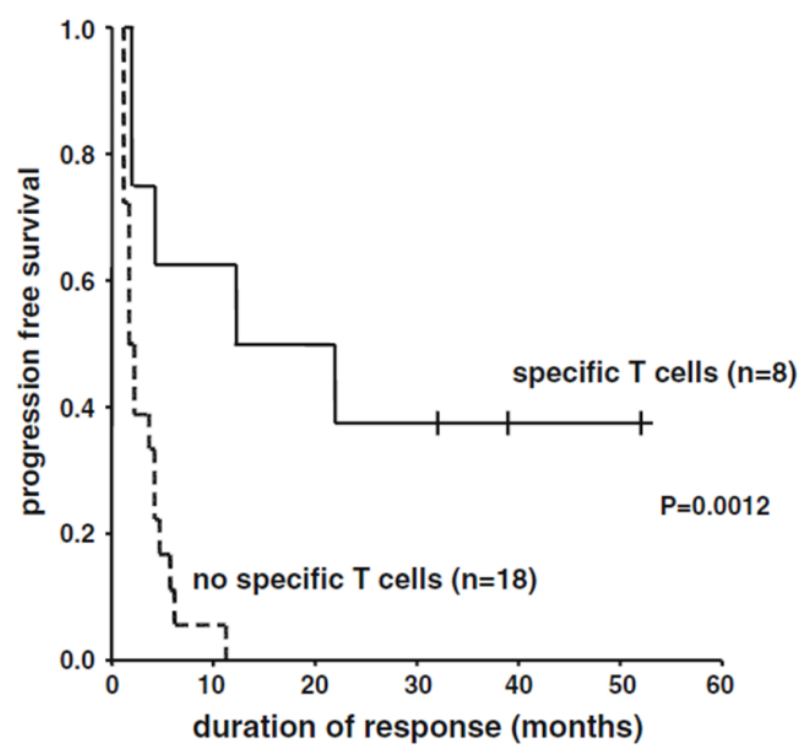

Figure 3. Presence of tetramer specific T cells highly correlates with progression free survival in melanoma patients. Correlation between the presence of specific T cells and clinical outcome is shown in this plot comparing the progression free survival of stage IV melanoma patients with (closed line) and without (hatched line) tumor-specific T cells in their DTH-infiltrated lymphocytes (For an updated version of this figure, see Chapter 11)

As both unloaded DC and DC loaded with KLH and/or peptides were positive, indurations at the DTH site were not predictive of vaccine-related T cell responses in our setting. However, as no DTH was detected after the first intradermal injection of the vaccine, the occurrence of a positive DTH reaction should be directly related to the vaccination. The reason for the DTH response to unloaded DC is not clear but could be explained by the vast amount of chemokines produced by mature DC (28). Punch biopsies (6 mm) were taken from positive DTH sites and divided in half. One part was used for histochemistry and the other part was used to isolate DTH-infiltrating leukocytes (DIL). Immune staining showed clusters of CD2+CD3+ infiltrating cells of which 50-70% were $CD4^+$ and 50-30% were CD8+ T cells. No clusters of infiltrating cells were observed in unchallenged control skin biopsies. DIL were generated by cutting the biopsies in pieces and culturing of the outgrowing cells for 2 to 3 weeks in the presence of low dose IL-2 (100 U/ml) without restimulation. Interestingly, DIL specific for KLH could easily be found in biopsies from KLH-pulsed DC, not in DIL from peptide or unpulsed DTH biopsies. Moreover, in 11 (6 stage III, 5 stage IV) out of 22 patients tested, gp100/tyr tetramer positive T cell populations were readily detected. In 5 additional patients, antigen-specific cytotoxic T cells in DIL cultures were detected after additional vaccination cycles.

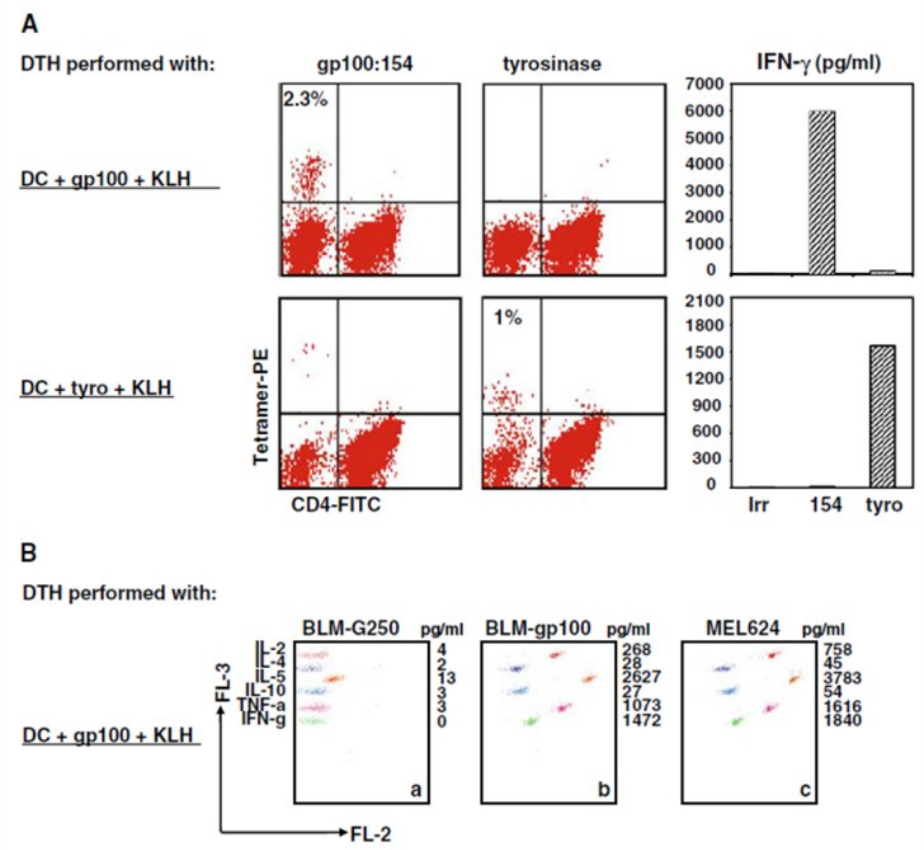

Figure 2. Specificity in DTH-infiltrated leukocyte (dil) cultures derived from patients vaccinated with peptide-loaded DC. In DIL cultured from a DTH performed with DC loaded with gp100 and KLH only T cells positive for the gp100 tetramers were observed. Tyrosinase tetramer positive cells were observed in the DIL derived from a DTH induced with tyrosinase peptide loaded DC. The production of IFNγ corresponded with the observed tetramer positivity.

No tetramer positive T cells were detected in DTH biopsies injected with unloaded DC or KLH loaded DC. Strikingly, in 6 of 7 patients in whom no tetramer positive cells were found in freshly isolated PBMC, significant numbers (up to 45%) of tetramer positive T cells were present in their cultured DTH biopsies taken at the same time point. Cytokine production and cytotoxicity of DIL upon co-culture with the appropriate target cells were fully correlated with the specificity in the tetramer analysis. Moreover, DTH reactions induced with DC pulsed with the gp100 peptides accumulated gp100 specific T cells and not tyrosinase and vice versa (Figure 2). Finally, *in situ* tetramer staining on cryo-sections revealed that gp100/tyr specific tetramers-positive cells were specifically present in the infiltrating T cell clusters. Control tetramers against MART-1, HIV or EBV were negative (50). Collectively, these data not only indicate that significant numbers of tetramer positive T cells accumulate in the DTH site, but also demonstrated that these T cells specifically produced cytokines (Figure 2) and/or are cytotoxic for tumor antigen expressing target cells (data not shown)(37). Next, we compared the clinical and immunological data of 26 stage IV melanoma patients (figure 3). Inclusion criteria of patients are described previously (19). Patients had documented progressive disease within 2 months before study entry, serum lactate dehydrogenase $\leq$ 2x the upperlimit of normal, no prior chemotherapy or immunotherapy within 3 months before study entry, and no residual toxicity from prior treatments. Of these patients, 15 patients had progressive disease (PD), 9 patients had stable disease with >4 months duration (SD), and 2 patients, one with multiple liver metastases at time of inclusion, are in complete remission (CR). No tumor-reactive DIL were found in 13 of the 15 patients with PD. Of the 9 patients with SD, 4 patients with specific T cells had a progression free survival of >42, 22, 12, and 4.5 months (median 12 months). In the 5 patients with SD without tumor-reactive DIL the median progression free survival was 6 months (range 11-4.5). Both patients in CR (>60 and >42 months) had tumor-specific T cells. Although the number of

patients in this study is limited, a statistically significant (p=0,0012) correlation was observed between the presence of tumor-specific T cell reactivity and progression free survival (37). The results were confirmed in 31 stage III melanoma patients.

Optimizing DC capabilities by RNA technology

Besides the production of highly reproducible GMP quality controlled batches of DC vaccines, *in vitro* and *in vivo* tools to analyze B and T cell responses are developed and injected DC can now be visualized in the patient by advanced imaging technology. Another major breakthrough is the application of RNA transfected DC that express complete tumor antigens. This has now proven to be effective and safe in patients and, in comparison to gene therapy, RNA transfection is much more straight forward. Cellular therapy with dendritic cells is still in its infancy, but a number of variables are recognized that can contribute to exploit its full potential. In particular monocyte derived DC may not seem optimally equipped for their task *in vivo*. In this context, RNA technology is a promising new tool to achieve temporarily expression or suppression of specific proteins to optimize DC function . Recent findings have shown that DC transfected with RNA encoding the full length tumor antigens, express the corresponding protein *in vivo* for a prolonged period of time. Moreover, these RNA transfected DC are able to induce anti-tumor responses in patients. But one can think of a broad range of applications of this technology to improve the functional capabilities of monocyte derived dendritic cells. During our investigations we observed that the majority of injected DC die early by apoptosis and necrosis. After injection the cells encounter hypoxic conditions and it is known that hypoxia inhibits migration of DC, likely because it blocks the production of metalloproteases (51). Similarly, Decoy receptor 3 was shown to be upregulated by DC that propagates apoptotic signals (52). Inhibition of this and other death inducing pathways may significantly increase DC survival. Secondly, migration of current monocyte derived DC *in vivo* is poor, their migration may be impaired due to limited chemokine receptor and cell adhesion receptor functioning. By exploiting RNA technology we might enhance expression of the chemokine CCR7, crucial for lymph node migration. Similarly, induced production of GM-CSF and IL-15 (53) might directly or indirectly enhance DC migration. Next, RNA technology can be exploited to improve DC maturation and T cell stimulation. Toll like receptors have been shown to be of key importance in DC maturation and subsequent induction of immunity through the upregulation of cytokines/chemokines and co-stimulatory molecules. To enhance DC maturation DC might be transfected with RNA encoding constitutively active TLRs or RNAs encoding co-stimulatory molecules, like CD70 and CD40L, can be introduced (K. Thielemans, personal communication). Expression of CD40L in DC has previously been reported to enhance the magnitude of CD4+ and CD8+ T cell responses in preclinical models (54, 55). Recently, CD70 has emerged as a key molecule for priming of CD8+ T cell responses (56). RNA interference to optimize T cell stimulation by *ex vivo* generated DC by another means is to induce expression of pro-inflammatory cytokines like interleukin-12 and type I interferons. Aside expression of activatory molecules in DC, it is becoming more and more evident that down regulatory mechanisms are in place that limit the DC's potential as a vaccine adjuvant. Recent murine data have demonstrated that SOCS1 (Suppressor of cytokine signaling 1) expression restricts the dendritic cells' ability to break tolerance and induce antitumor immunity (57, 58). We have recently demonstrated that upon human DC maturation SOCS1 as well as SOCS3 are also rapidly upregulated. Therefore, silencing of inhibitory molecules like SOCS 1 and IL-10 by RNA interference might be another means improve human DC-based cancer vaccines. Furthermore, one of the most potent factors limiting vaccine efficacy is the immune suppressive activity of the regulatory T cell (Treg). Remarkably, several reports indicate the rapid expansion of Treg following immunotherapy, including following DC vaccination. TGF is a cytokine required for the development of T regulatory T cells. Another Treg stimulatory molecule/pathway in DC as a candidate to silence concerns the enzyme indoleamine-2,3-dioxygenase (IDO). IDO1 appears most crucial for tryptophan catabolism and immune suppression (59, 60).

***In vivo* targeting of DC**

Direct targeting of antigens to DC surface receptors *in vivo* might replace laborious and expensive *ex vivo* culturing, and facilitate large-scale application of DC-based vaccination therapies. A major advantage of *in vivo* targeting strategies is that they can be produced in bulk quantities, whereas vaccines based on DC loaded with antigens *ex vivo* require tailor-made procedures for each individual. In addition, the opportunity to target natural DC subsets and at multiple sites *in vivo* might be preferable above loading more artificial *ex vivo* cultured DC. However, *ex vivo* culture conditions allow careful control of maturation and activation (61). Many of the receptors that are studied in targeting strategies belong to the C-type lectin receptor (CLR) family. The CLRs are a family of calcium-dependent lectins that share primary structural homology in their carbohydrate domain. Through this domain, CLRs bind to specific self or non-self sugar residues and are implicated in antigen capture and endocytosis. In our targeting studies we mainly investigated the targeting of DC-SIGN. DC-SIGN is predominantly expressed on immature DC and at lower levels on mature DC and macrophages (62-64). By cloning the hypervariable domains of a mouse antibody specific for human DC-SIGN into human framework regions, we obtained a humanized antibody. We demonstrated that this antibody efficiently targets myeloid APC *in vivo* and reached saturation with one single dose. The binding of the humanized antibody to DC-SIGN showed high affinity and facilitated endocytosis. Furthermore, targeted delivery to human monocyte-derived DC of a model antigen conjugated to the humanized DC-SIGN specific antibody leads to presentation of the antigen by MHC class I and II molecules and elicits both naïve and memory T-cell responses *in vitro* (65). The CLR targeting strategies that are most likely to enter the clinic in the near future target DC-SIGN, CD205 (DEC205) and the mannose receptor. Of these, DC-SIGN seems the most DC/macrophage lineage-specific receptor, which might be advantageous since the targeting vector will not be scavenged by other cell types that could result in lower targeting efficiencies and undesirable side-effects. The expression of CD205 for example is in humans less restricted than in mice. Although human CD205 expression levels are highest in mature DC, CD205 is also expressed by B cells, T cells, monocytes, macrophages and NK cells (66). CD205 however seems to be more potent in mediating cross-presentation *in vitro* compared to the other two receptors. Furthermore, due lack of direct control in these targeting strategies, the duration and stability of the vaccine following administration will be difficult to determine.

Conclusions and future prospects

Dendritic cell immunotherapy has been introduced in the clinic. It has proven to be feasible, non-toxic and effective in some cancer patients, particularly if the DC are appropriately matured and activated. However, many questions still remain. One of the concerns related to *ex vivo* generated DC is how to ensure effective migration to the T cell areas in the lymph node. In this context, we are pursuing the enhancement of migration of *ex vivo* generated DC by preconditioning the skin with inflammatory cytokines. The recent application of RNA technology in cellular therapy has paved the way to the next generation of dendritic cell based therapies. Different aspects of DC biology can now be optimized to enhance immunological and clinical responses. One can think of exploiting *ex vivo* generated DC equipped with enhanced expression of chemokine receptors to locate lymph nodes, silenced apoptotic pathways to increase longevity and upregulated production of pro-inflammatory cytokines to skew naïve T cells. These multiple approaches need to be investigated in small two-armed principle of concept trials with thorough immune monitoring, in order to increase the clinical efficacy of DC-based cancer vaccines. A second promising approach that circumvents many of the posed hurdles with *ex vivo* loaded DC is *in vivo* targeting. Targeting studies using members of the CLR family have paved the way to clinical studies.

References

1. Banchereau, J. and R.M. Steinman, *Dendritic cells and the control of immunity.* Nature, 1998. 392(6673): p. 245-52.
2. Jiang, W., et al., *The receptor DEC-205 expressed by dendritic cells and thymic epithelial cells is involved in antigen processing.* Nature, 1995. 375(6527): p. 151-5.
3. Sallusto, F. and A. Lanzavecchia, *Efficient presentation of soluble antigen by cultured human dendritic cells is maintained by granulocyte/macrophage colony-stimulating factor plus interleukin 4 and downregulated by tumor necrosis factor alpha.* J Exp Med, 1994. 179(4): p. 1109-18.
4. Matzinger, P., *Tolerance, danger, and the extended family.* Annu Rev Immunol, 1994. 12: p. 991-1045.
5. Adema, G.J., et al., *A dendritic-cell-derived C-C chemokine that preferentially attracts naive T cells.* Nature, 1997. 387(6634): p. 713-7.
6. Fernandez, N.C., et al., *Dendritic cells directly trigger NK cell functions: cross-talk relevant in innate anti-tumor immune responses in vivo.* Nat Med, 1999. 5(4): p. 405-11.
7. Kadowaki, N., et al., *Natural interferon alpha/beta-producing cells link innate and adaptive immunity.* J Exp Med, 2000. 192(2): p. 219-26.
8. Celluzzi, C.M., et al., *Peptide-pulsed dendritic cells induce antigen-specific CTL-mediated protective tumor immunity.* J Exp Med, 1996. 183(1): p. 283-7.
9. Mayordomo, J.I., et al., *Bone marrow-derived dendritic cells pulsed with synthetic tumour peptides elicit protective and therapeutic antitumour immunity.* Nat Med, 1995. 1(12): p. 1297-302.
10. Zitvogel, L., et al., *Therapy of murine tumors with tumor peptide-pulsed dendritic cells: dependence on T cells, B7 costimulation, and T helper cell 1-associated cytokines.* J Exp Med, 1996. 183(1): p. 87-97.
11. Steinman, R.M., *Dendritic cells: understanding immunogenicity.* Eur J Immunol, 2007. 37 Suppl 1: p. S53-60.
12. Liu, Y.J., *Dendritic cell subsets and lineages, and their functions in innate and adaptive immunity.* Cell, 2001. 106(3): p. 259-62.
13. Kalinski, P., et al., *T-cell priming by type-1 and type-2 polarized dendritic cells: the concept of a third signal.* Immunol Today, 1999. 20(12): p. 561-7.
14. Rescigno, M. and P. Borrow, *The host-pathogen interaction: new themes from dendritic cell biology.* Cell, 2001. 106(3): p. 267-70.
15. Jonuleit, H., et al., *Induction of interleukin 10-producing, nonproliferating CD4(+) T cells with regulatory properties by repetitive stimulation with allogeneic immature human dendritic cells.* J Exp Med, 2000. 192(9): p. 1213-22.
16. Sallusto, F. and A. Lanzavecchia, *Mobilizing dendritic cells for tolerance, priming, and chronic inflammation.* J Exp Med, 1999. 189(4): p. 611-4.
17. Dhodapkar, M.V., et al., *Antigen-specific inhibition of effector T cell function in humans after injection of immature dendritic cells.* J Exp Med, 2001. 193(2): p. 233-8.
18. Shevach, E.M., et al., *Control of T-cell activation by CD4+ CD25+ suppressor T cells.* Immunol Rev, 2001. 182: p. 58-67.
19. de Vries, I.J., et al., *Maturation of dendritic cells is a prerequisite for inducing immune responses in advanced melanoma patients.* Clin Cancer Res, 2003. 9(14): p. 5091-100.
20. Kalinski, P., et al., *Helper role of NK cells during the induction of anticancer responses by dendritic cells.* Mol Immunol, 2005. 42(4): p. 535-9.
21. Miller, J.S., et al., *Successful adoptive transfer and in vivo expansion of human haploidentical NK cells in patients with cancer.* Blood, 2005. 105(8): p. 3051-7.
22. Ruggeri, L., et al., *Effectiveness of donor natural killer cell alloreactivity in mismatched hematopoietic transplants.* Science, 2002. 295(5562): p. 2097-100.
23. Steinman, R.M. and J. Banchereau, *Taking dendritic cells into medicine.* Nature, 2007. 449(7161): p. 419-26.
24. Figdor, C.G., et al., *Dendritic cell immunotherapy: mapping the way.* Nat Med, 2004. 10(5): p. 475-80.
25. Parmiani, G., et al., *Melanoma immunology: past, present and future.* Curr Opin Oncol, 2007. 19(2): p. 121-7.
26. Banchereau, J., et al., *Immune and clinical outcomes in patients with stage IV melanoma vaccinated with peptide-pulsed dendritic cells derived from CD34+ progenitors and activated with type I interferon.* J Immunother, 2005. 28(5): p. 505-16.
27. Nestle, F.O., J. Banchereau, and D. Hart, *Dendritic cells: On the move from bench to bedside.* Nat Med, 2001. 7(7): p. 761-5.
28. de Vries, I.J., et al., *Phenotypical and functional characterization of clinical grade dendritic cells.* J Immunother, 2002. 25(5): p. 429-38.
29. Bakker, A.B., et al., *Melanocyte lineage-specific antigen gp100 is recognized by melanoma-derived tumor-infiltrating lymphocytes.* J Exp Med, 1994. 179(3): p. 1005-9.
30. Bakker, A.B., et al., *Analogues of CTL epitopes with improved MHC class-I binding capacity elicit anti-melanoma CTL recognizing the wild-type epitope.* Int J Cancer, 1997. 70(3): p. 302-9.
31. Brichard, V., et al., *The tyrosinase gene codes for an antigen recognized by autologous cytolytic T lymphocytes on HLA-A2 melanomas.* J Exp Med, 1993. 178(2): p. 489-95.
32. Scheibenbogen, C., et al., *Analysis of the T cell response to tumor and viral peptide antigens by an IFNgamma-ELISPOT assay.* Int J Cancer, 1997. 71(6): p. 932-6.
33. Herr, W., et al., *Frequency analysis of tumor-reactive cytotoxic T lymphocytes in peripheral blood of a melanoma patient vaccinated with autologous tumor cells.* Cancer Immunol Immunother, 1994. 39(2): p. 93-9.
34. Altman, J.D., et al., *Phenotypic analysis of antigen-specific T lymphocytes.* Science, 1996. 274(5284): p. 94-6.
35. Haanen, J.B., et al., *In situ detection of virus- and tumor-specific T-cell immunity.* Nat Med, 2000. 6(9): p. 1056-60.
36. Dunbar, P.R., et al., *Direct isolation, phenotyping and cloning of low-frequency antigen-specific cytotoxic T lymphocytes from peripheral blood.* Curr Biol, 1998. 8(7): p. 413-6.

37. de Vries, I.J., et al., *Immunomonitoring tumor-specific T cells in delayed-type hypersensitivity skin biopsies after dendritic cell vaccination correlates with clinical outcome.* J Clin Oncol, 2005. 23(24): p. 5779-87.
38. Boullart, A.C., et al., *Maturation of monocyte-derived dendritic cells with Toll-like receptor 3 and 7/8 ligands combined with prostaglandin E(2) results in high interleukin-12 production and cell migration.* Cancer Immunol Immunother, 2008.
39. Hoos, A., et al., *A clinical development paradigm for cancer vaccines and related biologics.* J Immunother, 2007. 30(1): p. 1-15.
40. Connerotte, T., et al., *Functions of Anti-MAGE T-cells induced in melanoma patients under different vaccination modalities.* Cancer Res, 2008. 68(10): p. 3931-40.
41. Palucka, A.K., et al., *Taming cancer by inducing immunity via dendritic cells.* Immunol Rev, 2007. 220: p. 129-50.
42. Fay, J.W., et al., *Long-term outcomes in patients with metastatic melanoma vaccinated with melanoma peptide-pulsed CD34(+) progenitor-derived dendritic cells.* Cancer Immunol Immunother, 2006. 55(10): p. 1209-18.
43. Lonchay, C., et al., *Correlation between tumor regression and T cell responses in melanoma patients vaccinated with a MAGE antigen.* Proc Natl Acad Sci U S A, 2004. 101 Suppl 2: p. 14631-8.
44. Britten, C.M., et al., *Toward the harmonization of immune monitoring in clinical trials: quo vadis?* Cancer Immunol Immunother, 2008. 57(3): p. 285-8.
45. Eggert, A.A., et al., *Biodistribution and vaccine efficiency of murine dendritic cells are dependent on the route of administration.* Cancer Res, 1999. 59(14): p. 3340-5.
46. De Vries, I.J., et al., *Effective migration of antigen-pulsed dendritic cells to lymph nodes in melanoma patients is determined by their maturation state.* Cancer Res, 2003. 63(1): p. 12-7.
47. Mackensen, A., et al., *Homing of intravenously and intralymphatically injected human dendritic cells generated in vitro from CD34+ hematopoietic progenitor cells.* Cancer Immunol Immunother, 1999. 48(2-3): p. 118-22.
48. Bulte, J.W. and D.L. Kraitchman, *Iron oxide MR contrast agents for molecular and cellular imaging.* NMR Biomed, 2004. 17(7): p. 484-99.
49. Verdijk, P., et al., *Sensitivity of magnetic resonance imaging of dendritic cells for in vivo tracking of cellular cancer vaccines.* Int J Cancer, 2007. 120(5): p. 978-84.
50. De Vries, I.J., et al., *In situ detection of antigen-specific T cells in cryo-sections using MHC class I tetramers after dendritic cell vaccination of melanoma patients.* Cancer Immunol Immunother, 2007. 56(10): p. 1667-76.
51. Zhao, W., et al., *Hypoxia suppresses the production of matrix metalloproteinases and the migration of human monocyte-derived dendritic cells.* Eur J Immunol, 2005. 35(12): p. 3468-77.
52. You, R.I., et al., *Apoptosis of dendritic cells induced by decoy receptor 3 (DcR3).* Blood, 2008. 111(3): p. 1480-8.
53. Ohteki, T., et al., *Essential roles of DC-derived IL-15 as a mediator of inflammatory responses in vivo.* J Exp Med, 2006. 203(10): p. 2329-38.
54. Diehl, L., et al., *CD40 activation in vivo overcomes peptide-induced peripheral cytotoxic T-lymphocyte tolerance and augments anti-tumor vaccine efficacy.* Nat Med, 1999. 5(7): p. 774-9.
55. French, R.R., et al., *CD40 antibody evokes a cytotoxic T-cell response that eradicates lymphoma and bypasses T-cell help.* Nat Med, 1999. 5(5): p. 548-53.
56. Borst, J., J. Hendriks, and Y. Xiao, *CD27 and CD70 in T cell and B cell activation.* Curr Opin Immunol, 2005. 17(3): p. 275-81.
57. Evel-Kabler, K., et al., *SOCS1 restricts dendritic cells' ability to break self tolerance and induce antitumor immunity by regulating IL-12 production and signaling.* J Clin Invest, 2006. 116(1): p. 90-100.
58. Shen, L., et al., *Silencing of SOCS1 enhances antigen presentation by dendritic cells and antigen-specific anti-tumor immunity.* Nat Biotechnol, 2004. 22(12): p. 1546-53.
59. Hill, M., et al., *IDO expands human CD4+CD25high regulatory T cells by promoting maturation of LPS-treated dendritic cells.* Eur J Immunol, 2007. 37(11): p. 3054-62.
60. Puccetti, P. and U. Grohmann, *IDO and regulatory T cells: a role for reverse signalling and non-canonical NF-kappaB activation.* Nat Rev Immunol, 2007. 7(10): p. 817-23.
61. Tacken, P.J., et al., *Dendritic-cell immunotherapy: from ex vivo loading to in vivo targeting.* Nat Rev Immunol, 2007. 7(10): p. 790-802.
62. Bozzacco, L., et al., *DEC-205 receptor on dendritic cells mediates presentation of HIV gag protein to CD8+ T cells in a spectrum of human MHC I haplotypes.* Proc Natl Acad Sci U S A, 2007. 104(4): p. 1289-94.
63. Geijtenbeek, T.B., et al., *Identification of DC-SIGN, a novel dendritic cell-specific ICAM-3 receptor that supports primary immune responses.* Cell, 2000. 100(5): p. 575-85.
64. Soilleux, E.J., et al., *Constitutive and induced expression of DC-SIGN on dendritic cell and macrophage subpopulations in situ and in vitro.* J Leukoc Biol, 2002. 71(3): p. 445-57.
65. Tacken, P.J., et al., *Effective induction of naive and recall T-cell responses by targeting antigen to human dendritic cells via a humanized anti-DC-SIGN antibody.* Blood, 2005. 106(4): p. 1278-85.
66. Kato, M., et al., *Expression of human DEC-205 (CD205) multilectin receptor on leukocytes.* Int Immunol, 2006. 18(6): p. 857-69.

Chapter 9

Imaging of cellular therapies

Srinivas M*

Aarntzen EH*

Bulte JW

Oyen WJ

Heerschap A

De Vries IJ

Figdor CG

* contributed equally

Adv Drug Deliv Rev. 2010;62(11):1080-93.

Abstract

Cellular therapy promises to revolutionize medicine, by restoring tissue and organ function, and combating key disorders including cancer. As with all major developments, new tools must be introduced to allow optimization. For cell therapy, the key tool is *in vivo* imaging for real time assessment of parameters such as cell localization, numbers and viability. Such data is critical to modulate and tailor the therapy for each patient. In this review, we discuss recent work in the field of imaging cell therapies in the clinic, including preclinical work where clinical examples are not yet available. Clinical trials in which transferred cells were imaged using magnetic resonance imaging (MRI), nuclear scintigraphy, single photon emission computed tomography (SPECT), and positron emission tomography (PET) are evaluated from an imaging perspective. Preclinical cell tracking studies that focus on fluorescence and bioluminescence imaging are excluded, as these modalities are generally not applicable to clinical cell tracking. In this review, we assess the advantages and drawbacks of the various imaging techniques available, focusing on immune cells, particularly dendritic cells. Both strategies of prelabeling cells before transplant and the use of an injectable label to target cells *in situ* are covered. Finally, we discuss future developments, including the emergence of multimodal imaging technology for cell tracking from the preclinical to the clinical realm.

1. Introduction

Cellular therapy is the use of transplanted cells, often autologous cells, to replace or renew damaged or diseased tissue. The idea of regulating the body's own resources to regenerate diseased tissue or to fight disease is very compelling; this can potentially reduce unpleasant side-effects caused by harsher, non-targeted treatments such as chemotherapy while exerting a strong healing effect. The field of cellular therapeutics is blossoming and may in the near future become standard treatment for a wide range of conditions involving damaged tissue, such as stem cell transplants in post myocardial-infarction tissue or neurodegenerative disease, and in regulating the immune system, as in dendritic cell (DC) vaccinations or the transfer of antigen-specific T cells in cancer therapy. Currently, over 17,000 ongoing clinical trials involve some form of cell therapy (www.clinicaltrials.gov). Despite this major effort, translation from preclinical studies to humans has been difficult and largely disappointing. While the task itself is immensely complex, one key reason for this failure is the lack of tools to study transplanted cells by non-invasively and longitudinally in humans. *In vivo* imaging is the foremost contender, and therefore, to move forward we urgently need novel imaging tools for qualitative and quantitative monitoring of transplanted cells to determine the anatomical location, cell numbers, and functional lifespan in patients.

Frequently, the function of the transplanted cells is measured by metabolic tests. Consider the example of cadaveric pancreatic islets transplanted to diabetic patients, generally in the hepatic portal vein (2): Transplant success is gauged by measuring blood glucose levels. However, since insulin levels are tightly regulated, loss of transplanted islets would simply upregulate insulin production by the remaining islets. In fact, type 1 diabetes itself results from a loss of both pancreatic islet mass and function to varying degrees. Thus, monitoring blood glucose levels alone does not provide an accurate picture of islet viability. This example clearly shows the need for assays to study the transferred islets directly, in terms of mass and function. For cell transplants in general, it is not sufficient to monitor cell numbers or cell function alone; both should be monitored simultaneously to accurately assess success of the therapy. In clinical studies, multimodal *in vivo* imaging can offer tools for monitoring with minimal invasive procedures.

The earliest *in vivo* imaging technique to study specific cells of interest in humans is leukocyte scintigraphy, which has now been used for about 30 years (3, 4). In this technique, leukocytes harvested from patient blood are labeled with radioactive tracers, commonly ^{111}In agents, and re-injected intravenously. The accumulation of these radiolabeled cells is used to locate foci of inflammation, for example in patients with fever of unknown origin (5). Imaging is done using a gamma camera or with single photon emission computed tomography (SPECT). Leukocyte scintigraphy is an example of diagnostic imaging, whereas the tracking of transplanted pancreatic islets is an example of therapeutic imaging. Diagnostic imaging has also been carried out exploiting other cell types including monocytes and macrophages (6).In this review we will focus on therapeutic imaging.

Tracking of transplanted therapeutic cells using imaging is a relatively recent development, and currently no standard clinically-approved imaging technique exists for the quantitative, longitudinal monitoring of cells after transfer. Hence, here we discuss the different imaging modalities applicable to humans and their most promising applications so far, focusing on immune cells used as therapeutics. We also consider future possibilities, in particular the development of more sensitive cell tracers and multimodal imaging. Finally, we discuss some important issues related to cell tracking *in vivo* and data reporting standards. Fig. 1 shows examples images after DC vaccination in melanoma patients using MRI, PET and scintigraphy.

1.1 Clinical imaging and cell tracking modalities

Several imaging modalities exist to track cells in animal models. However, only a few of these can be used in humans due to safety, technical and cost considerations. Table 1 lists common cell tracking modalities, their use in humans, their relative sensitivity using the most common imaging techniques and parameters and their application towards longitudinal use.

The imaging techniques relevant to clinical cell tracking include scintigraphy with gamma cameras, positron emission tomography (PET), SPECT and magnetic resonance imaging (MRI). Computed tomography (CT) is frequently used in conjunction with SPECT and PET to give anatomic context. In general, techniques dependant on radioactive isotopes are limited by the half-lives of the isotopes, and are thus difficult to apply towards longitudinal imaging. However, an intriguing approach that might be a good compromise is to use an injectable label, for example a radiolabeled antibody to track specific cells i.e. *in vivo* labeling (7) (see graphical abstract). This can then be repeatedly injected for longitudinal cell tracking (8). However, non-specific label uptake or slow clearance can confound data interpretation. Furthermore, techniques using radioactive isotopes or ionizing radiation can be restricted by exposure limits in humans. The absence of radiation is therefore one of the reasons why MRI is an attractive alternative. Other reasons include its extremely high resolution, tomographic ability and inherent soft tissue contrast. On the downside, MRI can be several orders of magnitudes less sensitive and less quantitative than techniques using radioactive isotopes. Similar to scintigraphy, for MRI cells are labeled before transfer to the patient, although labels can be targeted *in vivo* (6) or cells can also be transduced to express reporter genes (9).

Optical imaging techniques using fluorescence or bioluminescence, have proven invaluable in small animal models. These techniques are extremely fast and amenable to repeated sessions in the same animal. Existing markers such as green fluorescent protein (GFP) or luciferase expression can be exploited. In the case of bioluminescence imaging, a major advantage is the total absence of background allowing for data acquisition in a relatively quantitative manner. However, the limited depth penetration of these wavelengths of light currently restricts the techniques to small animals for non-invasive imaging. Accordingly, optical agents have not been applied to *in vivo* cell tracking in humans. Finally, the most widely-used imaging modality in the clinic does not exploit the visible light spectrum at all: Acoustic imaging, such as ultrasound imaging, is the most common structural imaging modality in the clinic. The technique gives real-time (4D) images with a limited field of view. Targeted labels have been developed for this technique (10), although human cell tracking has so far not been achieved. Due to resolution and penetration limits, ultrasound imaging is best-suited to gather structural data of superficial and echogenic structures, and appears less applicable to cell therapy.

1.2 The role of imaging in optimizing cellular therapeutics

The use of cell therapy brings us further into the realm of personalized medicine, as the therapeutic cells are often generated from the patients' own cells. The complex process of isolating and producing therapeutic cells generates a myriad of variables, all of which may affect the clinical outcome. Some of these variables are listed in Table 2. In effect therapeutic cells function as "drugs" and therefore require the study of many of the same variables that need to be optimized for drug trials; these are discussed in further detail in a review on stem cell transfers to treat Parkinson's disease (11). This level of personalization, where the whole procedure is optimized for each individual, requires a system for monitoring the transferred cells *in vivo*. A longitudinal, and in many cases, also a quantitative technique to monitor cell numbers *in vivo* will allow optimization of the cellular therapy specifically for each patient, maximizing the chance of success of these costly therapies. Overall, the application of *in vivo* imaging can allow for the development of the optimal cellular therapeutic regimen for each patient. Current clinical cell therapy protocols will need to be modified to include a labeling step or to include infusions of label after cell transfer, along with the

addition of imaging sessions at relevant time points. Longitudinal cell tracking could allow adjustments of some of the many variables involved as necessary to maximize therapeutic effect.

One important variable is the site of transfer. This plays a large role in cellular therapy. For example, the transfer site defines the local infrastructure including the availability of small blood vessels and lymphatics, and larger blood vessels with chemokine gradients that can influence the migration of transplanted cells. Any local inflammatory and immune response might lead to instant rejection of the cell graft. Moreover, the resident cells may direct maturation or differentiation of the transferred cells (12). For example, the local micro-environment is thought to contribute to a significant loss of pancreatic islets transplanted to the hepatic portal vein within the first few hours or days after transplant (2). From a more practical standpoint, certain transfer locations are more desirable simply because they are easy to access or easy to image, although not always both. For example, the liver is often the site of pancreatic islet transplants, but it can be difficult to image iron-labeled cells using MRI due to the large endogenous iron stores at the site (13). In the case of DC vaccinations, the role of the site of transfer was demonstrated in a study using ultrasound-guided injections of DC into a lymph node (LN); MR imaging of the injection site, revealed some misinjections which affected outcome (1). This study demonstrated both the importance of imaging in optimizing and validating cellular therapy, and the limitations of imaging modalities.

Another key variable is the treatment schedule of cell therapies. This is dependent on the availability of equipment and technology, number of cells required, planned frequency of transfer, cost and level of discomfort to the patient, amongst others. Transfer sites that are readily accessible, such as subcutaneous injections, are utilized more frequently. Sites such as LN may become damaged by the injection and thus cannot be injected repeatedly. Other than accessibility, oxygenation at the transfer site also plays a role. It has been demonstrated that a large proportion of DC simply die at or near the injection site likely because hypoxic conditions hinder migration or stimulate apoptosis. The frequency of transfer can be limited by the numbers of cells that can be cultured or purified. In general, it is thought that injections of large numbers of cells especially in a small volume, can lead to cell death in the bolus due to nutrient deprivation or hypoxia. One solution is to inject the cells in smaller numbers, or in a scaffold or gel to improve nutrient access, or simply to maintain mechanical properties of the tissue (14). Imaging the migration of labeled cells from the injection site has been used as a measure of cell viability after transfer (15). In this example, the cells were labeled for imaging during their *ex vivo* maturation and culturing process (see graphical abstract). Thus, the addition of an *ex vivo* labeling step did not require significant modification of existing cell culture protocol. Imaging data was then used to optimize the site of transfer, for example by pretreating the site with cytokines (16). Another plausible example on how cell tracking could be implemented in the process of clinical decision making involves a multimodality approach to image transplanted stem cells and their effect on the function of damaged myocardium: After injection of a fixed number of pre-labeled stem cells and an exact estimation of the number of engrafted cells, their effect on myocardium can readily be imaged. Imaging of myocardiac motion by ultrasound, metabolic activity by ^{18}F-FDG and myocardial perfusion by ^{201}Tl scans is routinely performed. This detailed information on the delivery of transplanted cells can help in the considerations for subsequent treatment options when the expected improvement in cardiac function is not reached.

Thus, the aim of *in vivo* imaging is to allow feedback on the success of the therapy in real time, so that the treatment schedule (i.e. variables such as the site of transfer and so on) can be modified to optimize the therapy in a patient. Table 2 lists several of the variables in cellular therapy that can be studied using imaging with relevant examples where available. In section 3 we discuss more specific examples of clinical cell tracking trials involving therapeutic immune cells.

2. Cell labeling

Cells must be suitably labeled for detection via imaging, to distinguish them from the surrounding cellular milieu. In both preclinical and clinical situations, cells are typically labeled *ex vivo*, before transfer to the host for cell tracking studies. Another option is *in vivo* labeling, for instance by labeled antibodies specific for the transferred cells (see graphical abstract for a summary of both strategies). Both techniques have pros and cons, as discussed in the following sections.

A recent review lists some general requirements for the use of novel agents for clinical cell tracking (17) namely that these cell labels must be shown to be non-toxic to cells in culture or animal models, that the labeled cells should be extensively characterized to determine any effect of labeling on cell functionality and that the label synthesis can be done in a reproducible manner in a GMP facility using compounds that are or can be approved for human use. They point out that the characterization of labeled cells in comparison to non-labeled controls must be repeated for each new cell type used. However, it is often difficult to study all the relevant features of cells *in vivo* using *in vitro* assays. One study on the effects of labeling human mesenchymal stem cells with a common MRI contrast agent found changes in the expression levels of several genes after labeling and exposure to a magnetic field (18). Such effects on cell function must be carefully investigated, especially in the case of long-lived cells that will persist and divide in the patient, such as stem cells.

2.1 In vitro labeling

Here, specific cell populations are purified from the patient and labeled for imaging before transfer (see graphical abstract). Advantages of this procedure include simplified removal of excess label and dead cells, and the possibility of conducting rigorous functional analyses on the labeled cells before transfer to the patient. Furthermore, non-specific labeling of irrelevant cells is greatly reduced if the relevant cell population is purified beforehand, and even cells that prove reluctant to take up label can be labeled using relatively harsh techniques such as electroporation or the use of transfection agents, especially positively charged peptides that can be used in the clinic. Many highly relevant therapeutic cells, such as stem cells, are not phagocytic and therefore need to be coaxed to take up imaging labels. One study on the biological effects of labeling mouse embryonic stem cells with three different transfection methods namely electroporation, protamine sulphate and poly-L-lysine, found that the transfection method used can affect factors such as cell differentiation and label uptake (19). Furthermore, transfection agents can result in non-specific uptake unless added to purified cells. *In vitro* labeling allows detailed characterization of the labeled cells before transfer, in terms of viability, gene expression and functional status using standardized assays. For example, in DC vaccination studies, levels of antigen presenting molecules (MHC class I and II) and chemokine receptors (e.g. CCR7) are determined before injection (20), or with T cell therapy using tumor antigen-specific cytotoxic T cells, cytotoxicity assays and intracellular IFN-gamma staining can be carried out (21). The homogeneity of label uptake within the population can also be determined.

As cells are labeled before transfer, any cell division that occurs *in vivo* would dilute the label between daughter cells. This can result in errors in quantification of cell numbers or even loss of detectability (22). This holds especially for rapidly dividing cells. Label retention within the cell must also be characterized as imaging modalities typically detect just the label regardless of whether the label is contained in the relevant cells, lost to the extracellular matrix or transferred to other cells. Intracellular localization of label can also be important, particularly when using MR labels where it has been shown that clustering of MR labels in dense vacuoles yields better local contrast enhancement than cytosolic distribution (8). Furthermore, clearance of label from dead cells must also be studied. For example, ^{99}Tc is not as suitable as ^{111}In for labeling immune cells due to higher leakage from the cells and subsequent clearance by the kidneys (23). Finally, on a more practical note, *ex vivo* labeling and cell culture requires the use of a clinical clean room, which makes it a labor intensive and costly procedure.

The radiolabels typically used to label cells have half lives ranging from about 2 hours to over 2 days. This restricts the length of time that they can be detected *in vivo*, often to a length of time much shorter than the lifetime of the transferred cells. It also introduces logistical issues in planning such trials, as the label needs to be synthesized shortly before use, and the cell labeling procedure itself also needs to be performed in a short period of time. MRI is an exception, since these labels comprise of very stable compounds such as super paramagnetic iron oxide (SPIO) or gadolinium agents. These heavy metals are polymer-coated to reduce toxicity. Such MRI labels are called "contrast agents" because they are not detected directly but instead through their effect on the local contrast. MRI contrast agents have already been used in several clinical cell tracking trials (17), allowing for high resolution, longitudinal cell tracking. Cells have been extensively characterized after labeling for MRI. For example, labeling with iron oxide and poly-L-lysine was found not to affect overall long-term gene expression in neural stem cells (24). Another study on mesenchymal stem cells labeled with clinically approved iron oxide and a 3T MRI scanner found no effect on cell viability, proliferation rate, migration and differentiation capacity, albiet expression levels of some genes were affected (18). Finally, although MRI-based cell tracking is not restricted by half-life decay as with radiolabels, they are generally less suitable for quantification of cell numbers using current imaging protocols.

2.2 In vivo labeling

In this procedure, the label is generally injected systemically and either taken up non-specifically by the relevant (phagocytic) cells or targeted specifically to the relevant cell type (second strategy in graphical abstract). This process eliminates the *ex vivo* purification and labeling of cells and therefore is much easier to apply and, in general, only viable or functional cells will be able to take up the label effectively. Furthermore, the use of an injectable label allows the use of radiolabels for longitudinal studies, as the agent can be injected before each imaging session and therefore a short halflife is less of a restriction. A simple example of such a label would be a specific antibody bound to a radioactive isotope for SPECT (7). Similarly, ultrasmall superparamagnetic iron oxide (USPIO) particles have been administered intravenously and were taken up by macrophages and transported to LN. Subsequent MR images show abnormal accumulation patterns in the case of LN metastases, where there was no infiltration of labeled macrophages (6). Common problems faced with systemic transfer of label include restricting uptake to the relevant cell population, accumulation in non-relevant areas such as liver or bladder, the requirement for larger doses to allow sufficient signal in the relevant cells leading to increased background signal, clearance of label and clinical exposure limits if the agent is radioactive. On the other hand, the technique can be significantly cheaper as there is no requirement for cell handling and purification *ex vivo*. This also makes *in vivo* labeling is less labor intensive and therefore more amenable to large scale studies. Long and colleagues exploited *in situ* labeling through cell-to-cell transfer (25). In a mouse model they injected irradiated tumor cells labeled with SPIO and examined the migration to and accumulation in draining lymph nodes of APC which captured antigen from the injection site.

An alternative labeling technique available to animal models is to transduce cells to express reporter genes, such as enzymes that trap tracers for PET; fluorescent proteins such as GFP for fluorescence imaging; luciferase for bioluminescence imaging; or iron transporters or CEST proteins for MRI contrast (9). Such reporter gene expression is well-suited for the detection of proliferative cells, as the label does not dilute with cell division. Furthermore, continued expression over the cell's lifetime allows longitudinal tracking, and can even be coupled to the expression of a particular gene of interest, or at the very least, to viability. However, the applicability of genetically modified cells to humans is not clear.

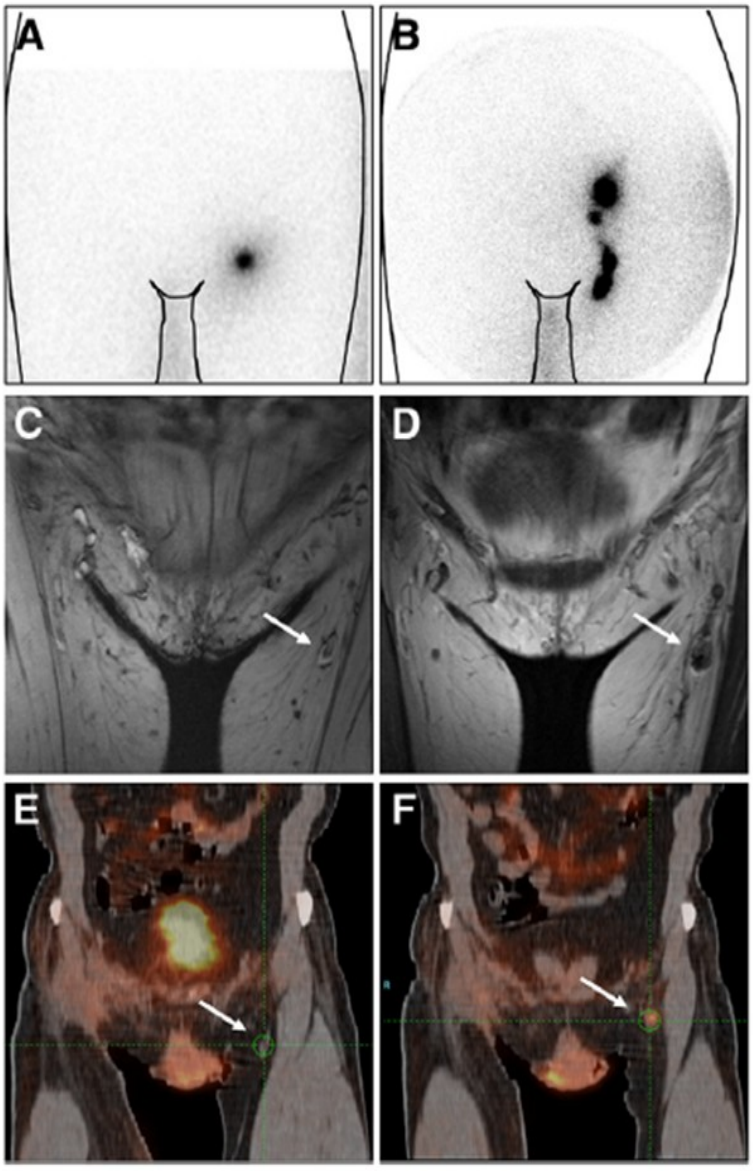

Figure 1. Examples of in vivo imaging of cellular therapy in clinical studies. Different modalities can be used to track pre-labeled dendritic cells after injection, or to image their effect on the local immune system. For example, phagocytic DC can be labelled with ^{111}Indium oxinate and visualized by scintigraphy directly after injection in the lymph node (A) and even 48 hours later (B). Distribution or spreading over a number of secondary lymph nodes indicates active migration to secondary lymphoid organs and the number of dendritic cells per spot can be calculated as percentage of total injected cells. In contrast to scintigraphy, MRI has excellent soft tissue contrast with highly detailed anatomical information. Here, DC were labelled with SPIO and injected i.n. in the same patient as (B), following scintigraphy, MRI scanning was performed directly after injection (C) and 48 hours later (D). MRI allows determination of the exact location of injected cells, e.g. in a lymph node or fatty tissue, and to an exact number of lymph nodes (1). In another patient, the metabolic activity of the target lymph node before (E) and after (F) a series of i.n. DC vaccinations was investigated using ^{18}F-FDG PET. An increase in glucose metabolism indicates activated lymphocytes, resulting from interaction with transplanted dendritic cells.

3. Tracking immune cells

Anti-cancer immunotherapy is an emerging approach to enhance endogenous tumor-directed immune responses. This strategy aims to avoid the harsh side effects that accompany chemotherapy by inducing toxicity to tumor cells in a highly selective manner. The immune system is designed to detect and eradicate pathogenic foreign and transformed body cells. Key players include professional antigen presenting cells (APC), e.g. DC and effector cells like $CD8^+$ cytotoxic T cells, $CD4^+$ helper T cells, $CD4^+CD25^+$ regulatory T cells and natural killer (NK) cells. Upon activation by pathogenic or abnormal cells, DC migrate to LN where they can activate effector cells, thus triggering an immune response (26). A long-term tumor-directed immune response is established upon concerted action of these diverse components of the immune system, and is the goal of clinical DV vaccination trials.

Most clinical studies exploit either *ex vivo* generated tumor antigen-loaded autologous DC or adoptively transferred tumor-specific cytotoxic T cells, i.e. the initiators or the final executors of the anti-tumoral response cascade. Even though the field of immunotherapy is rather new and numerous variables need further investigation, it has consistently shown immunological and clinical responses, albeit in a subset of patients (27). Other cellular therapeutics which have been used in clinical trials include stem cells, particularly in cardiomyopathy and neurological conditions, although imaging has been less commonly carried out. Here, we will focus on the role of imaging in the development of DC-based vaccines and adoptively transferred tumor-specific T cells in melanoma and discuss the use of imaging in optimizing stem cell therapy.

Table 1.

Modality	Used to track cells in humans	Relative sensitivity	Longitudinal cell tracking	Quantification of cell numbers	Assessment of cell viability or function	Reference
Nuclear medicine: Tracers, such as ^{111}In, ^{99}Tc or ^{18}F, or ionizing radiation for imaging						
Scintigraphy	Yes	+++	+	++	No	(4)
SPECT	Yes	++	+	+++	No	(4)
PET	Yes	+++	+	+++	Yes	(28)
Acoustic: Perfluorocarbon bubbles						
Ultrasound	Possible	+	+	+	No	(29)
MRI: Contrast agents such as iron oxide or gadolium, or ^{19}F cell tracers						
Metal-based contrast agents	Yes	+++	+++	+	No	(17) (30)
^{19}F MRI	Possible	+	+++	+++	No	(31)
Optical: Fluorescent dyes, proteins or quantum dots; bioluminescence detects luciferase activity						
Fluorescence	No	+	+++	+	Yes	(32)
Bioluminescence	No	++	+++	++	Yes	(32)
Two-photon	No	+++	++	++	Yes	(33)

3.1 Imaging DC therapy

DC used in therapy are autologous cells, generally purified and differentiated from the monocyte fraction of peripheral blood mononuclear cells. Alternatively, immature DC can be obtained from circulating CD34$^+$ progenitor cells. New techniques have become available to directly isolate specific DC populations from peripheral blood by positive selection using sorting beads. Immature DC can be activated by adding maturation stimuli like pro-inflammatory cytokines or pathogen-associated danger signals, resulting in upregulated expression of antigen-presenting molecules, co-stimulatory molecules and chemokine receptors (20, 26). Typically, DC are loaded with tumor antigens either by incubation or electroporation of encoding mRNA before transfer to induce antigen-specific responses. The influence of these parameters on the ensuing immune response is not fully understood. Other variables include those summarized in Table 2. In general, translocation to LN is considered an essential step in DC therapy and therefore *in vivo* imaging plays a key role in optimizing DC trials. Table 3 summarizes DC clinical studies, primarily with radioactively labeled DC.

DC migration to LN is a key step in the activation of the immune system, and has been extensively studied using scintigraphy. Scintigraphic imaging allows quantification of low numbers of cells; in general, 2x10^4 labeled cells can be reliably tracked. However, scintigraphy alone does not show whether the DC actually interact with lymphocytes in the LN. In our studies, we were able to determine the exact location of the labeled DC within the LN by concurrently labeling DC with ^{111}In for scintigraphy and iron oxide for MRI (1). High resolution MR on excised LN and immunohistological stainings further demonstrated interaction of these DC with T cells (34). The role of imaging in these studies has been critical- there is no other technique to monitor the efficacy of DC therapy in early stages, short of invasive tissue biopsies.

Effect of the route and site of transfer on DC biodistribution

DC have been administered by various routes in clinical trials: Intralymphatic (i.l.), intravenously (i.v.), intradermally (i.d.), subcutaneously (s.c.) or intranodally (i.n.), and combinations of these (Table 3). In i.l, i.n., i.d. and s.c. administration, specific LN are targeted (typically the draining LN), whereas in i.v. administration the DC are distributed over a large volume and available for entry to multiple LN.

Intradermal vaccinations are the most common. The dermis is richly permeated with lymphatic vessels with loose endothelium accessible to DC. Scintigraphic data shows that i.d. transfers result in

Table 2.

Variable	Imaging modality	Example	References
Delivery			
Route/site	MRI	SPIO-labeled DC monitored after i.v., s.c. or i.d. transfer	(35)
Real-time guided injections	MRI	Magnetocapsule-encapsulated islets, or with an MR-trackable injection cathether	(36, 37)
Number of cells	Scintigraphy	^{111}In-labeled DC monitored after intranodal or i.d. transfer	(15)
Pretreatment	Scintigraphy	Pretreatment of host environment with cyclofosfamide	(38)
Scaffolds	n/a	Embedding transplanted cells in biodegradable polymeric matrices, for example to increase access to nutrients	(39-44)
Cells			
Purification/culturing protocol	n/a	Cytokines used to culture DC	(45)
Status	Scintigraphy	Mature and immature ^{111}In-labeled DC	(15)
Cell treatment	MRI, scintigraphy	antigen loading of DC	(45) (25)

a reproducible delivery of up to 4% of the injected dose of mature DC to the LN, regardless of the maturation conditions or mode of antigen loading (Table 3). As discussed above, this relatively low number of emigration from the injection side is likely due to massive apoptosis from hypoxic conditions at the injection site and a high tissue density that prohibits migration. From the data in Table 3, it appears that more migration occurs when smaller numbers of cells are injected. As even these small numbers of cells that reach the LN are sufficient to induce tumor-directed immune responses (34), these DC are thought to display an optimal maturation phenotype. The results with s.c. administration are more variable, with only some studies detecting migration to LN, although always less than 4%. The subcutis consists of larger lymph vessels and has a different vasculature from the dermis, resulting in a less favorable milieu for DC. Variations in cell migration numbers upon s.c. injections might also be caused by differences in injection techniques.

Next to i.d. transfer, i.n. administration is the most common in clinical studies. As the LN is the site of immune activation, delivery of DC directly into the LN obviates the need for specific and optimized migratory capacities and directly thrusts the entire dose of cells to the LN. The percentage of cells that migrate from the primary injected node to secondary nodes ranges from 0-84%. This large variability cast doubt on the accuracy of i.n. injections, even when administered with ultrasound guidance. Therefore, we studied the migration and localization of a DC population dual-labeled with ^{111}In and iron oxide using scintigraphy and high resolution anatomic MRI (1). Surprisingly, in 4 out of 8 vaccinations we observed no migration to adjacent LN due to misinjection of the DC, even with ultrasound-guided injections by an experienced radiologist. Intralymphatic delivery of DC vaccines may be an alternative to i.n. injections as it would not affect LN architecture. However, this is technically challenging and therefore less suitable for routine clinical use.

Intravenous administration results in the same pattern of distribution in all clinical studies, starting with entrapment in the dense vasculature of the lungs. The lungs are the first network of small arterioles encountered after i.v. injection, and the entrapment may be caused by non-specific activation due to *ex vivo* handling of the cells. This is supported by the finding that mature DC are trapped in the lungs for a longer period than immature DC (46). In the next 24 hours, the DC redistribute mainly to the liver, spleen and bone marrow. No LN localization has been detected, as would have been expected based on studies using normal peripheral blood leukocytes (47). It is not clear whether DC actually do not reach the LN or whether SPECT or scintigraphy are not sensitive

enough to detect the small numbers of cells that might reach the LN. Hence, DC migration to LN upon i.v. transfer has not yet been demonstrated in humans.
Taken together, these studies demonstrate that i.d. vaccination results in a reproducible delivery of a small, but potent, number of DC to the LN. It should be noted that localized transfers, such as i.d. or i.n. injections, are much easier to image than systemic transfers, due to the higher cell densities at the site of injection and a more restricted migration range relative to systemic transfers.

DC dosage
A dose of 10-15 $x10^6$ cells per injection is typical for localized transfers. For i.v. administration, the cell numbers are larger, as is their distribution volume. The low rates of active migration observed (generally <4%) suggest that the conditions at the site of transfer are not optimal for emigration as discussed above. Analysis of the injection site of i.n. and i.d. vaccination revealed that SPIO-labeled DC die within the first 48 hours and are scavenged by macrophages (34).
Transferring larger numbers of cells increases the odds that the small percentage of migrating cells are detected, as the number of cells detected is limited by the sensitivity of the imaging technique. Ideally, the data should be confirmed by *ex vivo* analyses when tissue samples are available. Antigen capture by DC and subsequent migration to LN has been studied in animal models, where *ex vivo* isolation of *in situ* primed APC from the LN allowed validation and quantification of these cells (25).

3.2 Imaging T cell therapy
Another approach to actively enhance tumor-directed immune responses is to directly isolate endogenous tumor-specific immune cells (21). Malignancies are often infiltrated with tumor-specific cytotoxic T cells or NK cells which have been rendered impotent, likely due to the immunosuppressive tumor-microenvironment. Therefore, *ex vivo* expansion of purified tumor-specific immune cells offers opportunities to manipulate their avidity, cytotoxicity and specificity. Another approach is to engineer normal lymphocytes into tumor-specific lymphocytes by transfection of specific T cell receptors. In both strategies, the enriched population is then transferred back into the patient. The host environment can also be preconditioned by lympho-depletion with chemotherapy and/or irradiation. Several important issues need to be addressed when a new study like this is designed and imaging could help to optimize these variables. Most clinical studies that monitored transferred cells after direct labeling are over 20 years old as more recent work has focused on preclinical techniques to investigate indirect labeling of transferred cells.

Tracking transferred cells to tumor sites
Intravenous administration is the most widely used route, as the number of transferred tumor-specific T cells is usually large (>10^9 cells). In some studies intratumoral administration is used, although no imaging studies have been carried out in these investigations. In one study activated killer monocytes were administered intraperitoneally in patients with ovarian cancer and intraperitoneal tumor patches (54). No activity outside the peritoneum was detected up to 9 days after injection using scintigraphy on ^{111}In. However, this proves neither tumor specific localization of the transferred cells, nor their ability to evade the peritoneal cavity as *ex vivo* validation was not carried out. The distribution of T cells after i.v. administration follows a similar pattern to other immune cells; cells are first trapped in the lungs, after which they are distributed to the liver, spleen and bone marrow, as measured using scintigraphy (18, 55). However, activated tumor-specific T cells are expected to home to tumor cells to exert their action.

Table 3.

ref	source	activation status	Culture conditions	Antigen loading	Radioisotope	Route	No of cells (x10.6)	No of pts	Migration to LN, no pos/no total (range %)
(48)	monocyte	immature		Pulsing tumor lysate	^{111}In-oxine	i.d.	6	1	0.42
(48)	monocyte	immature		Pulsing tumor lysate	^{99}Tc-HMPAO	i.d.	6 – 9	3	3/3, 0.05 – 0.22
(49)	monocyte	immature		Electroporated RNA	^{111}In-oxine	i.d.	12.5	6	0
(49)	monocyte	immature		Electroporated RNA	^{111}In-oxine	i.d.	12.5	2	0.54
(23)	monocyte	immature		Pulsing tumor antigen	^{99}Tc-HMPAO	i.d.	10	3	1/3, 0.07
(15)	monocyte	immature		Pulsing tumor antigen	^{111}In-oxine	i.d.	10	8	0.2 – 0.4
(35)	monocyte	immature		Lipid transfected RNA	^{111}In-oxyquinoline	i.d.	1	4	Max 0.41
(50)	monocyte	immature		Pulsing tumor antigen	^{99}Tc-HMPAO	i.d.	1 – 7	5	"+"
(46)	monocyte	immature		Pulsing tumor antigen	^{111}In-oxine	i.d.	n/a	3	2/3, 0.48
(23)	monocyte	immature		Pulsing tumor antigen	^{111}In-oxine	i.d.	10	3	0/3
(35)	monocyte	immature		Lipid transfected RNA	^{111}In-oxyquinoline	s.c.	1	4	0/4
(46)	monocyte	immature		Pulsing tumor antigen	^{111}In-oxine	s.c.	n/a	3	1/3
(23)	monocyte	immature		Pulsing tumor antigen	^{111}In-oxine	s.c.	10	3	0/3
(23)	monocyte	immature		Pulsing tumor antigen	^{99}Tc-HMPAO	s.c.	10	3	0/3
(15)	monocyte	immature		Pulsing tumor antigen	^{111}In-oxine	i.n.	10	7	0.5 – 30
(35)	monocyte	immature		Lipid transfected RNA	^{111}In-oxyquinoline	i.v.	100	3	0/3
(46)	monocyte	immature		Pulsing tumor antigen	^{111}In-oxine	i.v.	33 – ^{18}0	3	0/3
(46)	monocyte	immature		Pulsing tumor antigen	^{18}F-FDG	i.v.	130 – 150	2	0/2
(23)	monocyte	mature	MPL	Pulsing tumor antigen	^{111}In-oxine	i.d.	10	3	1/3, 0.25
(46)	monocyte	mature	IFN-g, Imukin, FMKp	Pulsing tumor antigen	^{64}Cu-PTSM	i.d.	15.3 – 21.3	2	2/2, 0.06, 0.10
(49)	monocyte	mature	IL-1b, TNF-a, IL-6, PGE2	Electroporated RNA	^{111}In-oxine	i.d.	12.5	8	0.5 – 2.0
(46)	monocyte	mature	IFN-g, Imukin, FMKp	Pulsing tumor antigen	^{111}In-oxine	i.d.	n/a/	3	2/3, 1.08, 1.29
(23)	monocyte	mature	MPL	Pulsing tumor antigen	^{99}Tc-HMPAO	i.d.	10	3	0/3
(15)	monocyte	mature	IL-1b, IL-6, TNF-a, PGE2	Pulsing tumor antigen	^{111}In-oxine	i.d.	10	10	10/10, 0.5 – 3.9
(34)	monocyte	mature	IL-1b, IL-6, TNF-a, PGE2	Pulsing tumor antigen	^{111}In-oxine	i.d.	15	12	12/12, 0.1 – 3.7
(51)	monocyte	mature	IFNg, Ribomunyl	Pulsing tumor antigen	^{111}In-oxine	i.d.	8 – 34	6	2/6, 0 – 1.8
	monocyte	mature	IL-1b, IL-6, TNF-a, PGE2	Pulsing tumor lysate	^{111}In-oxine	i.d.	6.7 – 7	2	2/2, 0.95 – 3.14
	monocyte	mature	IL-1b, IL-6, TNF-a, PGE2	Pulsing tumor lysate	^{99}Tc-HMPAO	i.d.	4 – 12	5	5/5, 0.39 – 1.75
(46)	monocyte	mature	IFN-g, Imukin, FMKp	Pulsing tumor antigen	^{111}In-oxine	s.c.	n/a	3	3/3, 1.3, 0.73
(23)	monocyte	mature	MPL	Pulsing tumor antigen	^{111}In-oxine	s.c.	10	3	1/3, 0.25
(46)	monocyte	mature	IFN-g, Imukin, FMKp	Pulsing tumor antigen	^{64}Cu-PTSM	s.c.	17.6	2	1/2, 0.04
(23)	monocyte	mature	MPL	Pulsing tumor antigen	^{99}Tc-HMPAO	s.c.	10	3	0/3
(46)	monocyte	mature	IFN-g, Imukin, FMKp	Pulsing tumor antigen	^{64}Cu-PTSM	i.n.	n/a	2	0/2
(1)	monocyte	mature	IL-1b, IL-6, TNF-a, PGE2	Pulsing tumor antigen	^{111}In-oxine	i.n.	15	9	4/9, 1.7 – 17
(46)	monocyte	mature	IFN-g, Imukin, FMKp	Pulsing tumor antigen	^{111}In-oxine	i.n.	n/a	3	1/3
(15)	monocyte	mature	IL-1b, IL-6, TNF-a, PGE2	Pulsing tumor antigen	^{111}In-oxine	i.n.	10	7	0.4 – 84
(34)	monocyte	mature	IL-1b, IL-6, TNF-a, PGE2	Pulsing tumor antigen	^{111}In-oxine	i.n.	15	15	9/15, 0 – 56
(52)	monocyte	mature	IL-1b, IL-6, TNF-a, PGE2	RNA electroporated	^{111}In-oxine	i.n.	15	8	6/8, 0 – 65
(51)	monocyte	mature	IFNg, Ribomunyl	Pulsing tumor antigen		i.n.	7 – 25	5	2/5, 0 – 26
(53)	CD34+ proge	mature	TNF-a	Pulsing tumor antigen	^{111}In-oxine	i.v.	16 – 17	2	0/2
(46)	monocyte	mature	IFN-g, Imukin, FMKp	Pulsing tumor antigen	^{64}Cu-PTSM	i.v.	140 – 160	2	0/2
(46)	monocyte	mature	IFN-g, Imukin, FMKp	Pulsing tumor antigen	^{111}In-oxine	i.v.	110 – 250	3	0/3
(53)	CD34+ proge	mature	TNF-a	Pulsing tumor antigen	^{99}Tc-HMPAO	i.l.	10 – 13	3	"+"
(51)	monocyte	mature	IFNg, Ribomunyl	Pulsing tumor antigen	^{111}In-oxine	i.l.	33 – 50	4	4/4, "80"

Early imaging studies using ^{111}In-oxine labeled *ex vivo* expanded T cells and NK cells (56) indeed showed that tumor-specific T cells do traffic to tumor sites, (57-61) whereas normal lymphocytes do not. In a recent study using whole body SPECT in breast cancer patients, it was shown however that *ex vivo* ^{111}In-labeled tumor-specific T cells do not penetrate solid tumor masses, although they will attack loose tumor cells circulating in bone marrow (55). This observation might indicate either that not all tumors are susceptible to this treatment or that this treatment might be less effective in

patients with high tumor burden. Hence, combining this treatment with therapies that target tumor stromal cells, such as angiogenesis inhibitors, may probe beneficial. Another explanation is that the transferred cells lack specific homing receptors for effective localization to the tumor. Regardless, relocation to tumor sites is correlated with clinical response (60). In this respect, it would be tempting to investigate whether transferred cells can cross the blood brain barrier, since adoptive cell transfer can induce regression of brain metastasis (21). To conclude, active relocation of transferred immune cells to tumor sites is crucial for their therapeutic effect and incorrect delivery is one factor that hampers clinical efficacy. Imaging is well-suited to study cell distribution *in vivo.* However, molecular studies of adhesion and chemotactic factors are warranted to define a minimal set of homing receptors for immune cells in clinical adoptive cell transfer studies (57).

Pre-treatment

In the previous section, we concluded that therapeutic effect of adoptive cell transfer in cancer patients at least partly depends on the capacity of transferred T cells to home to the tumor. Different cell populations might have different intrinsic homing properties, which can be enhanced during *ex vivo* expansion. Another approach to improve clinical responses by improving homing to tumor site is demonstrated by the finding that pretreatment with cyclophosphamide increased the tumor localization of transferred cells (60). Furthermore, the concomitant administration of Interleukin-2 is known to induce homing of T cells to LN. Although this has not been demonstrated in imaging studies, it is likely that these pretreatments might explain the improved results of the combined treatment. Thus, one should consider using imaging techniques to support new combinations of adoptive cell transfer with immune modulating agents.

Optimizing dose and frequency

Thus far, the focus has been mainly on the quality and characteristics of transferred cells. However, dosage and frequency are important variables in immunotherapy. By using ^{111}In-labeled tumor-specific T cells, Pockaj *et al.* demonstrated an association between homing to the tumor site and the number of cells administered per transfer (60). As tumor destruction causes the release of inflammatory cytokines which attract immune cells, it is likely that this correlation is more complex than simple dose dependency.

To determine the optimal frequency of adoptive cell transfer, one should be informed about the persistence of transferred cells. This has mostly been done by using PCR to detect specific antigen receptors on cells purified from blood. PCR allows sensitive quantification of the number of circulating transferred cell, although not *in vivo*. Furthermore, isolated cells can be tested for phenotype and function *ex vivo*. However, as discussed above, homing to tumor sites of transferred cytotoxic and NK cells or homing to LN for DC is crucial, and these cells are not available for PCR detection, as tissue samples are not generally available. A recent preclinical study used quantitative *in vivo* ^{19}F MRI to longitudinally follow the increase and subsequent decrease of the number of antigen-specific T cells homing to a specific LN, over a period of 3 weeks in mice (62). This technique may be useful to track cell migration clinically in the near future. Currently, cells are labeled with radioisotopes, where the absence of excreted radioactivity suggests that the transferred cells have remained intact and survived in the host. It has been shown that ^{111}In-labeled allogeneic NK cells remain detectable in blood for as long as 6 days after transfer, with some accumulation in tumor tissue using whole body scintigraphy in humans (56). For tumor-specific cytotoxic T cells, transferred cells circulated up to two weeks after transfer, with unimpaired effector function for at least 24 hours (61). The next step in these developments is the use of transferred cells that express tumor-homing molecules or specific enzymes to trap imaging probes. The first report of this novel approach imaged a patient with glioblastoma multiforme who received cytotoxic T cells transduced with a tumor-homing, chimeric T cell receptor and the PET-reporter gene HSV1*tk*, which phosphorylates

and traps an ^{18}F PET probe (63). By combining MRI and PET, the authors showed specific localization of the transferred cells to the tumor lesion.

3.3 Imaging in the other cellular therapies

Another emerging application of cellular therapy is the transfer of stem cells to replace damaged cells in tissues that have a limited capacity to regenerate. Typically, these are cardiac myocytes in ischaemic myocardium, neuronal cells in ischaemic brain injury or degenerative diseases like Alzheimers' disease, and donor pancreatic islets in type I (autoimmune) diabetes. In this section we will discuss imaging in cardiac disease and the transplantation of pancreatic islets. Cardiac diseases like acute myocardial infarction and congestive heart failure are increasingly prevalent and current therapies aim to reduce stress on the remaining cardiomyocytes, although, no definitive therapeutic treatment is available. The engraftment of stem and progenitor cells has been extensively investigated in the recent years, with modest benefit in clinical outcome. Table 4 summarizes the clinical trials using radiolabeled cells to investigate their fate upon transfer. Intravenous transfer does not result in any accumulation of transferred cells to the myocardium (64), probably due to the lack of active homing and the poor perfusion of the injured sites. Furthermore, regardless of the type of cell that is used, transfer of cells into the coronary artery leads to only very low cell engraftment; maximum 39% after 1 hour and then decreasing in the next 24 hours. Optimizing the route of delivery, type of cell, timing after injury will improve results as revealed by these imaging studies.

The role of MRI in tracking progenitor cells in cardiac diseases is limited, although it obviates the use of radioisotopes in cells with high proliferative potential and long life span. Animal studies have shown that apart from the continuous motion of the heart, recent hemorrhages and nonspecific uptake of SPIO label by macrophages interferes with the SPIO-induced signal hypointensity of transferred cells (65).

However, in other cases, MRI does play an important role in the search for the optimal site of transfer, for example in the case of pancreatic islets (66, 67). Requirements for the site include a rich supply of oxygenated and nutrient-rich blood since islets are highly sensitive to hypoxia, drainage to the liver where the insulin acts, and local immune protection as type 1 diabetes is an autoimmune disorder. To the best of our knowledge, only one clinical study has been published using MRI to study transplanted islets longitudinally (13). In this study, iron-labeled allogeneic pancreatic islets were transplanted in the hepatic portal vein. It was shown *in vitro* that labeling with ferucarbotran did not affect cell function and this was supported by the *in vivo* finding that all patients became insulin independent. However, the naturally high iron load in the liver interfered with detection of transplanted islets and the number of hypointense spots in the liver did not correlate with the number of transplanted cells. Validation using tissue biopsies was not possible, as it would damage the remaining functional islets. A second clinical study on tracking iron-labeled pancreatic islets is currently ongoing. In succession of their *in vitro* and animal work (67, 68), Jirak and colleagues have initiated a clinical study in which 8 patients were enrolled at the time of writing *(personal communication)*.

4. Concerns and future perspectives

Clinical imaging is far behind preclinical animal studies in terms of the resolution, sensitivity and label availability. The same is true for the scanners themselves, for example animal MRI scanners can reach 16T or higher, while 7T is considered "high field" for human scanner, with most clinical scanners being less than 3T. Thus, most of the cutting-edge development occurs in animal models. Hence, in this section we examine current preclinical work that is potentially applicable to clinical cell tracking, as well as discuss some general concerns about *in vivo* clinical cell tracking.

Table 4

Ref	Disease stage	Source of cells	label	Site of transfer	# of patients	Distribution in myocardium, <2 hour (%)	Distribution in myocardium, 24 hours (%)
(69)	5 – 10 days after stent for AMI	Bone marrow cells, unselected	^{18}F-FDG	Intracoronary, infarct related artery	6	1.3 – 5.3	n/a
(69)	5 – 10 days after stent for AMI	CD34+ bone marrow cells	^{18}F-FDG	Intracoronary, infarct related artery	3	14 – 39	n/a
(70)	3 – 300 days after AMI	Peripheral HSC	^{18}F-FDG	Intracoronary artery	17	0.2 – 3.3	1 patient "present"
(71)	Congestive heart failure	Bone marrow MNC	^{99}Tc	Intracoronary artery	6	5.4 ± 1.7	2.3 ± 0.6
(72)	18 – 22 months after AMI	CD34+	^{18}F-FDG	Intracoronary artery	7	1.2 – 5	n/a
(73)	AMI	Bone marrow MNC	^{99}Tc-HMPAO	Intracoronary artery	12	16.14 ± 7.06	10.29 ± 6.88
(74)	5 days to 17 years after AMI	Proangiogenic progenitor	^{111}In-oxine	Intracoronary	17	1 – 19	1 – 3
(75)	>12 months after AMI	CD133+ peripheral blood stem cells	^{111}In-oxine	intracoronary	2	6.9 – 8 2	2.3 – 3.2
(76)	9 – 81 months after AMI	CD133+ / CD34+ bone marrow progenitor cells	^{99}Tc-HMPAO	Intracoronary, infarct related artery	8	9.2 ± 3.6	6.8 ± 2.4
(77)	7 – 21 days after AMI	Peripheral blood CD34+	^{18}F-FDG	intracoronary	6	4 – 7	n/a
(73)	AMI	Bone marrow MNC	^{99}Tc-HMPAO	Intracoronary vein	6	4.62 ± 1.40	3.13 ± 0.99
(70)	3 – 300 days after AMI	Peripheral HSC	^{18}F-FDG	intravenous	3	0	n/a
(69)	5 – 10 days after stent for AMI	Bone marrow cells, unselected	^{18}F-FDG	Intravenous	3	0	n/a

4.1 Developments on the horizon

Several promising new technologies have been developed in preclinical studies. Here, we discuss some techniques that might translate to clinical use in the near future.

Optical imaging techniques have not been applied to humans for cell tracking both because of light penetration limitations and the lack of FDA-approved agents specifically for cell labeling. However, preliminary *ex vivo* labeling has been done. For example, human embryonic stem cell-derived cardiomyocytes were labeled with an FDA-approved contrast agent *ex vivo*. The dye used, indocyanine green, is currently used to determine cardiac output, hepatic function and other factors via blood tests. The labeled stem cells remained fluorescent up to 48 hours after labeling, without any observed effect on viability or cell function (78). Dyes and microscopy are also commonly used in surgery, for example to locate LN. These clinical trials are reviewed elsewhere (79). It is conceivable that these techniques can be adapted to allow cell tracking, perhaps in conjunction with surgery. In all cases, the effects of labeling on cell function, especially in the case of long-lived cells must be fully characterized before clinical use.

One exciting development that might soon make the jump to clinical use is the application of non-proton MRI for cell tracking, primarily using ^{19}F MRI for quantitative, longitudinal cell tracking *in vivo* (80). The use of a tracer based on ^{19}F, instead of metal-based contrast agents such as iron oxides, allows for quantification of cell numbers directly from the image data. The use of such "hot-spot" imaging would also overcome the difficulty in positive identification of labeled cells using conventional metal-based contrast agents in MRI. Another recent development is the advent of imaging using chemical exchange saturation transfer (CEST) labels. These agents work by locally modifying the ^{1}H resonance frequency in a very specific manner, and can be made sensitive to factors such as temperature, pH or metabolite concentrations, thus possibly allowing detection of cell function *in vivo* (81, 82). CEST imaging has also been applied to reporter genes (9, 83). The recent interest in hyperpolarization, which results in a short-lived signal increase of several orders of

magnitude, has been used to study such elusive factors as the real time metabolism of substrates using MRI (84, 85). This technology may also allow the development of injectable agents for cell tracking, analogous to injectable agents used in SPECT or PET imaging- but without the radioactivity. Another recent study used labeled cells with iron for MRI contrast and also used the magnetic gradients in the scanner to direct the cells in a vascular bifurcation phantom (86). This opens the possibility of interactive manipulation of the labeled cells, perhaps using real time imaging and scanners without a closed bore that allow access to surgeons during imaging. Thus, the field offers great promise for *in vivo* imaging in the near future.

4.2 Multimodal imaging

Multimodal imaging is the use of different, complementary imaging modalities to study the same subject. These images might be of the same label or the same cells with different labels. Furthermore all imaging may occur in the same scanner or in different scanners with subsequent image registration. The main draw of multimodal imaging is the use of the strengths of one imaging modality to overcome the weaknesses of another. For example, tracer-specific SPECT or PET scans are commonly combined with CT to provide functional information with anatomic context.

The translation of this technology to the clinic is challenging. Technical challenges include the design and construction of safe, reliable multi-modal imaging scanners and the development of image registration algorithms when different scanners are used requiring patient repositioning. However, dual modality imaging has already become established in the diagnosis, staging and monitoring of response to treatment, especially with cancer patients, primarily using SPECT/CT and, more recently with PET/CT (87). Dual PET/CT imaging is relatively well-established in animal models, and has begun to be used in humans. A recent study demonstrated the clinical value of this technology in patients with thyroid carcinoma (88); after comparing the accuracy of diagnoses with PET, CT or PET/CT scan data, they found PET/CT data was far superior and allowed an accurate diagnosis of both the localization and characterization of lesions in all 18 of the patients imaged. Similarly, SPECT/CT scanners are used to provide functional data via SPECT and anatomic data via CT, generally in cancer and neurology (89). Although these techniques have not yet been applied to cellular therapies, further development of such technology will allow it in the future. Finally, it should be noted the use of techniques using injectable radioactive tracers for PET or SPECT will also require the identification of suitable (highly-specific) targets on the transplanted therapeutic cells.

Designing a dual functional scanner combining MRI with either PET or SPECT has proved more difficult due to the strong magnetic fields required for MRI. A prototype human PET/MRI scanner was tested to acquire images of the human brain in volunteers and patients (90). In this prototype scanner, PET acquisition did indeed interfere with the MR imaging, but further development may allow the simultaneous acquisition of morphologic (MRI) and functional (PET) data from the same scan. The development of PET/MR scanners is discussed elsewhere (91). One of the first clinical studies to use MRI to track injected DC in melanoma patients combined MRI with scintigraphy (1), although not in the same scanner. The injected cells were labeled with both iron oxide for MRI contrast and ^{111}In for quantitative scintigraphy. This was the first study that assessed both the localization of the transplanted cells (MRI) and quantified the percentage of migratory cells (scintigraphy). In addition, the cells were injected in the LN using ultrasound guidance.

In preclinical studies, *in vivo* cell tracking has been carried out with cells labeled with nanoparticles detectable by no less than four imaging modalities- MRI, PET, bioluminescence and fluorescence (92). Dual-modality probes are now increasingly common in preclinical models.

4.3 Are we imaging labeled cells or just label?

This is a vital question that must be considered. It is especially important in longer-lived, dividing and migratory cells that are pre-labeled before transfer. *In vivo* imaging modalities, in many cases, detect

only the presence of the contrast agent or the label, without being sensitive to whether the label is still associated with the relevant cells. In general, label retention in transferred cells is not a problem soon after transplant. The problem arises when labeled cells begin to divide, migrate or die. Label can also be transferred to neighboring cells or to the extracellular matrix. Thus, it is necessary that the clearance pathways and timelines of labels are well-studied beforehand. When bone marrow stromal cells were labeled with an MRI contrast agent, a fluorescent dye or with GFP and transferred to areas of inflammation or angiogenesis in a mouse model, it was found that the resident macrophages took up as much as 15% of these labels, regardless of the number of cells transferred or their viability (93). A similar study where iron-labeled cells were implanted in the ischemic myocardium in mice, found that there was no change in the signal voids observed in MRI scans in terms of their number, size or location regardless of whether the transferred cells were alive or dead at the time of transplant (94). Movement of label in the images suggests that the cells are alive and actively migrating, although it could be an artifact of bystander uptake of the label or of dead labeled cells by resident phagocytes, and reflect their movement. These studies show that the fate of label must be carefully characterized, generally using conventional histological techniques or flow cytometry, before conclusions can be made about cell numbers or even localization from *in vivo* image data alone.

Many cell therapy approaches utilize transfers of externally cultured cells, which may originate from the patient. This external phase is ideal for cell labeling with imaging agents, and it is the most common approach in both clinical and preclinical models. It also allows more effective label uptake in non-phagocytic cells, such as stem cells or T cells, which often do not take up imaging label effectively. In preclinical models, this low uptake can be countered through the use of transfection agents, which are generally not an option for clinical studies. Thus techniques such as electroporation or the use of positively charged peptides have been tested to improve cell loading (95, 96). Specific antibodies can also be used *in vitro* to increase cell loading (97). Regardless of the loading technique, cell loading needs to be reproducible and precise, such that the average amount of label per cell can be accurately quantified. This is vital for quantifying cell numbers from the *in vivo* image data. However, difficulties occur when the cells are transferred *in vivo* and the cell loading can then no longer be monitored. This is especially problematic with dividing cells where the label can either be lost or distributed between daughter cells. Cell division can also dilute the label down to undetectable levels. Often, these processes cannot be studied *in vitro* as many cell types cannot be cultured for long periods of time, for example pancreatic islets. However, quantitative cell tracking has been carried out for up for 3 weeks in actively dividing T cells using ^{19}F MRI "*in vivo* cytometry" in mice (62). In this case, the error due to the rate of cell division was considered tolerable.

4.4 Single cell imaging

Imaging single cells *in vivo* would allow quantitative and qualitative assessment of the success of the treatment, as each transferred cell could be monitored. Imaging a single cell *in vivo* using any technique other than microscopic approaches is a challenge even in preclinical models. Currently, MRI has the highest resolution for imaging soft tissue, and accordingly, single cells have been detected using MRI using clinical imaging parameters: Cells were labeled with low amounts of iron and imaged in a 1.5 T clinical MRI scanner with a voxel size of 60 μm^3 (98). Single cell *in vivo* imaging has thus far not been carried out in humans and will likely require significant further development of clinical MRI scanners, imaging techniques and cell labels.

From a more practical standpoint, it would be beneficial to be able to monitor small numbers of cells, or larger numbers of cells with lower label loading. For example, several studies have shown that only up to 4% of injected DC reached the LN, and that this migration is better when smaller numbers of cells are injected (see Table 3). This would mean much even lower cell numbers reaching the LN,

despite a higher percentage of migration, straining current detection limits with techniques such as scintigraphy.

4.5 Towards standardized reporting

Another key problem, that is perhaps simpler to solve, is the lack of a standardized reporting protocol for imaging and cell quantification studies. Thus, comparison and meta-analysis between studies is somewhat unnecessarily complicated, as illustrated by the incomplete data in Table 3. We suggest that in future imaging studies involving quantitative cell imaging it would be useful to include a minimal set of parameters, outlined in Table 5. This list is not exhaustive, but it includes some of the more common variables that need to be defined to allow inter-study analyses.

5 Conclusions

Medical imaging technology is already allowing the study of transplanted cells *in vivo*. One major hurdle that must be overcome is the cost of expensive imaging scanners - often multi-million dollar investments. Multimodal scanners are even more expensive. It would be ideal if the cheaper imaging techniques, such as ultrasound or fluorescence-based approaches, could be adapted to clinical cell tracking. For example, dyes are already used in more invasive procedures to identify LN or demarcate tumors (99, 100). Ultrasound has also been used with targeted imaging labels, particularly perfluorocarbon microbubbles (101). Such targeted contrast agents might allow the monitoring of transplanted cells noninvasively and in an extremely cost-efficient manner (101). However, much development is needed for these techniques to be adapted to cell tracking. Furthermore, the imaging modality or modalities selected must be carefully tailored to the model, in particular their detection thresholds must be considered.The incorporation of imaging in the clinical protocol is illustrated briefly in the graphical abstract. As described in the text, this would require both a labeling step (either *ex vivo* or *in vivo*), and one or more imaging steps at relevant time points after cell transfer. A control “before” image may also be necessary for background signal. The development of successful cell therapy is intricately coupled to the development of medical imaging technology that can allow non-invasive, longitudinal and quantitative monitoring of the transferred cells. This new technology might validate the old adage “seeing is believing”.

References

1. de Vries, I.J., et al., *Magnetic resonance tracking of dendritic cells in melanoma patients for monitoring of cellular therapy.* Nat Biotechnol, 2005. 23(11): p. 1407-13.
2. van der Windt, D.J., et al., *The choice of anatomical site for islet transplantation.* Cell Transplant, 2008. 17(9): p. 1005-14.
3. McAfee, J.G. and A. Samin, *In-111 labeled leukocytes: a review of problems in image interpretation.* Radiology, 1985. 155(1): p. 221-9.
4. Palestro, C.J., C. Love, and K.K. Bhargava, *Labeled leukocyte imaging: current status and future directions.* Q J Nucl Med Mol Imaging, 2009. 53(1): p. 105-23.
5. Bleeker-Rovers, C.P., J.W. van der Meer, and W.J. Oyen, *Fever of unknown origin.* Semin Nucl Med, 2009. 39(2): p. 81-7.
6. Barentsz, J.O., J.J. Futterer, and S. Takahashi, *Use of ultrasmall superparamagnetic iron oxide in lymph node MR imaging in prostate cancer patients.* Eur J Radiol, 2007. 63(3): p. 369-72.
7. Kim, J.A., et al., *Cellular immunotherapy for patients with metastatic colorectal carcinoma using lymph node lymphocytes localized in vivo by radiolabeled monoclonal antibody.* Cancer, 1999. 86(1): p. 22-30.
8. Thompson, M., et al., *In vivo tracking for cell therapies.* Q J Nucl Med Mol Imaging, 2005. 49(4): p. 339-48.
9. Gilad, A.A., et al., *MRI reporter genes.* J Nucl Med, 2008. 49(12): p. 1905-8.
10. Modo, M., *Noninvasive imaging of transplanted cells.* Curr Opin Organ Transplant, 2008. 13(6): p. 654-8.
11. Preynat-Seauve, O., et al., *Pluripotent stem cells as new drugs? The example of Parkinson's disease.* Int J Pharm, 2009. 381(2): p. 113-21.
12. Kiessling, F., *Noninvasive cell tracking.* Handb Exp Pharmacol, 2008(185 Pt 2): p. 305-21.
13. Toso, C., et al., *Clinical magnetic resonance imaging of pancreatic islet grafts after iron nanoparticle labeling.* Am J Transplant, 2008. 8(3): p. 701-6.
14. Bueno, E.M. and J. Glowacki, *Cell-free and cell-based approaches for bone regeneration.* Nat Rev Rheumatol, 2009. 5(12): p. 685-97.
15. De Vries, I.J., et al., *Effective migration of antigen-pulsed dendritic cells to lymph nodes in melanoma patients is determined by their maturation state.* Cancer Res, 2003. 63(1): p. 12-7.
16. Verdijk, P., et al., *Maximizing dendritic cell migration in cancer immunotherapy.* Expert Opin Biol Ther, 2008. 8(7): p. 865-74.
17. Bulte, J.W., *In vivo MRI cell tracking: clinical studies.* AJR Am J Roentgenol, 2009. 193(2): p. 314-25.
18. Schafer, R., et al., *Functional investigations on human mesenchymal stem cells exposed to magnetic fields and labeled with clinically approved iron nanoparticles.* BMC Cell Biol. 11(1): p. 22.
19. Suzuki, Y., et al., *In vitro comparison of the biological effects of three transfection methods for magnetically labeling mouse embryonic stem cells with ferumoxides.* Magn Reson Med, 2007. 57(6): p. 1173-9.
20. Figdor, C.G., et al., *Dendritic cell immunotherapy: mapping the way.* Nat Med, 2004. 10(5): p. 475-80.
21. Rosenberg, S.A., et al., *Adoptive cell transfer: a clinical path to effective cancer immunotherapy.* Nat Rev Cancer, 2008. 8(4): p. 299-308.
22. Walczak, P., et al., *Applicability and limitations of MR tracking of neural stem cells with asymmetric cell division and rapid turnover: the case of the shiverer dysmyelinated mouse brain.* Magn Reson Med, 2007. 58(2): p. 261-9.
23. Blocklet, D., et al., *111In-oxine and 99mTc-HMPAO labelling of antigen-loaded dendritic cells: in vivo imaging and influence on motility and actin content.* Eur J Nucl Med Mol Imaging, 2003. 30(3): p. 440-7.
24. Kedziorek, D.A., et al., *Gene expression profiling reveals early cellular responses to intracellular magnetic labeling with superparamagnetic iron oxide nanoparticles.* Magn Reson Med, 2010. 63(4): p. 1031-43.
25. Long, C.M., et al., *Magnetovaccination as a novel method to assess and quantify dendritic cell tumor antigen capture and delivery to lymph nodes.* Cancer Res, 2009. 69(7): p. 3180-7.
26. Banchereau, J. and A.K. Palucka, *Dendritic cells as therapeutic vaccines against cancer.* Nat Rev Immunol, 2005. 5(4): p. 296-306.
27. Lesterhuis, W.J., et al., *Dendritic cell vaccines in melanoma: from promise to proof?* Crit Rev Oncol Hematol, 2008. 66(2): p. 118-34.
28. Zhang, Y., et al., *Tracking stem cell therapy in the myocardium: applications of positron emission tomography.* Curr Pharm Des, 2008. 14(36): p. 3835-53.
29. Lindner, J.R., *Contrast ultrasound molecular imaging of inflammation in cardiovascular disease.* Cardiovasc Res, 2009. 84(2): p. 182-9.
30. Himmelreich, U. and T. Dresselaers, *Cell labeling and tracking for experimental models using magnetic resonance imaging.* Methods, 2009. 48(2): p. 112-24.
31. Srinivas, M., et al., *(19)F MRI for quantitative in vivo cell tracking.* Trends Biotechnol.
32. Sutton, E.J., et al., *Cell tracking with optical imaging.* Eur Radiol, 2008. 18(10): p. 2021-32.
33. Ng, L.G., et al., *Two-photon imaging of effector T-cell behavior: lessons from a tumor model.* Immunol Rev, 2008. 221: p. 147-62.
34. Verdijk, P., et al., *Limited amounts of dendritic cells migrate into the T-cell area of lymph nodes but have high immune activating potential in melanoma patients.* Clin Cancer Res, 2009. 15(7): p. 2531-40.
35. Morse, M.A., et al., *Migration of human dendritic cells after injection in patients with metastatic malignancies.* Cancer Res, 1999. 59(1): p. 56-8.
36. Barnett, B.P., et al., *Magnetic resonance-guided, real-time targeted delivery and imaging of magnetocapsules immunoprotecting pancreatic islet cells.* Nat Med, 2007. 13(8): p. 986-91.
37. Karmarkar, P.V., et al., *MR-trackable intramyocardial injection catheter.* Magn Reson Med, 2004. 51(6): p. 1163-72.

38. Lee, J.R., et al., *Combined treatment with intratumoral injection of dendritic cells and topical application of imiquimod for murine melanoma.* Clin Exp Dermatol, 2007. 32(5): p. 541-9.
39. Balakrishnan, B. and A. Jayakrishnan, *Self-cross-linking biopolymers as injectable in situ forming biodegradable scaffolds.* Biomaterials, 2005. 26(18): p. 3941-51.
40. Bensaid, W., et al., *A biodegradable fibrin scaffold for mesenchymal stem cell transplantation.* Biomaterials, 2003. 24(14): p. 2497-502.
41. Furth, M.E., A. Atala, and M.E. Van Dyke, *Smart biomaterials design for tissue engineering and regenerative medicine.* Biomaterials, 2007. 28(34): p. 5068-73.
42. Hannouche, D., et al., *Engineering of implantable cartilaginous structures from bone marrow-derived mesenchymal stem cells.* Tissue Eng, 2007. 13(1): p. 87-99.
43. Park, J.S., et al., *In vitro and in vivo test of PEG/PCL-based hydrogel scaffold for cell delivery application.* J Control Release, 2007. 124(1-2): p. 51-9.
44. Serban, M.A. and G.D. Prestwich, *Modular extracellular matrices: solutions for the puzzle.* Methods, 2008. 45(1): p. 93-8.
45. Pham, W., et al., *Dendritic cells: therapy and imaging.* Expert Opin Biol Ther, 2009. 9(5): p. 539-64.
46. Prince, H.M., et al., *In vivo tracking of dendritic cells in patients with multiple myeloma.* J Immunother, 2008. 31(2): p. 166-79.
47. Read, E.J., et al., *In vivo traffic of indium-111-oxine labeled human lymphocytes collected by automated apheresis.* J Nucl Med, 1990. 31(6): p. 999-1006.
48. Ridolfi, R., et al., *Evaluation of in vivo labelled dendritic cell migration in cancer patients.* J Transl Med, 2004. 2(1): p. 27.
49. Nair, S., et al., *Injection of immature dendritic cells into adjuvant-treated skin obviates the need for ex vivo maturation.* J Immunol, 2003. 171(11): p. 6275-82.
50. Thomas, R., et al., *Immature human monocyte-derived dendritic cells migrate rapidly to draining lymph nodes after intradermal injection for melanoma immunotherapy.* Melanoma Res, 1999. 9(5): p. 474-81.
51. Quillien, V., et al., *Biodistribution of radiolabelled human dendritic cells injected by various routes.* Eur J Nucl Med Mol Imaging, 2005. 32(7): p. 731-41.
52. Schuurhuis, D.H., et al., *In situ expression of tumor antigens by messenger RNA-electroporated dendritic cells in lymph nodes of melanoma patients.* Cancer Res, 2009. 69(7): p. 2927-34.
53. Mackensen, A., et al., *Homing of intravenously and intralymphatically injected human dendritic cells generated in vitro from CD34+ hematopoietic progenitor cells.* Cancer Immunol Immunother, 1999. 48(2-3): p. 118-22.
54. Stevenson, H.C., et al., *Fate of gamma-interferon-activated killer blood monocytes adoptively transferred into the abdominal cavity of patients with peritoneal carcinomatosis.* Cancer Res, 1987. 47(22): p. 6100-3.
55. Bernhard, H., et al., *Adoptive transfer of autologous, HER2-specific, cytotoxic T lymphocytes for the treatment of HER2-overexpressing breast cancer.* Cancer Immunol Immunother, 2008. 57(2): p. 271-80.
56. Brand, J.M., et al., *Kinetics and organ distribution of allogeneic natural killer lymphocytes transfused into patients suffering from renal cell carcinoma.* Stem Cells Dev, 2004. 13(3): p. 307-14.
57. Fisher, B., et al., *Tumor localization of adoptively transferred indium-111 labeled tumor infiltrating lymphocytes in patients with metastatic melanoma.* J Clin Oncol, 1989. 7(2): p. 250-61.
58. Faradji, A., et al., *Phase I trial of intravenous infusion of ex-vivo-activated autologous blood-derived macrophages in patients with non-small-cell lung cancer: toxicity and immunomodulatory effects.* Cancer Immunol Immunother, 1991. 33(5): p. 319-26.
59. Griffith, K.D., et al., *In vivo distribution of adoptively transferred indium-111-labeled tumor infiltrating lymphocytes and peripheral blood lymphocytes in patients with metastatic melanoma.* J Natl Cancer Inst, 1989. 81(22): p. 1709-17.
60. Pockaj, B.A., et al., *Localization of 111indium-labeled tumor infiltrating lymphocytes to tumor in patients receiving adoptive immunotherapy. Augmentation with cyclophosphamide and correlation with response.* Cancer, 1994. 73(6): p. 1731-7.
61. Meidenbauer, N., et al., *Survival and tumor localization of adoptively transferred Melan-A-specific T cells in melanoma patients.* J Immunol, 2003. 170(4): p. 2161-9.
62. Srinivas, M., et al., *In vivo cytometry of antigen-specific t cells using 19F MRI.* Magn Reson Med, 2009. 62(3): p. 747-53.
63. Yaghoubi, S.S., et al., *Noninvasive detection of therapeutic cytolytic T cells with 18F-FHBG PET in a patient with glioma.* Nat Clin Pract Oncol, 2009. 6(1): p. 53-8.
64. Kraitchman, D.L., et al., *Dynamic imaging of allogeneic mesenchymal stem cells trafficking to myocardial infarction.* Circulation, 2005. 112(10): p. 1451-61.
65. van den Bos, E.J., et al., *Magnetic resonance imaging of haemorrhage within reperfused myocardial infarcts: possible interference with iron oxide-labelled cell tracking?* Eur Heart J, 2006. 27(13): p. 1620-6.
66. Ahrens, E.T., et al., *Magnetic resonance imaging of embryonic and fetal development in model systems.* Methods Mol Med, 2006. 124: p. 87-101.
67. Jirak, D., et al., *Monitoring the survival of islet transplants by MRI using a novel technique for their automated detection and quantification.* MAGMA, 2009. 22(4): p. 257-65.
68. Kriz, J., et al., *Magnetic resonance imaging of pancreatic islets transplanted into the right liver lobes of diabetic mice.* Transplant Proc, 2008. 40(2): p. 444-8.
69. Hofmann, M., et al., *Monitoring of bone marrow cell homing into the infarcted human myocardium.* Circulation, 2005. 111(17): p. 2198-202.
70. Kang, W.J., et al., *Tissue distribution of 18F-FDG-labeled peripheral hematopoietic stem cells after intracoronary administration in patients with myocardial infarction.* J Nucl Med, 2006. 47(8): p. 1295-301.

71. Barbosa da Fonseca, L.M., et al., *Biodistribution of bone marrow mononuclear cells in chronic chagasic cardiomyopathy after intracoronary injection.* Int J Cardiol.
72. Dedobbeleer, C., et al., *Myocardial homing and coronary endothelial function after autologous blood CD34+ progenitor cells intracoronary injection in the chronic phase of myocardial infarction.* J Cardiovasc Pharmacol, 2009. 53(6): p. 480-5.
73. Silva, S.A., et al., *Autologous bone-marrow mononuclear cell transplantation after acute myocardial infarction: comparison of two delivery techniques.* Cell Transplant, 2009. 18(3): p. 343-52.
74. Schachinger, V., et al., *Pilot trial on determinants of progenitor cell recruitment to the infarcted human myocardium.* Circulation, 2008. 118(14): p. 1425-32.
75. Caveliers, V., et al., *In vivo visualization of 111In labeled CD133+ peripheral blood stem cells after intracoronary administration in patients with chronic ischemic heart disease.* Q J Nucl Med Mol Imaging, 2007. 51(1): p. 61-6.
76. Goussetis, E., et al., *Intracoronary infusion of CD133+ and CD133-CD34+ selected autologous bone marrow progenitor cells in patients with chronic ischemic cardiomyopathy: cell isolation, adherence to the infarcted area, and body distribution.* Stem Cells, 2006. 24(10): p. 2279-83.
77. Blocklet, D., et al., *Myocardial homing of nonmobilized peripheral-blood CD34+ cells after intracoronary injection.* Stem Cells, 2006. 24(2): p. 333-6.
78. Boddington, S.E., et al., *Labeling human embryonic stem cell-derived cardiomyocytes with indocyanine green for noninvasive tracking with optical imaging: an FDA-compatible alternative to firefly luciferase.* Cell Transplant, 2010. 19(1): p. 55-65.
79. Josephs, D., J. Spicer, and M. O'Doherty, *Molecular imaging in clinical trials.* Target Oncol, 2009. 4(3): p. 151-68.
80. Srinivas, M., et al., *Fluorine-19 MRI for visualization and quantification of cell migration in a diabetes model.* Magn Reson Med, 2007. 58(4): p. 725-34.
81. Aime, S., et al., *Paramagnetic lanthanide(III) complexes as pH-sensitive chemical exchange saturation transfer (CEST) contrast agents for MRI applications.* Magn Reson Med, 2002. 47(4): p. 639-48.
82. Aime, S., et al., *A paramagnetic MRI-CEST agent responsive to lactate concentration.* J Am Chem Soc, 2002. 124(32): p. 9364-5.
83. Gilad, A.A., et al., *Artificial reporter gene providing MRI contrast based on proton exchange.* Nat Biotechnol, 2007. 25(2): p. 217-9.
84. Viale, A. and S. Aime, *Current concepts on hyperpolarized molecules in MRI.* Curr Opin Chem Biol. 14(1): p. 90-6.
85. Viale, A., et al., *Hyperpolarized agents for advanced MRI investigations.* Q J Nucl Med Mol Imaging, 2009. 53(6): p. 604-17.
86. Riegler, J., et al., *Targeted magnetic delivery and tracking of cells using a magnetic resonance imaging system.* Biomaterials, 2010.
87. Zaidi, H., M.L. Montandon, and A. Alavi, *The clinical role of fusion imaging using PET, CT, and MR imaging.* Magn Reson Imaging Clin N Am. 18(1): p. 133-49.
88. Luster, M., et al., *Clinical value of 18-fluorine-fluorodihydroxyphenylalanine positron emission tomography/computed tomography in the follow-up of medullary thyroid carcinoma.* Thyroid. 20(5): p. 527-33.
89. Bybel, B., et al., *SPECT/CT imaging: clinical utility of an emerging technology.* Radiographics, 2008. 28(4): p. 1097-113.
90. Boss, A., et al., *Diffusion tensor imaging in a human PET/MR hybrid system.* Invest Radiol. 45(5): p. 270-4.
91. Herzog, H., et al., *The current state, challenges and perspectives of MR-PET.* Neuroimage. 49(3): p. 2072-82.
92. Hwang do, W., et al., *Development of a quadruple imaging modality by using nanoparticles.* Chemistry, 2009. 15(37): p. 9387-93.
93. Pawelczyk, E., et al., *In vivo transfer of intracellular labels from locally implanted bone marrow stromal cells to resident tissue macrophages.* PLoS One, 2009. 4(8): p. e6712.
94. Winter, E.M., et al., *Cell tracking using iron oxide fails to distinguish dead from living transplanted cells in the infarcted heart.* Magn Reson Med. 63(3): p. 817-21.
95. Kraitchman, D.L. and J.W. Bulte, *Imaging of stem cells using MRI.* Basic Res Cardiol, 2008. 103(2): p. 105-13.
96. Rogers, W.J., C.H. Meyer, and C.M. Kramer, *Technology insight: in vivo cell tracking by use of MRI.* Nat Clin Pract Cardiovasc Med, 2006. 3(10): p. 554-62.
97. Cruz, L.J., et al., *Targeted PLGA nano- but not microparticles specifically deliver antigen to human dendritic cells via DC-SIGN in vitro.* J Control Release.
98. Smirnov, P., et al., *In vivo single cell detection of tumor-infiltrating lymphocytes with a clinical 1.5 Tesla MRI system.* Magn Reson Med, 2008. 60(6): p. 1292-7.
99. Goetz, M. and T.D. Wang, *Molecular imaging in gastrointestinal endoscopy.* Gastroenterology. 138(3): p. 828-33 e1.
100. Singhal, S., S. Nie, and M.D. Wang, *Nanotechnology applications in surgical oncology.* Annu Rev Med. 61: p. 359-73.
101. Leong-Poi, H., *Molecular imaging using contrast-enhanced ultrasound: evaluation of angiogenesis and cell therapy.* Cardiovasc Res, 2009. 84(2): p. 190-200.

Chapter 10

Humoral anti-KLH responses in cancer patients treated with dendritic cell based immunotherapy are dictated by different vaccination parameters

Aarntzen EH

De Vries IJ

Göertz JH

Beldhuis-Valkis M

Brouwers HM

Van de Rakt MW

Van der Molen RG

Punt CJ

Adema GJ

Tacken PJ

Joosten I

Jacobs JF

Cancer Immunol Immunother. 2012;61(11):2003-11

Abstract

Keyhole limpet hemocyanin (KLH) attracts biomedical interest because of its remarkable immunostimulatory properties. Currently, KLH is used as vaccine adjuvant, carrier-protein for haptens and as local treatment for bladder-cancer. Since a quantitative human anti-KLH assay is lacking, it has not been possible to monitor the dynamics of KLH-specific antibody (Ab) responses after in vivo KLH-exposure. We designed a quantitative assay to measure KLH-specific Abs in humans and retrospectively studied the relation between vaccination parameters and the vaccine-induced anti-KLH Ab responses. Anti-KLH Abs were purified from pooled serum of melanoma patients who have responded to KLH as a vaccine adjuvant. Standard isotype-specific calibration curves were generated to measure KLH-specific Ab-responses in individual serum samples using ELISA.

KLH-specific IgM, IgA, IgG and all IgG-subclasses were accurately measured at concentrations as low as 20 µg/ml. The intra- and inter-assay coefficients of variation of this ELISA were below 6.7% and 9.9%, respectively. Analyses of 128 patients demonstrated that mature DC induced higher levels of KLH-specific IgG compared to immature DC, prior infusion with anti-CD25 abolished IgG and IgM production and patients with locoregional disease developed more robust IgG responses than advanced metastatic melanoma patients.

We present the first quantitative assay to measure KLH-specific Abs in human serum, which now enables monitoring both the dynamics and absolute concentrations of humoral immune responses in individuals exposed to KLH. This assay may provide a valuable biomarker for the immunogenicity and clinical effectiveness of KLH-containing vaccines and therapies.

Introduction

Keyhole limpet hemocyanin (KLH) is a high-molecular-weight glycoprotein, purified from a marine snail species called Megathura crenulata, which induces both cell-mediated and humoral responses in animals and humans. Because of its high immunogenicity and low toxicity, KLH is used for a variety of basic research and clinical applications (1). KLH was introduced into the clinic in 1967 to assess immunocompetence of individuals (2). Later, KLH became a standard carrier for the production of antibodies (Abs) to small molecule haptens such as peptides and oligosaccharides (1). Besides this, KLH is used as a local treatment for patients with bladder cancer (3). Finally, KLH has progressed into clinical trials as either adjuvant- or immunomonitoring tool in a variety of vaccines directed against cancer (4, 5) or infectious diseases (6). Dendritic cells (DCs) are potent antigen presenting cells and play a central role in the induction and maintenance of antigen-specific immunity. Antigen-specific immune responses in cancer patients can be induced by exploiting autologous DCs (7). In our institute, autologous DCs are activated *ex vivo* and loaded with tumor antigens. KLH is added to the vaccine both as a non-specific T helper cell stimulus and to facilitate monitoring of the vaccine-induced immune-responses (8-10). After DC injection, the cells migrate towards the lymph nodes where they present their processed antigens to the adaptive arm of the immune system, inducing antigen-specific T and B cell responses (11). In the last decade, several parameters of DC based therapy have been optimized to improve vaccine-induced immunological responses, particularly in melanoma patients (12). For example, it is well-accepted that the use of mature DC is superior to immature DC (13) and pretreatment with anti-CD25 antibodies does not improve immunological responses (14). The route of administration largely dictates the failure or success of the induced immunological responses (15, 16). Similarly, evidence is accumulating that the use of non-specific helper epitopes, such as KLH, is critical to the induction of effective anti-tumor responses (17). In these clinical trials, much effort has been put in the detection of tumor-antigen specific immune responses, e.g. ELIspots (18, 19), T cell receptor (TCR) frequency assessment (20) and analyses of skin test biopsies (21, 22). These assays have multiple disadvantages; the assays are laborious, have limited sensitivity, often lack association with clinical outcome and are difficult to standardize (23, 24). Strikingly, not much attention has been paid to the dynamics, levels and patterns of the vaccine-induced anti-KLH humoral responses in clinical trials, which could provide a simple and direct method for evaluation of vaccine-induced immune responses. Assays to monitor cellular (25, 26) and humoral (27-29) immune responses against KLH have been developed to facilitate optimal use of biomedical KLH applications. The enzyme-linked immunosorbent assay (ELISA) proved a simple and sensitive assay to measure serological Abs and in 1979 the first quantitative assay to detect KLH-specific Ab in mice was published (27). Five years later the first ELISA was developed to detect KLH-specific Ab in human serum (28). Currently, all published human anti-KLH ELISA's report Ab-responses in arbitrary units based on optical density-values, which yields relative units/values only. Because of the lack of a quantitative human anti-KLH assay, so far it has not been possible to monitor the dynamics of KLH-specific Ab-responses after in vivo KLH-exposure. It was neither possible to link the concentration of induced KLH-Abs to either the immunocompetence of an individual or to the immunogenicity of KLH-containing vaccines. In this study we present the first quantitative ELISA to measure KLH-specific Abs in human serum, measuring both IgG, IgA, IgM and all IgG-subclasses. We demonstrate that it is now possible to monitor the dynamics of both KLH specific Ab-levels and Ab class-switching in individuals that are repeatedly exposed to KLH. Furthermore, we retrospectively analyzed the humoral anti-KLH responses of melanoma patients enrolled in our clinical trials investigating dendritic cell based vaccinations. Our data confirm that individuals exposed to KLH react to it as a primary immunogen, inducing a characteristic primary immune response. Moreover, analyses of our clinical DC based vaccination protocols demonstrated that variations in the vaccination parameters dramatically influence both the quantity and the quality of the induced humoral response.

Materials and Methods

Preparation of serum-pool containing anti-KLH antibodies.

Serum was pooled from HLA-A*02:01 melanoma patients and colorectal cancer patients who were previously vaccinated with KLH-pulsed dendritic cells (DCs). To generate a serum pool with a broad spectrum of KLH-specific Abs, sera were obtained from 28 patients enrolled in different clinical trials within our institute in which the maturation status of the DCs and the route of vaccine administration varied per clinical trial (13-15, 30, 31). For the exact details regarding the vaccination protocols and the patient inclusion we refer to these individual studies. In all studies, KLH was added at day 3 of the DC culture at a concentration of 10 µg/ml and patients received maximum three vaccination cycles of 3 bi-weekly vaccinations at a 6 months interval. Informed consent was obtained from all patients and the study was approved by our Institutional Review Board.

Purification of KLH-specific antibodies

Using a KLH-coated column (Alpha Diagnostic International, San Antonio, Texas), 18 ml starting serum-pool of KLH-specific Abs was isolated from the above-mentioned trials. Prior to use, the column was extensively washed with elution buffer (0.1 M glycine HCl pH 2.5) to dissociate multimeric KLH and remove monomers that were not covalently linked to the sepharose bed. Subsequently, the column was equilibrated with PBS, followed by application of the pooled serum, washing with PBS and elution of the KLH-specific Abs with elution buffer and neutralized with Tris/HCL pH 9.0. The KLH-specific IgM-, IgA- and IgG-Abs in the eluate with a volume of 1380 µl were quantified using nephelometry on an Immage apparatus (Beckman Coulter, Brea, Ca), IgG subclasses were measured on a BNII (Siemens, Münich, Germany) using reagents of The Binding Site (Birmingham, UK) all according to the manufacturers protocol. Following this approach, a 1.4 ml polyclonal anti-KLH stock was obtained in which all major immunoglobulin isotypes and IgG subclasses were represented (Supplementary Table 1). This stock of purified and quantified KLH-specific Abs was stored at -80 °C and used to generate standard curves for the quantitative ELISA. All experiments in this manuscript were performed with one single calibrated work standard of 34 ml created from 28 different patients.

Quantitative anti-KLH ELISA

96-well plates were coated for 18 hours at 4°C with 5 µg/mL KLH (Biosyn, Carlsbad, CA) in PBS in a total volume of 120 µL per well and wells were subsequently blocked with skimmed milk powder. After washing the plates different concentrations of patient serum were added for 1 hour at room temperature. To prepare suitable standard curves for the anti-KLH ELISA's, the work-standard was serially diluted to establish a 7-point standard curve for each Ab-isotype (Supplementary Figure 1, available online). For analysis of individual patient samples, a standard curve was added to each plate. After washing, specific Abs against either human IgM or IgA or total IgG or IgG1 or IgG2 or IgG3 or IgG4 labeled with horseradish peroxidase (Invitrogen, San Diego, CA) at 1:500 were added to the wells as 100 µL aliquots. The isotype-specific secondary Abs allows quantification of both human IgM, IgA, total IgG, IgG1, IgG2, IgG3 and IgG4 KLH-specific Abs. After a further incubation for 1 hour at room temperature and a final washing with buffer, peroxidase activity was revealed using 3,3' 5,5-tetramethyl-benzide as substrate. The reaction was stopped with sulfuric acid and samples were measured in a microtiter plate reader at 450 nm. A uniform detection limit of the anti-KLH ELISA's was arbitrarily determined at 20 µg/ml. This detection limit falls within the lower linear part of all anti-KLH calibration curves. Precision and linearity were determined according to the Clinical and Laboratoy Standards Institute protocols EP5 and EP6, respectively.

Statistical analysis

Precision and linearity was analyzed using EP Evaluator 9 software, all other statistical analyses were performed by Graphpad Prism 5.0. For the comparison of different vaccination protocols, patients were grouped based on similar protocol characteristics, such as stage of disease on entry, route of administration, pretreatment with anti-CD25 antibodies, additional treatment with interleukin-2 (IL-2) or the method of tumorantigen loading. For the comparison of 2 groups all the above mentioned protocol characteristics should be similar, except for the single parameter under investigation. Maximum KLH-specific Ab responses, out of at least 3 samples obtained at standard time points during the first cycle, were compared, as this reflects the individual's competence to generate a humoral response. Nonparametric Mann-Whitney test was performed to compare the KLH-specific Ab-responses of similar isotypes in two groups of melanoma patients exposed to KLH. A two-tailed p-value <0.05 was considered significant.

Results

Assay performance and validation

To evaluate the precision of the assay, pooled serum samples were measured in 2 replicates per run, 1 run per day for a minimum of 20 runs. The resulting anti-KLH ELISA's have an intra-assay imprecision, denoted by the coefficient of variation (CV), that ranged from 4.3% to 6.7%. The inter-assay CV varied from 6.4% to 9.9% (Table 1). To test for assay-linearity we serially diluted 2 individual patient serum samples per KLH-assay isotype at a minimum of 5 levels, assayed in quadruplicate. The results yielded slopes ranging from 0.918 to 1.036 and the coefficients of determination (R2) ranged from 0.991 to 0.998 (Figure 1). A method-comparison analysis was not possible, as there is no golden standard quantitative human anti-KLH available.

Monitoring the dynamics of humoral anti-KLH responses in individual patients

Repetitive serum sampling of individual patients enrolled in clinical trials on dendritic cell based vaccinations allows in-depth monitoring of the kinetics of the KLH-specific Ab-responses during therapy. In the majority of patients, we detected the first KLH-specific Abs after the 2nd or 3rd vaccination. We show one representative melanoma patient who had detectable levels of KLH-specific IgM Abs after the second vaccination (Figure 2a). The IgM response was followed by KLH-specific IgG Abs and after four vaccinations also by IgA Abs. Ab titers were drastically decreased

Table 1 Performance assessment of the anti-KLH ELISA assays

	IgGtotal		IgG1		IgG2		IgG3		IgG4		IgAtotal		IgMtotal	
Mean	478.0		282.0		80.4		5.0		76.3		22.8		719.7	
Variat	Intra	Inter	Intra	Inter	Intra	Inter	Intra	Inter	Intra	Inter	Intra	Inter	Intra	Inter
Std.	22.1	30.5	13.6	25.1	5.4	7.1	0.22	0.40	4.1	5.1	1.1	2.2	44.4	71.6
CV	4.6	6.4	4.8	8.9	6.7	7.1	4.3	7.9	5.4	6.7	5.0	9.7	6.2	9.9

Abbreviations: CV, coefficient of variation; intra, intra-assay imprecision; inter, inter-assay imprecision

between vaccination cycles and after the last vaccination. IgG subclass analysis showed that IgG1 predominantly contributed to the KLH-specific IgG response in this patient (Figure 2b). This example demonstrates that the KLH Ab-response strongly depends on the schedule of KLH exposure and the time point of serum sampling. One vaccinated patient received 9 vaccinations that did not contain KLH, because of a severe shellfish allergy. We detected no KLH-specific Abs in this specific patient (Fig 2c,d), demonstrating that KLH-specific Ab-responses are caused specifically by the KLH added to the vaccine and not by the vaccine itself. The high specificity of the anti-KLH ELISA is further illustrated by

the fact that none of the 57 tested patients had detectable KLH-specific Abs prior to vaccination (Figure 3a, bars indicated by 'before').

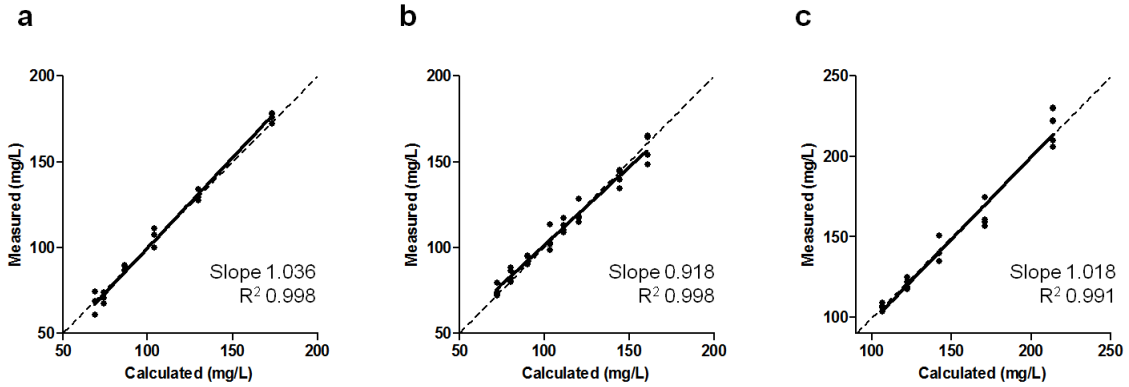

Figure 1. Serial dilution linearity of the anti-KLH ELISA. Serum samples of patients exposed to KLH were serially diluted with assay buffer and measured in quadruplicate. The results for linearity of the ELISA for the anti-KLH isotypes IgG (A) IgA (B) and IgM (C) are shown. Calculated concentrations are based on stock-concentration and dilution factor. Slopes and coefficients of determination (R2) are indicated in each panel. The line of identity is indicated by the dashed line.

Variations in vaccination parameters have major influence on the levels and patterns of humoral anti-KLH responses

Another application of this novel assay is that it allows the comparison of the humoral immunogenicity of different KLH-containing interventions. To demonstrate this, we performed subgroup analyses in a total of 118 melanoma patients, 43 stage III and 85 stage IV, who received dendritic cell based vaccinations according to different protocols (Table 2). Pretreatment with a single dose of intravenous humanized monoclonal anti-CD25 antibody (Daclizumab) significantly reduced the overall anti-KLH Ig responses (Figure 3a). The mean level of anti-KLH IgG without pretreatment (protocol 5, n=22) was 142 mg/L compared to 18 mg/L after pretreatment (protocol 4, n=13, p=0.0267). With regard to anti-KLH IgA, the mean levels were 5 mg/L with no pretreatment and 2 mg/L with pretreatment; for anti-KLH IgM this was 157 mg/L compared to 7 mg/L, respectively (p=0.0275). Vaccination with immature DC (protocol 1, n=9) barely induced anti-KLH antibodies compared to vaccination with mature DC (protocol 5, n=22)(Figure 3b). Anti-KLH IgG antibodies were detected in 2/9 patients upon immature DC vaccination and in 12/22 patients after vaccination with mature DC, mean 9 mg/L and 142 mg/L, respectively (p=0.0600). Anti-KLH IgM antibodies were induced in the same patients, 2/9 patients after immature DC vaccination and 9/22 patients after mature DC vaccination, to similar extend, 147 mean mg/L and 157 mg/L respectively (p=0.4157). As expected, the method of loading the tumor-antigens onto the dendritic cells, either pulsing with defined peptides (protocol 3, n=24) or electroporation with mRNA encoding the tumor antigens (protocol 2, n=17), did not affect the concentration or the pattern of vaccine-induced anti-KLH humoral responses (Figure 3c). Combined intravenous/intradermal vaccination (protocol 5, n=22) induced significantly more anti-KLH IgM antibodies as compared to intranodal vaccination (protocol 2 and 3, n=41), mean 157 mg/L and 27 mg/L respectively (p=0.0222), but no differences in IgG or IgA levels were noted (Figure 3d). We observed significantly higher anti-KLH IgG titers in melanoma patients who were vaccinated adjuvant to radical lymph node dissection (stage III) compared to melanoma patients with irresectable locoregional disease or distant metastatic disease (stage IV). Mean concentrations of all isotypes were at least two times higher in stage III patients compared to stage IV melanoma patients (Figure 3e). However, the most prominent was anti-KLH IgG, mean 310 mg/L in stage III patients (protocol 6, n=43) compared to 94 mg/L in stage IV patients (protocol 2 and 3, n=41), p=0.0002.

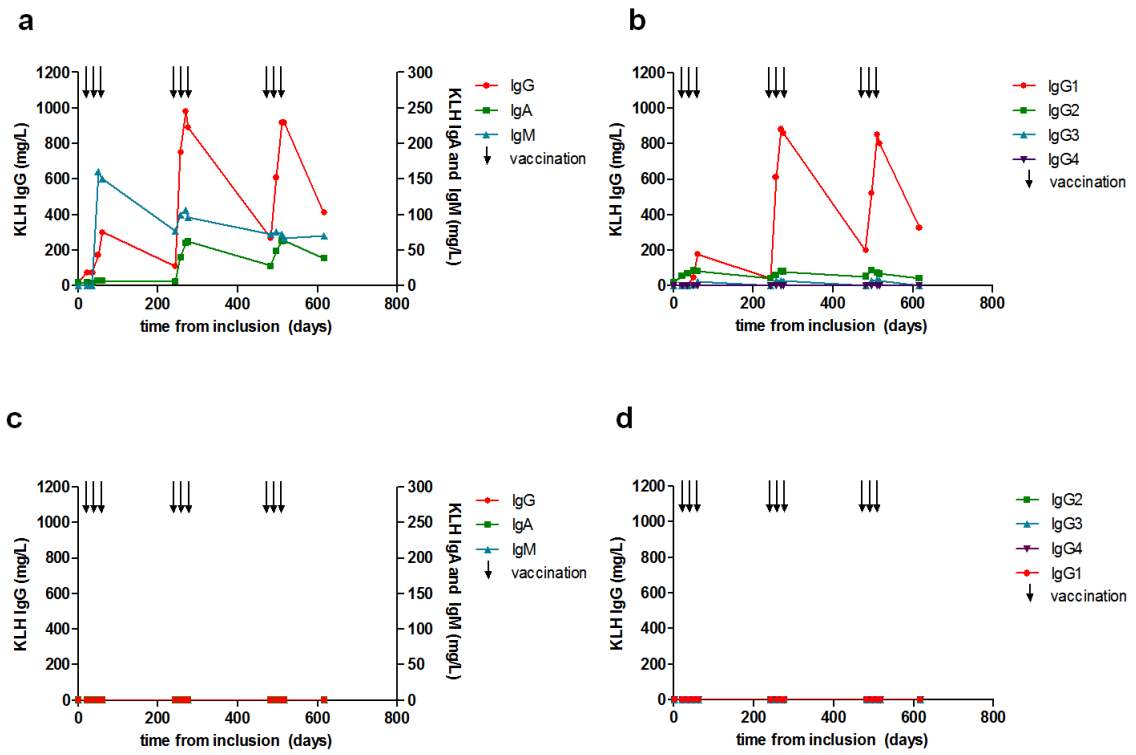

Figure 2. A detailed characterization of KLH-specific antibody responses in individual patients; two examples. Two patients who received 9 vaccinations of KLH loaded dendritic cells over a period of 18 months are characterized in detail for KLH-specific antibody responses. Each vaccination is indicated by a black arrow. One patient had a robust humoral response, the kinetics of the KLH-specific IgG, IgA and IgM responses are shown in (A). In (B) the IgG immune response is subdivided into the four IgG subclasses, demonstrating that IgG1 predominantly contributes to the KLH-specific immune response in this patient. The second patient received vaccinations with DC not loaded with KLH. In this patient KLH-specific antibody-responses were completely absent (C,D).

Discussion

KLH is widely used for biomedical applications because of its remarkable immunogenic properties. In the current study, we describe a novel, highly sensitive and quantitative, sandwich ELISA standardized to measure IgM, IgA and IgG Abs specific for KLH. We demonstrate that it is now possible to monitor the dynamics and concentrations of humoral KLH specific immune-responses in individuals exposed to KLH and in clinical trials. Importantly, we show that vaccine-induced KLH specific humoral responses largely depend on variations in vaccination parameters in DC based clinical trials. Using our novel anti-KLH ELISA we found that melanoma patients exposed to KLH loaded DCs often initially develop KLH specific IgM Abs, which is associated with a primary immune response as was expected from literature (32). After subsequent vaccinations in our patients, this is usually followed by class-switching and production of KLH specific IgG Abs, suggestive for a secondary immune response. This secondary immune response is accompanied by KLH specific IgA Abs in a minority of patients. In general, Ab isotype switching and the identity of the immunoglobulin subclasses is regulated by cytokines and B-cell activators (33). In this respect, Ab-responses in terms of isotype and subclass will be influenced by the route and conditions under which KLH is administered. In our studies, in which all individuals were exposed to KLH-loaded cytokine-matured DCs, IgG1 was the predominant subclass produced. We hypothesize that the method of KLH exposure and/or individual patient characteristics can result in significant skewing of the IgG subclass response. We further demonstrate that, using this novel assay, it is now possible to link the concentration of induced KLH specific Abs to the humoral immunogenicity of the KLH-containing DC

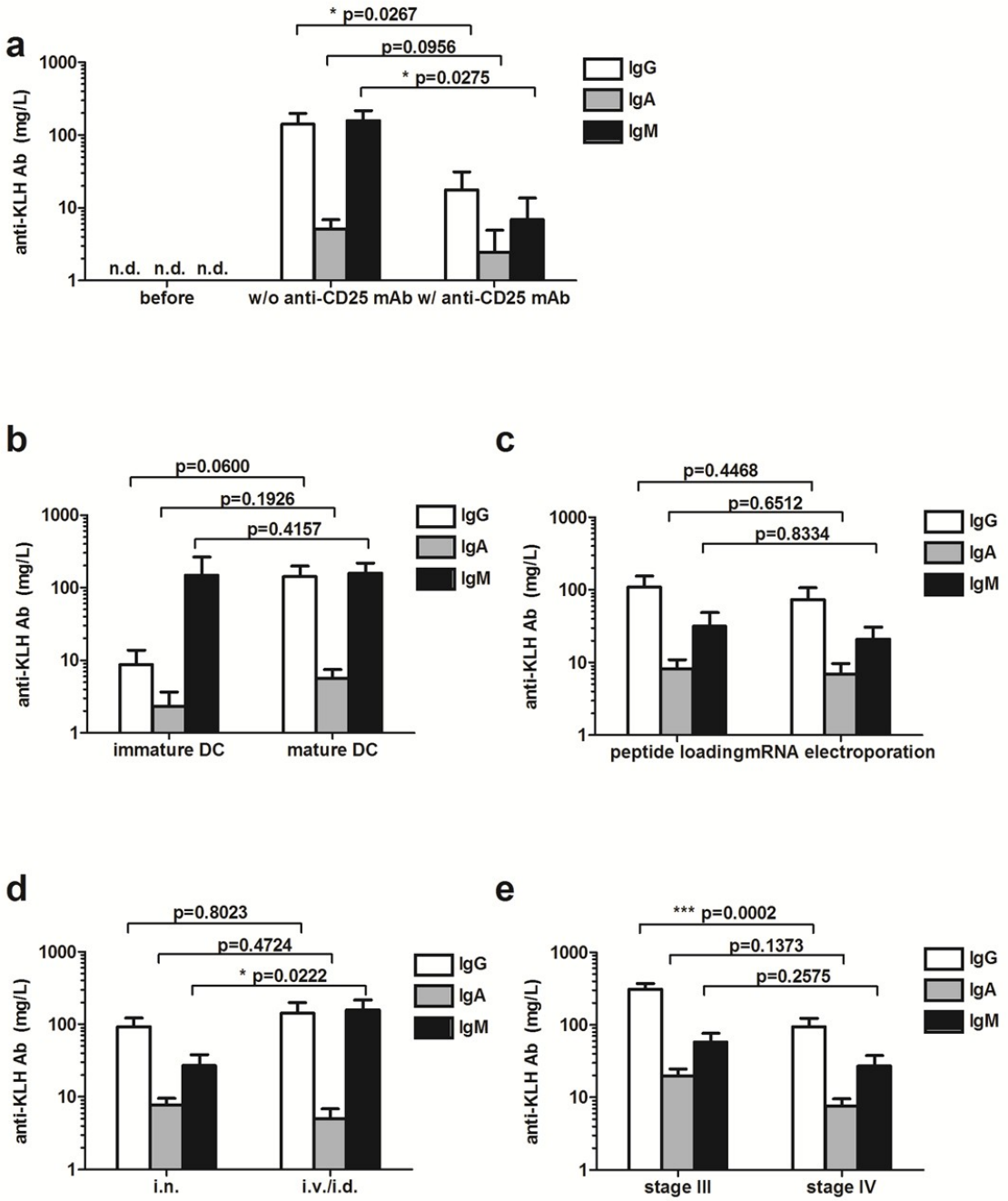

Figure 3. Variations in vaccination parameters induce different humoral anti-KLH responses. In total 128 melanoma patients were exposed to KLH by 3 bi-weekly vaccinations containing KLH loaded DC. None of the 35 patients tested (protocols 4 and 5) had KLH-specific antibodies prior to vaccination (a). KLH-specific Ab responses compared between (a) patients treated with or without daclizumab prior to the KLH exposure; (b) patients vaccinated with immature or mature KLH-loaded DC; (c) peptide-loaded or mRNA-transfected KLH-loaded DC; (d) intranodal or intravenous/intradermal routes of administration and (e) patients with locoregional metastatic disease or distant metastatic disease at inclusion. Mean levels of KLH-specific IgG (white bars), IgA (grey bars) and IgM (black bars) antibodies are shown in mg/L. Error bars indicate standard error of the mean; n.d., not detected.

based vaccines used in our institute. In our cohort of patients with metastatic melanoma we have found that adjustments in the vaccination protocol can significantly affect the humoral responses against KLH. We show for example that a single dose of daclizumab, a humanized monoclonal anti-CD25 Ab, prior to injection of KLH loaded DCs almost completely abolishes the KLH-specific humoral response. Blocking CD25 on activated T cells and regulatory T cells greatly reduces the capacity of the immune system to respond to de novo antigens. The in vivo effects of daclizumab on T cells are well documented (34), but the effects of daclizumab on humoral immune-responses were largely unexplored. Although injected prior to vaccination, circulating daclizumab may bind to CD25-expressing vaccinated DC, providing yet another possible explanation for the strongly reduced

vaccine-induced humoral responses to KLH. The maturation status of the DCs is another parameter that strongly affects humoral immunogenicity of the vaccine. We previously demonstrated that more effective cellular immune responses are induced with mature DCs compared to immature DCs (35). Now we demonstrate that mature DC also generate stronger humoral immune responses and are essential for efficient immunoglobulin class switching. In addition, we show that there is no significant difference in the KLH-specific IgG and IgA responses when the KLH-vaccine is administered intravenously/intradermally or intranodally in melanoma patients. However, intravenous/ intradermal injections tend to result in increased KLH-specific IgM responses compared to intranodal injection. In case of differential tumor-antigen loading onto the DC, we would not expect different KLH responses since in all protocols the DC are pulsed with KLH at day 3 after isolation, and loading with tumor-antigen occurs just before administration. Indeed, with regard to different methods of tumor-antigen loading we did not detect differences in levels or specificity of anti-KLH humoral reponses. Several lines of evidence demonstrate that tumor cells actively create a local and systemic immune suppressive environment (36-38). The level of tumorload may therefore negatively correlate with the competence of a patients' immune system to respond to antigens such as KLH (39). We investigated the humoral KLH responses in patients treated with DC based vaccinations adjuvant to radical lymph node dissection, and thus without macroscopic disease (stage III), and in patients with distant metastatic and measurable disease, stage IV melanoma. We indeed confirm that anti-KLH Ab production was higher in stage III patients compared to patients with stage IV melanoma, which argues in favour of applying immunotherapy at earlier stages of disease. Further analysis is warranted to investigate if the KLH-specific Ab-response in the context of anti-cancer vaccines can be used as a surrogate biomarker for tumor-specific immune-responses. The standardized ELISA presented here can facilitate in this effort as it allows inter-institutional comparisons of the humoral immunogenicity of KLH-containing vaccines. Although we initially developed the quantitative anti-KLH ELISA to monitor vaccine-induced immune responses, the assay allows quantification of humoral responsiveness as a measure of immunocompetence in individuals exposed to KLH. Since KLH elicits a primary immune response, intramuscular injection of KLH is the method of choice to investigate the capacity of an individual to respond to novel antigens, overcoming the confounding influence of previous exposure history (40). Finally, because of its capacity as a nonspecific immune stimulator, KLH has been investigated as an intravesical agent to treat superficial bladder cancer (3). Previously, it has been reported that the presence of anti-KLH antibodies was associated with treatment response (41). In this respect it is interesting to investigate whether in-depth analysis of the KLH-specific Ab-responses in these patients can be an early predictor of therapy outcome. In conclusion, we here present a sensitive and specific quantitative assay to measure KLH-specific Abs in human serum. We demonstrate that with this assay it is now possible to monitor both the dynamics and absolute concentrations of KLH-specific humoral responses in individuals exposed to KLH, for example to evaluate humoral immune competence. In addition, it may provide a valuable biomarker for the immunogenicity and clinical effectiveness of KLH-containing vaccines and therapies.

Table 2 Patients and protocol characteristics

Protocol nr.	Stage	Nr of patients	Maturation status	Route of administration	Anti-CD25 pretreatment	Method of Ag-loading
1	IV	9	immature	i.v./i.d.	no	peptide pulsing
2	IV	17	mature	i.n.	no	mRNA electroporation
3	IV	24	mature	i.n.	no	peptide pulsing
4	IV	13	mature	i.v./i.d.	yes	peptide pulsing
5	IV	22	mature	i.v./i.d.	no	peptide pulsing
	total	**85**				
6	III	43	mature	i.n.	no	peptide pulsing or mRNA electroporation
	total	**43**				

References

1. Harris, J.R. and J. Markl, *Keyhole limpet hemocyanin* (*KLH): a biomedical review.* Micron., 1999. 30(6): p. 597-623.
2. Swanson, M.A. and R.S. Schwartz, *Immunosuppressive therapy. The relation between clinical response and immunologic competence.* N.Engl.J.Med., 1967. 277(4): p. 163-170.
3. Perabo, F.G. and S.C. Muller, *Current and new strategies in immunotherapy for superficial bladder cancer.* Urology, 2004. 64(3): p. 409-421.
4. Schumacher, K., *Keyhole limpet hemocyanin* (*KLH) conjugate vaccines as novel therapeutic tools in malignant disorders.* J.Cancer Res.Clin.Oncol., 2001. 127 Suppl 2: p. R1-R2.
5. Krug, L.M., et al., *Immunization with N-propionyl polysialic acid-KLH conjugate in patients with small cell lung cancer is safe and induces IgM antibodies reactive with SCLC cells and bactericidal against group B meningococci.* Cancer Immunol Immunother, 2012. 61(1): p. 9-18.
6. Gandhi, R.T., et al., *A randomized therapeutic vaccine trial of canarypox-HIV-pulsed dendritic cells vs. canarypox-HIV alone in HIV-1-infected patients on antiretroviral therapy.* Vaccine, 2009. 27(43): p. 6088-94.
7. Melief, C.J., *Cancer immunotherapy by dendritic cells.* Immunity., 2008. 29(3): p. 372-383.
8. Leonhartsberger, N., et al., *Antigen-independent immune responses after dendritic cell vaccination.* Cancer Immunol.Immunother., 2007. 56(6): p. 897-903.
9. Scheibenbogen, C., et al., *Effects of granulocyte-macrophage colony-stimulating factor and foreign helper protein as immunologic adjuvants on the T-cell response to vaccination with tyrosinase peptides.* Int.J.Cancer, 2003. 104(2): p. 188-194.
10. Weide, B., et al., *Direct injection of protamine-protected mRNA: results of a phase 1/2 vaccination trial in metastatic melanoma patients.* J.Immunother., 2009. 32(5): p. 498-507.
11. Verdijk, P., et al., *Limited amounts of dendritic cells migrate into the T-cell area of lymph nodes but have high immune activating potential in melanoma patients.* Clin.Cancer Res., 2009. 15(7): p. 2531-2540.
12. Figdor, C.G., et al., *Dendritic cell immunotherapy: mapping the way.* Nat Med, 2004. 10(5): p. 475-80.
13. de, V.I., et al., *Maturation of dendritic cells is a prerequisite for inducing immune responses in advanced melanoma patients.* Clin.Cancer Res., 2003. 9(14): p. 5091-5100.
14. Jacobs, J.F., et al., *Dendritic cell vaccination in combination with anti-CD25 monoclonal antibody treatment, a phase I/II study in metastatic melanoma patients.* Clin Cancer Res.
15. Lesterhuis, W.J., et al., *Route of administration modulates the induction of dendritic cell vaccine-induced antigen-specific T cells in advanced melanoma patients.* Clin Cancer Res.
16. de Vries, I.J., et al., *Magnetic resonance tracking of dendritic cells in melanoma patients for monitoring of cellular therapy.* Nat Biotechnol, 2005. 23(11): p. 1407-13.
17. Engell-Noerregaard, L., et al., *Review of clinical studies on dendritic cell-based vaccination of patients with malignant melanoma: assessment of correlation between clinical response and vaccine parameters.* Cancer Immunol Immunother, 2009. 58(1): p. 1-14.
18. Kyte, J.A., et al., *Phase I/II trial of melanoma therapy with dendritic cells transfected with autologous tumor-mRNA.* Cancer Gene Ther, 2006. 13(10): p. 905-18.
19. Kyte, J.A., et al., *T cell responses in melanoma patients after vaccination with tumor-mRNA transfected dendritic cells.* Cancer Immunol Immunother, 2007. 56(5): p. 659-75.
20. Germeau, C., et al., *High frequency of antitumor T cells in the blood of melanoma patients before and after vaccination with tumor antigens.* J Exp Med, 2005. 201(2): p. 241-8.
21. de Vries, I.J., et al., *Immunomonitoring tumor-specific T cells in delayed-type hypersensitivity skin biopsies after dendritic cell vaccination correlates with clinical outcome.* J Clin Oncol, 2005. 23(24): p. 5779-87.
22. Lopez, M.N., et al., *Prolonged survival of dendritic cell-vaccinated melanoma patients correlates with tumor-specific delayed type IV hypersensitivity response and reduction of tumor growth factor beta-expressing T cells.* J Clin Oncol, 2009. 27(6): p. 945-52.
23. Britten, C.M., et al., *Minimal information about T cell assays: the process of reaching the community of T cell immunologists in cancer and beyond.* Cancer Immunol Immunother, 2011. 60(1): p. 15-22.
24. Janetzki, S., et al., *Results and harmonization guidelines from two large-scale international Elispot proficiency panels conducted by the Cancer Vaccine Consortium* (*CVC/SVI).* Cancer Immunol Immunother, 2008. 57(3): p. 303-15.
25. Neelapu, S.S., S. Baskar, and L.W. Kwak, *Detection of keyhole limpet hemocyanin* (*KLH)-specific immune responses by intracellular cytokine assay in patients vaccinated with idiotype-KLH vaccine.* J.Cancer Res.Clin.Oncol., 2001. 127 Suppl 2: p. R14-R19.
26. Spazierer, D., et al., *T helper 2 biased de novo immune response to Keyhole Limpet Hemocyanin in humans.* Clin.Exp.Allergy, 2009. 39(7): p. 999-1008.
27. Kelly, B.S., J.G. Levy, and L. Sikora, *The use of the enzyme-linked immunosorbent assay* (*ELISA) for the detection and quantification of specific antibody from cell cultures.* Immunology, 1979. 37(1): p. 45-52.
28. Korver, K., et al., *Measurement of primary in vivo IgM- and IgG-antibody response to KLH in humans: implications of pre-immune IgM binding in antigen-specific ELISA.* J.Immunol.Methods, 1984. 74(2): p. 241-251.
29. Oyelaran, O. and J.C. Gildersleeve, *Evaluation of human antibody responses to keyhole limpet hemocyanin on a carbohydrate microarray.* Proteomics.Clin.Appl., 2010. 4(3): p. 285-294.
30. Lesterhuis, W.J., et al., *Vaccination of colorectal cancer patients with CEA-loaded dendritic cells: antigen-specific T cell responses in DTH skin tests.* Ann.Oncol., 2006. 17(6): p. 974-980.
31. Lesterhuis, W.J., et al., *Wild-type and modified gp100 peptide-pulsed dendritic cell vaccination of advanced melanoma patients can lead to long-term clinical responses independent of the peptide used.* Cancer Immunol Immunother, 2011. 60(2): p. 249-60.

32. Lane, H.C., et al., *In vitro antigen-induced, antigen-specific antibody production in man. Specific and polyclonal components, kinetics, and cellular requirements.* J.Exp.Med., 1981. 154(4): p. 1043-1057.
33. Stavnezer, J., *Immunoglobulin class switching.* Curr.Opin.Immunol., 1996. 8(2): p. 199-205.
34. Waldmann, T.A., *Anti-Tac* (*daclizumab, Zenapax) in the treatment of leukemia, autoimmune diseases, and in the prevention of allograft rejection: a 25-year personal odyssey.* J.Clin.Immunol., 2007. 27(1): p. 1-18.
35. de Vries, I.J., et al., *Maturation of dendritic cells is a prerequisite for inducing immune responses in advanced melanoma patients.* Clin Cancer Res, 2003. 9(14): p. 5091-100.
36. Gajewski, T.F., et al., *Immune resistance orchestrated by the tumor microenvironment.* Immunol Rev, 2006. 213: p. 131-45.
37. Whiteside, T.L., *Inhibiting the inhibitors: evaluating agents targeting cancer immunosuppression.* Expert Opin Biol Ther, 2010. 10(7): p. 1019-35.
38. Munn, D.H. and A.L. Mellor, *Indoleamine 2,3-dioxygenase and tumor-induced tolerance.* J Clin Invest, 2007. 117(5): p. 1147-54.
39. Golub, S.H., D.M. Rangel, and D.L. Morton, *In vitro assessment of immunocompetence in patients with malignant melanoma.* Int J Cancer, 1977. 20(6): p. 873-80.
40. Grant, R.W., et al., *Cardiovascular exercise intervention improves the primary antibody response to keyhole limpet hemocyanin* (*KLH) in previously sedentary older adults.* Brain Behav.Immun., 2008. 22(6): p. 923-932.
41. Jurincic-Winkler, C.D., et al., *Antibody response to keyhole limpet hemocyanin* (*KLH) treatment in patients with superficial bladder carcinoma.* Anticancer Res., 1996. 16(4A): p. 2105-2110.

Skin-test infiltrating lymphocytes early predict clinical outcome of dendritic cell based vaccination in metastatic melanoma

Aarntzen EH

Bol K

Schreibelt G

Jacobs JF

Lesterhuis WJ

Van Rossum MM

Adema GJ

Figdor CG

Punt CJ*

De Vries IJ*

* contributed equally

Cancer Res. 2012;72(23):6102-10

Abstract

The identification of responding patients early during treatment would improve the capability to develop effective new immunotherapies more rapidly. Here we describe a bioassay that may link early T cell-mediated immune responses to later clinical benefits. This bioassay rests upon the tenet of immunotherapy that tumor-specific effector T cells capable of invading peripheral tissue can recognize tumor-antigens and exert cytotoxic functions there. To demonstrate its utility, we conducted a retrospective study of a large cohort of metastatic melanoma patients (n=91) enrolled in dendritic cell (DC)-based vaccination protocols to examine an hypothesized correlation of post-treatment skin-infiltrating lymphocytes (SKILs) with overall survival (OS). Stringent immunological criteria were defined to identify long-term survivors. The presence of TAA-specific CD8+ T cell populations within SKILs (criterion I) was highly predictive for long-term survival. Further restriction by selecting for the presence of TAA-specific $CD8^+$ T cells specifically recognizing tumor peptide (criterion II) were also associated with improved OS. Recognition of naturally processed antigen (criterion III), maximized the accuracy of the test, with a median OS of 24.1 versus 9.9 months ($p=0.001$). Our results show that detailed characterization of SKILs can permit an accurate selection of metastatic melanoma patients who benefit most from DC-based vaccination. This simple and robust bioassay integrates multiple aspects of cellular functions that mediate effective immune responses, thereby offering an effective tool to rapidly identify patients who are responding to immunotherapy at an early stage of treatment.

Introduction

The focus of treatment for metastatic cancer patients is shifting from a generalized approach based on population markers, to a personalized approach based on individual tumor and host characteristics (1). Immunotherapy is intrinsically a personalized treatment modality, as it acts via the patients' own immune system to induce anti-cancer immunity. Recent trials have underscored the potential of immunotherapy in metastatic cancers, especially in melanoma (2). Owing to their unique immune stimulatory properties, dendritic cells (DC) are an essential target for anti-cancer immunotherapy. We and others have explored DC-based therapy to induce tumor associated antigen (TAA)-specific immune responses in this population (3, 4). Interestingly, the reported rates of long-lasting responses in immunotherapy trials are generally low, but remarkably constant, regardless of the chosen regimen (5). This long-standing observation hints at a subgroup of 'immune reactive' patients. Identification of responding patients early during treatment would therefore greatly improve clinical efficacy of these novel and costly therapies. Thus, bioassays which accurately link immune responses to clinical outcome are warranted (1).

The mainstay of immunotherapy is to induce, enhance or sustain TAA-specific effector T cell immunity. Consequently, currently used bioassays focus on cellular immune responses at different time-points after immunotherapeutic intervention. For example, most vaccination studies include a control antigen like keyhole limpet hemocyanin (KLH) or tetanus toxoid (TT) as a surrogate marker for immune competence (6). However, the high immunogenicity of these control antigens often induce profound cellular and humoral responses, which do not accurately model the less abundant, and often self-antigens, TAA-specific cellular responses. Another widely used approach is ELIspot, which determines the production of a single cytokine upon antigenic stimulation, e.g. IFNγ ELIspots. Typically, ELIspots are performed on cell-samples obtained from peripheral blood, whereas anti-tumor effects can only be expected from immune cells capable of leaving the circulation and invading peripheral tissues. Although ELIspots are rather sensitive, they need careful standardization (7, 8). Moreover, they evaluate a single cytokine, whereas cytokine profiles better reveal the functional programming of effector cells. Imaging results from previous trials using adoptive cell transfer show that the migratory capacity of effector cells is positively correlated to clinical outcome (9), suggesting that this functionality should be incorporated in bioassays as well (10). Novel techniques have recently been developed that allow high throughput assessment of individual variations in many functional processes, e.g. differences in signaling pathways in immune cells (11). However, as of now these techniques lack validation and are not yet applicable in the evaluation for therapy-induced immune responses.

Previously, we reported that screening cultures from delayed type hypersensitivity (DTH) skin test biopsies, by using tetrameric MHC-peptide complexes, provides a valuable tool to link immune responses to clinical outcome in metastatic melanoma patients who underwent DC-based vaccinations (12). In this study, we extend these findings in a large cohort and demonstrate that detailed analysis of skin-test infiltrating lymphocyte (SKIL) cultures is a solid bioassay to predict survival in metastatic melanoma patients. This bioassay is simple, feasible and integrates multiple aspects of effector cell functions needed for effective immune responses.

Materials and methods

Patient characteristics

We retrospectively analyzed a cohort of 91 patients with irresectable locoregional or distant metastatic melanoma, who were enrolled in our vaccination studies between June 1999 and June 2008 (Table 1). Eligibility criteria included melanoma patients with irresectable locoregional or distant metastatic disease, according to the 2001 American Joint Committee on Cancer Staging criteria (13). Other inclusion criteria include HLA-A*02:01 phenotype, known HLA-DRB*01*04 status, melanoma expressing the melanoma-associated antigens gp100 and tyrosinase and World Health

Organization performance status 0 or 1. Patients with symptomatic brain metastases, serious concomitant disease or a history of second malignancy were excluded. The studies were approved by our Institutional Review Board and written informed consent was obtained from all patients.

Treatment schedule

All patients were vaccinated with cytokine-matured monocyte-derived autologous DCs loaded with tumor associated antigens (TAA) of gp100 and tyrosinase according to a schedule of 3 biweekly vaccinations followed in week 7-8 by delayed type hypersensitivity (DTH) skin test (Supplementary Figure 1). Differences in protocols included the route of administration (intranodal, intradermal or combined intradermal/intraveneously), method of antigen loading (detailed information below) and pretreatment with anti-CD25 antibody; described in Table 1. Unless progressive disease was documented, patients received a maximum of 3 vaccination cycles, each with a 6 month interval. For the exact details regarding the vaccination protocols we refer to these individual studies (14-18).

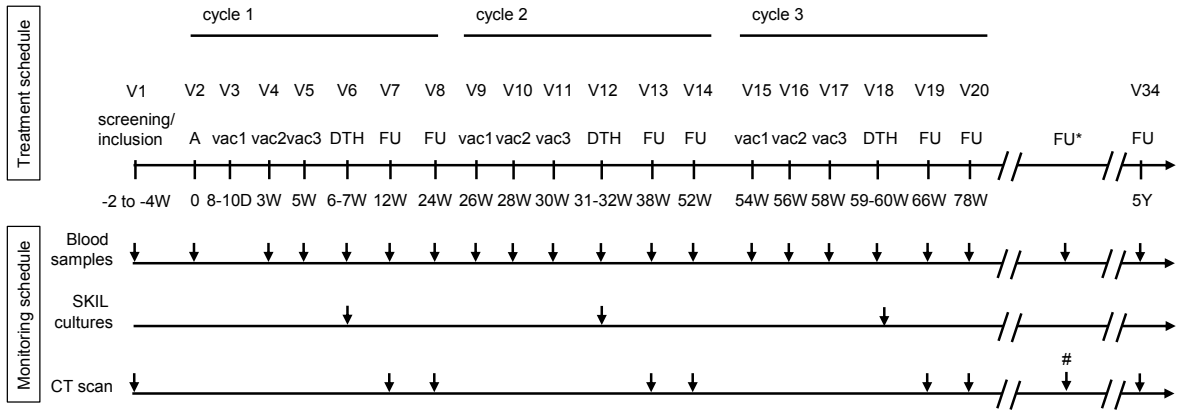

Supplementary Figure 1. Schedule of treatment and monitoring. Patients received 3 vaccinations a biweekly interval, followed a delayed type hypersensitivity (DTH) skin test. After completing one cycle and if no progression of disease was confirmed on CT-scan, patients were eligible to receive a maximum of two more cycles and were followed up to 5 years. Abbreviations: Vx = visit x; M = month, D = day, W = week, Y = year, vacx = vaccination x; FU = follow-up; * follow-up visits were planned every 3 months; # CT-scans were planned every 6 months.

Dendritic cell vaccine

Monocytes were enriched from leukapheresis products by counterflow centrifugation using Elutra-cell separator (Gambro BCT, Inc, Lakewood, CO) and single-use, functionally sealed disposable Elutra sets, as described before (19) and according to the manufacturer. Monocytes were cultured in the presence of interleukin (IL)-4 (500 U/ml) GM-CSF (800 U/ml) (both Cellgenix, Freiburg, Germany) and KLH (10 µg/ml, Calbiochem, Darmstadt, Germany). DC were matured with autologous monocyte-conditioned medium (30%, v/v) supplemented with prostaglandin E_2 (10 µg/ml, Pharmacia & Upjohn, Puurs, Belgium) and 10 ng/ml tumor necrosis factor-α (Cellgenix, Freiburg, Germany) for 48 hours as described previously (20). This procedure gave rise to mature DC meeting the release criteria described previously (3). DC were pulsed with the HLA class I gp100-derived peptides gp100:154-162, gp100:280-288 and the tyrosinase-derived peptide tyrosinase:369-377. DC from HLA-DRB*01*04–positive patients were also pulsed with HLA-DRB*01*04–binding peptides of both gp100 and tyrosinase (gp100:44-59 and tyro:448-462 analog (21, 22). Peptide-pulsing was performed as described previously (16). In the other protocols mature DC were electroporated with mRNA encoding gp100 or tyrosinase as described previously (23) and cells were resuspended in 0.1 mL for injection.

KLH-specific proliferation and IFNγ production

PBMC were isolated from heparinized blood by Ficoll-Paque density centrifugation, stimulated with KLH (4 μg/2×10^5 PBMC) in X-VIVO with 2% HS. After 3 days, cells were incubated with ^{3}H-thymidine for 8 hours, incorporation was measured with a β-counter. Experiments were performed in triplicate, non-specific proliferation upon stimulation with OVA was used as control. IFNγ production was measured in the supernatants after 24 hours by ELISA. Human IFNγ monoclonal antibody 2G1 was used for coating (0.75 μg/mL), human IFNγ biotin-labeled mAb M701B (0.05 mg/mL) was used for detection (all Thermo Scientific Inc). Recombinant human IFNγ RIFNG100 was used as standard. At least a two-fold increase compared to OVA was considered positive.

Skin-test infiltrating lymphocyte (SKIL) analyses

Skin tests were performed within 1-2 weeks after each vaccination cycle (Supplementary Figure 1) (24). Briefly, 2 to 10×10^5 DC pulsed with either gp100, tyrosinase or both epitopes or transfected with mRNA encoding either gp100 or tyrosinase or both (specifically indicated in the relevant text and figures) were injected intradermally in the skin of the back of the patient at different sites, 4 cm apart from each other. After 48 hours, the maximum diameter of induration was measured by palpation and punch biopsies (6 mm) were taken. Half of the biopsy was cryopreserved by snap freezing and the other part was manually cut and cultured or 2 to 4 weeks in RPMI-1640 containing 7% HS and IL-2 (100 U/ml), every 7 days half of the medium was replaced by fresh IL-2 containing RPMI-1640 7%HS.

Tetramer staining of SKILs

SKIL cultures were stained with tetrameric-MHC complexes containing the MHC-I epitopes gp100:154-162, gp100:280-288 or tyrosinase:369-377 (Sanquin, Amsterdam, The Netherlands) as described previously (12). Tetrameric-MHC complexes recognizing HIV were used as correction for background binding. Tetramer positivity was defined as at least two-fold increase in the double positive population.

Cytotoxic Acitivity of SKILs

Cytotoxic activity by SKILs in response to T2 cells pulsed with the indicated peptides or BLM (a melanoma cell line expressing HLA-A*02:01 and no endogenous expression of gp100 and tyrosinase), transfected with control antigen G250, or with gp100 or with tyrosinase, or an allogenic HLA-A*02:01-positive, gp100-positive, and tyrosinase-positive tumor cell line (Mel624) were measured. Target cells were incubated with 100 μCi $Na_2[^{51}Cr]O_4$ (Amersham, Bucks, UK) and, after washing, added to SKILs (1×10^5 cells) and unlabeled K562 cells (1×10^4 cells) in triplicate wells of a round bottom microtiter plate (E/T ratio 10/1). After 4 hours, supernatants were harvested and radioactivity was measured. The specific percentage of cytotoxicity was defined by the following formula:

$$\text{specific cytotoxicity} = \frac{(\text{experimental release [cpm]} - \text{spontaneous release [cpm]})}{(\text{maximum release [cpm]} - \text{spontaneous release [cpm]})} \times 100\%$$

Positive and specific cytotoxic activity was defined as a two-fold increase compared to stimulation with the same cell-lines pulsed with an irrelevant peptide.

Cytokine production profiles by SKILs

The production of IFNγ, TNFα, IL-10, IL-5, IL-4, IL-2 by SKILs was measured in supernatants after 16 hours of co-culture with different target cells to obtain a cytokine profile of post-vaccination SKILs. Target cells include T2 cells pulsed with the indicated peptides or BLM (a melanoma cell line

expressing HLA-A*02:01 and no endogenous expression of gp100 and tyrosinase), transfected with control antigen G250, or with gp100 or with tyrosinase, or an allogenic HLA-A*02:01-positive, gp100-positive, and tyrosinase-positive tumor cell line (Mel624) with SKILs, using the cytometric bead array (Th1/Th2 Cytokine CBA 1; BD Pharmingen), according to the manufacturer instructions. Positive and specific cytotoxic activity was defined as a two-fold increase compared to stimulation with the same cell-lines pulsed with an irrelevant peptide.

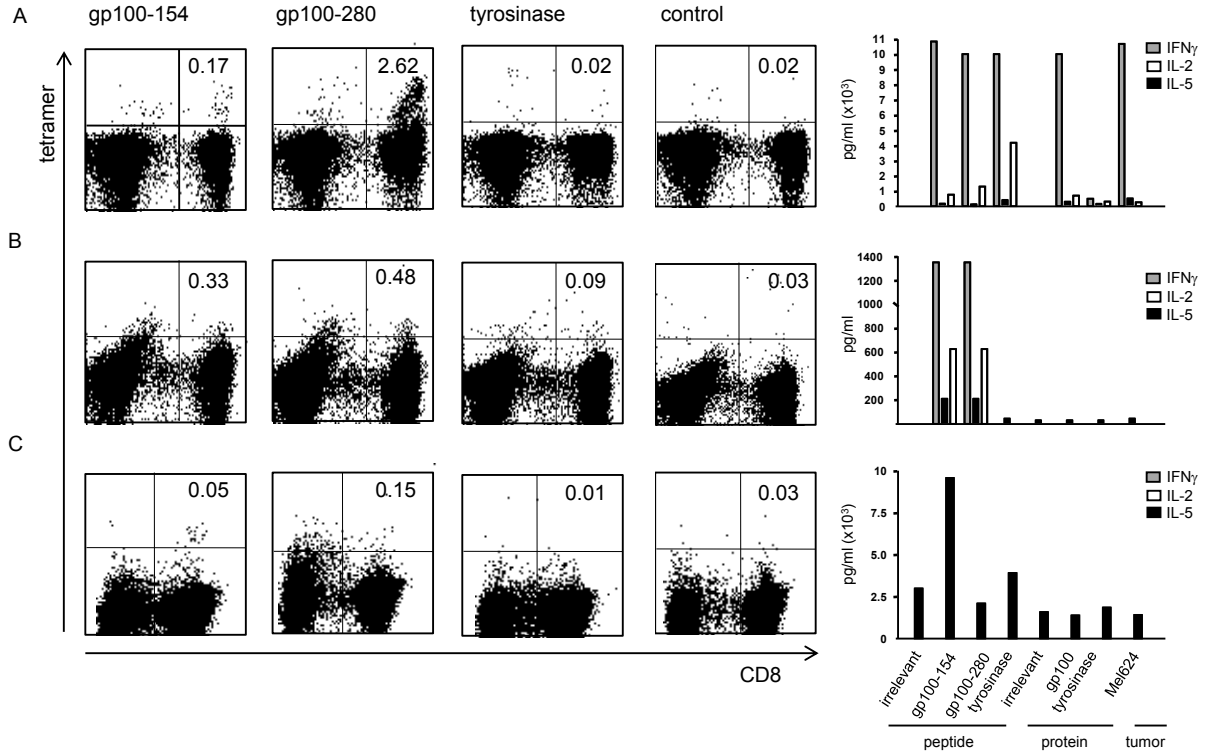

Supplementary Figure 2. Definition of criteria for SKIL culture evaluation. Three examples are shown to illustrate the definition of SKIL culture criteria. (A) Criterion III, one patient (IV-B-16-St) with a clear population of TAA-specific $CD8^+$ T cells in SKIL cultures, which produce high levels of IFNγ upon encounter of both the defined gp100 peptides and naturally processed gp100 presented by a HLA-A*02:01 positive melanoma cell line (Mel624). Moderate amounts of IL-2 are produced and minimal production of IL-5, representing a clear IFNγ dominant cytokine profile. (B) Criterion II, a patient (IV-B-11-Ro) with TAA-specific $CD8^+$ T cells in SKIL cultures which produce high levels of IFNγ and IL-2 upon encounter of the gp100 peptide, but fail to recognize the naturally processed gp100. (C) Criterion I, a patient (IV-A-07-Th) with a population of TAA-specific $CD8^+$ T cells in SKIL cultures, recognizing the g100-154 peptide, but not the naturally processed gp100. Furthermore, those TAA-specific $CD8^+$ T cells do not produce IFNγ but produce elevated levels of IL-5 instead, indicating that the immune system is skewed towards tumor tolerance.

Skin-test infiltrating lymphocyte culture evaluation

SKILs were evaluated according to increasingly stringent criteria; the presence of TAA-specific $CD8^+$ T cells by tetrameric MHC-peptide complexes (criterion I); peptide-recognition by specific production of Thelper 1 (Th1) cytokines (e.g. IFNγ and/or IL-2) or cytotoxicity and no Thelper 2 (Th2) cytokines (criterion II); or tumor-recognition of naturally processed TAA by specific production of Th1 cytokines or cytotoxicity and no Th2 cytokines (criterion III), an example is provided in Supplementary Figure 2. The best overall TAA-specific responses wasused for analyses, regardless of the time point at which the SKILs were obtained within the study, as this reflects the individual competence to generate a specific immune response.

Statistical analysis

Overall survival (OS) was calculated from the date of apheresis to date of death and analyzed by Kaplan-Meier estimation using SPSS19.0 (SPSS Inc, Chicago, IL). Statistical significance was evaluated using the log-rank test. Cox proportional hazard model was used to calculate hazard ratios (HR) for survival.

Table 1. Vaccination protocols and characteristics of SKIL cultures.

Protocol	Number of evaluable patients (total)	Method of antigen loading	Route of administration	Anti-CD25 mAb**	Number of cultures with outgrowth pos/total (%)	Mean ($x10^6$)	Range ($x10^6$)
1	1 (1)	Class I wt	i.d.	no	4/4 (100)	0.15	0.09 – 0.2
2	13 (17)	Class I wt	i.n.	no	48/48 (100)	0.50	0.03 – 5.6
3	17 (22)	RNA ¥	i.n.	no	115/126 (86)	0.53	0.01 – 7.0
4	13 (15)	Class I wt	i.v./i.d.	no	44/63 (70)	0.59	0.01 – 1.8
5	9 (10)	Class I mod †	i.v./i.d.	no	21/48 (44)	0.16	0.01 – 1.3
6	11 (11)	Class I/II wt ‡	i.n.	no	65/73 (89)	0.53	0.01 – 3.1
7	13 (15)	Class I wt	i.v./i.d.	yes	42/54 (78)	0.44	0.01 – 3.3
total	**77 (91)**				**339/416 (82)**		

Abbreviations: mAb, monoclonal antibody; wt, wild type; mod, modified, i.d., intradermal,; i.n., intranodal; i.v., intravenous
** Four or eight days prior to first vaccination, anti-CD25 antibody 0.5 mg/kg was administered intravenously
$ Class I wt; HLA class I-restricted wild-type gp100-derived peptides 154-162 and 280-288 and HLA class I-restricted tyrosinase-derived peptide 369-377
¥ mRNA; messenger RNA encoding full length gp100 and tyrosinase
† Class I mod; HLA class I-restricted modified gp100-derived peptides 154-162 Q→A and 280-288 A→V and HLA class I-restricted tyrosinase-derived peptide

Results

Vaccination protocols and SKIL cultures

Seventy-seven patients completed at least 1 scheduled cycle and were thus evaluable for immunological response (Table 1). Fourteen patients did not complete 1 scheduled cycle due to rapid progressive disease. The patients were vaccinated according to the various vaccination protocols, including intranodal, intradermal, intravenous/intradermal vaccinations; mode of antigen loading of DC was either pulsing with MHC Class I or MHC Class I and II defined epitopes derived from gp100 and tyrosinase, or electroporation with mRNA encoding these tumor associated antigens (25). In one protocol, patients received a single infusion of anti-CD25 antibody therapy prior to the first vaccination (14). To demonstrate that this procedure is feasible for large scale clinical studies, we determined the rate of successful SKIL cultures and their yield (Table 1). 329 out of 410 (80%) cultures yielded sufficient numbers of cells to allow further analysis, which results appear to be independent of the vaccination protocol (Table 1). On average, 4 successful cultures with different specificities were obtained per patient during complete course of 3 vaccination cycles.

KLH-specific T cell responses do not predict overall survival

Peripheral blood samples during and after completion of each vaccination cycle were available for 70 patients for testing of KLH-specific $CD4^+$ T cell proliferation. The maximum standard index (SI) compared to ovalbumin (OVA) was recorded and designated 'strong' if more than 40. No significant difference in median OS was observed for patients with or without strong KLH-specific $CD4^+$ T cell response; being 6.9 and 9.0 months respectively (p=0.95, Figure 1a, Table 2). We analyzed the cytokines produced upon KLH encounter and 9 out of 40 tested patients showed a clear IFNγ dominant response. However, this parameter did not significantly discriminate between patients with good and poor prognosis; median OS 16.7 and 11.0 months respectively, p=0.40 (Figure 1b, Table 2).

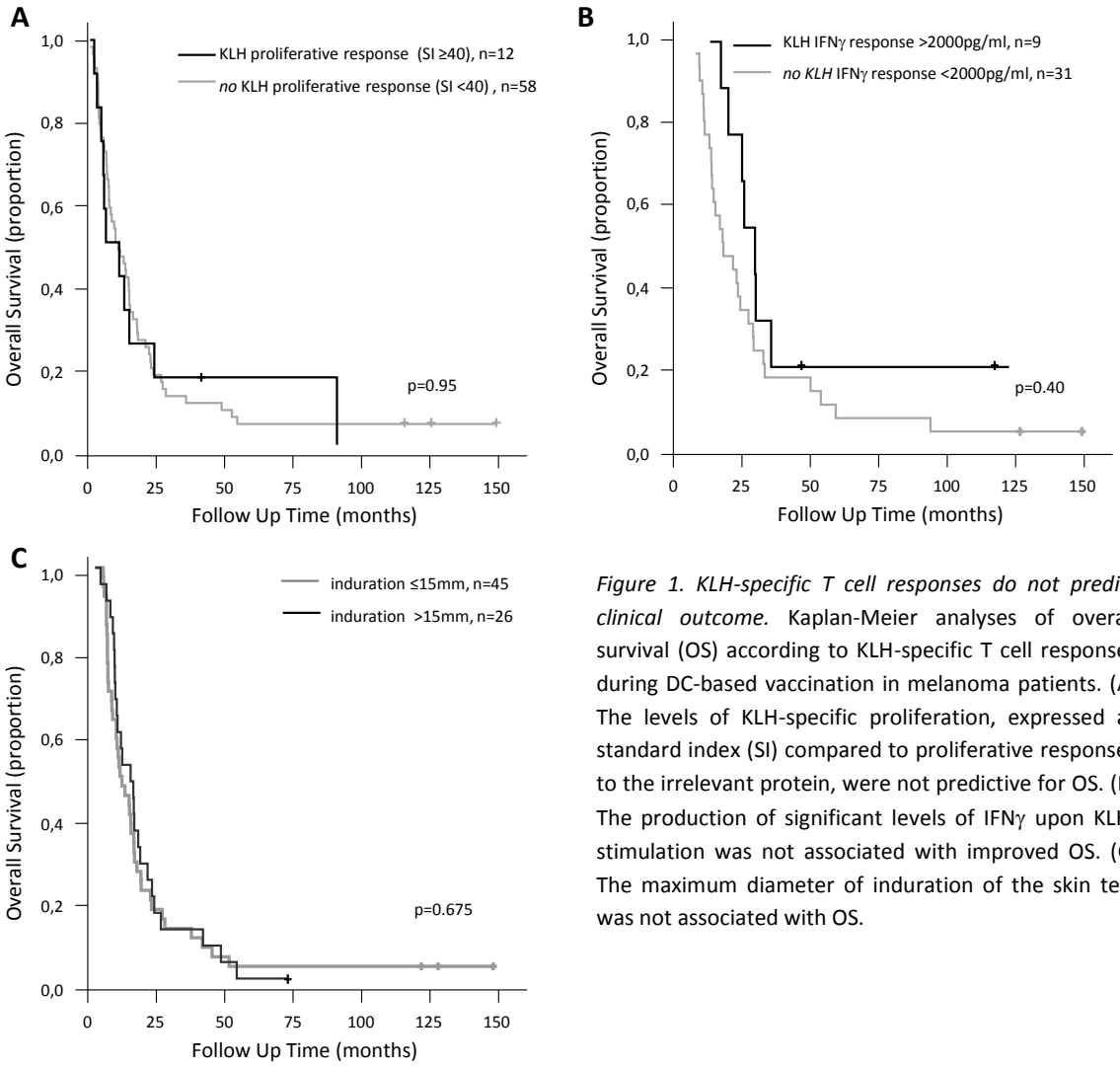

Figure 1. KLH-specific T cell responses do not predict clinical outcome. Kaplan-Meier analyses of overall survival (OS) according to KLH-specific T cell responses during DC-based vaccination in melanoma patients. (A) The levels of KLH-specific proliferation, expressed as standard index (SI) compared to proliferative responses to the irrelevant protein, were not predictive for OS. (B) The production of significant levels of IFNγ upon KLH-stimulation was not associated with improved OS. (C) The maximum diameter of induration of the skin test was not associated with OS.

Induration at the injection site is not predictive for clinical outcome

After completing the first cycle of three vaccinations, the induration in 70 evaluable patients upon intradermal challenge with DC expressing gp100 or tyrosinase was median 13mm (range 0 – 36mm) and 13mm (0 – 34mm) respectively. The degree of induration was not predictive for clinical outcome with a maximum induration >15mm corresponding with a median OS of 9.8 months and a maximum induration ≤15mm corresponding with 13.0 months, p=0.675 (Figure 1c).

SKIL procedure does not require the presence of defined epitopes

In some protocols we exploited DC transfected with mRNA encoding gp100 and tyrosinase, thus expressing multiple undefined epitopes. To investigate whether the results of tetramer screening of SKIL cultures depend on the presence of defined TAA epitopes, we performed parallel skin-test challenges within individual patients. In one cohort (n=17) we performed the delayed type hypersensitivity (DTH) procedure with intradermal injections of DC pulsed with defined epitopes (gp100:154-168, gp100:280-288 and tyrosinase:369-377) and DC transfected with mRNA encoding the same tumor antigens (full length gp100 and tyrosinase) within individual patients, who were vaccinated with mRNA-transfected DC. Cultures from SKILs obtained from DTH sites containing DC loaded with defined epitopes or mRNA-transfected DC, yielded equal numbers of cells and successful cultures. In total, 126 DTH challenges were performed in parallel, of these, 59 out of 63 mRNA-DC-challenged and 54 out of 63 peptide-DC-challenged skin-test biopsies yielded successful cultures. Comparable average yields per culture were obtained, 0.53 (range 0.01 – 7.0) $x10^6$ cells with mRNA-transfected DC and 0.40 (range 0.01 – 2.8) $x10^6$ cells for peptide pulsed DC. Furthermore, tetramer

screening for TAA-specific T cells showed that challenge with DC pulsed with defined epitopes or DC transfected with mRNA have similar sensitivity and specificity (data not shown). TAA-specific $CD8^+$ T cells directed against all 3 defined epitopes were detected in single SKIL cultures obtained from intradermal challenge with DC transfected with mRNA encoding both gp100 and tyrosinase (data not shown).

Table 2. Hazard Ratios associated with criteria for response

Response criterium	Hazard Ratio (95%CI)	P-value
Criterium III	0.30 (0.14 – 0.65)	0.002
Criterium II	0.42 (0.23 – 0.77)	0.005
Criterium I	0.60 (0.42 – 0.86)	0.005
Nr of epitopes (0, 1, 2 or 3)	0.60 (0.42 – 0.85)	0.004
KLH proliferation (SI >40)	0.93 (0.73 – 1.20)	0.583

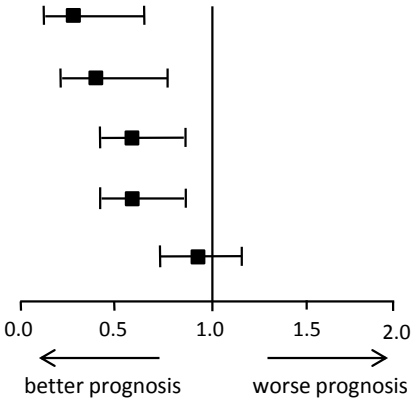

NOTE: A graphical representation of the hazard ratios associated with different response criteria were estimated using Cox proportional-hazard models. Hazard ratio <1 defines a positive correlation with overall survival if the criterion is met. Horizontal lines represent 95% confidence intervals. Abbreviations: KLH, keyhole limpet hemocyanin; IFNγ, interferon-gamma; SI, standard index compared to stimulation with Ovalbumin.

SKIL culture evaluation accurately predicts clinical outcome

To investigate the role of the breadth of response, we analyzed the clinical outcome in relation to the number of epitopes that were recognized. The presence of one TAA-specific $CD8^+$ T cell population in SKIL cultures was demonstrated in 14 patients, who had a median OS of 9.8 months (95%CI 7.3 – 12.3) compared to 10.9 months (95%CI 5.7 – 16.0) in 52 patients in whom no TAA-specific $CD8^+$ T cell populations were detected (Figure 2a). Two or 3 TAA-specific $CD8^+$ T cell populations were detected in 8 and 3 patients, respectively, corresponding with a median OS of 14.2 months (95%CI 0.4 – 30.7) and median not reached, respectively (Figure 2a). Overall, the presence of TAA-specific $CD8^+$ T cells in SKIL cultures (criterion I) was demonstrated in 25 patients and was associated with improved survival; median OS 14.1 months compared to 10.9 months in patients without TAA-specific $CD8^+$ T cells (Figure 2b) and HR 0.60 (95%CI 0.42 – 0.86, p=0.005, Table 2). Since patients were vaccinated with DC loaded with either multiple melanoma peptides or mRNA-transfected DC presenting multiple undefined antigens, T cell populations with different specificities could have been induced. In 18 patients with TAA-specific $CD8^+$ T cells we also demonstrated vaccine-specific peptide-recognition (criterion II), which was strongly associated with improved survival (median OS 14.2 months versus 10.2 months in patients without vaccine-specific peptide-recognition, Figure 2c and HR 0.42 (95%CI 0.23 – 0.77, p=0.005, Table 2). To even better identify immune responsive patients, we selected for SKILs responding to naturally processed antigen by producing Th1 cytokines, predominantly IFNγ. This was observed in 12 of these 18 patients who had a median OS of 24.1 versus 9.9 months in patients without SKILs responding to naturally processed antigen (Figure 2d) and HR 0.30 (0.14 – 0.65), p=0.002 (Table 2). As multiple cytokines were measured in SKIL cultures, we were able to identify functionally different cytokine profiles. As mentioned above and Supplementary Figure 2, in the majority of cases we detected IFNγ dominated cytokine production. However, in 2 patients we detected predominantly IL-5 production by SKILs responding to peptide-pulsed target cells, indicative

of Th2 skewing of the immune response. The detection of this response coincided with rapid progressive disease in both patients (Figure 3).

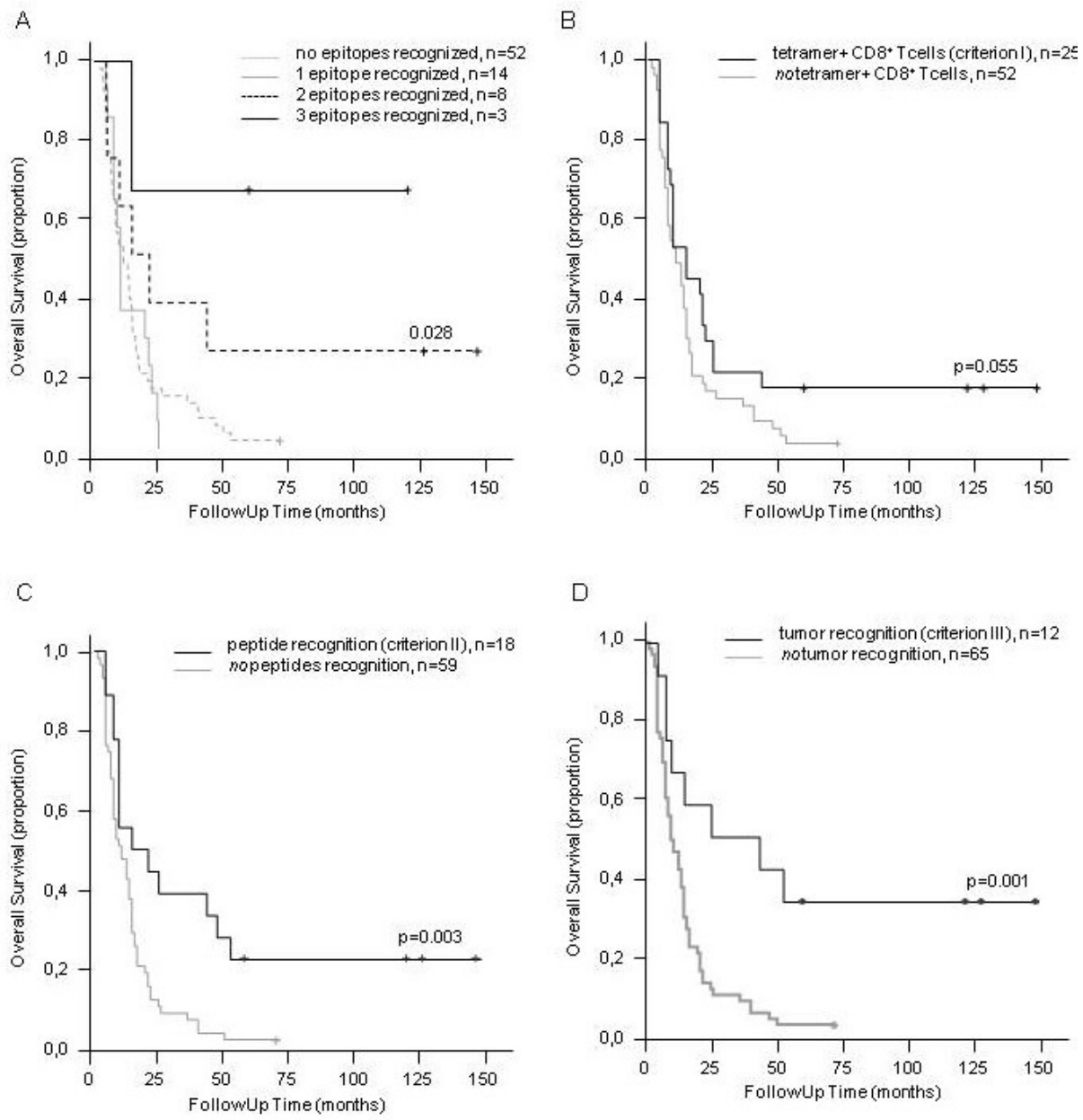

Figure 2. Analyses of SKIL cultures predict clinical outcome of DC-based therapy in metastatic melanoma patients. Kaplan-Meier analyses of overall survival (OS) according to different criteria for immune response in skin-test infiltrating lymphocyte (SKIL) cultures obtained during DC-based vaccination in melanoma patients. (A) The breadth of the vaccine-specific immune responses, measured as the number of vaccine-specific tetramer-positive populations in SKIL cultures, correlates with OS. (B) SKIL cultures were sampled with tetrameric MHC-peptide complexes for the presence of TAA-specific $CD8^+$ T cells (criterion I). (C) Next, SKIL cultures were evaluated for recognition of tumor-peptides by the production of IFNγ or cytotoxicity, but no IL-5 production (criterion II); improving the accuracy of this bioassay to select patients with a favourable clinical outcome. (D) Lastly, SKIL cultures were evaluated according to the most stringent criterion III, specific IFN production or cytotoxicity, but no IL-5 production upon recognition of naturally processed tumor antigen; which was highly associated with improved OS.

Discussion

Although the presence of tumor-specific cytotoxic T cells in cancer patients has been reported to associate with favourable clinical outcome (26), bioassays that accurately link vaccine-specific immune responses to survival are lacking. Although tetramer analysis or ELIspot assays of TAA-specific responses in peripheral blood are available, the low prevalence of TAA-specific T cells in peripheral blood makes this procedure less suitable for routine monitoring. Moreover, besides antigen specificity and effector activity, anti-tumor $CD8^+$ T cells must be able to extravasate and

migrate into peripheral target tissues. We addressed this issue by evaluating SKIL cultures. This bioassay integrates multiple facets of an effective immune response. First, it serves as a 'fitness test'; the *in vivo* intradermal challenge selects TAA-specific T cells that possess the migratory capacities to leave the circulation and penetrate peripheral tissue. Secondly, tetrameric MHC-peptide complexes allow sampling of different specificities (criterion I) within the SKIL population. Since SKILs are expanded *in vitro* in the absence of antigen, the composition of different specificities closely parallels the *in vivo* situation. Thirdly, more stringent recognition can be assessed by challenging SKILs either with target cells loaded with defined antigenic peptides (criterion II) or by target cells that express naturally processed TAA (criterion III). Finally, measuring cytokine profiles upon antigenic challenge reflects the *in vivo* programming of TAA-specific T cells either towards Th1 or Th2 immune responses. The latter is of crucial importance to interpret anti-tumor responses and eventual clinical outcome.

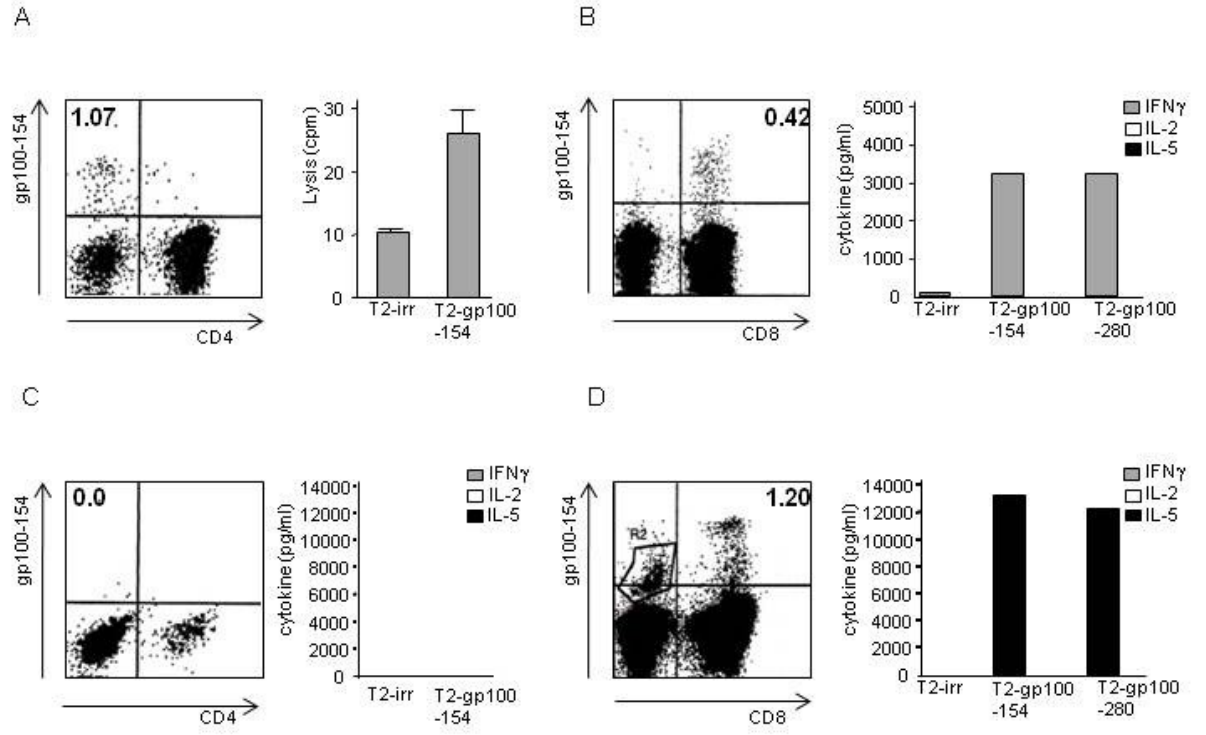

Figure 3. Immunological response closely relates to the individual clinical course of disease. Two patients are shown in whom the immunological evaluation predicted the course of their disease. (A) Data of IV-A-01 is depicted in whom TAA-specific $CD8^+$ T cell with specific cytotoxic capacity were detected after the first cycle of vaccinations. (B) After completing the third cycle of vaccinations, IFNγ-producing TAA-specific $CD8^+$ T cells were detected in SKIL cultures and no IL-5 was produced. As of May 2012, this patient survived 120+ months from start of vaccinations. (C) Data of IV-A-05 is shown in whom no TAA-specific $CD8^+$ T cells were detected after the first cycle of vaccinations. (D) However, SKIL culture evaluation upon the third cycle of vaccinations revealed TAA-specific $CD8^+$ T that produced high levels of IL-5 upon antigen encounter. Planned evaluation showed rapid progression of disease; the patient died shortly after the third vaccination series, 20 months after start of vaccination.

In most clinical studies a highly immunogenic non-tumor antigen is included in the vaccine, such as keyhole limpet hemocyanin (KLH) or tetanus toxoid (TT). The rationale for this approach is two-fold; it is used as a surrogate marker to which excessive humoral and proliferative responses will be induced, in that respect is serves to evaluate immune competence per individual. Secondly, these immunogenic proteins contain a multitude of predominantly T helper cell epitopes; ergo, it functions as a non-tumor specific adjuvant. We have previously investigated the magnitude and dynamics of humoral responses in this cohort of metastatic melanoma patients who underwent DC-based therapy (27). Our findings show that humoral anti-KLH responses are dictated by different vaccination parameters, such as route of administration and anti-CD25 mAb pretreatment. $CD8^+$ cytotoxic T cells (CTLs), as the endpoint effectors, represent a critical population for anti-cancer immunity. However, cellular responses to KLH are invariantly induced in the vast majority of patients,

regardless of the vaccination protocol (14-18, 28). In this study we show that neither the magnitude of KLH-specific T cell responses, nor the quality of the KLH-specific responses in terms of IFN production is predictive for clinical outcome. This demonstrates that loading *ex vivo* generated DC with KLH does not provide adequate means to assess anti-tumor cellular immune competence. This notion is further supported by the lack of correlation between the quality of vaccine-specific immune responses, as determined by the above mentioned SKIL criteria, and the magnitude of KLH-specific cellular responses (Supplementary Figure 2).

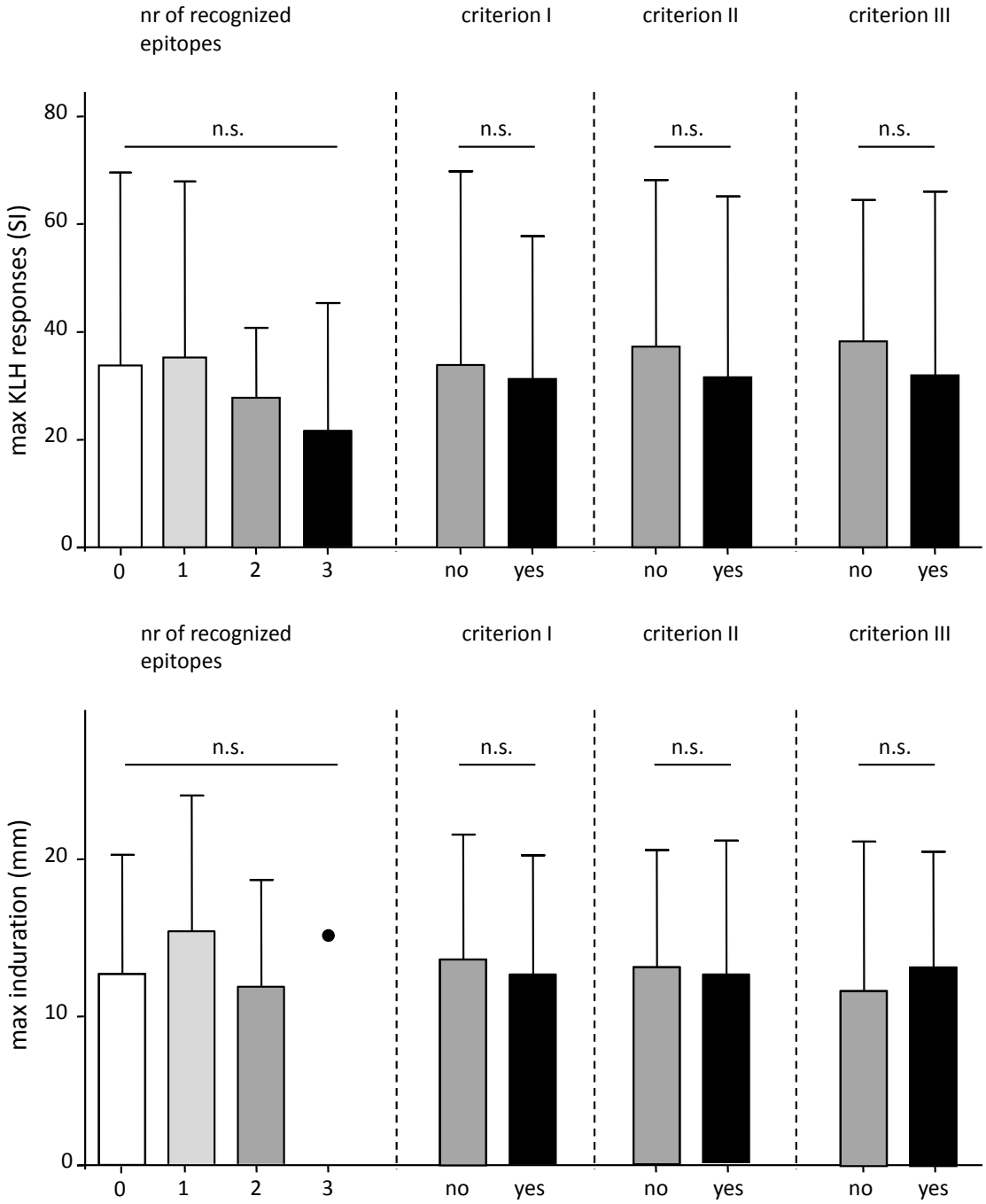

Supplementary Figure 3 and 4. KLH-specific T cell responses and levels of induration according to SKIL classification. Regardless of the number of epitopes or the increasingly stringent criteria for TAA-specific immune responses; the levels of KLH-specific T cell responses were similar and highly variable between individuals. One-way ANOVA was used for comparison of KLH-specific T cell responses in groups of patients with increasing breadth of TAA-specific $CD8^+$ T cell responses. Student t-test was used for comparison of KLH-specific T cell responses in groups of patients as defined by different SKIL criteria. Regardless of the number of epitopes or the increasingly stringent criteria for TAA-specific immune responses; the maximum induration at the injection site was similar in all groups. One-way ANOVA was used for comparison of induration in groups of patients with increasing breadth of TAA-specific $CD8^+$ T cell responses. Student t-test was used for comparison of induration in groups of patients as defined by different SKIL criteria.

It has been reported in some studies that the degree of induration at the injection site would reflect the individual capacity to mount a vaccine-specific immune response, and therefore correlate to therapy response. If so, the degree of induration would provide an easy and accessible measure for therapy evaluation. In general, induration is regarded as a typical $CD4^+$ T cell reaction. On the contrary, others have shown that intradermal injection site can be briskly infiltrated by $CD8^+$ T cells, suggesting that the level of induration would in fact show Th1 type immune induction. Our data clearly illustrate that induration is not associated with overall survival or with TAA-specific $CD8^+$ T cell responses (Supplementary Figure 3). Furthermore, the measurement of induration is subject to high inter-test variability which complicates standardization. Our increasing understanding of the complex interaction of an individuals' immune system and cancer and the development of immunotherapeutic interventions with clinical benefit, have drastically influenced the way we design and perform clinical studies on immunotherapy (29). From small proof-of-principal studies focussing on a single parameter (3), we now focus on large randomized prospective studies with adjusted endpoints, designed to evaluate potential biomarkers and specific clinical response patterns (1, 30).

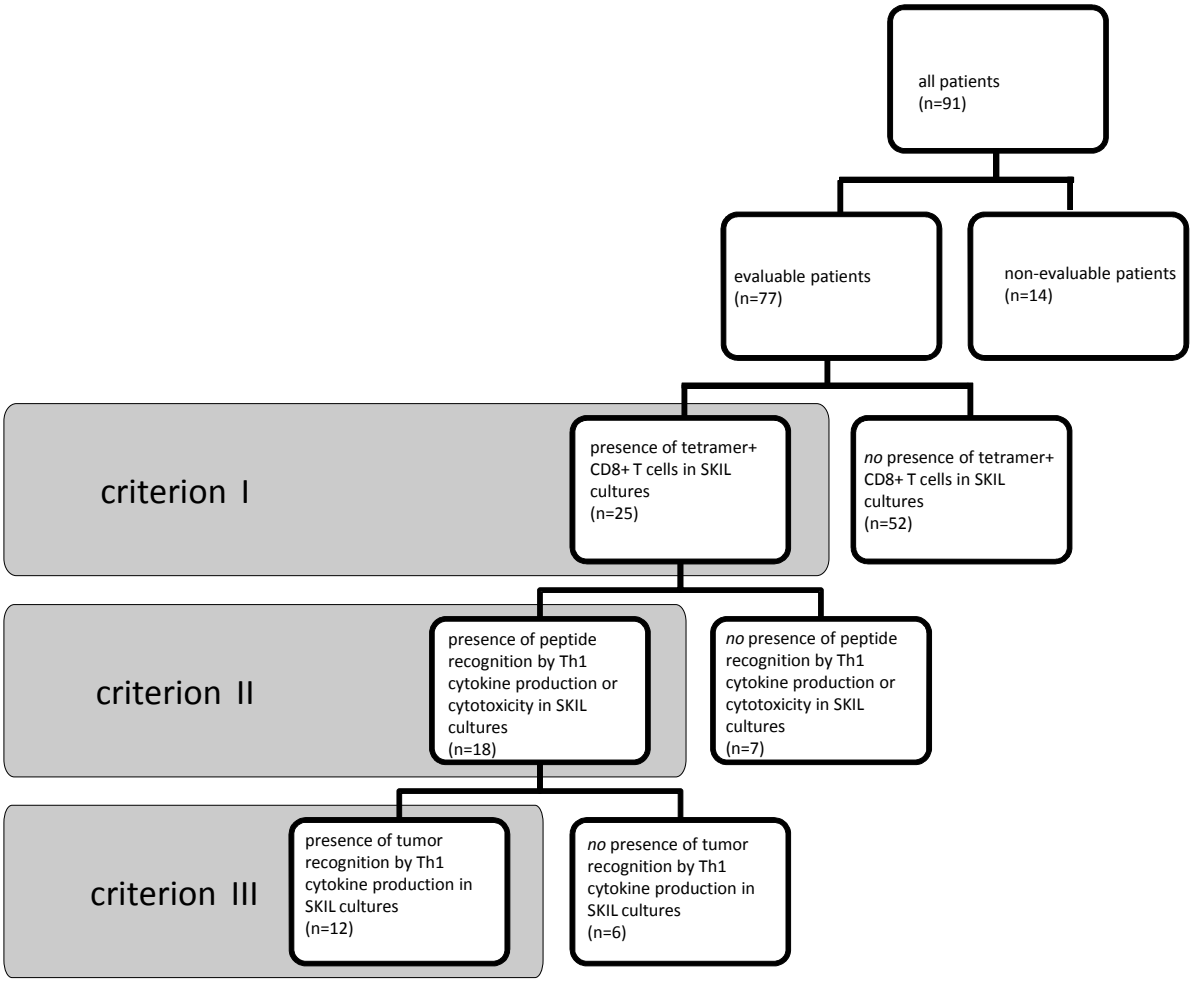

Supplementary Figure 5. Patient selection based on SKIL criteria. SKIL criteria are applied to select patients with immune responses meeting increasingly stringent criteria.

In this respect, we evaluated SKIL culture analyses for its feasibility in large studies. With notion of its invasive nature, this procedure is relatively easy to perform, does not need specialized personnel and is not labour intensive and is acceptable to the large majority of patients. Importantly, this procedure consistently yields sufficient numbers of SKILs to address the vaccine-specific immune response, which is independent of the vaccination protocol or intradermal challenge conditions. Even in patients vaccinated with DC loaded with modified tumor peptides to enhance MHC-binding efficacy, we detected $CD8^+$ SKILs directed against the tumor to similar extend as in other vaccination protocols. This is in line with our previous observation that modified peptides efficiently elicit

responses to wildtype peptides (31), resulting in comparable immunological responses *in vivo* as vaccination with wildtype peptide loaded DC (15).

The development of tools to monitor immune responses during immunotherapy is complicated by the evoluation of different effector T cell populations over time in response to vaccination and tumor changes. So far, it is not clear which time window after start of treatment reflects the vaccine-induced responses best and might be predictive of clinical outcome. Furthermore, the relevant effector populations are distributed over several body compartments, like draining lymph nodes, tumor tissue, bone marrow and peripheral blood; and it is debatable what compartment is best suitable to monitor vaccine-specific immune responses. The patients displayed in Figure 3 illustrate that the evaluation of both the kinetics and functional status of vaccine-specific responses is critical for correct correlation with clinical outcome. In the first patient, if only the percentage of vaccine-specific SKILs would have been assessed, it would have been a decline in vaccine-specific SKILs, However, the specific Th1 type responses after 1 and 3 cycles classifies this response as 'favourable'. In the second patient, the appearance of vaccine-specific SKILs could have been interpreted as a favourable response. However, since we measured a typical Th2 skewed functional status, this response was correctly classified as non-favourable. We acknowledge that further studies, incorporating multiple facets of tumor-specific immune responses at multiple time points after treatment, are warranted to elucidate the optimal time window to perform immune monitoring.

In conclusion, by evaluating the migratory-, antigen recognition-, as well as the effector function of SKILs, we are able to select for multifunctional $CD8^+$ T cells with high tumor recognition efficacy. We demonstrated that analyzing SKILs is a simple and robust, bioassay to predict overall survival in metastatic melanoma patients. Therefore, it represents an ideal candidate for immune monitoring in upcoming immunotherapy trials.

References

1. Sharma P, Wagner K, Wolchok JD, Allison JP. Novel cancer immunotherapy agents with survival benefit: recent successes and next steps. Nat Rev Cancer. 2011;11:805-12.
2. Lesterhuis WJ, Haanen JB, Punt CJ. Cancer immunotherapy - revisited. Nat Rev Drug Discov.10:591-600.
3. Figdor CG, De Vries IJ, Lesterhuis WJ, Melief CJ. Dendritic cell immunotherapy: mapping the way. Nat Med. 2004;10:475-80.
4. Palucka K, Ueno H, Banchereau J. Recent developments in cancer vaccines. J Immunol. 2011;186:1325-31.
5. Garbe C, Eigentler TK, Keilholz U, Hauschild A, Kirkwood JM. Systematic review of medical treatment in melanoma: current status and future prospects. Oncologist. 2011;16:5-24.
6. Schumacher K. Keyhole limpet hemocyanin (KLH) conjugate vaccines as novel therapeutic tools in malignant disorders. J Cancer Res Clin Oncol. 2001;127 Suppl 2:R1-2.
7. Britten CM, Janetzki S, Ben-Porat L, Clay TM, Kalos M, Maecker H, et al. Harmonization guidelines for HLA-peptide multimer assays derived from results of a large scale international proficiency panel of the Cancer Vaccine Consortium. Cancer Immunol Immunother. 2009;58:1701-13.
8. Janetzki S, Panageas KS, Ben-Porat L, Boyer J, Britten CM, Clay TM, et al. Results and harmonization guidelines from two large-scale international Elispot proficiency panels conducted by the Cancer Vaccine Consortium (CVC/SVI). Cancer Immunol Immunother. 2008;57:303-15.
9. Pockaj BA, Sherry RM, Wei JP, Yannelli JR, Carter CS, Leitman SF, et al. Localization of 111indium-labeled tumor infiltrating lymphocytes to tumor in patients receiving adoptive immunotherapy. Augmentation with cyclophosphamide and correlation with response. Cancer. 1994;73:1731-7.
10. Mauro C, Fu H, Marelli-Berg F. T cell trafficking and metabolism: novel mechanisms and targets for immunomodulation. Currt Opin Pharmacol. 2012.[Epub ahead of print]
11. Wang E, Panelli MC, Marincola FM. Gene profiling of immune responses against tumors. Curr Opin Immunol. 2005;17:423-7.
12. De Vries IJ, Bernsen MR, Lesterhuis WJ, Scharenborg NM, Strijk SP, Gerritsen MJ, et al. Immunomonitoring tumor-specific T cells in delayed-type hypersensitivity skin biopsies after dendritic cell vaccination correlates with clinical outcome. J Clin Oncol. 2005;23:5779-87.
13. Balch CM, Buzaid AC, Soong SJ, Atkins MB, Cascinelli N, Coit DG, et al. Final version of the American Joint Committee on Cancer staging system for cutaneous melanoma. J Clin Oncol. 2001;19:3635-48.
14. Jacobs JF, Punt CJ, Lesterhuis WJ, Sutmuller RP, Brouwer HM, Scharenborg NM, et al. Dendritic cell vaccination in combination with anti-CD25 monoclonal antibody treatment, a phase I/II study in metastatic melanoma patients. Clin Cancer Res. 2011;16(20):5067-78
15. Lesterhuis WJ, Schreibelt G, Scharenborg NM, Brouwer HM, Gerritsen MJ, Croockewit S, et al. Wild-type and modified gp100 peptide-pulsed dendritic cell vaccination of advanced melanoma patients can lead to long-term clinical responses independent of the peptide used. Cancer Immunol Immunother. 2011;60:249-60.
16. De Vries IJ, Lesterhuis WJ, Scharenborg NM, Engelen LP, Ruiter DJ, Gerritsen MJ, et al. Maturation of dendritic cells is a prerequisite for inducing immune responses in advanced melanoma patients. Clin Cancer Res. 2003;9:5091-100.
17. Verdijk P, Aarntzen EH, Lesterhuis WJ, Boullart AC, Kok E, van Rossum MM, et al. Limited amounts of dendritic cells migrate into the T-cell area of lymph nodes but have high immune activating potential in melanoma patients. Clin Cancer Res. 2009;15:2531-40.
18. Lesterhuis WJ, De Vries IJ, Schreibelt G, Lambeck AJ, Aarntzen EH, Jacobs JF, et al. Route of administration modulates the induction of dendritic cell vaccine-induced antigen-specific T cells in advanced melanoma patients. Clin Cancer Res. 2011;17:5725-35.
19. Berger TG, Feuerstein B, Strasser E, Hirsch U, Schreiner D, Schuler G, et al. Large-scale generation of mature monocyte-derived dendritic cells for clinical application in cell factories. J Immunol Methods. 2002;268:131-40.
20. De Vries IJ, Adema GJ, Punt CJ, Figdor CG. Phenotypical and functional characterization of clinical-grade dendritic cells. Methods Mol Med. 2005;109:113-26.
21. Topalian SL, Gonzales MI, Parkhurst M, Li YF, Southwood S, Sette A, et al. Melanoma-specific CD4+ T cells recognize nonmutated HLA-DR-restricted tyrosinase epitopes. J Exp Med. 1996;183:1965-71.
22. Li K, Adibzadeh M, Halder T, Kalbacher H, Heinzel S, Muller C, et al. Tumour-specific MHC-class-II-restricted responses after in vitro sensitization to synthetic peptides corresponding to gp100 and Annexin II eluted from melanoma cells. Cancer Immunol Immunother. 1998;47:32-8.
23. Schuurhuis DH, Verdijk P, Schreibelt G, Aarntzen EH, Scharenborg N, de Boer A, et al. In situ expression of tumor antigens by messenger RNA-electroporated dendritic cells in lymph nodes of melanoma patients. Cancer Res. 2009;69:2927-34.
24. Labtube.tv [internet], Sudbury (United Kingdom) Technology Networks Ltd, available from www.labtube.tv
25. Aarntzen EH, Schreibelt G, Bol K, Lesterhuis WJ, Croockewit AJ, de Wilt JH, et al. Vaccination with mRNA-electroporated dendritic cells induces robust tumor antigen-specific CD4+ and CD8+ T cells responses in stage III and IV melanoma patients. Clin Cancer Res. 2012 [Epub ahead of print]
26. Coulie PG, van der Bruggen P. T-cell responses of vaccinated cancer patients. Curr Opin Immunol. 2003;15:131-7.
27. Aarntzen EH, de Vries IJ, Goertz JH, Beldhuis-Valkis M, Brouwers HM, van de Rakt MW, et al. Humoral anti-KLH responses in cancer patients treated with dendritic cell-based immunotherapy are dictated by different vaccination parameters. Cancer Immunol Immunother. 2012.[Epub ahead of print]
28. Lesterhuis WJ, De Vries IJ, Schreibelt G, Schuurhuis DH, Aarntzen EH, De Boer A, et al. Immunogenicity of dendritic cells pulsed with CEA peptide or transfected with CEA mRNA for vaccination of colorectal cancer patients. Anticancer Res. 2010;30:5091-7.
29. Topalian SL, Weiner GJ, Pardoll DM. Cancer immunotherapy comes of age. J Clin Oncol. 2011;29:4828-36.

30. Wolchok JD, Hoos A, O'Day S, Weber JS, Hamid O, Lebbe C, et al. Guidelines for the evaluation of immune therapy activity in solid tumors: immune-related response criteria. Clin Cancer Res. 2009;15:7412-20.
31. Bakker ABH, van der Burg SH, Huijbens RJF, Drijfhout JW, Melief CJM, Adema GJ, et al. Analogues of CTL epitopes with improved MHC class-I binding capacity elicit antimelanoma CTL recognizing the wild-type epitope. Int J Cancer. 1997;70:302–309.

Chapter 12

Early identification of antigen-specific immune responses in vivo by ^{18}F-FLT PET imaging

Aarntzen EH

Srinivas M*

De Wilt JHW*

Jacobs JF

Lesterhuis WJ

Windhorst AD

Troost EG

Bonenkamp JJ

Van Rossum MM

Blokx WA

Mus RD

Boerman OC

Punt CJ

Figdor CG

Oyen WJ

De Vries IJ

* contributed equally

Proc Natl Acad Sci U S A. 2011;108(45):18396-9.

Abstract

Current biomarkers are unable to adequately predict vaccine-induced immune protection in humans with infectious disease or cancer. However, timely and adequate assessment of antigen-specific immune responses is critical for successful vaccine development. Therefore, we have developed a method for the direct assessment of immune responses *in vivo* in a clinical setting. Melanoma patients with lymph node (LN) metastases received dendritic cell (DC) vaccine therapy, injected intranodally, followed by ^{18}F-labeled 3'-fluoro-3'-deoxy-thymidine (^{18}F-FLT) PET at varying time points after vaccination. Control LNs received saline or DCs without antigen. De novo immune responses were readily visualized in treated LNs early after the prime vaccination, and these persisted for up to three weeks. This selective ^{18}F-FLT uptake was markedly absent in control LNs, although tracer uptake in treated LNs increased profoundly with as little as 4.5×10^5 DCs. Immunohistochemical staining confirmed injected DC dispersion to T cell areas and resultant activation of $CD4^+$ and $CD8^+$ T cells. The level of LN tracer uptake significantly correlates to the level of circulating antigen-specific IgG antibodies and antigen-specific proliferation of T cells in peripheral blood. Furthermore, this correlation was not observed with ^{18}F-FDG. Therefore, ^{18}F-FLT PET offers a sensitive tool to study the kinetics, localization and involvement of lymphocyte subsets in response to vaccination. This allows for early discrimination of responding from non-responding patients in anti-cancer vaccination and aid physicians in individualized decision-making.

Introduction

The field of vaccination has expanded over the last few years to include the development of therapeutic vaccines against infectious diseases such as AIDS (1,2) and tuberculosis (3); as well as conditions such as cancer (4,5). In particular, antigen-specific immunotherapy has recently progressed through the development of effective therapeutic vaccinations in advanced melanoma (6-8) and prostate cancer (5). Antigen-specific immune responses in cancer patients can also be induced by exploiting autologous dendritic cells (DCs) that are "educated" *ex vivo* i.e. DCs that are appropriately activated and loaded with tumor antigens (9). DCs are the most potent antigen presenting cells of the immune system and play a central role in the induction and maintenance of antigen-specific immunity (10). These cells capture and process antigen and migrate to the lymph nodes (LNs) where they present the antigen to the adaptive arm of the immune system, inducing antigen-specific T and B cell responses. This vaccine-induced immune protection cannot be adequately detected in humans, as most therapeutic vaccines have been characterized only in animal models (3, 11). The detection of vaccine-inducted immune responses *in vivo* using a clinically-applicable means is critical for the optimization of novel immunotherapies. Thus, we developed a technique for the direct assessment of immune responses *in vivo* during therapeutic vaccination. Positron emission tomography (PET) is a widely available, highly sensitive imaging modality for the *in vivo* visualization and quantification of molecular processes at a cellular level. Furthermore, whole body imaging allows localization in a longitudinal fashion. These features are necessary to measure immune responses by quantification of the low numbers of proliferating T and B cells early after vaccination in relevant LNs. Thus far, investigators have mainly exploited ^{18}F-labeled fluoro-2-deoxy-2-D-glucose (^{18}F-FDG) for PET imaging of proliferating cells, based on the increased glucose metabolism of these cells. Recently, novel tracers have been developed that facilitate imaging of other cellular processes: ^{18}F-labeled 3'-fluoro-3'-deoxy-thymidine (^{18}F-FLT) was designed as a tracer for cell proliferation (12) and is increasingly being applied in oncology. However, it has been recognized that enhanced nucleoside demand is not restricted to tumor cells (13). Indeed, a successful vaccination results in the proliferation of activated lymphocytes in a highly controlled manner within LNs. This proliferation is accompanied by a large metabolic switch in lymphocytes (14), and could serve as a marker of immune responsiveness. We hypothesized that PET imaging, exploiting ^{18}F-FLT, can specifically detect highly proliferative immune cell responses in proximal LNs upon vaccination and thus would allow *in vivo* assessment of vaccine-induced antigen-specific T and B cell responses. Such a 'detection system' would allow early discrimination of responding patients and therefore aid physicians in individualized decision-making.

Methods

Patients and treatment schedule

The presented data result from side-studies in two clinical trials in melanoma patients with regional lymph node metastases who are scheduled for radical lymph node dissection (ClinicalTrials.gov number NCT00243594 and NCT00243529). Eligibility criteria included stage III melanoma according to the 2001 American Joint Committee on Cancer Staging criteria (15), planned regional lymph node dissection (RLND) for lymph node metastases or interval <2 months after RLND, HLA-A*02:01 phenotype, melanoma expressing gp100 and tyrosinase, and World Health Organization performance status 0 or 1. Additional eligibility criteria have been described previously (16). The study was approved by our Regional Review Board, and written informed consent was obtained from all patients. In total, 14 patients were included for additional imaging studies. The vaccine consisted of autologous mature DCs, pulsed with tumor associated antigens and keyhole limpet hemocyanin (KLH). KLH is a highly immunogenic antigen that serves as a surrogate marker for immune competence and as a non-specific T helper cell stimulus. Similar DCs, but not loaded with KLH or tumor antigen, or sterile saline served as control vaccination. All injections were directly to the LN

(intranodally) by a highly experienced radiologist under ultra-sound guidance. All patients received three intranodal vaccinations at a biweekly interval; patients who remained free of disease progression were eligible for two maintenance cycles at 6 month intervals with the same schedule. One or two days prior to RLND, patients received one extra vaccination with DCs labeled with ^{111}In-oxine and superparamagnetic iron oxide (SPIO) for cell tracking studies in the region that was to be resected (17).

Dendritic cell vaccine

Monocytes were enriched from leukapheresis, as described previously (18) and cultured in the presence of interleukin (IL)-4, GM-CSF to induce differentiation to DC phenotype. DCs were matured with a cocktail of pro-inflammatory cytokines consisting of IL-1β, IL-6, TNFα supplemented with prostaglandin E_2 for 48 hours. This procedure gave rise to mature DCs meeting the release criteria (19). DCs were pulsed with the HLA class I gp100-derived peptides gp100:154-167, gp100:280-288 and the tyrosinase-derived peptide tyrosinase:369-376 directly after harvesting or thawing. Alternatively, mature DCs were electroporated with mRNA encoding gp100 or tyrosinase (20). Peptide pulsing or mRNA electroporation was performed under good manufacturing practice (GMP) conditions. More detailed description of the *ex vivo* culture methods are provided in Supplementary Text S1. Cells were resuspended in 0,1 mL saline for intranodal injection.

Positron emission tomography imaging

PET/CT scans were performed at varying time points after vaccination (Supplementary Table S1). Patients were instructed to drink 1 L of water, and received 10mg furosemide intraveneously to stimulate urinary tracer excretion. Emission images were acquired 1 hour after intravenous injection of 250 MBq ^{18}F-FLT. The images were corrected for attenuation using low-dose CT and reconstructed using the ordered-subsets expectation maximization (OSEM) algorithm. Low-dose CT scan was used for anatomical correlation. The image sets were reviewed in consensus by two observers. Three-dimensional regions of interest were placed manually over LNs by using a dedicated software program. Maximum standardized uptake values (SUVmax) were calculated for visible LNs of interest, according to the following formula: SUV = radioactivity concentration in tissue (Bq/kg)/(injected dose (Bq)/patient weight (kg)). Bone marrow SUVmax in the proximal part of the femoral bone served as internal positive control.

In vitro immune monitoring

Antibodies against KLH were measured in the serum of vaccinated patients using enzyme-linked immunosorbent assays (ELISA) (16). Microtiter plates were coated with KLH and different concentrations of patient serum were allowed to bind. After extensive washing, patient antibodies were detected with mouse antihuman IgG, IgA or IgM antibodies labeled with horseradish peroxidase; 3,3'-5,5-tetramethyl-benzidine was used as a substrate and plates were measured in a microtiter plate reader. An isotype-specific calibration curve for the KLH response was included in each microtiter plate. Cellular responses against KLH were measured in a proliferation assay; 1 x10^5 peripheral blood mononuclear cells taken at time points of scanning, were plated per well either in the presence of KLH or without. After 4 days of culture, 1 μCi/well of (^{3}H)thymidine was added and incorporation was measured in a β-counter.

^{111}In labeling and scintigraphy

DC were incubated with ^{111}In-oxine for 15 minutes at room temperature. *In vivo* planar scintigraphic images were acquired with a gamma camera equipped with medium energy collimators, at day 0 and 48 hours later. Migration was quantified by region-of-interest analysis of the individual nodes

visualized on the images and expressed as the relative fraction of ^{111}In-labeled DC that had migrated from the injection depot.

SPIO labeling and immunohistochemistry

Superparamagnetic iron oxide (SPIO) was added 3 days after onset of DCs culturing. The iron-content was previously determined to be 10-30pg of iron per cell in this standardized procedure (21) without affecting the viability. Sections (10 μm) of the resected LNs were stained with 2% potassium hexacyanoferrate (II)-trihydrate in 0.2 M HCl for 15 min and counterstained with 0.05% nuclear fast red in 5% aluminium sulphate. Immunohistochemistry was performed using antibodies against CD4, CD8, CD25. The slides were stained with Prussian Blue to detect SPIO-labeled cells.

Statistical analysis

The two-tailed paired t-test was applied for comparison of pre and post vaccination PET signals of LNs and bone marrow. Correlations between SUVmax of PET signal in LN and KLH specific *in vitro* monitoring were calculated using linear regression. All statistical analyses were calculated using GraphPad Prism (version 4.0). $p<0.05$ was regarded as statistically significant.

Results

^{18}F-FLT PET visualizes the immune response early after vaccination

To evaluate whether the ^{18}F-FLT PET signal of proliferating T and B cells co-localized with antigen-loaded DCs, we labeled the cells *ex vivo* with ^{111}In-oxine and SPIO. Planar scintigraphy was performed immediately following PET/CT scanning to localize and quantify the ^{111}In-labeled DCs. Three days after vaccination, up to four LN were revealed with retention of ^{18}F-FLT (Figure 1a). The scintigraphic images demonstrated that the PET signal intensity increased only in those LNs that contained antigen-loaded ^{111}In-labeled DCs (Figure 1b). Profound^{18}F-FLT uptake was observed even when very low numbers (4.5×10^5 cells) of antigen-loaded DCs were present. Immunohistochemical staining of the LNs revealed the presence of SPIO-labeled DC in the T cell areas and the activation of $CD4^+$ and $CD8^+$ T cells (Figure 1c-d).

^{18}F-FLT PET signal requires antigen-loaded dendritic cells

We observed a significant increase in ^{18}F-FLT signal early after the very first vaccination (Figure 1e,f), indicating that de novo immune responses are readily visualized. Vaccinated LNs remained positive up to 3 weeks after the last vaccination (Figure 1g,h). Bone marrow uptake served as internal positive control. Four patients underwent sequential scanning after vaccination. We observed a pronounced increase in^{18}F-FLT signal exclusively in vaccinated LNs from day 3 to 6 post-vaccination in 3 out of 4 patients (Figure 1i-l). We observed a further increase in ^{18}F-FLT accumulation ($p<0.05$) in LNs of who received three subsequent intranodal vaccinations, but not in control LNs which were either not injected, injected with saline or injected with DC not loaded with antigen (Figure 2a-c). This indicates that the observed increase in PET signal upon vaccination cannot be attributed solely to the effect of tissue damage by intranodal injection or to the presence of DCs alone, but that it requires the

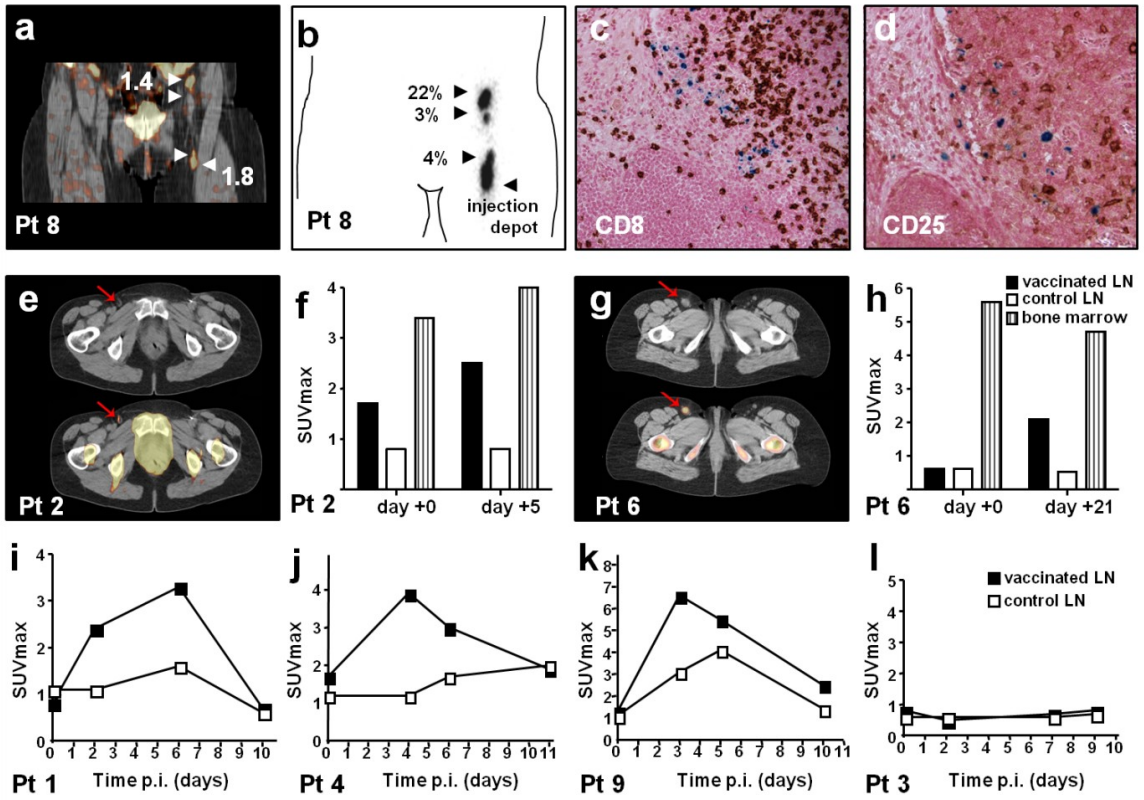

Figure 1. ^{18}F-FLT PET visualizes the immune response following vaccination. (A) Three days after intranodal delivery of the ^{111}In/SPIO-labeled and antigen-loaded DC, ^{18}F-FLT PET/CT scan was performed which showed tracer retention in the injected and three draining LNs. (B) Immediately prior to the PET/CT scan, the same LNs were visualized by scintigraphy, containing 4%, 3% and 22% of the injected radioactivity. (C,D) The same day a radical LN dissection was performed and ^{111}In-DC containing LNs were identified with a gamma probe. Immunohistochemical analyses of these LNs demonstrated a close interaction between injected SPIO-labeled DC and CD8$^+$ T cells, resulting in increased expression of activation marker CD25. (E,F) To show that *de novo* immune responses can also be imaged with ^{18}F-FLT we performed ^{18}F-FLT PET scans in one patient after the prime vaccination (pt 2). At day 5 post vaccination, ^{18}F-FLT signal had increased from SUVmax 1.7 to 2.5, whereas the control lymph node that received vaccination with DC not loaded with antigen did not show an increase in ^{18}F-FLT signal (SUVmax 0.9 to 0.8). (G,H) In patient 6, who received multiple vaccinations, a sustained ^{18}F-FLT signal was detected up to three weeks after the last vaccination, but not in the non-vaccinated control LN. (I-L) In order to find the optimal time point for ^{18}F-FLT PET imaging, sequential ^{18}F-FLT PET/CT scans were performed in 4 patients. We observed a profound increase in ^{18}F-FLT signal in vaccinated LNs (filled squares) but not in control LNs (open squares) between day 3 to 6 post injection with antigen-loaded DC. However, patient 3 received vaccination with DC loaded with tumor-antigen but not the control-antigen KLH. All patients received no other vaccinations 6 months prior to imaging.

presence of antigen. Interestingly, in one patient who did not detect PET signal in LN upon vaccination, the vaccine did include the melanoma-associated antigens but not KLH. Thus, these data support the notion that the measured ^{18}F-FLT signal is indeed antigen-specific.

^{18}F-FLT PET signal correlates with in vitro monitoring assays

To validate our findings, we compared tracer retention in the LNs with the presence of antigen-specific T and B cell responses in peripheral blood samples taken at the time of imaging. We observed a significant correlation between ^{18}F-FLT accumulation and the level of circulating KLH-specific IgG antibodies as well as KLH-specific proliferation of T cells (Figure 2d,e). In one patient (circle) we observed high ^{18}F-FLT uptake without apparent KLH-specific T cell proliferation. This patient not only showed exceptionally high KLH-specific IgG antibodies in the serum, but also profound levels of IgA and IgM antibodies, indicating that in this case the ^{18}F-FLT signal most likely reflects vigorous B cell proliferation. Vice versa, another patient, (triangle) exhibited modest B cell responses but pronounced T cell proliferation against KLH. Together, from these observations we

conclude that accumulation of ^{18}F-FLT in the vaccinated LNs reflects the sum of both antigen-specific T and antigen-specific B cell responses. This correlation is specific to the FLT tracer as it was not observed with ^{18}F-FDG.

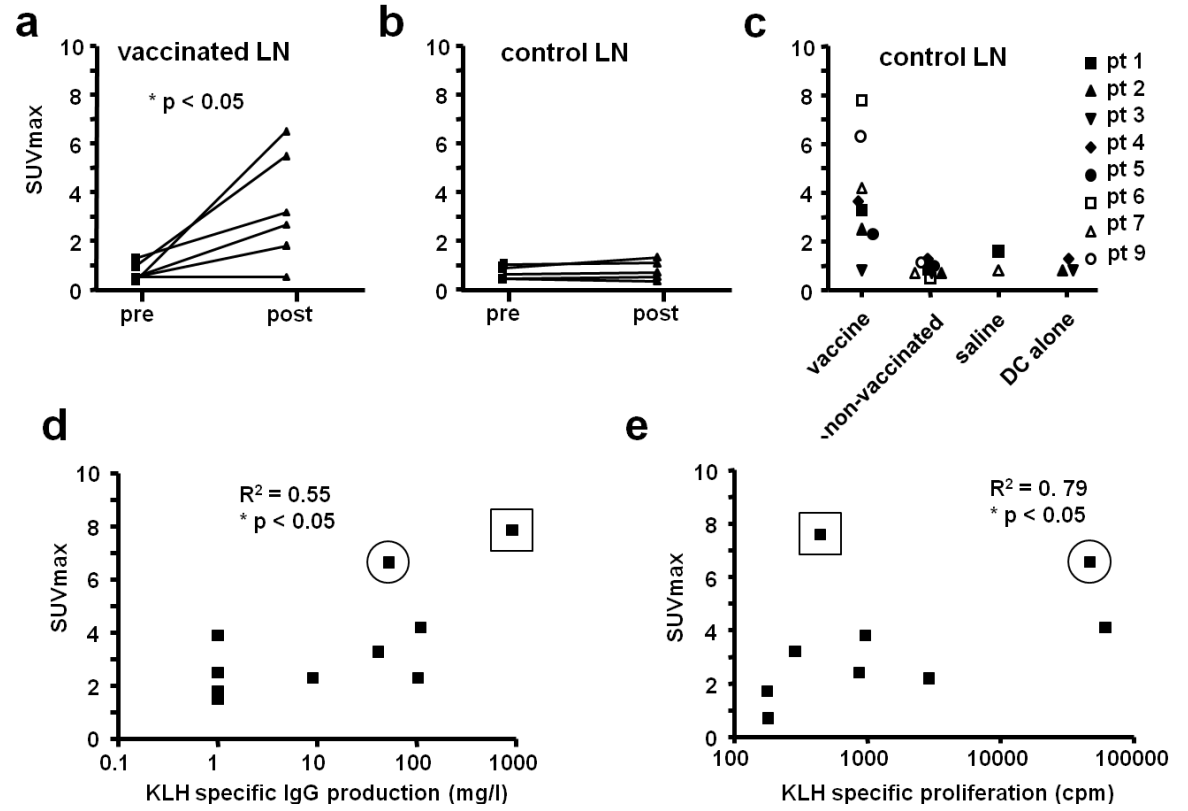

Figure 2. Increased ^{18}F-FLT PET signal directly correlates to antigen-specific immune responses. (A) A significant increase in ^{18}F-FLT signal ($p<0.05$) was detected in LNs after 3 intranodal vaccinations, except in one patient (pt 3). (B) In contrast, in control LNs no increase in tracer retention was observed. (C) Control LNs consisted of LNs at the contralateral side, either non-vaccinated LN or LN vaccinated with saline or DCs not loaded with antigen. An increase of ^{18}F-FLT signal was not observed in any of these cases. (D) Peripheral blood samples at the time point of the scan showed a significant correlation between the level of KLH-specific IgG antibodies and the intensity of ^{18}F-FLT uptake in the LNs, $p<0.05$. (E) Proliferation of peripheral blood mononuclear cells upon stimulation with KLH demonstrated a clear correlation between the intensity of ^{18}F-FLT signal and the KLH specific proliferation *in vitro*, $p<0.05$. One patient (square) showed high ^{18}F-FLT uptake (SUVmax 7.8) without accompanying KLH specific proliferation (403 ± 76 cpm), but showed pronounced humoral response to KLH (KLH IgG 918 mg/L), involving also KLH-specific IgA and IgM. In a second patient (circle), the observed ^{18}F-FLT PET signal (SUVmax 6.6) resulted from a modest KLH-specific IgG response (KLH IgG 118 mg/L) and a pronounced KLH-specific proliferation (45030 ± 12996 cpm).

Discussion

We here demonstrate that ^{18}F-FLT PET can be used to directly monitor antigen-specific immune responses *in vivo* shortly after therapeutic vaccination, as it offers a sensitive tool to study the kinetics, localization of induction of antigen-specific lymphocyte activation upon vaccination with antigen-loaded autologous DCs. For vaccination strategies in preventive settings, the established *in vitro* assays for proliferative and humoral responses are sufficient to predict adequate immunity. However, for a number of novel vaccination strategies that are designed as therapeutic intervention, no such established assays exist. To the contrary, for therapeutic vaccines that target major infectious diseases such as HIV, tuberculosis and malaria, or malignancies, the lack of tools to predict adequate immunity hampers translation of these vaccines to the clinic. We took the opportunity of our vaccination protocols that provide an unique setting in which we can control all elements required for a successful immune response; the antigen presenting cell is labeled and tracked *in vivo*, loaded with known antigens and delivered at the specific immune reactive site. Furthermore, the induced lymphocyte responses can be measured with established and well-validated assays. We used

this system as a model to systematically investigate the application of non-invasive *in vivo* nuclear imaging modality to evaluate antigen-specific immune responses upon therapeutic vaccination.

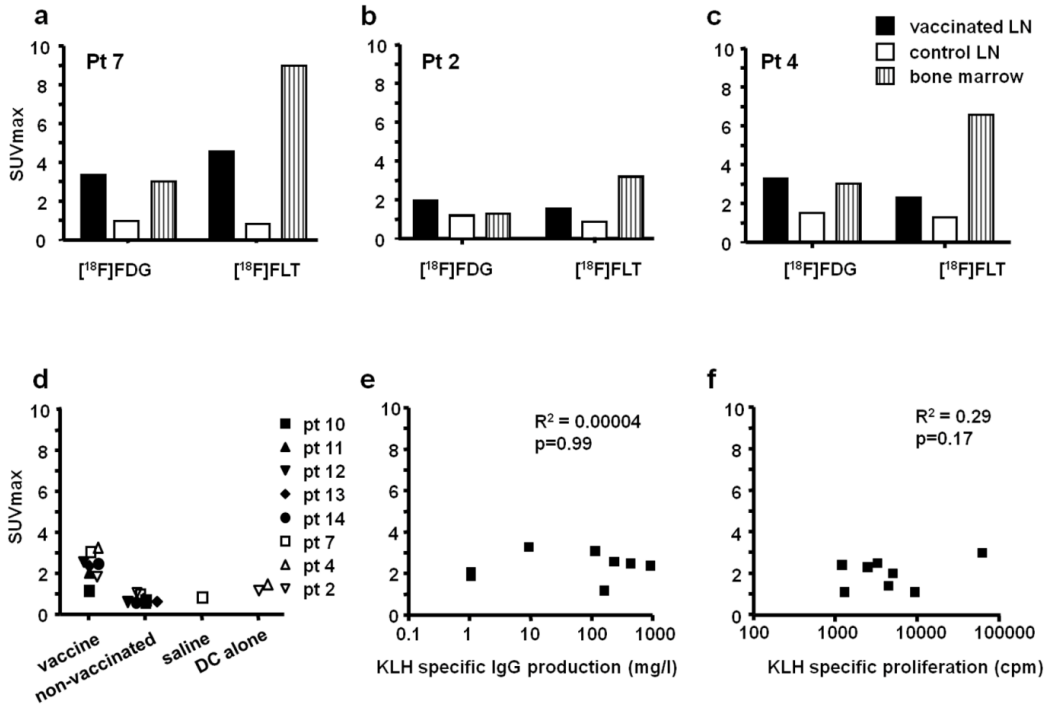

Supplementary Figure 3. ^{18}F-FDG PET does not target antigen-specific immune responses. (A-C) ^{18}F-FDG and ^{18}F-FLT PET were compared within individual patients for their imaging properties, at day 5 and 7 after last vaccination respectively. Both tracers target specifically vaccinated LN, but not control LNs, to equal extent. Bone marrow retention was higher for ^{18}F-FLT compared to ^{18}F-FDG, which is consistent with the known distribution pattern for both tracers. (D) Contralateral LNs served as negative controls within individual patients, no increase in ^{18}F-FDG PET signal was detected in non-vaccinated LNs, vaccinated with saline or DC not loaded with antigen. Notably, the ^{18}F-FDG signal intensity did not exceed SUVmax 3.3 even in LN vaccinated with antigen-loaded DC. (E,F) Consequently, no correlation was detected between ^{18}F-FDG signal intensity and KLH-specific IgG antibody production or proliferation response measured simultaneously *in vitro*.

In recently published large phase III trials, it has been demonstrated that immunotherapies can be effective even in advanced cancer patients. Both antigen-specific (5,7) and non-antigen specific agents (6) have now been approved by the FDA. Considering the amount of effort poured into the development of these novel agents, PET-based monitoring will advance our knowledge of the immunological processes that precede the failure or success of novel immunotherapies. Furthermore, it should vastly improve efficient application by aiding in individualized decision making. Most anti-cancer vaccines aim at inducing tumor-specific cytotoxic CD8$^+$ T cell responses. However, tumor-specific CD8$^+$ T cell responses occur at low precursor frequencies and might therefore contribute less to LN reactivity than vigorous KLH-specific responses8. To this end, we injected 3 patients with DCs loaded with KLH, but not with tumor-antigen. Interestingly, we measured markedly increased ^{18}F-FLT signals which cannot solely be attributed to KLH, since control vaccination with KLH-loaded DC in contralateral LNs induced only a modest ^{18}F-FLT signal (Figure S2). The challenge we now face is to further improve immune response imaging *in vivo*, and find tracers that are specific for different lymphocyte populations. Recently, in a preclinical model of mice challenged with an immunogenic sarcoma, ^{18}F-FDG accumulated mainly in cells of the innate immune system, whereas 2-fluoro-D-(arabinofuranosyl)-cytosine accumulated predominantly in CD8$^+$ T cells (22). Our findings that ^{18}F-FDG signal intensity does not correlated with immune reactivity (Figure S3), indicates that targeting glucose metabolism is not specific for antigen-specific immune activation. Hence, we have shown that ^{18}F-FLT is a sensitive and specific PET tracer for monitoring lymphocyte activation after DC vaccine therapy in a clinical setting.

Supplementary Table 1

Patient code	Method of antigen loading	Nr of vaccinations received total	Time of scan (day post vaccination)	Tracer	Control vaccination
1	mRNA electroporated	7	+2, +6, +10	(^{18}F)FLT	saline
2	mRNA electroporated	1	+5	(^{18}F)FLT	unpulsed DC
2	mRNA electroporated	6	+7	(^{18}F)FLT	unpulsed DC
3	mRNA electroporated *	4	+2, +7, +9	(^{18}F)FLT	unpulsed DC
4	mRNA electroporated	4	+4, +6, +11	(^{18}F)FLT	KLH pulsed DC
4	mRNA electroporated	9	+7	(^{18}F)FLT	unpulsed DC
9	mRNA electroporated	7	+3, +5, +10	(^{18}F)FLT	KLH pulsed DC
5	mRNA electroporated	7	+7	(^{18}F)FLT	non-vaccinated
6	mRNA electroporated	8	+5	(^{18}F)FLT	non-vaccinated
7	mRNA electroporated	6	+7	(^{18}F)FLT	saline
8	peptide pulsed	1	+3	(^{18}F)FLT	non-vaccinated
10	peptide pulsed	6	+21	(^{18}F)FDG	non-vaccinated
11	peptide pulsed	1	+6	(^{18}F)FDG	non-vaccinated
12	peptide pulsed	7	+6	(^{18}F)FDG	non-vaccinated
13	peptide pulsed	7	+5	(^{18}F)FDG	non-vaccinated
14	peptide pulsed	7	+5	(^{18}F)FDG	non-vaccinated
7	mRNA electroporated	6	+5	(^{18}F)FDG	saline
4	mRNA electroporated	9	+5	(^{18}F)FDG	unpulsed DC
2	mRNA electroporated	6	+5	(^{18}F)FDG	unpulsed DC

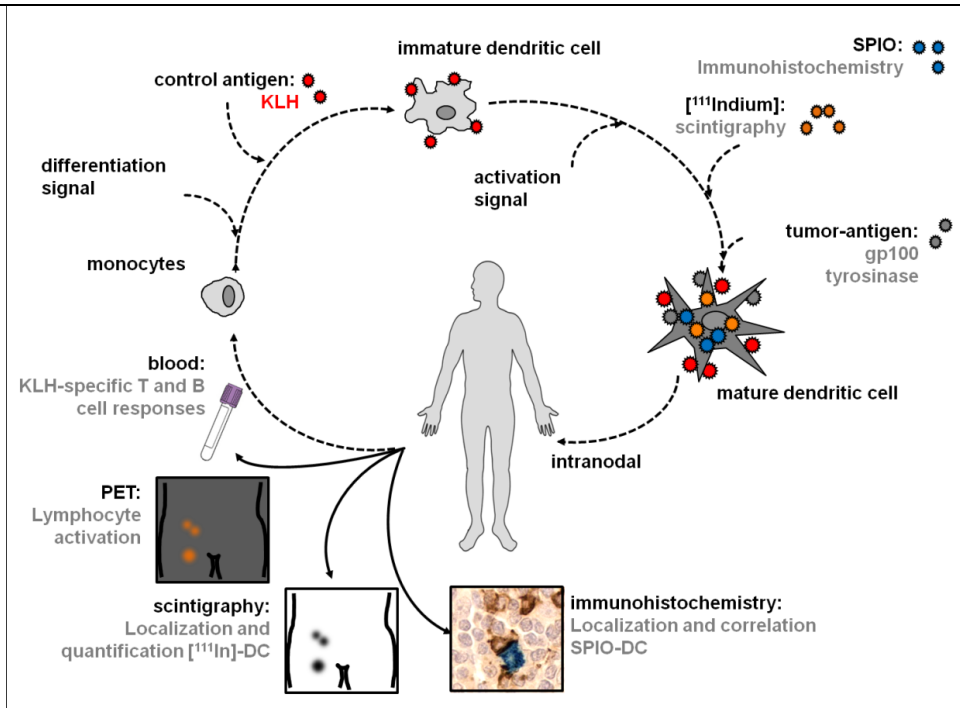

Supplementary Figure 1. Study design for multimodality imaging in DC-based cellular therapy. In our DC-based cellular therapy studies in melanoma patients, monocytes are obtained by apheresis and differentiated into immature dendritic cells (DC) by addition of interleukin-4 and GM-CSF. The control antigen KLH is added to the culture, which is spontaneously phagocytosed by immature DC. After six days, KLH-loaded immature DC are activated for two days by a cocktail of proinflammatory cytokines; interleukin-1b, interleukin-6, prostaglandin E_2 and tumor-necrosis-factor alpha, to induce a mature phenotype. Mature DC are either pulsed with peptides derived from melanoma-associated antigens gp100 and tyrosinase or electroporated with mRNA encoding these antigens. At this stage, SPIO particles are added for cell tracking by immunohistochemistry (IH) and (^{111}Indium) is added for tracking and quantification by scintigraphy. Upon intranodal delivery of the vaccine, immune responses are monitored in peripheral blood for KLH-specific responses, PET imaging for lymph node reactivity, scintigraphy for DC localization and immunohistochemistry for *in vitro* assessment of interaction DC with lymphocytes.

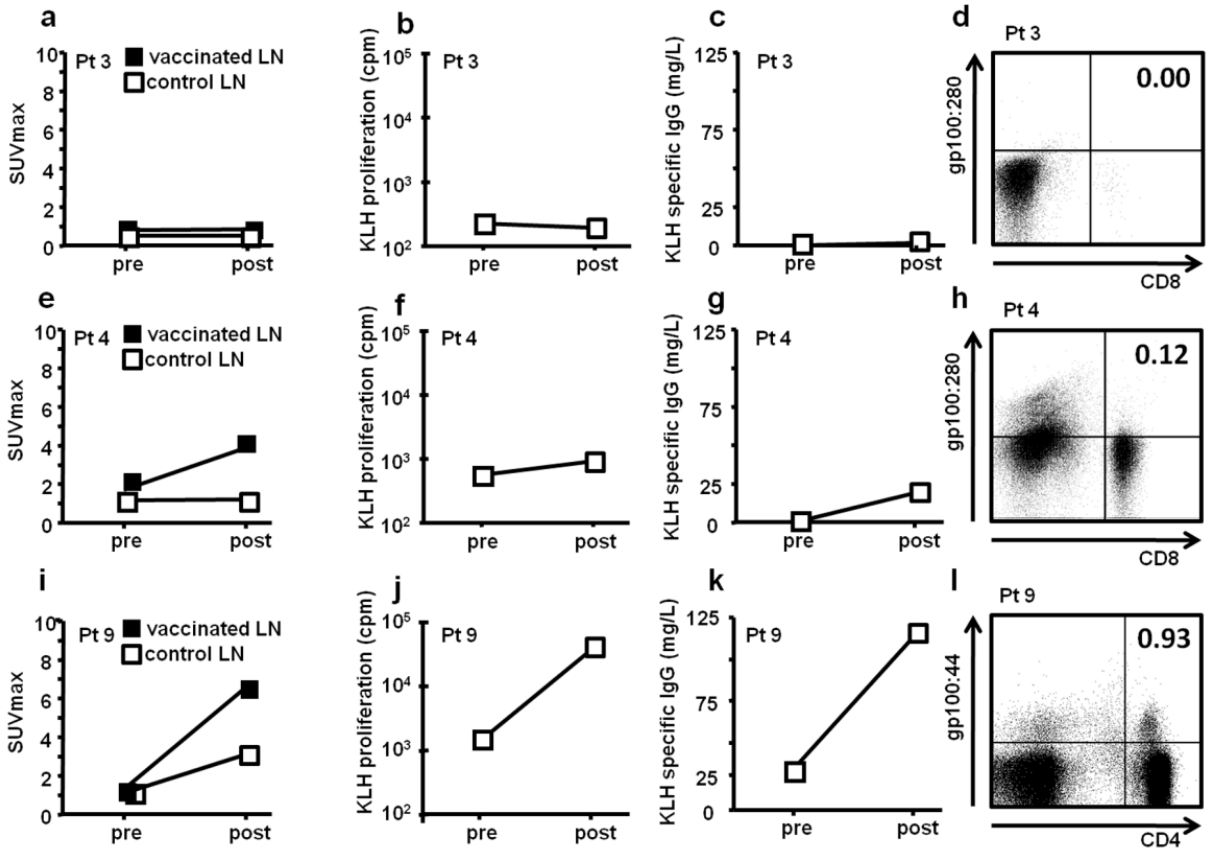

Supplementary Figure 2. *^{18}F-FLT PET signal increased in tumor-specific T cell responses.* (A) To investigate whether the observed increase in ^{18}F-FLT signal was attributable to tumor-specific immune responses, we analyzed three patients in detail. Patient 3 received vaccination with DC loaded with tumor antigen, but not loaded with KLH. No increase in ^{18}F-FLT signal intensity was observed. (B,C) Since the vaccinations did not include KLH, no KLH-specific responses were detected upon vaccination in peripheral blood. (D) However, also no tumor-specific T cell responses were induced, explaining the absence of increase in ^{18}F-FLT signal intensity. In two patients, control vaccinations consisted of dendritic cells loaded with KLH but not with melanoma-associated antigen. (E) In patient 4 no increase in the control LN was observed, whereas the LN vaccinated with DC loaded with both KLH and melanoma-associated antigens showed an enhanced ^{18}F-FLT signal, SUVmax 3.9. (F,G) In this patient no significant concurrent KLH-specific proliferative or IgG responses were detected, which is consistent with the absent ^{18}F-FLT signal in the control lymph nodes. (H) After completion of vaccination, tumor-specific CD8^{+} T cells were detected in cultures from delayed type hypersensitivity skin test biopsies, indicating that a tumor-specific immune response was indeed induced. (J) Similar investigations were performed in patient 9. The control LN vaccinated with DC loaded with KLH (but *not* melanoma-associated antigens) showed enhanced ^{18}F-FLT signal, SUVmax 3.1, albeit at a lesser extent than observed in the LN vaccinated with DC loaded with both KLH and melanoma-associated antigen. (J,K) We measured a profound proliferative response to KLH and an increased humoral response to KLH in concurrent blood samples, consistent with the induced ^{18}F-FLT signal in the lymph node vaccinated with KLH loaded DCs. (L) After completion of vaccinations, tumor-specific CD4^{+} T cells were detected in delayed type hypersensitivity skin test biopsies. From this we conclude that the measured ^{18}F-FLT signal intensity did not only result from KLH specific T and B cell responses, but can to a certain extent be attributed to tumor-specific T cells.

References

1. Buchbinder, S.P., et al., *Efficacy assessment of a cell-mediated immunity HIV-1 vaccine (the Step Study): a double-blind, randomised, placebo-controlled, test-of-concept trial.* Lancet, 2008. 372(9653): p. 1881-93.
2. Rerks-Ngarm, S., et al., *Vaccination with ALVAC and AIDSVAX to prevent HIV-1 infection in Thailand.* N Engl J Med, 2009. 361(23): p. 2209-20.
3. Wallis, R.S., et al., *Biomarkers and diagnostics for tuberculosis: progress, needs, and translation into practice.* Lancet. 375(9729): p. 1920-37.
4. Kenter, G.G., et al., *Vaccination against HPV-16 oncoproteins for vulvar intraepithelial neoplasia.* N Engl J Med, 2009. 361(19): p. 1838-47.
5. Kantoff, P.W., et al., *Sipuleucel-T immunotherapy for castration-resistant prostate cancer.* N Engl J Med. 363(5): p. 411-22.
6. Hodi, F.S., et al., *Improved survival with ipilimumab in patients with metastatic melanoma.* N Engl J Med. 363(8): p. 711-23.
7. Schwartzentruber, D.J., et al., *gp100 peptide vaccine and interleukin-2 in patients with advanced melanoma.* N Engl J Med. 364(22): p. 2119-27.
8. Lesterhuis, W.J., J.B. Haanen, and C.J. Punt, *Cancer immunotherapy - revisited.* Nat Rev Drug Discov. 10(8): p. 591-600.
9. Lesterhuis, W.J., et al., *Dendritic cell vaccines in melanoma: from promise to proof?* Crit Rev Oncol Hematol, 2008. 66(2): p. 118-34.
10. Banchereau, J. and A.K. Palucka, *Dendritic cells as therapeutic vaccines against cancer.* Nat Rev Immunol, 2005. 5(4): p. 296-306.
11. Appay, V., D.C. Douek, and D.A. Price, *CD8+ T cell efficacy in vaccination and disease.* Nat Med, 2008. 14(6): p. 623-8.
12. Shields, A.F., et al., *Imaging proliferation in vivo with [F-18]FLT and positron emission tomography.* Nat Med, 1998. 4(11): p. 1334-6.
13. Troost, E.G., et al., *18F-FLT PET Does Not Discriminate Between Reactive and Metastatic Lymph Nodes in Primary Head and Neck Cancer Patients.* J Nucl Med, 2007. 48(5): p. 726-735.
14. Fox, C.J., P.S. Hammerman, and C.B. Thompson, *Fuel feeds function: energy metabolism and the T-cell response.* Nat Rev Immunol, 2005. 5(11): p. 844-52.
15. Balch, C.M., et al., *Final version of the American Joint Committee on Cancer staging system for cutaneous melanoma.* J Clin Oncol, 2001. 19(16): p. 3635-48.
16. de Vries, I.J., et al., *Immunomonitoring tumor-specific T cells in delayed-type hypersensitivity skin biopsies after dendritic cell vaccination correlates with clinical outcome.* J Clin Oncol, 2005. 23(24): p. 5779-87.
17. de Vries, I.J., et al., *Magnetic resonance tracking of dendritic cells in melanoma patients for monitoring of cellular therapy.* Nat Biotechnol, 2005. 23(11): p. 1407-13.
18. de Vries, I.J., et al., *Phenotypical and functional characterization of clinical-grade dendritic cells.* Methods Mol Med, 2005. 109: p. 113-26.
19. Figdor, C.G., et al., *Dendritic cell immunotherapy: mapping the way.* Nat Med, 2004. 10(5): p. 475-80.
20. Schuurhuis, D.H., et al., *In situ expression of tumor antigens by messenger RNA-electroporated dendritic cells in lymph nodes of melanoma patients.* Cancer Res, 2009. 69(7): p. 2927-34.
21. Verdijk, P., et al., *Sensitivity of magnetic resonance imaging of dendritic cells for in vivo tracking of cellular cancer vaccines.* Int J Cancer, 2007. 120(5): p. 978-84.
22. Nair-Gill, E., et al., *PET probes for distinct metabolic pathways have different cell specificities during immune responses in mice.* J Clin Invest. 120(6): p. 2005-15.

Chapter 13

In vivo imaging of therapy-induced anti-cancer immune responses in humans

Aarntzen EH

Srinivas M

Radu CG

Punt CJ

Boerman OC

Figdor CG

Oyen WJ

De Vries IJ

Cell Mol Life Sci. 2012 Oct 5th (accepted)

Abstract

Immunotherapy aims to re-engage and revitalize the immune system in the fight against cancer. Research in the past decades has shown that the relationship between the immune system and human cancer is complex, highly dynamic and variable between individuals. Considering the complexity, enormous effort and costs involved optimizing immunotherapeutic approaches clinically applicable tool to monitor therapy-induced immune responses *in vivo* is most warranted. However, development of such a tool is complicated by the fact that a developing immune response encompasses several body compartments, e.g. peripheral tissues, lymph nodes (LN), lymphatic and vascular systems, as well as the tumour site itself. Moreover, the cells that comprise the immune system are not static but constantly circulate through the vascular and lymphatic system. Molecular imaging is considered the favourite candidate to fulfil this task. The progress in imaging technologies and modalities has provided a versatile toolbox to address these issues. This review focuses on the detection of therapy-induced anti-cancer immune responses *in vivo* and provides a comprehensive overview of clinically available imaging techniques as well as perspectives on future developments. In the discussion we will focus on issues that specifically relate to imaging of the immune system and we will discuss the strengths and limitations of the current clinical imaging techniques. The last section provides future directions that we envision to be crucial for further development.

1. Introduction

Immunotherapy aims to re-engage and revitalize the immune system in the fight against cancer. A recent series of successes has indicated the broad potential of this approach and has led to the approval of several novel immunotherapies (1-3). Although the recent progress is exciting, the underlying mechanisms are only partly understood (4). Considering the enormous effort and costs involved in developing, optimizing and applying an effective immunotherapeutic approach it is remarkable that a monitoring tool that accurately identifies a responding patient early during immunotherapeutic treatment is lacking. Research in the past decades has shown that the relationship between the immune system and human cancer is complex, highly dynamic and variable between individuals (5). Given the diversity in immune responses among individual patients to a single immunotherapeutic intervention, every clinical case potentially provides a unique opportunity to understand the crucial processes that precede the failure or success of immune responses. In this respect, individualized medicine is not only a goal in itself but rather a tool to develop successful therapy. Therefore, further progress can only be expected only if we manage to take this opportunity and learn how to guide therapy based on individual responses. The development of a clinically applicable tool to monitor therapy-induced immune responses *in vivo* is thus most warranted. However, development of such a tool is complicated by the fact that a developing immune response encompasses several body compartments, e.g. peripheral tissues, lymph nodes (LN), lymphatic and vascular systems, as well as the tumour site itself. Moreover, the cells that comprise the immune system are not static but constantly circulate through the vascular and lymphatic system. Current attempts to find such a monitoring tool often use surrogate markers, such as control antigens, or focus on a single functionality of immune effector cells, e.g. interferon gamma (IFNγ) enzyme-linked immunosorbent spots (ELIspots). In both cases, the results do not accurately link immune responses to clinical outcome. Furthermore, current immune monitoring assays are based on peripheral blood cells or tissue and are therefore invasive. Novel techniques allow high throughput assessment of individual variations in functional processes, e.g. differences in signalling pathways in immune cells (6). As of now, these techniques lack validation and are not yet applicable in the evaluation of therapy-induced responses. In general, the assays currently available provide only snapshots of a continuous and dynamic process. Moreover, most assays attempt to either extrapolate the findings in individual subjects to the general treated population, or to interpret findings in individual patients based on previous findings in the general population. Thus, in order development of a more complete picture, we require new tools; the ideal monitoring tool should be non-invasive, allow longitudinal data acquisition and reveal critical immunological processes that occur early during a treatment course on an individual basis. Quantification would be a further asset. Molecular imaging is considered the favourite candidate to fulfil this task. The progress in imaging technologies and modalities has provided a versatile toolbox (Figure 1) to address the issues mentioned above. Imaging modalities are available to image functional processes from a molecular scale to whole body levels. This review focuses on the detection of therapy-induced anti-cancer immune responses *in vivo* and provides a comprehensive overview of clinically available imaging techniques as well as perspectives on future developments. We begin with an overview of the de novo immune response and the current therapeutic approaches that intervene at a given phase of the response. Next, we describe the possible target processes and the imaging techniques available within each phase of the developing immune response. In the discussion we will focus on issues that specifically relate to imaging of the immune system and we will discuss the strengths and limitations of the current clinical imaging techniques. The last section provides future directions that we envision to be crucial for further development.

2. Current immunotherapy approaches

The immune system is a highly organized multi-cellular system designed to protect the host from invading pathogens and malignantly transformed cells (7). As such, the immune system acts with enormous specificity and great sensitivity, in concert with regulatory mechanisms, to avoid destructive self-reactivity. Many cell types from both innate (e.g. natural killer (NK) cells and macrophages) and adaptive (e.g. dendritic cells (DC), B cells and T cells) immunity contribute to immune competency. T cells are often considered to be the most critical effector cells in anti-cancer responses, since these cells are capable of developing antigen-specific memory responses. There are two major subsets of T cells, defined by the expression of the CD4 and CD8 surface markers. $CD4^+$ T cells are subdivided to T helper 1 (Th1) cells, which activate macrophages, antigen-presenting cells and cytotoxic $CD8^+$ T cells to promote cellular immunity. T helper 2 (Th2) cells promote antibody production by activating B cells. Within the $CD4^+$ T cell repertoire, a subset of T cells has the plasticity to become regulatory T cells (Treg), which mediate peripheral tolerance in physiological conditions. Although $CD8^+$ cytotoxic T cells (CTLs), as the endpoint effectors, represent a critical population for anti-cancer immunity, it has become clear that only a concerted action involving other cell types such as T helper cells and NK cells, can result in an effective anti-cancer clinical response. In that respect, the secretion of small molecules like cytokines and chemokines is an important means of short and long-distant communication between cells. Developing tumours are often infiltrated by lymphocytes that specifically recognize tumour associated antigens (TAA), but apparently are incapable of tumour eradication. However, these tumour-infiltrating lymphocytes can exert specific effector functions when disconnected from the suppressive tumour milieu. Based on this long-standing observation, the mainstay of immunotherapy is to induce, enhance or sustain such tumour-specific cellular immune responses in order to overcome the suppressive environment at the tumour site. To achieve this, a plethora of strategies have been tested in preclinical models. Current immunotherapy approaches which have been tested in clinical trials intervene at different phases of a developing immune response. The next sections provide an overview of a developing anti-cancer immune response, divided in phases, and the current immunotherapeutic strategies that intervene at these phases (Figure 2).

2.1. Phase I: Antigen encounter

The development of human tumours is a multistep process that occurs over an extended length of time (8). Since tumour cells originate from a normal cell and evade the immune system; human tumours express self-antigens that are poorly immunogenic, and lack pathogen associated molecular patterns (PAMPs). As such, they rarely trigger robust inflammatory responses, especially when compared to the response to invading pathogens. Peripheral tissues are constantly screened by specialized antigen presenting cells (APC) such as Langerhans cells and DC, which act as the sentinels of the immune system (7). These immature APC are phagocytic and capture antigens. Small numbers of APC migrate to draining LNs (LN) and present the processed TAA in major histocompatibility (MHC) complexes to effector cells. In the absence of inflammation, these APC remain in an immature state and ineffectively activate T cells. This absence of co-stimulatory signals and inflammatory cytokines leads to a tolerogenic T cell response. However, immature APC that encounter antigens under inflammatory conditions undergo a transformation to mature APC, which are highly migratory and potent orchestrators of adaptive immune responses.

2.1.1. Tumour antigen containing vaccines

Following the identification of several TAA, a series of clinical trials has evaluated cancer vaccines that deliver TAA to neutral sites like skin or muscle, similar to preventive vaccines, in order to be recognized and phagocytosed by endogenous APC. These vaccines can consist of TAA peptides alone, in combination with immune stimulatory adjuvants like TLR-agonists and chemical agents (e.g.

complete Freund's adjuvant (CFA) or Montanide) (9), or complexed with immunogenic viral particles. A recent single-arm clinical study demonstrated that vaccination with long-peptides derived from human papilloma virus (HPV)-16 E6 and E7 antigens induced complete tumour regressions in HPV-associated preneoplastic lesions (10). In order to use the full repertoire of possible immunogenic epitopes; autologous or allogeneic tumour cells can be modified to provide immunostimulatory signals together with TAA (11).

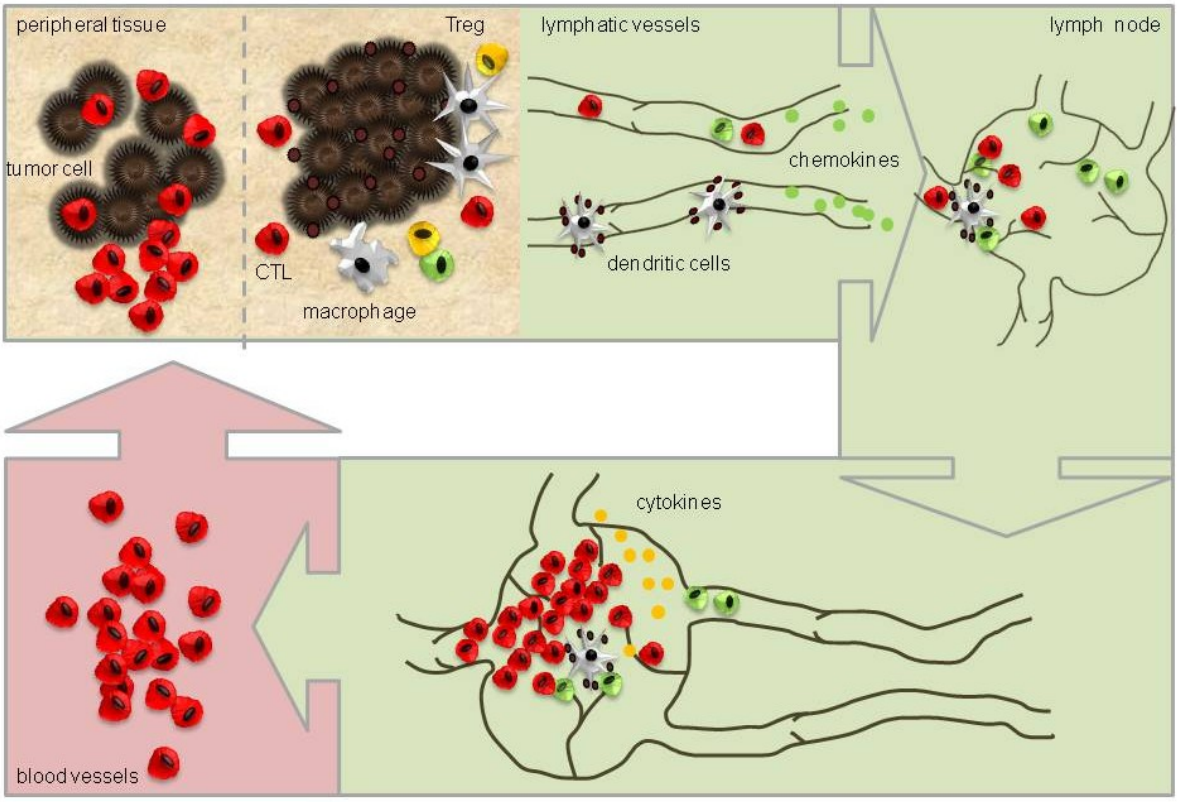

Figure 1: Overview of the developing immune response and possible targets for therapeutic strategies and imagin.g

2.1.2. Cellular vaccines

The isolation of specialized APC for *ex vivo* loading with antigen and activation, provides a more easily controlled setting (12). A recent phase III trial involving antigen-loaded antigen-presenting cells in patients with advanced prostate cancer, demonstrated improved overall survival with vaccinations compared to placebo (13). We have extensively studied the immunological responses to autologous antigen-loaded DC (14, 15). A highly interesting approach is the *in vivo* targeting of APC, which would replace laborious and expensive *ex vivo* culturing and facilitate large-scale application of DC-based vaccination therapies (16).

2.2. Phase II: Expansion of immune effector cells

2.2.1. Cytokine-based immunotherapy

Soluble signalling molecules, e.g. cytokines, play an important role in the induction of inflammatory responses, since they allow recruitment of lymphocytes and APC to the LN (LN). Next, in the interaction of APC with lymphocytes in LN, cytokines provide a directive signal to the immune effector cells to skew their differentiation. Lastly, cytokines may have a direct anti-tumour effect or at least induce inflammatory responses at the site of the tumour. The important role of cytokines prompted the administration of cytokines as anti-cancer immunotherapy. Interleukin-2 (IL-2), first described in 1976 as a T-cell growth factor (17), plays a central role in immune regulation and T-cell proliferation (18). IL-2 was approved by the US Food and Drug Administration (FDA) in 1998 for treatment of advanced metastatic melanoma and in 2005 for the treatment of metastatic renal cell cancer. High-dose bolus intravenous IL-2 injections demonstrated antitumour effects (19, 20). Long-

term follow-up of these studies demonstrated durable responses in 4% of the patients (21) suggesting the establishment of a memory T-cell response. However, the side effects associated with this treatment regimen are severe and often require hospitalization (22). Interferon alfa (IFN-α) was the first exogenous cytokine to demonstrate antitumour activity in advanced melanoma. Interferon α-2b, a type I IFN, is a highly pleiotropic cytokine with immunoregulatory, as well as direct antitumour properties in multiple malignancies (23). In 1995, interferon-α-2b became the first immunotherapy approved by the FDA for the adjuvant treatment of high-risk primary melanoma and objective responses were observed in approximately 15% of patients with metastatic melanoma. However, due to its multiple effects, tolerability is an issue with this regimen and has hampered widespread use. Moreover, both IL-2 and IFNα have not shown a clear benefit in overall survival, neither in the adjuvant setting nor in metastatic disease.

2.2.2. Adoptive T cell transfer

Other than strategies to prime TAA-specific T cells *in vivo*, by cellular vaccines or cytokines, TAA-specific T cells can be isolated from tumour tissue or peripheral blood and primed *in vitro* to enhance their effector function. Adoptive cell transfer (ACT) involves the administration of tumour-specific T cells. The earliest form of ACT that demonstrated effective anti-tumour immunity was allogeneic bone marrow transplantation for chronic myeloid leukemia (24, 25). Later studies have revealed that after T cells, alloreactive NK cells play a pivotal role in the graft versus leukemia effect (26). Following the finding that T cells isolated from tumour or tumour draining LNs can elicit specific anti-tumour effect *in vitro*, this approach has been investigated in solid tumours. Transferred TAA-specific T cells are either isolated from patient tumour biopsies and expanded *in vitro* under immune stimulating conditions, or peripheral blood T cells are endowed with antigen specific T cell receptors (TCRs) or fusion proteins termed chimeric activation receptors (CARs) (27, 28). The expanded numbers of TAA-specific T cells in ACT should break immune tolerance at the tumour level and regenerate a broad tumour-specific immune response. Clinical trials show that critical issues for further improvement of this approach are the *ex vivo* re-programming of TILs towards a pro-inflammatory phenotype, sufficient T cell homing to the tumour and the avidity of T cells involved for *in vivo* expressed TAA (29, 30).

2.3. Phase III: Targeting the tumour and its microenvironment

2.3.1. Monoclonal antibodies

Several immunotherapeutic strategies exploit direct anti-tumour effects, instead of indirectly by enhancing cellular immunity as mentioned above. The most prominent are monoclonal antibodies (mAbs) which can be divided in different classes according to their target (reviewed in (31)). First, mAbs are designed to activate the immune system by both antibody dependent cellular cytotoxicity (ADCC), such as anti-CD20 mAb (rituximab) and complement dependent cytotoxicity (CDC). Other mAbs inhibit cellular signalling pathways, such as the anti-Her2neu antibody trastuzumab, the anti-VEGF antibody bevacizumab and the anti-EGFR antibodies cetuximab and panitumumab. A novel promising antibody-based strategy is the use of bi-specific antibodies, which combine two different binding sites in order to bring specific effector cells in close proximity to specific target cells. For example, blinatomumab has a binding site for CD3, part of the TCR, and CD19, abundantly expressed on B cells. In a recent phase II study, has shown high response rates in patients with relapsed or refractory B-precursor acute lymphatic lymphoma (32).

2.3.2. Chemotherapy-induced immunogenic cell death

Evidence is accumulating that the immune system makes a crucial contribution to the antitumour effects of conventional chemotherapy-based and radiotherapy-based cancer treatments (33). It has

become clear that cell death induced by cytotoxic agents can be immunogenic and as such can trigger effective immune responses, reviewed in (34).

2.3.3. Overcoming tolerance

Strategies to neutralize immune suppressor mechanisms include chemotherapy (for example, low-dose cyclophosphamide), the use of antibodies (for example, CD25-targeted antibodies) in an attempt to deplete regulatory T cells and the use of antibodies against immune-checkpoint molecules (for example, cytotoxic T lymphocyte-associated protein 4 (CTLA4)-targeted antibodies and programmed cell death 1 (PD1)-targeted antibodies). Many of these strategies were recently reviewed (35, 36). Ipilimumab, a mAb that blocks the inhibitory signalling by CTLA-4 which is expressed on activated T cells has demonstrated significant clinical efficacy in two recent large phase III trials (37, 38). Based on these trials, ipilimumab has been approved by the FDA for metastatic melanoma (1, 39).

3. General issues in clinical imaging

The recent development of novel immunotherapies warrants monitoring tools that allow accurate and early prediction of therapy response and disclose the critical preceding immunological mechanisms of action. In order to address these needs in clinical immunotherapy trials, the ideal monitoring tool is an imaging modality that allows whole-body, non-invasive, quantitative and longitudinal visualization of functional processes on a molecular level. However, in practice, myriad factors affect the choice of label and imaging modality for a specific application. Matching the right imaging system, including modality and probe, to an application is essential to its success. Multimodality imaging can maximize the strengths of each imaging modality while minimizing its weaknesses (Table 1), and is therefore being extensively explored. The next section describes the basic properties of clinically applicable imaging modalities.

3.1 Scintigraphy

Planar scintigraphy is based on the detection of gamma radiation emitting radionuclides, yielding 2D images. Most cell-tracking studies use scintigraphy because of the ability to quantificatify signal, lower cost and wider availability. Scintigraphic imaging allows quantification of roughly greater than 104 labeled cells, dependent on the amount of activity that can be loaded per cell (40). However, scintigraphy lacks anatomic detail and is therefore increasingly being replaced by SPECT/CT. with a key issue that arises when using radionuclides is the half life of the label in relation to the life span of the transferred cells. The radiolabels that are typically used are ^{111}In and ^{99m}Tc, with half-lives of 2.8 days and 6 h, respectively, or ^{18}F with a half-life of 2 hours. This restricts the length of time that they can be detected *in vivo* (2-3 half-lives), often much shorter than the lifetime of the transferred cells. It also introduces logistic issues in planning such trials, as the entire process, from label synthesis to the final imaging, must be performed in a short period of time. Furthermore, label retention within cellular compartments must also be characterized, as imaging modalities typically detect just the label regardless of whether the label is contained in the relevant cells, lost to the extracellular matrix or transferred to other cells. For example, ^{99m}Tc is not as suitable as ^{111}In for labeling immune cells due to higher leakage of the ^{99m}Tc label from the cells (41) and subsequent accumulation in the intestine. ^{18}F-FDG has proven to be of little value in labeling transferred cells for *in vivo* tracking due to massive release from the cells (42), besides its short half-life.

3.2 Magnetic Resonance Imaging

MRI uses powerful magnets to polarize and excite single protons in water molecules, producing a detectable signal. It is a promising solution to the lack of anatomical detail in nuclear imaging modalities, since MRI provides excellent intrinsic contrast and high spatial resolution, even in soft

tissues. MRI labels comprise of very stable compounds such as superparamagnetic iron oxide (SPIO) or Gd agents. These heavy metals are chelated to reduce toxicity. Such labels are called "contrast agents" because they are not detected directly but instead through their effect on local contrast of mobile water in tissues. In this case, intracellular localization of label can also be important, particularly when using MRI labels where it has been shown that clustering of MRI labels in dense vacuoles yields better local contrast enhancement than cytosolic distribution (43). Contrast agents have already been used in several clinical cell tracking trials (44), allowing for high resolution, longitudinal cell tracking. Finally, although MRI-based cell tracking is not restricted by radioactive decay as with radiolabels, this method is less suitable for quantification of cell numbers using current imaging protocols. Furthermore, the effect of these metals on the cells must be considered. Therefore, a novel class of ^{19}F-based MRI contrast agents has been developed (45) with no physiological background and direct detection, which is suitable for quantification. The development of novel imaging protocols and pulse sequences has led to the functional assessment of the tissue using techniques such as dynamic contrast-enhanced MRI (DCE-MRI) and diffusion weighted imaging, which is dicussed in later sections. The combination of anatomical information and functional information using a single imaging modality is very powerful and therefore increasingly being investigated to monitor tumour responses to treatment.

Table 1. Characterization of clinically available imaging technologies for imaging immune responses.

modality	spatial resolution	temporal resolution	sensitivity	Label lifetime	functional information	cell tracking	anatomical information
MRI	50 micron – cm	s – min	variable, generally medium to low	variable	yes	*ex vivo* labeled cells	yes
PET	mm – cm	min – hr	extreme high (picomolar)	hr – days	yes	*in vivo*	no
SPECT	mm – cm	min – hr	extreme high	hr – days	yes	*ex vivo*	no
Planar Scintigraphy	mm – cm	min – hr	high	hr- days	yes	*ex vivo*	no

3.3 Positron Emission Tomography

PET reveals a three-dimensional image of functional processes as the system detects pairs of gamma rays emitted by a positron-emitting radionuclide. An advantage of PET tracers is that they are injected systemically, and then taken up by the relevant cells, as opposed to *ex vivo* labels as typically occurs with MRI, SPECT and scintigraphy. Thus the procedure can be carried out longitudinally (repeatedly), within the limits of radiation exposure. For example, patients were imaged with ^{18}F-FLT PET at various time points to determine the peak of the DC-induced response (46). However, *in situ* labeling requires high sensitivity detection, typically through PET (47). Another problem with systemic administration of tracer is the nonspecific accumulation in organs such as the kidneys or bladder, as well as uptake by irrelevant cell types, such as macrophages. ^{18}F-FDG for example accumulates in the myocardium and in the brain and ^{18}F-FLT accumulation is typically in the bone marrow. It is important to consider the dosage and penetration of these injectable tracers, particularly given their short lifetime. Furthermore, tumours or other lesions can be susceptible to permeability changes from vascular disruption or leakage and this can affect the perceived signal intensity.

3.4 Computed Tomography

CT scans generate a three-dimensional image from a large series of two-dimensional X-ray images taken around a single axis of a subject. Its use has dramatically increased in the past decades due to increased availability and the circumvention of superimposition compared to planar X-ray images. The use of contrast agents has increased its diagnostic accuracy even further. For monitoring therapy-induced responses, CT scans provide accurate assessment of tumour volumes. X-ray beams

are attenuated to different degrees by different tissue, resulting in image contrast. Based on the different attenuation of X-rays passing different tissues, a CT scan could provide information on the composition of tumours. Although, changes in tumour composition are often observed on CT scans after initiation of treatment, this is not standard used to evaluate treatment during clinical practice.

3.5 Ultrasound

Ultrasonography uses high frequency sound waves in the megahertz range that are reflected by tissue to varying degrees. While it may provide less anatomical detail than techniques such as CT or MRI, it has several advantages, in particular that it studies the function of moving structures in real-time, emits no ionizing radiation and is widely available, and relatively cheap. On the other hand, its short penetration depth (centimeter range) and poor reproducibility are drawbacks for studying deep structures and its use in clinical trials. Doppler capabilities on modern scanners allow the blood flow in arteries and veins to be assessed, which can be further enhanced by the use of intravenous contrast agents, such as gas microbubbles.

4. Immunological targets for imaging in humans

Given the enormous task of the immune system to maintain tolerance to self-antigens and yet induce immunity to potential harmful pathogens and malignantly transformed cells, it is obvious that immune responses are tightly regulated by intensive crosstalk between different immune cells. However, for the purpose of this overview, we have simplified this multistep process into a linear tri-phase sequel. The next section provides a description of immunological processes that have been used or potentially can be used as target for clinical imaging of developing immune responses. Each subsection highlights the specific contributions of the use of imaging to optimize therapy-induce immune responses.

4.1. Phase I: Antigen encounter

The recognition and phagocytosis of antigens that are expressed by tumour cells represents the first step to induce an immune response (Figure 2a). APC, e.g. DC, are specifically designed to fulfil this role. As such, APC are the main target for immunotherapeutic strategies exploiting TAA, either by *in vivo* loading or cellular therapy, using *ex vivo* generated antigen-loaded APC.

4.1.1 Labeling antigen presenting cells in vitro

DC used in vaccination therapy are autologous cells, generally purified and differentiated from monocytes or from bone marrow. These DC are typically activated *in vitro* by adding pro-inflammatory cytokines or pathogen-associated danger signals, resulting in a phenotype with enhanced immune stimulatory properties (12, 14). The therapeutic DC are loaded with tumour antigens before transfer back into the patient to induce antigen-specific responses. The *ex vivo* isolation of the DC allows convenient access for labeling before transfer, most clinical studies have used 99mTc or 111In to label the therapeutic cells for tracking *in vivo*, reviewed in (48). Preclinical models have shown that the site of delivery greatly influences the subpopulation of DC that is targeted (49). Moreover, the site of activation of lymphocytes dictates their preferential homing characteristics; skin-draining LNs induce skin-homing phenotypes in contrast to organ-draining LNs, which are involved in visceral homing lymphocytes (50, 51). Lastly, the route of administration is important for the *in vivo* biodistribution of the transferred cells. The dermis is richly permeated with lymphatic vessels with loose endothelium accessible to DC. The subcutis consists of larger lymphatic vessels and has a different vasculature from the dermis, resulting in a less favourable milieu for DC to migrate. Imaging the therapeutic DC upon vaccination has revealed important clues on how to optimize vaccination protocols.

Optimizing the route of administration

Therapeutic DC have been administered by various routes in clinical trials: Intralymphatic (i.l.), intravenously (i.v.), intradermally (i.d.), subcutaneously (s.c.) or intranodally (i.n.), and combinations of these. Intradermal vaccinations have been used commonly. Scintigraphic imaging of 111In-labeled DC shows that i.d. transfers result in a reproducible delivery of up to 4% of the injected dose of mature DC to the LN, regardless of the maturation conditions or mode of antigen loading. These small numbers of cells that reach the LN are sufficient to induce TAA-specific immune responses (52). The results with s.c. administration are more variable, with only some studies detecting migration to LN, and always less than 4%. Variations upon s.c. injections might be explained due to differences in injection techniques and the less favourable lymphatic structure of the subcutis. Intravenous administration results in a constant pattern of distribution in clinical studies, starting with entrapment in the capillaries of the lungs, which is most likely caused by non-specific activation and subsequent transient stiffening of cell membrane due to *ex vivo* handling of the cells. This is supported by the finding that mature DC are trapped in the lungs for a longer period of time than immature DC (53). Thereafter the DC redistribute mainly to the liver, spleen and bone marrow. No LN localization has been detected, as expected based on studies using normal peripheral blood leukocytes (54). It is not clear whether DC actually completely fail to reach the LNs or whether the techniques used are not sufficiently sensitive to detect the small numbers of cells that do reach the LNs. Hence, DC migration to LN upon i.v. transfer has not yet been demonstrated in humans. These studies demonstrate that i.d. injections result in a reproducible delivery of a small, but potent, number of DC to the LN. It should be noted that localized transfers, such as i.d. or i.n. injections, are much easier to image than systemic transfers, due to the higher local cell densities, at least at the injection site.

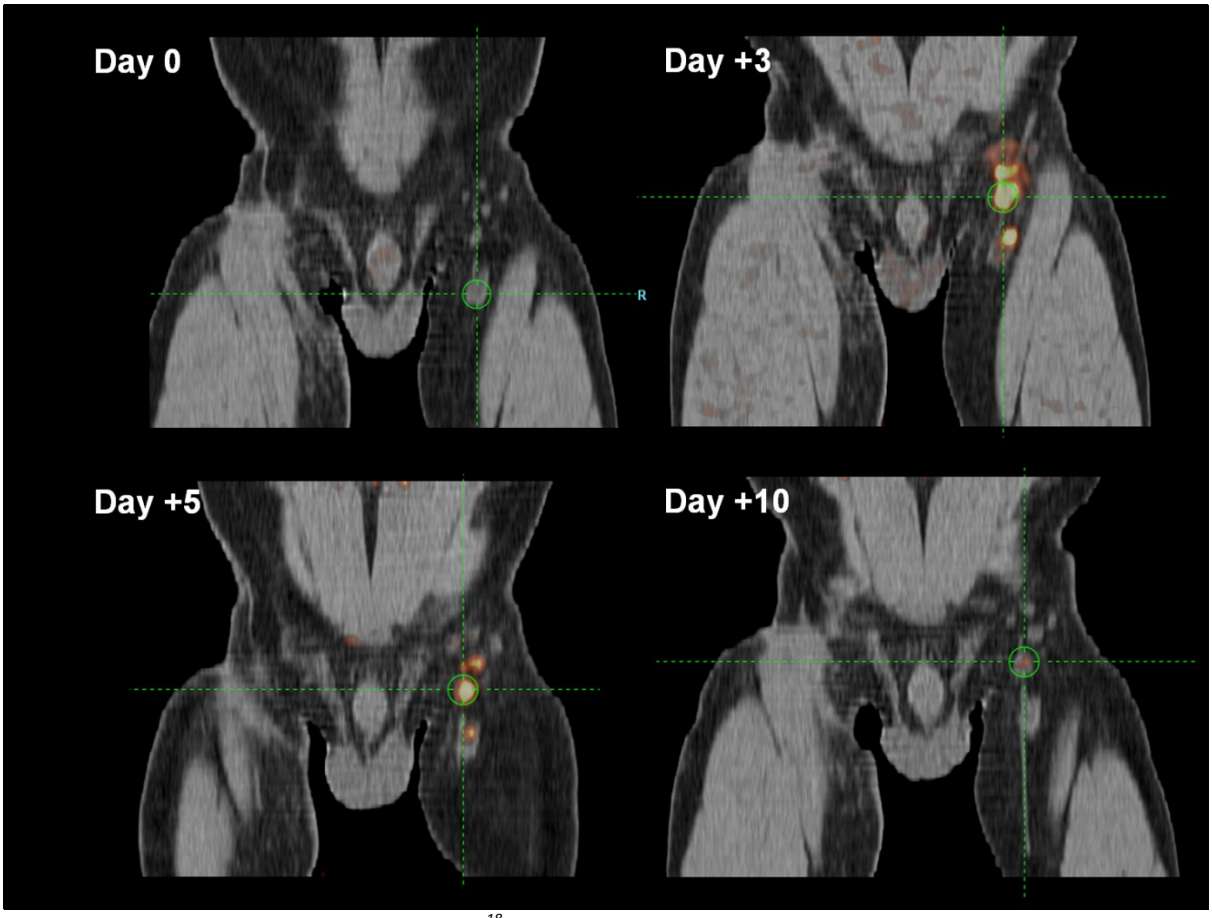

Figure 3. Example PET/CT scan of the dynamics of ^{18}F-FLT uptake in LN after vaccination

Confirming accurate delivery of the vaccine

Intranodal administration is the most common in clinical studies, after i.d. injections. As the LN is the site of immune activation, delivery of DC directly into the LN obviates the need for specific and optimized migratory capacities and directly thrusts the entire dose of cells to the optimal location. The percentage of cells that migrate from the primary injected node to secondary nodes ranges from 0-84%. This large variability cast doubts on the accuracy of i.n. injections, even when administered under ultrasound guidance. Therefore, we studied the migration and localization of a DC population dual-labeled with ^{111}In and iron oxide using scintigraphy and high resolution anatomic MRI (55). Surprisingly, in 4 out of 8 vaccinations we observed no migration to secondary LN, due to extranodal injection of the DC (confirmed using high resolution MRI).

4.1.2. Labeling *antigen-presenting cells in vivo*

More challenging is *in vivo* labeling of antigen presenting cells. Tagging DC *in vivo* through the use of labeled antigen is a convenient trick (56, 57). For example, a nasal vaccine consisting of ^{18}F-labeled botulinum neurotoxin was imaged in real-time and in a quantitative manner using PET in primates (58). In this study the investigators demonstrated that nasal administration is safe with respect to spreading antigens to the central nervous system. Furthermore, whole-body PET allowed detection of the degradation of the vaccine over a period of 4 hours. Long and colleagues exploited *in situ* labeling through cell-to-cell transfer. In a mouse model they injected irradiated tumour cells labeled with superparamagnetic iron oxide (SPIO), and tracked the subsequent migration of APCs, which had taken up the label to draining LNs (59). The cells could even be magnetically recovered *ex vivo*, allowing the investigators to study the phenotype and functionality of the transplanted cells after injection. In humans, this can be done using ^{111}In-labeled tumour antigen peptides and scintigraphy (60). In another approach, the label is injected systemically and either taken up non-specifically by the relevant (phagocytic) cells or specifically by the relevant cell type. This approach circumvents the *ex vivo* purification and labeling of cells and therefore is much easier to apply and more amenable to use in large scale studies. A simple example of such a label would be the use of a radiolabeled specific antibody bound to a radioactive isotope for SPECT (61). Preclinically, this can be done using several techniques including MRI (62) and multimodal nanoparticles (48, 63). However, in clinical practice it has been proven difficult to achieve sufficient signal in the relevant cells, which has so far hampered its use in human studies.

4.2. Second phase: expansion of immune effector cells

The LN are the key organ site in the interplay with DC for initiation of the ensuing immune response and remodelling of the LN infrastructure is an early event of this process (64, 65). Murine studies showed that this occurs via endothelial cell (EC) activation and proliferation (Figure 2b). VEGF is known to induce EC activation and is expressed on EC, DC, B cells and T cells, in response to inflammatory cytokines (66-71). Expansion of the LN infrastructure, e.g. lymphangiogenesis and angiogenesis, facilitates the recruitment of immune cells and their proliferation. Enhanced influx and entry of DC enhances the immune response by ensuring ample antigen presentation. Next, increased influx and screening by naïve T cells for specific antigens results in more potent responses (72-74). Thus lymphangiogenesis, APC – lymphocyte interaction and lymphocyte proliferation can serve as markers for immune responsiveness.

4.2.1. Remodelling of the LN vasculature

It has been shown that LN volume can change nearly 5-fold with induction of an immune response (75). Direct imaging for LN volume is relatively straightforward, and can be done using various techniques visualising the anatomy including MRI, CT and ultrasound (76). Recent data have shown that ultrasound imaging using targeted microbubbles improves the evaluation of the

microvasculature, even in 3 dimensions (77). The availability of Gadolinium (Gd) or (ultrasmall) SPIO based contrast agents, allows the use of dynamic contrast enhanced (DCE)-MRI to monitor angiogenesis on a functional level (78-81). DCE-MRI allows assessment of properties of LN vasculature such as expansion of LN size, total blood flow and blood volume, permeability of perfused capillaries and total surface of perfused capillaries. To date, the main application of diffusion weighted (DW)-MRI in imaging LNs is to detect metastatic LNs, for which it has proven high sensitivity. Accordingly, imaging reactive LNs in immune responses is logically the next application (75). It has recently been shown that MRI measures of vascularity using an injected iron based contrast agent, are comparable to those obtained from traditional histology, which has long been the gold standard to study angiogenesis (82), thus validating the technique.

Indirect imaging of LN vasculature

Alternatively, lymphangiogenesis can be measured by targeted imaging of molecular markers (83). The dominant events in the remodelling of newly formed blood- and lymph vessels, reviewed in (84), are coordinated by the expression of VEGF, and sprouting vessels abundantly express the □v□3 integrin. PET tracers have been developed to probe these specific targets. In our Institute, the anti-VEGF antibody bevacizumab, labeled with ^{111}In, is used for the scintigraphic detection of VEGF in tumours (85), but could easily be applied to image LN revascularisation. More recently, a new generation of protein-targeted contrast agents for multimodal imaging of the cell-surface receptor for VEGF was described (86). These probes are based on recombinant VEGF with a cysteine-containing tag that allows site-specific labeling with contrast agents for near-infrared fluorescence imaging, single-photon emission computed tomography (SPECT) or PET, reviewed in (87). It is expected that an integrin targeting probe for PET will be available for clinical use in the next few years. Importantly, integrin-targeted PET probes have already been tested for safety in humans (88), (89). $\alpha v\beta 3$ integrin has also been targeted by radiolabeled RGD-peptides which specifically bind the integrin, an example of which is ^{18}F-FPPRGD2 (89), ^{18}F-galactoRGD (90) or ^{18}F-Fluciclatide (91). In mice, similar PET probes have been shown to be sensitive to antiangiogenic therapy (91). Using a ^{124}I-labeled antibody against the lymphatic vessel endothelial hyaluronan receptor-1 (LYVE-1), Mumprecht et al imaged inflammation-induced expansion and regression of lymphatic networks *in vivo* in mice with PET (92). MRI is also being explored in preclinical models to specifically target molecular markers such as $\alpha v\beta 3$ integrin (93, 94). In clinical practice, enlargement of regional LN in response to preventive or therapeutic vaccination is a well-known phenomenon. Surprisingly, it has not yet been systemically investigated as a marker of immune responsiveness by using imaging modalities.

4.2.2. Imaging lymphocyte activation in LNs

In order to stimulate lymphocyte proliferation, antigen-bearing mature DC must come into direct contact with the lymphocytes. This cell-cell interaction is best imaged using microscopic techniques, including intravital microscopy, which allow direct viewing. Imaging such specific cell-cell interactions *in vivo* has not yet been performed in clinical studies. However, preclinical studies have revealed important information on the dynamics and kinetics of critical interactions and have paved the way for clinical applications.

Imaging chemotaxis

Aimed at facilitating influx of both APC and effector cells, reactive LN express and secrete chemokines in order for immune cells to relocate to the reactive LN (73, 95). Amongst others (96, 97), the presentation of chemokine CCR7 is dominant (98, 99) and provides a rational target for imaging. Chemotactic agents, which play a key role in directing trafficking, are also suitable imaging targets. CXCL12 is a key chemotaxis factor for lymphocytes, and is detected by CXCR4 on their cell

membrane. CXCR4 overexpression is thought to play a role in cancer (100). Thus, it has been explored as a potential imaging target. Imaging of surface receptors allows for *in situ* labeling of the lymphocytes, given that detection is highly specific and sensitive. Hence, PET is the most suitable approach, together with well-designed radioactive probes (101). CXCR4 expression has been assayed *in vivo* in a dynamic manner using tagged ligands (102, 103), showing that CXCR4 can reliably and specifically be targeted in a manner that correlates with cellular composition shown by immunohistochemistry.

APC – lymphocyte interaction

The *in situ* dynamics of DC/T cell interactions have been studied extensively using advanced microscopy methods which make it possible to study the kinetics of DC/T cell interactions (for example, (104)). Techniques such as intravital microscopy have enabled the study of immune cells in their native environment, with minimal external interference (105-109) . Single molecule techniques now facilitate direct study of the relevant receptors and cell components at the T cell synapse (110). It is now even possible to measure the forces generated by these molecular interactions *ex vivo* (98). From these studies, it became clear that DC/T cell interactions are highly complex and precisely regulated events that govern immune responses. Such findings contribute to the concept that immune activation occurs in separate stages (static, dynamic), emphasizing the importance of motility (e.g. CCR7 expression) and chemokine secretion by LN stroma/cells and DC. With respect to DC-based immune therapy, these studies show that the life-span of DC, prolonged antigen presentation and the migratory capacity are crucial for efficient immune induction. These extremely high-resolution techniques are obviously restricted to *ex vivo* use.

Lymphocyte proliferation

Efficient stimulation by APC should result in lymphocyte activation and the subsequent release of cytokines, such as IL-2, together with extensive proliferation, is an energy-consuming process. Activated, antigen-specific lymphocytes then emigrate from the LNs to antigen depots. In terms of detection of the immune response, these changes in cell metabolism are a candidate for imaging. In particular PET has been employed to study immune activation *in vivo*, as it allows the use of radiolabeled, injectable analogues of relevant metabolites, particularly glucose and nucleotides. Increased glucose uptake can be measured using ^{18}F-labeled fluoro-2-deoxy-2-D-glucose (^{18}F-FDG) PET, which is by far the most commonly used PET tracer. In hematolymphoid tissues however, increased levels of deoxycytidine (DCK) expression is found; DCK is the rate-limiting step in the deoxcycytidine salvage pathway. The tissue-specific expression of this enzyme allows more specific targeting by appropriate PET tracers (111). For example, ^{18}F–2-fluoro-d-(arabinofuranosyl)cytosine (^{18}F-FAC), a fluorinated deoxycytidine analog, has been shown in animal models to accumulate preferentially in $CD8^+$ T cells in mice studies. In contrast to ^{18}F-FDG, this preferentially accumulated in innate immune cells (112). The accumulation of nucleotide analogues, required for increased DNA synthesis during cell division, is another sensitive marker for antigen-specific lymphocytes, at least in melanoma patients vaccinated with antigen-loaded DC. ^{18}F-FLT is trapped intracellularly after phosphorylation by thymidine kinase 1 (TK-1). ^{18}F-FLT-phosphate is not incorporated into DNA since ^{18}F-FLT-monophosphate is a very poor substrate for the second kinase, thymidylate kinase (TMPK), and thus hampers procession to ^{18}F-FLT-triphosphate, which can be incorporated into the DNA. The accumulation of nucleotide analogues has also been studied using other radiolabels in humans. In one study, an ^{11}C-tagged thymidine analogue used for PET was compared to ^{18}F-FDG-PET in lung cancer (113). This study confirmed our results that nucleotide analogue ^{18}F-FLT, is more specific for detecting proliferation than ^{18}F-FDG. In our study, we directly compared the properties of ^{18}F-FDG and ^{18}F-labeled 3'-fluoro-3'-deoxy-thymidine (^{18}F-FLT) within individual patients and demonstrated that in terms of sensitivity and specificity, both tracers perform similarly (46). However, for ^{18}F-FDG

there was no correlation with the *in vitro* monitoring assays measuring concurrent antigen-specific T and B cell responses. Furthermore, ^{18}F-FDG uptake can be attributed to other factors, including other treatments such as vaccinations (114). In contrast, ^{18}F-FLT retention in the LNs of vaccinated patients only increased in the presence of antigen-loaded DC. Moreover, the degree of increase directly correlated to the magnitude of the induced antigen-specific T and B cell responses. This was the first clinical demonstration in that antigen-specific therapy-induced immune responses can be imaged *in vivo* early after treatment initiation (Figure 3. Example of a time course of ^{18}F-FLT uptake in vaccinated LN).

4.2.3. Imaging trafficking of immune effector cells

Activated lymphocytes must leave the LNs and migrate to sites where their cognate antigen is present. Imaging of lymphocyte trafficking is most easily achieved with *ex vivo* labeled cells, as in cases of ACT, but some clinical studies have explored *in vivo* labeling of effector cells as well.

Ex vivo labeling *of transferred cells*

Imaging of cells after ACT has recently been reviewed (115). Transfused cells often traffic initially to the lungs, bone marrow, liver and spleen (61), a process that is regulated by small molecules, primarily cytokines and chemokines. It has been demonstrated in early clinical trials that pretreatment with cyclophosphamide augments the trafficking of transferred cell to the tumor sites (116). In a similar way, IL-2 co-administration might positively contribute to the vaccination effect (117). The use of reporter gene expression, as another way to study small molecule expression, is particularly exciting. It detects the actual synthesis of the molecule and is independent of factors such as lifetime and distribution of the molecule itself. Furthermore, the use of an enzymatic reporter allows for amplification of a weak signal. Hence, mice have been transfected with luciferase linked to interferon-□ expression via plasmids for bioluminescence imaging (118). In this study, the plasmids were injected directly in the liver. Such technology can readily be adapted to other molecules of interest. For example, antigen specific T cells expressing a viral TK gene were tracked in recipient mice over a period of three weeks, using an ^{18}F-tagged probe specific to this variant of TK (119). Quantitative detection of the labeled T cells was possible, with a sensitivity limit in the order of 10^4 T cells – low enough to detect the milder immune response triggered by non-mutated self-antigens in cancer. However, nonspecific probe accumulation in the tumour complicated image interpretation.

In vivo imaging of effector cells

Imaging of lymphocytes, particularly T cells, has been carried out *in vivo* in preclinical models using several imaging modalities (120). Lymphocyte imaging requires a suitable target for the imaging probe, such as cell surface markers. For example, ^{99m}Tc-labeled IL-2 can be used to detect lymphocytes associated lesions in melanoma patients (121). This probe detects tumour-infiltrating lymphocytes, and such imaging can be used to study the effect of therapy. The technique can also be modified to target other immune cells, provided for example, with non-depleting ^{111}In-labeled anti-CD4 antibodies to track $CD4^+$ T cells, as in a murine model of colitis (122). The signal measured by SPECT in this model was found to correlate with standard pathologic measures, although unlike standard pathology, the SPECT/CT measurements are noninvasive and can be applied in humans. A recent example is the use of *in vivo* ^{19}F MRI to longitudinally and quantitatively track T cell homing to draining LN (123). Here, the numbers of antigen specific T cells in a relevant LN were quantified over a period of 3 weeks, in the same animal. Quantification errors arising from dilution of label due to cell division are unavoidable in such systems (124). A unique situation arises for *in vivo* clinical imaging of the immune system in humans in the cornea, where advanced microscopy techniques such as confocal and dual photon microscopy have been carried out on endogenous DC and

lymphocyte infiltration (125). The transparency and favourable optical properties of the eye makes this possible. However, the functionality of the immune system in the eye may not be directly comparable to that in other regions - it was long thought that the eye was “immune privileged” and lacked an immune system. *In vivo* imaging in the eye is more advanced in preclinical settings, which allows more manipulation and the use of pre-labeled cells (126).

4.3. Third phase: targeting the tumour and its microenvironment

Traditionally, measuring the change in tumour volumes according to the response evaluation criteria for solid tumours (RECIST) has been the key criterion upon the therapy effect is judged (127). The use of volume as a measure for response to treatment is based on a large body of evidence involving chemotherapy. Indeed, the direct cytotoxic mode of action of chemotherapy often translates into tumour shrinkage weeks to months after the start of treatment. This initial volume response is often correlated to clinical outcome and thus justifies its use in clinical decision-making. However, now that immunotherapeutic strategies have entered clinical practice, it has become clear that the traditional RECIST criteria are challenged by the advance of immunotherapy (128). In general, several factors need to be considered for the development and optimization of a clinical imaging protocol. For example, there are often no solid data to plan the optimal label or contrast dosage, timing and frequency of imaging and interaction with drugs or other interventions. Frequently there are not enough subjects to obtain results with statistical significance, especially given the high variability that can occur between patients. Thus, trials that incorporate novel imaging for response evaluation must be scrupulously planned beforehand, but can also yield valuable information on the mechanism of action of the applied therapy and on the early identification of responding subjects. The next sections describe several imaging strategies to dissect the relative contributions of tumour progression and on-site immune action.

4.3.1. Evaluation of tumour volume

Tumour shrinkage results from a complex interplay of various components of the immune system in different body compartments. In general, this takes weeks to months to develop and in this time frame the tumour will continue its expansive growth, giving misleading results when tumour size alone is measured. Secondly, in order to eliminate tumour cells, immune cells need to penetrate the tumour and its microenvironment to achieve cell-cell contact. This implies increased cellularity of the tumour and is, in terms of tumour volume, indicative for tumour progression. Wolchok et al (129) proposed a new response paradigm that addresses these issues, while using volume-based criteria. They evaluated a novel set of response criteria in a large series of patients with advanced melanoma who received ipilimumab, a fully human monoclonal antibody that blocks CTLA-4 (129). These immune-related response criteria now more accurately characterize new response patterns, especially those with delayed tumour shrinkage or initial tumour growth followed by tumour shrinkage. However, these novel criteria are designed to avoid preliminary termination of a possible effective immunotherapeutic treatment, but they fail to reveal cellular and molecular processes that precede a clinically meaningful response. Furthermore, as a result from the delayed volume responses that are associated with the indirect mode of action of immunotherapy, this information becomes available rather late after initiation of treatment.

4.3.2. Imaging tumour cellular composition

One rational approach to circumvent the above-mentioned issues is to measure the relative number of tumour cells in a suspected tumour-containing volume before and after start of treatment. Such an approach requires a highly sensitive and quantifiable tumour-specific marker, e.g. by using PET tracers. The developments in melanoma-specific markers is recently reviewed in (130). In this respect, novel compounds that target melanin biosynthesis and metallopeptides binding to

melanocortin type 1 receptor, which are overexpressed in melanoma, are promising agents (131-133). Changes that occur in the tumour due to an increased immune response can be imaged using MRI, for example through changes in relaxation times, contrast or apparent diffusion coefficient. These changes have been shown to correlate with conventional histological measure in mice (134). In this study, the immune response was induced by transferred cytotoxic T cells that expressed a modified TCR specific for a tumour antigen. However, to date there is no experience with the evaluation of responses to immunotherapy in particular.

4.3.2. Imaging tumour metabolic activity

Currently, ^{18}F-FDG is the most commonly used radiopharmaceutical for imaging tumour metabolism in clinical practice. Its use is based on the increased glycolytic rate in tumours compared to physiologic cells, known as the Warburg effect. Without doubt, imaging changes occurring in tumour metabolism early after treatment initiation by PET, has contributed to the optimization of clinical decision making in the management of patients with various types of cancer. However, the infiltration of effector immune cells, which are metabolically active as well, can be a confounder in the interpretation of tumour responses, leading to ^{18}F-FDG-positive tumour lesions due to activated immune cells rather than tumor cells (135). However, other studies have demonstrated otherwise, immunohistochemical staining showed highly ^{18}F-FDG avid lesions that were not regression showed indeed a high proliferative rate of tumor cells, whereas low 18F-FDG avid lesions were massively infiltrated by activated immune cells. There is increasing attention for the development of tracers which are more tumour-specific, in order to discriminate tumour metabolism from inflammatory responses. Potential candidates are amino acids, nucleotides, choline and σ-receptor ligands. In a preclinical model, Van Waarde *et al.*compared 2 σ-receptor ligands, ^{11}C-methionine and ^{11}C-choline with ^{18}F-FDG and found that one of the 18F-labeled σ-receptor ligands selectively targeted glioma metabolism; 30-fold tracer uptake compared to sterile inflammation (136). Further *in vitro* studies in this models showed that increased sigma-ligand binding and ^{11}C-choline uptake reflected active membrane repair upon chemotherapy-induced cell damage. Along the same lines, imaging nucleotide metabolism by ^{18}F-FLT, as a tracer for tumour cell proliferation in humans, has extensively been evaluated to show proliferation specifically. Effector immune cells that infiltrate tumours are mostly of a differentiated phenotype and show no proliferative activity on the spot. However, no comparative studies in humans have been performed to study the relative selectivity of ^{18}F-FLT for tumour cells compared to inflammation (137).

5. Discussion and future directions

Direct visualization is a powerful tool to push forward the understanding of complex processes, which has intrigued researchers for ages (Figure 1 Timeline). In the next section we describe particular issues concerning the application of imaging immune responses in clinical practice. Understanding those issues in the imaging of therapy-induced immune responses will hopefully improve the usage of these powerful tool in future clinical trials and thus contribute to the optimization of anti-cancer treatment.

5.1 General issues in imaging the immune system

Germain *et al.*eloquently stated that the imaging of the immune system is the biological equivalent of Heisenberg's principle, which implies that it is not possible to study the system without perturbing it (105). Indeed, the function of the immune system is to maintain cellular integrity and homeostasis; hence how can you label and probe it without affecting the system? Therefore, extra caution must be taken in the development of probes and labels for imaging. The highly mobile and rapidly changing nature of the immune system further complicates imaging studies. We have previously suggested two basic strategies for *in vivo* cell tracking (48). Briefly, cells can be pre-labeled before transfer or a

targeted label can be used to label the relevant cells *in situ*. Typically, the first strategy is used for MRI (pre-labeling with contrast agents), and the second for PET. This is a reflection of both the detectable lifetime of the labels and the sensitivity of the detection technique.

Ex vivo labeling of cells

From an imaging perspective, there are several advantages to this approach. First, the *ex vivo* isolation of the DC allows convenient access for labeling before transfer, and for detailed characterization of the labeled cells in terms of viability, gene expression and functional status (27, 48). Secondly, the homogeneity of label uptake within the population can also be determined and removal of excess label and dead cells is simpler. Furthermore, non-specific labeling of irrelevant cells is greatly reduced if the relevant cell population is purified beforehand. However, it can be an expensive and laborious process to purify, culture and label cells *ex vivo* before transfer. The effect of an imaging label on cells must be carefully considered. For example, radioactive probes can become highly concentrated locally and affect the labeled cells directly (138). This can be particularly deleterious for long-lived or highly proliferating cells, such as stem cells or activated T cells. MRI labels, such as those based on iron oxide have also been shown to impact cell migration (139) (140) and induce oxidative stress due to the catalytic iron moiety (141). The fate of the label, particularly its ability to stay with the relevant cell is crucial. It is known that cells can transfer their intracellular label to neighbouring cells, particularly when under stress leading to "secondarily labeled cells" which can confound imaging data (142). Hence, one always should ask – and answer – the question "What am I imaging?" These cellular effects must be considered in addition to any systemic side effects of the label, for example nausea or rashes; nephrogenic systemic fibrosis is a concern with Gd-based contrast agents for MRI.

In vivo labeling *of cells*

The alternatives to *ex vivo* labeling, using long-lived agents, are *in situ* labeling or genetic modification of the cells to express an imaging reporter gene. *In situ* labeling typically uses short-lived labels, as with injectable PET tracers. These tracers can even be generated from clinical applicable antibodies, for example ^{89}Zr-labeled Fresolimumab for PET detection of tumor necrosis factor (TNF)-α expression in mice (143). However, antibodies can neutralize or otherwise affect activity of the target molecule and/or cell. While that is often the purpose in antibody therapy, it is not necessarily desirable when imaging functionality or expression. In general, only viable or functional cells will be able to take up the label effectively, so non-specific labeling will not restrict its use. Furthermore, the use of an injectable label allows the use of radiolabels for longitudinal studies, as the agent can be injected (or re-injected) before each imaging session. However, the general problems faced with systemic transfer of label include limited uptake in the relevant cell population, accumulation in non-relevant tissues such as the liver or bladder, the requirement for higher activity doses to allow sufficient signal in the relevant cells, clearance of label and clinical radiation exposure limits for radioactive agents. The use of reporter genes is a powerful approach. This technique is well-suited for the detection of proliferative cells, as the label does not dilute with cell division. Furthermore, continued expression over the cell's lifetime allows longitudinal tracking, and can even be coupled to the expression of a particular gene of interest, or at the very least, to viable cells. Moreover, intrinsically labeled cells are attractive due to the absence of background from nonspecific uptake (56). However, the applicability of genetically modified cells to humans is not yet clear (144). Finally, it is always necessary to consider whether images are really specific to the relevant cells i.e. the specificity of detection. While this is typically more of a problem with injected labels or targeted agents that are injected systemically, it can also affect prelabeled cells through nonspecific transfer or loss of label from the transferred cells. The actual physical location of the label should be

confirmed using histology on tissue sections during the development and validation of such monitoring tools.

Figure 2: Timeline of development of immunotherapies and development of imaging tools.

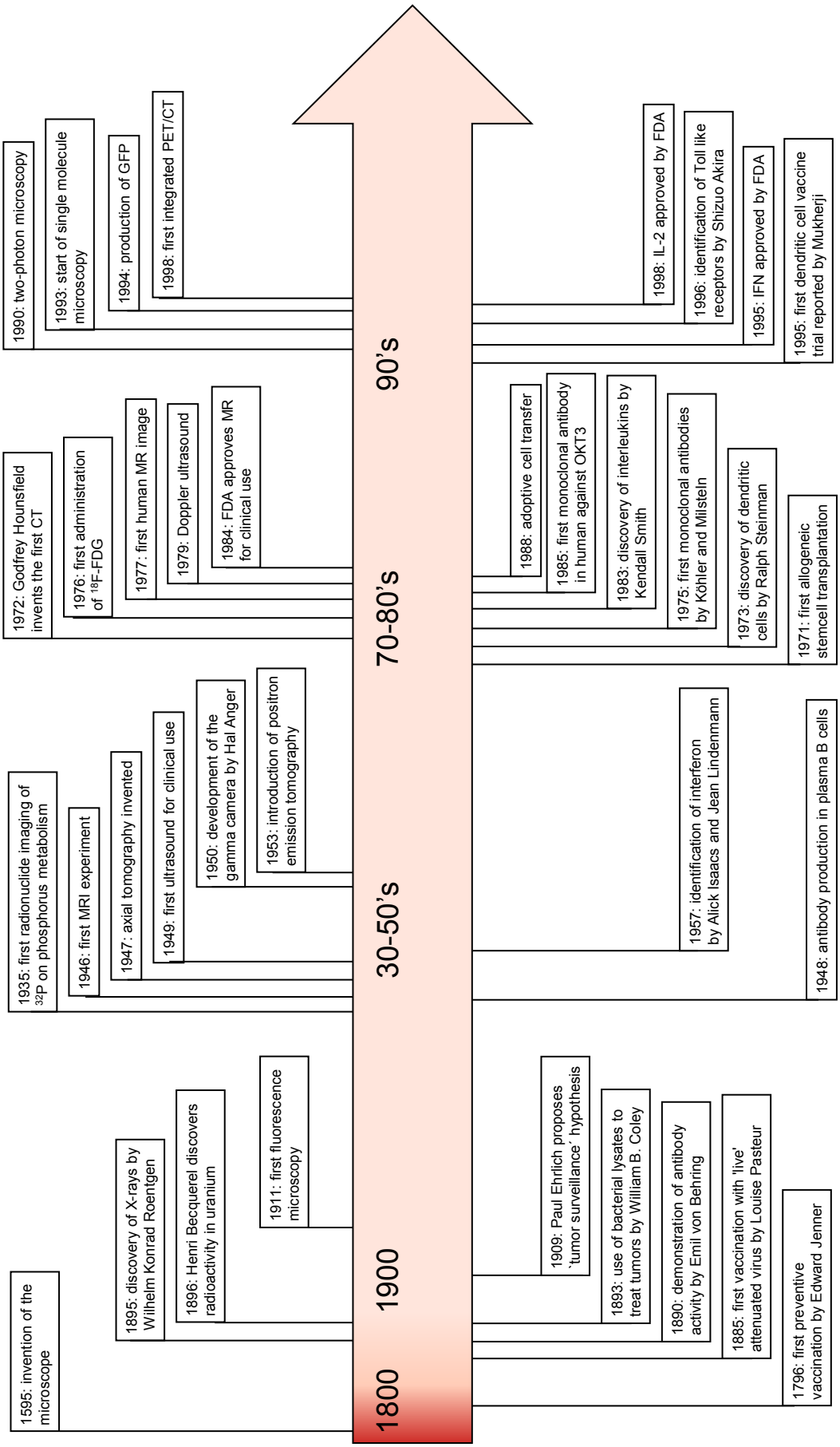

5.2 Future directions: How can imaging contribute?

The greatest challenge is to find a target process that is critical to successful immune activation, so that imaging this process accurately predicts response to intervention. Crucially, this must be done without disturbing the targeted process. Moreover, the imaging results should deliver important information as early after start of treatment as possible, to allow timely adjustment of treatment per individual. In this section we describe three possible solutions, using novel imaging tools fulfilling the needs described above.

Imaging specific functionalities

PET reporter gene (PRG)/probe (PRP) systems, recently reviewed in (145, 146) have proven their use in many preclinical models (119). PRG encodes a protein that mediates the accumulation of a specific reporter probe, labeled with positron-emitting radionuclide. These systems allow long-term whole-body visualization of the functional status of the transduced and transplanted cells, and can thus provide valuable information on the localization, the kinetics and the magnitude of transgene expression over time. The application in patients has long been hampered by safety concerns; the most commonly used transgenes are from viral origin and can trigger an immune attack against the transfected cells in humans (147). However, strategies to circumvent the safety concerns are being developed, paving the way to application in clinical trials. For example, therapeutic cells have genetically been modified to implement a suicide gene in ACT as a safety precaution. Another possibility to circumvent this immunogenicity is customizing the reporter gene, as has been done with thymidine kinase (TK) (144). TK gene therapy has been applied in small clinical trials (148, 149) and the cells used in ACT are frequently genetically modified (for example (150, 151)). Recently, humanized transgenes were described (144, 152, 153), based on a mutated form of the human thymidine kinase 2 (TK2). By using this PRG and a thymidine analog L-^{18}F-FMAU as PRP, the investigators could efficiently target and visualize nucleotide metabolism in proliferating cells, without perturbing the endogenous enzymes. In this study, the biodistribution of the used PRP and another probe, 18F-FHBG, were studied in patients, as a first step towards clinical application. This promising technique can easily be adjusted to target other functional processes; from the monitoring of cell-based therapies to anti-angiogenic treatment. In animal models, the relevant cells can be transduced to express reporter genes, such as enzymes that trap tracers for PET, fluorescent proteins such as green fluorescence protein (GFP) for fluorescence imaging, luciferase for bioluminescence imaging, or iron transporters or CEST proteins (154) for MRI contrast, and even for multimodality imaging using a triple reporter gene construct for fluorescence (eGFP), ^{18}F-FLT PET (TK 1 and 2) and luminescence (luciferase) (155).

Novel tracers that target specific effector cell populations

The activation and proliferation of immune effector cells is accompanied by an enormous metabolic switch. In a resting state the immune system maintains the existence of a diverse population of cells. Once danger is detected, specific populations need to shift to a highly activated state that runs specific transcriptional and translational programmes, within a time frame of hours, reviewed in (156, 157). In order to respond to these increased energy demands, T cells must actively acquire metabolites from their environment. For example, ligation of T cell receptor initiates cellular proliferation, whereas triggering of co-stimulatory molecules enables the uptake and usage of metabolites. Circulating growth factors, like cytokines and hormones, contribute to the ability of effector cells to switch between resting and activated states. Since the immune system comprises a multitude of different cell types and effector functions, it is of no surprise that in this tightly regulated process, specific effector functions are supported by specific metabolic pathways (157). In a preclinical study, Nair-Gill *et al.*investigated the immune cell specificity of PET probes for two different metabolic pathways: ^{18}F-FDG for glycolysis and ^{18}F-labeled 2-fluoro-d-

(arabinofuranosyl)cytosine (^{18}F-FAC) for deoxycytidine salvage; in response to a retrovirus-induced sarcoma (112). They demonstrated that the two probes had distinct patterns of accumulation: ^{18}F-FDG accumulated to the highest levels in innate immune cells, while ^{18}F-FAC accumulated predominantly in CD8^{+} T cells in a manner that correlated with cellular proliferation. Thus, innate and adaptive cell types differ in glycolytic and deoxycytidine salvage demands during an immune response, and this can be targeted with specific PET probes. In a similar fashion, Shu et al (158) develop PET probes with improved metabolic stability and specificity for rate-limiting enzyme in the deoxyribonucleoside salvage pathway: deoxycytidine kinase (dCK). Given the increased body of knowledge on the metabolic fates of different cell populations, it is just a matter of time before this will be translated to monitor immune responses in clinical trials.

Targeting on-site immune responses in tumour tissue

The transfer of technology from tumour and preclinical imaging holds great promise. One example of such technology transfer is in the detection of apoptosis *in vivo*. This might also be considered in non-immunotherapeutic regimen, since it has now been demonstrated that tumour regression at least partly results from chemotherapy-induced programmed cell death and the subsequent influx and activation of immune cells (34). The induction of tumour cell apoptosis by infiltrating immune cells precedes detectable tumour volume shrinkage (reviewed in (159)). Effective treatment should result in cell lysis, loss of membrane integrity and increased extracellular space. These physical changes can be detected and measured using MRI. MRI is already available in the clinic and could be applied to monitoring immune responses *in vivo*. Amongst others, Annexin-V, hydrophobic cations and caspase inhibitors have been tested as potential probes for imaging apoptosis in preclinical models. ^{99m}Tc-labeled Annexin-V has been tested in clinical trials (160). Indeed, the authors found that increased Annexin-V uptake in the tumour site early after start of platinum-based chemotherapy in non-small cell lung cancer (NSCLC) was associated with improved clinical response. Another apoptosis marker that has been tested in humans is ^{18}F-labeled 2-(5-fluoropentyhl)-2-methyl malonic acid (^{18}F-ML10) (161, 162). It is interesting to note that just 10 years ago, the field of *in vivo* imaging of the immune system was virtually non-existent. Five years ago, a review article covering imaging for cell tracking focused on the same techniques that we are still developing - SPIO labels for MRI, scintigraphy and PET visualizing TK activity (163). More recently, we have seen the preliminary introduction of these techniques in humans, the introduction of quantitative *in vivo* ^{19}F MRI, and the distinct possibility of imminent TK-based PET in humans. We have also learned that all these probes and imaging modalities are likely to perturb the cells we are imaging. Thus, although *in vivo* imaging is a new field, we are already beginning to see its applications in imaging the immune system. Together with improvements in labels and imaging hardware, and the advent of multimodal imaging scanners, the future of *in vivo* imaging of the immune system looks bright.

References

1. Sharma, P., et al., *Novel cancer immunotherapy agents with survival benefit: recent successes and next steps.* Nat Rev Cancer, 2011. 11(11): p. 805-12.
2. Morse, M.A., et al., *Recent developments in therapeutic cancer vaccines.* Nat Clin Pract Oncol, 2005. 2(2): p. 108-13.
3. Lesterhuis, W.J., J.B. Haanen, and C.J. Punt, *Cancer immunotherapy - revisited.* Nat Rev Drug Discov. 10(8): p. 591-600.
4. Egen, J.G., M.S. Kuhns, and J.P. Allison, *CTLA-4: new insights into its biological function and use in tumor immunotherapy.* Nat Immunol, 2002. 3(7): p. 611-8.
5. Ogino, S., et al., *Cancer immunology--analysis of host and tumor factors for personalized medicine.* Nat Rev Clin Oncol, 2011. 8(12): p. 711-9.
6. Wang, E., M.C. Panelli, and F.M. Marincola, *Gene profiling of immune responses against tumors.* Curr Opin Immunol, 2005. 17(4): p. 423-7.
7. Banchereau, J. and R.M. Steinman, *Dendritic cells and the control of immunity.* Nature, 1998. 392(6673): p. 245-52.
8. Hanahan, D. and R.A. Weinberg, *Hallmarks of cancer: the next generation.* Cell, 2011. 144(5): p. 646-74.
9. Schwartzentruber, D.J., et al., *gp100 peptide vaccine and interleukin-2 in patients with advanced melanoma.* N Engl J Med. 364(22): p. 2119-27.
10. Kenter, G.G., et al., *Vaccination against HPV-16 oncoproteins for vulvar intraepithelial neoplasia.* N Engl J Med, 2009. 361(19): p. 1838-47.
11. van den Eertwegh, A.J., et al., *Combined immunotherapy with granulocyte-macrophage colony-stimulating factor-transduced allogeneic prostate cancer cells and ipilimumab in patients with metastatic castration-resistant prostate cancer: a phase 1 dose-escalation trial.* Lancet Oncol, 2012.
12. Banchereau, J. and A.K. Palucka, *Dendritic cells as therapeutic vaccines against cancer.* Nat Rev Immunol, 2005. 5(4): p. 296-306.
13. Kantoff, P.W., et al., *Sipuleucel-T immunotherapy for castration-resistant prostate cancer.* N Engl J Med. 363(5): p. 411-22.
14. Figdor, C.G., et al., *Dendritic cell immunotherapy: mapping the way.* Nat Med, 2004. 10(5): p. 475-80.
15. Lesterhuis, W.J., et al., *Dendritic cell vaccines in melanoma: from promise to proof?* Crit Rev Oncol Hematol, 2008. 66(2): p. 118-34.
16. Tacken, P.J., et al., *Dendritic-cell immunotherapy: from ex vivo loading to in vivo targeting.* Nat Rev Immunol, 2007. 7(10): p. 790-802.
17. Taniguchi, T., et al., *Structure and expression of a cloned cDNA for human interleukin-2.* Nature, 1983. 302(5906): p. 305-10.
18. Smith, K.A., *Interleukin-2: inception, impact, and implications.* Science, 1988. 240(4856): p. 1169-76.
19. Atkins, M.B., et al., *High-dose recombinant interleukin 2 therapy for patients with metastatic melanoma: analysis of 270 patients treated between 1985 and 1993.* J Clin Oncol, 1999. 17(7): p. 2105-16.
20. Parkinson, D.R., et al., *Interleukin-2 therapy in patients with metastatic malignant melanoma: a phase II study.* J Clin Oncol, 1990. 8(10): p. 1650-6.
21. Abrams, J.S., et al., *High-dose recombinant interleukin-2 alone: a regimen with limited activity in the treatment of advanced renal cell carcinoma.* J Natl Cancer Inst, 1990. 82(14): p. 1202-6.
22. Bruton, J.K. and J.M. Koeller, *Recombinant interleukin-2.* Pharmacotherapy, 1994. 14(6): p. 635-56.
23. Gonzalez-Navajas, J.M., et al., *Immunomodulatory functions of type I interferons.* Nat Rev Immunol, 2012. 12(2): p. 125-35.
24. Porter, D.L., et al., *Induction of graft-versus-host disease as immunotherapy for relapsed chronic myeloid leukemia.* N Engl J Med, 1994. 330(2): p. 100-6.
25. Mackinnon, S., et al., *Adoptive immunotherapy evaluating escalating doses of donor leukocytes for relapse of chronic myeloid leukemia after bone marrow transplantation: separation of graft-versus-leukemia responses from graft-versus-host disease.* Blood, 1995. 86(4): p. 1261-8.
26. Velardi, A., *Role of KIRs and KIR ligands in hematopoietic transplantation.* Curr Opin Immunol, 2008. 20(5): p. 581-7.
27. Rosenberg, S.A., et al., *Adoptive cell transfer: a clinical path to effective cancer immunotherapy.* Nat Rev Cancer, 2008. 8(4): p. 299-308.
28. Berry, L.J., M. Moeller, and P.K. Darcy, *Adoptive immunotherapy for cancer: the next generation of gene-engineered immune cells.* Tissue Antigens, 2009. 74(4): p. 277-89.
29. Hughes, M.S., et al., *Transfer of a TCR gene derived from a patient with a marked antitumor response conveys highly active T-cell effector functions.* Hum Gene Ther, 2005. 16(4): p. 457-72.
30. Eggermont, A.M., *Therapeutic vaccines in solid tumours: can they be harmful?* Eur J Cancer, 2009. 45(12): p. 2087-90.
31. Adams, G.P. and L.M. Weiner, *Monoclonal antibody therapy of cancer.* Nat Biotechnol, 2005. 23(9): p. 1147-57.
32. Klinger, M., et al., *Immunopharmacological response of patients with B-lineage acute lymphoblastic leukemia to continuous infusion of T cell-engaging CD19/CD3-bispecific BiTE antibody blinatumomab.* Blood, 2012.
33. Apetoh, L., et al., *Toll-like receptor 4-dependent contribution of the immune system to anticancer chemotherapy and radiotherapy.* Nat Med, 2007. 13(9): p. 1050-9.
34. Zitvogel, L., et al., *Immunological aspects of cancer chemotherapy.* Nat Rev Immunol, 2008. 8(1): p. 59-73.
35. Schreibelt, G., et al., *Toll-like receptor expression and function in human dendritic cell subsets: implications for dendritic cell-based anti-cancer immunotherapy.* Cancer Immunol Immunother. 59(10): p. 1573-82.

36. Speiser, D.E. and P. Romero, *Molecularly defined vaccines for cancer immunotherapy, and protective T cell immunity.* Semin Immunol, 2010. 22(3): p. 144-54.
37. Hodi, F.S., et al., *Improved survival with ipilimumab in patients with metastatic melanoma.* N Engl J Med. 363(8): p. 711-23.
38. Robert, C., et al., *Ipilimumab plus dacarbazine for previously untreated metastatic melanoma.* N Engl J Med. 364(26): p. 2517-26.
39. Mellman, I., G. Coukos, and G. Dranoff, *Cancer immunotherapy comes of age.* Nature, 2011. 480(7378): p. 480-9.
40. Verdijk, P., et al., *Sensitivity of magnetic resonance imaging of dendritic cells for in vivo tracking of cellular cancer vaccines.* Int J Cancer, 2007. 120(5): p. 978-84.
41. Blocklet, D., et al., *111In-oxine and 99mTc-HMPAO* labeling *of antigen-loaded dendritic cells: in vivo imaging and influence on motility and actin content.* Eur J Nucl Med Mol Imaging, 2003. 30(3): p. 440-447.
42. Stojanov, K., et al., *(18F)FDG labeling of neural stem cells for in vivo cell tracking with positron emission tomography: inhibition of tracer release by phloretin.* Mol Imaging, 2012. 11(1): p. 1-12.
43. Thompson, M., et al., *In vivo tracking for cell therapies.* Q J Nucl Med Mol Imaging, 2005. 49(4): p. 339-48.
44. Bulte, J.W., *In vivo MRI cell tracking: clinical studies.* AJR Am J Roentgenol, 2009. 193(2): p. 314-25.
45. Srinivas, M., et al., *(19)F MRI for quantitative in vivo cell tracking.* Trends Biotechnol, 2010. 28(7): p. 363-70.
46. Aarntzen, E.H., et al., *Early identification of antigen-specific immune responses in vivo by (18F)-labeled 3'-fluoro-3'-deoxy-thymidine ((18F)FLT) PET imaging.* Proc Natl Acad Sci U S A, 2011. 108(45): p. 18396-9.
47. Laing, R.E., et al., *Visualizing cancer and immune cell function with metabolic positron emission tomography.* Curr Opin Genet Dev, 2010. 20(1): p. 100-5.
48. Srinivas, M., et al., *Imaging of cellular therapies.* Adv Drug Deliv Rev, 2010. 62(11): p. 1080-93.
49. Eggert, A.A., et al., *Biodistribution and vaccine efficiency of murine dendritic cells are dependent on the route of administration.* Cancer Res, 1999. 59(14): p. 3340-5.
50. Mullins, D.W., et al., *Route of immunization with peptide-pulsed dendritic cells controls the distribution of memory and effector T cells in lymphoid tissues and determines the pattern of regional tumor control.* J Exp Med, 2003. 198(7): p. 1023-34.
51. Mora, J.R., et al., *Selective imprinting of gut-homing T cells by Peyer's patch dendritic cells.* Nature, 2003. 424(6944): p. 88-93.
52. Verdijk, P., et al., *Limited amounts of dendritic cells migrate into the T-cell area of lymph nodes but have high immune activating potential in melanoma patients.* Clin Cancer Res, 2009. 15(7): p. 2531-40.
53. Prince, H.M., et al., *In vivo tracking of dendritic cells in patients with multiple myeloma.* J Immunother, 2008. 31(2): p. 166-179.
54. Read, E.J., et al., *In vivo traffic of indium-111-oxine labeled human lymphocytes collected by automated apheresis.* J Nucl Med, 1990. 31(6): p. 999-1006.
55. de Vries, I.J., et al., *Magnetic resonance tracking of dendritic cells in melanoma patients for monitoring of cellular therapy.* Nat Biotechnol, 2005. 23(11): p. 1407-13.
56. Bonetto, F., et al., *A novel (19)F agent for detection and quantification of human dendritic cells using magnetic resonance imaging.* Int J Cancer, 2011. 129(2): p. 365-73.
57. Baumjohann, D., et al., *In vivo magnetic resonance imaging of dendritic cell migration into the draining lymph nodes of mice.* Eur J Immunol, 2006. 36(9): p. 2544-55.
58. Yuki, Y., et al., *In vivo molecular imaging analysis of a nasal vaccine that induces protective immunity against botulism in nonhuman primates.* J Immunol, 2010. 185(9): p. 5436-43.
59. Long, C.M., et al., *Magnetovaccination as a novel method to assess and quantify dendritic cell tumor antigen capture and delivery to lymph nodes.* Cancer Res, 2009. 69(7): p. 3180-7.
60. Laverman, P., et al., *Development of 111In-labeled tumor-associated antigen peptides for monitoring dendritic-cell-based vaccination.* Nucl Med Biol, 2006. 33(4): p. 453-8.
61. Kim, J.A., et al., *Cellular immunotherapy for patients with metastatic colorectal carcinoma using lymph node lymphocytes localized in vivo by radiolabeled monoclonal antibody.* Cancer, 1999. 86(1): p. 22-30.
62. Ahrens, E.T., et al., *Receptor-mediated endocytosis of iron-oxide particles provides efficient labeling of dendritic cells for in vivo MR imaging.* Magn Reson Med, 2003. 49(6): p. 1006-13.
63. Bhirde, A., et al., *Nanoparticles for cell labeling.* Nanoscale, 2011. 3(1): p. 142-53.
64. Hay, J.B. and B.B. Hobbs, *The flow of blood to lymph nodes and its relation to lymphocyte traffic and the immune response.* J Exp Med, 1977. 145(1): p. 31-44.
65. Herman, P.G., I. Yamamoto, and H.Z. Mellins, *Blood microcirculation in the lymph node during the primary immune response.* J Exp Med, 1972. 136(4): p. 697-714.
66. Blotnick, S., et al., *T lymphocytes synthesize and export heparin-binding epidermal growth factor-like growth factor and basic fibroblast growth factor, mitogens for vascular cells and fibroblasts: differential production and release by CD4+ and CD8+ T cells.* Proc Natl Acad Sci U S A, 1994. 91(8): p. 2890-94.
67. Mor, F., F.J. Quintana, and I.R. Cohen, *Angiogenesis-inflammation cross-talk: vascular endothelial growth factor is secreted by activated T cells and induces Th1 polarization.* J Immunol, 2004. 172(7): p. 4618-23.
68. Baluk, P., et al., *Pathogenesis of persistent lymphatic vessel hyperplasia in chronic airway inflammation.* J Clin Invest, 2005. 115(2): p. 247-57.
69. Ruddell, A., et al., *B lymphocyte-specific c-Myc expression stimulates early and functional expansion of the vasculature and lymphatics during lymphomagenesis.* Am J Pathol, 2003. 163(6): p. 2233-45.
70. Zhang, M., et al., *Splenic stroma drives mature dendritic cells to differentiate into regulatory dendritic cells.* Nat Immunol, 2004. 5(11): p. 1124-33.
71. Angeli, V., et al., *B cell-driven lymphangiogenesis in inflamed lymph nodes enhances dendritic cell mobilization.* Immunity, 2006. 24(2): p. 203-15.

72. Webster, B., et al., *Regulation of lymph node vascular growth by dendritic cells.* J Exp Med, 2006. 203(8): p. 1903-13.
73. Angeli, V. and G.J. Randolph, *Inflammation, lymphatic function, and dendritic cell migration.* Lymphat Res Biol, 2006. 4(4): p. 217-28.
74. Soderberg, K.A., et al., *Innate control of adaptive immunity via remodeling of lymph node feed arteriole.* Proc Natl Acad Sci U S A, 2005. 102(45): p. 16315-20.
75. Klerkx, W.M., et al., *Longitudinal 3.0T MRI analysis of changes in lymph node volume and apparent diffusion coefficient in an experimental animal model of metastatic and hyperplastic lymph nodes.* J Magn Reson Imaging, 2011. 33(5): p. 1151-9.
76. Barrett, T., P.L. Choyke, and H. Kobayashi, *Imaging of the lymphatic system: new horizons.* Contrast Media Mol Imaging, 2006. 1(6): p. 230-45.
77. Streeter, J.E., et al., *Assessment of molecular imaging of angiogenesis with three-dimensional ultrasonography.* Mol Imaging, 2011. 10(6): p. 460-8.
78. Kusters, B., et al., *Differential effects of vascular endothelial growth factor A isoforms in a mouse brain metastasis model of human melanoma.* Cancer Res, 2003. 63(17): p. 5408-13.
79. Kusters, B., et al., *Vascular endothelial growth factor-A(165) induces progression of melanoma brain metastases without induction of sprouting angiogenesis.* Cancer Res, 2002. 62(2): p. 341-5.
80. Leenders, W., et al., *Vascular endothelial growth factor-A determines detectability of experimental melanoma brain metastasis in GD-DTPA-enhanced MRI.* Int J Cancer, 2003. 105(4): p. 437-43.
81. Leenders, W.P., et al., *Antiangiogenic therapy of cerebral melanoma metastases results in sustained tumor progression via vessel co-option.* Clin Cancer Res, 2004. 10(18 Pt 1): p. 6222-30.
82. Lemasson, B., et al., *In vivo imaging of vessel diameter, size, and density: A comparative study between MRI and histology.* Magn Reson Med, 2012.
83. Kurdziel, K.A., L. Lindenberg, and P.L. Choyke, *Oncologic Angiogenesis Imaging in the clinic---how and why.* Imaging Med, 2011. 3(4): p. 445-457.
84. Adams, R.H. and K. Alitalo, *Molecular regulation of angiogenesis and lymphangiogenesis.* Nat Rev Mol Cell Biol, 2007. 8(6): p. 464-78.
85. Stollman, T.H., et al., *Specific imaging of VEGF-A expression with radiolabeled anti-VEGF monoclonal antibody.* Int J Cancer, 2008. 122(10): p. 2310-4.
86. Backer, M.V., et al., *Molecular imaging of VEGF receptors in angiogenic vasculature with single-chain VEGF-based probes.* Nat Med, 2007. 13(4): p. 504-9.
87. Cai, W. and X. Chen, *Multimodality imaging of vascular endothelial growth factor and vascular endothelial growth factor receptor expression.* Front Biosci, 2007. 12: p. 4267-79.
88. Kim, J.H., et al., *Whole-body distribution and radiation dosimetry of (68)Ga-NOTA-RGD, a positron emission tomography agent for angiogenesis imaging.* Cancer Biother Radiopharm, 2012. 27(1): p. 65-71.
89. Mittra, E.S., et al., *Pilot pharmacokinetic and dosimetric studies of (18)F-FPPRGD2: a PET radiopharmaceutical agent for imaging alpha(v)beta(3) integrin levels.* Radiology, 2011. 260(1): p. 182-91.
90. Beer, A.J., et al., *PET Imaging of Integrin alphaVbeta3 Expression.* Theranostics, 2011. 1: p. 48-57.
91. Battle, M.R., et al., *Monitoring tumor response to antiangiogenic sunitinib therapy with 18F-fluciclatide, an 18F-labeled alphaVbeta3-integrin and alphaV beta5-integrin imaging agent.* J Nucl Med, 2011. 52(3): p. 424-30.
92. Mumprecht, V., et al., *In vivo imaging of inflammation- and tumor-induced lymph node lymphangiogenesis by immuno-positron emission tomography.* Cancer Res, 2010. 70(21): p. 8842-51.
93. Winter, P.M., et al., *Molecular imaging of angiogenesis in nascent Vx-2 rabbit tumors using a novel alpha(nu)beta3-targeted nanoparticle and 1.5 tesla magnetic resonance imaging.* Cancer Res, 2003. 63(18): p. 5838-43.
94. Wu, G., et al., *Novel peptide targeting integrin alphavbeta3-rich tumor cells by magnetic resonance imaging.* J Magn Reson Imaging, 2011. 34(2): p. 395-402.
95. Miyasaka, M. and T. Tanaka, *Lymphocyte trafficking across high endothelial venules: dogmas and enigmas.* Nat Rev Immunol, 2004. 4(5): p. 360-70.
96. Yopp, A.C., G.J. Randolph, and J.S. Bromberg, *Leukotrienes, sphingolipids, and leukocyte trafficking.* J Immunol, 2003. 171(1): p. 5-10.
97. Qu, C., et al., *Role of CCR8 and other chemokine pathways in the migration of monocyte-derived dendritic cells to lymph nodes.* J Exp Med, 2004. 200(10): p. 1231-41.
98. Braun, A., et al., *Afferent lymph-derived T cells and DCs use different chemokine receptor CCR7-dependent routes for entry into the lymph node and intranodal migration.* Nat Immunol, 2011. 12(9): p. 879-87.
99. Bao, X., et al., *Endothelial heparan sulfate controls chemokine presentation in recruitment of lymphocytes and dendritic cells to lymph nodes.* Immunity, 2010. 33(5): p. 817-29.
100. Laverman, P., et al., *Radio*labeled *peptides for oncological diagnosis.* Eur J Nucl Med Mol Imaging, 2012. 39 Suppl 1: p. S78-92.
101. Demmer, O., et al., *Design, synthesis, and functionalization of dimeric peptides targeting chemokine receptor CXCR4.* J Med Chem, 2011. 54(21): p. 7648-62.
102. Gourni, E., et al., *PET of CXCR4 expression by a (68)Ga-labeled highly specific targeted contrast agent.* J Nucl Med, 2011. 52(11): p. 1803-10.
103. Woodard, L.E. and S. Nimmagadda, *CXCR4-based imaging agents.* J Nucl Med, 2011. 52(11): p. 1665-9.
104. Kastenmuller, W., M.Y. Gerner, and R.N. Germain, *The in situ dynamics of dendritic cell interactions.* Eur J Immunol, 2010. 40(8): p. 2103-6.
105. Germain, R.N., et al., *Dynamic imaging of the immune system: progress, pitfalls and promise.* Nat Rev Immunol, 2006. 6(7): p. 497-507.

106. Klauschen, F., et al., *Quantifying cellular interaction dynamics in 3D fluorescence microscopy data.* Nat Protoc, 2009. 4(9): p. 1305-11.
107. Bousso, P., *T-cell activation by dendritic cells in the lymph node: lessons from the movies.* Nat Rev Immunol, 2008. 8(9): p. 675-84.
108. Celli, S., et al., *Decoding the dynamics of T cell-dendritic cell interactions in vivo.* Immunol Rev, 2008. 221: p. 182-7.
109. Jusforgues-Saklani, H., et al., *Antigen persistence is required for dendritic cell licensing and CD8+ T cell cross-priming.* J Immunol, 2008. 181(5): p. 3067-76.
110. Dustin, M.L. and D. Depoil, *New insights into the T cell synapse from single molecule techniques.* Nat Rev Immunol, 2011. 11(10): p. 672-84.
111. Brewer, S., et al., *Epithelial uptake of (18F)1-(2'-deoxy-2'-arabinofuranosyl) cytosine indicates intestinal inflammation in mice.* Gastroenterology, 2010. 138(4): p. 1266-75.
112. Nair-Gill, E., et al., *PET probes for distinct metabolic pathways have different cell specificities during immune responses in mice.* J Clin Invest, 2010. 120(6): p. 2005-15.
113. Minamimoto, R., et al., *4'-(Methyl-11C)-Thiothymidine PET/CT for Proliferation Imaging in Non-Small Cell Lung Cancer.* J Nucl Med, 2012. 53(2): p. 199-206.
114. Burger, I.A., et al., *Incidence and intensity of F-18 FDG uptake after vaccination with H1N1 vaccine.* Clin Nucl Med, 2011. 36(10): p. 848-53.
115. Rabinovich, B.A. and C.G. Radu, *Imaging adoptive cell transfer based cancer immunotherapy.* Curr Pharm Biotechnol. 11(6): p. 672-84.
116. Pockaj, B.A., et al., *Localization of 111indium-labeled tumor infiltrating lymphocytes to tumor in patients receiving adoptive immunotherapy. Augmentation with cyclophosphamide and correlation with response.* Cancer, 1994. 73(6): p. 1731-7.
117. Hancock, B.W. and R.C. Rees, *Interleukin-2 and cancer therapy.* Cancer Cells, 1990. 2(1): p. 29-32.
118. Zhou, Y., et al., *Noninvasive molecular imaging of interferon beta activation in mouse liver.* Liver Int, 2012. 32(3): p. 383-91.
119. Shu, C.J., et al., *Quantitative PET reporter gene imaging of CD8+ T cells specific for a melanoma-expressed self-antigen.* Int Immunol, 2009. 21(2): p. 155-65.
120. Gross, S., B.L. Moss, and D. Piwnica-Worms, *Veni, vidi, vici: in vivo molecular imaging of immune response.* Immunity, 2007. 27(4): p. 533-8.
121. Signore, A., et al., *99mTc-interleukin-2 scintigraphy as a potential tool for evaluating tumor-infiltrating lymphocytes in melanoma lesions: a validation study.* J Nucl Med, 2004. 45(10): p. 1647-52.
122. Kanwar, B., et al., *In vivo imaging of mucosal CD4+ T cells using single photon emission computed tomography in a murine model of colitis.* J Immunol Methods, 2008. 329(1-2): p. 21-30.
123. Srinivas, M., et al., *In vivo cytometry of antigen-specific t cells using 19F MRI.* Magn Reson Med, 2009. 62(3): p. 747-53.
124. Srinivas, M., et al., *Customizable, multi-functional fluorocarbon nanoparticles for quantitative in vivo imaging using 19F MRI and optical imaging.* Biomaterials, 2010. 31(27): p. 7070-7.
125. Mantopoulos, D., A. Cruzat, and P. Hamrah, *In vivo imaging of corneal inflammation: new tools for clinical practice and research.* Semin Ophthalmol, 2010. 25(5-6): p. 178-85.
126. Spencer, D.B., et al., *In vivo imaging of the immune response in the eye.* Semin Immunopathol, 2008. 30(2): p. 179-90.
127. Therasse, P., E.A. Eisenhauer, and J. Verweij, *RECIST revisited: a review of validation studies on tumour assessment.* Eur J Cancer, 2006. 42(8): p. 1031-9.
128. Hoos, A., et al., *Improved Endpoints for Cancer Immunotherapy Trials.* J Natl Cancer Inst.
129. Wolchok, J.D., et al., *Guidelines for the evaluation of immune therapy activity in solid tumors: immune-related response criteria.* Clin Cancer Res, 2009. 15(23): p. 7412-20.
130. Minn, H. and P. Vihinen, *Melanoma imaging with highly specific PET probes: ready for prime time?* J Nucl Med, 2011. 52(1): p. 5-7.
131. Guo, H., et al., *Effects of the amino acid linkers on the melanoma-targeting and pharmacokinetic properties of 111In-labeled lactam bridge-cyclized alpha-MSH peptides.* J Nucl Med, 2011. 52(4): p. 608-16.
132. Denoyer, D., et al., *High-contrast PET of melanoma using (18)F-MEL050, a selective probe for melanin with predominantly renal clearance.* J Nucl Med, 2010. 51(3): p. 441-7.
133. Denoyer, D., et al., *Improved detection of regional melanoma metastasis using 18F-6-fluoro-N-(2-(diethylamino)ethyl) pyridine-3-carboxamide, a melanin-specific PET probe, by perilesional administration.* J Nucl Med, 2011. 52(1): p. 115-22.
134. Lazovic, J., et al., *Imaging immune response in vivo: cytolytic action of genetically altered T cells directed to glioblastoma multiforme.* Clin Cancer Res, 2008. 14(12): p. 3832-9.
135. Strauss, L.G., *Fluorine-18 deoxyglucose and false-positive results: a major problem in the diagnostics of oncological patients.* Eur J Nucl Med, 1996. 23(10): p. 1409-15.
136. van Waarde, A., et al., *Comparison of sigma-ligands and metabolic PET tracers for differentiating tumor from inflammation.* J Nucl Med, 2006. 47(1): p. 150-4.
137. Brockenbrough, J.S., et al., *Tumor 3'-deoxy-3'-(18)F-fluorothymidine ((18)F-FLT) uptake by PET correlates with thymidine kinase 1 expression: static and kinetic analysis of (18)F-FLT PET studies in lung tumors.* J Nucl Med, 2011. 52(8): p. 1181-8.
138. Gholamrezanezhad, A., et al., *Cytotoxicity of 111In-oxine on mesenchymal stem cells: a time-dependent adverse effect.* Nucl Med Commun, 2009. 30(3): p. 210-6.
139. Cromer Berman, S.M., et al., *Cell motility of neural stem cells is reduced after SPIO-labeling, which is mitigated after exocytosis.* Magn Reson Med, 2012.

140. de Chickera, S.N., et al., Labeling *dendritic cells with SPIO has implications for their subsequent in vivo migration as assessed with cellular MRI.* Contrast Media Mol Imaging, 2011. 6(4): p. 314-27.
141. Novotna, B., et al., *Oxidative damage to biological macromolecules in human bone marrow mesenchymal stromal cells labeled with various types of iron oxide nanoparticles.* Toxicol Lett, 2012. 210(1): p. 53-63.
142. Silva, A.K., et al., *Cellular Transfer of Magnetic Nanoparticles Via Cell Microvesicles: Impact on Cell Tracking by Magnetic Resonance Imaging.* Pharm Res, 2012.
143. Oude Munnink, T.H., et al., *PET with the 89Zr-labeled transforming growth factor-beta antibody fresolimumab in tumor models.* J Nucl Med, 2011. 52(12): p. 2001-8.
144. Campbell, D.O., et al., *Structure-guided engineering of human thymidine kinase 2 as a positron emission tomography reporter gene for enhanced phosphorylation of non-natural thymidine analog reporter probe.* J Biol Chem, 2012. 287(1): p. 446-54.
145. Yaghoubi, S.S., et al., *Positron emission tomography reporter genes and reporter probes: gene and cell therapy applications.* Theranostics, 2012. 2(4): p. 374-91.
146. Brogan, J., et al., *Imaging molecular pathways: reporter genes.* Radiat Res, 2012. 177(4): p. 508-13.
147. Berger, C., et al., *Analysis of transgene-specific immune responses that limit the in vivo persistence of adoptively transferred HSV-TK-modified donor T cells after allogeneic hematopoietic cell transplantation.* Blood, 2006. 107(6): p. 2294-302.
148. Schwarzenberg, J., et al., *Human biodistribution and radiation dosimetry of novel PET probes targeting the deoxyribonucleoside salvage pathway.* Eur J Nucl Med Mol Imaging, 2011. 38(4): p. 711-21.
149. Sangro, B., et al., *A phase I clinical trial of thymidine kinase-based gene therapy in advanced hepatocellular carcinoma.* Cancer Gene Ther, 2010. 17(12): p. 837-43.
150. Davis, J.L., et al., *Development of human anti-murine T-cell receptor antibodies in both responding and nonresponding patients enrolled in TCR gene therapy trials.* Clin Cancer Res, 2010. 16(23): p. 5852-61.
151. Di Stasi, A., et al., *Inducible apoptosis as a safety switch for adoptive cell therapy.* N Engl J Med, 2011. 365(18): p. 1673-83.
152. Likar, Y., et al., *PET imaging of HSV1-tk mutants with acquired specificity toward pyrimidine- and acycloguanosine-based radiotracers.* Eur J Nucl Med Mol Imaging, 2009. 36(8): p. 1273-82.
153. Likar, Y., et al., *A new pyrimidine-specific reporter gene: a mutated human deoxycytidine kinase suitable for PET during treatment with acycloguanosine-based cytotoxic drugs.* J Nucl Med, 2010. 51(9): p. 1395-403.
154. Gilad, A.A., et al., *MRI reporter genes.* J Nucl Med, 2008. 49(12): p. 1905-8.
155. Pei, Z., et al., *A multimodality reporter gene for monitoring transplanted stem cells.* Nucl Med Biol, 2012.
156. Fox, C.J., P.S. Hammerman, and C.B. Thompson, *Fuel feeds function: energy metabolism and the T-cell response.* Nat Rev Immunol, 2005. 5(11): p. 844-52.
157. Gerriets, V.A. and J.C. Rathmell, *Metabolic pathways in T cell fate and function.* Trends Immunol, 2012. 33(4): p. 168-73.
158. Shu, C.J., et al., *Novel PET probes specific for deoxycytidine kinase.* J Nucl Med, 2010. 51(7): p. 1092-8.
159. Reshef, A., et al., *Small-molecule biomarkers for clinical PET imaging of apoptosis.* J Nucl Med, 2010. 51(6): p. 837-40.
160. Kartachova, M., et al., *Prognostic significance of 99mTc Hynic-rh-annexin V scintigraphy during platinum-based chemotherapy in advanced lung cancer.* J Clin Oncol, 2007. 25(18): p. 2534-9.
161. Hoglund, J., et al., *18F-ML-10, a PET tracer for apoptosis: first human study.* J Nucl Med, 2011. 52(5): p. 720-5.
162. Haimovitz-Friedman, A., et al., *Imaging radiotherapy-induced apoptosis.* Radiat Res, 2012. 177(4): p. 467-82.
163. Zhou, R., P.D. Acton, and V.A. Ferrari, *Imaging stem cells implanted in infarcted myocardium.* J Am Coll Cardiol, 2006. 48(10): p. 2094-106.

The incidence of cancer is rising at fast pace; it is estimated that in the year 2030 22.2 million people will experience cancer, representing a 75% increase from the year 2008 (1). Anti-cancer treatments have evolved accordingly and at this point, surgery, radiotherapy and chemotherapy offer considerable response rates in many types of cancer, even in metastatic stage of disease. However, for some cancers, these classical treatment modalities have reached their potential. Metastatic or irresectable melanoma is one of them. By summing up 20 trials from 2002 to 2010 on chemotherapy and combinations of chemotherapy with novel biological or immunotherapies in metastatic melanoma, Garbe et al brutely demonstrate this notion; median overall survival still does not exceed 10 months regardless of the regimen (2).

"If there is anything I (*first person singular*) could do..." is a recurrent thought of many metastatic melanoma patients who enter the stage of 'no standard systemic treatment with proven benefit'.
"Imagine your own immune cells harnessed in a vaccine to fight cancer" is a thought that has probably crossed the mind of Ralph Steinman many times when he performed his early experiments. Notwithstanding other important contributions to the development of anti-cancer immunotherapy by others, Ralph Steinman discovered dendritic cells as the orchestrators of immune responses. He has pursued the role of dendritic cells since their discovery in 1973, leading to the first vaccination of a B-cell lymphoma patient in 1996 (3). As of June 2012, 151 clinical trials on dendritic cell vaccination are open for inclusion worldwide (www.clinicaltrials.gov). The rapid development from discovery to clinical application is unprecedented in medical history. Apart from his tenacious drive, he exemplifies the 'from bed to benchside' paradigm by demonstrating that translation of experimental data to clinical cases and careful clinical observation for validation of experimental data is an inexhaustible source of motivation. Lastly, the story of dendritic cell based vaccination seems to answer to the hope of many patients who face the limits of standard medical care that there must be a reasonable option beyond 'standard'.

Have dendritic cell based vaccination saved many lives? No. In line with the reported responses rates in literature, our studies demonstrate that only a small minority of patients survive >24 months and in most cases we could show an active role for the immune system. However, it has provided a unique platform to study interventions in a complex organ that encompasses several body compartments, e.g. peripheral tissues, lymph nodes, lymphatic and vascular systems and the tumour site. Moreover, the cells that comprise the immune system are not static but constantly circulate through the vascular and lymphatic system while they undergo many stages of differentiation during their life span.

The lesson from the latter is that every clinical case potentially provides a unique opportunity to learn about the critical processes that precede the failure or successful induction of an immune response. Progress of anti-cancer immunotherapy is only to be expected only if we manage to take this opportunity and learn how to guide therapy based on individual characteristics. The acknowledgement of the lack of biomarkers as the major hurdle for improved efficacy of immunotherapy has drastically influenced the way we design and perform clinical studies. Instead of performing small proof-of-principal studies in academic centres, focussing on a single parameter; large sponsor-driven randomized prospective studies are designed to find potential biomarkers. However, the approach of finding biomarkers for personalized medicine based on statistical analyses

of a general population has one demerit; it has lost its link to the individual case. Functional *in vivo* multimodal imaging is an ideal candidate to fulfill this thrilling task. It allows longitudinal assessment of the presence, specificity, phenotype, localization and multiple functionalities of immune cells in real-time in an individual case, linking therapeutic interventions to clinical outcome. In this respect the old adagium 'seeing is believing', is an undeniable truth.

References

1. Bray, F., et al., *Global cancer transitions according to the Human Development Index (2008-2030): a population-based study.* Lancet Oncol, 2012.
2. Garbe, C., et al., *Systematic review of medical treatment in melanoma: current status and future prospects.* Oncologist, 2011. 16(1): p. 5-24.
3. Hsu, F.J., et al., *Vaccination of patients with B-cell lymphoma using autologous antigen-pulsed dendritic cells.* Nat Med, 1996. 2(1): p. 52-8.

Het afweersysteem

Ons afweersysteem is een goed georganiseerd systeem dat bestaat uit een grote verscheidenheid van cellen, met elk een unieke functie. Het is zó ontworpen dat het bij uitstek geschikt is om ons lichaam te beschermen tegen indringers van buitenaf, zoals virussen en bacteriën, of tegen ontregelde cellen uit ons lichaam zelf, zoals kankercellen. Om deze ingewikkelde maar uiterst belangrijke taak te kunnen verrichten werkt ons afweersysteem met een enorme precisie; alleen gevaarlijke cellen worden aangepakt, óók als dat maar een enkele cel is. In het geval dat gevaarlijke cellen van buitenaf ons willen indringen, zoals een virus bij een fikse keelverkoudheid, reageert ons afweersysteem vaak heel adequaat; we worden er een beetje ziek van, maar het levert geen echt gevaar op. Hoe gaat een dergelijke afweerreactie in zijn werk? Het begint met het herkennen van virusdeeltjes als 'gevaar', hiervoor zijn dendritische cellen heel geschikt. Dendritische cellen zijn uitgerust met speciale herkenningsmoleculen (receptoren) op de buitenkant van hun celwand, bedoelt om unieke stukjes eiwit (antigenen) te herkennen. Daarnaast zijn dendritische cellen gelokaliseerd op strategische plaatsen, waar er contact is met de buitenwereld, zoals slijmvliezen en de huid. Deze dendritische cellen zijn continu op zoek naar alles wat *niet* in het lichaam thuishoort, en wat dus misschien wel gevaarlijk kan zijn. Wanneer zij iets herkennen als vreemd, en hierdoor gealarmeerd worden, zullen ze naar de lymfeklieren bewegen en de informatie die zij ergens opgepikt hebben zullen ze dan meenemen. De lymfklieren zijn een ontmoetingsplaats voor afweercellen; doorlopend komen dendritische cellen binnen met informatie over indringers die mogelijk een gevaar vormen. In de lymfeklier zijn ook andere afweercellen te vinden, dit zijn de cellen die het eigenlijke opruimwerk moeten doen, de T cellen. Deze afweercellen herkennen elk één specifiek uniek stukje eiwit (antigeen), en wanneer hun dit unieke stukje eiwit aangeboden wordt door een gealarmeerde dendritische cel, zullen zij in actie komen. Dat betekent dat zij zich zullen gaan vermenigvuldigen en de lymfeklier verlaten, om in grote getallen door het lichaam te zwerven, op zoek naar dat unieke stukje eiwit, …om het vervolgens op te ruimen. Dit proces werkt 24 uur per dag, 7 dagen per week. In het geval van een keelverkoudheid herkennen we deze stappen; ons slijmvlies van de keel wordt binnengedrongen, we krijgen keelpijn; vervolgens komen onze dendritische cellen in actie en nemen stukjes eiwitten mee naar de lymfeklieren. Gelukkig zijn er genoeg T cellen die deze antigenen herkennen en er begint een afweerreactie op gang te komen, onze lymfeklieren in de hals

zwellen dan ook op om ruimte te maken voor deze grote aantallen afweercellen. Na een paar dagen is ons afweersysteem op volle sterkte en wordt het virus opgeruimd. Ons afweersysteem kent ook een aantal regelsystemen, waardoor de afweerreactie weer wordt geremd wanneer het gevaar geweken is en er geen onnodige schade wordt aangedaan aan de gezonde weefsels.

Het afweersysteem en kanker

Wanneer bij iemand kanker wordt vastgesteld, is de afweerreactie niet adequaat genoeg geweest. Ons afweersysteem is blijkbaar onvoldoende in staat geweest om de kankercellen te herkennen als 'gevaar' en onze gezondheid is ernstig bedreigd. De kankercellen zijn op sommige punten in het voordeel; zij zijn van oorsprong lichaamseigen cellen en worden dus veel minder snel als 'gevaarlijk' herkend. Daarnaast maken kankercellen slim gebruik van de normale regelmechanismen om de afweercellen af te remmen in hun aanval op de kankercellen. Het ontwikkelen van kanker is een kat-en-muis spel tussen kankercellen en het afweersysteem. En op het moment dat bij patiënten kanker wordt ontdekt is vaak de kanker aan de winnende hand. Hoewel we ons goed moeten realiseren dat het hebben van kanker verre van kinderspel is, laat het onderwerp van dit proefschrift zich wel goed uitleggen door een vergelijking te maken met een strategisch spel.

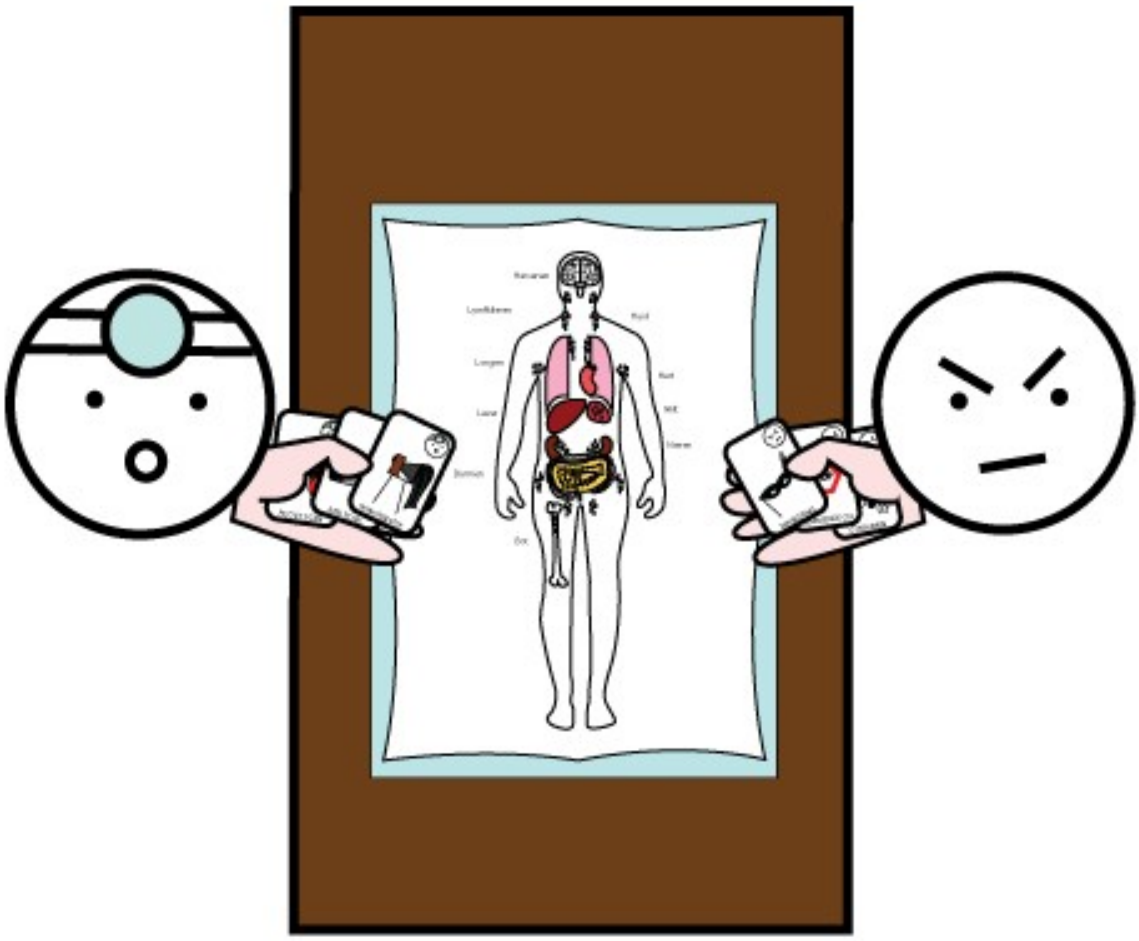

Het spel

In dit strategisch spel zijn kanker en het afweersysteem elkaars tegenspelers, en het doel is de controle over het lichaam te veroveren. Beide spelers hebben de beschikking over een set speelkaarten; mogelijkheden die zij op elk gewenst moment in kunnen zetten om de tegenspeler te slim af te zijn.

De speelkaarten

Aan de kant van het afweersysteem zijn dit de belangrijkste speelkaarten.

Dendritische cellen. Zoals hierboven beschreven hebben dendritische cellen een tweeledige rol, zij zijn in eerste instantie ‘verkenners’, continu op zoek naar gevaar. Maar wanneer zij ‘gevaar’ ontdekt hebben, ondergaan dendritische cellen een verandering; zij worden enorm goed in het activeren van juist die afweercellen die voor dàt specifieke gevaar op dàt moment in actie moeten komen. Het worden zogenaamde professionele antigeen-presenterende cellen, oftewel de ‘generaals’ van ons afweersysteem.

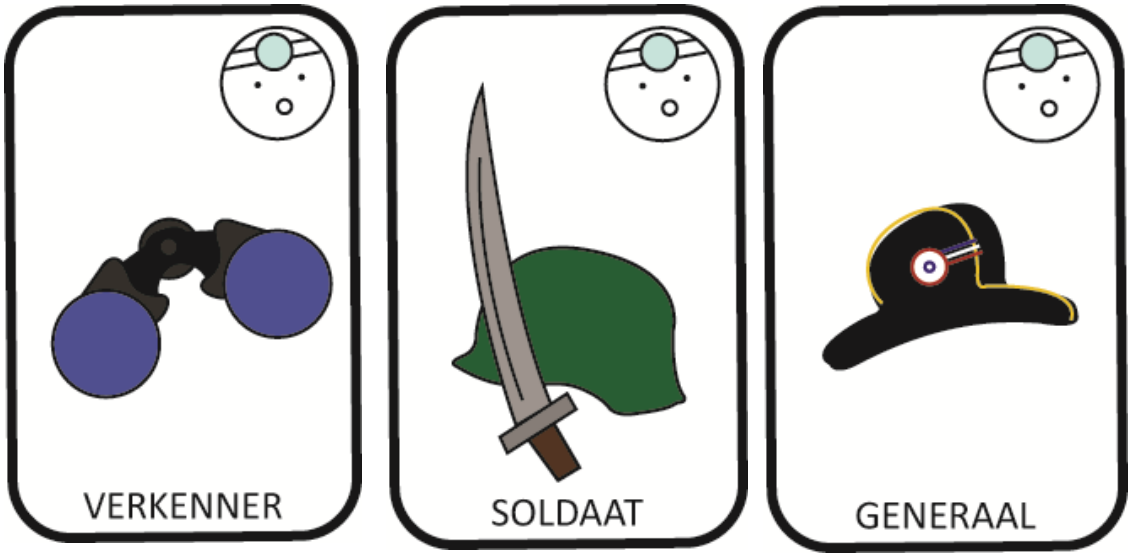

T cellen. Er zijn ook afweercellen die het opruimwerk moeten doen, deze zou je de ‘soldaatcellen’ kunnen noemen. Zij kunnen elk 1 stukje eiwit herkennen, maar vervolgens zich meer dan een duizendvoud vermenigvuldigen. Er zijn veel verschillende klassen en soorten T cellen, maar voor het opruimen van kanker zijn $CD8^+$ en $CD4^+$ T cellen het belangrijkst.

Andere soldaatcellen. Ons afweersysteem bestaat uit veel meer ‘soldaatcellen’, sommigen komen pas in actie wanneer ze door dendritische cellen geactiveerd worden, omdat zij hun de bijbehorende unieke stukjes eiwit presenteren, bijvoorbeeld B cellen. Andere ‘soldaatcellen’ komen ook zonder tussenkomst van dendritische cellen in actie en herkennen minder unieke stukjes eiwit, zoals NK cellen of macrofagen. Deze ‘soldaatcellen’ vallen buiten het onderwerp van dit proefschrift.

De tegenspeler, kanker, heeft een ander set speelkaarten. Kankercellen zijn kwaadaardig ontregelde lichaamseigen cellen, ze lijken dus in veel opzichten nog op de normale cellen binnen een bepaald weefsel. Het belangrijkste verschil is dat zij zich continu vermenigvuldigen, zonder zich iets aan te trekken van de terugkoppeling uit het weefsel. Daarnaast houden kankercellen zich niet aan de natuurlijke grenzen, en zullen zij zich dus door het lichaam willen verspreiden (metastaseren).

Maskering. Kankercellen lijken weliswaar voor het grootste deel op normale cellen, echter door hun mutaties kunnen er unieke stukjes eiwit ontstaan (antigen), waardoor ze te herkennen zijn door het afweersysteem. Door deze unieke stukjes eiwit niet te laten zien, kan de kankercel zich voor het afweersysteem onzichtbaar maken.

Remmende cellen. Onderdeel van een normaal werkend afweersysteem zijn de remmende cellen, regulatoire T cellen genoemd. Zij zijn één van de regelmechanismen die het afweersysteem kent om geen schade aan gezonde weefsels toe te brengen. Kankercellen trekken bij voorkeur deze remmende cellen aan en creëren op die manier een barrière voor soldaatcellen.

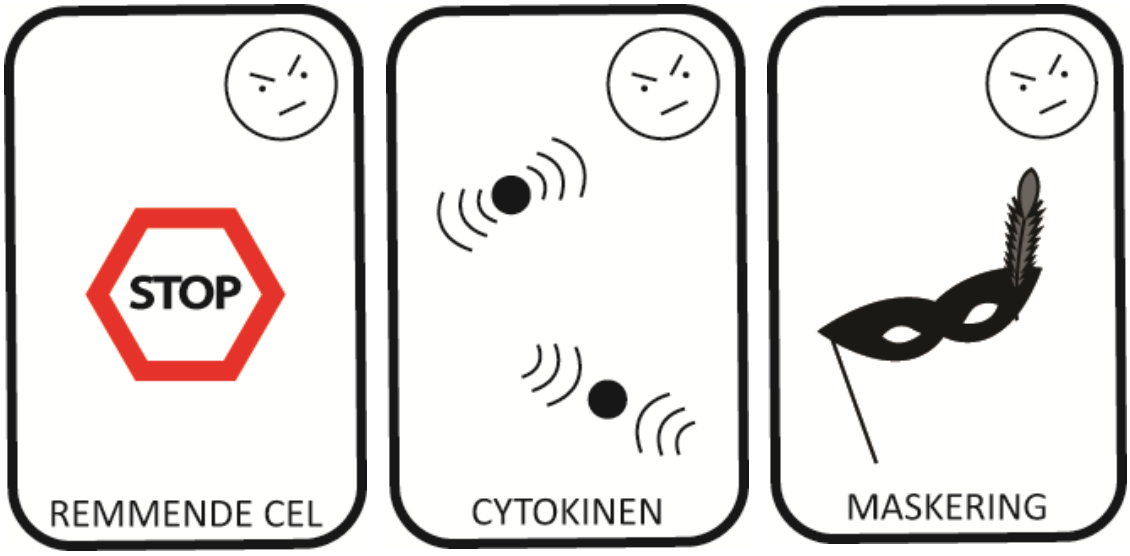

Signaalstoffen. Al die verschillende cellen van het afweersysteem moeten met elkaar communiceren, dit doen ze niet alleen door fysiek met elkaar contact te maken, zij scheiden ook signaalstoffen af (cytokinen). Sommige van deze signalen zullen activerend werken, andere juist remmend. Kankercellen gebruiken juist de remmende signaalstoffen om een aanval van soldaatcellen te weerstaan.

Het spelbord

De huid. Dit proefschrift gaat over de behandeling van kanker, dat is ontstaan uit de pigmenthoudende cellen (melanoom). In principe kan deze vorm van kanker overal ontstaan, maar het gebeurt veruit het vaakst vanuit de pigmenthoudende cellen van de huid; een moedervlek. Vandaar uit kan het zich uitspreiden door het hele lichaam. Melanoom is een vorm van kanker dat zich al in een vroeg stadium via het bloed door het lichaam kan verspreiden, mede hierom noemen we dit een 'agressieve' vorm van kanker.

Lymfeklieren. Boven zijn lymfeklieren beschreven als de ontmoetingsplaats tussen afweercellen; vooral dendritische cellen en T cellen. Om die reden zijn ook lymfeklieren strategisch gelegen en hebben we er veel van; hun aantal wordt geschat tussen 500 en 600. Een normale lymfeklier is slechts 8 tot 10mm groot.

Andere organen. Ons lichaam bestaat uit veel verschillende weefsels en organen, sommige hiervan zijn van essentieel belang. Van het melanoom weten we dat er verschil in ernst bestaat wanneer het zich heeft verspreidt naar verschillende organen; de overleving van patiënten is slechter wanneer het melanoom zich niet alleen in de huid of in de lymfeklieren heeft verspreid, maar ook naar de longen. Uitzaaiingen naar de lever of andere organen maakt de overleving van deze patiënten opnieuw nog slechter.

De troefkaarten; immunotherapie

De rol van het afweersysteem bij het herkennen en het opruimen van kankercellen, heeft ertoe geleid dat onderzoekers en artsen het gebruik van het afweersysteem als behandeling tegen kanker zijn gaan onderzoeken. Een behandeling waarin gebruik wordt gemaakt van ons afweersysteem noemen we immunotherapie; en dat kan aangrijpen op verschillende afweercellen. De studies die in dit proefschrift worden beschreven richten zich op vaccinaties met dendritische cellen, vanwege hun centrale rol in het opstarten van een afweerreactie. De dendritische cellen van een patiënt worden meestal verzameld uit afweercellen die veel voorkomen in het bloed, zogenaamde monocyten. Van deze cellen worden dendritische cellen gekweekt, deze worden in het Tumor Immunologisch Laboratorium geactiveerd door toevoeging van alarmsignalen en ze worden opgeladen met unieke

stukjes eiwit van een melanoom (antigenen) waarvan bij de patiënt is getest of deze inderdaad ook op zijn of haar melanoom voorkomen. Vervolgens wordt dit vaccin, de geactiveerde en met melanoom antigenen beladen lichaamseigen dendritische cellen, geïnjecteerd in de patiënt, vaak direct in de lymfeklier. Van daaruit zouden deze dendritische cellen hun natuurlijke rol weer op moeten pakken; ze zouden opzoek moeten gaan naar de 'soldaatcellen' die dit specifieke melanoom herkennen. Op deze manier wordt het afweersysteem wakker geschud en getraind op het herkennen en opruimen van kankercellen. Er zijn meer soorten troefkaarten, allemaal vormen van immunotherapie die buiten het onderwerp van dit proefschrift vallen. Maar het belangrijkst is dat met deze kaarten het afweersysteem een troef in handen heeft die de kankercellen niet hebben. We moeten er dus ons voordeel mee doen! Het nadeel echter, is dat de troefkaarten 'immunotherapie' moeten worden uitgespeeld zonder dat de behandelaar een goed zicht heeft op het spelbeloop.

De tactiek kaarten; immuno monitoring

Als je je troefkaarten blind moet uitspelen, is de kans groot dat je ze niet optimaal in kunt zetten. En zoals eerder gezegd, als kanker je tegenstander is, dan is het cruciaal om zo effectief mogelijk te spelen. Het onderwerp van dit proefschrift is het vinden van manieren om tòch zicht te krijgen op het spelbeloop; dit noemen we 'immuno monitoring'. In sommige gevallen is dat letterlijk 'zicht krijgen op', want met behulp van scantechnieken kunnen belangrijke processen in een afweerreactie gevolgd worden, zonder dat dit proces verstoord hoeft te worden. Andere technieken bestaan uit het verkrijgen van informatie over de afweerreactie door afweercellen af te nemen van strategische plaatsen, zoals lymfeklieren, bloed of de huid. Deze 'tactiek' kaarten worden hier kort uitgelegd.

Scintigrafie. De eerste stap in een succesvolle dendritische cel vaccinatie is het bereiken van de lymfeklier. In de studies in dit proefschrift wordt het vaccin via de huid ingespoten en zullen de dendritische cellen zelf hun weg naar de lymfeklier moeten vinden; slechts weinig cellen zullen de lymfeklier daadwerkelijk bereiken. Het vaccin kan ook direct in een lymfeklier worden geïnjecteerd, wat gezien de grootte van een lymfeklier technisch erg moeilijk is. Tijdens het maken van het vaccin kunnen de dendritische cellen een radioactief label meekrijgen, dat door middel van een gamma-camera gevolgd kan worden, dit heet scintigrafie. De scans zijn niet gedetailleerd, maar zijn wel erg gevoelig en in staat om te berekenen hoeveel dendritische cellen er daadwerkelijk in de lymfeklieren zijn aangekomen.

MRI scan. Een MRI scan staat voor Magnetic Resonance Imaging, en maakt in tegenstelling tot radioactieve scans gebruik van minuscule verstoringen in magnetische velden. Wanneer dendritische cellen met een ijzer-label of een ^{19}F-label gemerkt worden, kunnen ze met een MRI scan gevolgd worden. Het voordeel boven scintigrafie is dat deze scan veel gedetailleerder is. Als nadeel geldt echter, dat ijzer-labels niet geteld kunnen worden, en dus het aantal dendritische cellen niet

berekend kan worden. ^{19}F is een nieuw label, waarmee dit wel kan en daarmee kan dit nadeel omzeild worden. In dit proefschrift demonstreren wij dat op deze manier onderzocht kan worden wat de meest effectieve manier is om het vaccin toe te dienen.

Bloedtesten. Behalve dat het belangrijk is om te weten of het vaccin goed in de lymfeklieren aan is gekomen, is het van cruciaal belang dat je in kunt schatten wat het effect is op de afweercellen. Afweercellen die in een lymfeklier geactiveerd zijn, zullen de lymfeklier verlaten en via het bloed in de rest van het lichaam opzoek gaan naar de kankercellen waarop ze getraind zijn. De afweercellen in het bloed kunnen dus een blauwdruk zijn van wat er in een lymfeklier gebeurd is. In de praktijk is het echter vaak zo dat er in ons bloed enorm veel afweercellen zijn, en het aandeel van afweercellen die door de dendritische cel vaccinaties geactiveerd zijn is dan ook erg klein. Het kan dus erg moeilijk zijn om naar een paar specifieke afweercellen te zoeken. Daarnaast wil je eigenlijk niet alleen weten dat deze afweercellen er zijn, maar vooral wat ze tegen de kanker kunnen uitrichten. Er zijn tot op heden geen testen die je op grote schaal kunt toepassen om naast de aanwezigheid van deze melanoom herkennende afweercellen, ook hun functie te bepalen.

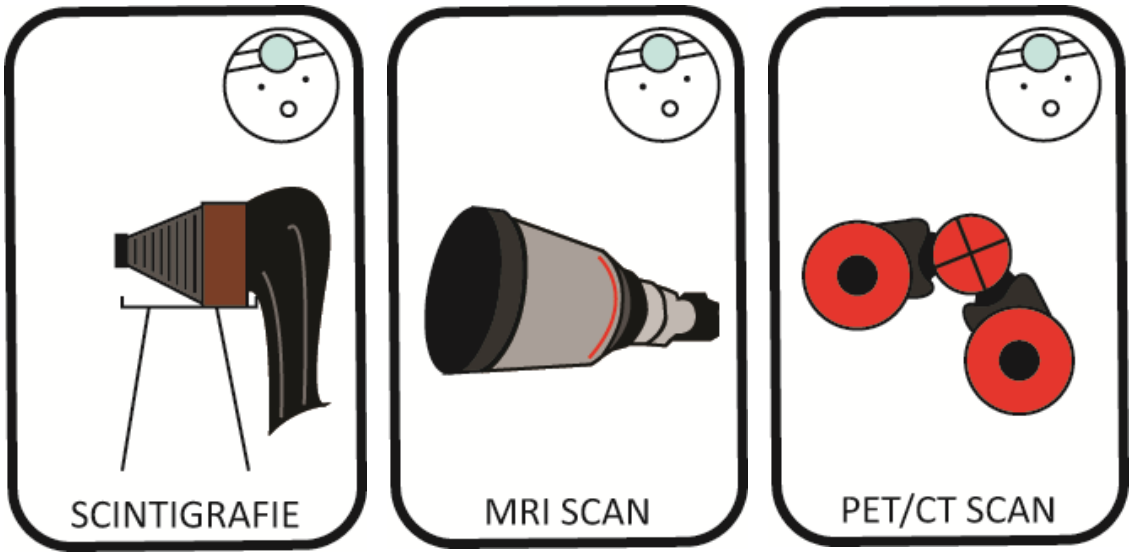

Huidtest. Met deze test wordt eigenlijk een oefensituatie opgezet; dendritische cellen die met unieke stukjes eiwit van het melanoom (antigenen) zijn beladen worden in de huid gespoten. Als alles goed is gegaan, zullen na de vaccinaties afweercellen door het lichaam zwerven die deze antigenen kunnen herkennen. Om deze antigenen te vinden, zullen de afweercellen de bloedbaan moeten verlaten en de huid binnen dringen. Na het afnemen van zo'n stukje huid (biopt) kunnen deze afweercellen in het laboratorium aan testen van verschillende moeilijkheidsgraad worden onderworpen. Zo kan heel gedetailleerd in kaart worden gebracht hoe functioneel de afweercellen zijn. In dit proefschrift tonen wij aan dat deze test goed kan voorspellen hoe de afweercellen in het lichaam hun werk doen.

PET/CT scan. Een PET/CT scan staat voor Positron Emitting Tomography/Computed Tomography, een combinatie van scans waarbij enerzijds radioactieve straling wordt gemeten en anderzijds een anatomische afbeelding wordt gemaakt. Met behulp van chemische technieken kunnen veel stofjes een radioactief label krijgen en zo zichtbaar worden voor een PET scan. Als je deze stofjes slim kiest, kun je heel precies naar functionele lichaamsprocessen kijken. In dit proefschrift worden twee van die stofjes gebruikt; ^{18}F-gelabeld FDG en ^{18}F-gelabeld FLT. FDG is een suiker, dat door heel actieve cellen gebruikt wordt als brandstof om energie uit vrij te maken. Zowel kankercellen als afweercellen zijn heel actieve cellen en zullen dus veel suiker opnemen. Met behulp van een PET scan kun je deze actieve cellen dan ook opsporen. FLT is een bouwsteen van ons genetisch materiaal (DNA), cellen die zich vermenigvuldigen moeten de helft van hun DNA meegeven aan hun nakomelingen en zelf weer

aanvullen. Vermenigvuldigende cellen zullen dus veel DNA-bouwstenen nodig hebben. Opnieuw kun je met een PET scan dan ook zien waar cellen zich bevinden die snel aan het vermenigvuldigen zijn. In dit proefschrift hebben wij uitgezocht of je door FDG of FLT te gebruiken met een PET scan kunt zien of er in de lymfeklieren daadwerkelijk activatie en/of vermenigvuldiging van afweercellen plaatsvindt na vaccinatie met dendritische cellen. Het blijkt dat dit wel met FLT, maar niet met FDG, kan en dat dit ook overeenkomt met andere manieren om de effecten na vaccinatie te meten.

De afloop

Hoe de afloop van de strijd tussen het afweersysteem en de kanker zal zijn, is niet te voorspellen. In het geval van patiënten met een uitgezaaide vorm van melanoom is de kans op overleving erg klein. Helaas hebben tot op heden dendritische celvaccinatie, of andere vormen van immunotherapie, hierop nog weinig invloed gehad. De afgelopen jaren hebben echter wel laten zien dat door het vaccin te verbeteren, we steeds beter in staat zijn om het afweersysteem ook goed te activeren; we hebben dus betere troefkaarten in handen. Daarnaast hebben we nu, door gebruik te maken van tactiek kaarten, ook de mogelijkheid gekregen om al in een vroeg stadium inzicht te krijgen in de effecten van vaccinaties. Op deze manier zouden we de vaccinaties zo efficiënt mogelijk in kunnen zetten, en belangrijker, zo zouden we de behandeling per patiënt aan kunnen passen om zijn of haar kansen zo groot mogelijk te maken.

Dankwoord

Dit proefschrift zou niet zijn geworden wat het nu is, zonder de inzet van de patiënten die deel hebben genomen aan de vaccinatie studies. Het contact met hen tijdens de vaccinatie poli was vaak intensief en persoonlijk. Er zijn veel momenten die me als dierbare herinneringen bij zullen blijven en me nog lang zullen motiveren om onderzoek te doen binnen de oncologie. Keer op keer, hebben zij mij versteld doen staan van de veerkracht van mensen, een les waarvoor ik ze heel dankbaar ben.

Een tweede groot woord van dank gaat uit naar mijn promotoren en co-promotor, die elk op zijn of haar eigen wijze een kritische bijdrage heeft geleverd aan dit proefschrift. Professor Punt, beste **Kees**, je hebt een enorm scherp inzicht in het doen van klinische studies. Jouw rechtlijnigheid en vastberaden manier van onderzoek doen heb ik erg gewaardeerd, al was het voor een over-enthousiaste jongeling zoals ik niet altijd goed in te voelen. Daarnaast heb je me doen inzien dat wij allemaal eens de Nachttrein naar Lissabon zouden moeten nemen. Professor Figdor, beste **Carl**, je hebt me laten zien dat goed onderzoek een team effort is. Als geen ander weet je mensen te motiveren en over grenzen heen te kijken, om vervolgens je eigen creatieve lijn te volgen. Een goed voorbeeld doet goed volgen? Jouw feedback is direct en altijd raak. Professor De Vries, beste **Jolanda**, ik ken niemand die zo snel kan schakelen en zoveel ballen tegelijk in de lucht kan houden als jij. Voor ik het in de gaten heb, denk jij al tien stappen vooruit. Je hebt me veel vrijheid gegeven om mijn eigen ideeën uit te voeren en tegelijkertijd kon ik altijd binnen lopen om de meest uiteenlopende zaken te bespreken. Doctor Jacobs, beste **Hans**, sinds mijn eerste kennismaking met het TIL hebben onze wegen spontaan vaak parallel gelopen. Al zijn de gekke gezichten bij de flowkasten alweer even geleden, de momenten op het werk of privé zijn nog altijd even inspirerend! Je rol als co-promotor heb je dubbel en dwars verdiend.

De 'klinische club' en oudgedienden; **Nicole**, **Mandy**, **Annemiek**, **Gerty**, **Jurjen**, **Kalijn**, **Tjitske**, **Jeanette**, **Michel**, **Danita**, **Pauline**, **Mangala**, **Eric**, **Marieke**, **Joost**, **Daniël**, **Mary-lène**, jullie zijn de motor achter deze studies. Het was fantastisch om met jullie samen te werken! Ik heb veel van jullie geleerd: van pipetteren en dendritische cellen kweken, tot het opvoeden van kinderen. Het zou goed zijn om af en toe te beseffen hoe uniek het is om met zoveel verschillende individuen zo'n goed team te vormen.

Gerty en **Kalijn**, met jullie als paranimfen hoef ik geen nacht wakker te liggen om mijn promotie, jullie zijn veel nauwkeuriger in het plannen en voorbereiden dan ik! Gerty, bedankt voor alle 'puntjes-op-de-i', en het was een eer om met de winnaar van de abstract-prijs terug te vliegen uit Budapest… Kalijn, bij jou is de vaccinatiepoli in goede handen, volgens mij zie je onderzoek als topsport!

Mangala, vanaf het begin ben je de perfecte sparring-partner geweest; je denkt standaard out-of-the box. Als we samen aan een artikel werken is het af binnen 2 weken… of binnen 2 jaar!

Daarnaast had ik het voorrecht om met nog heel veel anderen samen te werken, elk van hen maakte dat ik dit proefschrift met heel veel plezier heb geschreven. Zo waren er de **Tillers**, die zulke ongelooflijk goede afdelingsfeesten kunnen vieren, dat ik ze, voor zover ik me kan herinneren, nooit meer zal vergeten! Een speciale knipoog naar de TIL-band **Under DC**, die meer belachelijke foto's hebben opgeleverd dan me lief is… Ook wil ik de dames van Poli Rood bedanken, in het bijzonder **Christel**, **Maritha**, **Maartje**, **Michiel, Mirjam**, **Iris** en **Karin**, die er voor zorgden dat de vaccinatie poli ook in roerige tijden altijd soepel bleef lopen. De aferese-dames, **Gaby**, **Corry**, **Mariëtte** en **Monique**,

die in ruil voor een zak drop altijd wel een gaatje wisten te vinden in het afereseprogramma. De dames van het Onco secretariaat, **Carola**, **Jolanda**, **Tonnie**, **Brechje** die creatief meedachten zodat we de logistiek van de vaccinaties altijd weer rond kregen en die stapels met statussen gezocht hebben. De (oud-)**bewoners van De Villa**, die van een gehorige, koude, of juist snikhete, oude barak toch een gezellige plek wisten te maken. De vaccinatie studies hebben bij uitstek een multidisciplinair karakter, en zonder de inzet van de afdeling Heelkunde, **Han**, **Hans**, **Annelies**, de afdeling Pathologie, **Willeke**, **Han**, **Arie**, **Peter**, de afdeling Dermatologie, **Michelle**, **Rianne**, **Wilmy**, de afdeling Hematologie, **Sandra**, de afdeling Radiologie, **Roel**, **Simon** en de **echo-laboranten**, de afdeling Nucleaire Geneeskunde, **Peter**, **Eddy**, **Maichel**, **Miranda**, **Michel**, **Martin**, en de apotheek, **Marieke**, zou het resultaat zijn echte glans nooit gekregen hebben.

De afdeling Nucleaire Geneeskunde verdient hier een speciale plaats. Allereerst **Wim** en **Fee**, bedankt voor het vertrouwen dat jullie in mij stellen om te mogen beginnen aan de opleiding terwijl er nog een proefschrift af te ronden viel en voor de ruimte die jullie hebben gegeven om dit goed te doen. Volgens mij bevat dit proefschrift genoeg potentie om binnen de Nucleaire Geneeskunde het onderzoek een vervolg te kunnen geven; maar nu eerst op volle kracht vooruit! Daarnaast aan mijn collega-aios, **Ben**, **Rick**, **Michelle**, **Elske**, **Jeroen**, **Dennis**, **Sabine L.** en **Sabine H.** ook een groot dankjewel voor jullie geduld en gezelligheid. Mede door jullie zit ik nu op een goede plek!

Ook buiten het werk zijn er veel mensen die op meer of minder zichtbare manier hun bijdrage hebben gehad aan dit proefschrift. Vanaf De Intro van de studie Geneeskunde en soms al eerder zijn er 'De Jongens', inmiddels aangevuld met wederhelften. Op één of andere manier weten we elkaar toch elke keer weer te vinden, hoever we soms ook uitwaaieren. De spelletjesavonden, de jam-sessies op krappe Vosseveld kamertjes, de optredens, de wandeltochten, de discussies en de biertjes; ik hoop ze nooit te hoeven missen. **Anthony**, **Jurrian**, **Esther**, **Michiel**, **Ilker**, **Ivar**, **Leonoor**, **Anil**, **Jenny**, **Johan**, super jongens! Ook 'de volleybal club', dat nu eigenlijk alleen nog maar een dekmantel is voor het doen van spelletjes, het voeren van politieke discussie en tegenwoordig ook het bespreken van de obstakels die jonge ouders tegen komen. **Joost**, **Nienke**, **Remco**, **Maaike**, **Rianne** en **Christian**, bedankt voor jullie gezelligheid en interesse! Ook het thuisfront, **Koen**, **Monique**, **Bram**, **Lizan**, maar ook **Hans** en **Bertha**, **Mirjam**, **Tom**, **Arjan** en **Lieke**, en eigenlijk ook **Lotte**, **Wessel**, **Len** en **Fenna**, horen hier. Jullie zijn al bij veel mooie momenten geweest en ik ben heel blij dat jullie er nu ook weer bij zijn. Als we als 'family' wat ondernemen en voelt dat altijd als 'thuis', bedankt daarvoor.

Pa en **ma**, jullie onvoorwaardelijke steun heeft mij het zelfvertrouwen gegeven om dit proefschrift tot een goed eind te brengen. 'Volg je eigen kop' en 'pratende mensen zijn te helpen', hebben jullie ooit gezegd, en dat blijken telkens weer wijze lessen te zijn. Van de trein naar Eindhoven waar het ooit begon, tot het oppassen op de jongens in de laatste maanden, jullie staan altijd voor me klaar en daar kan ik jullie niet genoeg voor bedanken.

Duuk en **Tibbe** en ons derde **kleine wonder**, jullie hebben mij de mooiste titel gegeven van allemaal!

Lieve **Sabrina**, jou ontmoeten is het beste wat mij ooit is overkomen, we overlappen, we vullen elkaar aan, je stuurt me, je remt me en je motiveert me, je bedenkt wat ik nooit had kunnen bedenken en je zegt de goeie dingen op het goede moment; en in alles geldt '*better together*'. Zonder jou zou ik niet zijn wie ik nu ben, bedankt lief, ik hou van je!

Erik Hendrikus Johannes Gregorius Aarntzen werd geboren op 28 juni 1981 in Angeren, waar hij opgroeide en een fantastische jeugd beleefde. In 1993 begon hij aan het Voortgezet Wetenschappelijk Onderwijs (VWO) aan het Olympus College in Arnhem, waar hij in 1999 zijn examen behaalde. In dat jaar begon hij aan de opleiding Biomedische Technologie aan de Technische Universiteit in Eindhoven. Na een jaar besloot hij over te stappen naar de opleiding Geneeskunde aan de Radboud Universiteit Nijmegen. Dit bleek een goede keus; in 2001 haalde hij *cum laude* zijn propedeuse. Tijdens zijn doctoraal blijkt er al een grote interesse voor onderzoek, hij volgde een aantal extra cursussen binnen de Immunologie en de Medische Biotechnology en deed hij als student onderzoek op de afdeling Pathologie. Na het afronden van zijn doctoraal in 2004, maakte hij voor het eerst kennis met de afdelingen Tumor Immunologie en Medische Oncologie. Onder supervisie van prof.dr. G.J. Adema deed hij zijn Wetenschappelijke Stage met als titel '*Clinically applicable dendritic cells combining high migratory and IL-12 producing functions*'. Deze proeve smaakte naar meer. Na het afronden van zijn co-schappen, onder andere in het Holy Family Hospital in Berekum (Ghana), startte hij als arts-onderzoeker op de afdelingen Tumor Immunologie en Medische Oncologie binnen de dendritische celvaccinatie studies. Intussen was hij aangenomen voor de opleiding Algemeen Inwendige Ziekten en was hij vastbesloten zijn wetenschappelijke stage voort te zetten binnen een Agiko constructie. Deze werd hem in oktober 2008 toegekend. Sindsdien heeft hij tussen de opleiding Algemeen Inwendige Ziekten (prof.dr. J. de Graaf), de kliniek van de afdeling Medische Oncologie (prof.dr. C.J.A. Punt) en het lab van de afdeling Tumor Immunologie (prof.dr. C.G. Figdor) het onderzoek verricht dat heeft geleid tot dit proefschrift. De term Translationeel Ondezoek heeft hij onder andere invulling gegeven door dirigeren van twee professionele video's, waarin de studies uit dit proefschrift vertaald worden voor een breed publiek.

Het besluit om in Nijmegen Geneeskunde te gaan studeren was niet alleen om wetenschappelijke redenen een schot in de roos. Tijdens de opleiding ontmoette hij Sabrina, een mooier toeval bestaat niet. Vanaf dat moment kon het nooit meer stuk. De buitenlandse reizen, de ontbijtjes op het studentenbalkon, het enthousiaste 'ja'-woord, de geboorte van hun twee fantastische zoons Duuk en Tibbe en alle momenten daartussen, zijn een aaneenschakeling van geluk.

Aarntzen EH, Srinivas M, Bonetto F, RicondoCruz LJ, Verdijk P, Schreibelt G, Van de Rakt MM, Lesterhuis WJ, Van Riel M, Punt CJ, Adema GJ, Heerschap A, Figdor CG, Oyen WJ, De Vries IJ. Targeting of ^{111}In-labeled dendritic cell human vaccines improved by reducing number of cells. *Clin Cancer Res. 2012* [submitted]

Aarntzen EH, Srinivas M, Walczak P, Janowski M, Heerschap A, De Vries IJ, Figdor CG, Bulte JW, Oyen WJ. *In Vivo* Tracking Techniques for Cellular Regeneration, Replacement, and Redirection. *J Nucl Med. 2012 Dec 1;53(12):1825-1828.*

Tel J, **Aarntzen EH**, Baba T, Schreibelt G, Schulte BM, Benitez-Ribas D, Boerman OC, Croockewit A, Oyen WJ, Van Rossum MM, Winkels G, Coulie PG, Punt CJ, Figdor CG, De Vries IJM. *Cancer Res. 2012* [submitted]

Aarntzen EH, de Vries IJ, Lesterhuis WJ, Schuurhuis D, Jacobs JF, Bol K, Schreibelt G, Mus R, De Wilt JH, Haanen JB, Schadendorf D, Croockewit S, Blokx WA, van Rossum MM, Kwok WW, Adema GJ, Punt CJ, Figdor CG. Targeting CD4+ T helper cells improves the induction of anti-tumor responses in dendritic cell based vaccination. *Cancer Res. 2012 Oct 18.* [accepted]

Aarntzen EH, Srinivas M, Radu CG, Punt CJ, Boerman OC, Figdor CG, Oyen WJ, de Vries IJ. *In vivo* imaging of therapy-induced anti-cancer immune responses in humans. *Cell Mol Life Sci. 2012 Oct 5.* [accepted]

Aarntzen EH, Bol K, Schreibelt G, Jacobs JF, Lesterhuis WJ, van Rossum MM, Adema GJ, Figdor CG, Punt CJ, de Vries IJ. Skin-test infiltrating lymphocytes early predict clinical outcome of dendritic cell based vaccination in metastatic melanoma. *Cancer Res. 2012 Dec 1;72(23):6102-6110.*

Aarntzen EH, Srinivas M, Punt CJ, Figdor CG, Oyen WJ, de Vries IJ. Insight into the dynamics, localization and magnitude of antigen-specific immune responses by ^{18}F-FLT PET imaging. *Oncoimmunology. 2012 Aug 1;1(5):744-745.*

Aarntzen EH, Schreibelt G, Bol K, Lesterhuis WJ, Croockewit AJ, de Wilt JH, van Rossum MM, Blokx WA, Jacobs JF, Duiveman-de Boer T, Schuurhuis DH, Mus R, Thielemans K, de Vries IJ, Figdor CG, Punt CJ, Adema GJ. Vaccination with mRNA-Electroporated Dendritic Cells Induces Robust Tumor Antigen-Specific CD4+ and CD8+ T Cells Responses in Stage III and IV Melanoma Patients. *Clin Cancer Res. 2012 Oct 1;18(19):5460-5470.*

Weide B, Zelba H, Derhovanessian E, Pflugfelder A, Eigentler TK, Di Giacomo AM, Maio M, **Aarntzen EH,** de Vries IJ, Sucker A, Schadendorf D, Büttner P, Garbe C, Pawelec G. Functional T cells targeting NY-ESO-1 or Melan-A are predictive for survival of patients with distant melanoma metastasis. *J Clin Oncol. 2012 May 20;30(15):1835-41.*

Aarntzen EH, de Vries IJ, Göertz JH, Beldhuis-Valkis M, Brouwers HM, van de Rakt MW, van der Molen RG, Punt CJ, Adema GJ, Tacken PJ, Joosten I, Jacobs JF. Humoral anti-KLH responses in cancer patients treated with dendritic cell-based immunotherapy are dictated by different vaccination parameters. *Cancer Immunol Immunother. 2012 Nov;61(11):2003-11.*

Aarntzen EH, Srinivas M, De Wilt JH, Jacobs JF, Lesterhuis WJ, Windhorst AD, Troost EG, Bonenkamp JJ, van Rossum MM, Blokx WA, Mus RD, Boerman OC, Punt CJ, Figdor CG, Oyen WJ, de Vries IJ. Early identification of antigen-specific immune responses in vivo by [18F]-labeled 3'-fluoro-3'-deoxy-thymidine ([18F]FLT) PET imaging. *Proc Natl Acad Sci U S A. 2011 Nov 8;108(45):18396-9.*

Lesterhuis WJ, de Vries IJ, Schreibelt G, Lambeck AJ, **Aarntzen EH**, Jacobs JF, Scharenborg NM, van de Rakt MW, de Boer AJ, Croockewit S, van Rossum MM, Mus R, Oyen WJ, Boerman OC, Lucas S, Adema GJ, Punt CJ, Figdor CG. Route of administration modulates the induction of dendritic cell vaccine-induced antigen-specific T cells in advanced melanoma patients. *Clin Cancer Res. 2011 Sep 1;17(17):5725-35.*

Lesterhuis WJ, De Vries IJ, Schreibelt G, Schuurhuis DH, **Aarntzen EH**, De Boer A, Scharenborg NM, Van De Rakt M, Hesselink EJ, Figdor CG, Adema GJ, Punt CJ. Immunogenicity of dendritic cells pulsed with CEA peptide or transfected with CEA mRNA for vaccination of colorectal cancer patients. *Anticancer Res. 2010 Dec;30(12):5091-7.*

Lesterhuis WJ, de Vries IJ, **Aarntzen EH**, de Boer A, Scharenborg NM, van de Rakt M, van Spronsen DJ, Preijers FW, Figdor CG, Adema GJ, Punt CJ. A pilot study on the immunogenicity of dendritic cell vaccination during adjuvant oxaliplatin/capecitabine chemotherapy in colon cancer patients. *Br J Cancer. 2010 Oct 26;103(9):1415-21.*

Aarntzen EH, van der Graaf WT, van Laarhoven HW. Scrotal and inguinal mass. Neth J Med. 2010 Sep;68(9):367-70.

Srinivas M, **Aarntzen EH**, Bulte JW, Oyen WJ, Heerschap A, de Vries IJ, Figdor CG. Imaging of cellular therapies. *Adv Drug Deliv Rev. 2010 Aug 30;62(11):1080-93.*

Schuurhuis DH, Verdijk P, Schreibelt G, **Aarntzen EH**, Scharenborg N, de Boer A, van de Rakt MW, Kerkhoff M, Gerritsen MJ, Eijckeler F, Bonenkamp JJ, Blokx W, van Krieken JH, Boerman OC, Oyen WJ, Punt CJ, Figdor CG, Adema GJ, de Vries IJ. *In situ* expression of tumor antigens by messenger RNA-electroporated dendritic cells in lymph nodes of melanoma patients. *Cancer Res. 2009 Apr 1;69(7):2927-34.*

Verdijk P, **Aarntzen EH**, Lesterhuis WJ, Boullart AC, Kok E, van Rossum MM, Strijk S, Eijckeler F, Bonenkamp JJ, Jacobs JF, Blokx W, Vankrieken JH, Joosten I, Boerman OC, Oyen WJ, Adema G, Punt CJ, Figdor CG, de Vries IJ. Limited amounts of dendritic cells migrate into the T-cell area of lymph nodes but have high immune activating potential in melanoma patients. *Clin Cancer Res. 2009 Apr 1;15(7):2531-40.*

Schuurhuis DH, Lesterhuis WJ, Kramer M, Looman MG, van Hout-Kuijer M, Schreibelt G, Boullart AC, **Aarntzen EH**, Benitez-Ribas D, Figdor CG, Punt CJ, de Vries IJ, Adema GJ. Polyinosinic polycytidylic acid prevents efficient antigen expression after mRNA electroporation of clinical grade dendritic cells. *Cancer Immunol Immunother. 2009 Jul;58(7):1109-15.*

Aarntzen EH, Figdor CG, Adema GJ, Punt CJ, de Vries IJ. Dendritic cell vaccination and immune monitoring. *Cancer Immunol Immunother. 2008 Oct;57(10):1559-68.*

Verdijk P, **Aarntzen EH**, Punt CJ, de Vries IJ, Figdor CG. Maximizing dendritic cell migration in cancer immunotherapy. *Expert Opin Biol Ther. 2008 Jul;8(7):865-74.*

Jacobs JF, **Aarntzen EH**, Sibelt LA, Blokx WA, Boullart AC, Gerritsen MJ, Hoogerbrugge PM, Figdor CG, Adema GJ, Punt CJ, de Vries IJ. Vaccine-specific local T cell reactivity in immunotherapy-associated vitiligo in melanoma patients. *Cancer Immunol Immunother. 2009 Jan;58(1):145-51.*

Boullart AC, **Aarntzen EH**, Verdijk P, Jacobs JF, Schuurhuis DH, Benitez-Ribas D, Schreibelt G, van de Rakt MW, Scharenborg NM, de Boer A, Kramer M, Figdor CG, Punt CJ, Adema GJ, de Vries IJ. Maturation of monocyte-derived dendritic cells with Toll-like receptor 3 and 7/8 ligands combined with prostaglandin E2 results in high interleukin-12 production and cell migration. *Cancer Immunol Immunother. 2008 Nov;57(11):1589-97.*

Lesterhuis WJ, **Aarntzen EH**, De Vries IJ, Schuurhuis DH, Figdor CG, Adema GJ, Punt CJ. Dendritic cell vaccines in melanoma: from promise to proof? *Crit Rev Oncol Hematol. 2008 May;66(2):118-34.*

Aarntzen EH, Barrera P. Short digits...what's up? Arthritis Rheum. 2007 Dec 15;57(8):1568-71.

Jacobs JF, Hoogerbrugge PM, de Rakt MW, **Aarntzen EH**, Figdor CG, Adema GJ, de Vries IJ. Phenotypic and functional characterization of mature dendritic cells from pediatric cancer patients. *Pediatr Blood Cancer. 2007 Dec;49(7):924-7.*

Van Bokhoven MM, **Aarntzen EH**, Tan AC. Metastatic melanoma of the common bile duct and ampulla of Vater. Gastrointest Endosc. 2006 May;63(6):873-4.

Aarntzen EH, Van Riel PL, Barrera P. Refractory adult onset Still's disease and hypersensitivity to non-steroidal anti-inflammatory drugs and cyclo-oxygenase-2 inhibitors: are biological agents the solution? *Ann Rheum Dis. 2005 Oct;64(10):1523-4.*